KOMUNIKÁCIE

COMMUNICATIONS

SCIENTIFIC LETTERS OF THE UNIVERSITY OF ŽILINA

Volume 24

UNIVERSITY OF ŽILINA

ISSN 1335-4205

3/2022

UNIVERSITY OF ŽILINA
EDIS-Publishing House
UNIZA

EDIS-Publishing House of the University of Žilina (UZ) is one of the University of Žilina's consituents. The beginning of its existence dates back to 1990. In the course of its work, the publishing house has published more than 4 700 titles of book publications, especially university textbooks, scientific monographs, scripts, prose, but also enriched the book market with titles of regional, children's and popular literature.

Students and professional public have the opportunity to purchase published titles in the „Selling Study Literature" directly on the premises of the University of Žilina, in the EDIS shop or upon order on a „cash on delivery" basis. All published titles are available at: www.edis.uniza.sk.

EDIS-Publishing House of the University of Žilina offers book titles in English

Lenka Černá, Jozef Daniš
APPLICATION OF COST CALCULATIONS IN THE TARIFF POLICY FORMATION IN RAILWAY TRANSPORT
ISBN 978-80-554-1391-4 Price 7.61 €

Jozef Gašparík et al.
RAILWAY TRAFFIC OPERATION
ISBN 978-80-554-1281-8 Price 15.80 €

Eva Nedeliaková, Jana Sekulová
EVALUATION OF QUALITY IN RAILWAY TRANSPORT
ISBN 978-554-1272-6 Price 8.00 €

Anna Tomová
ECONOMICS OF AIR NAVIGATION SERVICES
ISBN 978-80-554-0905-4 Price 14.30 €

Felix Fedorovič Rybakov, Alexander Nikolaevič Lyakin, Štefan Cisko et.al.
GLOBALIZATION AND DEVELOPMENT OF INFRASTRUCTURE
ISBN 978-80-554-0719-7 Price 19.80 €

Marica Mazurek
MODELS OF BRANDING AND THEIR APPLICATION
ISBN 978-80-554-1705-9 Price 9.00 €

Ján Bujňák, Ružica Nikolić, Jelena Djoković
STEEL STRUCTURES COLLECTION OF SOLVED PROBLEMS WITH EXCERPTS FROM THEORY
ISBN 978-80554-0404-2 Price 9.34 €

Martin Bugaj
Aeromechanics 1
ISBN 978-80-554-1675-5 Price 14.50 €

Michal Kvet, Karol Matiaško, Marek Kvet
USB - BECOME EXPERT IN MYSQL PRACTICES FOR DATABASE SYSTEMS IN MYSQL
ISBN 978-80-554-1786-8 Price 13.50 €

Tetiana Hovorushchenko et.al.
CD - INTELLIGENT INFORMATION-ANALYTICAL TECHNOLOGIES...
ISBN 978-80-554-1729-5 Price 3.50 €

Karol Matiaško, Michal Kvet, Marek Kvet
CD - Practices for database systems
ISBN 978-80-554-1397-6 Price 2.20 €

Jozef Melcer
Dynamics of structures
ISBN 978-80-554-1698-4 Price 19.00 €

EDIS-Publishing House UNIZA
Univezitná 8215/1
010 26 Žilina
e-mail: edis_objednavky@uniza.sk, edis@uniza.sk
www.edis.uniza.sk

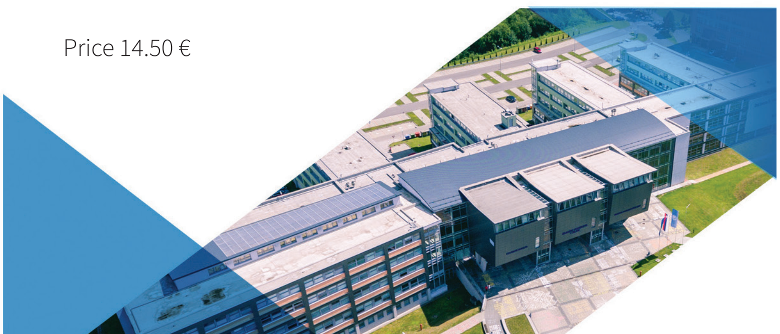

A - OPERATION AND ECONOMICS

CONTROL OVER DRIVING BEHAVIOUR AND ACCIDENT INVOLVEMENT: A CASE AMONG YOUNG DRIVERS IN MALAYSIA A88
S. H. Harith

CHANGE IN THE MOBILITY OF POLISH RESIDENTS DURING THE COVID-19 PANDEMIC A100
P. Gorzelańczyk

MOBILITY IN THE DEVELOPING COUNTRY. THE CASE STUDY OF BANGKOK METROPOLITAN REGION A112
K. Wilinski, S. Pathak

EMPIRICAL MEASUREMENT OF ELECTROMOBILITY EFFICIENCY IN THE ENVIRONMENT OF THE EUROPEAN UNION A123
J. Kubás, M. Ballay, J. Ristvej, K. Zábovská

APPLICATION OF MULTI-CRITERIA DECISION MAKING METHODS FOR EVALUATION OF SELECTED PASSENGER ELECTRIC CARS: A CASE STUDY A133
O. Stopka, M. Stopková J. Pečman

EFFECT OF PERIODIC TECHNICAL INSPECTIONS OF VEHICLES ON TRAFFIC ACCIDENTS IN THE SLOVAK REPUBLIC A142
J. Hudec, B. Šarkan

B - MECHANICAL ENGINEERING

ECONOMIC AND ENVIRONMENTAL BENEFITS OF USING CAVITATION TREATED FUEL IN VEHICLES OF INTERNAL COMBUSTION ENGINES B158
I. Aftanaziv, M. Malovanyy, L. Shevchuk, O. Strogan, L. Strutynska

ANALYSIS OF INFLUENCE OF THE LOAD PLANE COMBINED WITH PRELOAD ON DURABILITY OF BEARING B170
J. Kaczor

ULTRASONIC UNIT FOR REDUCING THE TOXICITY OF DIESEL VEHICLE EXHAUST GASES B189
A. Kadyrov, B. Sarsembekov, A. Ganyukov, S. Suyunbaev, K. Sinelnikov

EXPERIMENTAL AND THEORETICAL PERFORMANCE EVALUATION OF BASIN SOLAR STILL WITH LID AFLOAT IN EGYPT CONDITIONS B199
A. Mesalem, A. Walaa, A. Elweetedy, S. Elshamarka

DEVELOPMENT OF A MODEL FOR CALCULATING THE SLIP COEFFICIENTS OF A MECHANICAL WHEELED VEHICLE WITH TWO STEERING AXLES B211
T. N. Bekenov, Z. T. Nussupbek, Z. T. Tassybekov, Z. K. Sattinova

RESEARCH INTO THE LOADING OF THE TANK CAR FRAME CONCEPT WITH FILLER IN THE COMPOSITE CENTER SILL B219
O. Fomin, J. Gerlici, A. Lovska, K. Kravchenko

PREDICTION OF THE ULTRA-LARGE CONTAINER SHIPS' PROPULSION POWER AT THE INITIAL DESIGN STAGE B228
P. K. Korlak

METHODS FOR IDENTIFICATION OF COMPLEX INDUSTRIAL CONTROL OBJECTS ON THEIR ACCELERATING CHARACTERISTICS B239
A. Abdullayeva, A. Kalabayeva, A. Ivanov, S. Abdullayev, G. Bakyt

METHODOLOGY OF FORCE PARAMETERS JUSTIFICATION OF THE CONTROLLED STEERING WHEEL SUSPENSION B247
B. Sokil, O. Lyashuk, M. Sokil, Y. Vovk, I. Lebid, I. Hevko, M. Levkovych, R. Khoroshun, A. Matviyishyn

CALCULATION OF BASIC INDICATORS OF RUNNING SAFETY ON THE EXAMPLE OF A FREIGHT WAGON WITH THE Y25 BOGIE B259
J. Dižo, M. Blatnický, D. Molnár, A. Falendysh

A MATHEMATICAL MODEL OF OPERATION OF A SEMI-TRAILER TRACTOR POWERTRAIN B267
J. Dižo, M. Blatnický, R. Melnik, O. Kravchenko

D - CIVIL ENGINEERING IN TRANSPORT

SMOTE VS. RANDOM UNDERSAMPLING FOR IMBALANCED DATA- CAR OWNERSHIP DEMAND MODEL D105
W. Chaipanha, P. Kaewwichian

THE COMPARISON OF DYNAMIC EFFECTS ACTING IN THE COMMON CROSSING AND SWITCH UNIT OF A TURNOUT D116
J. Smutný, D. Jánoštík, V. Nohál

A SIMULATION APPROACH FOR EVALUATING CONGESTION AND ITS MITIGATION MEASURES ON URBAN ARTERIALS OPERATING WITH MIXED TRAFFIC CONDITIONS D126
CH. S. Bari, T. V. Gunjal, A. Dhamaniya

ENERGY-SAVING THERMAL STABILIZATION SYSTEM AND ASSESSMENT OF TEMPERATURE LOADINGS OF A BRIDGE DECK PAVEMENT D141
S. A. Kostenko, A. A. Piskunov, N. A. Ganin, G. A. Emelianova

E - MANAGEMENT SCIENCE AND INFORMATICS

REVIEWING THE COMPONENTS OF TECHNOLOGY ACCEPTANCE BEHAVIOR IN TRANSPORTATION SECTOR E96
W. Ahmed, S. M. Hizam, I. Sentosa

DEVELOPMENT OF MODE-WISE SPEED PREDICTION MODELS FOR URBAN ROADS WITH SIDE FRICTION CHARACTERISTICS E108
S. G. Singh, S. V. Kumar

F - SAFETY AND SECURITY ENGINEERING IN TRANSPORT

ANALYSIS AND EVALUATION OF THE EFFECTIVENESS OF SAFETY SYSTEMS AT RAILROAD CROSSINGS IN POLAND F46
P. Gorzelańczyk, A. Borkowska, P. Szubert, T. Kalina, M. Jurkovič

ASSESSING THE PROPENSITY TO CAR SHARING SERVICES IN UNIVERSITY CITIES: SOME INSIGHTS FOR DEVELOPING THE CO-CREATION PROCESS G46
V. Torrisi, T. Campisi, M. Ignaccolo, G. Inturri, G. Tesoriere

CONTROL OVER DRIVING BEHAVIOUR AND ACCIDENT INVOLVEMENT: A CASE AMONG YOUNG DRIVERS IN MALAYSIA

Siti Hawa Harith

Department of Human Resource Management, School of Business Management, Universiti Utara Malaysia, Kedah, Malaysia

*E-mail of corresponding author: sitihawa@uum.edu.my

Resume

Human factors specifically, perceived behavioural control (PBC) is among the accident causation factors leading to risky driving behaviour among young drivers. Therefore, this paper aims to investigate the relationship between PBC and young drivers' risky driving behaviour, PBC and accident involvement as well as the mediating role of risky driving behaviour to mediate the relationship between the PBC and accident involvement. The sample of this study involved active young drivers aged between 18 and 25, possess valid driving license, with at least six months of driving experience and have been involved in a road accident for the past 12 months. Results showed a significant relationship between PBC and young drivers' risky driving behaviour as well as the PBC and accident involvement. Moreover, risky driving behaviour was proved to mediate the relationship between PBC and accident involvement.

Article info

Received 12 September 2021

Accepted 27 October 2021

Online 29 March 2022

Keywords:

perceived behavioural control

risky driving behaviour

accident involvement

young drivers

Available online: https://doi.org/10.26552/com.C.2022.3.A88-A99

ISSN 1335-4205 (print version)

ISSN 2585-7878 (online version)

1 Introduction

Over the years, Malaysia has reported a high number of road accidents as well as fatality cases. In 2018 alone, a total of 536,250 accident cases and 6284 fatalities have been reported [1]. This figure exceeded the initial expectation made by the Malaysian government. Reports show that majority of road accidents occurred due to the drivers' and riders' failure to abide by the traffic rules and regulations [2-3]. Violation of traffic law leads to accidents not only in Malaysia but also in other countries around the world. Despite other factors that could contribute toward road accidents like technical factors of road faulty and vehicle faulty as well as the environmental factors of adhering weather, human factors of traffic violation behaviour and risky driving behaviour indeed top the issue factors [4]. Human factors are the most avoidable factors for the road accidents since drivers and riders are highly and solely responsible for their own driving behaviour [3]. Moreover, it has been reported that most road accidents occur due to the drivers' and riders' irresponsible driving behaviour.

Scholars further summarized that to overcome the issue of drivers' and riders' risky driving behaviour and their involvement in road accidents, an independent variable namely perceived behavioural control (PBC) should be used as one of the important elements that need to be considered [5-7]. The PBC believes in on the concept of self-control where drivers and riders can control their own driving behaviour. This means that, any driving decisions made by drivers and riders are solely based on their own discretion without any coercion from other parties. As a result, drivers and riders are basically in total control over the course of driving whether or not to drive dangerously and jeopardize their own life as well as other road users. Given the important role of PBC as one of the key antecedents of risky driving behaviour, this study aimed to investigate the relationship between the drivers' and riders' PBC toward risky driving behaviour and their involvement in a road accident as well as the mediating role of risky driving behaviour to mediate the relationship between the PBC and accident involvement.

1.1 Road accident involvement among young drivers around the world

Road accident involvement among the young and novice drivers has been seen higher compared to other age group drivers. The term "young driver" is being defined as a driver aged between 18 to 25 years old [8]. In contrast, Cordellieri et al. [9] define "young driver" as a driver aged between 18 to 22 years old, whereas Mohamed and Bromfield [10] describe "young driver" as those aged between 18 to 24 years old. Jamaluddin et al. [11] in their research for the Malaysian Institute of Road Safety and Research (MIROS) highlighted that young driver aged between 15 and 25 are the highly risky accident group in Malaysia. Thus, in this research, the operational definition for the term "young driver" is defined as a driver aged between 18 and 25 years old.

Literature consistently revealed that younger drivers tend to commit more traffic violations including speeding and using mobile phones while driving despite their lack of driving experience [12]. This fact was further supported by other studies, which also highlighted the high traffic violations and accident involvements among the young drivers and riders in Australia and other European countries like the UK, Belgium and Italy [13-14]. In an investigation involving six European countries such as Germany, Finland, Italy, Netherlands, Sweden and the United Kingdom, reported that drivers' misjudgement over the time and distance during the course of driving has been reported as one of the contributors of accident occurrence and involvement among drivers [15].

A relevant review of the literature demonstrated that 2681 younger drivers from nine European countries namely Italy, Austria, Bulgaria, Cyprus, Germany, Ireland, Latvia, Lithuania and Poland tend to perceive a higher level of risks associated with driving [9]. Younger drivers are lacking in driving skills since the improvement of the skills eventually increases with age [11]. Similar situation had occurred in Asian countries, particularly Malaysia. Based on a study conducted by MIROS, age was considered one of the significant factors influencing the road accidents in the Klang Valley [11]. The study further highlighted that driver between the age of 15 to 25 years old are highly involved in traffic crashes [11]. It is further highlighted that young driver aged between 16 to 25 years old had caused 46% of fatal and non-fatal accidents in Malaysia [16].

In the road safety study, individual factors play a significant role to explain the occurrence of road accidents. Individual factors are the determinant identified within the individual himself/herself [17]. The factors include human attitude and personal characteristics [17]. To further identify the factors leading to accident involvement, a systematic review was conducted in this study on four academic databases namely Emerald, Scopus, Web of Science and Wiley Online Library. Through the review, an individual factor of perceived behavioural control (PBC) was identified as the possible significant contributor of accident involvement [5-6]. Therefore, this study further investigates the impact of the PBC on young drivers' risky driving behaviour and involvement in road accidents.

2 Literature review

2.1 Perceived behavioural control (PBC) and risky driving behaviour

The PBC applies the self-efficacy concept that explains a person's ability to control his or her own behaviour. PBC can also be interpreted as a belief where an outcome or consequence of the behaviour is influenced by the person himself. To promote the safe driving and reduce road accident statistics, PBC is used as one of the highly applicable indicators. In the concept of road safety, PBC is interpreted as to what extent drivers and riders can control their driving behaviour by not committing any wrongful traffic acts such as speeding, close following, use of mobile phone, dangerous overtaking and driving while intoxicated [5, 6, 18]. Risky driving behaviour is also known as traffic violation behaviour. This risky driving behaviour is considered as the drivers' and riders' intentional failure to abide by the traffic rules and regulations despite having knowledge of the wrongdoing. By breaking the traffic rules and regulations, drivers and riders are jeopardizing not only their life but also lives of other road users. Among the common risky driving behaviours committed by drivers and riders are driving over the speed limit, illegal use of mobile phone while driving, tailgating and running through the red light [5, 19-20]. In some of the serious cases, drivers and riders fail to control their vehicles and cause casualty.

A study conducted in Australia reported that the PBC can influence the drivers' behaviour to text while driving [21]. It was further mentioned that drivers with a high level of PBC were found to not engage with such violation behaviour [21-22]. Similarly, another study conducted in Australia also highlighted the importance of self-control to restraint one's behaviour from illegal use of mobile phones while driving [22]. Furthermore, a study conducted among Spain university students showed that texting while driving is a typical traffic violation committed by the students [12]. Students with good self-control were able to restrain themselves from using mobile phones and kept their full attention on driving.

Besides that, the PBC is also an important element to curb drivers' and riders' speeding behaviour. This has been further confirmed in two studies conducted in France, which highlighted PBC as the significant predictors to explain the risky driving behaviour of speeding [5, 23]. Similar findings have also been reported in two studies conducted in Taiwan which reported that PBC is a significant factor that can influence the drivers' speeding behavior [24-25]. Drivers' PBC increased alongside their driving experience [26]. Years of driving experience increase the drivers' driving skill and knowledge as well as their ability to control the vehicle. It has been reported that older drivers are more likely to engage in speeding compared to young drivers since they have good ability and skills to control their vehicle and can ensure that they arrive at the destination safely [26].

Moreover, a study by Cristea and Gheorghiu [27] utilizing the sample of cyclists reported that PBC was able to influence the cyclists' riding behaviour. Cyclists with a high level of self-control were found able to stop themselves from running through the red light and switching on the turning signal [27]. Researchers further emphasized that a high level of PBC can increase the use of safety equipment or helmet in Turkey [28]. Such behaviour was found to help avoid the occurrence of severe traffic crashes and protect the riders from fatal accidents. A similar finding has been also reported in a study carried out in Malaysia where the PBC can influence the riders' behaviour to wear safety helmets before starting their journey [29].

Nevertheless, it has been reported that PBC does not necessarily avoid motorcyclists' risky driving behaviour. A study conducted in Turkey reported that PBC failed to overcome the motorcyclists' speeding and performing stunt behaviour while riding [28]. A similar finding has also been reported in a study conducted in Thailand which revealed that PBC was unable to restraint university students from breaking the traffic rules and regulations [30]. It has been reported that most university students illegally ran through the red light, especially at the road junction. In addition, a study by Warner and Aberg [31] using the sample of driver test participants reported that participants only portrayed their intention to abide by the speed limit during the initial data collection however, during the driving test, the participants were driving above the speed limit, which contradicts their initial intention. Overall, it can be summarized that there are various results over the effectiveness of the PBC in overcoming the drivers' and riders' risky driving behaviour. Therefore, further study needs to be conducted to confirm the effectiveness of PBC in restraint the drivers and riders from breaking the traffic rules and regulations. Hypothesis developed for this study is:

H1: There is a significant relationship between PBC and risky driving behaviour.

2.2 Perceived behavioural control (PBC) and accident involvement

A road accident is defined as the collision between one or more vehicles on the road causing vehicle damage, injury or even fatality [32]. Meanwhile, accident involvement is defined as the number of road accidents caused by the drivers and riders due to their fault or not [10]. Recently, there is an emerging number of road accidents due to drivers' egotistic acts of using the mobile phone while driving. This selfish act indeed disturbs the drivers' and riders' concentration and consequently increases the risk of an accident [33-34]. Wilson and Stimpson [35] reported that drivers failed to fix their eyes on the road when texting and reading a message. The illegal use of mobile phones has been reported to contribute to approximately 30% of road fatalities in the US [35].

Backer-Grondahl and Sagberg [36] further emphasized that the use of hand-held phones while driving has become a significant contributor to traffic crashes among road accident victims. A similar finding has also been highlighted by Horsman and Conniss [33], who reported the illegal use of hand-held phone as the key attributor in drivers' distraction problems. The urge to answer a call and read messages as soon as they receive it while driving has led to a greater accident risk [37]. Moreover, Bin Islam and Kanitpong [38] reported that the bus driver's loss of control in making the right decision and judgment when a sudden incident happened has resulted in a road accident between a bus and a pickup truck in Thailand. Further analysis revealed that this fatal accident could have been avoided if the bus driver has reduced the speed when driving on the curve upstream. Overall, it was proven that PBC is the key factor in road accident causation and involvement. The clear relationship between these two variables led towards the development of a hypothesis of:

H2: There is a significant relationship between PBC and accident involvement.

2.3 Mediating role of risky driving behaviour to mediate the relationship between perceived behavioural control (PBC) and accident involvement

Several studies have shown that risky driving behaviour occurs due to the drivers' and riders' poor PBC and that this aberrant driving behaviour has significantly led to accidents [5, 27]. Chen and Chen [24] highlighted PBC as the significant factor towards drivers' risky driving behaviour of speeding, which has become the main contributor of road accidents [26]. Similarly, a study by Cristea and Gheorghiu [27] reported that cyclists with poor PBC are more likely to cycle at a high speed although when passing a road junction that requires them to stop. Apart from that, it was also reported that these cyclists failed to stop at the road junction and were more likely to make a sudden left or right turn. This selfish act indeed becomes a major road accident contributor involving cyclists.

In addition, drivers and riders with poor PBC also tend to use their phones while driving regardless of knowing that this action can distract their focus when driving [21-22]. Wilson and Stimpson [35], Muehlegger and Shoag [34] and Horsman and Conniss [33] revealed that drivers and riders who illegally use their phones while driving are indeed more likely to be involved in road accidents. In summary, it has been proven that risky driving behaviour help to explain the effects of the

Figure 1 *Research Framework*

Table 1 *Number of registered vehicles up to year 2019 and number of road accident according to states within the year 2012 to 2019*

States	No. of registered vehicles up to 2019	No. of road accident							
		2012	2013	2014	2015	2016	2017	2018	2019
Perlis	116,231	1,881	1,895	1,888	1,861	2,062	1,925	2,093	2,098
Kedah	1,380,952	19,935	20,228	20,159	22,016	23,200	23,262	23,239	24,867
Penang	2,673,907	37,851	39,408	38,747	39,856	42,244	43,007	45,734	47,198
Perak	2,274,725	34,714	39,361	35,131	36,736	38,531	38,587	38,278	39,720
Selangor	2,931,203	129,106	135,024	137,809	140,957	151,253	154,958	163,078	168,222
Kuala Lumpur	6,441,342	61,872	64,527	63,535	64,664	68,866	72,940	72,284	73,771
Negeri Sembilan	970,371	22,146	23,066	23,748	22,939	24,428	24,941	25,123	25,838
Malacca	864,194	15,195	16,083	16,375	17,069	18,601	18,771	19,120	19,593
Johor	3,638,857	62,316	64,600	64,473	67,112	73,116	76,121	78,812	82,502
Pahang	1,066,464	20,554	20,130	19,071	19,635	20,465	20,813	20,641	21,196
Terengganu	641,736	10,861	9,748	10,326	10,381	10,793	10,713	10,607	11,355
Kelantan	905,024	9,968	10,996	9,383	9,960	10,544	10,786	10,983	11,295
Sabah	1,238,538	17,446	18,700	17,693	17,290	17,298	17,244	18,006	18,520
Sarawak	1,804,251	18,578	17,438	17,858	19,130	20,065	19,807	20,600	21,341

relationship between the independent variable of PBC and the dependent variable of accident involvement. The hypothesis that has been developed by this study is:

H3: Risky driving behaviour mediate the relationship between the PBC and accident involvement.

Figure 1 shows the research framework that been investigated in this study. PBC is the independent variable, risky driving behaviour is the mediator and finally, accident involvement is the dependent variable.

2.4 Underpinning theory: attribution theory

Attribution Theory is used to explain the purpose or motive of human behaviour. Two factors that lead towards individual behaviour, namely internal attribution and external attribution. Internal attribution, also known as dispositional attribution, is a factor within the individual himself/herself that causes the person to act in a certain manner. An example of internal attribution is personality and attitude. Meanwhile, the external attribution, also known as situational attribution, is the outside factor that causes a person to act accordingly. An example of external attribution is the surrounding situation and the influence of other people.

For this study, the internal attribution was used to underpin the relationship between the PBC and the young drivers' and riders' risky driving behaviour, as well as their accident involvement. The young drivers' and riders' ability to control their driving decision is something within themselves. They have the power to avoid risky driving behaviour such as driving above the permitted speed, overtaking at the double lines, running through the red light, as well as illegal use of mobile phones to type and read text while driving.

Drivers and riders who make the right driving decision and comply with the traffic rules and regulations would be subsequently able to avoid being involved in road accidents. For example, driving while using mobile phones will distract the drivers' or riders' attention. Thus, drivers and riders must be able to restraint themselves from reading and replying to the text message once they received it. This is because the text message they received may involve some emotional or personal feeling that would distract their attention. Moreover, there is also an example where the drivers or riders feel the urge to read or reply to the text message as soon as they received it however, their mobile phones are not within the possible place to reach, such as in the backpack or at the back of their trousers. The drivers' or riders' first action to reach for their mobile phones has already distracted the course of driving.

3 Methodology

This study was carried out using the quantitative research design through the deductive approach. The minimum sample size for this study was determined using the G*Power calculation with the anticipated effect size of 0.15, the desired alpha level at 0.05 and the desired statistical power of 0.80. As a result, the minimum sample size of this study became 98 samples. This study is a cross -sectional study conducted using 193 young drivers and riders. This study employed the purposive sampling method. Young drivers and riders are defined as those from within the age 18 to 25 years. Other criteria for sample selection in this study were that they must possess a valid driving license, with at least six months of driving experience, actively drive for the past six months (must drive at least 3-4 times a week) and be involved in any road accident for the past 12 months in either Selangor, Johor, or Kuala Lumpur. Data released by the Malaysian Ministry of Transportation reported that these three states recorded the highest number of accidents for the past eight consecutive years. Table 1 shows the number of registered vehicles up to year 2019 and number of road accidents according to states within the year 2012 to 2019 (the latest data that has been published by the Ministry of Transportation Malaysia).

All the items in the modified questionnaire measured each of the risky driving behaviour: (1) speeding, (2) close following, (3) use of mobile phone while driving or riding, (4) failure to switch on the turning signal, (5) run through the red light and (6) dangerous overtake. These are among the common risky driving behaviour committed by the drivers and riders within the context of Malaysia setting as discussed in studies by Abdul Manan [39] and Abdul Manan and Várhelyi [40], as well as Harith and Mahmud [41].

Questionnaire items for the PBC were adapted from several scholars namely Gauld et al. [21], Eyssartier et al. [5] and Prat et al. [12]. A study by Prat et al. [12] reported reliability of 0.87, whereas a study by Eyssartier et al. [5] reported reliability of 0.77. The researchers used the five - point trueness - based Likert scale, which ranged from "*Strongly disagree* (1); *Disagree* (2); *Neutral* (3); *Agree* (4); to *Strongly Agree* (5)". All the modified questionnaire items used in this study were categorized as negative items. Six PBC questionnaire items used to collect the data are: -

i) For me, I have complete control over whether or not I would drive above the speed limit.
ii) For me, I can take the risk to follow the car closely.
iii) For me, I am confident to use a mobile phone while driving.
iv) For me, I am confident to change the lane without switching on the turning indicator.
v) For me, if I wanted to, I can run through the red light.
vi) For me, I am confident to overtake other cars.

Meanwhile, questionnaire items for the risky driving behaviour were adapted from Castanier et al. [42] and Chung and Wong [43]. All the adapted questionnaire items reported reliability of more than 0.70 (6). The researchers used the five - point frequency - based Likert scale, which ranged from "*Never* (1); *A few times* (2); *Frequently* (3); *Often* (4); to *Very Often* (5)". Six questionnaire items for the variable of risky driving behaviour used to collect the data were: -

Please indicate how often you have carried out each of the behaviour during the past 12 months:

i) Excessive speeding
ii) Following car too closely
iii) Using a phone while driving
iv) Not switching on the turning signal
v) Run through the red light
vi) Dangerous overtake

Finally, questionnaire items for accident involvement were adapted from Mohamed and Bromfield [10] with a reliability of 0.75. The researchers used the combination of five - point frequency - based Likert scale, which ranged from "*Never* (1); *Only once* (2); *Twice* (3); *Three times* (4); to *More than three times* (5)" and the five - point trueness - based Likert scale, which ranges from "*Strongly disagree* (1); *Disagree* (2); *Neutral* (3); *Agree* (4); to *Strongly Agree* (5)". Five questionnaire items for the variable of accident involvement used to collect the data were: -

i) Estimation of accident involvement for the past 12 months *(five - point frequency - based Likert scale)*
ii) Most of the accidents happened because of my own fault *(five - point trueness - based Likert scale)*
iii) Estimation of accident involvement happened because of my own fault *(five - point frequency - based Likert scale)*
iv) Most of the accidents happened because of other road users' fault *(five - point trueness - based Likert scale)*
v) Estimation of accident involvement happened because of other road users' fault *(five - point frequency - based Likert scale)*

4 Results

From the overall 300 questionnaires distributed, a total of 145 questionnaires were returned, representing 48% of the response rate. For the online questionnaire, a total of 53 questionnaires were retrieved and four questionnaires with more than 20% missing data were excluded. As a result, the total number of usable questionnaires for this study became 193. Table 2 shows the summary of distributed and returned questionnaires.

***Table 2** Summary of distributed and returned questionnaires*

Questionnaire Returned (paper)	Incomplete and Excluded (paper)	Total Usable Questionnaire
145	1	144
Online Questionnaire	Incomplete and Excluded (online)	Total Usable Questionnaire
53	4	49
Grand Total	193	

***Table 3** Demographic Information*

Personal Characteristics (n = 193)	Frequency	Percentage (%)
Respondent age		
18 - 19 years old	41	21.2
20 - 21 years old	89	46.1
22 - 23 years old	33	17.1
24 - 25 years old	30	15.5
Gender		
Male	99	51.3
Female	94	48.7
Marital status		
Married	17	8.8
Single	176	91.2
States of accident		
Kuala Lumpur	65	33.7
Selangor	62	32.1
Johor	66	34.2
Employment status		
Full time employee	21	10.9
Part time employee	2	1.0
Student	168	87.0
Unemployed	2	1.0
Driving frequency per week		
3 - 4 times	87	45.1
5 - 6 times	31	16.0
Everyday	75	38.9
Driving experience		
6 months - 1 year	51	26.4
1 - 2 years	45	23.3
2 - 3 years	29	15.0
More than 3 years	68	35.2
Mode of transport		
Car	104	53.9
Motorcycle	86	44.6
Bicycle	3	1.5
Location of accident		
Straight and flat road	56	29.0
Curve and steep road	53	27.5
Road junction	74	38.3
Ring road	10	5.2
Weather condition during accident		
Sunny	93	48.2
Rainy	79	40.9
Windy	21	10.9

Table 4 *Results of direct relationship between variables*

Hypothesis	Relationship	Std. Beta	t-value	P Value	Decision
H1	PBC → Risky Driving Behaviour	0.201	3.728	0.00	Supported
H2	PBC → Accident Involvement	0.039	2.103	0.01	Supported

Table 5 *Result of indirect relationship between variables*

Hypothesis	Relationship	Std. Beta	t-value	P Value	Decision
H3	PBC → Risky Driving Behaviour → Accident Involvement	0.039	1.948	0.05	Supported

Table 3 shows the respondents' demographic information. The majority of respondents (n = 89) were aged between 20 - 21 years old, followed by 21.2% within the age of 18 to 19 years old, 17.7% within the age of 22 to 23 years old and finally 15.5% within the age of 24 to 25 years old. Next, about 51.3% of the respondents were male, whereas, the remaining 48.7% were female. For the employment status, most of the respondents were students (n = 168). The remaining were full time employees (n = 21), part-time employees (n = 2) and only two unemployed respondents. Moreover, 87 respondents were reported to drive at least 3 - 4 times a week, followed by 75 respondents driving daily and 31 respondents driving 5 to 6 times per week. The majority of the respondents (n = 68) have more than three years of driving experience followed by 51 respondents with six months to one year of driving experience.

Meanwhile, the statistics of road accidents distribution, based on states, was almost similar with 65 accidents occurring in Kuala Lumpur, 62 accidents occurring in Selangor and 66 accidents occurring in Johor. Subsequently, most of the respondents (n = 104) drove a car when the accident occurred, followed by 86 respondents who rode a motorcycle and only three respondents who rode a bicycle when the accident happened. For the location of the accident, the majority of the accidents occurred at the road junction (n = 74), followed by straight and flat road (n = 56), curve and steep road (n = 53) as well as ring road (n = 10). Finally, in terms of the weather condition during the accident, about 93 cases were reported to have occurred during the sunny weather followed by 79 accident cases that happened during the rainy condition and finally, only 21 accident cases were reported to have occurred during the windy weather.

Harman's Single - Factor test result reported that the data set did not suffer from the common method bias issue as the variance explained by the single factor was only 23.7%, which is lesser than the cut-off point of 50% [44]. The results of Average Variance Extracted (AVE) and Composite Reliability (CR) were also greater than the cut-off point of 0.5 and 0.7 respectively. Meanwhile, the result of Fornell and Larcker's criterion reported that the average variance of own constructs was larger than the other constructs, which confirmed the discriminant validity. The model also did not suffer from multi-collinearity problems since the inner Variance Inflation Factor (VIF) values for the exogenous variables were less than 5.0 [45].

Three hypotheses were developed to measure the relationship between the *(1)* PBC and risky driving behaviour, *(2)* PBC and accident involvement and *(3)* the mediating role of risky driving behaviour to mediate the relationship between the PBC and accident involvement. Table 4 shows the results of the two direct relationships between the PBC and risky driving behaviour as well as PBC and accident involvement. The t-value of the relationship between the PBC and risky driving behaviour was ≥ 1.28 and significant at level of significance 0.10, ($\beta = 0.201$, $p < 0.10$). Meanwhile, the t-value of the relationship between PBC and accident involvement was ≥ 1.28 and significant at level of significance 0.10, ($\beta = 0.039$, $p < 0.10$). Therefore, it can be summarized that the first and second hypotheses are supported.

The mediating role of risky driving behaviour was analysed using the Preacher and Hayes Method. The mediating analysis was analysed through the indirect effect or also known as "bootstrapping the indirect effect". Table 5 shows the result of bootstrapping analysis on the indirect relationship on the mediating role of risky driving behaviour to mediate the relationship between the PBC and accident involvement. From the tabulated result, it can be identified that the indirect effect of PBC → Risky Driving Behaviour → Accident Involvement was significant ($\beta = 0.039$, t - value of 1.948). The 90% Boot CI Bias Corrected for the significant indirect effects was [LL = 0.013, UL = 0.074]. Therefore, it can be summarized that the third hypothesis is supported.

5 Discussion and conclusion

The result of this study demonstrated that the young drivers' and riders' PBC significantly influenced their risky driving behaviour of speeding, tailgating, use of mobile phone while driving, failure to switch on the turning signal, running through the red light and dangerous overtake. Based on the finding, it can be identified that the young drivers and riders who can control themselves to follow the traffic rules and regulations would subsequently avoid committing the risky driving behaviour. Apart from that, PBC was also proved to act as a vital variable in the young drivers' and riders' involvement in road accidents. Various studies from Western and European countries, like Australia and France, confirmed the significant relationship between PBC and the drivers' risky driving behaviour [21-22, 27]. It was further reported that drivers with a high level of PBC can restrain themselves from violating the traffic rules including illegal use of mobile phones while driving and speeding.

Meanwhile, studies conducted in Taiwan reported similar findings where the PBC was proven as one of the influential antecedences toward the drivers' speeding behaviour [24-25]. Besides, in Malaysia, PBC is considered an important element in cultivating the culture of wearing a helmet and reducing the drivers' violation of speeding [46-47]. As a result, it was shown that the young drivers' and riders' poor PBC has significantly caused them to commit risky driving behaviour and become involved in road accidents. Based on the demographic information, it was demonstrated that the majority of the respondents were students who still are pursuing their tertiary education. They are the future human capital with bright opportunities awaiting them. The consequences of being involved in a road accident would cause a loss not only to the country but also to the individual himself/herself. Therefore, these young drivers and riders need to put greater attention to their safety while driving.

Apart from that, past literature revealed that 10% of road accidents occurred due to technical and environmental factors [48-49]. Based on the data gathered from demographic information, it was identified that more than half (51.8%) of the accidents occurred during rainy and windy weather. Besides the human factors, this variable should be investigated in future research. This is because the young drivers and riders have limited driving experiences and vehicle handling skills which would cause them difficulty in controlling their vehicles, especially during the bad weather. The probability of skidding and lapsing occurring during the adverse weather was very high thus, drivers with limited driving skills and experience would most probably become panic and anxious. As a result, their poor emotion and lack of self-control to handle such situations would eventually cause them to be involved in road accidents.

Moreover, another aspect that needs to be emphasized to avoid the occurrence of road accidents is through the regular vehicles' technical inspections. A recent study conducted in 10 EU states summarized the requirement for regular technical inspection with the vehicles age [50]. As noted, the older the age of a vehicle, the higher the tendency for the vehicle faulty. Thus, through a regular inspection, the probability of vehicle faulty that could lead toward the occurrence of road accidents can further be minimized.

Another reason that can be investigated in future studies, related to the occurrence of road accidents, is the technical factor in terms of road condition [4]. Data gathered from the questionnaires distributed to the respondents revealed that 38.3% of the accident occurred at the road junction, 27.5% occurred at the curvy and steep road and 5.2% occurred at the ring road. Accidents at road junctions can occur either due to the drivers' carelessness, negligence towards traffic rules and regulations like running through the red light or the conditions of the road itself. Not all the road junctions have installed a traffic light to control the traffic. The existence of a traffic light at road junctions would help the drivers to take turn to cross over the road, which subsequently helps to minimise the occurrence of road accidents. Besides that, several accidents have been reported on curvy and steep roads. Driving on these roads requires good vehicle handling skills, which is one of the young drivers' disadvantages. A study by Jamaluddin et al. [11] further emphasised that the empowerment of driving skills goes along with driving experience. The more experience the drivers have, the more vehicle handling skills they will possess, which can be subsequently used to avoid road accidents regardless of the location or type of the road.

This study has several limitations. Firstly, this study was conducted using the purposive sampling method, which included several criteria such as age limitation, driving frequency, driving experience and the respondents must be involved in at least one road accident. As a result, the findings of this research cannot be generalized to all drivers and riders in Malaysia. Apart from that, this study only covered the states of Selangor, Kuala Lumpur and Johor, which further limited the generalization of findings, where the results were only applicable to these three states. Overall, it can be summarized that the PBC is indeed an important individual trait that will help young drivers and riders, who are mostly university students in Malaysia, to restraint themselves from breaking the traffic rules and regulations. Therefore, young drivers and riders must develop good self-control. This inner strength requires high perseverance as they are fighting with themselves to follow the traffic rules and regulations. When the young drivers and riders can strengthen their self-control, they would not be easily influenced by other road users or even peer passengers who encourage them to drive aberrantly, run through the red light and even overtake at the double line.

Moreover, other related parties like NGOs, Police and the Ministry of Transportation also need to play an active role to increase the drivers' and riders' awareness towards the road safety. When handling young drivers, different approaches are needed to address this issue compared to those of older drivers. World Health Organization (WHO) reported that the road safety education and training are among the best intervention plans that can help to curb the drivers' and riders' risky driving behaviour and subsequently reduce the number of road accidents.

MIROS chairman, Tan Sri Lee Lam Thye highlighted that imposing higher fines by the authorities is no longer the significant solution to reduce the number of road accidents in Malaysia [51]. Malaysian citizens are seen unaffected by the traffic compound and summonses issued by the authorities [51]. For example, the use of automated enforcement system (AES) cameras installed throughout the Malaysian highway. AES is one of the self-regulated methods used by the authority to control the drivers and riders speeding violations. It is shown that drivers would tend to decrease their vehicle speed only at certain locations where the cameras are installed, while at other locations, they would still drive above the permitted speed limit. This is because the drivers know exactly where these cameras are installed. The notification on the location of AES cameras is publicised through the media of television, newspaper, radio and other social media including Facebook and Twitter before it is enforced. As a result, another approach should be emphasized by the government to curb this issue as soon as possible.

To achieve that, it is recommended for the Malaysian government to put more initiative on delivering the road safety message to the public especially the young drivers and riders through the communication campaign of meaningful and significant slogans such as "*Value Your life*", and "*Better safe than sorry*". This younger generation is prone to social media platforms like Facebook, Tiktok and Instagram. Thus, the government should aim to deliver road safety awareness through these platforms to ensure such a message can be delivered successfully. Since the majority of the respondents are still pursuing their tertiary education, related authorities, like the Road Safety Department, police and MIROS, can focus on conducting the road safety campaign at the public and private universities in Malaysia.

Moreover, another important aspect that needs to be emphasized is to include the right propensity of fear into the road safety message such as the use of real accident pictures and the true story of the accident victims. More road safety campaign needs to be organized with enhanced content accordingly to increase the level of fear among the drivers and riders. When the right propensity of fear is delivered to the road users through the road safety campaign, education and training, the drivers and riders would be able to perceive the message correctly and subsequently increase their self-control to abide by the traffic rules and regulations. "An ounce of precaution is better than a pound of cure", thus, we should avoid such incidents from happening rather than dealing with their consequences.

In addition, the road safety education delivered during the driving schools' training should be revised and the study plan also should be added with a more comprehensive road safety knowledge. A study conducted in the Slovak Republic further summarized that the inspection conducted by the Slovak Republic Ministry of Transport and Construction reported high incidents of fraud involving the driving participants to which the driving licenses were issued although they did not even complete the training in driving schools [52]. This illegal act caused a significant impact on the government, the other road users and the drivers themselves. Those drivers are not competent enough to drive on roads. Thus, such incident needs to be avoided for the better road safety condition in the future.

Acknowledgement

This research received funding from Universiti Utara Malaysia.

References

[1] General Road accident data in Malaysia (1997-2016) - Official website of Malaysian Institute of Road Safety Research [online] [accessed 2021-05-10]. 2017. Available from: https://www.miros.gov.my/1/page.php?id=17

[2] ASHRAF, I., HUR, S., SHAFIQ, M., PARK, Y. Catastrophic factors involved in road accidents: underlying causes and descriptive analysis. *PLOS ONE* [online]. 2019, **14**(10), e0223473 [accessed 2021-06-03]. ISSN 1932-6203. Available from: https://doi.org/10.1371/journal.pone.0223473

[3] HU, L., BAO, X., WU, H., WU, W. A study on correlation of traffic accident tendency with driver characters using in-depth traffic accident data. *Journal of Advanced Transportation* [online]. 2020, **2020**, p. 1-7. [accessed 2021-05-30]. ISSN 0197-6729. Available from: https://doi.org/10.1155/2020/9084245

[4] HAGHI, A., KETABI, D., GHANBARI, G., RAJABI, H. Assessment of human errors in driving accident; analysis of the causes based on aberrant behaviors. *Life Science Journal*. 2014, **11**(9), p. 414-420. ISSN 2372-613X.

[5] EYSSARTIER, C., MEINERI, S., GUEGUEN, N. Motorcyclists' intention to exceed the speed limit on a 90 km/h road: effect of the type of motorcycles. *Transportation Research Part F: Traffic Psychology and Behaviour* [online]. 2017, **45**, p. 1831-93. [accessed 2021-05-30]. ISSN 1873-5517. Available from: https://doi.org/10.1016/j.trf.2016.12.009

[6] MOAN, I. S. Whether or not to ride with an intoxicated driver: predicting intentions using an extended version of the theory of planned behaviour. *Transportation Research Part F: Traffic Psychology and Behaviour* [online]. 2013, **20**, p. 193-205. [accessed 2021-05-30]. ISSN 1873-5517. Available from: https://doi.org/10.1016/j.trf.2013.08.001

[7] MOAN, I. S., RISE, J. Predicting intentions not to "drink and drive" using an extended version of the theory of planned behaviour. *Accident Analysis and Prevention* [online]. 2011, **43**(4), p. 1378-1384. [accessed 2021-05-30]. ISSN 1879-2057. Available from: https://doi.org/10.1016/j.aap.2011.02.012

[8] CESTAC, J., PARAN, F., DELHOMME, P. Drive as I say, not as I drive: influence of injunctive and descriptive norms on speeding intentions among young drivers. *Transportation Research Part F: Traffic Psychology and Behaviour* [online]. 2014, **23**, p. 44-56. [accessed 2021-05-30]. ISSN 1873-5517. Available from: https://doi.org/10.1016/j.trf.2013.12.006

[9] CORDELLIERI, P., BARALLA, F., FERLAZZO, F., SGALLA, R., PICCARDI, L., GIANNINI, A. M. Gender effects in young road users on road safety attitudes, behaviours and risk perception. *Frontiers in Psychology* [online]. 2016, **7**, 1412 [accessed 2021-05-30]. ISSN 1664-1078. Available from: https://doi.org/10.3389/fpsyg.2016.01412

[10] MOHAMED, M., BROMFIELD, N. F. Attitudes, driving behavior, and accident involvement among young male drivers in Saudi Arabia. *Transportation Research Part F: Traffic Psychology and Behaviour* [online]. 2017, **47**, p. 59-71. [accessed 2021-05-30]. ISSN 1873-5517. Available from: https://doi.org/10.1016/j.trf.2017.04.009

[11] JAMALUDDIN, N., HO, J. S., SHABADIN, A., MEGAT JOHARI, N., AMEER BATCHA, W. Exposure work commuting: case study among commuting accidents in Klang Valley, Malaysia. *Journal of Civil Engineering and Architecture* [online]. 2015, **9**, p. 51-56. [accessed 2021-05-30]. ISSN 2332-1121. Available from: https://doi.org/10.17265/1934-7359/2015.01.006

[12] PRAT, F., GRAS, M. E., PLANES, M., GONZALEZ-IGLESIAS, B., SUNMAN, M. J. M. Psychological predictors of texting while driving among university students. *Transportation Research Part F: Traffic Psychology and Behaviour* [online]. 2015, **34**, p. 76-85. [accessed 2021-05-30]. ISSN 1873-5517. Available from: https://doi.org/10.1016/j.trf.2015.07.023

[13] CARPENTIER, A., BRIJS, K., DECLERCQ, K., BRIJS, T., DANIELS, S., WETS, G. The effect of family climate on risky driving of young novices: the moderating role of attitude and locus of control. *Accident Analysis and Prevention* [online]. 2014, **73**, p. 53-64. [accessed 2021-05-30]. ISSN 1879-2057. Available from: https://doi.org/10.1016/j.aap.2014.08.005

[14] ROWE, R., ANDREWS, E., HARRIS, P. R., ARMITAGE, C. J., MCKENNA, F. P., NORMAN, P. Identifying beliefs underlying pre-drivers' intentions to take risks: an application of the theory of planned behaviour. *Accident Analysis and Prevention* [online]. 2016, **89**, p. 49-56. [accessed 2021-05-30]. ISSN 1879-2057. Available from: https://doi.org/10.1016/j.aap.2015.12.024

[15] THOMAS, P., MORRIS, A., TALBOT, R., FAGERLIND, H. Identifying the causes of road crashes in Europe. *Annals of Advances in Automotive Medicine*. 2013, **57**, p. 13-22. ISSN 1943-2461.

[16] RAMLI, R., OXLEY, J., NOOR, F. M., ABDULLAH, N., MAHMOOD, M. S., TAJUDDIN, A., K., MCCLURE, R. Fatal injuries among motorcyclists in Klang Valley, Malaysia. *Journal of Forensic and Legal Medicine* [online]. 2014, **26**, p. 39-45. [accessed 2021-05-30]. ISSN 1878-7487. Available from: https://doi.org/10.1016/j.jflm.2014.06.007

[17] MALLE, B. F. Attribution theories: how people make sense of behaviour. In: *Theories in social psychology*. DEREK, C. (Ed.). Hoboken: Wiley-Blackwell, 2011. ISBN 978-1-444-33122-6, p. 72-95.

[18] ELLIOTT, M. A. Predicting motorcyclists' intentions to speed: effects of selected cognitions from the theory of planned behaviour, self-identity and social identity. *Accident Analysis and Prevention* [online]. 2010, **42**(2), p. 718-725 [accessed 2021-05-30]. ISSN 1879-2057. Available from: https://doi.org/10.1016/j.aap.2009.10.021

[19] CESTAC, J., PARAN, F., DELHOMME, P. Drive as i say, not as i drive: influence of injunctive and descriptive norms on speeding intentions among young drivers. *Transportation Research Part F: Traffic Psychology and Behaviour* [online]. 2014, **23**, p. 44-56. [accessed 2021-05-30]. ISSN 1873-5517. Available from: https://doi.org/10.1016/j.trf.2013.12.006

[20] ABERG, L., WALLEN, W. H. Speeding-deliberate violation or involuntary mistake? *Revue Europeenne de Psychologie Appliquee* [online]. 2008, **58**(1), p. 23-30 [accessed 2021-05-30]. ISSN 1162-9088. Available from: https://doi.org/10.1016/j.erap.2005.09.01

[21] GAULD, C. S., LEWIS, I., WHITE, K. M. Concealing their communication: exploring psychosocial predictors of young drivers' intentions and engagement in concealed texting. *Accident Analysis and Prevention* [online]. 2014, **62**, p. 285-293 [accessed 2021-05-30]. ISSN 1879-2057. Available from: https: https://doi.org/10.1016/j.aap.2013.10.016

[22] NEMME, H. E., WHITE, K. M. Texting while driving: psychosocial influences on young people's texting intentions and behaviour. *Accident Analysis and Prevention* [online]. 2010, **42**(4), p. 1257-1265 [accessed 2021-05-30]. ISSN 1879-2057. Available from: https://doi.org/10.1016/j.aap.2010.01.019

[23] CRISTEA, M., PARAN, F., DELHOMME, P. Extending the theory of planned behavior: the role of behavioral options and additional factors in predicting speed behavior. Transportation Research Part F: Traffic Psychology and Behaviour [online]. 2013, **21**, p. 122-132 [accessed 2021-05-30]. ISSN 1873-5517. Available from: https://doi.org/10.1016/j.trf.2013.09.009

[24] CHEN, C. F., CHEN, C. W. Speeding for fun? Exploring the speeding behavior of riders of heavy motorcycles using the theory of planned behavior and psychological flow theory. *Accident Analysis and Prevention* [online]. 2011, **43**(3), p. 983-990 [accessed 2021-05-30]. ISSN 1879-2057. Available from: https://doi.org/10.1016/j.aap.2010.11.025

[25] TSENG, C. M., CHANG, H. L., WOO, T. H. Modelling motivation and habit in driving behavior under lifetime driver's license revocation. *Accident Analysis and Prevention* [online]. 2013, **51**, p. 260-267. [accessed 2021-05-30]. ISSN 1879-2057. Available from: https://doi.org/10.1016/j.aap.2012.11.017

[26] CESTAC, J., PARAN, F., DELHOMME, P. Young drivers' sensation seeking, subjective norms, and perceived behavioral control and their roles in predicting speeding intention: how risk-taking motivations evolve with gender and driving experience. *Safe Science* [online]. 2011, **49**(3), p. 424-432 [accessed 2021-05-30]. ISSN 0925-7535. Available from: https://doi.org/10.1016/j.ssci.2010.10.007

[27] CRISTEA, M., GHEORGHIU, A. Attitude, perceived behavioral control, and intention to adopt risky behaviors. *Transportation Research Part F: Traffic Psychology and Behaviour* [online]. 2016, **43**, p. 157-165 [accessed 2021-05-30]. ISSN 1873-5517. Available from: https://doi.org/10.1016/j.trf.2016.10.004

[28] OZKAN, T., LAJUNEN, T., DOGRUYOL, B., YILDIRIM, Z., COYMAK, A. Motorcycle accidents, rider behaviour, and psychological models. *Accident Analysis and Prevention* [online]. 2012, **49**, p. 124-132 [accessed 2021-05-30]. ISSN 1879-2057. Available from: https://doi.org/10.1016/j.aap.2011.03.009

[29] AMBAK, K., ISMAIL, R., ABDULLAH, R. A., BORHAN, M. N. Prediction of helmet use among Malaysian motorcyclist using structural equation modelling. *Australian Journal of Basic Applied Sciences*. 2010, **4**(10), p. 5263-5270 [accessed 2021-05-30]. ISSN 1991-8178.

[30] SATIENNAM, W., SATIENNAM, T., TRIYABUTRA, T., RUJOPAKARN, W. Red light running by young motorcyclists: Factors and beliefs influencing intentions and behavior. *Transportation Research Part F: Traffic Psychology and Behaviour* [online]. 2018, **55**, p. 234-245 [accessed 2021-05-30]. ISSN 1873-5517. Available from: https://doi.org/10.1016/j.trf.2018.03.007

[31] WARNER, H. W., ABERG, L. Drivers' decision to speed: a study inspired by the theory of planned behavior. *Transportation Research Part F: Traffic Psychology and Behaviour* [online]. 2006, **9**(6), p. 427-433 [accessed 2021-05-30]. ISSN 1873-5517. Available from: https://doi.org/10.1016/J.TRF.2006.03.004

[32] MAMADY, K., ZOU, B., MAFOULE, S., QIN, J., KEITA, H., KEITA, F. L., HU, G. Fatality from road traffic accident in guinea: a retrospective descriptive analysis. *Open Journal of Preventive Medicine* [online]. 2014, **4**, p. 809-821 [accessed 2021-05-30]. ISSN 2162-2485. Available from: https://doi.org/10.4236/ojpm.2014.411091

[33] HORSMAN, G., CONNISS, L. R. Investigating evidence of mobile phone usage by drivers in road traffic accidents. *Digital Investigation* [online]. 2015, **12**(Supplement 1), p. S30-S37 [accessed 2021-05-30]. ISSN 1742-2876. Available from: https://doi.org/10.1016/j.diin.2015.01.008

[34] MUEHLEGGER, E., SHOAG, D. Cell phones and motor vehicle fatalities. *Procedia Engineering* [online]. 2014, **78**, p. 173-177 [accessed 2021-05-30]. ISSN 1877-7058. Available from: https://doi10.1016/j.proeng.2014.07.054

[35] WILSON, F. A., STIMPSON, J. P. Trends in fatalities from distracted driving in the United States, 1999 to 2008. *American Journal of Public Health* [online]. 2010, **100**(11), p. 2213-1129 [accessed 2021-05-30]. ISSN 1541-0048. Available from: https://doi10.2105/AJPH.2009.187179

[36] BACKER-GRONDAHL, A., SAGBERG, F. Driving and telephoning: relative accident risk when using hand-held and hands-free mobile phones. *Safe Science* [online]. 2011, **49**(2), p. 324-330 [accessed 2021-05-30]. ISSN 0925-7535. Available from: https://doi10.1016/j.ssci.2010.09.009

[37] O'CONNOR, S. S., WHITEHILL, J. M., KING, K. M., KERNIC, M. A., BOYLE, L. N., BRESNAHAN, B. W., MACK, CH. D., EBEL, B. E. Compulsive cell phone use and history of motor vehicle crash. *Journal of Adolescent Health* [online]. 2013, **53**(4), p. 512-519 [accessed 2021-05-30]. ISSN 1879-1972. Available from: https://doi.org/10.1016/j.jadohealth.2013.05.015

[38] BIN ISLAM, M, KANITPONG, K. Identification of factors in road accidents through in-depth accident analysis. *IATSS Research* [online]. 2008, **32**(2), p. 58-67 [accessed 2021-05-30]. ISSN 0386-1112. Available from: https://doi.org/10.1016/S0386-1112(14)60209-0

[39] ABDUL MANAN, M. M. Motorcycles entering from access points and merging with traffic on primary roads in Malaysia: behavioral and road environment influence on the occurrence of traffic conflicts. *Accident Analysis and Prevention* [online]. 2014, **70**(2014), p. 301-313 [accessed 2021-05-30]. ISSN 1879-2057. Available from: https://doi.org/10.1016/j.aap.2014.04.009

[40] ABDUL MANAN, M. M., VARHELYI, A. Exploration of motorcyclists' behavior at access points of a Malaysian primary road - a qualitative observation study. *Safe Science* [online]. 2015, **74**(2015), p. 172-183. [accessed 2021-05-30]. ISSN 0925-7535. Available from: https://doi.org/10.1016/j.ssci.2015.01.005

[41] HARITH, S. H., MAHMUD, N. Human risk factors and road accident causation among motorcyclists in Malaysia: a review article. In: International Conference on Industrial Engineering and Operations Management: proceedings. 2018. ISSN 2169-8767. p. 2202-2209.

[42] CASTANIER, C., DEROCHE, T., WOODMAN, T. Theory of planned behaviour and road violations: the moderating influence of perceived behavioural control. *Transportation Research Part F: Traffic Psychology and Behaviour* [online]. 2013, **18**, p. 148-158 [accessed 2021-05-30]. ISSN 1873-5517. Available from: https://doi.org/10.1016/j.trf.2012.12.014

[43] CHUNG, Y. S., WONG, J. T. Beyond general behavioral theories: structural discrepancy in young motorcyclist's risky driving behavior and its policy implications. *Accident Analysis and Prevention* [online]. 2012, **49**, p. 165-176 [accessed 2021-05-30]. ISSN 1879-2057. Available from: https://doi.org/10.1016/j.aap.2011.04.021

[44] NUNNALLY, J. C. *Psychometric theory*. 3 ed. New York: McGraw-Hill, 1994. ISBN 9780070478497.

[45] TEHSEEN, S., RAMAYAH, T., SAJILAN, S. Testing and controlling for common method variance: a review of available methods. *Journal of Management Sciences* [online]. 2017, **4**(2), p. 146-175 [accessed 2021-05-30]. ISSN 2313-0113. Available from: https://doi.org/10.20547/jms.2014.1704202

[46] OXLEY, J., RAVI, M. D., YUEN, J., HOAREAU, E., HASHIM, H. H. Identifying contributing factors to fatal and serious injury motorcycle collisions involving children in Malaysia. In: Annual Scientific Conference Annals of Advances in Automotive Medicine: proceedings. Association for the Advancement of Automotive Medicine. 2013. ISNN 1943-2461. p. 329-336.

[47] NIK, A. R. N. H., BAHARUDDIN, K. A., MOHAMAD, S. M. S. Burden of motorcycle-related injury in Malaysia. *International Journal of Emergency Medicine* [online]. 2015, **8**(17), p. 1-6 [accessed 2021-05-30]. ISSN 1865-1380. Available from: https://doi.org/10.1186/s12245-015-0065-4

[48] FONG, M. C., MEASELLE, J. R., DWYER, J. L., TAYLOR, Y. K., MOBASSER, A., STRONG, T. M., WERNER, S., OUANSAVANH, S., MOUNMINGKHAM, A., KASUAVANG, M., SITTIPHONE, D., PHOUMESY, K., SYSAYTHONG, K., KHANTYSAVATH, K., BOUNNAPHONE, S., VILAYSOM, A., TOUVACHAO, S. MOUNMEUANGXAM, S., SOURALAY, S., LIANOSAY, B., LIA, T., SPECTOR J. M. Rates of motorcycle helmet use and reasons for non-use among adults and children in Luanfg, Prabang, Lao People's Democratic Republic. *BMC Public Health* [online]. 2015, **15**(970), p. 1-6 [accessed 2021-05-30]. ISSN 1471-2458. Available from: https://doi.org/10.1186/s12889-015-2304-2

[49] LEE, C. F. Miros statistics say human error causes 80% of traffic accidents. The Sun Daily [online] [accessed 2021-05-30]. 2015. Available from: https://www.thesundaily.my/archive/1333889

[50] HUDEC, J., SARKAN, B., CZODOROVA, R. Examination of the results of the vehicles technical inspections in relation to the average age of vehicles in selected EU states. *Transportation Research Procedia* [online]. 2021, **55**, p. 2-9 [accessed 2021-10-15]. ISSN 2352-1465. Available from: https://doi.org/10.1016/j.trpro.2021.07.063

[51] SINGH, R. Enforcement and road safety campaign the answer not higher fines. The Sun Daily [online] [accessed 2021-05-30]. 2016. Available from: https://www.thesundaily.my/archive/1692677-YSARCH350136

[52] HUDEC, J., SARKAN, B., CABAN, J., STOPKA, O. The impact of driving schools' training on fatal traffic accidents in the Slovak Republic. *Scientific Journal of Silesian University of Technology. Series Transport* [online]. 2021, **110**, p. 45-57 [accessed 2021-10-15]. ISSN 2450-1549. Available from: https://doi.org/10.20858/sjsutst.2021.110.4

CHANGE IN THE MOBILITY OF POLISH RESIDENTS DURING THE COVID-19 PANDEMIC

Piotr Gorzelańczyk

Stanislaw Staszic University of Applied Sciences in Pila, Pila, Poland

*E-mail of corresponding author: piotr.gorzelanczyk@puss.pila.pl

Resume

The aim of the article is to analyze the mobility of Polish residents and a change caused by the COVID-19 pandemic. For this purpose, a questionnaire study was conducted on changes in the mobility of Polish residents before and during the COVID-19 pandemic. It was carried out in December 2020, when the second wave of cases of the above-mentioned virus was ongoing in Poland. During the study of Polish residents, questions were asked about the purpose of their trip, means of transport, distance to the destination and duration of the trip, as well as the place of making purchases before and during the pandemic. In addition, respondents were asked whether the COVID-19 pandemic had affected their mobility. During the COVID-19 pandemic, the mobility of citizens, especially in the cities, has changed. Instead of using the public transport, they used cars, bicycles and walk.

Article info

Received 3 December 2021
Accepted 21 January 2022
Online 29 March 2022

Keywords:

mobility
Poland
COVID-19
coronavirus
pandemic

Available online: https://doi.org/10.26552/com.C.2022.3.A100-A111

ISSN 1335-4205 (print version)
ISSN 2585-7878 (online version)

1 Introduction

With the development of civilization, more and more cars are registered each year (Figure 1), as more and more people use private cars to quickly reach their destination, mainly work or school. Over the last 10 years, the number of registered cars in Poland has increased by almost 50%. Efficient and fast communication is very important due to the ability to easily change position and move from place to place in a short time. Many elements affect efficient communication.

The transport needs of residents depend on the efficient communication of residents. One can divide their activities, among others on: professional, social, existential and physical. The activity of the inhabitants depends, among others, on the place of residence. Various activities occur in large cities, others in small cities and thus affect the direction of mobility. In addition to the above-mentioned activities, the way and place of movement of Polish residents changed a lot in March 2020, when the first cases of COVID-19 appeared in Poland. The number of cases of this virus was increasing day by day. In December 2020 it was almost 1.2 million cases and almost 26,000 people have died (Figure 2).

COVID-19 is an infectious disease caused by the acute respiratory syndrome coronavirus 2 (SARS-CoV-2), the seventh coronavirus that can be transmitted from person to person [3]. On March 11, 2020, the World Health Organization (WHO) classified the COVID-19 epidemic as a global pandemic [4]. The new form of the coronavirus has reached the economic world and society on an unprecedented scale since the Great Depression (1929-1933) and is an epidemic compared to the Spanish flu of 1918 [5-6]. The spread of COVID-19 has limited the economic activity and has led to a significant threat to the financial stability of many countries around the world [7].

The development of the COVID-19 pandemic has reduced the mobility of people around the world on an unprecedented scale, Warren and Skillman [8]. Measures have been put in place to restrict travel, movement and participation in activities in many countries around the world as yet unseen [9]. These include, among others: staying at home, distance education, closed public institutions and workplaces, canceled mass events and public gatherings, as well as restrictions on public transport, affected about 90% of the world's population [10]. In articles [11-13] is indicated a significant relationship between the human mobility and the tightening of government restrictions to contain the COVID-19 pandemic. Mobility restrictions varied by nation and region due to their initial mobility

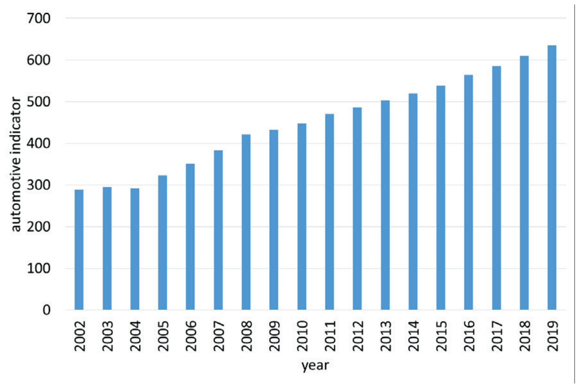

Figure 1 *Automotive index in 2002 ÷ 2019 [1]*

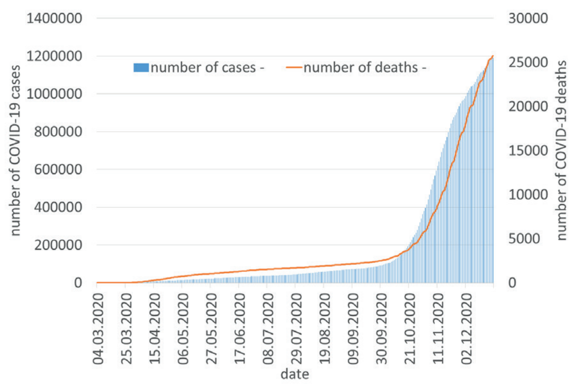

Figure 2 *Diseases and deaths caused by COVID-19 in Poland [2]*

structure [14]. Schlosser et al. [15] found that the COVID-19 pandemic caused a reduction in long-distance travel, which influenced the spread of the epidemic by "flattening" the epidemic curve and delaying spread to geographically distant regions.

Mobility is defined differently by different authors. Szoltysek [16] treats mobility as a daily, routine movement and activities resulting from the reorganization of the personal life, which may include changing the place of residence or work. It can be equated with the movement and any activity of people performed by means of transport outside the place of residence [17-18]. On the other hand, Menes [19] presents mobility as mobility related to the daily movement of residents, mainly to work or school.

In accordance with the Treaty on the Functioning of the European Union [20] and the resulting EU transport policy, mobility is understood as an element of human activity that depends on the person traveling, the person managing the infrastructure and other users of the transport system related to this mobility [21-22]. The concept of sustainable development is closely related to the issue of mobility and covers the following issues: economic, environmental and social [23-26].

When analyzing the mobility of inhabitants, transport challenges should be taken into account, which in the 2011 White Paper [27] and in the Action Plan on Urban Mobility [28]. Bearing in mind the behavior of urban residents, a policy of sustainable transport development in urban areas should be created. This policy creates plans for development of sustainable transport in cities where sustainable urban mobility is the most important element. It is the main goal of the transport policy of the 21st century [25-26, 29-30]. A transport sustainability plan requires, inter alia, restrictions on the use of passenger cars in daily travel to increase the use of public transport, bicycles or walking [31].

To sum up they assumed that mobility can be treated as a daily movement of inhabitants related to their existence. He assumed it in the article. Before COVID-19 pandemic went off he conducted research on this field. It was made in 2019 [32].

2 Study of changes in the mobility of Polish residents caused by COVID-19

2.1 Purpose and scope of research

The aim of this article was to assess changes in the mobility of Polish residents caused by the introduction of COVID-19. The obtained research results may constitute the basis for adopting the mobility directions of the inhabitants of Poland, when a similar situation arises in the future. Due to the prevailing pandemic, the study was conducted using the survey method on a representative group of Polish residents in December 2020.

2.2 Research methodology

The study was conducted using a questionnaire. Initially, a preliminary study was conducted, which helped to refine the questions in the survey. The only possible form of conducting this type of research during the prevailing COVID-19 pandemic. The research was conducted in an open manner, while maintaining the anonymity of the respondents. It was preceded by a pilot study aimed at fully understanding the questions asked by the respondents. Then, the actual research was carried out using the Internet. The questionnaire included 18 questions about age, sex, number of inhabitants, place of residence, level of education, manner of performing professional work and professional status. The main questions in the survey were concerned with the destination of Polish residents, means of transport, distance to the destination and duration of the trip, as well as the place of shopping before and during the pandemic. They were also asked if the respondents had plans to change their communication habits in the event of another pandemic. At the end of the survey, respondents had the opportunity to express their views on mobility before and during the outbreak. For the sake of the correctness of the research results, the questionnaire was addressed to various groups of recipients. Incomplete surveys have been rejected. An important step during the research was the calculation of the sample selection. For Poland (38162000 residents), assuming a confidence level of 90% and a maximum error of 5%, the required number of people in the study was 384 respondents. Therefore, the survey was conducted with the participation of 1130 people [33-34].

2.3 Research object

The subjects of the research were the inhabitants of Poland, taking into account the place of residence, sex, number of inhabitants and their status on the labor market. The study was conducted on a group of

Table 1 *Socio-demographic characteristics of survey respondents*

Category	number	%	Female		Male	
			number	%	number	%
Sex:						
Female	647	57.26	--	--	--	--
Male	483	42.74	--	--	--	--
Age:						
under 18 years	55	4.87	7	1.08	48	9.94
18-25 years	120	10.62	63	9.74	57	11.80
26-35 years	306	27.08	185	28.59	121	25.05
36-45 years	358	31.68	213	32.92	145	30.02
46-55 years	181	16.02	114	17.62	67	13.87
over 55 years	110	9.73	65	10.05	45	9.32
Place of residence:						
urban area	616	54.51	336	51.93	280	57.97
rural area	514	45.49	311	48.07	203	42.03
Educational level:						
no education	6	0.53	3	0.46	3	0.62
primary	53	4.69	8	1.24	45	9.32
basic vocational	11	0.97	6	0.93	5	1.04
secondary technical	99	8.76	51	7.88	48	9.94
secondary	120	10.62	61	9.43	59	12.22
higher	841	74.42	518	80.06	323	66.87
Status on the labour market:						
pupil	71	6.28	16	2.47	55	11.39
student	49	4.34	27	4.17	22	4.55
employed	935	82.74	551	85.16	384	79.50
unemployed	22	1.95	15	2.32	7	1.45
pensioner	19	1.68	15	2.32	4	0.83
other	34	3.01	23	3.55	11	2.28
Number of inhabitants:						
up to 5.000	463	40.97	275	42.50	188	38.92
5.000 - 10.000	116	10.27	72	11.13	44	9.11
10.000 - 15.000	49	4.34	32	4.95	17	3.52
15.000 - 20.000	42	3.72	23	3.55	19	3.93
20.000 - 50.000	57	5.04	42	6.49	15	3.11
50.000 - 100.000	129	11.42	80	12.36	49	10.14
100.000 - 150.000	31	2.74	25	3.86	6	1.24
150.000 - 200.000	14	1.24	5	0.77	9	1.86
200.000 - 500.000	23	2.04	14	2.16	9	1.86
over 500.000	206	18.23	79	12.21	127	26.29

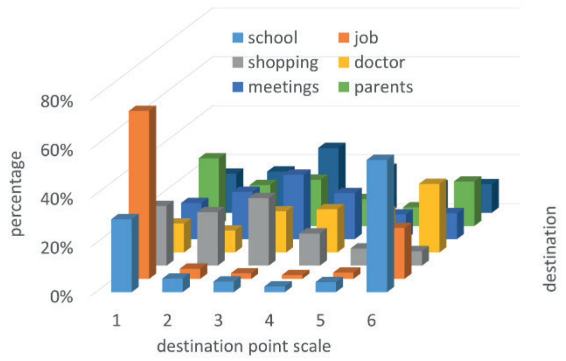

Figure 3 *Purpose of daily travel before the pandemic*

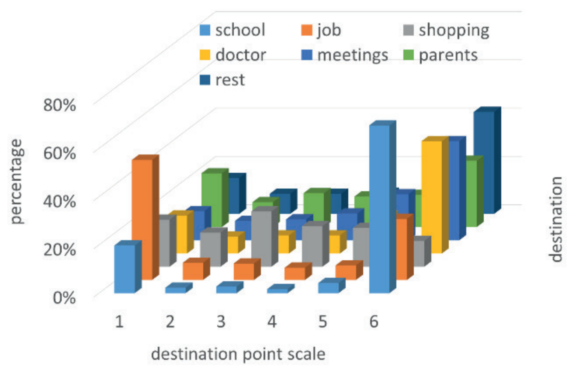

Figure 4 *The purpose of daily travel during the pandemic*

3,598 respondents, but only 1,130 correctly completed questionnaires were used for further analysis. Women constituted 57% of the respondents and men 43%. Most people were adults. 37% of them were young people aged 18-35. Respondents aged 36-55 accounted for almost 48% and 10% were over 55 years old. Almost 5% of people were under 18 years of age. The majority of women (33%) and men (30%) were aged 36-45 years.

Most of the respondents lived in cities with up to 5,000 inhabitants, almost 41% of the respondents and over 500,000 – 18%. The remaining 41% of respondents lived in cities of 5-500 thousand. 55% of the respondents lived in the city and 45% in the countryside. The majority of women (43%) and men (39%) lived in cities with up to 5,000 inhabitants (Table 1).

Another question was related to the statute on the labor market. Over 83% are working people and 6% are pupils. 85% of women and 80% of men were working. The remaining group consisted of, respectively: the unemployed, students, working students, retirees and pensioners, people running a business and farmers.

Among the respondents, over 74% were people with higher education. 80% of the women surveyed had a tertiary education, compared to 67% of the men. Currently, the respondents work in a traditional way, 44% in the workplace, 21% remotely. On the other hand, 35% replied that they work as a hybrid. To the question: Has your professional situation changed after the outbreak of the coronavirus epidemic? 78% of respondents said they did not.

Table 2 *Purpose of women's daily travel before and during the pandemic*

Destination	Before the pandemic, %						During the pandemic, %					
	1	2	3	4	5	6	1	2	3	4	5	6
school	31.07	5.41	4.02	2.63	4.02	52.86	16.54	2.32	2.94	2.01	4.79	71.41
work	71.25	3.71	2.32	1.08	2.32	19.32	49.77	6.80	7.88	5.26	7.11	23.18
shopping	28.28	22.57	25.81	11.44	5.72	6.18	20.40	12.36	22.87	16.69	17.16	10.51
doctor	10.05	8.35	20.71	20.40	18.24	22.26	13.60	7.42	9.89	8.35	18.08	42.66
meetings	14.84	19.94	28.44	17.77	9.89	9.12	11.44	6.18	8.19	10.20	18.70	45.29
parents	29.83	18.24	17.31	9.43	7.42	17.77	21.48	11.90	12.98	12.36	14.53	26.74
leisure	14.37	17.62	28.59	16.23	11.90	11.28	12.06	6.96	7.42	8.81	17.31	47.45
max	71.25	22.57	28.59	20.40	18.24	52.86	49.77	12.36	22.87	16.69	18.70	71.41

Table 3 *Purpose of men's daily travel before and during the pandemic*

Destination	Before the pandemic, %						During the pandemic, %					
	1	2	3	4	5	6	1	2	3	4	5	6
school	28.36	5.59	4.55	2.07	4.35	55.07	24.22	2.48	2.69	1.45	3.11	66.05
work	63.35	4.97	2.28	2.28	3.11	24.02	48.24	7.87	5.59	5.80	5.18	27.33
shopping	18.63	21.33	28.99	15.32	9.32	6.42	18.22	17.18	22.98	16.98	13.87	10.77
doctor	14.70	8.90	11.80	13.04	15.53	36.02	19.46	6.42	4.55	6.21	12.84	50.52
meetings	13.66	18.01	25.05	19.05	11.39	12.84	13.25	10.56	9.94	13.25	20.29	32.71
parents	24.84	14.49	20.29	12.01	8.70	19.67	22.77	9.52	15.53	12.63	12.01	27.54
leisure	16.98	16.36	25.26	18.22	10.56	12.63	18.63	10.77	9.73	8.90	17.18	34.78
max	63.35	21.33	28.99	19.05	15.53	55.07	48.24	17.18	22.98	16.98	20.29	66.05

2.4 Results

The first substantive question of the survey was to indicate the purpose of daily travel, before and during the pandemic. In this case, the respondents had the option to choose one of seven answers, specifying the importance of the target. In the analyzed case: 1 was the most common target, 6 the rarest. Before the pandemic, the most important destination for the respondents was work, then shopping, social meetings, a doctor and

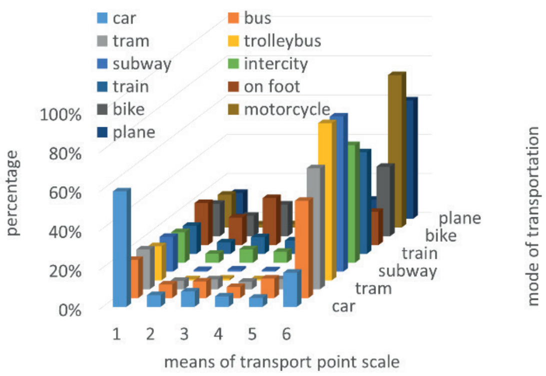

Figure 5 *Means of transport before the pandemic*

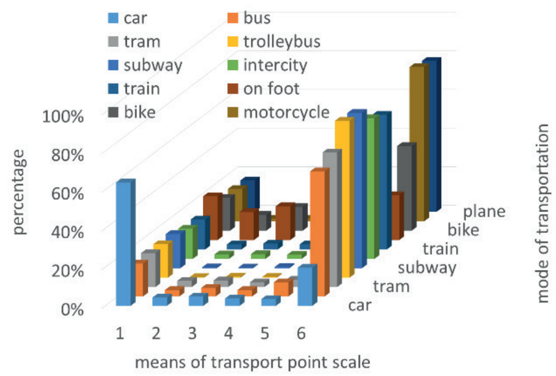

Figure 6 *Means of transport during the pandemic*

Table 4 *A means of transporting women before and during the pandemic*

Means of transport	Before the pandemic, %						During the pandemic, %					
	1	2	3	4	5	6	1	2	3	4	5	6
car	63.68	4.79	7.26	3.86	4.79	15.61	69.40	3.71	4.33	2.32	2.47	17.77
Bus	17.16	8.04	7.42	5.41	9.12	52.86	14.99	2.47	3.55	2.94	7.11	68.93
Tram	18.70	4.33	3.71	3.09	4.33	65.84	15.61	3.55	1.55	2.16	3.25	73.88
Trolleybus	14.99	0.93	0.77	0.62	0.62	82.07	14.84	0.46	0.46	0.31	0.62	83.31
Metro	15.15	1.39	0.62	0.31	0.46	82.07	15.15	0.77	0.15	0.46	0.15	83.31
Intercity transport	13.60	5.10	7.73	4.79	6.80	61.98	13.60	2.32	2.01	2.16	4.33	75.58
Train	13.76	5.72	7.73	6.80	11.13	54.87	14.22	2.01	2.47	1.08	6.18	74.03
By foot	22.87	14.84	23.03	11.59	8.96	18.70	23.96	13.45	16.54	10.82	9.12	26.12
Bike	13.76	9.43	16.85	10.36	9.89	39.72	13.91	6.65	13.29	7.88	9.43	48.84
Motorbike	14.06	1.24	1.55	0.62	1.24	81.30	13.91	1.08	1.39	0.31	0.46	82.84
Plane	12.21	2.78	8.04	5.41	9.89	61.67	13.45	1.70	0.77	0.62	2.47	80.99
max	63.68	14.84	23.03	11.59	11.13	82.07	69.40	13.45	16.54	10.82	9.43	83.31

Table 5 *A means of transporting men before and during the pandemic*

Means of transport	Before the pandemic, %						During the pandemic, %					
	1	2	3	4	5	6	1	2	3	4	5	6
car	51.35	7.87	8.28	7.25	5.59	19.67	55.90	5.18	5.18	5.59	5.80	22.36
Bus	22.57	7.25	9.52	6.63	10.56	43.48	20.91	4.55	4.76	4.14	8.70	56.94
Tram	23.60	4.76	6.42	4.14	5.80	55.28	21.33	2.48	5.59	3.31	4.55	62.73
Trolleybus	21.53	0.41	1.04	0.21	0.41	76.40	18.63	14.08	24.64	14.91	12.84	14.91
Metro	21.53	0.62	1.86	1.04	0.62	74.33	22.15	0.21	0.62	0.83	1.04	75.16
Intercity transport	19.46	4.35	6.21	6.63	7.25	56.11	19.46	2.69	2.90	2.07	6.00	66.87
Train	16.36	6.42	9.52	7.66	13.25	46.79	18.43	3.52	3.93	4.14	7.66	62.32
By foot	18.63	14.08	24.64	14.91	12.84	14.91	20.50	15.32	18.63	12.84	12.84	19.88
Bike	20.29	11.80	15.53	11.18	10.14	31.06	21.33	9.94	10.97	8.28	11.39	38.10
Motorbike	21.53	2.07	1.45	1.66	0.83	72.46	21.53	1.66	1.24	1.04	0.00	74.53
Plane	15.73	5.80	6.00	5.59	10.56	56.31	21.53	1.04	1.86	1.24	2.28	72.05
max	51.35	14.08	24.64	14.91	13.25	76.40	55.90	15.32	24.64	14.91	12.84	75.16

finally school. However, during the pandemic, a different hierarchy of respondents' goals emerged. In the first place, there is still work and shopping, while socializing has passed and the school has moved up. During the pandemic, the respondents dropped out of visiting a doctor, resting or visiting their parents. The above data correspond to the previous questions concerning the age and professional situation of the respondents. The above data are presented in the Figures 3 and 4.

The main purpose of women's trips was work. This was 71% before the pandemic and 50% during the pandemic. The same was true for men: before the pandemic, work accounted for 63% and during the pandemic 48%. This is confirmed by the age of the respondents and also by the fact that 35% of them worked in a hybrid mode (Table 2, 3).

Then, respondents were asked which means of transport they use. As in the previous case: 1 was the most common target, 6 the rarest. When asked, before the pandemic, the respondents most often used the car and walked and least often - trolleybus and motorbike. Not much has changed during the pandemic and respondents chose the car and walked over it. However, it can be noticed that the respondents gave up public transport as much as possible. The above results are mainly concerned with the activity of people, such as the workplace or school and shopping. The data is presented in Figures 5 and 6. Due to the pandemic, more men and women started using their own cars instead of public transport (Table 4, 5).

Another question was about the distance from home to destination before and during the pandemic. Most of the respondents before the outbreak of the pandemic indicated a distance of 1-5 km (26%) as the main goal, this is due to the workplace and the additional goal was a distance of more than 20 km (36 %), mainly trips related to leisure and family visits. After the outbreak of the pandemic, a distance of 1-5 km appeared as the main and additional destination. This is largely due to commuting and shopping. Following the outbreak of the pandemic, respondents gave up visiting relatives and resting, spending most of their time at home. The data is shown in Figure 7. Before the swap, women were 1-5 km away from their main destination, while men were more than 20 km away. During the pandemic, women's distance remained the same, while men's decreased to 5 km (Table 6).

Another question was how long it would take to travel to the primary and secondary destinations before and during the pandemic? In this case, before the outbreak of the pandemic, most people reached their primary destination, usually work, within 15-30 minutes (32%) and the secondary destination, shopping, within 15 minutes (41 %). During an epidemic and a decrease in traffic on the roads, the time for both cases is up to 15 minutes. A small number of respondents targeted more than 2 hours. This correlates with the distance of the place of residence from the primary and secondary travel destination, as shown in Figure 8. For the main goal before the pandemic outbreak, women had up to 15 minutes (33%) and men between 15 and 30 minutes (35 %). During the pandemic, the main target for women and men was up to 15 minutes (41%) (Table 7).

The next questions were about where to shop before the pandemic. When asked about this question, before the pandemic was announced, the respondents indicated large stores as the most popular place to buy: a supermarket, hypermarket, market and the third place was only the internet, while after the epidemic was announced, the respondents most often made purchases on the Internet and in the local stores. This is confirmed by responses to the reduction in distance and time to destination after the declaration of a pandemic. The data is presented in Figures 9 and 10. Before the pandemic, women shopped mainly in supermarkets and hypermarkets, but during the pandemic the situation changed and more women shopped online (Table 8). There was a similar situation among men (Table 9).

Subsequent questions were related to the change of communication habits in the event of another pandemic (Figure 11). This question was answered by the largest number of respondents, almost 77%, (woman 75.73%, men 78.05 %). These are the people who use the car most often because of the comfort, safety, isolation from other people, or the inability to use public transport, especially in rural areas and the pandemic did not affect

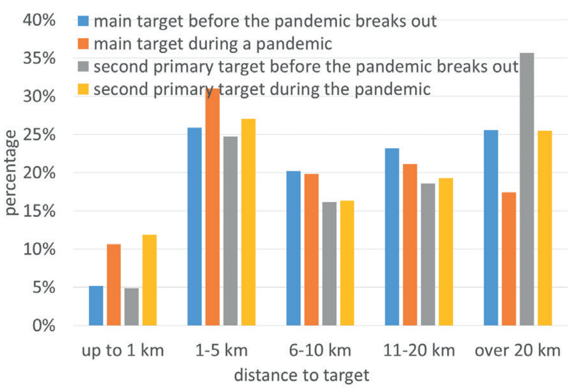

***Figure 7** Distance to destination before and during the pandemic*

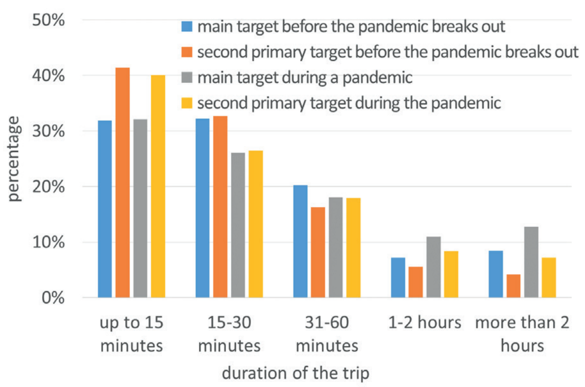

***Figure 8** Duration of the trip before and during the pandemic*

Table 6 *Distance to target for female and male before and during the pandemic*

Distance	Female					Male				
	do 1km	1-5km	6-10km	11-20km	pow. 20km	do 1km	1-5km	6-10km	11-20km	pow. 20km
primary objective before the outbreak of a pandemic	5.26	27.51	20.09	22.57	24.57	4.97	24.43	20.50	23.60	26.50
second main objective before the outbreak of a pandemic	4.48	22.10	14.68	19.47	39.26	5.59	29.19	18.01	18.01	29.19
primary objective during the pandemic	9.58	32.46	20.87	20.56	16.54	11.80	28.99	19.25	21.74	18.22
second main objective during pandemic	11.59	25.97	17.00	20.09	25.35	12.01	28.99	15.73	17.81	25.47

Table 7 *Distance to travel time for female and male before and during the pandemic*

Travel time	Female					Male				
	up to 15 minutes	15-30 minutes	31-60 minutes	1-2 hours	over 2 hours	up to 15 minutes	15-30 minutes	31-60 minutes	1-2 hours	over 2 hours
primary objective before the outbreak of the pandemic	32.61	31.53	18.39	7.88	9.58	30.23	35.20	22.98	5.59	6.00
second main objective before the outbreak of the pandemic	28.59	25.35	18.86	11.28	15.92	37.06	28.16	17.18	10.35	7.25
primary objective during the pandemic	41.27	32.61	14.99	6.80	4.33	40.58	34.58	17.39	3.73	3.73
second main objective during the pandemic	36.79	26.89	18.55	9.43	8.35	43.69	26.71	16.77	7.45	5.38

the way of traveling in this case. Furthermore, some of the respondents have changed the way of traveling since the epidemic was introduced, i.e. for 9 months. First of all, fearing for their health, it was abandoning the public transport in favor of a car, some were even forced to buy a car, bicycle or walk. However, especially persons from large cities, that were forced to use the public transport due to the lack of parking spaces at work. In addition, about 11% of respondents said that in the event of a prolonged pandemic, they would change their mobility in the main one and adequately measured their decision to the existing situation.

The next question was an open-ended question in which respondents had the opportunity to determine the impact of how the coronavirus changed their mobility. Most of the respondents wrote that its impact was significant. Apart from the comments mentioned in the above question, it is worth noting that there has been a decrease in the number of public transport passengers. They mainly use cars or other means of

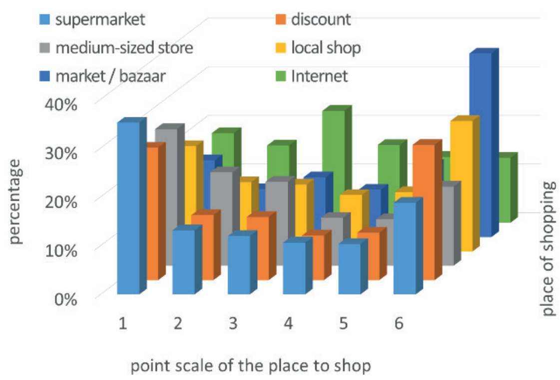

Figure 9 *Place of shopping before the pandemic*

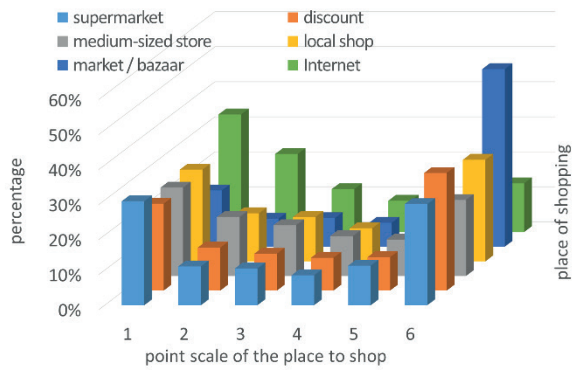

Figure 10 *Place of making purchases during the pandemic*

Table 8 *Women's shopping space before and during the pandemic*

place of shopping	Before the pandemic , %						During the pandemic, %					
	1	2	3	4	5	6	1	2	3	4	5	6
super- and hypermarket	38.02	10.82	11.28	10.51	9.58	19.78	30.14	9.27	9.74	7.73	10.97	32.15
discount store	27.36	12.83	10.97	8.19	10.51	30.14	23.34	11.59	8.66	8.81	10.05	37.56
medium-sized shop. so-called market	29.52	18.24	18.24	8.50	8.96	16.54	25.04	16.85	14.99	10.20	11.13	21.79
estate shop	22.41	13.76	12.83	10.36	13.29	27.36	27.67	12.36	11.13	9.27	9.27	30.29
marketplace/ bazaar	14.99	10.05	14.06	10.36	14.68	35.86	14.06	7.42	9.89	6.49	9.89	52.24
Internet	19.63	14.53	22.87	17.47	12.06	13.45	38.95	23.03	9.74	7.73	6.96	13.60
max	38.02	18.24	22.87	17.47	14.68	35.86	38.95	23.03	14.99	10.20	11.13	52.24

Table 9 *Men's shopping space before and during the pandemic*

place of shopping	Before the pandemic, %						During the pandemic, %					
	1	2	3	4	5	6	1	2	3	4	5	6
super- and hypermarket	31.06	15.32	13.04	10.97	11.18	18.43	28.78	13.66	11.80	9.94	11.80	24.02
discount store	27.33	13.66	14.29	10.77	8.70	25.26	16.36	17.81	23.19	13.87	15.73	13.04
medium-sized shop. so-called market	25.88	18.84	17.18	12.22	10.35	15.53	25.26	15.73	15.11	13.66	9.32	20.91
estate shop	20.29	14.29	15.53	13.25	10.97	25.67	22.57	16.15	13.66	10.97	9.73	26.92
marketplace/ bazaar	17.81	9.94	10.35	9.32	14.49	38.10	19.88	8.49	6.83	7.25	10.77	46.79
Internet	16.36	17.81	23.19	13.87	15.73	13.04	26.71	20.91	15.11	10.56	12.84	13.87
max	31.06	18.84	23.19	13.87	15.73	38.10	28.78	20.91	23.19	13.87	15.73	46.79

individual communication, including by bike or walking. This is due to the safety of passengers, the introduction of restrictions on the number of people in the vehicle and in some cases also the increase in ticket prices and the liquidation of connections. The above state is also confirmed by the author's observations regarding public transport.

A smaller number of people, due to work and study at home, as well as the closure of cultural institutions and restaurants, as well as restraining from travel and social visits, limited their mobility to a practically minimum. They also reduced the frequency of purchases: once every few days instead of everyday purchases. The air transport in the initial phase of the pandemic has practically been extinguished to zero. All over the world, many airlines have suspended regular flights. This situation caused a radical decline in tourist and business traffic not only in Poland, but all over the world.

The respondents also stated that in cities, COVID-19 affected the mobility of residents, while in rural areas, slightly, because the primary means of transport there is a car. The above state is also confirmed by the author's observations.

The next step was to correlate the answers given

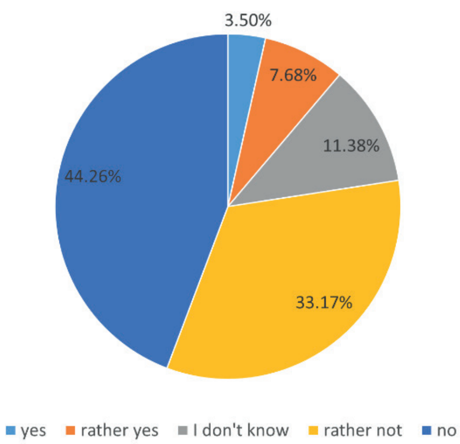

Figure 11 *Changing communication habits*

Table 10 *Correlation of answers given by gender*

Criterion	*df*	α	χ^2	χ^2_d	Conclusion
Age range	5	0.05	50.26	11.07	There is a correlation
Place of residence	1	0.05	4.07	3.84	There is a correlation
Number of residents	9	0.05	50.64	16.92	Correlation exists
Education	5	0.05	48.48	11.07	Correlation exists
Labour market status	5	0.05	42.36	11.07	Correlation exists
Occupational situation after the coronavirus outbreak	1	0.05	0.01	3.84	No correlation
Professional work	2	0.05	11.16	5.99	Correlation exists
Change in communication habits	4	0.05	5.18	9.48	no correlation

where:
df - the degrees of freedom,
α - the significance level,
χ^2 - the Chi-square statistic,
χ^2_d - the critical Chi-square value.

by the respondents according to their gender. Based on the research, it can be concluded that the gender of the respondents depended on the age range, place of residence, population, education, labour market status and professional work (Table 10).

In the next step, correlations were made between the factors found in the questionnaire. Based on the Table 11, a very strong positive correlation can be found between the following factors: main destination before and during the pandemic (r = 0.9823, p < 0.001), mode of transport before and during the pandemic (r = 0.9953, p < 0.001) and travel time to destination before and during the pandemic (r = 0.9879, p < 0.001).

In contrast, a very strong negative correlation is found between the following factors: mode of work and education (r = - 0.9598, p = 0.002), main destination before pandemic and distance to main destination before pandemic (r = - 0.9756, p = 0. 001), main destination before pandemic vs distance to main destination during pandemic (r = -0.9959, p < 0.001), age vs travel time before pandemic (r = - 0.9804, p = 0.001) and age vs travel time during pandemic (r = - 0.9756, p = 0.001).

Based on e Table 11, there is no correlation between the following factors: main destination before the pandemic and education (r = -0.0930) and labour market status (r = -0.0947); main destination during the pandemic and population (r = 0.0898) and education (r= -0.0676); mode of transport before the pandemic and labour market status (r = - 0.0917) and main destination during the pandemic (r = - 0. 0211); mode of transport during the pandemic and main destination before the pandemic (r = 0.0515) and during the pandemic (r = - 0.0765); distance to the main destination before the pandemic and labour market status (r = - 0.0226); distance to the main destination during the pandemic and age (r = 0.0593) and place of shopping during the pandemic and labour market status (r = - 0.0350).

2.5 Discussion of the results

At the beginning of the announcement of the epidemic, the mobility of residents practically decreased. Currently, the difference is not very noticeable, but the travel times in rush hour traffic have shrunk slightly. In the evenings and on weekends, it increased in turn. This is mainly due to working and distance learning up to the afternoon hours.

Most of the respondents use a car, but quite often, due to the prevailing situation, they choose an active

Table 11 *Correlation factors in the survey (bp- before the pandemic; dp- during the pandemic)*

	Factors	1	2	3	4	5	6	7	8	9	10	11	12	13	14	15	16
1	age	1															
2	number of inhabitants	-0.6997	1														
3	education	-0.2753	-0.1240	1													
4	labour market status	0.4488	-0.2388	-0.2814	1												
5	way of working	-0.1097	0.6843	-0.9598	0.1633	1											
6	main destination bp	-0.4966	0.2189	-0.0930	-0.0947	-0.8811	1										
7	main destination dp	-0.3603	0.0898	-0.0676	-0.1141	-0.9250	0.9823	1									
8	mode of transport bp	-0.5198	0.8715	-0.3536	-0.0917	0.7969	0.1078	-0.0211	1								
9	mode of transport dp	-0.5277	0.8678	-0.3123	-0.1447	0.7919	0.0515	-0.0765	0.9953	1							
10	distance to main destination bp	0.3704	-0.8205	0.5929	-0.0226	-0.9756	0.4751	0.6323	-0.8999	-0.9045	1						
11	distance to main destination dp	0.0593	-0.5856	0.5342	-0.2577	-0.9959	0.6985	0.8275	-0.7057	-0.7124	0.9436	1					
12	time of travel to destination bp	-0.9804	0.8361	-0.6889	-0.2261	0.2967	0.5609	0.3932	0.7696	0.7404	-0.4618	-0.1817	1				
13	travel time to main destination dp	-0.9574	0.9059	-0.7164	-0.2188	0.4902	0.4265	0.2481	0.8580	0.8331	-0.5928	-0.3258	0.9879	1			
14	shopping place bp	-0.2679	0.7210	-0.5249	0.2980	0.8436	0.3825	0.2993	0.7927	0.7484	-0.7497	-0.5614	0.9041	0.9471	1		
15	shopping place dp	-0.2840	0.4269	0.5532	-0.0350	0.8288	0.1464	0.1551	0.2747	0.2818	-0.9265	-0.7761	0.5525	0.6687	0.3505	1	
16	change in COVID habits	0.4608	-0.5950	0.9284	-0.3181	-0.4139	-0.6371	-0.5646	-0.5718	-0.5164	0.3407	0.1451	-0.9107	-0.8785	-0.9449	-0.7749	1

lifestyle: walking or cycling, walking, giving up the public transport for safety reasons. The most important destination for respondents before the pandemic was work, then shopping, socializing, a doctor and finally school. In the midst of the pandemic, it is still mostly work and shopping, while socializing has gone and the school has moved up. During the pandemic, the respondents did not visit the doctor, rest or visit their parents. They cover the distance of up to 5 km and it takes them up to 15 minutes and they do their shopping less often, once every few days in smaller stores and on the Internet.

In addition, the study found a strong negative correlation between: mode of work and education; main destination before the pandemic and distance to the main destination before the pandemic; main destination before the pandemic and distance to the main destination during the pandemic; age and travel time before the pandemic; and age and travel time during the pandemic.

3 Summary

After the outbreak of the COVID-19 epidemic, the mobility of Polish residents has changed, especially in cities where there was public transport and people stayed at home or started using their own cars. In smaller towns and villages, where there is no public transport, people still mainly use cars because they are dependent on it. The above statement is confirmed by the results of the surveys. Based on the research, it can be concluded that the gender of the respondents depended on the age range, place of residence, population, education, labour market status and professional work. In addition, respondents were asked whether the COVID-19 pandemic had affected their mobility. During the COVID-19 pandemic, the mobility of citizens, especially in the cities, has changed. Instead of using public transport, they use cars, bicycles and walk. In smaller towns and villages, the communication behavior of the inhabitants has practically not changed, as they mainly use cars.

References

[1] Central register of vehicles and drivers „The number of means of transport in Poland" [online] [accessed 2019-02-21]. Available from: http://www.cepik.gov.pl/statystyki

[2] Number of COVID-19 cases and deaths [online] [accessed 2019-02-21]. Available from: https://koronawirusunas.pl/

[3] ANDERSEN, K., RAMBAUT A., LIPKIN W. I., HOLMES E., GARRY R. The proximal origin of SARS-CoV-2. *Nature Medicine* [online]. 2020, **26**, p. 450-452. ISSN 1078-8956, eISSN 1546-170X. Available from: https://doi.org/10.1038/s41591-020-0820-9

[4] MAIER, B. F., BROCKMANN D. Effective containment explains subexponential growth in recent confirmed COVID-19 cases in China. *Science* [online]. 2020, **368**, p. 742-746. ISSN 0036-8075. Available from: https://doi.org/10.1126/science.abb4557

[5] BARRO, R., URSUA, J., WENG, J. The coronavirus and the great influenza pandemic: lessons from the "Spanish Flu" for the Coronavirus's potential effects on mortality and economic activity [online]. NBER Working Papers 26866. Cambridge, MA, USA: National Bureau of Economic Research, 2020. Available from: https://doi.org/10.3386/w26866

[6] LAING, T. The economic impact of the coronavirus 2019 (Covid-2019): implications for the mining industry. *The Extractive Industries and Society* [online]. 2020, **7**(2), p. 580-82. ISSN 2214-790X. Available from: https://doi.org/10.1016/j.exis.2020.04.003

[7] BOOT, A., CARLETTI, E., HASELMANN, R., KOTZ, H. H, KRAHNEN, J. P. PELIZZON, L., SCHAEFER, S., SUBRAHMANYAM, M. The coronavirus and financial stability. SAFE Policy Letter 78. Frankfurt: Leibniz Institute for Financial Research SAFE, 2020.

[8] WARREN, M. S., SKILLMAN, S.W. Mobility changes in response to COVID-19. arXiv:2003.14228. 2020.

[9] JONAS, D. V. The effect of COVID-19 and subsequent social distancing on travel behavior. *Transportation Research Interdisciplinary Perspectives* [online]. 2020, **5**, 100121. ISSN 2590-1982. Available from: https://doi.org/10.1016/j.trip.2020.100121

[10] GOSSLING, S., SCOTT, D. HALL. C. M. Pandemics, tourism and global change: a rapid assessment of COVID-19. *Journal of Sustainable Tourism* [online]. 2021, **29**(1), p. 1-20. ISSN 0966-9582, eISSN 1747-7646. Available from: https://doi.org/10.1080/09669582.2020.1758708

[11] GIOVANNI, B., PIERRI, F., CINELLI, M., FLORI, A., GALEAZZI, A., PORCELLI, F., SCHMIDT, A. L., VALENSISE, C. M. SCALA, A., QUATTROCIOCCHI, W. Economic and social consequences of human mobility restrictions under COVID-19. *Proceedings of the National Academy of Sciences of the United States of America* [online]. 2020, **117**(27), p. 15530-15535. ISSN 0027-8424, eISSN 1091-6490. Available from: https://doi.org/10.1073/pnas.2007658117

[12] GIULIA, P., VALDANO, E., SCARPA, N., RUBRICHI, S., COLIZZA. V. Population mobility reductions during COVID-19 epidemic in France under lockdown - *medRxiv* [online]. 2020, 2020.05.29.20097097. Available from: https://doi.org/10.1101/2020.05.29.20097097

[13] QUEIROZ, L., MELO, J. L., BARBOZA, G., URBANSKI, A. H. NICOLAU, A., OLIVA, S., NAKAYA. H. Large-scale assessment of human mobility during COVID-19 outbreak - OSF Preprints [online]. 2020. Available from: https://doi.org/10.31219/osf.io/nqxrd

[14] GALEAZZI, A., CINELLI, M., BONACCORSI, G., PIERRI, F., SCHMIDT, A.L. SCALA, A., PAMMOLLI, F., QUATTROCIOCCHI. W. Human mobility in response to COVID-19 in France, Italy and UK. *Scientific Reports* [online]. 2021, **11**, 13141. eISSN 2045-2322. Available from: https://doi.org/10.1038/s41598-021-92399-2

[15] SCHLOSSER, F., MAIER, B. F., HINRICHS, D., ZACHARIAE, A., BROCKMANN, D. COVID-19 lockdown induces structural changes in mobility networks. *Proceedings of the National Academy of Sciences of the United States of America* [online]. 2020, **117**(52), p. 32883-32890. ISSN 0027-8424, eISSN 1091-6490. Available from: https://doi.org/10.1073/pnas.2012326117

[16] SZOLTYSEK, J. *Creating mobility of city dwellers*. Warsaw: Wolters Kulwer, 2011. ISBN 978-83-264-1549-4.

[17] ZALOGA, E., DUDEK, E. Selected problems of European society mobility. *Problemy Transportu i Logistyki / Problems of Transport and Logistics*. 2009, **9**, p. 99-109. ISSN 1644-275X, eISSN 2353-3005.
[18] FLEJTERSKI, S., PANASIUK, A., PERENC, J., ROSA, G. *Contemporary economics of services*. Warsaw: PWN Scientific Publisher, 2005 ISBN: 83-01-14488-2
[19] MENES, E. Socio-economic aspects of the development of individual motorization in Poland. *Przeglad Komunikacyjny / Communication Review*. 2001, **01**. ISSN 0033-2232, eISSN 2544-6037.
[20] Treaty on the functioning of the European union. Official Journal of the European Union. C 326/49 of 26.10.2012.
[21] KRUSZYNA, M. Railway station as a mobility node. *Przeglad Komunikacyjny / Communication Review*. 2012, **10**, p. 34-37. ISSN 0033-2232, eISSN 2544-6037.
[22] KRUSZYNA, M. Traffic engineering and shaping mobility. *Przeglad Komunikacyjny / Communication Review*. 2010, **11-12**, p. 52-53. ISSN 0033-2232, eISSN 2544-6037.
[23] BORYS, T. Measurement of sustainable transport development. In: *Ecological problems of sustainable development*. KIELCZEWSKI, D., DOBRZANSKA, B. (eds.). Bialystok: Wydawnictwo Wyzsza Szkola Ekonomiczna in Bialystok, 2009. ISBN 978-83-61247-07-4.
[24] LITMAN, T. Developing indicators for comprehensive and sustainable transport planning. *Transportation Research Record: Journal of the Transportation Research Board* [online]. 2007, **2017**(1), p. 10-15. ISSN 0361-1981, eISSN 2169-4052. Available from: https://doi.org/10.3141/2017-02
[25] CHAMIER-GLISZCZYNSKI, N. Sustainable urban mobility as part of the transport plan Koszalin University of Technology. *Logistyka / Logistics*. 2015, **4**. ISSN 1231-5478.
[26] BANISTER, D. The sustainable mobility paradigm. *Transport Policy* [online]. 2008, **15**(2), p. 73-80. ISSN 0967-070X. Available from: https://doi.org/10.1016/j.tranpol.2007.10.005
[27] White paper on transport - plan for creating a single European transport area - striving for a competitive and resource-efficient transport system. European Commission, Directorate-General for Mobility and Transport. 2011.
[28] European Parliament resolution of 23 April 2009 on an action plan for urban mobility 2008/2217 (INI).
[29] CERVARO, R. Paradigm shift: from automobility to accessibility planning. Working Paper No. 677. Berkeley CA, 1996.
[30] KOMSTA, H. DROZDZIEL, P., OPIELAK, M. The role of urban public transport in creating mobility of residents. *Logistyka / Logistics*. 2019, **1-2**. ISSN 1231-5478.
[31] KLOS-ADAMKIEWICZ, Z. Mobility plan as a tool for implementing sustainable transport development in cities. *Logistyka / Logistics*. 2014, **2**. ISSN 1231-5478.
[32] GORZELANCZYK, P. Mobility of Polish residents. In: *Research and the Future of Telematics*. 2020. p. 3-15. ISBN978-3-030-59269-1.
[33] BABBIE, E. R. *The practice of social research*. Belmont: Wadsworth Cengage, 2010. ISBN 9780495598411.
[34] Research sample selection [online] [accessed 2020-02-21]. Available from: https://www.naukowiec.org/dobor.html

MOBILITY IN THE DEVELOPING COUNTRY. THE CASE STUDY OF BANGKOK METROPOLITAN REGION

Kamil Wilinski [1], **Shubham Pathak** [2,*]

[1]School of Languages and General Education (SOLGEN), Walailak University, Tha Sala, Nakhon Si Thammarat, Thailand
[2]College of Graduate Studies (CGS) Center of Excellence in Sustainable Disaster Management (CESDM), Walailak University, Tha Sala, Nakhon Si Thammarat, Thailand

*E-mail of corresponding author: sitihawa@uum.edu.my

Resume

Significant economic growth visible in recent decades in Thailand contributed to a huge demand for private vehicles, which was not followed by a sufficient growth of transport infrastructure, consequently leading to permanent congestion, increase in the number of accidents, high carbon emission and thus a decline in the air quality. This research was conducted in the capital of Thailand, Bangkok using key informant interviews to examine socio-economic determinants of 3 different modes choice: car, motorcycle and public transport. The major findings included the lack of use of public transportation due inadequate transportation schemes and policies at the local and national level in Thailand. Further analytical findings include the social, cultural and economic factors affecting the choices of the mode of transportation in Thailand.

Article info

Received 7 July 2021
Accepted 7 March 2022
Online 9 May 2022

Keywords:

travel mode choice
travel behaviour
Bangkok
Thailand

Available online: https://doi.org/10.26552/com.C.2022.3.A112-A122

ISSN 1335-4205 (print version)
ISSN 2585-7878 (online version)

1 Travel behavior

1.1 Mobility trends

Promoting the low carbon transport and reducing the need for private vehicle travel can be a major solution for the increasing problems caused by transit, such as environmental pollution, public health issues, road safety and rising costs of building and modernizing transport infrastructure. Research from several western countries present shifts in the mobility trends between generations in favour of public transit and other more sustainable transport modes [1-4]. This phenomenon is also known as a "peak car" theory and represents a decline in the car ownership, driver's licence ownership and kilometres travelled [5]. Explanations for that phenomenon vary by different studies, conducted in different countries. Some studies have ascribed the reversal in car dependence to changes in the economy as financial crises and rising fuel prices [6]. Another present social changes such as lower incomes, global preference for less car-dependent inner-city living, increasingly restrictive driving license regimes and delay in the life stage of millennials, in areas such as full-time work, home ownership, marriage and child-rearing, which do not induce them to own a private car in comparison to the previous generations [7]. It is also argued that changes are caused by attitudes and preferences change triggered by increased use of information communication technology (ICT) and its' services such as e-commerce, social networks and mobility as a service (MaaS) [8]. Trends towards decreased car dependence can be also explained by shifts in the increased multimodality [9-10]. On the other hand, environmental awareness about the impact of transit on the environment has proven to be the minor reason for the licencing decline and travel mode change [7, 11].

Regardless of the noticeable changes in the developed countries, constant preference for private transit, mainly based on cars and motorcycles, has been still strongly visible in the Southeast Asian economies; in some of those countries, motorization rates exceed both the population growth and urbanization rate [12]. For the main cause of unsustainable transport practices in Bangkok Metropolitan Region is monocentric urban development, high income gap between social classes causing uneven spatial distribution of housing and employment and thus different commuting possibilities

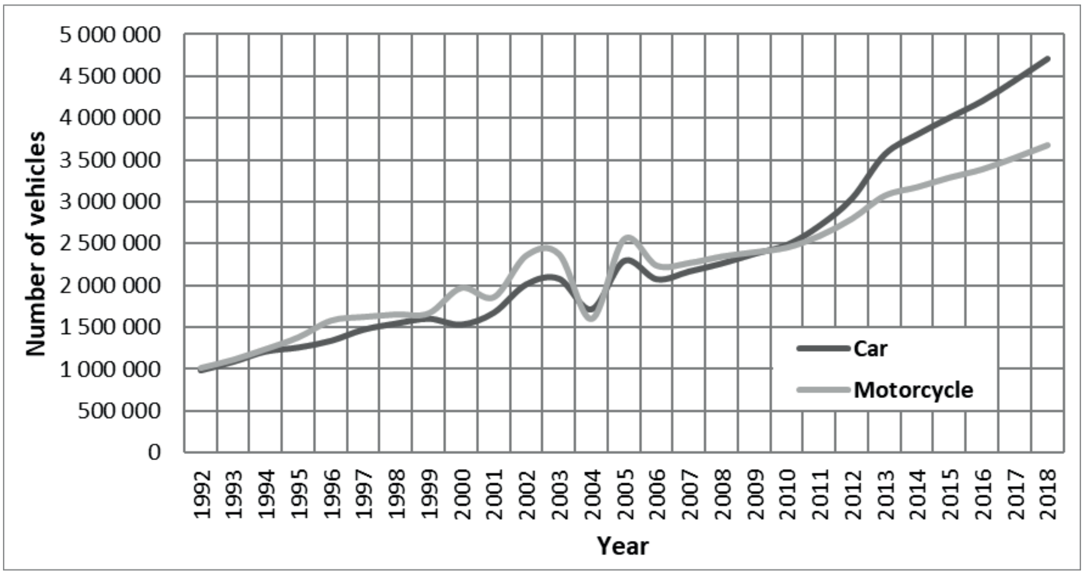

***Figure 1** Accumulated number of private vehicles registered in Bangkok Metropolitan Region between 1992 and 2018*

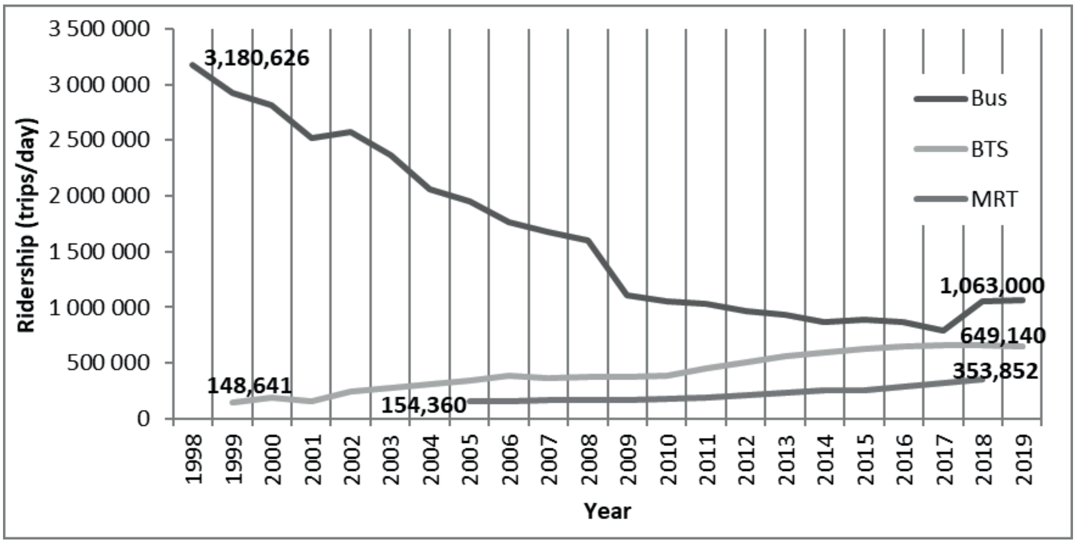

***Figure 2** Share of public transport journeys in Bangkok Metropolitan Region between 1998 and 2019*

for different social groups [13]. Furthermore, research presents unfavourable opinions of the elderly, disabled and indigent travellers regarding the accessibility, safety, connectivity and affordability of the metro system in Bangkok Metropolitan Region [14].

On the other hand, studies emphasise the importance of cultural differences between developing and developed economies and hence different factors important for travellers in the travel mode choice. Diversity in culture and social life among Asian countries reflect how people think about private transportation versus public transit [15]. In some of the developing countries private vehicle is considered as much more attractive mode of transport, providing more status and pleasure than other modes [15]. In order to prevent from further superiority of private vehicles in many Asian countries, “push and pull” strategies have been implemented using price mechanisms and usage management strategies to reduce the demand for motorized vehicles, as well as the quality improvement strategies of the public transport service, to attract more passengers and to reduce the market share of motorized vehicles [16]. Nevertheless, mobility management strategies focused on communication and persuasion, providing detailed travel information and incentives through marketing techniques in order to reduce the car use and increase use of public transit among specific socio-economic groups, have not been widely considered [17].

1.2 Transport environment in Bangkok Metropolitan Region

Thailand is a developing, upper-middle income country [18]. In 2019 the population of Thailand was more than 66.59 million people [19], with 39,160,454 vehicles

Table 1 *Thematic layers for content analysis*

Serial number	Factors	References	Sub theme
1.	Gender	[23] [24] [25]	Demographic
2.	Age	[26] [27] [25]	
3.	Education	[27]	Personal
4.	Occupation	[28]	
5.	Commuting mode	[29] [15]	
6.	Income	[25]	Economic
7.	Number of owned cars	[30]	
9.	Number of owned motorcycles	[16]	
10.	Travel time	[31] [32]	External
11.	Travel cost	[33] [32]	

registered and an increase of 2.05 % or approximately 0.97 million vehicles per year between 2015-2019 [20]. Private motorcycles accounted for 53.96 % (21,130,663), whereas private passenger cars for 42.43 % (16,616,848) of the total number of vehicles on the roads of Thailand. Furthermore, in 2019 total number of driving licences was 31,575,798 and growing by 2.32 % or about 0.87 million licenses per year between 2014-2018.

The capital of Thailand, Bangkok, with the surrounding provinces, known as Bangkok Metropolitan Region, is inhabited by more than 10.890 million people [19]. Data compilation and analysis concerning trips made in Bangkok and its vicinities [21]. showed that private-vehicle trips, both by cars and motorcycles have grown steadily (Figure 1). Registered cars surged from 987,999 in 1992 to 4,714,916 in 2018, an average increase of 6.58 % per year. In the same period, number of registered motorcycles has risen from 1,006,302 in 1992 to 3,669,600 in 2018, an average increase of 6.10 % per year.

Bangkok is the only city in Thailand equipped with the developed public transport systems that has continually been invested by the government in order to address the traffic problems. The city is served by many public and private transport providers from which the most important are bus-lanes (Bangkok Mass Transit Authority), BTS Sky Trains (Bangkok Mass Transit System) and MRT (Metropolitan Rapid Transit) accounting for 91.47 % of passenger ridership in 2018 [21]. Public bus transportation recorded substantial ridership decrease from 4,073,883 trip/day in 1992 to 1,063,000 trip/day in 2019 (exclusive of free user), BTS Sky Train between 2019-2020 carried 649,140 passengers per day with an upward trend since the beginning of the system's operation, while MRT in 2018 carried 337,000 passengers daily, also presenting a growing tendency (Figure 2). Presently, the city authorities urge the Bangkok Metropolitan Region network's expansion and emphasize the connection of different transport modes.

From the above-mentioned data, it is concluded that travel by private vehicle is likely to grow based on the increase in the number of vehicles registered, while travel by public transportation as a whole will continue to fall, thereby intensifying traffic problems within the Bangkok Metropolitan Region. Although travel by BTS and MRT has grown steadily, such ridership growth is still behind the expected number. According to the government forecasts, in 2029 57.6 % of trips in the Bangkok Metropolitan Region are expected to be made by private vehicles, including private cars 41.1 % and motorcycles 12.4 %, whereas the public transport use will compose of 42.4 % [21].

1.3 Theoretical framework

Travel mode choice studies are often based on the utility maximization theory assuming that the travel mode choice is made rationally and travellers choose the mode with the highest utility among the alternatives, as determined by their socio-economic characteristics (income, employment status, gender, number of children etc.) and the service attributes of modes (travel time, travel cost, availability etc.) [16, 22].

The conceptual framework for this study has been derived through previous literature, responses from the respondents and findings among new studies in the transportation research (see Table 1).

Gender: In the traditional societies and developing economies women tend to both make less trips and use passenger car less frequently than men do. Study conducted among indigent people living in Bangkok, found that male commuters are more dependent on private motorcycles and less on public transport than female commuters.

Age: Research from western countries confirm the existence of differences between generations in terms of travel behavior, caused by wide variety of factors. In Bangkok, dependence on private transportation modes increases and dependence on public transport decreases with age.

Education: Current millennials have the highest level of participation in higher education of any generation in the USA. Higher levels of education through the bachelor's degree level are associated with higher levels of daily vehicle kilometers travelled per capita along. Additionally, workforce participation is associated with significantly higher per capita daily vehicle kilometres travelled.

Occupation: The changes in residence and employment contribute to a great extent to changes in the commuting patterns, with private mode of transport becoming more frequently used, while use of other modes decline.

Commuting mode choice: Social-role and self-identities are important predictors of mode choice and may prevent travel behaviour change. According to [15] attitude toward car and public transit provide valuable insights regarding the commuting mode choice in Asian countries. In Thailand, the intention and desire to use the car for commuting is found to be high.

Income: Travel behavior of indigent people living in Bangkok depends not only on income but also on public transport availability, job location and place of residence. Suburban residents with limited public transport accessibility tend to use private transportation modes, mainly motorcycles, regarding their greater affordability and spend a large portion of household expenditures on vehicle and fuel. Study emphasizes importance of low-cost public transport to vulnerable subgroups of the urban poor.

Number of owned car: The habitual behavior of private vehicle use hinders an individual's intention to switch from a car or motorcycle to public transit. Furthermore, motorcycle commuters are more likely than car commuters to switch to a public transit through their reasoned evaluation process.

Number of owned motorcycles: It is found that in the motorcycle dependent region travellers with higher motorcycle ownership rates or lower incomes are more likely to use motorcycles. In the motorcycle-dependent area without a good public transportation system, motorcyclists might be more likely to switch to a car, rather than to public transport.

Travel cost and time: Thai travellers' mode choice behavior on mass transit is significantly affected by the total travel cost in private transport, total travel time in public transport and distance range from home to mass transit station. Moreover, studies emphasize the importance of social equity in long-term urban transport plans regarding access to jobs reachable by marginalized groups within a defined travel time threshold and a fare policy eliminating social exclusion from particular public transport modes because of travellers' financial status by the implementation of a fair fare system. In regard to the value of travel time to work, it is higher in high-income groups. As income increases value of travel time also increases. Furthermore, as trip length increases, the value of travel time increases.

2 Materials and methods

2.1 Procedure

In order to acquire travel behavior information, the interview checklist was divided into 2 parts. Part 1 consists of the respondent's socio-demographic information such as gender, age, education, occupational status, income, number of owned cars and motorcycles. Part 2 presents the information about the travel mode choice and details of travel cost and time.

2.2 Data collection

To gather data from the respondents' key informant interviews were used. The interviewees were chosen through random purposive sampling among the general population, with one restriction, respondents had to be more than 18 years old as this is the minimum required age to drive a motor vehicle in Thailand, thus entitling to use all the studied transportation modes. The process of reaching out to the respondents was carried out over a period of 2 months. A total of 42 inclusive of 35 Thai nationals and 7 foreign residents were interviewed for this research. The sample size is adequate in terms of the randomly selected daily commuters to examine the travel behavioural choices, risk perceptions and factors involved through the detailed data collected among the respondents [34-36].

2.3 Profile of the respondents

The respondents for this research belonged to several varied levels of each factor. The respondents involved the overall perception and behaviour of the commuters. The factors are supported by the literature review and 42 key informant interviews. These key informant interviewees were selected based upon their inclusivity with major sectors of the Thai economy and societal set up (see Table 2).

The demographic and socio-economic factors are presented together in order to provide the scenario of the systems among commuters where these factors result in

Table 2 Sector-wise respondents

Number	Career/ Professional	Sector	Gender	
			M	F
1	Student	Education	5	3
2	Employee	Administration	4	2
3	Government official	Policy makers	5	3
4	Entrepreneur	Business	5	4
5	Elderly	Retired	3	3
6	Other	Social	3	2

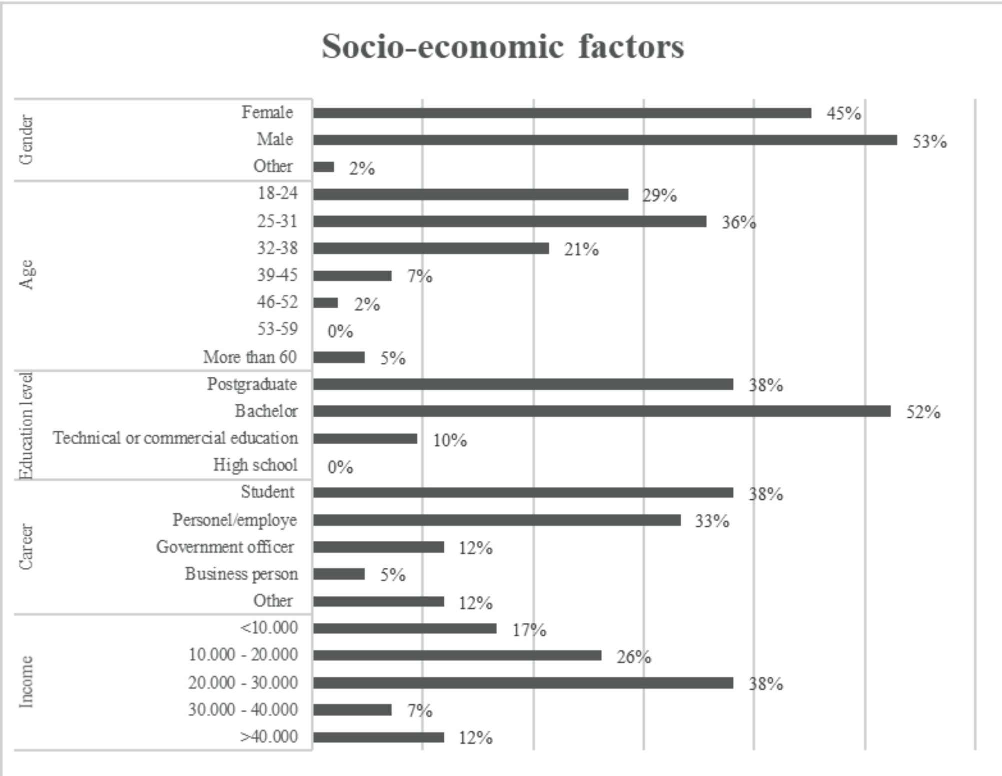

Figure 3 *Prolife of the Respondents*

the choices between the mode of transportation. These factors included gender, age, education levels, career and income levels of the respondents. The following chart provides for the detailed description of the profile of the respondents (Figure 3).

The gender in Thailand is divided into male, female and the third gender. The respondents belonged to all three types of gender. The male respondent was 53 %, female respondents were 45 % and others were 2 %. The factor of age was rearranged into range of years of age, in order to understand and analyse the different behaviours among different age groups. The respondents among the age group or 25 years of age to 31 years of age were highest with 36 %, followed by age group of 18 years of age to 24 years of age with 29 %, age group of 32 years of age to 45 years of age with 7 %, age group of more than 60 years of age with 5 %, age group of 46 years of age to 52 years of age with 2 %, however, there were no respondent between age group of 53 years of age to 59 years of age.

In terms of the education level, it was found that all the respondents were over the education level of high school. It was found that higher education is pertinent among all age groups of respondents. The education level was found to be highest with the bachelors at 52 % followed by post-graduates with 38 % and technical or commercial education with 10 %.

The economic profile of the respondents was found among their distinctive careers and income levels. The career factor was depicted in terms of professional employment of the respondents. It was found that students were 38 % of the total respondents, followed by employees with 33 % respondents, government officers were 12 % followed by business entrepreneurs at 5 %, other employment careers were found to be 12 % of the total respondents. Similarly, the income levels among

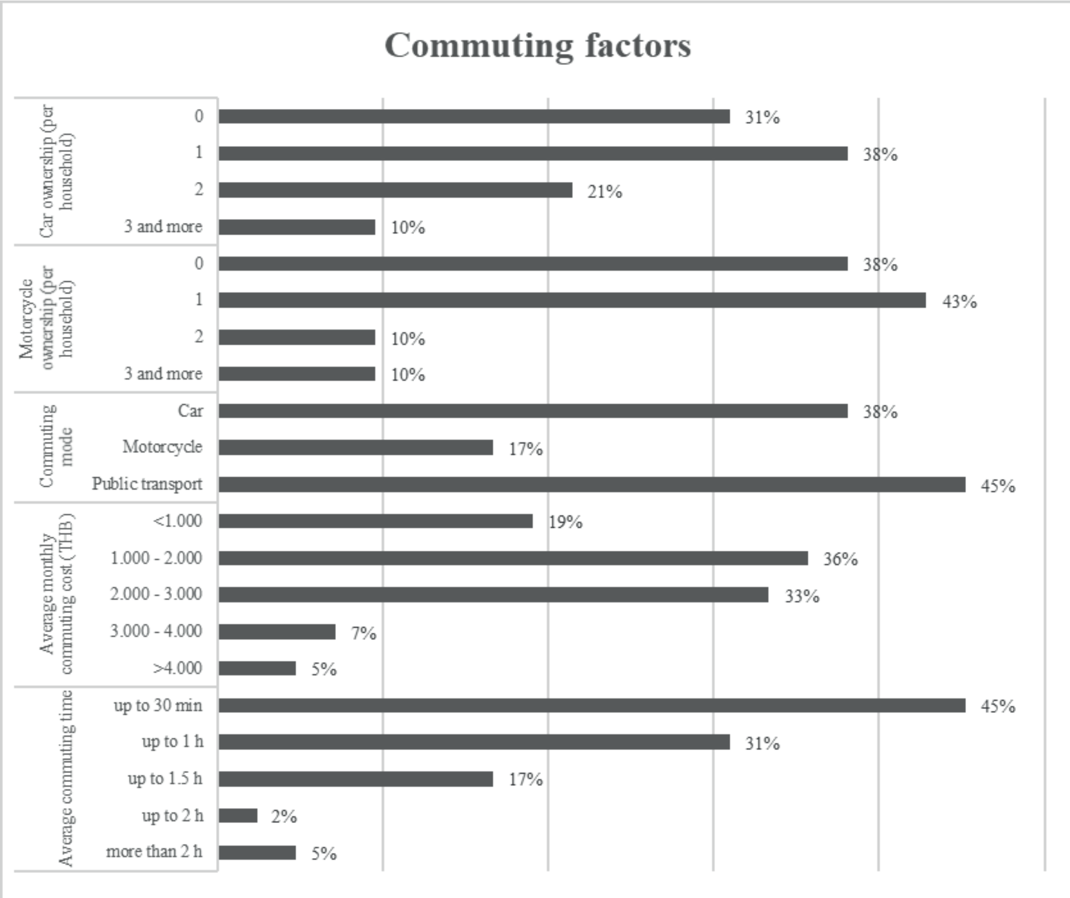

Figure 4 *Survey results among commuting factors*

the respondents were found to varied. The highest number of respondents were found in the range of 20,000 to 30,0000 Thai baht ($579.22-$868.84) earnings per month with 38 % respondents. The other composition of respondent in their respective income range involved in the range of 10,000 to 20,0000 Thai baht ($289.61-$579.22) earnings per month with 26 % respondents, less than 10,0000 Thai baht ($289.61) earnings per month with 17 % respondents, more than 40,0000 Thai baht ($1158.45) earnings per month with 12 % respondents and in the range of 30,000 to 40,0000 Thai baht ($868.84-$1158.45) earnings per month with 7 % respondents.

The survey results pertaining to the commuting factors depicted that each factor contributes towards the behavioural approach and decision-making process to choose the mode of transportation. The data presents the gap among the financial status of the respondents, which in turn provided for the overall perception, understanding and choices of the daily commuters (see Figure 3).

In terms of car ownership, it was found that there are 31 % of the respondents who do not own car. The remaining 69 % of the respondents were found to own one (38 %), two (21 %) and 3 (10 %) or more cars.

It was found that respondents who do not own a motorcycle were 38 % of the total respondents. One of the major reasons for not utilizing the motorcycle was the fact that respondents do not find it a secure mode of transportation [37]. The respondents owning one motorcycle were found to be 42 % of the total respondents, followed by respondents who owned two motorcycles with 10% and respondents with 3 or more than 3 motorcycles were 10 % of the total respondents.

The commuting mode choice depicted the findings towards the usage of public transportation as the first choice with 45 % of the total respondents. The second choice of daily commuting was found to be a car with 38 % and motorcycle with 17 % as the third choice of commuting (Figure 4). This was in line of the fact that Thailand has a sound network and infrastructure towards the public transportation. This effectiveness provides for the timely and ease of travel in the public transportation. However, public transportation such as sky train system are expensive but faster. In comparison, the public bus service is cheaper mode of transportation, however, it is more time consuming and uncomfortable, depending upon the air conditioning and/or seat quality [38].

The average monthly commuting costs in Thai Baht were divided into five ranges. The findings depicted that highest range of transportation expenses was 1,000 to 2,000 THB ($28.96-$57.92) with a total of 36 % respondents. The remaining range were inclusive of

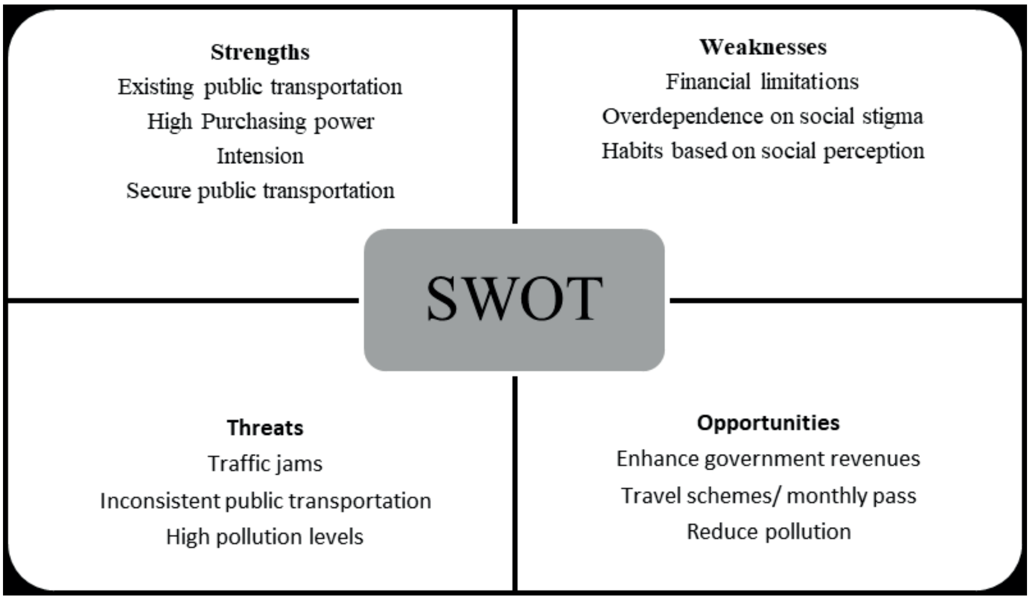

Figure 5 *SWOT analysis for selecting mode of the transportation in Thailand*

less than 1,000 THB (19 %), 2,000- 3,000 THB ($57.92-$86.88) (33 %), 3,000 to 4,000 THB ($86.88-$115.84) (7 %) and more than 4,000 THB ($115.84) (5 %). The findings depicted that costs of commuting are the major factor, which affects the behavioural approach towards choosing the mode of transportation [32].

The travel time is also an important factor affecting the commuter's choice as discussed and presented in the literature review. The average commuting time was divided into five range of time slots to understand the value of travel time among daily commuters. The findings depicted that the respondents do not prefer to travel for longer time periods, for instance that travel time with less than 30 minutes was preferred by 45 % of respondents. Similarly, travel time between 30 minutes to 1 hour was preferred by 31 % respondents, followed by respondents who preferred travel time between 1 hour to 1.5 hours with 17 %, remaining 7 % respondents preferred between 1.5 hours to 2 hours and more than 2 hours with 2 % and 5 %, respectively.

The important factors were found to be travel time and travel costs [39]. The significant relationship was found between the economic capacities of the travellers and their income level. The findings depicted that the travel time is a significant factor in overall behaviour and selection of the mode of transportation.

3 Discussion

The findings depicted the various interconnected and interdependent factors, which contributes towards the behavioural patterns and approaches of the daily commuters. The financial situation, socially accepted standard of living, habits pertaining to the age, gender and demographic factors, were found to be significant in choosing the mode of transportation between a car, motorcycle of public transportation. Bangkok is equipped with sky trains and underground rail network, which provides for faster mode of transportation. On the other hand, individual vehicle owner found it difficult to travel with consistent traffic jams and high pollution levels.

These findings support the previous literatures among the other countries and were found to be related with studies from European countries [40-42], developing economies such as Mexico [43-44] and Asian countries [45]. The comparative analysis between the other countries enhances the adequacy towards the adoption of accurate governmental initiatives to enhance the ease and comfort of the daily commuters in Thailand. It was observed that Thailand lacks the governmental planning to tap upon the daily commuters. Integrated combined efforts from the governmental factors, as well as demographic, social and economic factors, provided for the in-depth analysis from this research [46-47].

The following is the SWOT analysis performed to ascertain the situational analysis based on the content analysis of the selected factors (r Figure 5).

Strengths: One of the major strengths in Thailand is its developed public infrastructure with existing public transportation structure in almost every corner of the country. The connectivity is adequate due to the high reliance on the tourism and logistics sector of the economy. In terms of paying capacities of the general population, Thailand enjoys high purchasing power among its citizens. This provides for positive intension among general population in Thailand to spend adequately for transportation expenses. However, the income level of each individual results in different behavioural approach towards choosing the mode of transportation. Another strength of public and private transportation is the security [48]. The public transportation inclusive sky trains and underground train system are very secure with government policies for screening of each passenger.

Weaknesses: The major factor that affects the choice of the daily commuter, is the travel time and travel costs. There are several financial limitations in the public transportation system. The factor, which affects directly upon the choice of mode of transportation is the overdependence on social stigma. The social perceptions have an adverse impact on the habits of the daily commuters as they are drawn more towards the individually owned vehicles rather than using the public transportation.

Opportunities: The government interventions through adequate policies would positively impact the commuters and they would in turn enhance government revenues. Several schemes could be adopted by the public and private transportation. For instance, economical monthly pass for the students, daily commuters and frequent travellers. The government could utilize the public transportation mediums as a means of reducing and minimizing the environmental issues in the Bangkok Metropolitan Area. The reduced vehicles on the roads reduced carbon emissions, reduce probability of road accidents and enhance the overall traffic management system of the area.

Threats: Despite all the current policies, efforts and presence of the defined public transportation system, there is a gap between the adequate transportation behaviour, which results in mismanaged traffic jams and inconsistent public transportation. The recent high pollution levels are major concerns as the population in Bangkok Metropolitan Area had to wear facemasks even before the COVID-19 pandemic occurred. The overall perception of the private vehicle ownership is deeply imbedded among the general population in Thailand. This diminishes the attractiveness of the public transportation channels.

The SWOT analysis provided for the distinctive factors that would be essential to improve the sustainable travel choices among the Thai population [49]. The factors included the demographic, economic, social and policy level implications that were observed during the research. The interdependent factors are analysed with the interconnected factors for the overall analysis and recommendations.

4 Recommendations

The results of this study provided for following recommendations, which are divided into policymakers and daily commuters, government and individuals, respectively.

4.1 Recommendations for government

1. Revision of public transportation policies in terms of economic viability of recurring travel.
2. Empowerment or provision of beneficial travel schemes for daily commuters.
3. Improvement of the public transportation vehicles in order to attract the daily commuters.
4. Reduction of the travel time and travel costs through adequate travel route planning inclusive of suburban areas.
5. Enhanced affordability, accessibility and connectivity of public transportation to avoid social exclusion.

4.2 Recommendations for individuals

1. Awareness of environmental impacts rather than the societal status through being owner of a private vehicle.
2. Economic benefit analysis of all the public mode of transportation available.
3. Usage of monthly pass and student discount travel card in the public transportation systems in Bangkok Metropolitan Region.
4. Education regarding the environmental, economic and social impacts of individual mode of transportation.
5. Enhanced usage of carpooling.

5 Conclusion

The study finds out that the most significant factors under the perception of the daily commuters are travel time, travel cost and the comfort level of the individuals. Thailand has been dealing with transportation issues and corresponding environmental degradation in the recent times. Therefore, this research presents the analytical approach towards reduction of pollution and effective traffic management through analyzed travel behaviors of the daily commuters. The government must implement adequate policies and schemes towards enhancing the participation of daily commuters towards the public transport. This needs to be amalgamated along with reduced travel time to cover maximum travel distance at the most economical price and highest comfort level. Such an adequate policy and effective implementations would benefit daily commuters as well the development of the government infrastructures and growth of the Thai economy. This paper contributes to the academic literature of travel studies, through a consideration of the developing, Southeast Asian country's environmental and cultural aspect.

6 Way ahead

The research paves the way for micro level quantitative research and leads up further research into the environmental impacts of planned travel behaviours and overall implications leading to the high pollution in the Bangkok Metropolitan area. Likewise, the study could be further analysed for different demographic, social and economic set up among the developing countries.

References

[1] KUHNIMHOF, T., BUEHLER, R., DARGAY, J. A new generation: travel trends for young Germans and Britons. *Transportation Research Record* [online]. 2011, **2230**(1), p. 58-67. ISSN 0361-1981, eISSN 2169-4052. Available from: https://doi.org/10.3141/2230-07

[2] MCDONALD, N. C. Are millennials really the "go-nowhere" generation? *Journal of the American Planning Association* [online]. 2015, **81**(2), p. 90-103. ISSN 0194-4363, eISSN 1939-0130. Available from: https://doi.org/10.1080/01944363.2015.1057196

[3] NEWBOLD, K. B., SCOTT, D. M. Insights into public transit use by Millennials: the Canadian experience. *Travel Behaviour and Society* [online]. 2018, **11**, p. 62-68. ISSN 2214-367X. Available from: https://doi.org/10.1016/j.tbs.2017.12.009

[4] OAKIL, A. T. M., MANTING, D., NIJLAND, H. Determinants of car ownership among young households in the Netherlands: the role of urbanisation and demographic and economic characteristics. *Journal of Transport Geography* [online]. 2016, **51**, p. 229-235. ISSN 0966-6923. Available from: https://doi.org/10.1016/j.jtrangeo.2016.01.010

[5] GOODWIN, P., VAN DENDER, K. "Peak car" - themes and issues. *Transport Reviews* [online]. 2013, **33**(3), p. 243-254. ISSN 0144-1647, eISSN 1464-5327. Available from: https://doi.org/10.1080/01441647.2013.804133

[6] BASTIAN, A., BORJESSON, M., ELIASSON, J. Explaining "peak car" with economic variables. *Transportation Research Part A: Policy and Practice* [online]. 2016, **88**, p. 236-250. ISSN 0965-8564. Available from: https://doi.org/10.1016/j.tra.2016.04.005

[7] DELBOSC, A., CURRIE, G. Causes of youth licensing decline: a synthesis of evidence. *Transport Reviews* [online]. 2013, 33(3), p. 271-290. ISSN 0144-1647, eISSN 1464-5327. Available from: https://doi.org/10.1080/01441647.2013.801929

[8] LYONS, G. Transport's digital age transition. *Journal of Transport and Land Use* [online]. 2015, **8**(2), p. 1-19. ISSN 1938-7849. Available from: https://doi.org/10.5198/jtlu.2014.751

[9] KUHNIMHOF, T., ARMOOGUM, J., BUEHLER, R., DARGAY, J., DENSTADLI, J. M., YAMAMOTO, T. Men shape a downward trend in car use among young adults - evidence from six industrialized countries. *Transport Reviews* [online]. 2012, **32**(6), p. 761-779. ISSN 0144-1647, eISSN 1464-5327. Available from: https://doi.org/10.1080/01441647.2012.736426

[10] KUHNIMHOF, T., BUEHLER, R., WIRTZ, M., KALINOWSKA, D. Travel trends among young adults in Germany: increasing multimodality and declining car use for men. *Journal of Transport Geography* [online]. 2012, **24**, p. 443-450. ISSN 0966-6923. Available from: https://doi.org/10.1016/j.jtrangeo.2012.04.018

[11] SIMONS, D., CLARYS, P., DE BOURDEAUDHUIJ, I., DE GEUS, B., VANDELANOTTE, C., DEFORCHE, B. Why do young adults choose different transport modes? A focus group study. *Transport Policy* [online]. 2014, **36**, p. 151-159. ISSN 0967-070X. Available from: https://doi.org/10.1016/j.tranpol.2014.08.009

[12] STEAD, D., POJANI, D. The urban transport crisis in emerging economies: a comparative overview. In: *The urban transport crisis in emerging economies* [online]. POJANI, D., STEAD, D. (eds.). The Urban Book Series. Cham: Springer, 2017. ISBN 978-3-319-82924-1, eISBN 978-3-319-43851-1. Available from: https://doi.org/10.1007/978-3-319-43851-1_14

[13] PEUNGNUMSAI, A., MIYAZAKI, H., WITAYANGKURN, A., KIM, S. M. A grid-based spatial analysis for detecting supply-demand gaps of public transports: a case study of the Bangkok Metropolitan Region. *Sustainability* [online]. 2020, **12**(24), 10382. eISSN 2071-1050. Available from: https://doi.org/10.3390/su122410382

[14] PRASERTSUBPAKIJ, D., NITIVATTANANON, V. Evaluating accessibility to Bangkok Metro Systems using multi-dimensional criteria across user groups. *IATSS Research* [online]. 2012, 36(1), p. 56-65. ISSN 0386-1112. Available from: https://doi.org/10.1016/j.iatssr.2012.02.003

[15] VAN, H. T., CHOOCHARUKUL, K., FUJII, S. The effect of attitudes toward cars and public transportation on behavioral intention in commuting mode choice - a comparison across six Asian countries. *Transportation Research Part A: Policy and Practice* [online]. 2014, **69**, p. 36-44. ISSN 0965-8564. Available from: https://doi.org/10.1016/j.tra.2014.08.008

[16] CHEN, C. F., LAI, W. T. The effects of rational and habitual factors on mode choice behaviors in a motorcycle-dependent region: evidence from Taiwan. *Transport Policy* [online]. 2011, **18**(5), p. 711-718. ISSN 0967-070X. Available from: https://doi.org/10.1016/j.tranpol.2011.01.006

[17] BURNETT, K. P., THRIFT, N. J. New approaches to understanding traveller behaviour. In: *Behavioural Travel Modelling* [online]. London: Routledge, 2021. eISBN 9781003156055, p. 116-134. Available from: https://doi.org/10.4324/9781003156055

[18] Country classification - United Nations [online] [accessed 2021-20-06]. Available from: https://www.un.org/en/development/desa/policy/wesp/wesp_current/2012country_class.pdf

[19] Department of Provincial Administration, Thailand Population: Official Statistics Registration Systems [online] [accessed 2021-21-06]. Available from: https://stat.bora.dopa.go.th/new_stat/webPage/statByYear.php

[20] Department of Land Transportation [online] [accessed 2021-21-06]. Available from: https://web.dlt.go.th/statistics/

[21] Annual Report 2019 - Mass Rapid Transit Authority of Thailand [online] [accessed 2021-22-06]. Available from: https://www.mrta.co.th/media/780084/mrta-annual-report-2019.pdf

[22] KAMPF, R., GASPARIK, J., KUDLACKOVA, N. Application of different forms of transport in relation to the process of transport user value creation. *Periodica Polytechnica Transportation Engineering* [online]. 2012, **40**(2), p. 71-75. ISSN 0303-7800, eISSN 1587-3811. Available from: https://doi.org/10.3311/pp.tr.2012-2.05

[23] BASARIC, V., VUJICIC, A., SIMIC, J. M., BOGDANOVIC, V., SAULIC, N. Gender and age differences in the travel behaviour - a Novi Sad case study. *Transportation Research Procedia* [online]. 2016, **14**, p. 4324-4333. ISSN 2352-1465. Available from: https://doi.org/10.1016/j.trpro.2016.05.354

[24] ELIAS, W., BENJAMIN, J., SHIFTAN, Y. Gender differences in activity and travel behavior in the Arab world. *Transport Policy* [online]. 2015, **44**, p. 19-27. ISSN 0967-070X. Available from: https://doi.org/10.1016/j.tranpol.2015.07.001

[25] RATANAWARAHA, A., CHALERMPONG, S. How the poor commute in Bangkok, Thailand. *Transportation Research Record* [online]. 2016, **2568**(1), p. 83-89. ISSN 0361-1981, eISSN 2169-4052. Available from: https://doi.org/10.3141/2568-13

[26] JAMAL, S., NEWBOLD, K. B. Factors associated with travel behavior of millennials and older adults: a scoping review. *Sustainability* [online]. 2020, **12**(19), 8236. eISSN 2071-1050. Available from: https://doi.org/10.3390/su12198236

[27] POLZIN, S. E., CHU, X., GODFREY, J. The impact of millennials' travel behavior on future personal vehicle travel. *Energy Strategy Reviews* [online]. 2014, **5**, p. 59-65. ISSN 2211-467X. Available from: https://doi.org/10.1016/j.esr.2014.10.003

[28] BEIGE, S., AXHAUSEN, K. W. The dynamics of commuting over the life course: Swiss experiences. *Transportation Research Part A: Policy and Practice* [online]. 2017, **104**, p. 179-194. ISSN 0965-8564. Available from: https://doi.org/10.1016/j.tra.2016.04.005

[29] HEINEN, E. Identity and travel behaviour: a cross-sectional study on commute mode choice and intention to change. *Transportation Research Part F: Traffic Psychology and Behaviour* [online]. 2016, **43**, p. 238-253. ISSN 1369-8478. Available from: https://doi.org/10.1016/j.trf.2016.10.016

[30] CHEN, C. F., CHAO, W. H. Habitual or reasoned? Using the theory of planned behavior, technology acceptance model and habit to examine switching intentions toward public transit. *Transportation research part F: Traffic Psychology and Behaviour* [online]. 2011, **14**(2), p. 128-137. ISSN 1369-8478. Available from: https://doi.org/10.1016/j.trf.2010.11.006

[31] ATHIRA, I. C., MUNEERA, C. P., KRISHNAMURTHY, K., ANJANEYULU, M. V. L. R. Estimation of value of travel time for work trips. *Transportation Research Procedia* [online]. 2016, **17**, p. 116-123. ISSN 2352-1465. Available from: https://doi.org/10.1016/j.trpro.2016.11.067

[32] WITCHAYAPHONG, P., PRAVINVONGVUTH, S., KANITPONG, K., SANO, K., HORPIBULSUK, S. Influential factors affecting travellers' mode choice behavior on mass transit in Bangkok, Thailand. *Sustainability* [online]. 2020, **12**(22), 9522. eISSN 2071-1050. Available from: https://doi.org/10.3390/su12229522

[33] EL-GENEIDY, A., LEVINSON, D., DIAB, E., BOISJOLY, G., VERBICH, D., LOONG, C. The cost of equity: Assessing transit accessibility and social disparity using total travel cost. *Transportation Research Part A: Policy and Practice* [online]. 2016, **91**, p. 302-316. ISSN 0965-8564. Available from: https://doi.org/10.1016/j.tra.2016.07.003

[34] MARSHALL, B., CARDON, P., PODDAR, A., FONTENOT, R. Does sample size matter in qualitative research?: a review of qualitative interviews in IS research. *Journal of Computer Information Systems* [online]. 2013, **54**(1), p. 11-22. ISSN 0887-4417, eISSN 2380-2057. Available from: https://doi.org/10.1080/08874417.2013.11645667

[35] NEUBURGER, L., EGGER, R. Travel risk perception and travel behaviour during the COVID-19 pandemic 2020: a case study of the DACH region. *Current Issues in Tourism* [online]. 2021, **24**(7), p. 1003-1016. ISSN 1368-350, eISSN 1747-7603. Available from: https://doi.org/10.1080/13683500.2020.1803807

[36] TROTTER II, R. T. Qualitative research sample design and sample size: resolving and unresolved issues and inferential imperatives. *Preventive Medicine* [online]. 2012, **55**(5), p. 398-400. ISSN 0091-7435. Available from: https://doi.org/10.1016/j.ypmed.2012.07.003

[37] PONGPRASERT, P., KUBOTA, H. Switching from motorcycle taxi to walking: a case study of transit station access in Bangkok, Thailand. *IATSS Research* [online]. 2017, **41**(4), p. 182-190. ISSN 0386-1112. Available from: https://doi.org/10.1016/j.iatssr.2017.03.003

[38] POMLAKTONG, N., JONGWILAIWAN, R., THEERAWATTANAKUL, P., PHOLPANICH, R. Road transport in Thailand. In: *Priorities and pathways in services reform: Part II - Political economy studies*. World Scientific, 2014. ISBN 978-981-4504-68-3, p. 227-243. Available from: https://doi.org/10.1142/9789814504690_0009

[39] METZ, D. Time constraints and travel behaviour. *Transportation Planning and Technology* [online]. 2021, **44**(1), p. 16-29. ISSN 0308-1060, eISSN 1029-0354. Available from: https://doi.org/10.1080/03081060.2020.1851445

[40] IVANOVA, M., IVANOV, I. K., IVANOV, S. Travel behaviour after the pandemic: the case of Bulgaria. *Anatolia* [online]. 2021, **32**(1), p. 1-11. ISSN 1303-2917, eISSN 2156-6909. Available from: https://doi.org/10.1080/13032917.2020.1818267

[41] MOLLOY, J., SCHATZMANN, T., SCHOEMAN, B., TCHERVENKOV, C., HINTERMANN, B., AXHAUSEN, K. W. Observed impacts of the Covid-19 first wave on travel behaviour in Switzerland based on a large GPS panel. *Transport Policy* [online]. 2021, **104**, p. 43-51. ISSN 0967-070X. Available from: https://doi.org/10.1016/j.tranpol.2021.01.009

[42] NOSAL HOY, K., PULAWSKA-OBIEDOWSKA, S. The travel behaviour of Polish women and adaptation of transport systems to their needs. *Sustainability* [online]. 2021, **13**(5), 2693. eISSN 2071-1050. Available from: https://doi.org/10.3390/su13052693

[43] CALONGE-REILLO, F. Travel behaviour in contexts of security crisis. Explaining daily use of car in non-central districts in Guadalajara metropolitan area, Mexico. *Travel Behaviour and Society* [online]. 2021, **24**, p. 1-9. ISSN 2214-367X. Available from: https://doi.org/10.1016/j.tbs.2021.01.006

[44] IRAKOZE, B., ALI, A. Enhancing the mobility services by the implementation of real-time passenger information system in the capital city of Kigali, Rwanda. Master´s thesis. Gothenburg, Sweden: Chalmers University of Technology, 2021.

[45] NAN, Z., JIA, W., WANG, P., DUNG, CH.-H., ZHAO, P., LEUNG, K., SU, B., CHENG, R., LI, Y. Changes in local travel behaviour before and during the COVID-19 pandemic in Hong Kong. *Cities* [online]. 2021, **112**, 103139. ISSN 0264-2751. Available from: https://doi.org/10.1016/j.cities.2021.103139

[46] KONTOGEORGOPOULOS, N. Community-based ecotourism in Phuket and Ao Phangnga, Thailand: partial victories and bittersweet remedies. *Journal of Sustainable Tourism* [online]. 2005, **13**(1), p. 4-23. ISSN 0966-958, eISSN 1747-7646. Available from: https://doi.org/10.1080/17501220508668470

[47] SORNSARUHT, P., DEEBHIJARN, S. A social impact assessment using a SWOT-based framework to determine the factors for free train transportation in Thailand. *Humanities, Arts and Social Sciences Studies (former name Silpakorn University Journal of Social Sciences, Humanities and Arts)* [online]. 2017, **17**(1), p. 41-68. eISSN 2630-0079. Available from: https://doi.org/10.14456/sujsha.2017.2

[48] SIPUS, D., ABRAMOVIC, B. The possibility of using public transport in rural area. *Procedia Engineering* [online]. 2017, **192**, p. 788-793. ISSN 1877-7058. Available from: https://doi.org/10.1016/j.proeng.2017.06.136

[49] MIKUSOVA, N., FEDORKO, G., MOLNAR, V., HLATKA, M., KAMPF, R., SIRKOVA, V. Possibility of a solution of the sustainability of transport and mobility with the application of discrete computer simulation - a case study. *Sustainability* [online]. 2021, **13**(17), 9816. eISSN 2071-1050. Available from: https://doi.org/10.3390/su13179816

EMPIRICAL MEASUREMENT OF ELECTROMOBILITY EFFICIENCY IN THE ENVIRONMENT OF THE EUROPEAN UNION

Jozef Kubás [1,*], Michal Ballay [1], Jozef Ristvej [2], Katarína Zábovská [1]

[1]University Science Park, University of Zilina, Zilina, Slovakia
[2]Department of Crisis Management, Faculty of Security Engineering, University of Zilina, Zilina, Slovakia

*E-mail of corresponding author: jozef.kubas@uniza.sk

Resume
The article presents an assessment of the use of alternative fuels in Europe with an emphasis on electromobility. In this regard, the impact of political intentions, ambitions and goals are analyzed, in relation to the current situation. Based on the results of empirical measurements, the efficiency of implementation of a European publicly accessible infrastructure for charging electric vehicles was determined. Using the method, the efficiency of electromobility in all the countries of the European Union was investigated. The resulting parameters are comparable in the context of the objectives of the Green Deal and the expected impact of electric cars. Using the results of the DEA model, one can point out the efficiency of countries and suggest ways to improve it.

Article info
Received 20 October 2021
Accepted 21 January 2022
Online 30 May 2022

Keywords:
electromobility
efficiency
DEA model
charging infrastructure
European Union

Available online: https://doi.org/10.26552/com.C.2022.3.A123-A132

ISSN 1335-4205 (print version)
ISSN 2585-7878 (online version)

1 Introduction

Transportation in the 19th century was a century of steam, the 20th century was a century of oil and it is more than likely that the 21st century will be a century of alternative propulsion, including electric vehicles. Electromobility is growing every year and has a significant share. However, compared to internal combustion engines, the current market share of electric cars is low. Within electric cars, one can encounter several problems, out of which the main one is relatively low energy efficiency. These vehicles are not a full-fledged alternative to internal combustion vehicles. The age of technology is upon us and we should be able to find a solution for any possible disadvantage. However, with each new technology come new challenges and, in general, electromobility is the future.

Many expert studies estimate the number and overall share of the electric car market in the future. In these cases, one encounters different information, depending on the area in which these studies come from. Some are about the breakdown of their production costs and assumptions about how these components will evolve over time, others are directly related to the environment. At the same time, there are various strategies at national or international level that promote alternative fuels in relation to the environment. In this article, authors point out the support mechanisms in relation to political ambitions and goals. Is assessed the planned (future) state with the current state in the field of electromobility. The important fact is that electromobility cannot be without the necessary infrastructure, which means that it does not impose the new demands on the road infrastructure, but it does require the construction of a charging network.

2 Ambitions and targets of the European Union in relation to electric vehicles

Popularity of alternative fuel vehicles has been rising in recent years based on effort on maximizing fuel efficiency and minimizing negative environmental impacts. A transport system is gradually being set up, which aims at the efficient use of resources and eliminating oil dependence. In this article, in order to deal with alternative fuels, there must be an appropriate definition, which clearly identifies what these terms represent. Directive 2014/94 / EU of the European Parliament and of the Council of 22 October 2014 defines the concept of alternative fuels. “Alternative fuels” are fuels or energy sources, which serve at least

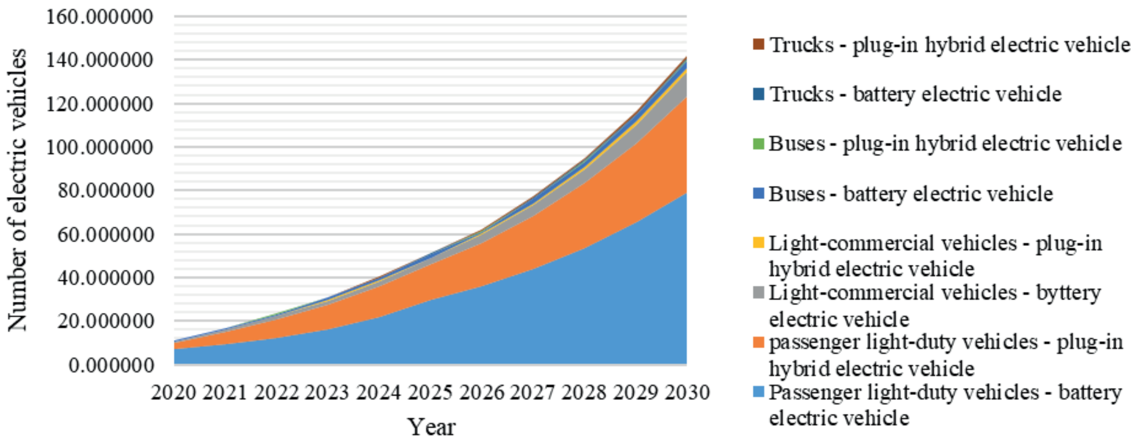

Figure 1 *Global electric vehicles stock by mode in the Stated Policies Scenario, 2020-2030 [6]*

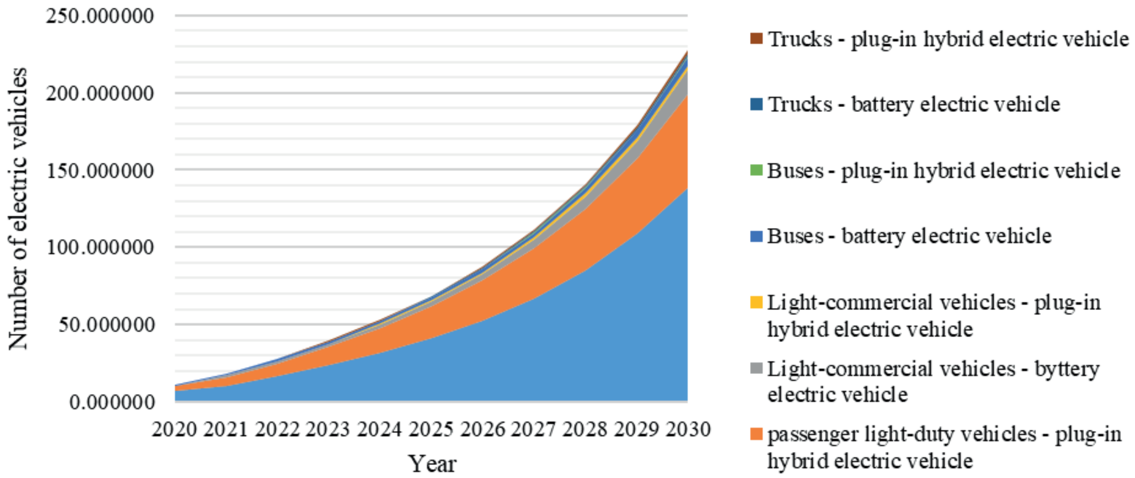

Figure 2 *Global electric vehicles stock by mode in the Sustainable Development Scenario, 2020-2030 [7]*

in part to replace fossil oil sources in the supply of energy to transport and which have the potential to contribute to its decarbonisation and to improve the environmental performance of the transport sector. Defined alternative fuels include the following: natural gas, including biomethane in gaseous form (compressed natural gas) and liquefied gas (liquefied natural gas), biofuels, electricity, liquefied petroleum gas, hydrogen and synthetic/paraffin fuels [1-2].

Road transport is an important part of all social processes. Nowadays, it is significantly affected by technological advances and societal change. Besides that, due to the growing demand for mobility, there is an overload. Road infrastructure in some cases is not able to provide sufficient traffic flow throughput and not fast enough to increase traffic. Additional expansion of road infrastructure is not possible, especially in urban areas and the construction of new infrastructure is very demanding. In this respect, it is therefore necessary to look for new, progressive tools, which, when applied, will make the transport system safer and more efficient [3].

At the same time, it must be emphasized that there is a constant increase in means of transport. The current trend in road transport is electric mobility, which also reflects existing policy frameworks and intentions, based on the developed strategies, whose main goal is to meet the global climate goals and achieve significant reductions in air pollutant emissions. By 2070, net-zero emissions should be achieved. These ambitions and goals contribute to a significant increase in the number of electric vehicles. This is largely due to growing enlargement in China. Worldwide, the number of electric vehicles for all the vehicle categories in the world will increase from 11 million in the current year to 145 million by 2030. The average annual growth is almost 30% (Figure 1).

The main goal stated in the Sustainable Development Scenario, 2020-2030, is reduction of carbon intensity of electricity generation and utilization of public transport. This represents a significant increase in the number of electric cars, which should reach the level of 230 million vehicles (Figure 2) [4-5].

All electric vehicles related targets and ambitions

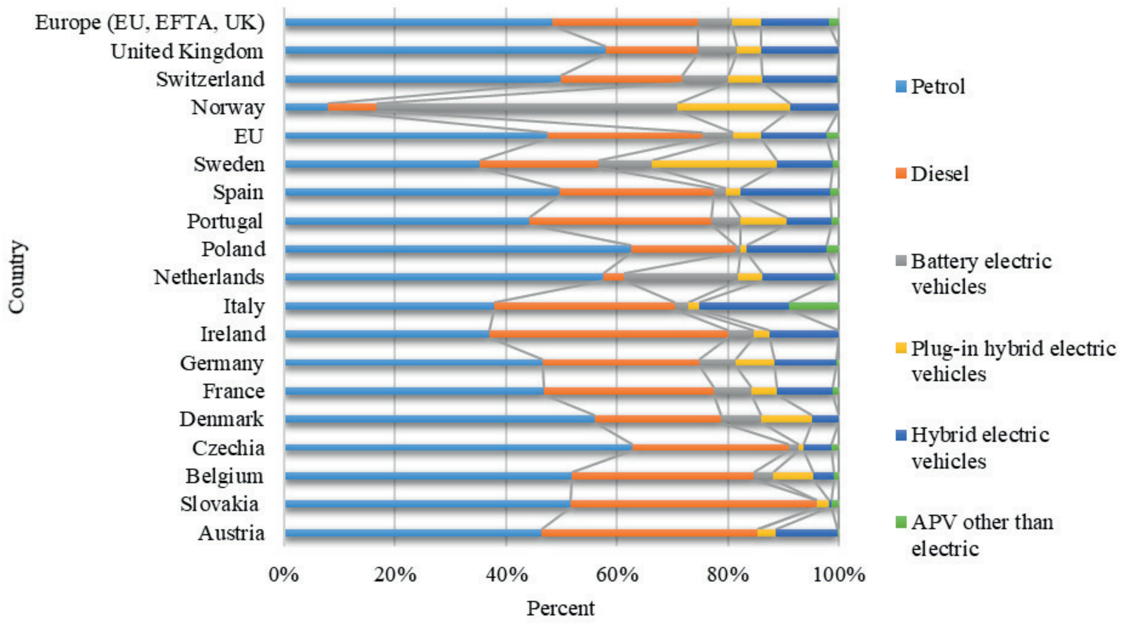

Figure 3 *Passenger car sales in selected European countries in 2020, by fuel type [8]*

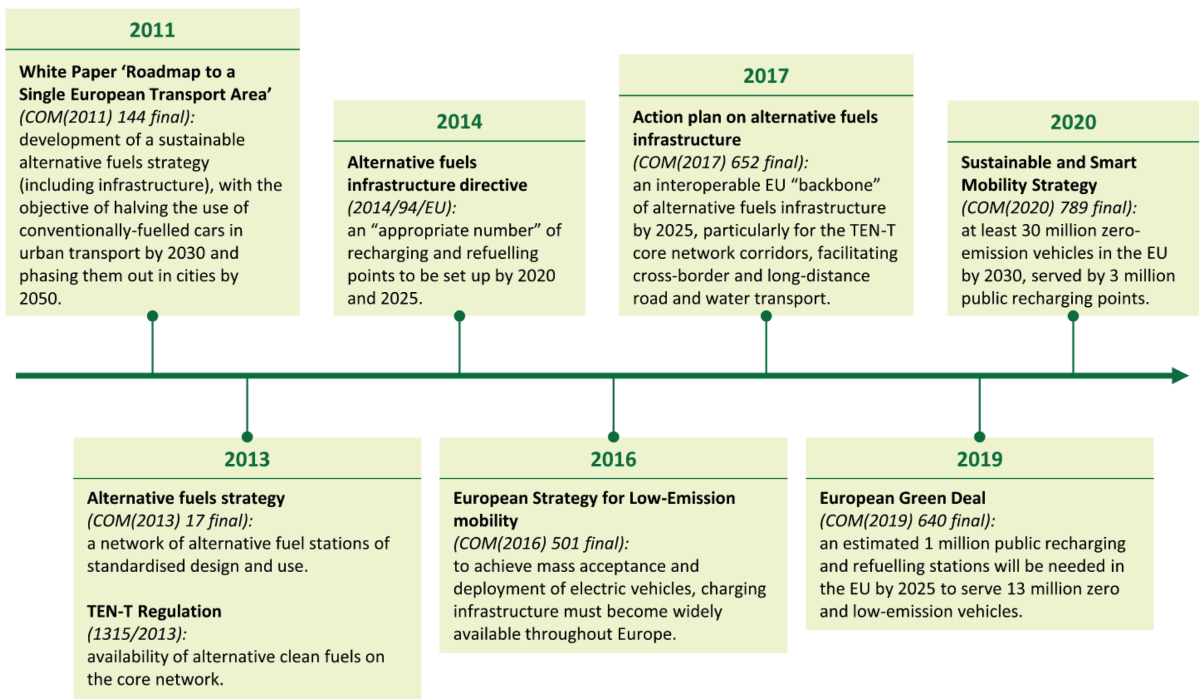

Figure 4 *EU policy documents on alternative fuel infrastructure [9]*

are met, even if the current policy measures are not deemed sufficient to stimulate such adoption rates. Number of electric vehicles in Europe is still small and largely dependent on support policies. Most electric road vehicles are concentrated in a few northern and western Member States, although the southern and eastern ones have recently recorded the biggest sales growth.

Each Member State is responsible for developing and implementing its own alternative fuels policy within the framework set by EU legislation. Countries that offer generous incentives and have developed a good charging infrastructure have a higher share of electric road vehicles on transport routes.

There are measures at European Union level that support:

- assistance in the development and standardization of charging infrastructure,

- the use of renewable electricity and intelligent charging
- the battery research [9].

In relation to alternative fuels, several strategies have been developed at European Union level since 2011 and directives issued, which are gradually leading to the ambitious goal of becoming a climate-neutral continent. **The Green Deal**, which is the latest in a series of EU policy documents on development of the alternative fuels infrastructure, should also contribute to this goal (Figure 3). Alternative fuels are very important in this regard, as transport in Europe produces almost a quarter of greenhouse gas emissions. At the same time, we are facing a major challenge in the field of alternative fuels infrastructure. In this regard, it is important to adopt the common standards to ensure interoperability, coordinate and support Member States' deployment of electrical charging infrastructure [9-11]. Figure 4 shows the timeline of EU policy documents on alternative fuel infrastructure.

The 2014 directive on alternative fuels infrastructure is the key policy tool within the overall EU strategy to develop publicly accessible electrical charging infrastructure. It aims to overcome a market failure best described as the "'chicken-and-egg" problem: on one hand, vehicle uptake will be constrained until charging infrastructure is available, while on the other hand, investments in infrastructure require more certainty of vehicle uptake levels [9, 11].

3 Electric vehicles charging infrastructure

Electric vehicles require access to charging points, which are not the sole choice of their owners. For this reason, electric car infrastructure plays a very important role, especially with regard to urbanism, energy companies and technological change. The number of charging stations is affected by the location, distribution and types of electric vehicles. Charging infrastructure for electric vehicles can be considered from the three perspectives:

- Home charging - is the most readily available, with charging options technically at level 1 (portable charger) and level 2 (more powerful unit).
- Workplaces - the availability of charging stations depends on regional or national policies.
- Publicly available chargers - needed where charging from home and in the workplace is not available or not enough to meet needs (for example, when traveling long distances).

The number of charging stations is increasing every year. The largest increase and share was recorded by private charging points (domestic charging). Slow charging is prevalent worldwide and this is mainly due to the fact that fast charging stations make up the smallest share. On average, the expansion of charging stations (infrastructure) increases by 30% every year. The distribution between the fast and slow charging points is determined by various factors. These are interconnected and dynamic, such as charging behavior, population density, battery capacity, housing and local government policy. Sustainable and Smart Mobility Strategy identifies infrastructure expansion forecast for electric vehicles (Figure 5).

Sustainable and Smart Mobility Strategy identified the need to expand charging stations for 3 million public charging points by 2030. Uncertainty prevails with this prediction, to reach the set targets. If the deployment of infrastructure continues to follow the 2014-2020

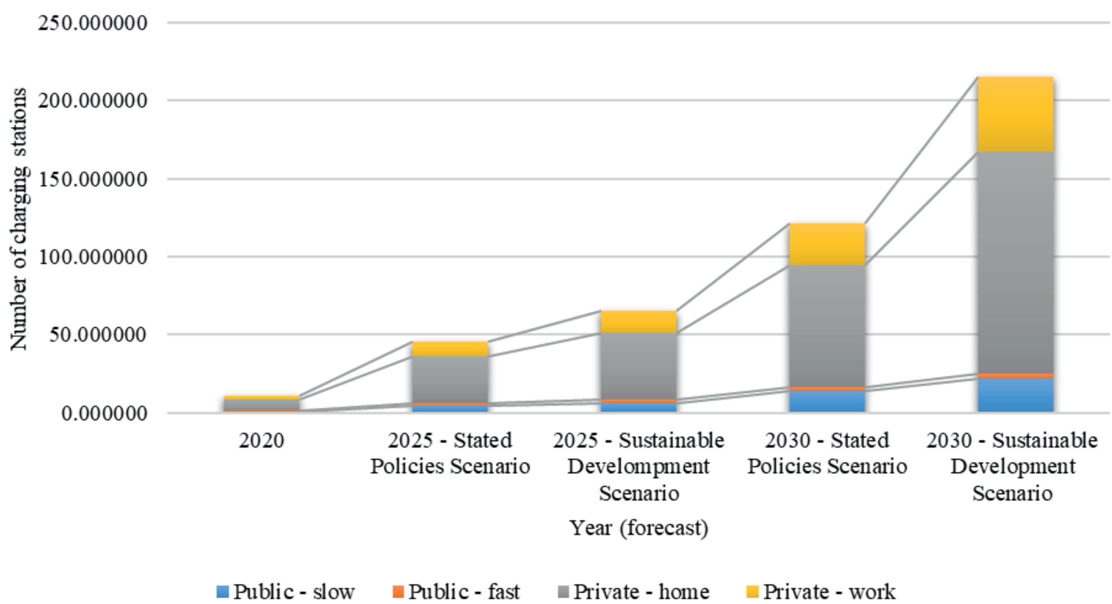

Figure 5 *Number of electric LDV chargers by scenario, 2020-2030 [13]*

trend, there will be a significant risk that the target of 1 million public charging points by 2025 will be unfulfilled [4, 11-12].

4 Evaluation of the efficiency of electromobility in EU countries with regard to charging infrastructure

One major problem that slows down the electric car is the impression that they cannot travel the required distance without the need to recharge. The cause may be a lack of charging infrastructure or insufficient awareness of its existence. Although the charging infrastructure for electric cars is increasing at different speeds across the EU, as is the use of electric vehicles, in some Member States there is still a lack of differences between countries. The very loss of supplied energy is also a problem with electromobility. Despite the documentation of the cars, which states the technical parameters such as power and range, irregularities may occur. In some cases, the incomplete use of energy does not allow the necessary range and it is necessary to recharge the car more often [14]. That is why it is necessary to examine how the infrastructure is available in individual states. These states need to be compared to each other and the efficiency of electricity infrastructure examined with regard to possibilities of individual states. Various methods can be used to measure efficiency. The popular and frequently used methods are as follows:

- DEA (Data Envelopment Analysis) method - is a non-parametric-deterministic method of estimating efficiency, which has recently become more and more popular in the banking environment. This approach was proposed by Farrell [15] who seeks to find better ways to assess productivity. Thanks to Charnes, Cooper and Rhodes [16], Farrell's concept was later refined into a practical research tool used in various areas of economic research.
- SFA (Stochastic Frontier Analysis) method - This method is one of the best known parametric-stochastic methods used to estimate the efficiency of financial institutions. It was independently developed by several authors [17-18] and subsequently introduced into the banking environment in 1990. The basic approach is a direct estimate of the production function using the profit and cost function. Recently, the multiproduction logarithmic transformation of the costs/profit function has been widely used. Cost and profit efficiency are important economic goals - minimizing costs and maximizing profits. Some authors have also used this method to measure energy efficiency [19].
- Ordinary Least Squares (OLS) method - The main task of this method is that the sum of the error squares they try to minimize is considered as a criterion for the accuracy of the problem. Numerical and analytical approaches can be used using the method. In particular, the numerical least squares implementation method involves the largest possible dimension of an unknown random variable. In addition, the more calculations, the more the solution itself. Additional sets of predicted solutions are obtained from the set of calculations (initial data), from which the best were selected. If the solution file is parameterized, the least squares method decreases to achieve the optimal parameter value [20].

According to several authors, the DEA method is the most suitable of all the methods for measuring efficiency [21-22]. Iliyasu et al. summarized the possibilities of available software suitable for use in the academic environment [23]. The DEA method chosen by authors in this research is one of the nonparametric methods and it represents a model of linear programming. The DEA method used to analyse the relative efficiency of a production unit in a selected group of production units that use identical aggregated inputs and produce aggregated outputs. Arranged units (DMUs- Decision-making unit's) maximize their efficiency for each DMU_i, i ę ⊂ {1 , ... , n}. The optimized unit is called DMU_o, o ⊂{1 ,. . . , n}. The vector of inputs is recorded, as well as of the organizational unit as $x_i = (x_{i1}, \dots, x_{im})$ T and the vector of outputs $y_i = (y_{i1}, \dots, y_{is})$ T. Every single input and output has some evaluation, i.e. values that are denoted by vectors $u = (u_1, \dots, u_m)$ T for inputs and $v = (v_1, \dots, v_s)$ T for outputs. In this case, u_i (i = 1, ... , m) is the value of the i-th input and v_k (k = 1, ... , s) is a certain value of the k-th output [24-26]. For DMU_o, the efficiency measure E_o (u, v) is determined based on the following equation:

$$E_0(u,v) = \frac{\sum_{k=1}^{s} v_k y_{ok}}{\sum_{j=1}^{m} u_k x_{oj}} = \frac{v^T y_o}{u^T x_0} \quad (1)$$

In order for the DMU to be effective, there is the so-called optimal solution in the form (u *, v *) in the problem, where E * (u *, v *) = v * T y_o = 1 au *> 0, v *> 0. If a different case occurred, the DMU would be inefficient. The CRR model was chosen for the work, in which it is necessary to enter individual inputs (CCR-I) and individual outputs (CRR-O). Some authors also point out the suitability of using this model [27-28]. Authors in this research have focused on the CCR output model, as it is easier to change the outputs in the parameters that were chosen.

When selecting indicators used to measure efficiency, the focus was primarily on inputs and outputs that need to be determined before entering into the calculation method. This method was used to determine the efficiency of the electrical infrastructure with respect to charging stations. The principle of this method is that the calculation will show which of the compared countries works most effectively (i.e. which would achieve 100% efficiency) and based on the results, other countries were then compared to it. Under the name of DMU are the organizational units, i.e. states whose goal is to maximize their efficiency. For each organizational unit (DMU), it is important to determine the inputs and outputs, which should neither be zero nor negative.

In the case of the DEA analysis, it is important to determine the input (CRR-I) and output (CRR-O) data. Gross domestic product (GDP) per capita in Purchasing Power Standards (PPS) was chosen as the input data. It is the spending of funds needed to create improvement issues with regard to development and security in transport [29]. Among the output data, the Recharging points for 100,000 people and High-Power Public Recharges for 100 km Highway were chosen. Those data for the European Union states (DMU) are shown in Table 1; all the data are from year 2020.

The data from Table 1 are then entered into the DEA model with a focus on the CCR output model. Therefore, it was necessary to correctly determine the inputs and outputs. The correct designation made it possible to evaluate the efficiency of states with regard to electromobility and charging infrastructure. The results are shows in Figure 6. The number 1 means 100% efficiency. The DMUs are fully (100%) effective based on the available data for other units if and only if their performance does not indicate that some of the inputs or outputs of a given DMU could be improved without compromising the level of other inputs or outputs [32].

Figure 6 shows the efficiency of the European Union countries. Efficiency was evaluating based on selected inputs and outputs. Of the countries compared, only the two countries were 100% efficient, namely the Netherlands and Estonia. Greece and subsequently Malta had the least efficiency in terms of charging infrastructure. If the focus is on efficiency of Slovakia, it can be seen that it was in 5th place with an efficiency rate of 52%. The efficiency of all compared countries is shown in Table 2.

Table 2 shows the efficiency of all the European countries, compared to each other. The advantage of

***Table 1** Input and output data to the DEA method [30-31]*

State - DMU	(CCR-I) GDP per capita in PPS	(CCR-O) Recharging points per 100.000 people	(CCR-O) High-Power Public Recharges per 100 KM Highway
Netherlands	128	383.1	79
France	106	68.4	35
Germany	120	53.7	57
Italy	96	22.4	18
Sweden	119	100.8	75
Belgium	118	73.6	27
Austria	126	92.5	77
Spain	91	17.3	14
Finland	111	67.5	54
Denmark	130	55.9	42
Portugal	79	24	16
Poland	73	4.4	25
Hungary	73	13	15
Czechia	93	11	49
Ireland	193	22.2	32
Luxembourg	260	589	7
Slovakia	70	16.9	56
Slovenia	89	35.6	17
Croatia	65	16.5	14
Romania	70	2.6	24
Estonia	84	32	131
Greece	73	4.4	4
Latvia	69	16.5	14
Bulgaria	53	2.8	10
Lithuania	84	6.4	31
Malta	100	19.6	0
Cyprus	90	7.9	9

the calculation is that it can point out to the necessary changes so that the efficiency of other states is 100%. In the considered case, the focus was on the output-oriented CCR model, as the outputs can change under certain conditions while maintaining the same inputs. If the focus is, for example on Slovakia, which was on fifth place, it is possible to see in the table exactly how the outputs could change so that its efficiency becomes 100%. Recharging points per 100000 people would have to change from 16.9 to 32.33. The High-Power Public Recharges per 100km Highway would have to change from the original 56 to 107.12.

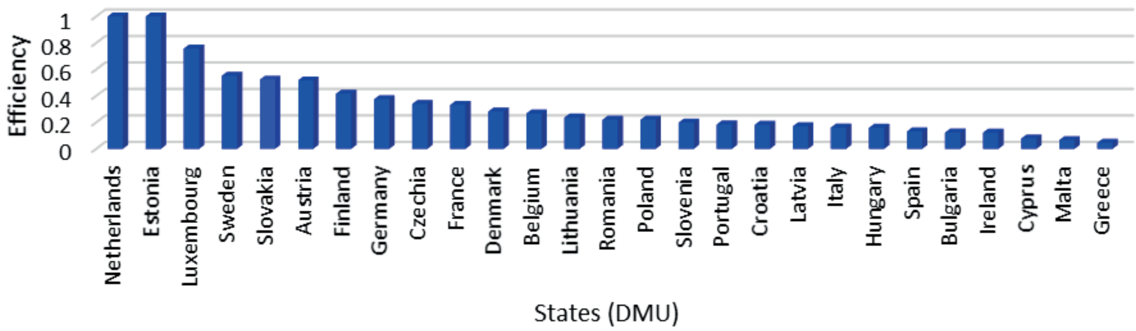

Figure 6 *Efficiency of the states of the European Union with regard to charging infrastructure*

Table 2 *Results of the DEA - CCR output model method*

Ranking of state	DMU	Efficiency	Inputs	outputs		Effective pattern (inputs)	Effective pattern (outputs)	
1.	Netherlands	1	128	383.1	79	128	383.1	79
1.	Estonia	1	84	32	131	84	32	131
3.	Luxembourg	0.76	260	589	7	260	778.17	160.47
4.	Sweden	0.55	119	100.8	75	119	182.78	136
5.	Slovakia	0.52	70	16.9	56	70	32.33	107.12
6.	Austria	0.52	126	92.5	77	126	179.2	149.17
7.	Finland	0.42	111	67.5	54	111	162.27	129.82
8.	Germany	0.38	120	53.7	57	120	143.18	151.98
9.	Czechia	0.34	93	11	49	93	35.43	145.04
10.	France	0.33	106	68.4	35	106	206.17	105.5
11.	Denmark	0.28	130	55.9	42	130	198.37	149.04
12.	Belgium	0.27	118	73.6	27	118	275.2	100.96
13.	Lithuania	0.24	84	6.4	31	84	32	131
14.	Romania	0.22	70	2.6	24	70	26.67	109.17
15.	Poland	0.22	73	4.4	25	73	27.81	113.85
16.	Slovenia	0.2	89	35.6	17	89	180.16	86.03
17.	Portugal	0.18	79	24	16	79	130.48	86.99
18.	Croatia	0.18	65	16.5	14	65	91.22	77.39
19.	Latvia	0.17	69	16.5	14	69	96.83	82.16
20.	Italy	0.16	96	22.4	18	96	139.91	112.43
21.	Hungary	0.16	73	13	15	73	81.79	94.37
22.	Spain	0.13	91	17.3	14	91	131.98	106.81
23.	Bulgaria	0.12	53	2.8	10	53	22.87	81.69
24.	Ireland	0.12	193	22.2	32	193	181.73	261.95
25.	Cyprus	0.08	90	7.9	9	90	101.82	115.99
26.	Malta	0.07	100	19.6	0	100	299.3	61.72
27.	Greece	0.05	73	4.4	4	73	97.55	88.68

5 Conclusion

Alternative fuels play an important role in an environmentally friendly environment modernization. There are many types of alternative propulsion and electromobility has an important place among them. With the rise of electromobility, the need for charging infrastructure is evolving in direct proportion. In the article, the focus was on important documents that address the development of electromobility in the European Union. Subsequently, a space was creating to examine the efficiency of spending funds on building infrastructure with regard to electromobility and available resources. The efficiency could be investigated using the DEA model. In order to evaluate the efficiency correctly, it was necessary to correctly determine the inputs and outputs that enter the DEA model. The input data selected were the GDP per capita in PPS of individual countries. The output data were Recharging points per 100,000 people and High-Power Public Recharges per 100 km Highway in each state. All the Member States of the European Union were considered in this research. Using the DEA method, it was possible to determine which state has 100% efficiency with respect to the specified parameters. From those states was then derived the efficiency of other states. The results of the method also show how it is possible to achieve 100% efficiency, while maintaining inputs and adjusting outputs. Countries that do not achieve 100% efficiency should focus on outputs and thus increase efficiency. This article also creates space for new research into the efficiency of electromobility in such a way that efficiency could be examined from the global perspective. Efficiency could also be examined in the terms of use of all the available alternative fuels and with them the availability of publicly accessible places to replenish the necessary raw materials. For the purposes of the article, authors have focused on the European Union countries, as they have the same strategic documents in the field of electromobility and similar conditions. Nevertheless, it is possible to examine differences in efficiency.

Acknowledgement

This publication was realized with support of Operational Program Integrated Infrastructure 2014 - 2020 of the project: Innovative Solutions for Propulsion, Power and Safety Components of Transport Vehicles, code ITMS 313011V334, co-financed by the European Regional Development Fund.

References

[1] Directive 2014/94/eu of the European Parliament and of the council of 22 October 2014 on the deployment of alternative fuels infrastructure [online], Available from: https://eur-lex.europa.eu/legal-content/EN/TXT/?uri=celex%3A32014L0094

[2] BALLAY, M., MONOŠI, M. Electric vehicle technologies in relation to the implementation fire service rescue operations. *Journal Crisis Management / Casopis Krizovy Manazment* [online]. 2016, **2**, p. 18-25. [accessed 2021-09-12]. ISSN 1336-0019. Available from: https://www.fbi.uniza.sk/uploads/Dokumenty/casopis_km/archiv/2016_02/06O1%20Ballay%20Monosi.pdf

[3] Global EV outlook - International Energy Agency [online]. 2021 [accessed 2021-09-12]. Available from: https://www.iea.org/reports/global-ev-outlook-2021

[4] World energy model - International Energy Agency [online]. 2020 [accessed 2021-09-13]. Available from: https://www.iea.org/reports/world-energy-model

[5] Electric road vehicles in the European Union. Trends, impacts and policies - European Parliament [online]. 2019. [accessed 2021-09-12]. Available from: https://www.europarl.europa.eu/RegData/etudes/BRIE/2019/637895/EPRS_BRI(2019)637895_EN.pdf

[6] Global EV stock by mode in the Stated Policies Scenario, 2020-2030 - International Energy Agency [online]. 2020 [accessed 2021-09-14]. Available from: https://www.iea.org/data-and-statistics/charts/global-ev-stock-by-mode-in-the-stated-policies-scenario-2020-2030

[7] Global EV stock by mode in the Sustainable Development Scenario, 2020-2030 - International Energy Agency [online]. 2020. Available from: https://www.iea.org/data-and-statistics/charts/global-ev-stock-by-mode-in-the-sustainable-development-scenario-2020-2030

[8] WAGNER, I. Passenger car sales in selected European countries in 2020, by fuel type - Statista [online]. 2021 [accessed 2021-09-13]. Available from: https://www.statista.com/statistics/500546/share-of-fuel-types-of-passenger-car-fleet-in-europe-by-country/

[9] Special Report 05/2021: Infrastructure for charging electric cars is too sparse in the EU - European Court of Auditors [online]. 2021. [accessed 2021-09-15]. Available from: https://op.europa.eu/webpub/eca/special-reports/electrical-recharging-5-2021/en/

[10] State of the art on alternative fuels transport systems in the European Union - European Commission, B-1049 Brussels [online]. 2020. [accessed 2021-09-15]. Available from: https://op.europa.eu/en/publication-detail/-/publication/fd62065c-7a0b-11ea-b75f-01aa75ed71a1

[11] Alternative fuels for sustainable mobility in Europe. Clean transport, Urban transport - European Commission [online]. 2021 [accessed 2021-09-15]. Available from: https://ec.europa.eu/transport/themes/urban/cpt_en
[12] Alternative fuel infrastructures for heavy - duty vehicles. Requested by the TRAN Committee, PE 690.888 - European Parliament [online]. 2021 [accessed 2021-09-15]. Available from: https://erticonetwork.com/wp-content/uploads/2020/06/KL0420116ENN.en_.pdf
[13] Number of electric LDV chargers by scenario, 2020-2030 - International Energy Agency [online]. 2020 [accessed 2021-09-15]. Available from: https://www.iea.org/data-and-statistics/charts/number-of-electric-ldv-chargers-by-scenario-2020-2030
[14] SYNAK, F., KUCERA, M., SKRUCANY, T. Assessing the energy efficiency of an electric car. *Communications - Scientific Letters of the University of Zilina* [online]. 2021, **23**(1), p. A1-A13 [accessed 2021-09-15]. ISSN 1335-4205, eISSN 2585-7878. Available from: https://doi.org/10.26552/com.C.2021.1;.A1-A13
[15] FARRELL, M. J. The Measurement of productive efficiency. *Journal of the Royal Statistical Society. Series A (General)* [online]. 1957, **120**(3), p. 253-290 [accessed 2022-01-15]. ISSN 00359238, eISSN 23972327. Available from: https://doi.org/10.2307/2343100
[16] CHARNES, A., COOPER, W. W., RHODES, E. Measuring the efficiency of decision making units. *European Journal of Operational Research* [online]. 1978, **2**(6), p. 429-444 [accessed 2022-01-15]. ISSN 0377-2217. Available from: https://doi.org/10.1016/0377-2217(78)90138-8
[17] AIGNER, D. J., LOVELL, C. A. K., SCHMIDT, P. Formulation and estimation of stochastic frontier production function models. *Journal of Economics* [online]. 1977, **6**, p. 21-37 [accessed 2022-01-15]. ISSN 0304-4076. Available from: http://dx.doi.org/10.1016/0304-4076(77)90052-5
[18] BATTESE, G., CORRA, G. S. Estimation of a production frontier model: with application to the Pastoral Zone of Eastern Australia. *Australian Journal of Agricultural Economics* [online]. 1977, **21**, p. 169-179 [accessed 2022-01-15]. eISSN 1467-8489. Available from: https://doi.org/10.22004/ag.econ.22266
[19] KINACI, H., NAJJARI, V., ALP, I. Using data envelopment analysis and stochastic frontier analysis methods to evaluate efficiency of hydroelectricity centres. *Gazi University Journal of Science*. 2016, **29**(1), p. 167-176. eISSN 2147-1762.
[20] If the least squares method is applied - Stuklopechat.Sk (in Slovak) [online]. 2018. [accessed 2022-01-15]. Available from: https://sk.stuklopechat.com/obrazovanie/81411-gde-primenyaetsya-metod-naimenshih-kvadratov.html
[21] ALBORES, P., PETRIDIS, K., DEY, P. K. Analysing efficiency of waste to energy systems: using data envelopment analysis in municipal solid waste management. *Procedia Environmental Sciences* [online]. 2016, **35**, p. 265-278 [accessed 2021-09-20]. ISSN 1878-0296. Available from: https://doi.org/10.1016/j.proenv.2016.07.007
[22] CHOI, K. S., KIM, W. J. An Analysis on the efficiency of low-cost airlines in Korea. *Journal of The Korean Society for Aeronautical and Space Sciences* [online]. 2018, **46**, p. 436-444 [accessed 2021-09-25]. ISSN 2093-274X, eISSN 2093-2480 Available from: https://doi.org/10.5139/JKSAS.2018.46.5.436
[23] ILIYASU, A., MOHAMED, Z. A., TERANO, R. Data envelopment analysis models and software packages for academic purposes. *Pertanika Journal of Scholarly Research Reviews* [online]. 2015, **1**(1), p. 27-32 [accessed 2021-09-25]. eISSN 2462-2028. Available from: https://core.ac.uk/download/pdf/234560142.pdf
[24] MALIK, M., EFENDI, S., ZARLIS, M. Data envelopment analysis (DEA) model in operation management. *IOP Conference Series: Materials Science and Engineering* [online]. 2018, **300**, 012008. ISSN 1757-8981, eISSN 1757-899X. Available from: https://doi.org/10.1088/1757-899X/300/1/012008
[25] JABLONSKY, J Solving DEA models in spreadsheets and modelling languages. In: 8th International Conference on Modelling, Simulation and Applied Optimization ICMSAO: proceedings [online]. IEEE. 2019. Available from: https://ieeexplore.ieee.org/document/8880322
[26] KUBAS, J., SOLTES, V., MISIK, J., STOFKOVA, Z. Efficiency of using financial resources and their impact on security in a local context. *Procedia Engineering* [online]. 2017, **192**, p. 498-503 [accessed 2021-09-25]. ISSN 1877-7058. Available from: https://doi.org/10.1016/j.proeng.2017.06.086
[27] MOZAFFARI, M. R., DADKHAH, F., JABLONSKY, J., WANKE, P. F. Finding efficient surfaces in DEA-R models. *Applied Mathematics and Computation* [online]. 2020, **386**, 125497. ISSN 0096-3003. Available from: https://doi.org/10.1016/j.amc.2020.125497
[28] YILMAZ, B., YURDUSEV, M. A. Use of data envelopment analysis as a multi criteria decision tool - a case of irrigation management. *Mathematical and Computational Applications* [online]. 2011, **16**(3), p. 669-679 [accessed 2021-09-30]. eISSN 2297-8747. Available from: https://doi.org/10.3390/mca16030669
[29] PRIEVOZNIK, P., STRELCOVA, S., SVENTEKOVA, E. Economic security of public transport provider in a three-dimensional model. *Transportation Research Procedia* [online]. 2021, **55**, p. 1570-1577 [accessed 2021-09-25]. ISSN 2352-1465. Available from: https://doi.org/10.1016/j.trpro.2021.07.146
[30] Alternative fuels. Electricity - year 2020 - European Alternative Fuels Observatory [online]. 2021. [accessed 2021-09-30]. Available from: https://www.eafo.eu/alternative-fuels/electricity/charging-infra-stats#

[31] GDP per capita in PPS - year 2020 - Eurostat [online]. 2021. [accessed 2021-09-30]. Available from: https://ec.europa.eu/eurostat/databrowser/view/tec00114/default/table?lang=en

[32] SILANC, P. A valuation of the eco-efficiency using the DEA models - a double stage (in Slovak). *EAPG Working Paper Series* [online]. 2013, WP No. 8. [accessed 2021-09-25]. ISSN 1338-2632. Available from: https://nhf.euba.sk/www_write/files/katedry/khp/eapg/wp008.pdf

APPLICATION OF MULTI-CRITERIA DECISION MAKING METHODS FOR EVALUATION OF SELECTED PASSENGER ELECTRIC CARS: A CASE STUDY

Ondrej Stopka *, Mária Stopková , Jan Pečman

Department of Transport and Logistics, Institute of Technology and Business in Ceske Budejovice, Ceske Budejovice, Czech Republic

*E-mail of corresponding author: stopka@mail.vstecb.cz

Resume

The article deals with the analysis of selected technical and economic aspects that influence decision making process when choosing a car with an electric drive - an electric car. Environmental friendliness is beginning to be one of the key aspects in the context of electric vehicle selection, but its final choice is still affected by the standards offered by internal combustion vehicles. In our case, the relevant standards were defined when using the results of a questionnaire survey, the criteria of scales, which are used to compare selected types of electric passenger cars in the conditions of the Czech Republic. The aim of the article is to select an appropriate electric car by using specific techniques of multi-criteria decision making - the Basic Variant method and the Analytic Hierarchy Process (AHP). The scientific value of the article lies primarily in its applicability to the global environment and the variability possibilities of criteria set and their significance.

Available online: https://doi.org/10.26552/com.C.2022.3.A133-A141

Article info

Received 28 February 2022
Accepted 24 May 2022
Online 21 June 2022

Keywords:

individual automobile transport
passenger car
electric car
multi-criteria decision making

ISSN 1335-4205 (print version)
ISSN 2585-7878 (online version)

1 Introduction

Electromobility is gradually building its strong position in the transport market Although it is not possible to clearly determine the sense of the emergence of modern electromobility, the environmental aspect is considered to be the most important, influenced in particular by the following regulations:

- The UN Framework Convention on Climate Change was adopted by the 1992 UN Conference on Environment and Development in Rio de Janeiro [1].
- Kyoto Protocol to the United Nations Framework Convention on Climate Change (hereinafter only "the Protocol"), adopted in December 1997 [2].
- Paris Agreement [3].

These regulations impose the protection of the climate system for the benefit not only of the present but also of future generations, on the basis of four basic principles [4]:

- principle of intergenerational justice,
- common but differentiated responsibilities,
- the need to protect in particular those parts of the planet which are more susceptible to the negative effects of climate change,
- preliminary caution.

The development of electric cars in the last two decades is one of the reactions of the automotive industry to the above-mentioned regulations and a manifestation of the effort to maintain the experienced user concept of the passenger car. From this point of view, it is clear that if the current electric car is to replace or even offer better standards than a car with an internal combustion engine, it will be necessary to define and evaluate customer requirements and, based on them, to develop the car and assess its suitability in accordance with the above regulations. If so, it will be possible to adhere this concept, and if not, it will be necessary to look for a different and perhaps completely different concept for this type of transport. The aim of the article is to select an electric vehicle under current conditions using scientific methods and on the basis of defined criteria.

2 Literature review

The topic of electromobility has long been dealt with by scientific teams around the world, not only from a technical point of view. In particular, the environmental, social and economic factors influenced by electromobility and which must be taken into account in its development are examined. The electric vehicle's propulsion unit itself is at a relatively high level in terms of available technology, efficiency and reliability, both the Battery Management System (BMS), which is discussed, for example, by Ayob et al [5], including the subject of recharging, which is addressed, e.g., in [6]. However, regarding the issue of electromobility, the storage of electrical energy in fuel cells remains. These possibilities were investigated in collaboration with Volkswagen AG Groger et al [7] or Mouli et al [8], whose study compares different charging options. The issues of recycling and charging or exchange stations are also presented, the possibilities of which are described by Buzoverov and Zhuk [9] in their extensive study.

Putting electric cars into practice, i.e., to their end users, carries with it multiple partial topics. From the point of view of economics and legislation, it is therefore mainly up to the individual states how they will react to the topic of electromobility, or in what ways they will support it. Territorial differences in relation to the approach to electromobility are addressed, for example, by Zhao, which compares world leaders - Germany and China [10]. This study takes into account specific territorial and political requirements as a basis for the development of batteries or fuel cells. The social aspects of electromobility lie, for example, in the so-called environmental responsibility, i.e., the effort of consumers to reduce their eco-footprint, with the aim of achieving so-called carbon-free urban mobility [11-12]. However, the issue of reducing the eco-footprint leads back to the technology and operation itself, because in the analysis of the life cycle of an electric vehicle, it is necessary to consider its components, their impact on environment and possible recyclability. Helmers in [13] and Wuschke et al in [14] addressed this issue in detail.

As mentioned, the market is an important factor for the further development of passenger electric cars, although its current strength is not comparable to the market for cars with internal combustion engines. It is not known what the climatic conditions and the car market will be in the coming decades. In addition to a series of technological, raw material and economic uncertainties, we often find opinions that electromobility will affect movement in urban areas and change the behavior of the automotive industry, energy and public administration [15].

There is a wide array of electromobility development programs in countries around the world that motivate the purchase of electric cars with varying degrees of success, for instance in [16-18]. Due to these programs, it is possible to observe an increasing share of electric cars in the total number of sold cars, but the same tendency cannot be expected even after their termination. Electromobility is also closely linked to the development of the smart energy networks of the future [19]. In terms of production itself, the electric car needs up to 30% fewer components than vehicles with internal combustion engines, as stated, e.g., in [20-23]. With the greater development of electromobility, this factor can contribute to influencing supply chains and production logistics, but also to the demise of some component manufacturers. In light with the above remarks, it is already clear that even the current concept of electric cars does not guarantee an improvement in the climate, if it is developed for these purposes, even without mentioning the fact regarding the share of passenger car transport in generation of harmful gases, life cycle of electric cars and so forth. However, as discussed in [20, 24], those who are interested in buying an electric car can also be motivated by other factors.

During the research, it was identified that the current requirements imposed by the customer on the electric car are mainly influenced by the standards imposed on cars with internal combustion engines, which was also examined, for example, by Metso et al [25]. From the environmental-technical standpoint, the customer's questions relating to the electric car are mainly focused on the safety of operation, the efficiency of the propulsion system and the service life of its components. It was not identified that the customer was interested in the possible advantages of an electric car over a car with an internal combustion engine in terms of user comfort - such as automatic preparation before driving, including defrosting windows in winter and heating or cooling the cabin from external power supply when connected to the charging network. Such equipment represents an indisputable advantage over a car with an internal combustion engine, especially when it is possible to program it or control it remotely [26].

The multi-criteria evaluation in this article therefore applies to the most frequently asked questions of potential customers to whom weights for the overall evaluation were assigned.

3 Materials and methods

For the purposes of this case study, six types of electric cars of comparable categories in terms of equipment and parameters coming from various manufacturers were objectively selected. By applying the Basic Variant method and the AHP method [27-28], the most appropriate model is then specified. As already mentioned, the most frequently asked customer questions concern the comparability of an electric car and an internal combustion engine car. Six basic factors were selected for the multi-criteria evaluation process. The foundation for the very evaluation was, on the one hand, a questionnaire survey among sellers of Hyundai, Kia and Nissan electric cars. To provide relevant information on this particular issue, data provided by CEZ were also used, which can already be ranked among the largest providers of services in the area of electromobility. The company operates in the operation

***Table 1** Variants of the criteria of the Basic variant method*

Vehicle	Price [CZK]	Mileage [km]	Power [kW]	Energy need [kWh.100km-1]	Max. speed [km.h-1]	Trunk volume [l]
Hyundai IONIQ	899 999	270	100	11.5	165	357
Nissan Leaf	950 000	240	80	15	144	435
VW e-Golf	959 000	180	85	12.7	140	341
BMW i3	954 000	260	125	13.1	150	260
Kia Soul EV	849 950	212	8	14.7	145	281
Renault ZOE	735 000	350	80	13.3	135	338
significance value	0.3	0.25	0.2	0.05	0.06	0.14
criterion	MIN	MAX	MAX	MIN	MAX	MAX

Explanatory note: CZK stands for the Czech crow/koruna and exchange rate of CZK to EUR is 0.04 € (May 30, 2022)

***Table 2** Determination of the base in the Basic Variant method*

Vehicle	Price [CZK]	Mileage [km]	Power [kW]	Energy need [kWh.100km-1]	Max. speed [km.h-1]	Trunk volume [l]
Hyundai IONIQ				1	1	
Nissan Leaf						1
VW e-Golf						
BMW i3			1			
Kia Soul EV						
Renault ZOE	1	1				
Significance value	0.3	0.25	0.2	0.05	0.06	0.14
criterion	MIN	MAX	MAX	MIN	MAX	MAX
B - basis	735 000	350	125	11.5	165	435

of charging infrastructure as well as in the field of sales of electric vehicles themselves. The construction and operation of charging infrastructure is dealt with by the Clean Technology Department branch of the enterprise Ceske energeticke zavody (CEZ CTD), while the sale of electric cars is dealt with by the CEZ Energy Service Company (CEZ ESCO) branch. According to CEZ ESCO's sales department, potential customers and their interest in purchasing an electric vehicle are most influenced by the following factors [20]:

- purchase price of an electric car,
- maximum distance,
- engine power,
- energy need,
- maximal speed,
- luggage compartment volume.

The aim is to select a compromise vehicle with electric drive for purchase. When assessing a significant number of criteria, the following methods are very effective, especially in the case where neither variant is optimal in all respects.

3.1 Basic variant method

This technique is based, like the weighted sum method, on maximizing utility. In principle, on the contrary, it is the target method, i.e., with the best values in all criteria. In the case of this method, 2 key equations are given, which are formulated in the manuscript methodology, and which can be partially modified. The modified relation for the yield (maximization) criteria shows Equation (1) [29]:

$$u_{ij} = \frac{original\ value}{base}\ [-], \tag{1}$$

where the benefit of a given variant is denoted as u_{ij}.

A modified relation for cost (minimization) criteria is shown in Equation (2).

$$u_{ij} = \frac{base}{original\ value}\ [-]. \tag{2}$$

The total benefit of the i-th variant is again calculated as a weighted sum of the partial benefits.

Individual selection variants together with criteria are shown in Table 1. The vehicles were selected according to two parameters - a range of more than 150 km and availability on the Czech market. The values of the criteria were determined according to the data provided by the manufacturers. Significance weights were thereafter determined by interviewing 6 experts who specialize in the sale of electric cars at CEZ. These experts defined the input weights of all the criteria independently of the other persons. Then, the sum of the obtained results was counted, and the weights of

Table 3 Calculated values of individual criteria

Vehicle	Price [CZK]	Mileage [km]	Power [kW]	Energy need [kWh.100km-1]	Max. speed [km.h-1]	Trunk volume [l]
Hyundai IONIQ	0.817	0.771	0.800	1	1	0.821
Nissan Leaf	0.774	0.686	0.640	0.767	0.873	1
VW e-Golf	0.766	0.514	0.680	0.906	0.848	0.784
BMW i3	0.770	0.743	1	0.878	0.909	0.598
Kia Soul EV	0.865	0.606	0.648	0.782	0.879	0.646
Renault ZOE	1	1	0.640	0.865	0.818	0.777
Significance value	0.3	0.25	0.2	0.05	0.06	0.14
criterion	MIN	MAX	MAX	MIN	MAX	MAX
B - basis	735 000	350	125	11.5	165	435

Table 4 Scalar product of selected variants

Vehicle	Price [CZK]	Mileage [km]	Power [kW]	Energy need [kWh.100km-1]	Max. speed [km.h-1]	Trunk volume [l]	w
Hyundai IONIQ	0.817	0.771	0.800	1	1	0.821	0.822
Nissan Leaf	0.774	0.686	0.640	0.767	0.873	1	0.762
VW e-Golf	0.766	0.514	0.680	0.906	0.848	0.784	0.700
BMW i3	0.770	0.743	1	0.878	0.909	0.598	0.799
Kia Soul EV	0.865	0.606	0.648	0.782	0.879	0.646	0.723
Renault ZOE	1	1	0.640	0.865	0.818	0.777	0.879
Significance value	0.3	0.25	0.2	0.05	0.06	0.14	
Criterion	MIN	MAX	MAX	MIN	MAX	MAX	
B - basis	735 000	350	125	11.5	165	435	

individual criteria significance were determined using the arithmetic mean.

The first step is to determine the base that represents the optimal value in the column according to the nature of the criterion. It is necessary to distinguish whether these are maximization or minimization criteria.

The following is the designation of the relevant places where the individual most advantageous values of the base are located by the number 1. The determination of the individual bases is shown in Table 2.

Subsequently, the values of the other criteria are calculated using two modified equations for the maximization and minimization criteria given in the introduction of this chapter [30]. The calculation of partial values is shown in Table 3.

After calculating the individual values, a column marked "w" is added to the table, which shows the scalar product between the individual values of the variants and the weights of the individual criteria - Table 4. The compromise variant is then represented by the variant with the highest scalar product.

According to Table 4, the electric vehicle Renault Zoe was chosen by the method of Basic Variant as compromise

3.2 AHP method

The second method used is the Analytic Hierarchy Process method, which was designed by Thomas L. Saaty in 1980. This method seeks to simplify the complex decision-making problems that it presents as a hierarchical structure. By this term is meant a linear structure comprising several levels, each of which contains several elements. The arrangement of individual levels goes from the general to the specific. The principle of this method is to quantify the intensity of interaction of individual elements in the system using Saaty's method of quantitative pairwise comparison, which is used at each level of the hierarchical structure [31].

In the initial stage of the method, it is again necessary to determine the possible variants along with the given criteria. The possible variants, the given criteria and the determined weights are the same as for the method of the Basic Variant mentioned in the previous chapter. The input data are provided in Table 5.

The subsequent procedure consists in creating as many tables as there are specified criteria. In this case it

***Table 5** criteria of the AHP method*

Vehicle	Price [CZK]	Mileage [km]	Power [kW]	Energy need [kWh.100km-1]	Max. speed [km.h-1]	Trunk volume [l]
Hyundai IONIQ	899 999	270	100	11.5	165	357
Nissan Leaf	950 000	240	80	15	144	435
VW e-Golf	959 000	180	85	12.7	140	34
BMW i3	954 000	260	125	13.1	150	260
Kia Soul EV	849 950	212	81	14.7	145	281
Renault ZOE	735 000	350	80	13.3	135	338
Significance value	0.3	0.25	0.2	0.05	0.06	0.14
criterion	MIN	MAX	MAX	MIN	MAX	MAX

***Table 6** Saaty scale*

1	variants are equally important both compared	both variants compared have the same property
3	the variant is slightly more important than the other variant	the first variant is slightly more significant than the other
5	the variant is much more important than the other variant	the first variant is strongly more significant than the other
7	the variant is significantly more important than the other variant	the first variant is very strongly more important than the other
9	extreme significance of one variant over another	the first variant is even more than strongly significant than the other

***Table 7** Cost criterion - complete table*

Price	Hyundai IONIQ	Nissan Leaf	VW e-Golf	BMW i3	Kia Soul EV	Renault ZOE	geom. mean	N weight	x weight
Hyundai IONIQ	1	3	5	7	0.2	0.142	1.172	0.110	0.033
Nissan Leaf	0.333	1	3	1	0.111	0.111	0.48	0.045	0.014
VW e-Golf	0.2	0.333	1	0.333	0.111	0.111	0.254	0.024	0.007
BMW i3	0.143	1	3	1	0.143	0.111	0.435	0.041	0.012
Kia Soul EV	5	9	9	7	1	0.2	2.876	0.270	0.081
Renault ZOE	7	9	9	9	5	1	5.425	0.510	0.153

is about 6 criteria = 6 tables. Each table will contain, in addition to the variants being compared, the geometric mean, the standard weight and the final weight.

The AHP method is based on the Saaty method, which is partially modified here. It will be based on the Saaty scale of preferences, which is shown in the following Table 6.

The value of 1 is the main diagonal in the tables, as it represents the equivalence of the same variants. Subsequently, 2 variants are always compared against one criterion. Preferences are determined according to the Saaty scale in Table 6. For illustration, Table 7 below compares the purchase price criterion with respect to all specified variants. The method of calculation is the same for all 5 remaining criteria (mileage, engine power, energy need, max. speed and luggage compartment volume = trunk volume).

Subsequently, the values are calculated into the geometric mean column.

After calculating the individual geometric means, it is necessary to standardize the given weights. Normalization of values is performed by dividing the individual geometric means by their sum for the given column. Subsequently, it is only necessary to multiply the individual standardized weights by the weights of the individual criteria and add them to the last column. Entire this process is presented, for instance, in [32]. Table 8 shows the calculated values of the geometric mean, the standard weight and the multiplication by the respective weight for the purchase price criterion.

Table 8 *The resulting values of the AHP method*

Vehicle	Price [CZK]	Mileage [km]	Power [kW]	Energy need [kWh.100 km-3]	Max. speed [km.h-1]	Trunk volume [l]	Sum
Hyundai IONIQ	0.033	0.043	0.048	0.021	0.028	0.029	0.202
Nissan Leaf	0.014	0.023	0.01	0.002	0.006	0.073	0.128
VW e-Golf	0.007	0.005	0.02	0.012	0.004	0.015	0.063
BMW i3	0.012	0.045	0.102	0.007	0.013	0.004	0.183
Kia Soul EV	0.081	0.011	0.012	0.002	0.007	0.006	0.119
Renault ZOE	0.153	0.122	0.008	0.006	0.002	0.014	0.305

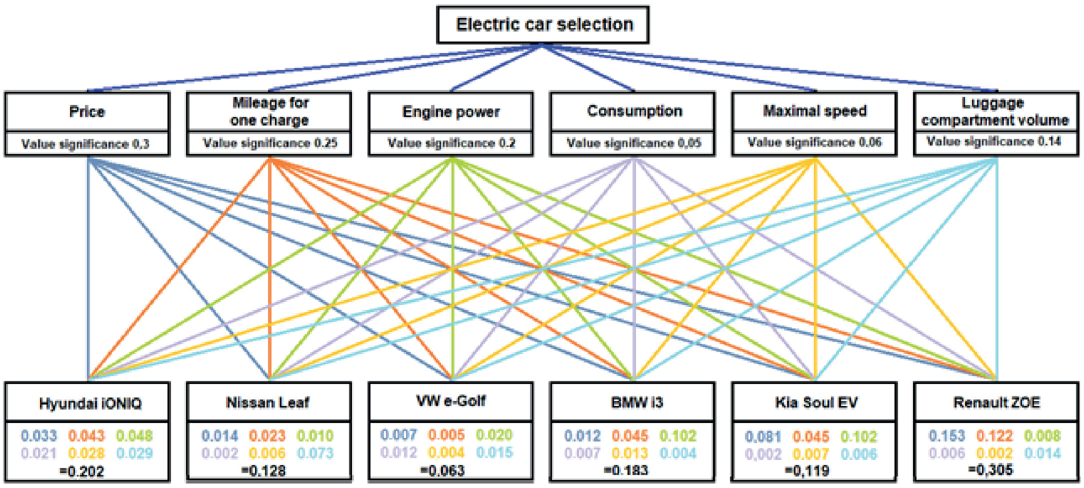

Figure 1 *Graphic representation of the AHP method*

The calculation for the remaining 5 criteria (mileage, engine power, energy need, max. speed and luggage compartment volume) is the same. The final step is to enter the individual values from the "x weight" columns to the individual variants. The values are then summed for each variant. The variant that reaches the highest value is again selected from the given values. The highest value was obtained by Renault ZOE, which, according to the AHP method, represents a compromise variant.

The AHP method also includes a graphical representation of the decision-making process in Figure 1.

Figure 1 graphically shows the dependence of the weights of individual criteria and their effect on the overall result. It is also clear from the figure that when calculating with the AHP method, it is possible to easily apply other criteria or adjust the value of the weights.

4 Results and discussion

The article is focused on the evaluation of economic and technical aspects relevant to the selection of a passenger electric car in the conditions of the Czech Republic. Questionnaire methods, discussions with experts and studies of scientific literature [7-11] were used to select aspects, on the basis of which relevant vehicle parameters influencing their selection were defined by comparative methods. Furthermore, the two most suitable scientific methods of evaluation were selected and the weights of criteria for individual parameters were determined. After performing and evaluating two exact methods [30-32], it was found that according to the Basic Variant method, the compromise variant is Renault ZOE.

The AHP method also reached the same result. The chosen electric car achieves very favorable results regarding the purchase price, mileage and the volume of the luggage compartment. According to the weights of these criteria, the purchase price and mileage are among the most important, which is why the vehicle achieved the best results. On the contrary, it reaches low values in terms of maximum speed and power of the electric engine. A possible alternative to the Renault ZOE electric car is the Hyundai IONIQ electric car. This electric car was placed according to the method of the Basic Variant in second place with a very small difference in values. The vehicle also took second place according to the AHP method.

Comparing the best Renault ZOE and the second Hyundai IONIQ, it can be stated that the Renault ZOE dominates in the two most important criteria, namely the purchase price and mileage. The difference in purchase prices is CZK 164,999 [33]. In terms of mileage, the Renault ZOE dominates by a considerable 80 kilometers.

On the other hand, the Hyundai IONIQ has a 20 kW more powerful electric motor, which allows it to reach speeds of up to 165 km / h, while its need is 1.8 kWh / 100 km lower. The difference in luggage compartment volumes is 19 liters in favor of Hyundai IONIQ. Here, it would depend on the specific customer whether to choose a cheaper vehicle with a higher mileage, or to opt for a vehicle with a more powerful electric motor and lower energy need, which at the same time allows a higher maximum speed to be achieved. If the vehicle were purchased by a family, a luggage compartment almost 20 liters larger could also play a large role [34]. Hence, in the conditions of the Czech Republic, the applied methods and performed procedures in connection with electric cars confirmed to be very useful and adequate.

The proportion of newly registered electric vehicles is only 0.3% of the total number of newly registered vehicles [35]. Nevertheless, sales in Western European countries reach tens of percent. For this reason, the methods are presented and outline the possibility of how a potential car applicant can compare the current offer of electric vehicles and choose the best compromise variant according to his preferences. Completely different criteria can be set, or the same can be used. Each buyer achieves a different result, as it depends very much on the criteria that affect the buyer, as well as on the weight he attributes to each criterion [36].

5 Conclusion

In the article, a compromise variant of the vehicle recommended for purchase was selected using two exact methods used in operational research. Six objectively selected vehicles with similar values of individual parameters were available. The comparison was made using six criteria and weights, which were determined following a questionnaire survey, discussions with car dealers and experts. As a compromise variant, the Renault ZOE was used using the methods. The result is influenced by the set criteria and their assigned weights as an example for use. Customer requirements that motivate the purchase of an electric car are mainly in the provision of comparable standards, such as a car with an internal combustion engine.

However, this comparison can only be considered temporary, until electric cars offer a better standard than cars with internal combustion engines. The criteria and their weights as well as the electric car model can be changed, in which case completely different results can be obtained. The current trend for changing the significance of individual criteria or their change may also be influenced by the latest knowledge and environmental and social trends. Manufacturers of electric cars, as well as the public administration and the customers themselves, thus having the opportunity to use decision-making methods to influence the vehicle market and the demand for them.

As for a crucial advantage, this study proved that various techniques of multi-criteria decision making in order to evaluate and choose passenger electric cars can be applied. On the other hand, as far as the major disadvantage is concerned, it is very difficult to determine the proper set of criteria taken into consideration as well as appropriate evaluated variants (i.e., passenger electric cars in our case).

In regard to the future research steps, these types of approaches can be successfully introduced to other transport-related issues to a greater or lesser extent and should be examined even more comprehensively. Therefore, further research can focus in particular on the following issues. Various telematics applications or other information technologies should be taken into account when addressing the analogous topics. Moreover, a negative impact of such solutions on environment needs to be investigated as well. And last but not least, it also would be reasonable to deal with the economic aspects of these proposals and approaches in more detail, such as time return on individual investments, overall profitability of the planned project and so forth.

Acknowledgment

The article is published within the solution of the research project TAČR: CK03000085 “Implementation of city logistics into the process of sustainable urban mobility planning”.

References

[1] United Nations framework convention [online] [accessed 2021-12-02]. 1992. Available from: https://unfccc.int/process-and-meetings/the-convention/what-is-the-united-nations-framework-convention-on-climate-change

[2] Kyoto protocol to the United Nations framework convention on climate change - Ministry of the Environment of the Czech Republic [online] [accessed 2021-12-02]. 2019. Available from: https://www.mzp.cz/cz/ramcova_umluva_osn_zmena_klimatu

[3] Paris agreement on climate change - Council of the European Union. [online] [accessed 2022-01-30]. 2018. Available from: http://www.consilium.europa.eu/cs/policies/climate-change/timeline

[4] LIU, K, KANG, L., AND PENG, Q. A brief review on key technologies in the battery management system of electric vehicles. *Frontiers of Mechanical Engineering* [online]. 2019, **14**(1), p. 47-64. ISSN 2095-0233, eISSN 2095-0241. Available from: https://doi.org/10.1007/s11465-018-0516-8

[5] AYOB, A., WAN MOHD, F., AZAH, M., MOHD, I. Review on electric vehicle, battery charger, charging station and standards. *Research Journal of Applied Sciences, Engineering and Technology* [online]. 2014, **7**(2), p. 364-373. ISSN 2040-7459, eISSN 2040-7467. Available from: https://doi.org/10.19026/rjaset.7.263

[6] MAHESWARI, S., SHARAN, V., SHALINI, V., SOWNDARABARANI, D., DINESH KUMAR, S. Improved battery management system for hybrid electric vehicle using supercapacitor. *AIP Conference Proceedings* [online]. 2021, **2387**, 120005. ISSN 0094-243X, eISSN 1551-7616. Available from: https://doi.org/10.1063/5.0068644

[7] GROGER, O., HUBERT A., GASTEIGER, J. AND SUCHSLAND, H. Review electromobility: batteries or fuel cells? *Journal of The Electrochemical Society* [online]. 2015, **162**(14), p. A2605-A2622. ISSN 0013-4651, eISSN 1945-7111. Available from: https://doi.org/10.1149/2.0211514jes

[8] MOULI, G., KAPTEIN, Z., BAUER, P., ZEMAN, M. Implementation of dynamic charging and V2G using Chademo and CCS/Combo DC charging standard. In: 2016 IEEE Transportation Electrification Conference and Expo (ITEC): proceedings [online]. 2016. p. 1-6. Available from: https://doi.org/10.1109/ITEC.2016.7520271

[9] BUZOVEROV, E., ZHUK, A. Comparative economic analysis for different types of electric vehicles. *International Journal of Sustainable Energy Planning and Management* [online]. 2020, **29**, p. 57-68. ISSN 2246-2929. Available from: https://doi.org/10.5278/ijsepm.3831

[10] ZHAO, Q. Electromobility research in Germany and China: structural differences. *Scientometrics* [online]. 2018, **117**, p. 473-493 ISSN 0138-9130, eISSN 1588-2861. Available from: https://doi.org/10.1007/s11192-018-2873-9

[11] SECHILARIU, M., MOLINES, N., RICHARD, G., MARTELL-FLORES, H., LOCMENT, F., BAERT, J. Electromobility framework study: infrastructure and urban planning for EV charging station empowered by PV-based microgrid. *IET Electrical Systems in Transportation* [online]. 2019, **9**(4), p. 176-185. eISSN 2042-9746. Available from: https://doi.org/10.1049/iet-est.2019.0032

[12] MACIEL FUENTES, D. A.; GONZALEZ, E. G. Technoeconomic analysis and environmental impact of electric vehicle introduction in taxis: a case study of Mexico City. *World Electric Vehicle Journal* [online]. 2021, 12, 93. eISSN 2032-6653. Available from: https://doi.org/10.3390/WEVJ12030093

[13] HELMERS, E. Electric car life cycle assessment based on real-world mileage and the electric conversion scenario. *The International Journal of Life Cycle Assessment*. [online]. 2015, **22**(1), p. 15-30. ISSN 0948-3349, eISSN 1614-7502. Available from: https://doi.org/10.1007/s11367-015-0934-3

[14] WUSCHKE, L., JACKEL, H. G., LEISSNER, T., PEUKER, U. A. Crushing of large li-ion battery cells. *Waste Management* [online]. 2019, **85**, p. 317-326. ISSN 0956-053X. Available from: https://doi.org/10.1016/j.wasman.2018.12.042

[15] ATIAS, D. *The automobile revolution: towards a new electro-mobility paradigm* [online]. Cham Switzerland: Springer, 2017. ISBN 978-3-319-45838-0. Available from: https://books.google.cz/books?id=AgYtDQAAQBAJ&printsec=frontcover&hl=cs&source=gbs_ge_summary_r&cad=0#v=onepage&q&f=false

[16] SCHMOCH, U., BECKERT, B., SCHAPER-RINKEL, P. Impact assessment of a support programme of science-based emerging technologies. *Scientometrics* [online]. 2019, **118**, p. 1141-1161. ISSN 0138-9130, eISSN 1588-2861. Available from: https://doi.org/10.1007/s11192-018-03002-x

[17] KIRSANOVS, V., BARISA, A., SAFRONOVA, A. Cost-benefit assessment of electric vehicle vs internal combustion engine in Latvia. In: IEEE 61st Annual International Scientific Conference on Power and Electrical Engineering of Riga Technical University RTUCON: proceedings [online]. IEEE. 2020. Art. no. 9316610. Available from: https://doi.org/10.1109/RTUCON51174.2020.9316610

[18] LUSZCZYK, M., SULICH, A., SIUTA-TOKARSKA, B., ZEMA, T., THIER, A. The development of electromobility in the European Union: evidence from Poland and cross-country comparisons. *Energies* [online]. 2021, **14**(24), 8247. eISSN 1996-1073. Available from: https://doi.org/10.3390/en14248247

[19] VADIRAJ, A. Infrastructure development and its management for future sustainable mobility. *SAE Technical Papers* [online]. 2016, **28**, 0252. ISSN 0148-7191, eISSN 2688-3627. Available from: https://doi.org/10.4271/2016-28-0252

[20] DIZO, J., BLATNICKY, M., SEMENOV, S., MIKHAILOV, E., KOSTRZEWSKI, M., DROZDZIEL, P., STASTNIAK, P. Electric and plug-in hybrid vehicles and their infrastructure in a particular European region. *Transportation Research Procedia* [online]. 2021, **55**, p. 629-636. ISSN 2352-1465. Available from: https://doi.org/10.1016/j.trpro.2021.07.029

[21] STOMA, M., DUDZIAK, A., CABAN, J., DROZDZIEL, P. The future of autonomous vehicles in the opinion of automotive market users. *Energies* [online]. 2021, **14**(16), 4777. eISSN 1996-1073. Available from: https://doi.org/10.3390/en14164777

[22] SETTEY, T., GNAP, J., SYNAK, F., SKRUCANY, T., DOCKALIK, M. Research into the impacts of driving cycles and load weight on the operation of a light commercial electric vehicle. *Sustainability* [online]. 2021, **13**(24), 13872. eISSN 2071-1050. Available from: https://doi.org/10.3390/su132413872

[23] MARCZAK, H., DROZDZIEL, P. Analysis of pollutants emission into the air at the stage of an electric vehicle operation. *Journal of Ecological Engineering* [online]. 2021, **22**(8), p. 182-188. ISSN 2299-8993. Available from: https://doi.org/10.12911/22998993/140256

[24] THILINA, D., GUNAWARDANE, N. The effect of perceived risk on the purchase intention of electric vehicles: an extension to the technology acceptance model. *International Journal of Electric and Hybrid Vehicles* [online]. 2019, **11**(1), p. 73-84. ISSN 1751-4088, eISSN 1751-4096. Available from: https://doi.org/10.1504/ijehv.2019.098717

[25] METSO, L., HAPPONEN, A., RISSANEN, M., EFVENGREN, K., OJANEN, V., KARRI, T. Data openness based data sharing concept for future electric car maintenance services [online]. In: *Smart Innovation, Systems and Technologies*. BALL, A., GELMAN, L., RAO, B. (Eds.). Vol. 166. Cham: Springer, 2020. ISBN 978-3-030-57744-5, eISBN 978-3-030-57745-2, p. 429-436. Available from: https://doi.org/10.1007/978-3-030-57745-2_36

[26] JIN, L. Q, SONG, C. X, WANG, Q. N. Evaluation of influence of motorized wheels on contact force and comfort for electric vehicle. *Journal of Computers* [online]. 2011, **6**(3), p. 497-505. ISSN 1796-203X. Available from: https://doi.org/10.4304/jcp.6.3.497-505

[27] EJEM, E. A., UKA, C. M., DIKE, D. N., IKEOGU, C. C., IGBOANUSI, C. C., CHUKWU, O. E. Evaluation and selection of Nigerian third-party logistics service providers using multi-criteria decision models. *LOGI - Scientific Journal on Transport and Logistics* [online]. 2021, **12**(1), p. 135-146. eISSN 2336-3037. Available from: https://doi.org/10.2478/logi-2021-0013

[28] KAYA, O., ALEMDAR, K. D., ATALAY, A., CODUR, M. Y., TORTUM, A. Electric car sharing stations site selection from the perspective of sustainability: A GIS-based multi-criteria decision making approach. *Sustainable Energy Technologies and Assessments* [online]., 2022, **52**(A), 102026. ISSN 2213-1388. Available from: https://doi.org/10.1016/j.seta.2022.102026

[29] WANG, X., ZHANG, H., ZHANG, S., WU, L. Impacts of joint operation of wind power with electric vehicles and demand response in electricity market. *Electric Power Systems Research* [online]. 2021, **201**, 107513. ISSN 0378-7796. Available from: https://doi.org/10.1016/j.epsr.2021.107513

[30] FIALA, P., MANAS, M. *Multicriterial decisions*. Prague: VSE, 1994. ISBN 80-707-9748-7.

[31] FOTR, J., DEDINA, J., HRUZOVA, H. *Managerial decisions*. 3. ed. Prague: Ekopress, 2003. ISBN 80-861-1969-6.

[32] CARNY, S., SPERKA, A., ZITRICKY, V. Multi-criteria evaluation of railway transport using evaluation method. *LOGI - Scientific Journal on Transport and Logistics* [online]. 2020, **11**(2), p. 88-99. eISSN 2336-3037. Available from: https://doi.org/10.2478/logi-2020-0018

[33] ZMESKAL, Z. Application of decomposition multi-attribute methods AHP and ANP in financial decision-making. In: International Scientific Conference Managing and Modelling of Financial Risks: proceedings [online]. Vol. 6. 2012. p. 689-699.

[34] Electrical vehicles specification [online] [accessed 2022-01-21]. Available from: https://www.renault.cz/elektricke-vozy/zoe.html

[35] LINA, X, ZEJUN, K. driving style recognition model based on nev high-frequency big data and joint distribution feature parameters. *World Electric Vehicle Journal* [online]. 2021, 12(3), 142. eISSN 2032-6653. Available from: https://doi.org/10.3390/wevj12030142

[36] GLOSER-CHAHOUD, S., HUSTER, S., ROSENBERG, S., BAAZOUZI, S., KIEMEL, S., SINGH, S., SCHNEIDER C., WEEBER M., MIEHE R., SCHULTMANN, F. Industrial disassembling as a key enabler of circular economy solutions for obsolete electric vehicle battery systems. *Resources, Conservation and Recycling* [online]. 2021, **174**, 105735. ISSN 0921-3449. Available from: https://doi.org/10.1016/j.resconrec.2021.105735

EFFECT OF PERIODIC TECHNICAL INSPECTIONS OF VEHICLES ON TRAFFIC ACCIDENTS IN THE SLOVAK REPUBLIC

Juraj Hudec [1,2], **Branislav Šarkan** [2,*]

[1]Ministry of Transport and Construction of the Slovak Republic, Bratislava, Slovak Republic
[2]The Faculty of Operation and Economics of Transport and Communications, University of Zilina, Zilina, Slovakia

*E-mail of corresponding author: sarkan@fpedas.uniza.sk

Resume
The article presents a search for links between the Periodic Technical Inspections of Vehicles (TI) and traffic accidents due to vehicle technical defects in the Slovak Republic. Based on these links, it is sought to assess the justification for TI regarding the road safety. For this purpose, statistical data on traffic accidents, caused by vehicle technical defects as well as data concerning TI carried out were examined. The first finding was that the approaching end of the validity of the TI, the probability of traffic accidents due to technical defects increases for vehicles. The second finding was that with the increasing number of vehicles assessed at the Periodical Technical Inspection Stations (PTI) as temporarily roadworthy and not roadworthy, the number of accidents due to vehicle technical defects was decreasing. The results formulated in this paper show that the TI have a measurable effect on traffic accidents caused by vehicle technical defects, thus positively affecting the road safety and thus having a demonstrable justification.

Available online: https://doi.org/10.26552/com.C.2022.3.A142-A159

Article info
Received 27 January 2022
Accepted 27 19 May 2022
Online 21 June 2022

Keywords:
periodic technical inspections
technical condition of vehicles
vehicle technical defects
road safety
traffic accident

ISSN 1335-4205 (print version)
ISSN 2585-7878 (online version)

1 Introduction

Development of the automotive industry due to the growing demand for vehicles for private or business purposes also contributes to the need for technical inspections of these vehicles, which contributes to the safe operation of means of transport. Vehicles in good technical condition are then a prerequisite for carrying out their transport task [1].

One of the functions of the state is to protect the lives and property of its citizens. Therefore, every civilized state has an interest in ensuring that vehicles in traffic do not endanger road safety and the environment. Consequently, the minimum technical requirements to be met by each vehicle in the road traffic have been laid down and this includes the introduction of periodic technical inspections and regular emission measurements.

Although there are still various discussions being held on this topic in some countries (especially in the US and Australia), most countries in the world have introduced mandatory technical inspections into their jurisdictions. In all the EU countries, this is an obligation and technical inspections of vehicles registered in the EU Member States are carried out at regular intervals in a harmonized way [2].

One of the causes of traffic accidents is the technical condition of vehicles. However, according to national statistics, the proportion of such accidents in the overall causes of traffic accidents varies considerably, ranging from a few tenths of a percent to double digits. Despite the various statistics, there is a common view that the system of periodic technical inspections and vehicle technical defects affect the road safety and the number of traffic accidents. However, this is countered by the views that systems of periodic technical inspections of vehicles are costly for vehicle operators and provide negligible benefits for society. These views are often justified by the fact that development of the automotive technology is progressing considerably and more complex passive and active safety systems are being used. Likewise, the production of more sophisticated cars is facing increasingly stringent type-approval requirements.

However, the effectiveness of national systems of periodic technical inspections, at first sight, appears to be difficult to measure and the input data depend on the sources and methodology of their collection and may vary from one another. Several different studies have already been written on this topic using different research methods, sometimes with conflicting conclusions. That is because it is very difficult to establish a direct causal link between periodic technical inspections of vehicles and the reduction in the accident rate.

This article, therefore, presents an examination, in an original way, of the periodic technical inspections effect on the occurrence of traffic accidents due to vehicle technical defects, namely in the environment of the Slovak Republic and thus the impact on road safety. Based on the above, it also assesses the effectiveness of periodic technical inspections of vehicles in this state.

2 Literature review

The reason for introducing the obligation to subject vehicles to regular technical inspections is the presumption of eliminating vehicles from the road traffic with serious and dangerous defects that could potentially result in a traffic accident and thus endanger people's health, lives and property. However, the fundamental question is to what extent the poor technical condition of vehicles affects and may affect the accident rate and what are its consequences. Whether it is actually necessary to take measures at a national level to eliminate the consequences of road accidents caused by vehicle technical defects and therefore whether the effort and attention spent on systems of periodic technical inspection of vehicles have a measurable impact on road safety. Discussions are taking place on this topic, either at a scientific level or government level of some countries.

This part of the paper thus deals with the available world literature, articles and studies, which deal with vehicle technical defects as the cause of traffic accidents and the effect of periodic technical inspections on the reduction in accident rate due to vehicle technical defects and which are also looking for answers to questions concerning the justification of periodic technical inspection systems. Due to the complex concept of the issue, the literature was sorted according to selected criteria and from the most recent to the oldest.

2.1 Effect of vehicle technical defects on causes of the traffic accidents in the light of the results of various studies and research projects

The following part focuses on the issue of vehicle technical defects as the cause of traffic accidents. In this

Table 1 *Percentage of vehicles with technical defects that directly caused the traffic accident*

Study	Share
Fazzalaro (2007), USA [3]	1%
Asander (1992) [4]	23% (direct causes or increasing damage or injury) (Finland)
	7-9% (major causal role, a contributing cause, or by increasing the consequences of the accident) (Denmark)
RACQ (1990) [5]	5%
Rompe and Seul (1985) [6]	3-24%
	1.3% (Japan)
Grandel (1985) [7]	2-10%
McLean et al. (1979), Australia [8]	1.5% motorcycles
	2.9% passenger cars
Treat (1977), USA [9]	4.5% passenger cars

Table 2 *Percentage of vehicles with technical defects that contributory caused the traffic accident*

Study	Share
Haworth et al. (1997) (motorcycle crashes), Australia [10]	12% in total
	28% of accidents involving single vehicle
	7% of accidents involving multiple vehicles
Haworth et al. (1997) (single vehicle crashes), Australia [11]	3%
Asander (1993) [4]	23% (direct causes or increasing damage or injury) (Finland)
	7-9% (significant impact, related impact, or increase in connections with traffic accidents) (Denmark)
Case et al. (1991) [12]	5.8%
Rompe & Seul (1985) [6]	4 - 19% (possibly up to 33%)
Grandel (1985), Germany [7]	6.5% traffic accidents involving passenger cars
	5% traffic accidents involving two-wheeled vehicles
CCRAM (1978) Melbourne (Forest and Youngman) [13]	5.8%
	(0.6-1.8% of these defects can be detected by a technical inspection)
Treat (1977), USA [9]	12.6% vehicles

respect, the results of studies of the relevant worldwide scientific literature concerning the traffic accidents caused by vehicle technical defects, as well as other links, were summarized.

In the course of time, several studies, or research projects were carried out in various countries, focusing on the effect of vehicle technical defects on the occurrence of traffic accidents. For the purposes of this paper, 28 of them were examined. In the case of publications in which their results were explicitly quantified, in order to simplify their interpretation, they were summarized in the Table 1 and Table 2 by means of the percentages of vehicles with technical defects that directly caused the traffic accident and the proportions of vehicles whose technical defects only contributed to the occurrence of the traffic accident.

Table 1 shows results of world studies, research and publications focuses on the issue of vehicle technical defects as a main causes of traffic accidents with their percentages expression.

Table 2 shows results of world studies, research and publications focuses on the issue of vehicle technical defects that contributory caused of traffic accidents with their percentages expression.

Table 1 shows clearly that 1.3% to 24% of the vehicles involved in the traffic accident had technical defects that caused the accident [8]. Based on studies in which in-depth accident investigations were carried out [9], technical defects played a causal role in 2.9% to 4.5% of car accidents.

Furthermore, from Table 2 it can be seen that between 3% and 19% of the vehicles involved in the accident had technical defects that played a contributory role in the accidents [7]. Perhaps the most comprehensive studies on the subject show that vehicle defects are a contributing factor in 6.5% to 12.6% of traffic accidents. For motorcycles, it is 5% to 12% of accidents [9].

Research, therefore, shows that the share of traffic accidents arising directly or indirectly from vehicle technical defects, in relation to all accidents, is relatively low, but not negligible. In absolute terms and especially in terms of possible fatality of the consequences, it may even be perceived as significant.

2.2. Effect of introduction of the periodic technical inspections system on reduction in accident rate in the light of the results of various studies and research projects

One of the methods for assessing the effectiveness, and thus the justification for introducing systems of periodic technical inspections for vehicles, as a measure to reduce the number of accidents due to technical defects of vehicles, is to examine their effect on these accidents. The aim of these systems constitutes the preventive removal of defects from a vehicle fleet through a periodic technical inspection of vehicles on a compulsory basis, as well as fixation of any found defect before the vehicle is allowed to operate on public roads [14]. It is assumed that if periodic technical inspections reduce the number of technical defects in the vehicle fleet of a given state, then this will also result in a reduction in the accident rate caused by technical defects of the vehicles.

This section summarizes information on the relevant scientific literature and publications concerning the effects of systems of technical inspections on accident rate, as well as their other related consequences. Studies or research projects were focused on:

- a comparison of states that have the periodic technical inspection of vehicles mandatory with states, where there is no such obligation,
- a comparison of states before and after the introduction of the obligation to conduct periodic technical inspection of vehicles,
- a comparison of countries following the withdrawal of the obligation for periodic technical inspection,
- a comparison of accident rates of vehicles that have undergone periodic technical inspections with vehicles that have not been subject to such inspections within the jurisdiction of the same state,
- an analysis of the accident rate of vehicles undergoing periodic technical inspections, during the time in between such inspections.

For the purposes of this paper, 18 publications have been reviewed. Their results mostly support the positive effect of periodic technical inspections, but in certain cases, they show some differences [15]. One of the reasons may be that the results are influenced by methodological and statistical shortcomings. This is stated by reviewers [16], as well as by the authors of the articles themselves [17].

Another reason for differences in results may be the influence of other factors, such as different levels and types of road safety measures, various traffic intensity in different countries, level of public roads or vehicles operation in different climatic conditions, collection of data based only on police registers, different methodologies of such data collection and assessment of causes of traffic accidents, methodological shortcomings and age of these studies [18]. These factors were not considered in the analyses of the various studies [19]. Differences in vehicle fleets or vehicle wrecks available for the study may also have had an impact on data obtained for a particular jurisdiction [6]. Likewise, the different levels of quality of the periodic technical inspection systems of the countries studied may make it difficult to compare studies [20].

Another major problem when it comes to determining the effect of systems of technical inspections of vehicles on the reduction in accident rate is that the related studies did not directly address this issue. Only study [21] was the closest to it. According to the cited studies, provided that the PTI detect defects in vehicles that must subsequently be rectified, this eliminates the

Table 3 *Effect of periodic technical inspection on the reduction in traffic accident rates*

Study	Percentage reduction in accident rates
Schulz and Franck (2021) [20]	in fatal accident rate and accident rate with no proportion figures given in Punjab (Pakistan)
European Commission (2019) [23]	5% (in accident rate of mopeds in Spain) 18% (in fatalities in Spain)
Schulz and Scheler (2019) [24]	40% (in accident rate in Costa Rica)
Hoagland et al. (2018) [25]	0% following the abolition of compulsory technical inspections in the state of New Jersey
Schulz and Scheler (2016) [26]	10% (in accident rate in Tukey)
Keall & Newstead (2013), New Zealand [27]	8% (during the transition from an annual to a semi-annual frequency of technical inspections)
Rune Elvik (2001), Norway [13]	5-10% (with an increase in the frequency of technical inspections by 100%)
Fosser (1992), Norway [28]	0% (Norway has significant random roadside inspection program)
Asander (1992), Sweden [4]	16% (in accident rate with serious injury)
NHTSA (1989), USA [16]	10% (in accident rate) 0% (in fatal accident rate)
White (1986), New Zealand [29]	10-15% (in accident rate)
Rompe & Seul (1985) [6]	50% (in accident rate)
Loeb and Gilad (1984), USA [18]	in fatal accident rate and accident rate with no proportion figures given
Berg et al. (1984), Sweden [30]	14% (in police reported accidents) 15% (in accident rate with serious injury)
Crain (1981), USA [31]	reduction in accident rate, but no figures given
Schroer and Peyton (1979), USA [19]	9.1% (in accident rate, after technical inspection, compared to uninspected vehicles) 21% (in accident rate, after periodic technical inspection, compared to uninspected vehicles) 5.3% (in accident rate for inspected vehicles compared to accident rates of vehicles before the inspection)
Little (1971), USA [32]	5% (in death rates)

Table 4 *Effect of periodic technical inspections on the incidence of defects on vehicles*

Study	Figures
Asander (1992) [4]	7-8% of vehicles with serious defects replaced with new vehicles
NHTSA (1989), USA [16]	0.25-2.5% higher proportion of crashed vehicles with technical defects in countries without a system of regular technical inspection compared to countries having such a system 2.5% Higher rate of tyre failure in states without a system of regular technical inspections

incidence of at least part of the accidents that are caused by vehicle technical defects [22]. It also suggests that periodic technical inspections address only part of this problem [19].

Table 3 provides a summary of changes in accidents' rate due to periodic technical inspections of vehicles, resulting from the results of related publications.

Table 4 provides an effect of periodic technical inspections of vehicles on vehicle defects resulting from the results of related publications.

Table 3 demonstrates that the effect of the technical inspection system on accident rate ranged from no effect to a 16% reduction and up to 21% in case of periodic technical inspections. The study [6] with reference to US studies suggests that a system of periodic technical inspections could reduce the accident rate of vehicles with a technical defect by about 50%.

The effect of the system of periodic technical inspections of vehicles on the incidence of vehicle defects is shown in Table 4. Here it can be seen that the system of periodic technical inspections of vehicles reduces the incidence of defects in a vehicle fleet by up to 2.5% [16]. In Sweden, it was found that 7-8% of vehicles with serious defects were replaced with new vehicles after the introduction of a system of periodic technical inspections [4].

Some new studies have shown an important correlation between the PTI and the accidents decrease and improvement of road safety [33]. According to one study, the PTI avoid more than 400 fatalities per year, about 12,000 injured and almost 8,500 accidents during the period 1998-2006 [34]. This study was an update, which demonstrates that vehicle technical failures contribute about a 6% of the total number of car accidents and an 8% of motorcycles accidents, which annually represents 2,000 fatalities in the European Union and a much higher number of injuries. According to this work, PTI avoided 11,000 traffic accidents, about 11,000 injured and 170 fatalities, which represents an economic benefit of 300 million Eur [35]. Other studies show similar results [36].

Several new studies have also examined the economic effect of introduction of PTI. For example, introduction of the PTI in Costa Rica show that there are considerable economic gains from having such a system in place with high cost-benefit ratios [24]. In the case of Punjab, the introduction of a regulated PTI system has a significant benefit. As already stated in the analysis, about 335 accidents can be avoided by a regulated introduction of a PTI system, 198 of which would be fatal. The economic loss of 198 fatal accidents amounts to 11.6 million USD, which is a considerable amount for a region like Punjab, whose economic power fades in comparison to that of a developed country [20]. A PTI system would also help in preventing the costs associated with serious or minor injuries. Consequently, the economic damage associated with road accidents is incredibly significant. It has been shown in other countries that the introduction of PTI has a significant positive impact on the number of traffic accidents [26]. The purpose of another study carried out for European Commission is to assess the benefit of including two- and three wheelers and light trailers within the framework of periodic inspection of vehicles and to propose the precise way to do so. For the two- and three-wheelers, the study considers the impact of introducing inspection of mopeds in Spain between 2007 and 2010 depending on the region. The report demonstrates that the benefit of this initiative is 4.73 times greater than the costa. With all the considerations taken into account, the costs and benefit analysis has been undertaken with the data of Croatia resulting in a benefit 6.32 times greater than the costs [23].

Thus, the majority of research projects and statistics demonstrate that periodic technical inspection systems, by reducing technical defects in a vehicle fleet, have an impact on the reduction in accident rate of vehicles that could otherwise occur due to technical defects and are therefore justified [30]. However, the numerical expression of this impact is presented differently in various research projects, as well as that it is not always possible to accurately quantify it. Nevertheless, none of the publications directly examined the incidence of accidents in the period between the performance of technical inspections and their end of validity, as well as the link between the results of periodic technical inspections given by the temporary roadworthiness and not roadworthiness and the number of accidents, what was examined in this article.

3 Material and methods

The present article provides an analysis of data concerning the traffic accident rates due to technical defects of vehicles in the Slovak Republic, as well as research on the incidence of traffic accidents in the period in between the performance of technical inspections and the end of their validity. Furthermore, the article examined the effect of the results of periodic technical inspections given by temporary roadworthiness and not worthiness of vehicles on the number of traffic accidents due to a technical defect.

The basic materials and resources for analysis and research consisted of:

- statistical data on all the traffic accidents in the period 2012 - 2020, provided by the Presidium of the Police Force of the Slovak Republic,
- detailed data on traffic accidents caused primarily by a technical defect of vehicles in the period 2016-2020, obtained from the information system of traffic accidents of the Presidium of the Police Force of the Slovak Republic,
- data from the Slovak central automated information system of technical inspections, in which all data on technical inspections of vehicles for the period 2016-2020 are stored,
- up-to-date statistics on the results of the vehicle assessments by the PTI,
- up-to-date statistics on the traffic accidents due to a technical defect provided by the foreign authorities of selected states that have the above-mentioned issue in their competence.

MS Excel and the Data Analysis tool were used for graphical data processing and for correlation and regression analysis.

Processed documents did not contain data on damage events, that is traffic accidents due to technical defects of vehicles, which were not reported to the Police Force, but only to insurance companies.

4 Technical defects of vehicles as the major cause of traffic accidents in the Slovak Republic

The most common major causes of traffic accidents in the Slovak Republic are a violation of driver's duty, illegal speeding, improper driving through an intersection and so on. Their exact ratio is shown in Figure 1.

The exact ratio of the causes of traffic accidents that resulted in the death of a person in 2020 is shown in Figure 2.

From the presented graphs it is clear that vehicle technical defects, as the major cause of traffic accidents (even fatal ones), is listed in the last places in the Slovak Republic. The same applies to other countries.

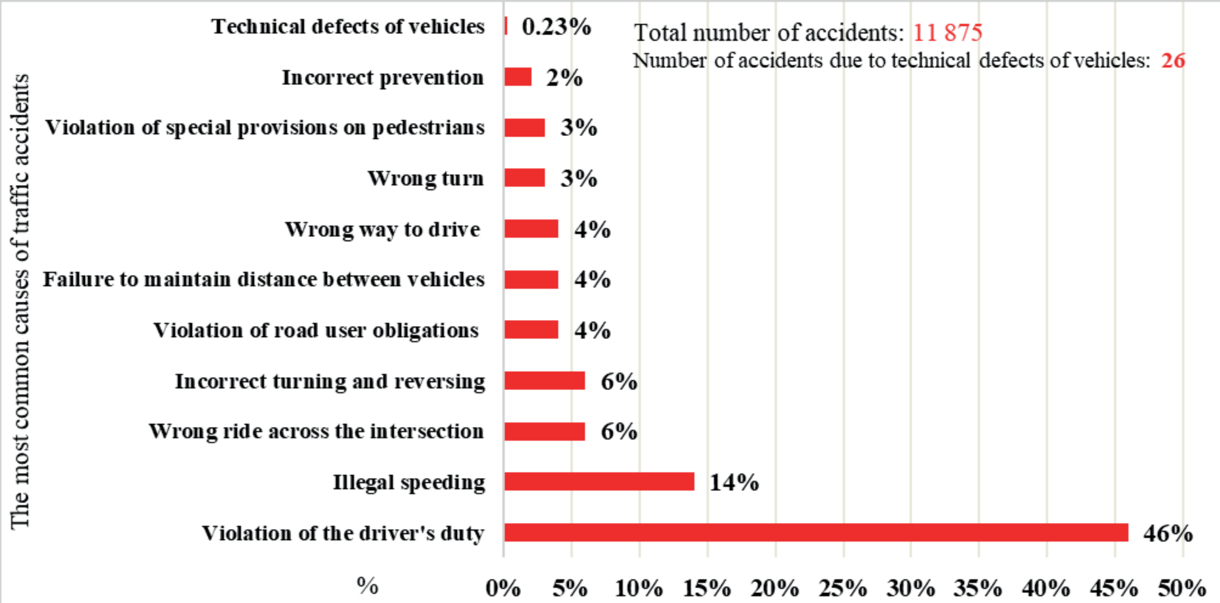

Figure 1 *The most common major causes of traffic accidents in the Slovak Republic in 2020*

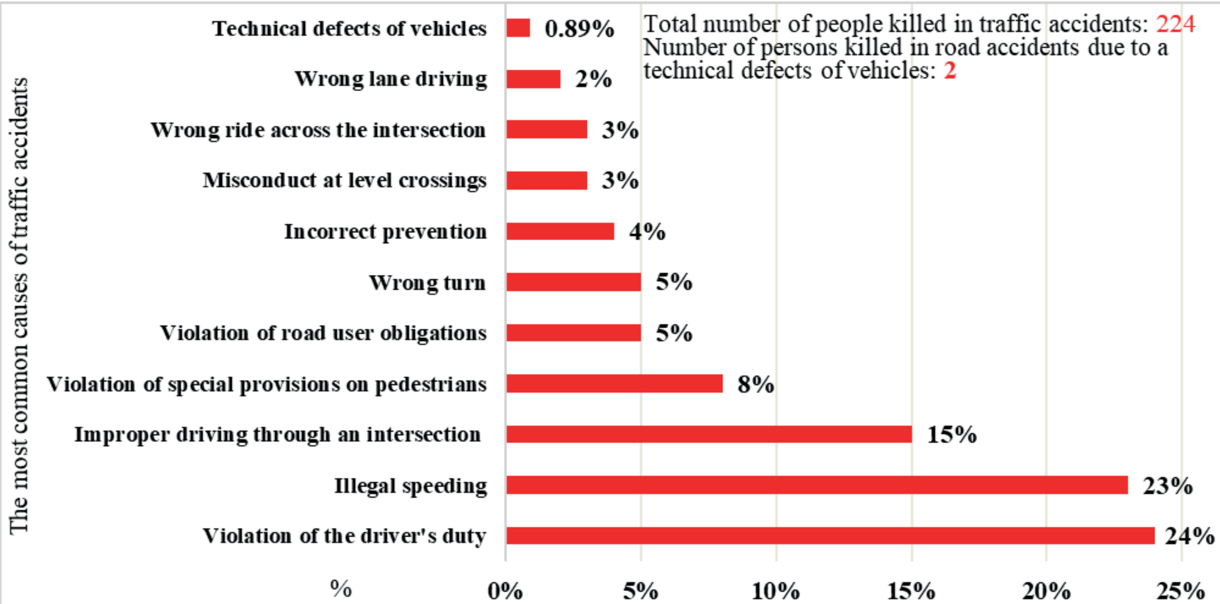

Figure 2 *The most common major causes of traffic accidents in the Slovak Republic that resulted in the death of a person in 2020*

However, their rates vary considerably from one country to another.

Table 5 shows the percentage of traffic accidents caused by vehicle technical defects in selected states and periods.

The presented Table 5 shows that the rate of traffic accidents, caused by vehicle technical defects, as reported by individual countries, varies from one state to another, just as the differences between individual states. For example, in Austria and Germany, the reported accident rate is three times higher than in the Slovak Republic and in contrast to the Slovak Republic, only the traffic accidents that result in injuries are included in it. Likewise, the age of vehicle fleets is different. The reason for this phenomenon is that each state, when determining the cause of the traffic accident, uses a different methodology for assessing technical defects of vehicles as well as assesses these causes differently. For example, in the event of a traffic accident in the Slovak Republic, if a vehicle technical defect is suspected, a court expert from the department of road transport is called in to investigate the cause of the traffic accident. If the expert identifies a technical defect of a vehicle as a major cause of the accident, which, however, has manifested itself on the vehicle for a long time and the driver could and should have eliminated it, the police force will ultimately assess this as a failure to comply with the duties of the driver who used the vehicle that was not supposed to be operated in the road traffic. The same applies to tires. If an accident occurs

***Table 5** Percentage of accidents caused by vehicle technical defects in selected countries and periods*

Country (year)	Proportion of accidents caused by technical defects of vehicles [%]
Slovak Republic (2020)	0.23
Czech Republic (2020)	0.4
Austria (2020)	1.1 (only with injuries)
Germany (2020)	1.2 (only with injuries)
Great Britain (2020)	3.84
USA (average of all the states without the obligation of periodic TI) (2017)	0.83
USA (average of all the states with the obligation of periodic TI) (2017)	0.61

in the Slovak Republic due to loss of adhesion of tires of a vehicle on the road surface in a causal connection with insufficient or inappropriate tire tread, or other wear and tear, or with the vehicle equipped with wheels of the wrong tire size, such a road accident is classified as a non-adjustment of driving to the condition and nature of the road and thus a breach of the driver's duties. Conversely, in Germany, the United Kingdom, the USA and so on, a technical defect of a vehicle is considered to be the cause of road accidents resulting from worn tires with insufficient tread, etc. In the Slovak Republic, only a vehicle technical defect that occurred suddenly and without the possibility of being influenced by a driver, for example by the maintenance of a vehicle, is considered to be the cause of an accident due to a vehicle technical defect. The possible invalidity of the technical inspection and the related non-roadworthiness of the vehicle for road traffic are also not considered. Furthermore, in the Slovak Republic, statistics on the road accidents due to technical defects does not include the so-called damage events, i.e. the traffic accidents, which, under certain conditions, do not have to be reported to the Police, but only to insurance companies (if a person has not been killed or injured, there has been no damage to the road or public utility equipment, there has been no spill of dangerous goods, or some of the vehicles involved, including transported goods, or other property has suffered material damage not exceeding one and a half times the greater damage according to the Criminal Code of the Slovak Republic (in 2021 it was 3,990 euros)). Due to such a procedure, the share of vehicle technical defects in the causes of traffic accidents in the Slovak Republic will inevitably be reflected in the statistics by a low percentage. However, far more such accidents are expected to occur but are not classified as such for the statistical purposes.

For the sake of objectivity, it should also be mentioned that most of the data listed in Table 5 come from countries where the system of periodic technical inspections is in place, which may also have an impact on the declared low accident rates. As far as the USA is concerned, Table 5 contains two figures concerning the USA states. One of them is the proportion of accidents caused by vehicle technical defects, represented by an average percentage for all the US states where the system of periodic technical inspection is not in place and the other is the proportion for all the US states where the system of mandatory periodic technical inspection is in place. The data shows that in the US states where the obligation of technical inspections is in place, the average annual rate of traffic accidents caused by vehicle technical defects was 36% lower in 2017 than in the US states where there is no such obligation. The difference between the two data groups is statistically significant.

5 Analysis of data on traffic accidents due to vehicle technical defects in the Slovak Republic

Based on data provided by the Presidium of the Police Force of the Slovak Republic on vehicles and traffic accidents caused by vehicle technical defects in the period 2016-2020, as well as other related documents from insurance companies, a detailed analysis was performed. The analysis showed that in the monitored period, 260 technical defects were detected in 183 vehicles that were involved in traffic accidents, which were directly caused by these defects. Specific technical defects that have been identified on vehicles as the main cause of road accidents can be broken down according to Figure 3.

It is clear from the graph above that the most common vehicle technical defect that caused the traffic accidents in the Slovak Republic over a period of five years was tire damage with sudden air leakage (90 cases). It is followed by a wheel failure (44 cases) and steering failure (31 cases). Technical defects that caused the least traffic accidents were taillights failure (3 cases), followed by windscreen damage (5 cases) and a wheel lock-up from a mechanical failure (6 cases). Regarding a service brake failure, which is one of the most essential elements of active safety and directional stability of vehicles and the work of technicians of PTI is of great importance in this respect, as the cause of traffic accidents ranks seventh out of twelve with 23 cases. In comparison to other countries, it should be noted that the most common vehicle technical defects that caused traffic accidents in Germany in 2020 were tires and breaks. In the UK it was brakes, tires, vehicle overload

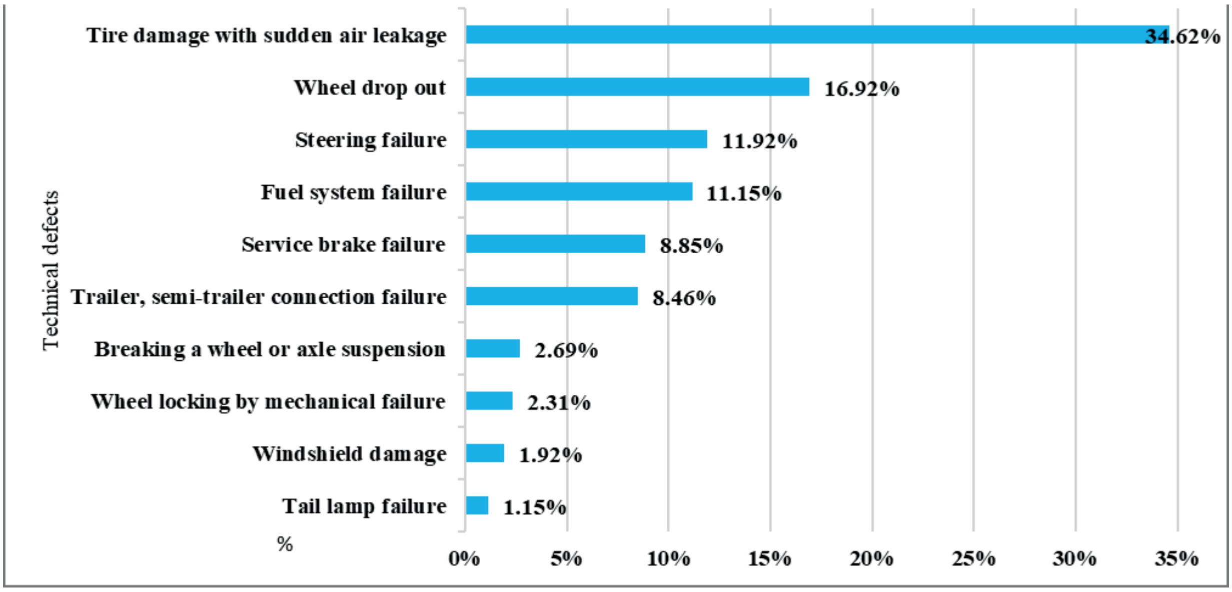

Figure 3 *Technical defects of vehicles that directly caused traffic accidents in the period 2016-2020*

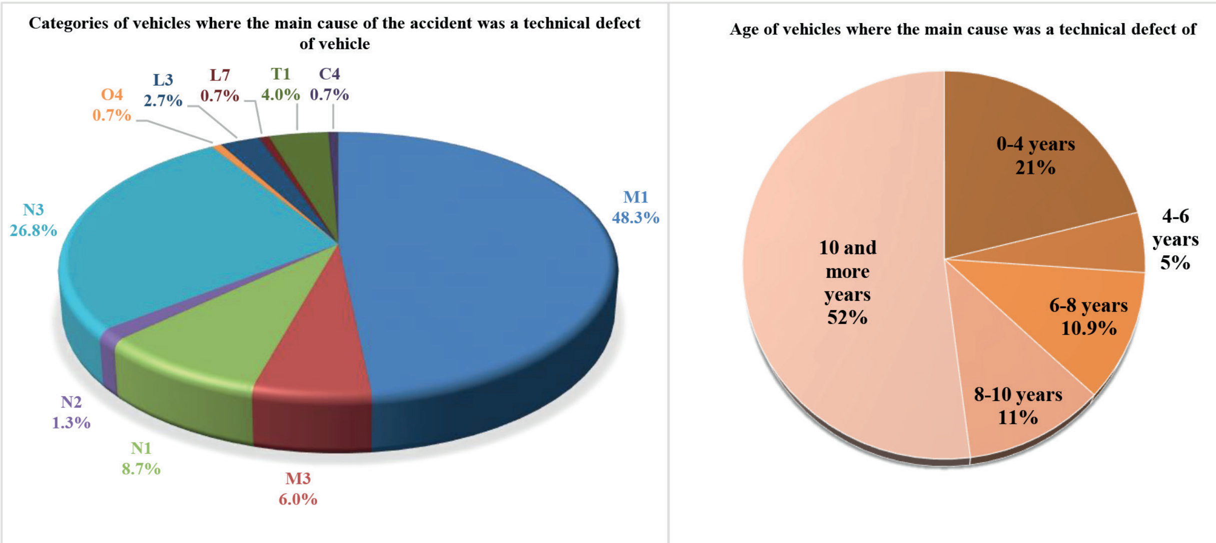

Figure 4 *Percentage of categories of vehicles and age of vehicles, which were involved in traffic accidents due to vehicle technical defects*

and lighting systems, while in the USA it was tires, the so-called other causes, lights (main, brake), steering, brakes and direction indicator lamps. In comparison to the results of PTI, in the Slovak Republic the most frequently detected vehicle defects were in the category of the braking system (almost half of all the detected defects), lighting and reflective electrical equipment, as well as vehicle chassis and its accessories. Defects of axels, wheels, tires and axle suspensions were found in the fifth place only (just 5% of all detected defects).

As regards the categories of vehicles involved in the traffic accidents due to a technical defect, their breakdown is shown in Figure 4.

It is clear from the first graph that majority of the accidents due to vehicle technical defects were caused by vehicles of categories M1 (passengers cars), N3 (commercial trucks) and N1 (light goods vehicles). Categories O4 (heavy goods trailers), C4 (tracked tractors) and L7 (heavy quadricycle) caused the least accidents. The above-mentioned distribution largely also replicates the distribution of the number of registered vehicles in the Slovak Republic and thus the rate of occurrence of the categories of vehicles in question in road traffic, as well. Regarding the age of vehicles involved in the traffic accidents due to technical defects, the second figure clearly shows that majority of such accidents were caused by vehicles older than 10 years (52 %). The second most numerous age category of vehicles that was involved in traffic accidents was surprisingly the category 0 to 4 years, i.e. new vehicles (21 %).

The distribution of age and odometer status of vehicles involved in traffic accidents due to a technical defect are illustrated in Figure 5.

The average age of all the vehicles that caused a traffic accident due to a technical defect was 11.01

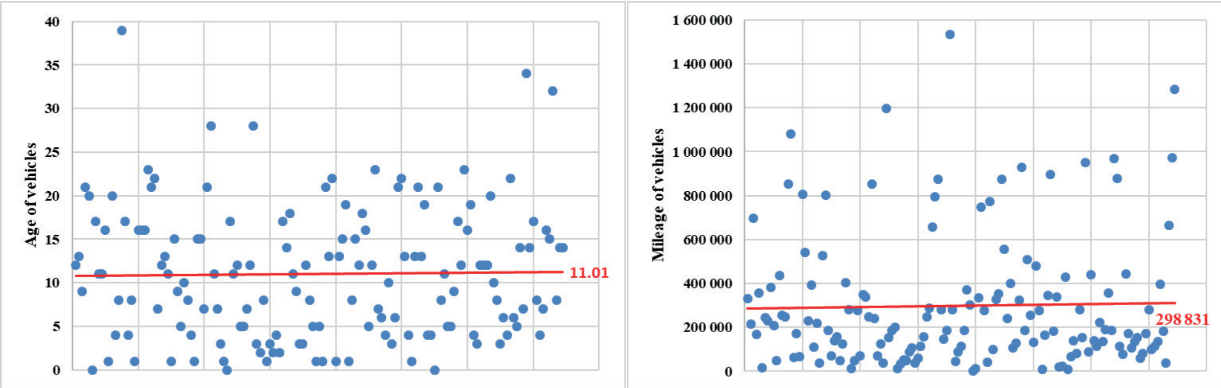

Figure 5 *Distribution of age and odometer status of vehicles involved in traffic accidents due to a technical defect*

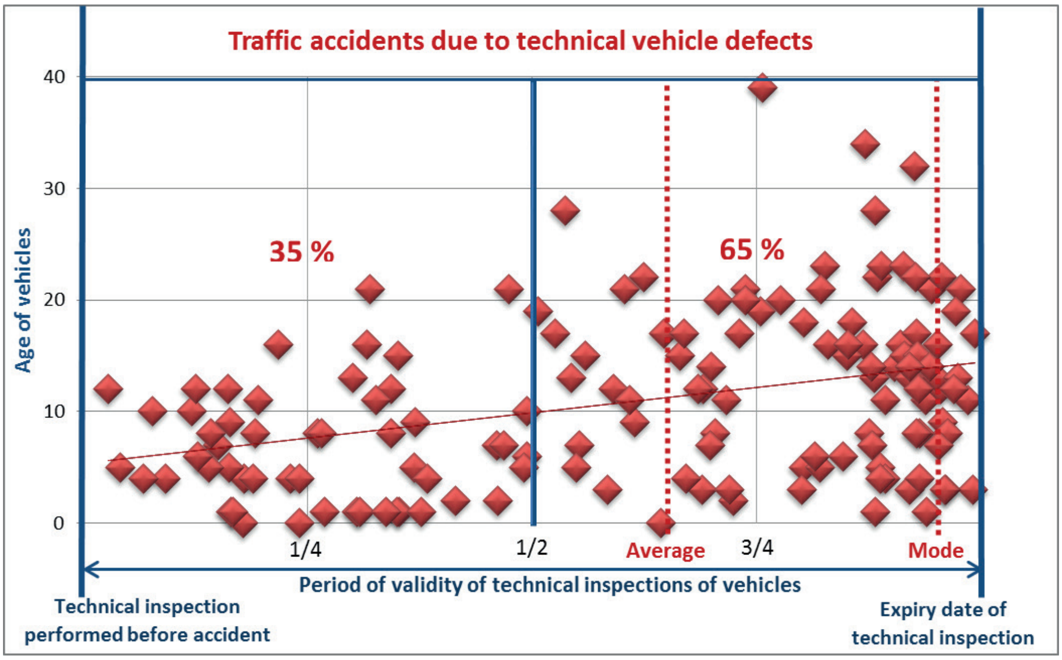

Figure 6 *Temporal distribution of all the accidents due to vehicle technical defects in the period from the performance of the technical inspection prior to the accident until the end of its validity*

years (10.5 years for vehicle categories M1 and N1), which is less than the average age of the vehicle fleet in Slovak Republic (13.03 years). However, the graph also shows that technical defect occurred in the new vehicles, as well and was the main cause of the accident when it comes to these vehicles.

In terms of the odometer status of vehicles, for which a technical defect was the main cause of the traffic accident, it is clear from the graph that the average mileage that all those vehicles had at the time of an accident was 298 831 (171 343 km for category M1 and N1). Here too, however, the graph shows that even the vehicles with low mileage in many cases had technical defects that caused the traffic accident.

In terms of the consequences of traffic accidents due to vehicle technical defects, the statistics for 2016-2020 showed that 73 people were slightly injured, 10 people were seriously injured, 3 people were killed and a total of EUR 2,529,690 of damage was quantified in these road accidents.

6 Examination of traffic accidents due to vehicle technical defects in terms of their temporal distribution during the period of validity of the technical inspection and the age of the vehicles

Based on the data on the exact dates of traffic accidents due to technical defects of the examined vehicles in the period 2016-2020, it was determined when the vehicles were last subjected to the periodic technical inspection prior to the date of the accident and what was the validity period of this inspections. In the case of new vehicles which, according to the legal regulations of the Slovak Republic, were not yet subject to periodic technical inspection, the date of the first registration was considered to be the date of the technical inspection before the traffic accident. Based on determination of the period of validity of technical inspection of examined vehicles at the time of traffic accidents due to technical defects of these vehicles,

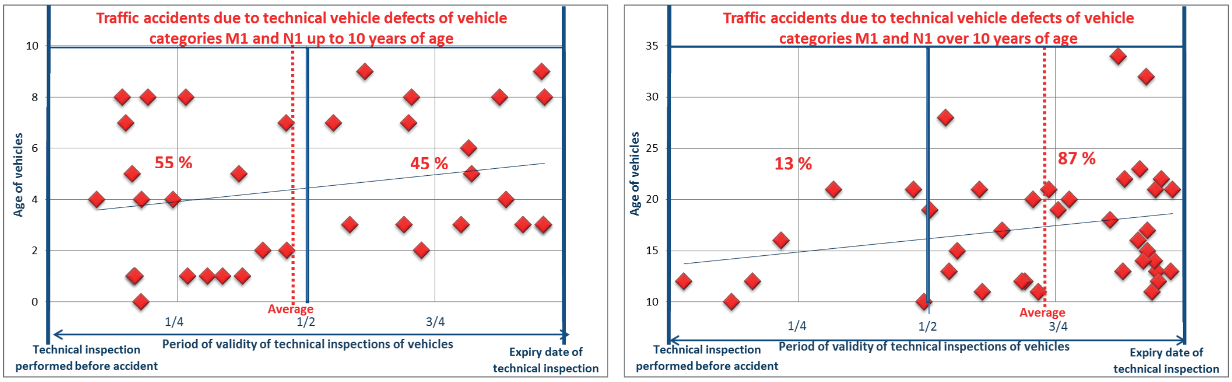

Figure 7 *Temporal distribution of traffic accidents due to technical defect of M1 and N1 category of vehicles aged up to 10 years and over 10 years in the period from the performance of technical inspection before the accident to the end of its validity*

the scatter graph (Figure 6) was subsequently created, into which data were transferred on the exact time of traffic accidents caused by technical defects of examined vehicles, which happened in the period from the latest technical inspection before the accident to its validity period.

The temporal distribution of all accidents due to vehicle technical defects in the period from the performance of the technical inspection before the accident until the end of its validity is illustrated in Figure 6.

The visual display of the data in the graph showed that vehicle accidents due to a technical defect occurred throughout the period of validity of their technical inspections, but the largest clusters were formed before the end of the validity of technical inspections. The calculated accident modus due to a vehicle technical defect is located in the graph approximately one month before the end of the validity of technical inspections. Thus, during that period happened majority of the traffic accidents due to vehicle technical defects. On average, however, traffic accidents due to vehicle technical defects occurred at the end of the second third of the period of validity of the technical inspection. Of all the traffic accidents caused by a vehicle technical defect, 35% occurred in the first half of the period of validity of the technical inspection and 65% of them occurred in the second half.

Subsequently, the same was done, but for vehicle categories M1 and N1. In fact, compared to other categories, most road accidents due to vehicle technical defects were recorded in the case of category M1 vehicles, which pose the greatest risk in terms of road safety. Moreover, the N1 vehicle category is similar to the M1 category. Therefore, special attention had to be paid to such vehicles. Those vehicle categories were therefore separately divided into two groups. The first group consisted of all the traffic accidents involving vehicles of categories M1 and N1, which were less than 10 years old at the time of the traffic accident. The second group consisted of all the accidents involving M1 and N1 vehicles, which were older than 10 years at the time of the accident. For these two groups, the two graphs were prepared (Figure 7), which depicted the temporal distribution of traffic accidents in the period from the performance of the technical inspection before the traffic accident to the end of its validity.

The temporal distribution of traffic accidents due to technical defect of M1 and N1 category of vehicles aged up to 10 years and over 10 years in the period from the performance of technical inspection before the accident to the end of its validity is illustrated in Figure 7.

The visual display of the data in the graph showed that traffic accidents due to technical defects of M1 and N1 vehicles with an age of less than 10 years usually occurred proportionally throughout the period of validity of their technical inspections, with a slight predominance in the first half of the period of validity of the periodic technical inspection, during which occurred 55% of traffic accidents. In the second half, on the other hand, occurred 45% of accidents. *Ratione temporis*, during the period of validity of the periodic technical inspection and age distribution, no anomalies or clumps occurred during traffic accidents. It could therefore be deduced from the above that newer vehicles have not yet been involved in traffic accidents due to technical defects, which would be affected by the technical inspection or its impending expiry date and the associated deterioration of the technical condition of the vehicles. Likewise, it is not possible to observe a clear dependence on vehicle age when it comes to occurrence of defects on vehicles. Only modest, as there is a slight increase in traffic accidents involving older vehicles in the second half of the period of validity of the periodic technical inspection. Traffic accidents due to vehicle technical defects of categories M1 and N1 aged up to 10 years are therefore probably due to other reasons, in particular, manufacturing defects found in certain vehicle components.

The situation was diametrically different in the case of vehicle categories M1 and N1 that are aged over 10 years. In this group, the traffic accidents due to vehicle technical defects were occurring to an incomparably greater extent only in the second half of the period of validity of their technical inspection. According to the

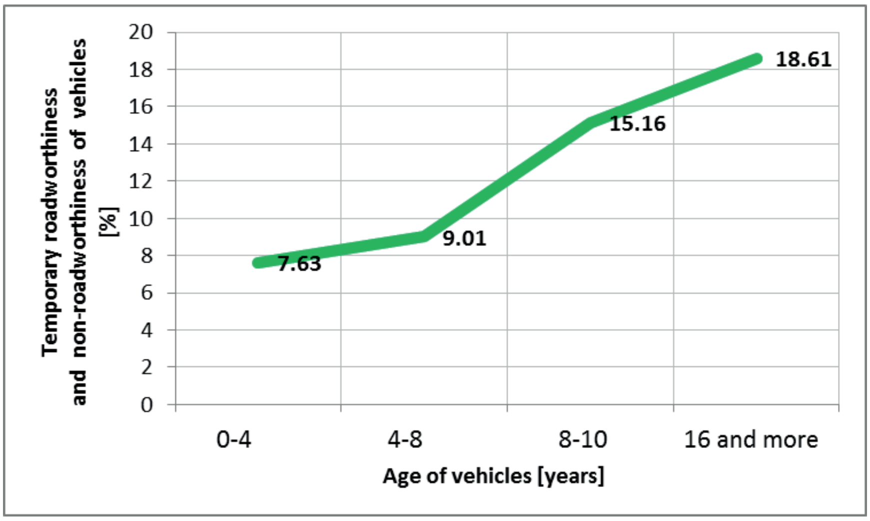

Figure 8 *Dependence of occurrence of the vehicle defects on the age of the vehicle in the Slovak Republic in the period 2019 - 2021*

legislation of the Slovak Republic, vehicle categories M1 and N1 are to be subjected to periodic technical inspections for the first time four years after the first registration and then at two-year intervals. The transformation of the period of validity of technical inspections of vehicles over 10 years of age into two-year periods showed that in the first year after the periodic technical inspections were carried out occurred only 13% of traffic accidents involving these vehicles. However, in the second year of validity of the technical inspection occurred up to 87% of traffic accidents due to technical defects on the vehicles cited.

Based on the above visual displays of the temporal distributions of traffic accidents due to technical defects in vehicles, it could be concluded that periodic technical inspections of vehicles have a demonstrable justification. With the approaching end of the period of validity of the periodic technical inspection, the incidence of traffic accidents due to vehicle technical defects and, consequently, the probability of their occurrence also increased rapidly. Moreover, since, according to Figure 4, the most traffic accidents due to vehicle technical defects involved vehicles of category M1 and at the same time the average age of vehicles of categories M1 and N1 that had a traffic accident due to a technical defect was 10.5 years, it could be deduced that by halving the validity of the periodic technical inspection for vehicles of categories M1 and N1 that are over 10 years of age, i.e. to one-year intervals, the number of traffic accidents due to technical defects of these vehicles could also fall by at least a half.

In this context, it should be noted that the age of vehicles constitutes a very strong factor that influences the incidence of vehicle defects. This can be empirically demonstrated. Data for the period 2019 – 2021, concerning the results of the assessment of the technical condition of vehicles at the PTI in the Slovak Republic, were selected from the information system of technical inspections of the Slovak Republic, namely the sum of percentages of temporary roadworthiness and non-roadworthiness of vehicles for the road traffic (i.e. the proportion of vehicles in which at least one serious or dangerous defect was detected) according to age bands. The above was selected from a total of all 3,554,432 periodic technical inspections and the related data are recorded in Figure 8.

From the graphic course of temporary roadworthiness and non-roadworthiness of vehicles, which was assessed on average by PTI in the Slovak Republic, it is visually clear that, in correlation with the increasing age of vehicles, the number of major and dangerous defects found on these vehicles during the technical inspections is also increasing. Thus, 7.63% of major and dangerous defects were found in vehicles aged 4 years and under and up to 18.61% of major and dangerous defects were found in vehicles over 16 years of age [37].

The above can also be verified through the correlation analysis. The value of the Pearson's correlation coefficient r(*X, Y*) of two variables *X*, *Y*, which is defined as the ratio of the covariance S_{XY} and the product of their standard deviations S_x S_y, is calculated according to:

$$r(X,Y) = \frac{S_{XY}}{S_X S_Y} = \frac{\sum_{i=1}^{n}(X_i - \bar{X})(Y_i - \bar{Y})}{\sqrt{\sum_{i=1}^{n}(X_i - \bar{X})^2}\sqrt{\sum_{i=1}^{n}((Y_i - \bar{Y}))^2}}. \quad (1)$$

The correlation coefficient of the dependence of the occurrence of vehicle defects (dependent variable) on the age of the vehicle (independent variable) in the Slovak Republic was calculated as r(*X, Y*) = 0.98, which is interpreted as a very strong correlation. The significance of this correlation coefficient was verified by the p-value test. Statistical P-value = 0.020346 < α (0.05), i.e. the null hypothesis H0 is rejected and the alternative

***Table 6** Assessment of the technical condition of vehicles by the PTI as temporarily roadworthy and not roadworthy and the number of traffic accidents caused by vehicle technical defects in each year in the period 2012 - 2020*

Year		2012	2013	2014	2015	2016	2017	2018	2019	2020
Temporarily roadworthy and not roadworthy vehicles	Quantity	30 757	40 835	58 130	98 689	97 114	70 627	84 711	162 836	165 629
	%	3.16	3.79	5.42	8.64	7.96	5.7	6.8	13.03	13.58
Accidents due to technical defects	Quantity	48	49	46	39	37	47	37	35	26

hypothesis H1 is accepted that there is a statistically significant linear relationship among y a x at the level of significance α = 0.05.

This phenomenon is also evidenced by other studies conducted with a similar focus in other EU countries. In Finland, for example, over the period 2011-2015, on a sample of 13 million vehicles that underwent technical inspections, carried out research on the dependence of the number of major and dangerous defects found during technical inspections on vehicles on their age. It also follows from the above that as the age of vehicles increases, so does, quite significantly, the number of serious and dangerous defects found on vehicles during the technical inspections. In addition, in Germany, a survey was conducted in 2004 focusing on the effect of vehicle age on vehicle defect rate on a sample of 3 million vehicles during technical inspections and it was shown that 10% of major defects were found in vehicles around 4 years of age. In the case of vehicles older than 9 years, the defect rate increased to more than 31% [36]. However, this phenomenon is not accidental and does not concern only one year or one state. Studies from Sweden and Great Britain also prove it [36]. Passenger cars in Sweden and the so-called heavy vehicles from Great Britain show very similar trends.

It is therefore clear from the above that the factor that most influences the occurrence and number of technical defects found on vehicles during the technical inspection is the age of the vehicles and therefore shortening the interval of periodic technical inspections for older vehicles and categories, which suffered the most traffic accidents due to vehicle technical defect, would be highly justified. The PTI exclude from traffic a number of old vehicles with major and dangerous defects that pose a threat to road safety. These one-year periods of periodic technical inspections of M1 and N1 vehicles also apply in other EU countries, such as Finland, Latvia, the Netherlands, Spain, Estonia, Belgium, Bulgaria, Austria, etc.

7 Correlation of results of vehicles' technical inspections with traffic accidents due to vehicle technical defects

The purpose of periodic technical inspections of vehicles is to identify defects in vehicles, their parts, systems, components, or separate technical units in order to exclude from the road traffic technically non-roadworthy vehicles that pose a risk to health, lives, property and the environment. This leads to the hypothesis that the operation of PTI prevents the incidence of traffic accidents and thus has a positive effect on the road safety. However, this assumption cannot be unambiguously quantified. It is very difficult to identify and measure the direct causal link between the operation of PTI and the number of accidents caused by vehicle technical defects. Especially when technical inspections of vehicles have been carried out on the territory of the Slovak Republic for more than 70 years and therefore it is not possible to compare the state of accident rate before and after the introduction of these PTI. Similarly, statistics on traffic accidents due to vehicle technical defects do not create an objective picture of reality.

For this reason, a simple pairwise correlation and regression analysis was used to identify and measure the effect of periodic technical inspections of vehicles on accident rate due to vehicle technical defects. Within this framework, the correlation of the results of technical inspections of vehicles with the number of traffic accidents caused by vehicle technical defects in the period 2012 - 2021 was examined. The results of technical inspections of vehicles are represented by the number and percentage of temporary roadworthiness and non-roadworthiness of vehicles, which were assessed on average by the PTI in each year of the monitored period. Given that in the Slovak Republic the methodology for assessing traffic accidents due to vehicle technical defects did not change during the period under examination and therefore the data examined were not influenced by unknown variables. The monitored data (temporarily roadworthy and not roadworthy vehicles and traffic accidents due to technical defects) are recorded in Table 6.

The Pearson correlation coefficient was used to calculate the correlation rate between the temporarily roadworthy and not roadworthy vehicles (independent variable X) and the number of accidents due to vehicle technical defects (dependent variable Y). In order to eliminate doubts about the data of the independent variable, two correlation coefficients were calculated. The first was based on the number of temporarily roadworthy and not roadworthy vehicles and the second on the percentage rate of temporarily roadworthy and not roadworthy vehicles.

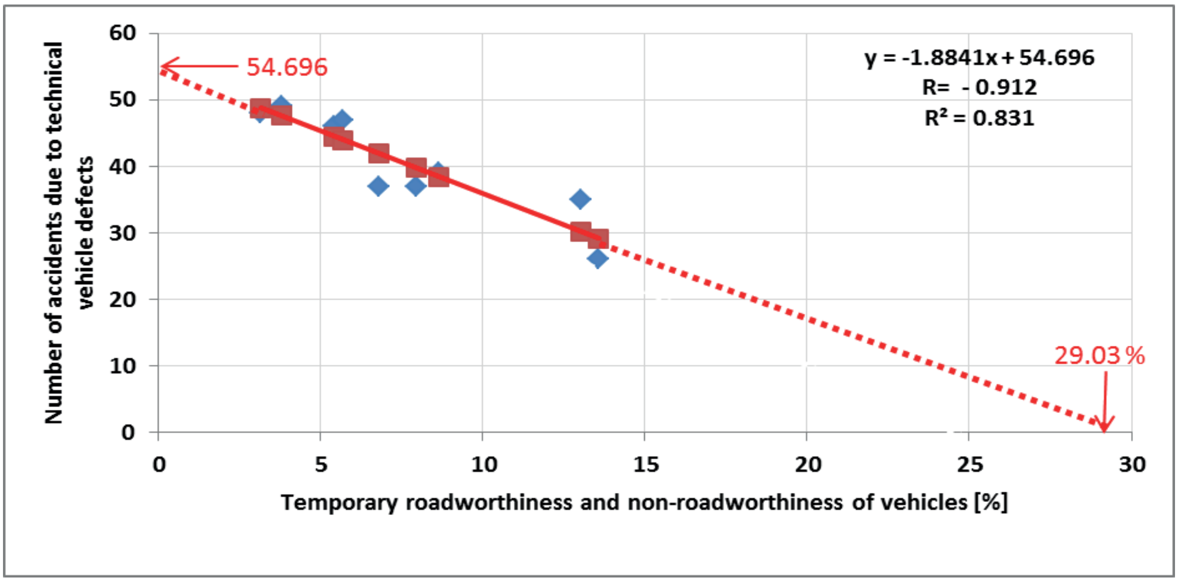

Figure 9 *Regression line and function*

The first correlation coefficient was calculated as r(*X, Y*) = -0.91, when the independent variable was the number of temporarily roadworthy and not roadworthy vehicles and the second correlation coefficient was calculated as r(*X, Y*) = - 0.912, when the independent variable was the percentage rate of temporarily roadworthy and not roadworthy vehicles. In both cases, this is interpreted as a very strong negative correlation. The significance of these correlation coefficients was verified by the p-value test. Statistical p-value = 0.000641 <α (0.05) if the independent variable was the number of temporarily roadworthy and not roadworthy vehicles and p-value = 0.000614 <α (0.05) if the independent variable was the percentage rate of temporarily roadworthy and not roadworthy vehicles. In both cases, therefore, the null hypothesis H0 was rejected and the alternative hypothesis H1 was accepted, i.e. there is a statistically significant linear relationship between *X* and *Y* (between the number of temporarily roadworthy and not roadworthy vehicles and the number of accidents due to vehicle technical defects) at the level of significance α = 0.05. This means that with the increasing number of vehicles assessed at the PTI as temporarily roadworthy and not roadworthy, the number of traffic accidents due to vehicle technical defects decreases. In view of the almost identical values of the calculated correlation coefficients, in order to simplify the interpretation of the results, only the correlation coefficient calculated from the percentage rate of temporary roadworthiness and non-worthiness was used for further mathematical modeling.

As a very high degree of correlation between the results of technical inspections given by the percentage rate of temporary roadworthiness and non-worthiness of vehicles and the number of traffic accidents due to vehicle technical errors with a statistically significant linear relationship was demonstrated, it was possible to determine a regression function.

The linear regression function is represented by a straight line that describes the linear relationship between the dependent variable Y and the independent variable X. The regression model of this line is estimated by the least-squares method, which minimizes the sum of squares of the residual deviations. The line estimated by the least-squares method is as close as possible to all actual values. The result is graphically recorded in Figure 9.

The regression function was determined in the form y = -1.8841x + 54.696. The value of R^2 (R Square) is the value of the coefficient of determination and in this case, it has a value of 0.831. This value, after multiplying by 100, indicates that the selected regression function explains the variability of the number of road accidents due to vehicle technical defects to approximately 83.1%. The other part presents unexplained variability, the influence of random factors and other unspecified influences.

The null hypothesis H0 was tested in ANOVA, which states that the regression model chosen to explain the dependence (in this case a linear regression line) is not suitable. The alternative hypothesis H1 claims the opposite. An F test was used to evaluate this claim. Significance F = 0.000614 <0.05 (α - significance level), i.e. H0 is rejected and H1 is selected, which means that the regression model was selected correctly.

Based on the regression function, it was subsequently calculated by what rate of temporary roadworthiness and non-worthiness of vehicles would have to PTI in the Slovak Republic assess on average vehicles so that the number of road accidents due to technical defect would fall to zero. The value of this locating constant is 29.03%. In the graph, this is expressed by extending the regression line shown by the dashed line to the intersection with the X-axis. Value of the second locating constant is 54.696 (the number of road accidents due to technical defect, if the rate of temporary roadworthiness and non-worthiness of vehicles would by zero).

8 Conclusion and discussion

In connection with the elaboration of the topic, research of world literature was carried out, consisting of articles and studies that dealt with the issue of vehicle technical defects as the cause of traffic accidents and the effect of periodic technical inspections on the reduction of traffic accidents due to a vehicle technical defect. At the same time, some of these studies sought answers to questions about the justification for periodic technical inspection systems. Publications concerned showed that the proportion of traffic accidents caused by a direct causal link with vehicle technical defects to all the traffic accidents ranged from 1% to 24% and by an indirect causal link from 0.6% to 28%. Furthermore, the studies examining the effect of periodic technical inspections on traffic accidents showed that the effect of the system of technical inspection on accident rate ranged from no effect to a reduction in accident rate from 16% to 21%, or up to 50% and therefore periodic technical inspections are justified. However, some studies have argued the exact opposite [38].

The problem of the publications dealing with the technical defects of vehicles was that they covered a long period from 1967 to 2021 and the period, in which the older studies were created, which were the most numerous, were based on the period conditions (level of a vehicle fleet, roads, technical inspections, etc.), which were different from the current ones. These publications are therefore not entirely up to date as regards the empirical nature of the data and their direct use, but are definitely worth noting. Another problem was that just a few studies dealt purely with the mentioned topic, the sources of the data used in publication suffered from heterogeneity and were methodically differently processed. However, none of the publications examined the incidence of the traffic accidents in the period between the performance of technical inspections and the end of their validity, as well as the link between the results of the PTI of vehicles given by the temporary roadworthiness and non-roadworthiness of vehicles and the number of traffic accidents, what was examined in this article.

Regarding the publications, it should also be noted that, in particular, recent US studies (but also the older ones), differ significantly from European ones in that they increasingly call into question the system of mandatory periodic technical inspections of vehicles, which are gradually being abolished in individual US states [31]. This phenomenon largely reflects the social setting in the US, where there has long been controversy over whether the periodic technical inspections of vehicles are a cost-effective way to increase the road safety [25]. In particular, the analysis of changes in technical control procedures (in the US called security inspections), carried out in the US in 2017, raised many doubts about the effectiveness of these controls. According to the above analysis, the number of fatal accidents due to vehicle technical defects has been steadily decreasing over the last two decades, as well as due to the safer technology of newer vehicles [25]. However, the economic dimension plays a major role in this, because periodic technical inspections and subsequent repairs of vehicles represent financial costs for the inhabitants of the given states and thus their abolition, i.e. their absence is a politically popular topic.

As regards the traffic accidents due to vehicle technical defects in the Slovak Republic, it is clear that from the statistics that their rate is reported very low, as in other EU countries. The reason for that is the strict methodology of their assessment, according to which only a vehicle technical defect, which occurred suddenly and which the driver of the vehicle could not influence in any way, is to be considered the main cause of the traffic accident. Moreover, this must also be established by a court expert. The main goal of the police in investigating the cause of the traffic accident is to try to assign responsibility for the traffic accident due to a specific person and not to the technical condition of the vehicle, because if the vehicle is to be blamed, no penalty is imposed. In the event of a failure to comply with a person's obligations, a fine is imposed on that person. Therefore, it is assumed that the actual number of traffic accidents due to vehicle technical defects is higher than the one in reported statistics. Moreover, each country has its own methodology for assessing the technical defects as the main cause of accidents. For this reason, statistics on the number of traffic accidents due to vehicle technical defects suffer from heterogeneity, do not reflect reality and therefore it is not possible to marginalize the importance of the periodic technical inspection only based on their reported low rate.

Despite the low amount of information, data on traffic accidents due to vehicle technical defects in the Slovak Republic in the period of five years (2016-2021) were comprehensively processed. Their analysis showed that more than a half of the accidents due to vehicle technical defects were caused by tires (sudden air leakage and wheel failure), especially in terms of older vehicles with high mileage and vehicles of the M1 category. The above also corresponds to the most common vehicle technical defects that caused accidents abroad. Conversely, according to the statistical results of the assessment of the technical condition of vehicles at PTI in the Slovak Republic, the most frequent defects on vehicles were found on brake systems (almost half of all detected defects), lighting, reflective electrical equipment and chassis and its accessories. Defects of axels, wheels, tires and axle suspensions were found in the fifth place only (just 5% of all the detected defects). This may also be since inspection operations during which the tires are being checked at the PTI (inspection items of group no. 5 axles, wheels, tires and suspension [2]) cannot be objectively inspected at the level of inspection bodies [39]. Although cameras are installed at the PTI in the Slovak Republic, for the purposes of supervision by the inspection bodies, through their use, however, it is not possible to check mainly essential inspection operations, for example how a technician of a PTI assesses braking systems. This then has a significant effect on the operation of the PTI, where in inspection items of group no. 1 (braking systems) technicians detect the most serious and dangerous defects on vehicles.

Furthermore, the article examined traffic accidents due to vehicle technical defects in terms of their temporal distribution during the period of validity of the technical inspection and the age of the vehicle. The purpose of that examination was to seek evidence confirming or refuting the justification for periodic technical inspections of vehicles. As a part of this, graphs were drawn up in which data on traffic accidents due to vehicle technical defects were set into the period of validity of the technical inspection, which was limited along the x-axis by the date of the technical inspection before the accident. At the same time, these accident data were also distributed in terms of the vehicle's age along the y-axis. Three of these graphs were constructed. The first graph (Figure 6) covers all the traffic accidents and all the categories of vehicles for the period 2016 - 2021, the other two graphs (Figure 7) show data on traffic accidents of only categories M1 and N1 on the grounds that category M1 had the largest share of these traffic accidents and vehicle category N1 is similar to category M1. With regard to vehicle categories M1 and N1 up to 10 years of age, according to Figure 7, accidents generally occurred proportionally throughout the period of validity of their technical inspections, with a slight predominance in the first half of the period of validity of the periodic technical inspection. Here, 55% of traffic accidents occurred, compared to 45% in the second half. Newer vehicles have therefore not yet been subject to traffic accidents due to vehicle technical defects that would be affected by technical inspection, i.e. its approaching expiry date and the associated deterioration of the technical condition of the vehicles, but for other reason, such as manufacturing defects in different vehicle components. According to Figure 7, the proportion of the traffic accidents due to technical defects of M1 and N1 vehicles over 10 years of age was only 13% in the first year since the performance of the technical inspection and in the second year of the validity of the technical inspection that share was up to 87%. On average, traffic accidents were occurring in this category no more than half a year before the end of the validity of the periodic technical inspection. It follows from the above that with the approaching end of the period of validity of periodic technical inspection, the occurrence of traffic accidents due to vehicle technical defects was rapidly increasing and thus also the probability of their occurrence. By reducing the mandatory two-year periods of periodic technical inspections of M1 and N1 vehicles that are older than 10 years by half, could hypothetically also reduce by more than half the number of traffic accidents due to technical defects of this group of vehicles. It is, however, debatable in this case whether the actual occurrence of defects in the vehicles, which cause the accidents at most in the period before the end of the validity of technical inspection was affected by the expiring period of the validity of the technical inspection or was that a random phenomenon. However, in this case, it should be noted that this phenomenon has a rational justification, as after a successful technical inspection, an owner of a vehicle is no longer motivated to have the vehicle inspected and defects fixed since he does not have to. For this reason, over time, within the period limited by the previous and the following periodic technical inspection, dangerous technical defects may occur (especially in the older ones), which are not known to the vehicle owner and which cause a traffic accident.

In the last part of the present article, an empirical identification and measurement of the effect of periodic technical inspection of vehicles on accident rate due to vehicle technical defects were carried out by means of a simple pairwise correlation and regression analysis. In particular, the links between the results of technical inspections of vehicles and traffic accidents due to technical defects were examined. The Pearson correlation coefficient was used to calculate the correlation rate between temporarily roadworthy and not roadworthy vehicles and the number of accidents due to vehicle technical defects in the period 2012-2021. The above correlation coefficient was calculated as $r(X, Y) = -0.912$. This is interpreted as a very strong negative correlation and its significance was confirmed by a statistical test by means of a p-value. It follows from the above that as the number of vehicles assessed as temporarily roadworthy and not roadworthy by PTI increases, the number of traffic accidents due to vehicle technical defects decreases. Subsequently, the regression function in the form $y = -1.8841x + 54.696$ was determined and graphically portrayed together with the regression line (Figure 9). Based on the cited function, it was calculated that with an 83.1% probability, if vehicles in the Slovak Republic are to be assessed at PTI by an average of 29.03% rate of temporary roadworthiness and not roadworthiness, the number of traffic accidents due to vehicle technical defects will drop to zero. However, the question, in this case, could be whether the strong correlation found between the percentage of temporarily roadworthy and not roadworthy vehicles and the number of accidents due to vehicle technical defects is in fact the result of causal links, or only causality. The temporal link of phenomena does not always mean that there is a causal link between them. Many correlations are purely random and contain other hidden or intervening variables. However, in the case of the calculated correlation between the results of the assessment of vehicles at PTI and the number of traffic accidents, there are logical causal links that militate against the time coincidences in trends.

The results formulated in this paper show that periodic technical inspections of vehicles have a measurable effect on traffic accidents due to vehicle technical defects and therefore have demonstrable justification. As the consequences of traffic accidents due to technical defects tend to be fatal, it is not appropriate to perceive mandatory technical inspections as just a financial burden for citizens, but as one of the effective tools for improving road safety. At the same time, periodic technical inspections of vehicles fulfil their purpose indirectly through the psychological effect that they have on vehicle operators. Awareness of the obligation to undergo a periodic technical inspection of a vehicle causes that certain defect on vehicles are being preventively fixed by the vehicle owners even before the performance of such inspection, thereby contributing in this manner to their safety as well as others [40]. Without this, they probably would not have any incentive to behave like this.

However, a prerequisite for an effective system of periodic technical inspection is that PTI will carry out their duty with better quality and realistically identify all the serious and dangerous defects on vehicles during the periodic technical inspections, which could endanger road safety. In this way, they could prevent traffic accidents that occur due to vehicle technical defects. Therefore, instead of calling the systems of periodic technical inspections into question, national authorities should rather take more stringent measures to improve the performance of PTI (especially at the EU level), such as the introduction at PTI of compulsory accreditation under ISO 17020 [41], which has a demonstrably positive effect on the quality of the PTI activity [42], as well as pay attention to inspections of PTI. As an example may serve the Slovak Republic, where inspection bodies effectively control the activities of technicians through cameras, thanks to which, after the introduction of this control system, the rate of temporary roadworthiness and non-worthiness in the assessment of vehicles at PTIs increased significantly and, in correlation with this, decreased the number of traffic accidents due to vehicle technical defects.

Acknowledgment

This research was funded by the project of institutional research of the Faculty of Operation and Economics of Transport and Communications, University of Zilina no. 2/KCMD/2021 Research on the impact of urban logistics on the environment.

This publication was realized with support of Operational Program Integrated Infrastructure 2014 - 2020 of the project: Innovative Solutions for Propulsion, Power and Safety Components of Transport Vehicles, code ITMS 313011V334, co-financed by the European Regional Development Fund.

References

[1] Roadworthiness package. Regulation of the European Parliament and of the Council on periodic roadworthiness tests for motor vehicles and their trailers and repealing. Directive 2009/40/EC and Regulation of the European Parliament and of the Council on the technical roadside inspections of the roadworthiness of commercial vehicles circulating in the Union and repealing Directive 2000/30/EC and Regulation of the European Parliament and of the Council amending Council Directive 1999/37/EC on the registration documents for vehicles. Brussels: European Commission, 2012. SWD(2012) 206 final.

[2] Directive 2014/45/EU of the European Parliament and of the Council on periodic roadworthiness tests for motor vehicles and their trailers and repealing Directive 2009/40/EC.

[3] FAZZALARO, J. Periodic motor vehicle safety inspections. Connecticut General Assembly Office of Legislative Research, 2007. 2007-R-0591.

[4] ASANDER, S. Vehicle safety inspection systems. In: Conference and Workshop Wheels ’92: proceedings. 1992.

[5] RACQ submission to travelsafe committee. Does Queensland need compulsory periodic inspections of passenger vehicles? Queensland: RACQ, 1990.

[6] ROMPE, K., SEUL, E. Advantages and disadvantages of conducting roadworthiness tests to monitor the mechanical condition for private cars, the impact of such tests on road safety, environmental protection and the renewal of the vehicle fleet and the scope for introducing roadworthiness testing throughout the European community. Final report commissioned by the Directorate-General for Transport, VII/G-2 of the Commission of the European Communities, Drawn up by the TUV Rheinland, 1985.

[7] GRANDEL, J. Investigation of the technical defects causing motor vehicle accidents. *SAE International Congress and Exposition* [online]. 1985, 850434. ISSN 0148-7191, e-ISSN 2688-3627. Available from: https://doi.org/10.4271/850434

[8] MCLEAN, A. J., AUST, H. S., BREWER, N. D., SANDOW, B. L. Adelaide in-depth accident study. Part 6: Car accidents. Adelaide: The University of Adelaide, 1979. ISBN 0-908204-02-7.

[9] TREAT, J. R. Tri-level study of the causes of traffic accidents: an overview of final results. In American Association for Automotive Medicine Annual Conference 1997: proceedings. Vol. 21. 1997. p. 391-403.

[10] HAWORTH, N., SMITH, R., BRUMEN, I., PRONK, N. Case-control study of motorcycle crashes. Australia: Federal Office of Road Safety, 1997. Report CR 174.

[11] HAWORTH, N., VULCAN, P., BOWLAND, L., PRONK, N. Estimation of risk factors for fatal single vehicle crashes. Victoria, Australia: Monash University Accident Research Centre, 1997. Reports No. 121.

[12] CASE, M., DE FOREST, R., YOUNGMAN, J. H. R. Compulsory periodic vehicle inspections. Technical Paper SAE. 1991. No. 912587.

[13] RECHNITZER, G., HAWORTH, N., KOWADLO, N. the effect of vehicle roadworthiness on crash incidence and severity. Victoria, Australia: Monash University, Accident Research Centre, 2000.

[14] FILIPCZYK, J., MAKAROVA, I., BELYAEV, E. Analysis of periodical technical inspection systems in automotive transport. The experiences of Poland and Russia. *Transport Problems* [online]. 2015, **10**(4), p. 121-128. eISSN 2300-861X. Available from: https://doi.org/10.21307/tp-2015-053

[15] WOLFE, A. C., O'DAY, J. Cost-effectiveness of periodic motor vehicle inspection (PMVI): a review of the literature. Washington, DC: National Highway Traffic Safety Administration [online]. Available from: http://deepblue.lib.umich.edu/bitstream/2027.42/158/2/71884.0001.001.pdf

[16] NHTSA. Study of the effectiveness of state motor vehicle inspection programs. Final report. USA: US Department of Transportation, 1989.

[17] WHITE, W. T. A theory of how the period of vehicle inspection affects the evolution of defects and the probability of accidents. In: Road Traffic Safety Seminar: proceedings. Vol. 1. 1988. p. 14-16

[18] LOEB, P. D., GILAD, B. The efficacy and cost-effectiveness of vehicle inspection. A state specific analysis using time series data 1984. *Journal of Transport Economics and Policy*. 1984, **18**(2), p. 145-164. ISSN 0022-5258.

[19] SCHROER, B. J., PEYTON, W. F. The effects of automobile inspections on accident rates. *Accident Analysis and Prevention* [online]. 1979, **11**(1), p. 61-68. ISSN 0001-4575. Available from: https://doi.org/10.1016/0001-4575(79)90040-X

[20] SCHULZ, W. H., FRANCK, O. An empirical study to estimate the economic effects of the introduction of a periodical technical inspection (PTI) for motor vehicles in Punjab (Pakistan). *The Open Transportation Journal* [online]. 2021, **15**(1), p. 182-193. ISSN 2667-1212, eISSN 1874-4478. Available from: http://doi.org/10.2174/1874447802115010182

[21] WHITE, W. T. Relaxation of PMVI: scenario selection. Wellington, New Zealand: Traffic Research Branch, Ministry of Transport, 1986.

[22] BUYVOL, P. A,. GABSALIKHOVA, L. M., MAKAROVA, I. V., MUKHAMETDINOV, E.M. Increase in the efficiency of the operation of vehicle inspection companies (in Spanish). *Contemporary Dilemmas - Politacal Education and Values / Dilemas Contemporaneos - Education Politica y Valores*. 2018, **6**(90), p. 1-13. eISSN 2007-7890.

[23] Study on the inclusion of light trailers and two- or three- wheel vehicles in the scope of the periodic roadworthiness testing. Final report - Publications Office of the European Union [online]. 2019. Available from: https://op.europa.eu/en/publication-detail/-/publication/366a32b6-34c2-11e9-8d04-01aa75ed71a1

[24] SCHULZ, W. H., SCHELER, S. Reducing the death toll of road accidents in Costa Rica through the introduction of roadworthiness inspections by the government. *SSRNElectronic Journal* [online]. 2019, p. 1-27. ISSN 1556-5068, eISSN 1556-5068. Available from: http://dx.doi.org/10.2139/ssrn.3420341

[25] HOAGLAND, A., WOOLLEY, T. It's no accident: evaluating the effectiveness of vehicle safety inspections. *Contemporary Economic Policy* [online]. 2018, **36**(2), p. 607-628. eISSN 1465-7287. Available from: https://doi.org/10.1111/coep.12284

[26] SCHULZ, W. H., SCHELER, S. Getting ready for Europe: an empirical assessment for the introduction of periodical technical inspections of road vehicles in Turkey. *SSRN Electronic Journal* [online]. 2020, p. 1-26. ISSN 1556-5068, eISSN 1556-5068. Available from: http://dx.doi.org/10.2139/ssrn.3420341

[27] KEALL, M. D., NEWSTEAD, S. An evaluation of costs and benefits of a vehicle periodic inspection scheme with six-monthly inspections compared to annual inspections. *Accident Analysis and Prevention* [online]. 2013, **58**, p. 81-87. ISSN 0001-4575. Available from: https://doi.org/10.1016/j.aap.2013.04.036

[28] FOSSER, S. An experimental evaluation of the effects of periodic motor vehicle inspection on accident rates. *Accident Analysis and Prevention* [online]. 1992, **24**(6), p. 599-612. ISSN 0001-4575. Available from: https://doi.org/10.1016/0001-4575(92)90012-8

[29] WHITE, W. T. Does periodic vehicle inspection prevent accidents? *Accident Analysis and Prevention*. 1986, **18**(1), p. 51-62. ISSN 0001-4575.

[30] BERG, G., DANIELSSON, S., JUNGHARD, O. Traffic safety and periodic vehicle inspections / Trafiksakerhet och periodisk fordonskontroll (in Swedish). VTI rapport 281. 1984. ISSN 0347-6030.

[31] CRAIN, W. M. *Vehicle safety inspection systems. How effective?* Washington DC: American Enterprise Institute for Public Policy Research, 1980. ISBN 0-8447-3361-X.

[32] LITTLE, J. W. Uncertainties in evaluating periodic motor vehicle inspection by death rates. *Accident Analysis and Prevention* [online]. 1971, **2**(4), p. 301-313. ISSN 0001-4575. Available from: https://doi.org/10.1016/0001-4575(71)90043-1

[33] GARCIA-CORDONIE, J., IZQUIERDO, P., VILAN, J. A., SEGADE, A., CASAREJOS, E., LAGO, M. L. Definition and implementation of an integrated management plan (IMP) applied to the equipment at periodical technical inspection (PTI) stations. In: 6th International Conference of Integrity-Reliability-Failure IRF2018: proceedings. 2018. p. 785-794.

[34] GARCIA, S. R., BABE, G. A., LOPEZ, D. V. Contribution of the technical inspection of vehicles to road safety / Contribucion de la inspeccion tecnica de vehiculos a la seguridad vial (in Spanish). Madrid: Fundacion Instituto Tecnologico para la Seguridad del Automovil (FITSA), Instituto de Seguridad de los Vehiculos Automoviles (ISVA), Universidad Carlos III, 2007.

[35] GARCIA, S. R., BABE, G. A., LOPEZ, D. V. Contribution of periodic motor vehicle inspection (PMVI) to vehicle safety. Madrid: Fundacion Instituto Tecnologico para la Seguridad del Automovil (FITSA), Instituto de Seguridad de los Vehiculos Automoviles (ISVA), Universidad Carlos III, 2012.

[36] Autofore: Study on the future options for vehicle roadworthiness enforcement in the European Union - International Motor Vehicle Inspection Committee (CITA) [online]. Available from: http://citainsp.org/wp-content/uploads/2016/01/PressReleaseEN.pdf

[37] HUDEC, J., ŠARKAN, B., CZODOROVÁ, R. Examination of the results of the vehicles technical inspections in relation to the average age of vehicles in selected EU states. *Transportation Research Procedia* [online]. 2021, **55**(6), p. 2-9. ISSN 2352-1465. Available from: https://doi.org/10.1016/j.trpro.2021.07.063

[38] JAROSINSKI, W. Periodic technical inspections of vehicles and road traffic safety with the number of road accidents involving fatalities. *Eksploatacija i Niezawodnosc - Maitenance and Reliability* [online]. 2014, **16**(1), p. 105-111. ISSN 1507-2711. Available from: https://doi.org/10.17531/ein.2014

[39] DUBRETA, N., MIKULIC, I. Subjectivity and technology in work of technicians in periodical technical inspection stations. *Interdisciplinary Description of Complex Systems* [online]. 2019, **17**(3), p. 640-658. ISSN 1334-4684, eISSN 1334-4676. Available from: https://doi.org/10.7906/indecs.17.3.18

[40] MIKULIC, I., BOSKOVIC, I., ZOVAK, G. Effects of driving style and vehicle maintenance on vehicle roadworthiness. *Promet - Traffic and Transportation* [online]. 2020, **32**(5), p. 667-667. ISSN 0353-5320. Available from: https://doi.org/10.7307/ptt.v32i5.3443

[41] ZOVAK, G., CALA, I., SISKO, I. Applilacion of standards in auditing of stations for technical inspection of vehicles. *Promet - Traffic and Transportation* [online]. 2009, **21**(3), p. 191-198. ISSN 0353-5320, eISSN 1848-4069. Available from: https://doi.org/10.7307/ptt.v21i3.225

[42] HUDEC, J., SARKAN, B., CZODOROVA, R., CABAN, J. The influence of quality management system on the operation of periodical technical inspection stations. *Applied Sciences* [online]. 2021, **11**(11), 4854. eISSN 2076-3417. Available from: https://doi.org/10.3390/app1111485

ECONOMIC AND ENVIRONMENTAL BENEFITS OF USING CAVITATION TREATED FUEL IN VEHICLES OF INTERNAL COMBUSTION ENGINES

Ivan Aftanaziv [1], Myroslav Malovanyy [2,*], Lilija Shevchuk [3], Orysia Strogan [1], Lesia Strutynska [5]

[1]Department of Descriptive Geometry and Engineering Graphics, Institute of Applied Mathematics and Fundamental Sciences, Lviv Polytechnic National University, Lviv, Ukraine
[2]Department of Ecology and Sustainable Environmental Management, Viacheslav Chornovil Institute of Sustainable Development, Lviv Polytechnic National University, Lviv, Ukraine
[3]Department of Organic Products Technology, Institute of Chemistry and Chemical Technologies, Lviv Polytechnic National University, Lviv, Ukraine
[5]Department of Human Resourse Management and Adminislration, Lviv Polytechnic National University, Lviv, Ukraine

*E-mail of corresponding author: mmal@lp.edu.ua

Resume

The results of an experimental study of efficiency of the cavitation treatment of a fuel mixture, based on A-95 gasoline and distilled water, for automobile internal combustion engines are presented. Cavitation treatment of this fuel mixture at a percentage of water/gasoline of 17/83% allows increasing the cost of gasoline up to 15-20% when operating engines on flat and sloping sections of roads and in traffic jams. Due to the cavitation treatment, the engine power is reduced by only 6÷7%. The design of the created automobile electromagnetic vibrating cavitator is described. Its application will not only save fuel, but increase the completeness of combustion of water-gasoline fuel mixture, i.e. improve the environment, as well %.

Article info

Received 10 August 2021
Accepted 27 20 January 2022
Online 25 March 2022

Keywords:

cavitation disturber
electromagnetic drive
gasoline economy
completeness of fuel combustion
ecology

Available online: https://doi.org/10.26552/com.C.2022.3.B158-B169

ISSN 1335-4205 (print version)
ISSN 2585-7878 (online version)

1 Introduction

The defining feature of modernity is intensive research on introduction of the energy-saving technologies and aspects of the renewable energy sources use. It is necessary to note the use of energy-saving technologies in industry [1], the development of thermal modernization in the communal sphere [2], the synthesis of biogas as an efficient energy source [3], the use of energy for the synthesis of aquatic organisms [4], particularly microalgae [5-6]. An important aspect of these problems is introduction of the energy-saving technologies in transport.

The rapid development of electric vehicles, however, does not eliminate the need to improve internal combustion engines. Gasoline engines will be widely used for a long time to drive large vehicles, including military special equipment, as well as for various motorized household devices. Therefore, research aimed at improving the performance of gasoline engines will still be relevant.

Of particular importance today are the studies aimed at preserving the environment, including through the maximum reduction of emissions from the products of incomplete combustion of engine fuel. It is known that the incomplete combustion of fuel in the chambers of engine cylinders is the main reason for the formation of carbon dioxide, harmful to the atmosphere, which contributes to formation of the atmospheric “greenhouse effect”.

It is known that the quality of the air-fuel mixture prepared for injection into the working chamber, along with the quality of gasoline, has a decisive influence on the completeness of combustion in the working chamber of the fuel. Mainly the deterioration of fuel combustion conditions and the consequent insufficient completeness of its combustion are caused by insufficient oxygen in the air-fuel mixture. The dispersion of the fuel, i.e. the degree of scattering of its micro-droplets provided by the carburettor or injection nozzles, is important. It is generally accepted that the higher the scattering dispersion of gasoline given in the combustion chamber, the higher the degree of its mixing with air [7]. Accordingly, the best conditions for complete combustion of fuel are provided. As a result, higher engine power and a lower degree of environmental pollution will be guaranteed [8].

To achieve this effect, scientists from the National University "Kyiv Polytechnic Institute" of Sikorsky created cavitation ultrasonic devices to increase the dispersion of the air-injected mixture injected into the working chambers of the cylinders of engines [9]. The principle of operation of these devices is based on the additional dispersion of fuel jets by vibrating high-frequency ultrasonic dispersants. This is done just before the pre-prepared air-fuel mixture enters the combustion chamber of the engines [10]. The authors note that "… Ultrasonic cavitation treatment of fuel can improve its energy and consumer performance." At the same time, they rightly claim that this is ensured due to the fact that "in the process of flattening cavitation bubbles in micro volumes high temperatures and pressures develop, which create preconditions for appearance of electric charges rich in the energy of dissociated and ionized molecules, as well as atoms and free radicals that improve the process of fuel combustion", [11]. Vibrating ultrasonic dispersants were installed directly in the devices for preparing the air-fuel mixture. Therefore, the authors of this development successfully increased the power of engines by 10-15 % without increasing their size and weight. It has also reduced emissions of harmful carbon dioxide by almost a quarter.

At the end of the last century, scientists at the "Kyiv Polytechnic Institute" made quite successful attempts to use cavitation to improve the quality of diesel and gasoline fuels for internal combustion engines. Under the leadership of Prof. Fedotkina I. M., a study of the effect of cavitation on fuel quality was conducted there. Their theoretical and experimental studies have shown quite good results [12]. In particular, the ability of cavitation to positively affect the improvement of fuel quality was established. Researchers explain this by the destructive effect of cavitation on fuel clots, as well as the degassing of fuel from dissolved non-combustible gases. At the same time, cavitation also contributes to the qualitative mixing of certain fuel fractions [12]. However, it turned out that the improvement of fuel characteristics as a result of its cavitation treatment is quite short-lived. In a few days after the cavitation treatment, the fuel poured into the storage tanks lost the acquired characteristics, which had improved its quality. According to its characteristics, the fuel almost completely returned to its initial state prior to the cavitation treatment [12]. Unfortunately, the researchers then failed to organize the cavitation treatment of fuel just before it is fed into the working chambers of the engines. This is what hindered the widespread production use of cavitation fuel processing.

Different methods have been tried to improve the completeness of fuel combustion in the working chamber of the cylinders of internal combustion engines. In particular, due to the admixture of distilled water in certain proportions to the air-fuel mixture supplied to the working chamber of the engines. This idea was prompted by the fact that under the action of high combustion temperatures of carbon compounds, including gasoline, water molecules decompose, forming a number of gases when interacting with their environment. Along with water vapour, a number of combustible gas compounds are formed here. Among them are combustible compounds of oxygen and hydrogen, as well as their possible combinations. That is why in the case of fires caused by the combustion of carbon compounds, in particular oils, diesel and gasoline, it is never recommended to use water as a fire extinguisher.

However, the problem of clear dosing of the ratios of gasoline, water and air and ensuring their quality mixing with each other is still unresolved and is the main obstacle to the industrial implementation of this progressive idea.

The aim of this study was to create a low-frequency vibration-resonant device for cavitation treatment of water-fuel mixture before its direct supply to the combustion chamber of gasoline engines.

The objectives of the research were as follows:

- study of the influence of the percentage of fuel components in the water-gasoline mixture on the stability of the internal combustion engine;
- creation of an experimental installation for the low-frequency cavitation treatment of water-gasoline fuel mixture;
- development of a technological scheme for preparation of the water-fuel mixture for automobile internal combustion engines.
- development of design of the automobile vibrocavitator for the cavitation treatment of water-fuel mixture or fuel before their supply to the combustion chamber of the engine.

2 Data and methods

The study of influence of the cavitation treatment on the performance characteristics of the water-gasoline fuel mixture was carried out on a carburettor internal combustion engine model VAZ-21083 car brand VAZ-21099. The study involved two stages. First, in the experimental low-frequency vibration-resonant cavitator, distilled water and A-95 gasoline supplied to its working area were mixed in certain proportions. This mixture was subjected to cavitation treatment for a fixed time. In the second stage of research, the water-gasoline fuel mixture treated in the cavitator was sent to the carburettor of the running engine of the car. According to the readings of the indicator devices on the car panel, certain parameters of the engine operation were recorded.

Since the main difference of the method of preparation of the fuel mixture for internal combustion engines, proposed in this article, is the use at the stage of preparation of the mixture cavitation treatment of its components, hereinafter describes the nature and mechanisms of formation in the treated fluids cavitation phenomena and their accompanying effects.

Based on the experience of the authors in the field of research of cavitation phenomena and their effects [13-14], it can be argued that three main factors determine the preconditions for the perturbation of cavitation in the fluid thickness or in the liquid flow. These are:

- the presence of cavitation embryos in the liquid. In particular, small mechanical inclusions and most importantly - dissolved in the liquid gases and air, the volumes of which are close to the maximum possible quantities specified by Henry-Dalton' law;
- insignificant, within (0.9-1.5) $\cdot 10^3$ kg/m^3, density of liquid or total density of its components;
- providing the fluid with external energy sufficient to break the intermolecular bonds in the fluid thickness or in the fluid streams. In the first case, it may be the supplied kinetic energy, such as magnetic field or ultrasound, in the second - pre-provided to the liquid reserve of potential energy released during the flow of fluid through obstacles, accompanied by a change in the nature of the laminar fluid flow to turbulent.

Accordingly, in the process of experimental research the main attention was paid to control over the presence and intensity of the cavitation process in the water-gasoline mixture, as well as the parameter of the engine of a car powered by cavitation-treated fuel.

The presence of cavitation treatment here was investigated by the kinetics of chemical reactions of the potassium permanganate reduction in the environment of cavitation-treated water. At concentrations of CH_3O_4 equal to 0.5 mol and KM_nO_4, respectively 4x10^{-3} mol, such a reaction occurs at a low rate, which allows monitoring its course and changes in colour shades. Due to the colour changes of the permanganate ion, the reaction can be monitored photometrically using a colorimeter model KFK-2. 1. 1 $\cdot 10^{-6}$ m^3 of methanol, 2.10^{-6} m^3 of sulphuric acid (2 molar concentration) and untreated distilled water or water after cavitation treatment were added to a 50$\cdot 10^{-6}$ m^3 volumetric flask. Subsequently, 0.2$\cdot 10^{-6}$ m^3 of potassium permanganate was added to the volumetric flask and, after vigorous stirring, it was photometered. At the same time, such a liquid mix with usual water not only reacts with insignificant speed, but also practically does not change transparency and colour. In the presence of cavitation-treated water in a volumetric flask, the rate of the oxidation reaction increases significantly by about 3.5 times, the colour of the liquid mixture changes intensely from colourless to deep blue.

According to the test colour tables of the control liquid mixture, comparing it to the reference, where the ultrasonic cavitation treatment was used, one can judge not only about the presence of cavitation treatment of the test batch of water, but also the intensity of the cavitation field in which this treatment took place. Subsequent experiments showed that the most effective for the combustion of gasoline-fuel mixture was the intensity of the cavitation field of the treatment zone in the range of (1.0-1.5)$\cdot 10^6$ KW/m^3.

The volumes of liquids in the storage tanks of the working area of the cavitator, water and gasoline tanks in the cavitator, as well as in the working tanks of the direct supply of gasoline or water-gasoline mixture to the carburettor of the test engine of the car were measured by filling them in volumetric flasks with experimental liquids with the volumes of 50$\cdot 10^{-6}$ m^3 and 100$\cdot 10^{-6}$ m^3.

The volumes of water and gasoline content in the finished cavitation-treated fuel mixture were determined from calculations of the mass content of the initial ingredients. For example, to provide 10% water content in the finished mixture with a volume of 2 10^{-3} m^3, the storage tanks of the cavitator were filled by 1.8 10^{-3} m^3 with gasoline and 0.2 10^{-3} m^3 with water.

The parameters of cavitation treatment, which regulate the level of external energy provided to the treated liquids, are important for the quality of the finished cavitation-treated water-gasoline fuel mixture. The main of these parameters are the amplitude and frequency of harmonic oscillations of cavitation perturbators and, of course, the time of cavitation processing. The oscillation frequency of cavitation perturbators on the described devices was set and regulated by a standardized frequency regulator of the supply voltage of the windings of their drives. The model of this AES-120 frequency regulator has a frequency control range from 0 to 150 s^{-1}. The main frequency range of the AC supply voltage used in this experimental study was 40-60 s^{-1}. The measurement of the supply voltage frequency, which determines the oscillation frequency of disk cavitation perturbators in our cavitators, was carried out with an accuracy of 0.5-1.0 s^{-1}.

The amplitude of oscillations of cavitation perturbators was measured in stroboscopic light using a ruler digitized in millimetres. The amplitude was determined as a half of the path that the disk cavitation perturbator will travel during its reciprocating oscillating motion along the geometric axis of the oscillation drive rod. The amplitude of oscillations is regulated by the magnitude of the pulling force of the electromagnetic cavitator's armature with the cavitation perturbators fixed to its electromagnet. The magnitude of this pulling force is determined by the magnitude of the current supplied to the windings of the coil of the electromagnet. The range of studied amplitudes of oscillations of cavitation perturbators was (0.5-3.5)$\cdot 10^{-3}$ m. The amplitude of oscillations was measured in each of the experiments with an accuracy of (0.10-0.15)$\cdot 10^{-3}$ m.

The cavitation time of the water-gasoline fuel mixture, the duration of the car engine operation at a certain unit of volume of the treated mixture, was measured with a chronometer with an accuracy of 5-10 s.

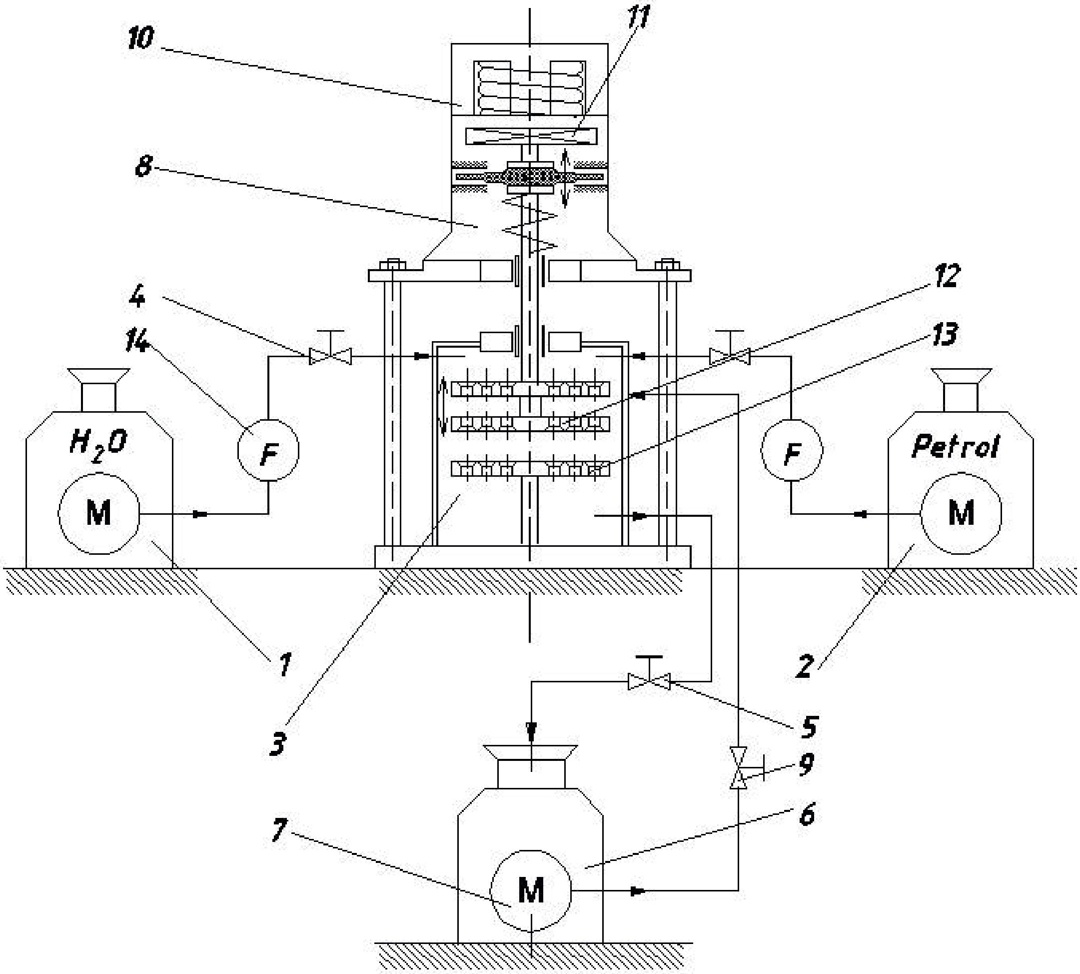

Figure 1 *Technological scheme of laboratory experimental unit for mixing and the cavitation treatment of water-gasoline fuel mixture for internal combustion engines*

The engine crankshaft speed of the experimental car was measured according to the readings of the tachometer installed on the interior panel of the car. Its standard measurement error is (1-1.5) s^{-1}.

The most important of the engine's quality indicators, the level and composition of emissions of the car, were evaluated by comparing the emissions of carbon monoxide, carbon dioxide and hydrocarbons when the engine runs on traditional gasoline A-95 and prepared by the proposed vibratory cavitary water-gasoline. The gas analyzer was used to measure harmful emissions in engine exhaust gases. The main measurements of the emission composition were carried out on an automotive one-component gas analyzer model DOZOR-C (manufacturer - Ukraine). It controlled the volume percentage of CO_2 and carbon dioxide in the emissions of CO. For a more complete analysis of the composition of emissions, a gas analyzer of combustible gases model WINTACT WT8823 was used, which allows the analysis of a wider range of nomenclature of combustible gases, including nitrogen and its oxide, oxygen, water vapour and the like. The measurement accuracy when using both control devices was proportional and was in the range of 0.05-0.1 vol.%.

The data of all the measurements are averaged and indirectly reflected in the text and reference Tables 1, 2 and 3.

Figure 1 shows a flow chart of an experimental laboratory unit for the cavitation treatment of the water-gasoline fuel mixture. In accordance with this scheme, from storage tanks 1 and 2 (Figure 1) gasoline and distilled water in certain percentages were pumped into the working area of the cavitator 3. After filling the working area of the cavitator with water and gasoline control, the valves 4 were closed. Control throttle 5 opened the closed water-gasoline mixture circulation network. Simultaneously, the electromagnetic drive 8 of the vibrating cavitation 3 and the pump 7 located in the storage tank 6 were started. Adjusting throttles 5 and 9 provided uniform circulation of water-gasoline mixture between the storage tank 6 and the working chamber of the cavitator. The technological cycle of the cavitation treatment of the fuel mixture here provided continuous circulation of the mixture between the storage tank 6 and the working area of the vibrocavitator 3. Due to that, gasoline and water were continuously mixed with each other and were subjected to cavitation treatment. The duration of the cavitation treatment of water-gasoline fuel mixture varied in the range from 3 to 10 minutes.

The main components of a vibration-resonant cavitator (Figure 2) are the electromagnetic actuator 10, which is connected to its elastically mounted oscillating armature 11, as well as the rod with oscillating disk cavitation perturbators 12. The stationary disk cavitation perturbators 13 are installed on the basis of the cavitation coaxially to the oscillating ones. Both oscillating and stationary cavitation perturbators are located in a common cylindrical case 3. That case is equipped with fittings for gasoline and water, as well as for the removal of cavitation-treated fuel mixture. To clean liquids from mechanical contaminants, the supply network to the working chamber of the cavitator of distilled water and gasoline is equipped with filters 14. The main elements of the control panel of the cavitator power supply network are the frequency regulator of the electric supply voltage of its electromagnetic drive model AFC120 and the timer o the duration of processing liquids [13-14].

The uniqueness of the technological capabilities of cavitation is primarily due to the periodic time (up to $1.5 \cdot 10^6$ KW/m^3) energy impact on the treated water-gasoline fuel mixture. This is accompanied by concomitant phenomena of shock microwave formation, phase transitions occurring on the surfaces of cavitation microbubbles and certain chemical transformations. All this does not only accelerate the course of chemical reactions, especially redox, but enables to change the structure of the ingredients of the fuel mixture submitted to the cavitation zone, as well [14]. As a result, in the finished cavitation-treated fuel mixture, water molecules not only change their structure but also partially disintegrate. As a result of a decay, the H_2O_2 molecules are formed from a certain part of its molecules, which are short-lived in time and, in turn, disintegrate into hydrated e^-_{hydro} ions and free H^0 and O^0H radicals. It is these decomposition products and especially radicals, that have increased oxidative capacity, which helps to improve the conditions of complete combustion of the gasoline component of the newly formed fuel mixture.

In addition, which is very important, the cavitation field actively mixes these newly formed components of water with gasoline molecules. This is how cavitation forms the finished fuel mixture. That is, with a certain degree of approximation, one can say that after the cavitation treatment of the components of the fuel mixture of pure water in the traditional perception no longer exists. And this is very positive. After all, the newly formed fuel mixture will not have a detrimental effect on the parts of the fuel system and the combustion chamber of the engines. On the contrary, due to the complete combustion of fuel in the fuel system of the engine, the amount of scale will decrease.

Field studies were performed in the following sequence. A storage tank filled with cavitation treated water-gasoline fuel mixture was fixed above the engine of the car on a special device. The storage tank was connected to the carburettor of the engine by a pipeline and the car engine was started at idle mode. On the dashboard of the car, according to the tachometer, changes in the speed of the engine crankshaft were observed. Using a timer, the duration of the engine to burn a fixed amount of fuel mixture with a volume of 0.001 m^3 was monitored.

3 Results and discussion

Variable parameters in the study of the cavitation treatment of water-gasoline fuel mixture were the percentage of water and gasoline in the fuel mixture, the duration of treatment and vibration parameters of cavitation perturbators, namely their amplitude (A, m) of oscillations and frequency (f, Hz)

The results of the experimental study of the cavitation treatment of water-gasoline fuel mixture are shown in Table 1.

In field studies, the stability of the engine when using cavitation-treated water-gasoline mixture was observed. The results of field studies are shown in Table 2.

Experimental research has shown that in the "idle" modes of operation of the car engine, the presence of up to 15% of distilled water in its fuel does not significantly affect the stability of the engine. At the same time, the crankshaft speed is reduced by only 5÷7%. In addition, it was found that as the water content increases by 6÷8%, the duration of the engine at a fixed 10^{-3} m^3 volume of the fuel mixture is reduced.

***Table 1** Investigation of the cavitation treatment of the water-gasoline fuel mixture*

No.	Percentage of fuel mixture components		Duration of cavitation treatment of fuel mixture, s.	Vibration parameters of cavitation perturbators	
	Gasoline, %	Distilled water, %		Frequency, Hz	Amplitude, 10^{-3} m
1	95	5	5400	48	1.0
2	90	10	5160	45	1.1
3	85	15	4800	50	1.2
4	83	17	4500	52	1.0
5	80	20	4200	47	1.2

Table 2 *The results of the study of the car engine when using cavitation-treated water-gasoline mixture*

No.	Percentage of gasoline and water in the fuel mixture, %	Engine crankshaft speed, s^{-1}	Engine life duration per 10^{-3} m^3 fuel mixture, s	Engine stability
1	95/5	18.33	90	stable
2	90/10	17.51	86	stable
3	85/15	16.67	80	stable
4	83/17	16.17	77	unstable
5	80/20	15.83	75	with interruptions

4 Suggestions for using the proposed method

The obtained results of experimental researches give the basis for constructive development of the vibrocavitator built in a fuel supply network. The functions of this vibrocavitator are the task of cavitation treatment of gasoline fuel and the formation of water-gasoline fuel mixture. This vibrator can be installed directly on the engine. To power its electric drive, it is appropriate to use a standard voltage regulator which is electrically connected to the car battery. The vibrating cavitation modes can be adjusted and switched on and off by the car's on-board computer. Schematic structural diagram of such a vibrocavitation is shown in Figure 2.

The components of the car vibrating cavitation are rigidly fixed in the lower part of the case 3 electromagnet 1 with the winding 2. An anchor 5 of the electromagnet and a rod 6 are fixed on the elastic membrane 4 above the electromagnet 1. On this rod 6, disk cavitation perturbators 7 are mounted. Through the flanges, the cover 8 of the case, located above the membrane 4, is tightly connected to the lower part 3 of the case, for example, with a bolted connection.

In the cover 8 of the case 3 there are two inlet valves 9. For example, spring-loaded 10 petal valves. The inlet openings of the valves are equipped with a fitting 11 for connection to the supply pipe to the cavitator water or gasoline. On the upper part of the cover 8 of the case, namely above the oscillating cavitation perturbators 7, there is a discharge valve 12. This valve is connected through a fitting to the pipe connecting the cavitator with the carburettor or the fuel rail of the car engine.

From theoretical and experimental studies of the cavitation processes is known that the perturbation of cavitation in a liquid flow is possible only under full conditions of energetic influence on the liquid or a rapid change in the nature of the flow. For example, exposure of fluid to ultrasound of a certain intensity or the rapid transition from laminar to turbulent fluid flow. It is generally accepted that the conditions of perturbation in the cavitation fluid are regulated by the Reynolds number. The critical value of this indicator, which relates the characteristics and physical properties of the fluid and the speed of its flow (or movement of solids in it) regulates changes in the nature of fluid flow. Thus, for the water-based liquids at values of the critical Reynolds

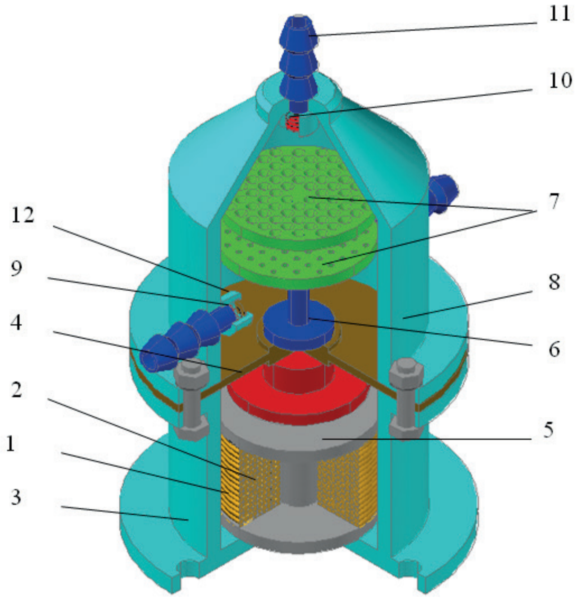

Figure 2 *Schematic structural diagram of the vibrocavitator for preparation of the water-gasoline fuel mixture for the car engine*

number R_e > 2300, the laminar regime is transformed into turbulent, which is characterized by manifestations of the cavitation phenomena.

The values of the critical Reynolds number are the main criterion for calculating the energy parameters and velocities of the cavitation perturbators in the proposed devices for the cavitation treatment of water-gasoline fuel mixture.

The classical formula for calculating the value of the critical Reynolds number in this case relates the physical parameters of the treated fluid with the speed of movement of cavitation perturbators in it. Namely

$$R_e = \frac{\rho u l}{\eta} = \frac{ul}{\upsilon} \cdot > 2300, \quad (1)$$

where $\eta = \upsilon \cdot \rho$ is dynamic viscosity of the treated water-gasoline mixture ;
ρ is the density of the liquid mixture;
υ is the kinematic viscosity of the liquid mixture;
u is the speed of oscillating movements in the liquid mixture of cavitation perturbators;
l *is* the characteristic total length of the circles of the holes for the flow of liquid in the cavitation perturbators.

When calculating the main design parameters of the cavitator for the treatment of water-gasoline fuel mixture, substituting the numerical values of the physical parameters of the treated liquid mixture in Equation (1), velocity u of oscillatory movements in the liquid mixture of cavitation, required for cavitation perturbation, is determined. The numerical value of the critical Reynolds number is given from the condition $R_{e\,cr.}$ > 2300.

The vibrating electromagnetic drive provides cavitation perturbators in our device with oscillating spatial movements. The speed of oscillating movements of cavitation exciters provided by it is defined as so-called "vibration speed" and is equal to $\upsilon = A \cdot f$ where A is the amplitude of oscillations of cavitation perturbators; f is the oscillation frequency of cavitation perturbators.

Equating the required critical velocity for cavitation perturbation with the vibration velocity provided by the vibrocavitation υ and setting the amplitude of oscillations of cavitation perturbators in the range of A = (0.5-1.5)$\cdot 10^{-3}$, m, the oscillation frequency f (H_Z) required for cavitation perturbation is determined..

According to the values of the required indicators υ, (m/s) of vibration velocity of cavitation perturbators, their amplitude A, (m) and frequency f, (H_Z) of oscillations, the energy parameters of the cavitation vibration drive are calculated. In particular, the traction force of the drive electromagnet P, (H) required to overcome the resistance of the fluid, which is expended on the oscillating movements in the fluid of the cavitation perturbators.

According to the values of the force P, (H), the amplitude A, (m) and the oscillation frequency f, (H_Z) of the cavitation perturbators, the power parameters of the electromagnetic drive of the cavitator are chosen.

When the alternating sinusoidal voltage, transformed by the converter of the voltage frequency regulator, is applied to the winding 2 of the electromagnet 1, the iron of the electromagnet is magnetized. Overcoming the elasticity of the membrane 4, the electromagnet attracts the armature 5. Simultaneously with the armature, the rod 6, rigidly connected to it and the cavitation perturbators 7 attached to it, are moved. When the sinusoidal supply voltage of the electromagnet decreases from its maximum value to zero, the elastic force of the elastic membrane 4 returns the armature anchor 5 to its original initial location. At the same time, the rod 6 and the cavitation perturbators 7 move with the armature to the upper initial position. The spatial movements of the membrane 4, the armature 5, the rod 6 and the cavitation perturbators 7 are repeated in a similar order in each subsequent half-cycle of the sinusoidal alternating supply voltage of the electromagnet winding. Eventually, these movements are transformed into a harmonic oscillating motion of the armature 5 of the electromagnet and the associated cavitation perturbators. The frequency of these oscillating movements is twice the frequency of the AC supply voltage of the electromagnet winding. Cavitation perturbators 7 are discs made of stainless steel or other cavitation-resistant material. The surface of the cavitation perturbators 7 of the device is permeated with a large number of conical holes. With oscillating rectilinear sequential movements of these disks, water and gasoline penetrate into their conical holes, which are actively mixed with each other. Penetrating in a confined space into the conical holes of the disks, liquid microjets, due to changes in their shape and speed, form microturbulent flows. In a liquid medium where the water is present, microturbulent flows appear as centres of self-perturbation of the cavitation region.

Cavitation microjets intensively mix liquids available in the working area of the cavitator with each other, forming a homogeneous fuel mixture. In addition, under the action of self-perturbed cavitation, hydrogen peroxide ions $H_2O'_2$ are formed in the water present here. Since hydrogen peroxide is a good oxidant, its presence will contribute to a better combustion of the fuel mixture in the combustion chambers of the engine cylinders. Cavitation also has a positive effect on the gasoline present in the working chamber of the cavitator. Cavitation microbubbles and microjets destroy the fuel clots present in gasoline, thereby improving its complete combustion. Through the outlet valve 12 cavitation-treated in the working chamber of the cavitator, the water-gasoline fuel mixture is pushed into the carburettor of the engine or its fuel distribution rail.

Cavitation-treated in the working chamber of the cavitator water-gasoline fuel mixture through the outlet valve 12 is pushed into the outlet pipe, from which it enters the carburettor of the engine or its distribution fuel bar.

In terms of its design dimensions, the design of the car cavitator is quite small. In terms of weight,

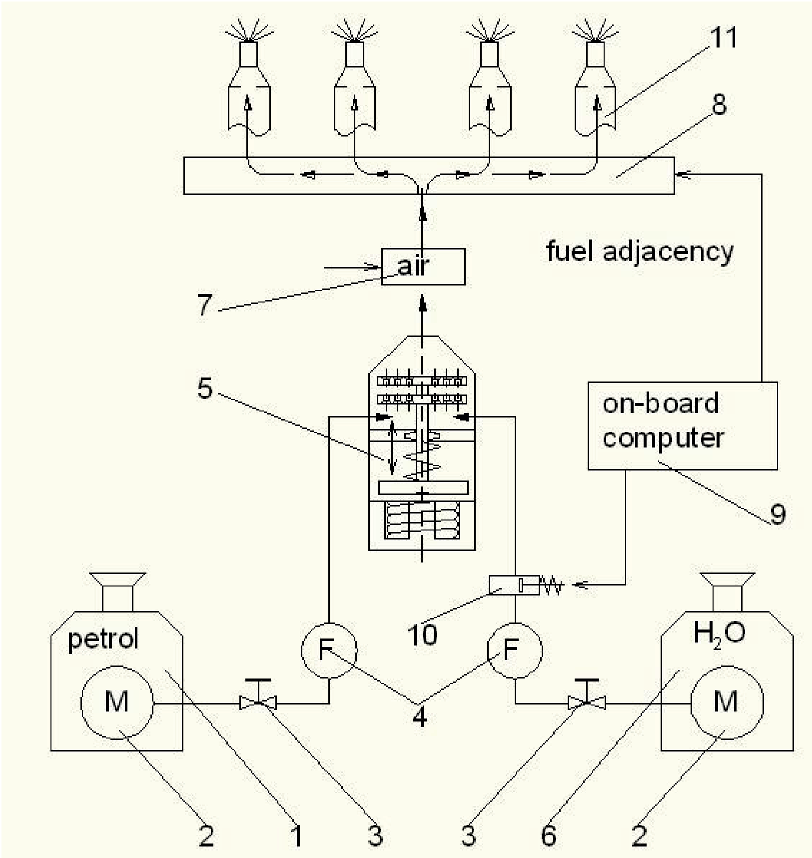

Figure 3 *Technological scheme of the preparation and supply network of the cavitation-treated water-fuel mixture in the combustion chambers of the engine cylinders*

appearance and size, this car cavitator is commensurate with the car electrical distributor. That is why it can be mounted directly on the car engine.

The electrical circuit for converting the 12-volt voltage of the car battery into the alternating 220-volt supply voltage of the cavitator electromagnet can be borrowed from the circuit of the electric converter. Such converters are used to transform accumulated wind or solar 12-volt electricity into alternating 220-volt electricity for domestic power grids.

Figure 3 shows an upgraded technological scheme of the network of preparation and supply of fuel to the combustion chamber of the engine cylinders.

A typical fuel supply network here is supplemented by a water-gasoline fuel mixture cavitator, a water supply subsystem and its control equipment. As well as the traditional fuel supply scheme, the proposed one includes a storage tank 1, a gasoline pump 2, a control throttle 3 and a filter 4. However, here the gasoline is not fed into the carburettor, but first into the cavitator 5. A similar portion of distilled water is fed into the cavitator simultaneously from the additionally arranged storage tank 6 via a similarly arranged network with a pump, an adjusting throttle and a filter. To ensure a predetermined percentage of water and gasoline in the fuel mixture, the volume of water supply is regulated at the stage of adjustment by the control throttle 3. In the cavitator, distilled water and gasoline are subjected to cavitation treatment, mixed with each other and fed through the exhaust pipe to the carburettor of the car or its distribution bar 8. As with the traditional fuel supply scheme, for example, when using an injector scheme of fuel mixture injection, the water-gasoline fuel mixture formed in the cavitator 5 is saturated with air and through the injectors 11 enters the combustion chamber of the engine cylinders.

It is reasonable to assume that with the addition of distilled water to the fuel mixture in difficult modes of engine operation, its torque and certain dynamic characteristics may decrease. Therefore, it is advisable in cases of forced engine operation to temporarily abandon the water supply and return to the classic scheme of gasoline supply. In modern cars, it is advisable to put this function on the on-board computer 9, which at certain moments of load changes will turn on or off the solenoid valve 7 of the water supply network.

5 Analysis of the advantages of using the proposed method

It is clear that the main points of the water-gasoline mixture using would be the so-called light modes of engines operation. These can be periods when the engine is idling, when the engine is warming up, when driving on flat and descending sections on the slopes and so on. But most often these are periods of the slow movement of the car in the so-called “car traffic jams” inherent in modern cities. It is in such fairly frequent road transport situations that the modes of operation of automobile engines for the development of high power are completely unnecessary and the cost of this expensive fuel is inappropriate. Here it would be appropriate to switch to e use the cheaper fuel mixtures. For example, the proposed water-gasoline. After all, the cost savings of gasoline provided in the range of 10-15% will be guaranteed to cover the cost of equipping cars with the proposed system of cavitation preparation of the water-gasoline mixture. Fuel savings would be even more noticeable if one organically combines the cavitation preparation of water-gasoline fuel mixture with devices of cavitation fuel spraying at the stages of its injection into the working chambers of engine cylinders [15].

It may seem that the simplified modes of operation of car engines, which are characterized by operation at close to “idling” modes, in the general period of operation of the car, take up a small percentage of time. These are the periods of operation of cars in the conditions of driving on flat and descending sections of routes, at their idle time in city traffic jams, etc. However, this is a misconception, although it is quite common. The indisputable experience of the so-called “hybrid” cars, operated on both fuel and electric drives, suggests otherwise. Namely, in urban conditions of car operation in modern cities, the periods of operation of their drive electric motors and internal combustion engine are almost the same. After all, the fuel engine is switched on automatically and only for the heavy-duty modes of operation, i.e. acceleration, uphill, overtaking and poor quality road surfaces.

This gives grounds to conclude that in the so-called “light modes of operation of engines” modern cars are operated up to 50% of their operation duration. Similarly, if one takes into account the statistics, according to which the average annual mileage of a car is about twenty thousand kilometres, one can predict that half of this mileage will fall on “light” engine conditions. Thus, with a certain degree of approximation, one can assume that during the year of operation, the mileage of a car on a water-gasoline fuel mixture can be about 10 thousand kilometres. If one assumes, for an approximate calculation, that the indirect fuel consumption here is about 10 litres per 100 km and take into account that 15% of this fuel can be replaced by water, the annual savings on one car from the installation of its vibrocavitation will reach $ 150. This is at the indirect cost of A-95 gasoline, which is about $ 1 per 1 litre of fuel.

For the practical arrangement on the car engine of the proposed system of preparation of the water-gasoline fuel mixture, first of all, the vibrocavitation device, for cavitation processing and mixing of the mixture components, will be required. To provide power to its drive, one would need a voltage converter from a constant 12-volt to a change of 220-volt. Additional storage capacity would also be required to store distilled water and pipelines with control equipment to supply water and gasoline to the cavitator and transfer the formed fuel mixture to the carburettor or the fuel rail. Component pipelines, their control valves, solenoid valves and a storage tank are manufactured industrially and their total cost, according to the estimates, will not exceed $ 50. Unfortunately, vibrocavitators for preparation of the water-gasoline fuel mixtures are not manufactured by industry. Therefore, at this stage they would have to be made individually. However, given that their production will not require expensive scarce materials, we can assume that the manufacture of one cavitator will cost about $ 150. Thus, the total cost of equipping one car with a system of preparation of the water-gasoline fuel mixture will be approximately $ 200. The same proportional annual savings are provided by use of 15% of water in the water-gasoline fuel mixture to power the car engine when operating the engine in light modes, in particular when working at idle. Therefore, equipping the car with a system of preparation of the water-gasoline fuel mixture will pay off in one year of the car operation. Considering that systems of this type are designed for a 5-year service life, one can assume that during this period, the car owners would be able to save about $ 700 on the cost of partial replacement of gasoline with water. It is taken into account that part of the savings will have to be spent on purchase of the distilled water and maintenance and routine inspections and minor repairs of the system.

It is undeniable that the economic factors of any of the proposed technical solutions are important. However, with regard to the road transport, which has flooded almost all the populated cities and towns around the world, no less important is the problem of reducing the harmful emissions of fuel combustion products into the atmosphere. This environmental problem is multifaceted. First of all, it is a problem of active consumption of atmospheric oxygen by automobile engines for the maintenance of the fuel combustion process. It is known that 2.5 kg of oxygen is absorbed from the atmosphere to burn $1 \cdot 10^{-3}$ m^3 of gasoline in a car engine. To some extent, this means that by equipping the car's engine with the proposed system of preparation of the water-gasoline fuel mixture, one reduces the annual consumption of atmospheric oxygen by such a car by approximately 300 kg.

Another, even more important problem for mankind, caused by operation of the automobile internal combustion engines, is their harmful emissions into the atmosphere of combustion products of carbon fuel. After all, it is generally accepted that for every 10 thousand kilometres a car on average burns a ton of gasoline, consuming (absorbing from the atmosphere!) 3.5 tons of oxygen and emitting 16 tons of exhaust gases, including very toxic 80 kg of CO, 10 kg of nitrogen oxides, 20 kg

***Table 3** Comparative studies of the content of automotive emissions*

No.	Controlled gases of automobile emissions	The content of harmful emissions in volume percentages, vol. %		The difference in performance, %
		Gasoline A-95	Cavitation-treated water-gasoline fuel mixture	
1	CO	5	4	20
2	CO_2	16	13	19
3	NO_x	0.5	0.4	20

of hydrocarbons. Keep in mind that each $1 \cdot 10^{-3}$ m^3 of gasoline burns causes formation of 16 m^3 of a mixture of different exhaust gases.

Therefore, the reduction of 15÷17% of gasoline costs for the engine of the car in light modes, which provides the proposed system of cavitation preparation of water-gasoline fuel mixture, guarantees a proportional reduction of approximately the same 15% of emissions in exhaust gases.

At this stage of the active struggle of the world community and especially Europe, for environmental protection and reduction of greenhouse gas emissions, the standard for emissions in fuel combustion products, the so-called "Euro 6" standard, introduced here, reduces the carbon dioxide emissions from $120 \cdot 10^{-6}$ kg/m^3 to $90 \cdot 10^{-6}$ kg/m^3. At the same time, recognizing the importance of reducing car emissions, the world-renowned SAE study has shown that one of the most effective ways to reduce car emissions is by "injecting water into the combustion chamber." This reduces emissions of nitrogen oxides and other toxic components by up to 90%.

Of course, all these statements need to be tested experimentally. Therefore, a number of experimental studies were conducted aimed at comparative study of the cavitation-treated water-gasoline fuel mixture effect on the volume of harmful emissions during its combustion. For measurements, a single-component gas analyzer model DOZOR-C was used, which measured the content of carbon monoxide in the exhaust gases and a multi-component gas analyzer model WINTACT WT8823, which was used to measure the content of carbon dioxide CO_2 and nitrogen oxide in the exhaust gases. Measurements were performed under the similar operating conditions of the car engine at "idling" at the same temperatures of the engine coolant (90 ± 2) ^{0}C and the environment (22 ^{0}C). By adjusting the degree of opening of the carburettor throttle, the same numerical values of crankshaft speed were achieved. According to the readings of the car tachometer, they were (20±1) s^{-1}. Comparative measurements of the content of automotive emissions were performed when using gasoline grade A-95 and the cavitation-treated water-gasoline fuel mixture, formed on its basis with the addition of 15% of distilled water The results of comparative studies are shown in Table 3.

Thus, the data of a comparative study of the content of harmful emissions of the engine model VAZ-21083 car VAZ-2199 when burning traditional gasoline brand A-95 or the cavitation-treated water-gasoline mixture with 15% of distilled water in the fuel mixture, show that the presence of water in the cavitation-treated fuel mixture reduces the amount of harmful carcinogenic gases in car emissions by about 19-20%.

Therefore, using the proposed system of cavitation treatment of water-gasoline fuel mixture can have undeniable environmental benefit.

It consists in the fact that a car equipped in this way will not burn about 150 litres of gasoline during the year due to its replacement with water. And for a city with a million inhabitants, where, according to statistics, there is one car for every four inhabitants, the environment will not be polluted by the products of combustion of almost 18 million litres of gasoline. It is conventionally taken into account that the number of cars with gasoline and diesel engines in the city is about the same.

6 Conclusions

1. Experimental research has confirmed the ability to use cavitation treatment for intensive mixing of difficult to mix water and gasoline in certain mass ratios. The water-gasoline fuel mixture formed by cavitation treatment is suitable for ensuring stable operation of automobile engines in the facilitated modes, for example, "idling". The range of stable operation of the engine on the water-gasoline cavitation-treated fuel mixture is in the ratio of 15-17% of water to 85-83% of gasoline in the formed fuel mixture.
2. It is experimentally established that when the mass of water in the water-gasoline cavitation-treated fuel mixture increases, the engine crankshaft speed decreases by 15-20 percent. This will be accompanied by a proportional decrease in its torque and, accordingly, engine power.
3. The working chamber with the disk cavitation perturbators placed in it is the basis of the proposed design of a low-frequency vibration-resonant cavitator for mixing and cavitation treatment of the water-gasoline fuel mixture. The electromagnetic drive healed by the car battery provides oscillating movements to cavitation disturbers. It is established that the optimum modes of oscillatory displacements of cavitation perturbators are the amplitude of oscillations of (1.0-1.5) 10^{-3} m at the frequency of

their oscillations in the range of 47-52 Hz.

4. The improved technological scheme of a power supply of the automobile internal combustion engine' cylinders with the cavitation-treated water-gasoline fuel supply includes supplementation of a traditional gasoline supply network with an electromagnetic vibrating cavitator for mixing the water-gasoline mixture and an additional water supply network with its accumulation tank.
5. The so-called "facilitated" modes of engine operation, including idling, traffic jams, driving on flat and descending sections of highways, etc. are the main periods of use of the water-gasoline fuel mixture during the operation of cars.
6. The use of the water-gasoline fuel mixture during one-year operation of the car can save up to 150 litres of gasoline worth about $ 150. In addition, along with the economic benefits, there is also an environmental component. It is the reduction of the amount of gasoline burned.

References

[1] SHATOKHA, V., MATUKHNO, E., BELOKON, K., SHMATKOV, G. potential means to reduce CO_2 emissions of iron and steel industry in Ukraine using best available technologies. *Journal of Sustainable Metallurgy* [online]. 2020, **6**(3), p. 451-462. ISSN 2199-3823. Available from: https://doi.org/10.1007/s40831-020-00289-0

[2] MALOVANYY, M., ZYCZYNSKA, A. Minimization of energy consumption for heating houses by thermal modernization (on the example of educational buildings) / Minimizatsiia enerhovytrat na opalennia budynkiv shliakhom termomodernizatsii (na prykladi navchalnykh korpusiv) (in Ukrainian). *Ekolohichna Bezpeka ta Zbalansovane Resursokorystuvannia* [online]. 2016, **2**, p. 135-140. ISSN 2415-3184. Available from: http://library.nung.edu.ua/ekolog%D1%96chna-bezpeka-ta-zbalansovane-resursokoristuvannya.html

[3] VOYTOVYCH, I., MALOVANYY, M., ZHUK, V., MUKHA, O. Facilities and problems of processing organic wastes by family-type biogas plants in Ukraine. *Journal of Water and Land Development* [online]. 2020, **45**(IV-VI), p. 185-189. ISSN 2083-4535. Available from: https://doi.org/ *10.24425/jwld.2020.133493*

[4] MALOVANYY, M., TYMCHUK, I., BALANDIUKH, IU., SOLOVIJ, KH., ZHUK, V., KOPIY, M., STOKALYUK, O., PETRUSHKA, K. Optimum collection and concentration strategies of hydrobionts excess biomass in biological surface water purifying technologies. *Environmental Problems* [online]. 2021, **6**(1), p. 40-47. ISSN 2414-5955. Available from: https://doi.org/10.23939/ep2021.01.040

[5] NYKYFOROV, V., MALOVANYY, M., KOZLOVSKA, T., NOVOKHATKO, O., DIGTIAR, S. The biotechnological ways of blue-green algae complex processing. *Eastern-European Journal of Enterprise Technologies* [online]. 2016, **5**(10), p. 11-18. ISSN 1729-3774. Available from: https://doi.org/10.15587/1729-4061.2016.79789

[6] MALOVANYY, M., ZHUK, V., NYKYFOROV, V., BORDUN, I., BALANDIUKH, J., LESKIV, G. Experimental investigation of Microcystis aeruginosa cyanobacteria thickening to obtain a biomass for the energy production. *Journal of Water and Land Development* [online]. 2019, **43**(X-XII), p. 113-119. ISSN 2083-4535. Available from: https:// doi.org/10.2478/jwld-2019-0069

[7] LUHOVSKOI, A. F. The use of piezoelectric converters as a way to improve the systems for the preparation and supply of fuel to the internal combustion engine / Primenenie pezoelektricheskih preobrazovateley kak put sovershenstvovaniya sistem podgotovki i podachi topliva v DVS (in Russian). *Vestnik Natsionalnogo Tehnicheskogo Universisteta Ukrainyi "KPI". Mashinostroenie.* 1997, **32**, p. 34-38. ISSN 2305-9001.

[8] LUHOVSKOI, A. F. Preparation of a fuel mixture in an internal combustion engine using ultrasound / Podgotovka toplivnoy smesi v DVS s pomoschyu ultrazvuka (in Russian). *Vestnik Natsionalnogo Tehnicheskogo Universisteta Ukrainyi "KPI". Mashinostroenie.* 1997, **32**, p. 209-213. ISSN 2305-9001.

[9] LUHOVSKOI, A. F. Ultrasonic spraying in fuel-air mixture preparation systems / Ultrazvukovoe raspyilenie v sistemah podgotovki toplivno-vozdushnoy smesi (in Russian). *Tekhnika v Silskohospodarskomu Vyrobnytstvi, Haluzeve Mashynobuduvannia, Avtomatyzatsiia. Zbirnyk Naukovykh Prats Kirovohradskoho Derzhavnoho Tekhnichnoho Universytetu*. 2000, **7**, p. 30-33. ISSN 2409-9392.

[10] LUHOVSKOI, A. F., CHOPNYIY, V. I., EPEMENKO, A. I. Preparation of a fuel mixture in carburetor power systems for internal combustion engines using an ultrasonic dispenser with radial-bending vibrations / Podgotovka toplivnoy smesi v kapbyupatopnyih sistemah pitaniya DVS s pomoschyu ultpazvukovogo dispepgatopa s padialno-izgibnyimi kolebaniyami (in Russian). In: International Scientific and Technical Conference Ppohpesyvna Tekhnika i Tekhnolohiia Mashynobuduvannia, Ppyladobuduvannia i Zvapiuvalnoho Vyrobnytstva: proceedings. Vol. 3. 1998. p. 341-346.

[11] CHORNYI, V. I., LUHOVSKYI, O. F., PRYLYPKO, Y. S. Ultrasonic fuel treatment device in internal combustion engines/ Prystrii ultrazvukovoi obrobky palyva v dvyhunakh vnutrishnoho zghoriannia (in Ukrainian) [online]. Patent Ukrainy UA 42827. Available from: https://base.uipv.org/searchINV/search.php?action=viewdetails&IdClaim =17353

[12] FEDOTKIN, I. M., GULYIY, I. S. *Cavitation: Cavitation technique and technology, their use in industry / Kavitatsiya: Kavitatsionnaya tehnika i tehnologiya, ih ispolzovanie v promyishlennosti* (in Russian). Kyiv: Polihrafknyha, 2000. ISBN 5-7763-2417-3.
[13] SHEVCHUK, L. I., STARCHEVSKYI, V. L. *Cavitation. Physical, chemical, biological and technological aspects / Kavitatsiia. Fizychni, khimichni, biolohichni ta tekhnolohichni aspekty* (in Ukrainian). Lviv: Vydavnytstvo Lvivskoi politekhniky, 2014. ISBN 978-617-607-666-7.
[14] SHEVCHUK, L. I., AFTANAZIV, I. S., STROHAN, O. I., STARCHEVSKYI, V. L. *Low-frequency vibration-resonant cavitators / Nyzkochastotni vibrorezonansni kavitatory* (in Ukrainian). Lviv: Vydavnytstvo Lvivskoi politekhniky, 2013. ISBN 978-617-607-509-7.
[15] LUGOVSKOY, A. F., CHUHRAEV, N. V., CHORNYIY, V. I., PRILIPKO, Y. S. Ultrasonic cavitation technologies in mechanical engineering and medicine / Ultrazvukovyie kavitatsionnyie tehnologi v mashinostroenii i meditsine (in Russian). *Vestnik Natsionalnogo Tehnicheskogo Universisteta Ukrainyi "KPI". Mashinostroenie*. 2006, **48**, p. 228-233. ISSN 2305-9001.

ANALYSIS OF INFLUENCE OF THE LOAD PLANE COMBINED WITH PRELOAD ON DURABILITY OF BEARING

Jaroslaw Kaczor

Institute of Sanitary Engineering and Building Installations, Technical University of Lodz, Lodz, Poland

*E-mail of corresponding author: jaroslaw.kaczor@p.lodz.pl

Resume

Angular ball bearings are commonly used whenever there is a demand to increase stiffness of a bearing. The aforementioned increase of stiffness can be achieved by obtaining proper preload in bearings. In common belief, preload has a negative consequence: it increases the load of rolling elements, which must lead to lower durability of bearing compared to the situation before the preload use.

The objective of the research was to analyse how a change of load plane, while applying the preload, affects durability of angular ball bearings. In calculations of durability of bearings, besides elasticity of a shaft, radial, axial and bending elasticities of bearings were taken into consideration, as well.

Article info

Received 27 October 2021
Accepted 2 February 2022
Online 5 April 2022

Keywords:

angular ball bearings
preload
durability of bearing
bearing life

Available online: https://doi.org/10.26552/com.C.2022.3.B170-B188

ISSN 1335-4205 (print version)
ISSN 2585-7878 (online version)

1 Introduction

In modern scientific literature there can be found a lot of information concerning the effect of preload on bearings and bearing systems. The preload is applied not only in the case of angular contact ball bearings but also in the case of other bearings; e.g. [1] presents a generalization of previous works developed by the authors in the field of calculation and selection of slewing bearings where a theoretical model for estimation of the static load-carrying capacity of four-contact-point slewing bearings was obtained.

Authors of [2] present the results of experimental studies on the effects of mechanical preload and bearing clearance on the rotor dynamic performance of lobed gas foil bearings (GFBs) for oil-free turbochargers (TCs).

Great attention was paid to the effect of the preload on stiffness of machine tool spindles in relation to thermal effects; e.g. [3] presents a unified method to predict nonlinear thermal characteristics of a high-speed spindle bearing subjected to a preload. Based on the quasi-static model and finite difference method the change of thermal contact resistance, bearing parameters and heat source with temperature per second is completely analyzed using a new algorithm. As a result, the thermal effects on contact angles, contact forces, the preload and stiffness of the bearing are found. Moreover, analysis results show that the estimated preload and bearing stiffness nonlinearly vary with the increase in temperature. In [4], a multi-criteria optimization was performed for systems bearing-spindle. Many objectives were considered in this work, including vibration frequencies, static stiffness and total friction torque. Bearing preload and bearing position were selected as variable factors.

Then, in [5] are presented the effects of the preload and preload method on the rotational performance of the spindle-bearing system is explored experimentally to reveal the role of preload and preload method in spindle rotational performances under different speeds.

The angular contact ball bearing preload is very important for the high-speed spindles and has a very large effect on the dynamic and thermal characteristics of the spindles [6], vibrations [7], the performance of the spindle system and bearings in a machine tool [8-9], dynamic characteristics of a rotor [10], on the dynamic performance of bearing system [11] and of spindles [12]. In [11] the maximum compliance of the spindle tool tip was found to occur at the bending vibrations of a spindle shaft and vary with the preload amount of a spindle bearing.

The preload has a significant effect on the axial stiffness of the machine tool spindle, as shown in [13-14], where the axial stiffness softening and hardening

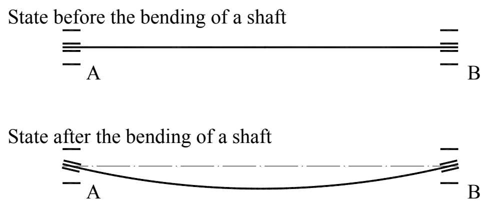

Figure 1 *Tilting of the rings in the bearings due to angular deflection of the shaft [16-17]*

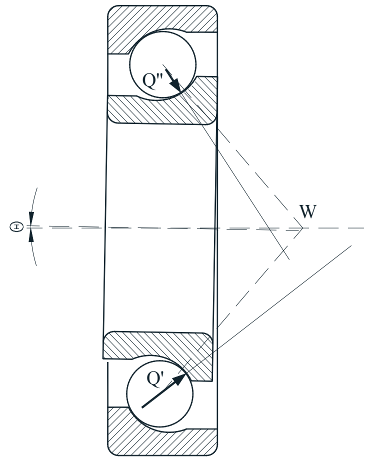

Figure 2 *Direction of internal forces acting in a bearing due to tilting of rings in the bearing by an angle θ: Q' - internal force of the lower ball, Q" - internal force of the upper ball, W - nodal point*

Figure 3 *The emergence of reactionary bending moments in bearings*

characteristics of machine tool spindle are studied. "The results show that when bearing preload reaches a certain relatively large threshold, a "sag" shape occurs in the axial stiffness curve, indicating the "stiffness hardening" characteristic of the spindle. On the other hand, for a small preload no "sag" shape occurs in spindle stiffness curve, indicating the "stiffness softening" characteristic of the spindle. This phenomenon is of great significance for the acquisition of the excellent spindle stiffness properties." [13].

Wear between the rolling elements and raceways has a significant effect on the dynamic characteristics of the bearing, which is the main cause of a bearing failure. The proposed computational models have been developed to investigate the dynamic characteristics of the bearing [15]. However, bearing wear has rarely been studied due to the complexity of the contact load and wear mechanism.

Currently used solutions to the problem define the bearing reaction forces and moments in bearings, assuming that the shaft is perfectly stiff.

However, the susceptibility of the bearings is overlooked. Bearings are considered to be perfectly rigid articulated supports when the reality is different: in most types of bearings, the rings in the bearing tilt relative to each other (Figure 1), which results in contact deformation in the bearing.

Figure 2 shows the tilt of the ring in the bearing. This tilting causes contact deformation where the rolling element is in contact with the raceways, leading to additional internal forces in the bearing. Development of those additional forces in the bearing causes an increase in the pressure Q forces of the rolling elements on the raceways and a change in the action of these forces.

Due to the bearing rings being tilted by an angle θ (Figure 2), the lines of action of the internal force vectors Q 'and Q" pass the nodal point Won the right and as a result create moments of the same signs.

In addition, the lines of action of the forces from all the rolling elements are deflected and this deflection occurs to varying degrees depending on the position of the rolling element on the bearing circumference, resulting in a resultant bending moment in the axial plane of the bearing and shaft. This moment emerges

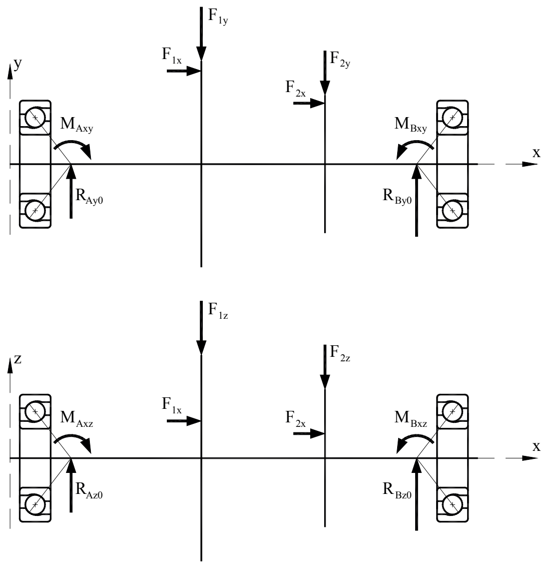

***Figure 4** Calculation of transverse reactions of bearings*

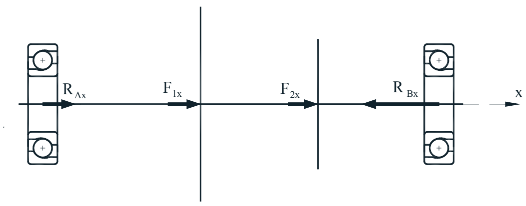

***Figure 5** Calculation of axial reactions of bearings*

simultaneously with the increase of Q forces in relation to the state with no deflection. These bending moments are the bearing's reaction to angular deflection of the shaft and occur in both bearings (Figure 3).

The occurrence of these bending reaction moments in the bearings results in the fact that the bearings are actually loaded completely differently from the simple model based on external forces and support's reactions. Moreover, the resulting reaction bending moments additionally load the shaft and change its deflection line and this affects the bending moment distribution and changes in the reaction of the supports.

In fact, the following loads are exerted on the shaft: (Figure 4 and Figure 5):

- external loads in the form of external forces and moments,
- loads of supports in the form of reaction forces and reaction moments of supports.

All the aforementioned loads have been included in the static equations.

As proven, the values of reaction bending moments are dependent on the shaft deflection line, which means that they are dependent on its stiffness.

If the shaft is loaded in different planes, the shaft deflection line is a three-dimensional line, the shape of which is relatively complicated. Determining the shaft deflection parameters with the use of commonly used formulas is not practical in the case under consideration.

In practice, two methods are used for such complex cases. In the case of many simple shaft loads, the superposition principle can be used, which consists in putting together of the deflection coming from individual forces. Another method used for the complex shaft loads and applied in manuscript, is Mohr's method, based on differential equations describing the geometric parameters of deformations and relationships between loads.

The reaction moments generated in the bearings are the bearings reaction to shaft angular deflection. The values of the reaction bending moments depend on the shaft deflection line and therefore they depend on its stiffness.

When calculating the bearing service life, in addition to shaft elasticity, bearing radial, axial and bending elasticity must be taken into account. The radial and axial elasticity is determined by the dependence of the radial and axial force acting on the bearing and the radial and axial displacement of the rings in the bearings.

On the other hand, bending elasticity is expressed by the dependence of the bending moment, developed in the bearing, on the angular deflection of the rings in the bearing.

Not only the radial and axial reaction, but the reaction moment of each bearing is considered in the static equations of the system, as well. It is worth noting that there is a feedback: the radial displacements in the bearings correspond to the deflections of the shaft on the

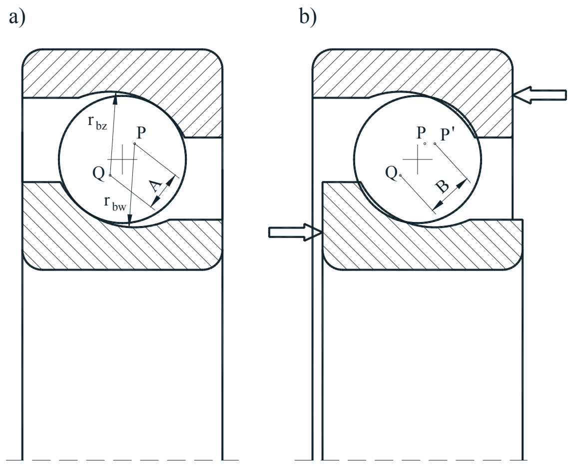

Figure 6 *Ring displacement due to loading and preload*

supports and the angular deflections of the bearing rings are determined by the deflection line of the shaft and this deflection line is affected by the reaction moments of the bearings, which affect the angular deflections of the rings.

The bearing reactions result from the internal forces acting between the bearing elements, which in turn depend on the mutual displacements of the bearing elements.

The pressure force between the rolling part (ball) and the raceway of the ring of the ball bearing is the cause of the contact deformation. This deformation is spatial, i.e. three-dimensional. The area of the deformed surface can be considered elliptical and the profile - parabolic. There is a close correlation between the force Q and the dimensions of the contact ellipse and the depth of deformation in both contacting elements.

Figure 6 shows a half section of the bearing. Figure 6a shows the unloaded condition. In this condition, the ball adheres to both rings without distortion. The center of curvature of the inner ring raceway is at point P and the outer ring is at point Q. The spacing between them is A.

Figure 6b shows the condition after the axial loading of the bearing (obviously greatly exaggerated) and due to the application of preload. The inner ring has been shifted relative to the outer ring and the center of its raceway curvature has moved to the point P ‘. The circle symbolizing the ball now penetrates a certain depth into the profiles of both rings, which causes contact deformation. The contact strains can be determined from the formula:

$$\delta = B - A = P'Q - PQ\,. \tag{1}$$

This principle determines the normal contact deformation for an arbitrarily positioned ball due to a displacements of the inner ring relative to the outer ring. Before presenting this spatial analysis, it is necessary to define the geometrical design features of the bearing.

The calculation of deformations in the contact between any sphere and rings can be done using the vector calculus. It will be more correct to explain this procedure in a three-dimensional drawing showing all the displacements. The method shown is used in this procedure and is illustrated in Figure 7. The starting point is an approximation of the rings in the bearing (inner relative to outer) on which this ball is located. The measure of this approximation is the local distance between the circles OK_p and OK_q. This can be delineated by considering the change in position of point P to position P’. This transition consists in the displacement of the inner ring in the x, y, z directions and its deflection about around the y and z axes:

- shift in the x direction: f_x
- shift in the y direction: f_y
- shift in the z direction: f_z
- tilt with respect to y axis: $r_p \cdot \Theta_y \cdot \sin\psi$
- tilt with respect to z axis: $r_p \cdot \Theta_z \cdot \cos\psi$.

The point P’ has a different axial plane from the point P because it experiences some circumferential shift. This new plane is indicated in Figure 7 by the vertices of ae triangle BP’Q’. Therefore, the distance between the circles OK_p and OK_q, is the distance between the points P’ and Q’ to be measured. For a more accessible illustration of the components of the displacement of point P to P’, an additional Figure 8 is provided, showing the plane BP’Q’, where point P is converted to point PP. The displacements f_y and f_z are projected onto the plane BP’Q’. The difference between the distances P’Q’ and PP Q’ defines the value of the ring approximation.

After determining the rapprochement of the rings δ and the Hertzian parameters of the contact δ* and Σρ, it is now possible to determine the force Q at the contact point under consideration.

Knowing the Q forces acting between the balls and rings allowed to determine the reaction forces and the reaction moments for the spatial force system. The notation of the reactions is shown in Figure 9.

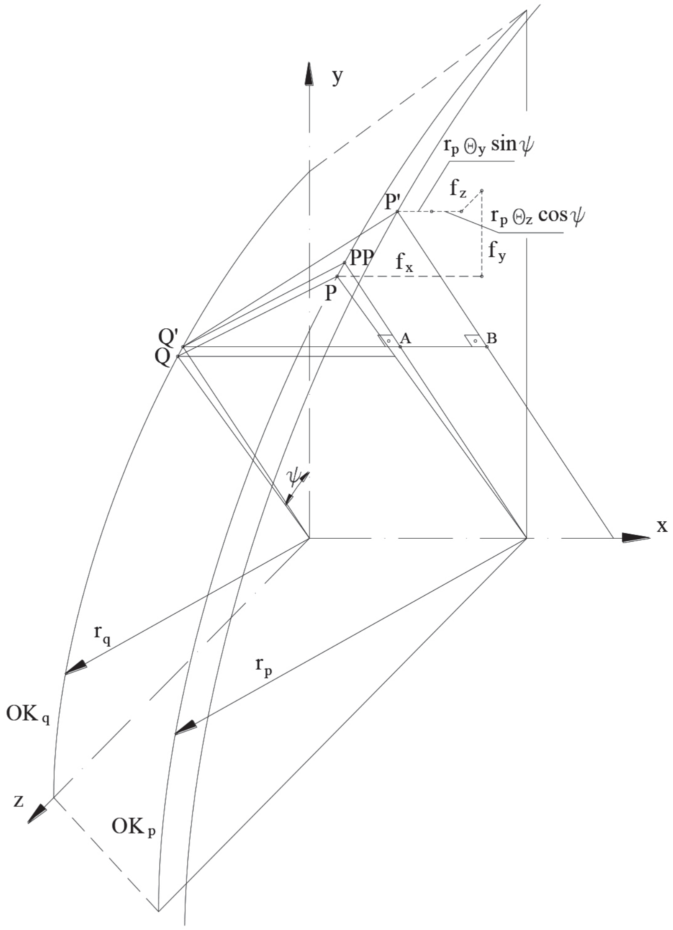

***Figure 7** Local approximation of rings*

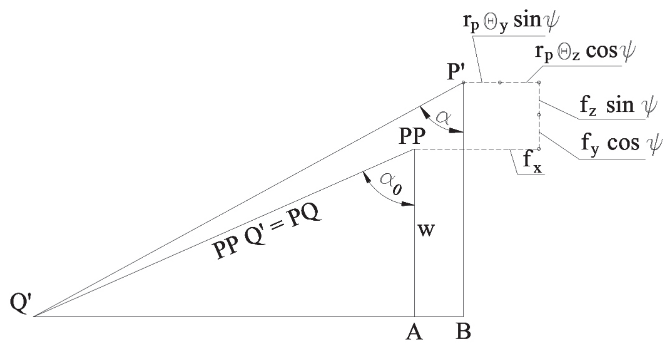

***Figure 8** Illustration in the BP 'Q' plane of the principle of calculating the local rapprochement of the rings*

The upper figure in the perspective view shows the arc of the centers of curvature of the outer ring raceway. The Q forces are applied to the points on this arc, which act between the rolling elements and the bearing raceway. They are deviated from the y-z plane by the angle α. As a result of the projection of the Q forces on the assumed axes of symmetry, one obtains the following formulas:

$$Q_x = Q \cdot \sin\alpha \,, \tag{2}$$

$$Q_r = Q \cdot \cos\alpha \,, \tag{3}$$

$$Q_y = Q_r \cdot \cos\psi = Q \cdot \cos\alpha \cdot \cos\psi \,, \tag{4}$$

$$Q_z = Q_r \cdot \sin\psi = Q \cdot \cos\alpha \cdot \sin\psi \,, \tag{5}$$

$$M_{xz} = Q \cdot \frac{r_q \cdot (r_{bw} + r_{bz} - D_k)}{w} \cdot \sin(\alpha - \alpha_0) \cdot \sin\psi \,, \tag{6}$$

$$M_{xy} = Q \cdot \frac{r_q \cdot (r_{bw} + r_{bz} - D_k)}{w} \cdot \sin(\alpha - \alpha_0) \cdot \cos\psi \,. \tag{7}$$

Equations (2) ÷ (7) define the loads occurring on one, arbitrary, rolling element.

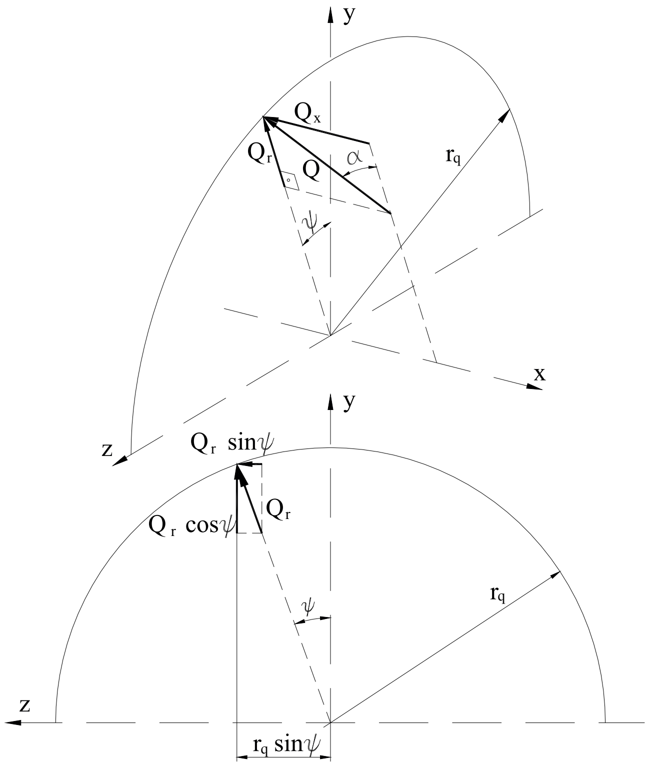

Figure 9 *Determining the reaction of bearing*

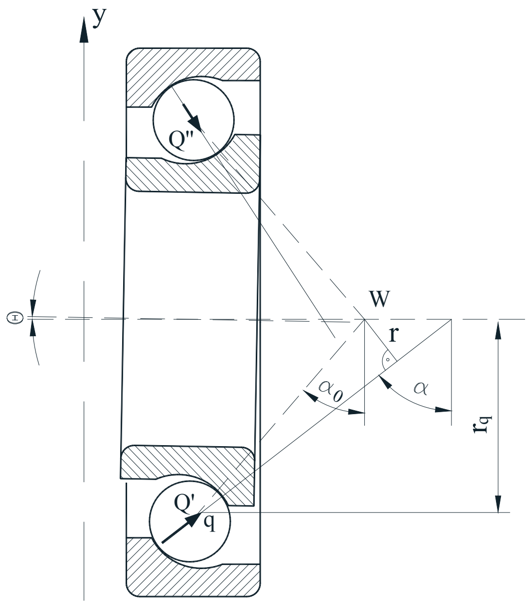

Figure 10 *Determining the reaction moment of a bearing [18-19]*

The moment from the force Q is to be determined with respect to the point W, which is measured at the point of support of the shaft on the bearing. This calculation is shown in Figure 10. The force Q is applied at the center of the outer ring raceway curve, denoted as q. The moment of force Q coming out of any sphere (here a sphere lying in the plane of the diagram is chosen) is:

$$M = Q \cdot r \,. \tag{8}$$

The total bearing reactions and reaction moments are the result of the interaction of each rolling element in the bearing and are determined by adding the forces and moments resulting from rolling elements under the normal deformation:

$$R_x = \sum (Q \cdot \sin\alpha) \,, \tag{9}$$

$$R_r = \sum (Q \cdot \cos\alpha) \,, \tag{10}$$

$$R_y = \sum(Q \cdot \cos\alpha \cdot \cos\psi), \tag{11}$$

$$R_z = \sum(Q \cdot \cos\alpha \cdot \sin\psi), \tag{12}$$

$$M_{xz} = \sum\left[Q \cdot \frac{r_q \cdot (r_{bw} + r_{bz} - D_k)}{w} \cdot \sin(\alpha - \alpha_0) \cdot \sin\psi\right], \tag{13}$$

$$M_{xy} = \sum\left[Q \cdot \frac{r_q \cdot (r_{bw} + r_{bz} - D_k)}{w} \cdot \sin(\alpha - \alpha_0) \cdot \cos\psi\right]. \tag{14}$$

The formulas presented here allowed the reactions of the two shaft bearings to be determined separately, based on their separate internal deformations.

The above shows determination of the shaft support reactions based on the shaft loads and determination of the bearing reactions as a response to the deformations taking place in them. The shaft supports are, of course, the bearings. Both reactions must therefore be respectively equal to each other. It is one of the components of the bearing balance. The first is the equilibrium of the reaction in the directions perpendicular to the shaft axis, i.e. y and z. If the lateral reaction, calculated as the support reaction, was greater than the bearing reaction resulting from internal deformations in it, for example:

$$R_{Ay0} > R_{Ay}, \tag{15}$$

or $R_{Az0} > R_{Az}$, (16)

or $R_{By0} > R_{By}$, (17)

or $R_{Bz0} > R_{Bz}$, (18)

then the calculation procedure increases the internal displacement in the corresponding bearing (A or B) in the appropriate direction (x or y), so as to satisfy all the above equations. In the event of the opposite sign of inequality, the corresponding displacement in the corresponding bearing is reduced.

In the direction of the shaft axis, the balance of the axial external forces and the axial reactions of the bearings is checked. The resultant of these forces:

$$W_x = R_{Ax} + \sum F_{ix} - R_{Bx}, \tag{19}$$

should be zero. If it is less than zero, the calculation procedure shifts the shaft along with the inner rings of the bearings to the left in order to increase the left bearing deformation and consequently increase the R_{Ax} force and at the same time reduce the R_{Bx}. If, on the other hand, this resultant $W_x > 0$, then the calculation procedure shifts the shaft along with the inner rings of the bearings to the right in order to reduce the R_{Ax} force and at the same time increase the R_{Bx}.

The iterative process presented above, used in the computer program, makes it possible to calculate such displacements and tilts of the inner rings in relation to the outer rings in both bearings, that all the equilibrium equations are simultaneously satisfied.

The absolute equivalent load on the ring, moving in relation to the load, is equivalent to the time-averaged load of the ball circling the bearing Q_{sr}. This value is calculated in the computer program according to the known dependence taking into account the equivalent effort of the material subjected to variable loads:

$$Q_{sr} = \frac{1}{Z}\sum_{i=1}^{Z} Q_i^3. \tag{20}$$

The equivalent load of a point contact radial bearing is calculated from the formula:

$$P = \frac{0.2288}{0.5625} \cdot Z \cdot Q_{sr} = 0.4068 \cdot Z \cdot Q_{sr}. \tag{21}$$

The angular contact ball bearing belongs to the deep groove bearings with point contact. The fatigue strength of the raceways and balls of an angular contact bearing depends in the same way on their averaged load as in a deep groove ball bearing, provided that the total load is taken into account, not only its radial component. In the developed procedure, the total loads are calculated. Therefore, the formula was adopted for the angular contact ball bearing.

Based on the Weibull theory, an expression was obtained:

$$L = \left(\frac{C}{P}\right)^p. \tag{22}$$

The number L is the number of million revolutions the bearing can make before the raceway or rolling elements are damaged. The exponent of the power p is a number with different values depending on the bearing type. For the ball bearings, p = 3.

2 The calculation method used

In order to solve the problem, it was necessary to combine such issues as: deflection line of machine shaft for the complex external load, dislocations of inner rings in relation to the outer ones as a result of loads and of preload, elastic contact deformations in the points of contact of rolling parts with the track in both bearings of the system, calculations of contact forces in bearings, based on contact deformations, balance between inner (contact) forces and outer loading of the whole bearing, calculations of durability of bearings based on these contact forces.

The adoption of a correct computational model is a crucial step towards finding a theoretical solution to the problem. On the correctness of the model depends the scope of the considered phenomena, the degree

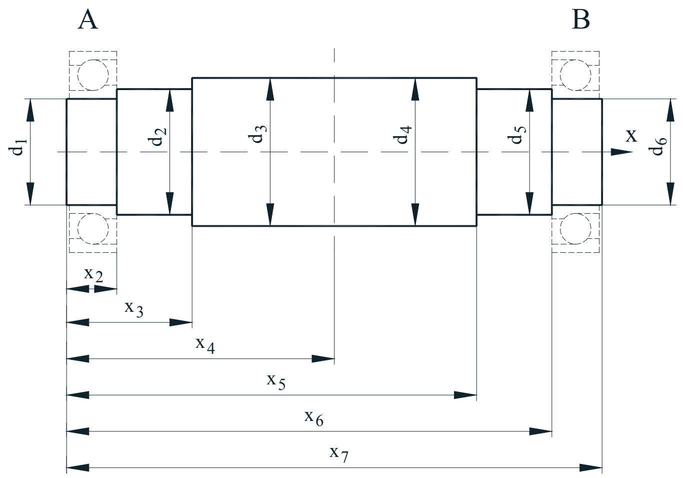

Figure 11 *Sketch of a model shaft*

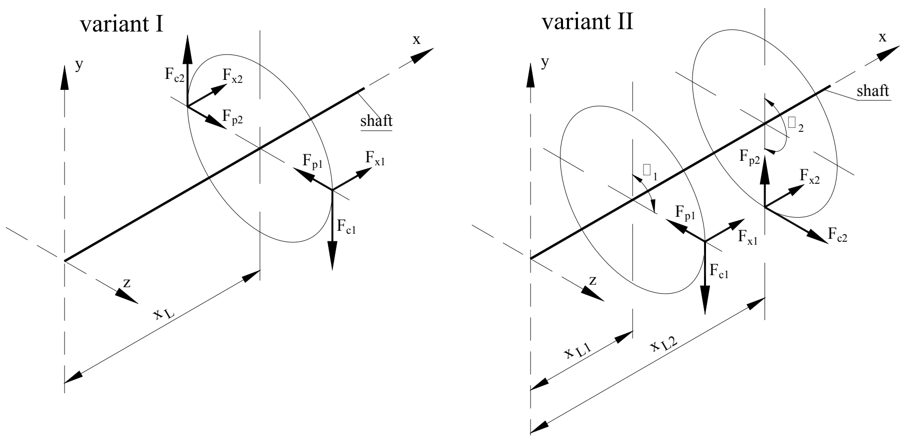

Figure 12 *Load variants adopted*

of approximation to reality and the amount of work needed to apply the solution. For the present study, used a method developed by the author, which was applied in papers [20-24] and others.

3 Analytical considerations

These types of bearings work in arrangements and must be considered in arrangements. Forces that occur in bearings depend, among others, on the load bearing, shaft deflection. The bearing load or the shaft deflection line depends again on the way the external shaft is loaded. Possibilities are endless, therefore a specific construction had to be assumed by the author.

The assumed construction was a model shaft (Figure 11) with two 7212B angular ball bearings of a dynamic capacity of C=57200 N, according to [25].

The model shaft has the following dimensions: x_2 = 22 mm, x_3 = 100 mm, x_4 = 200 mm, x_5 = 300 mm, x_6 = 371 mm, x_7 = 400 mm, d_1 = 60 mm, d_2 = 67 mm, d_3 = 75 mm, d_4 = 75 mm, d_5 = 67 mm, d_6 = 60 mm. The bearing was a subject to calculations for loadings different in values and differently placed. Variants of locations are shown in Figure 12. In one variant of location (variant I) it is assumed the load is assumed to be on either side of a single gear located at a distance x_L distance from the end of the shaft. In another variant (variant II) loads are applied on two gears placed at x_{L1} and x_{L2} distances from the end of the shaft. Location of points of application is defined by angles β_1 and β_2.

The locations of the load planes were taken in relation to the shaft length L_w, which corresponds to dimension x_7:

For variant I of the location (Figure 12 - left): $x_L = 0.3\ L_w$, $x_L = 0.4\ L_w$, $x_L = 0.5\ L_w$, $x_L = 0.6\ L_w$ or $x_L = 0.7\ L_w$.

For variant II of the location (Figure 12 - right): $x_{L1} = 0.4\ L_w$, $x_{L2} = 0.6\ L_w$, for the angles: $\beta_1 = \beta_2 = 90^{\circ}$ and $\beta_1 = 90^{\circ}$, $\beta_2 = 180^{\circ}$ or $\beta_1 = 90^{\circ}$, $\beta_2 = 270^{\circ}$.

Diameter of the rolling: D_t = 200 mm.

It has been assumed, that loads in both the points presented in Figure 12 are identical. ($F_{c1} = F_{c2}$, $F_{p1} = F_{p2}$, $F_{x1} = F_{x2}$). The diameters of the gears are the same.

The circumferential load F_{c1} on the alleged gear F_{c1} depends on dynamic capacity of the bearing and will be assumed as 0.1 C, when F_{p1}=0.36 F_{c1}.

Characteristics of durability of bearings, when considering the preload for the obtained values, are presented in the Figures 13÷19:

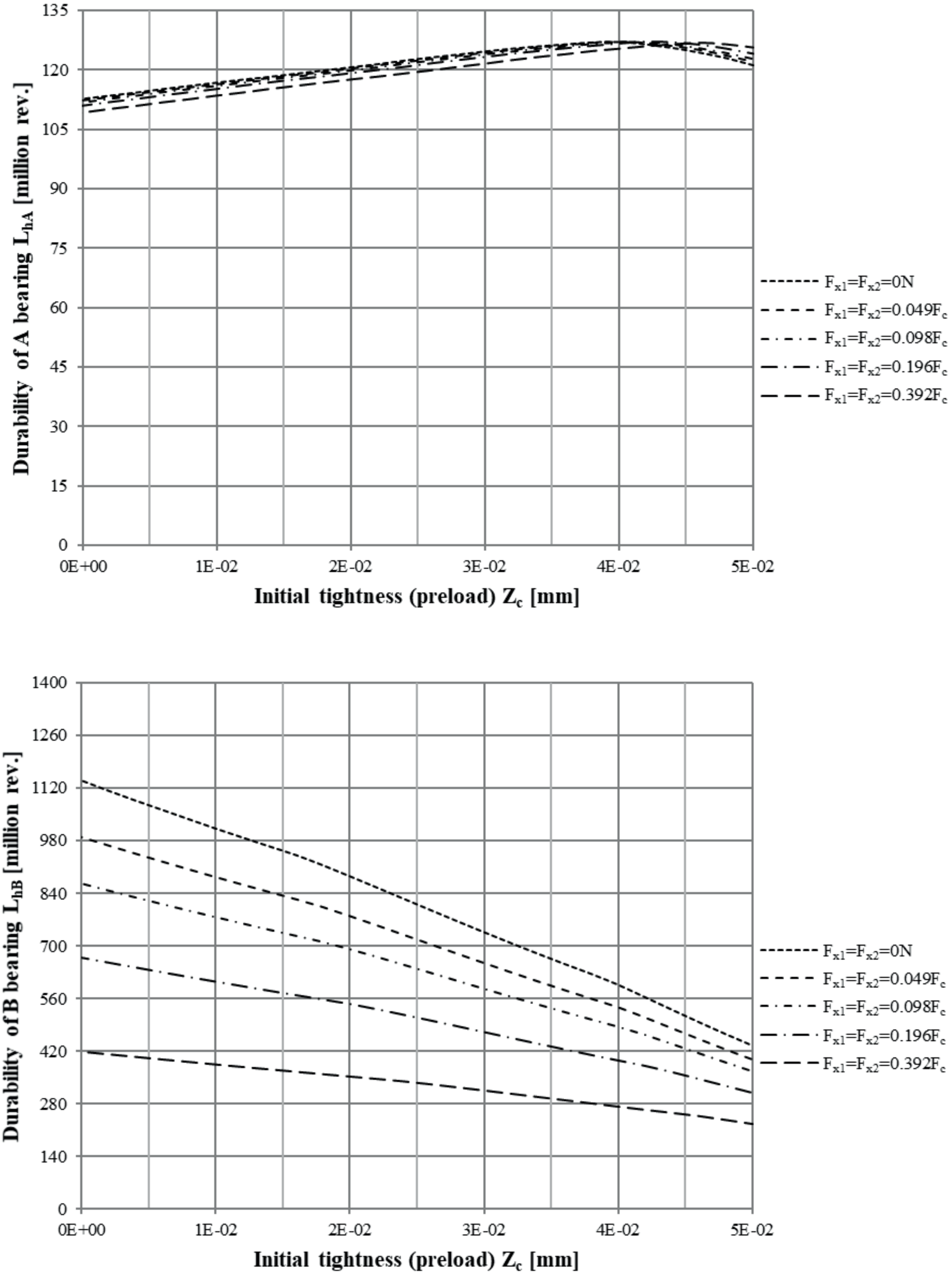

Figure 13 *Durability of bearings A and B for the load plane x_L = 0.3 L_W for variant I of the load*

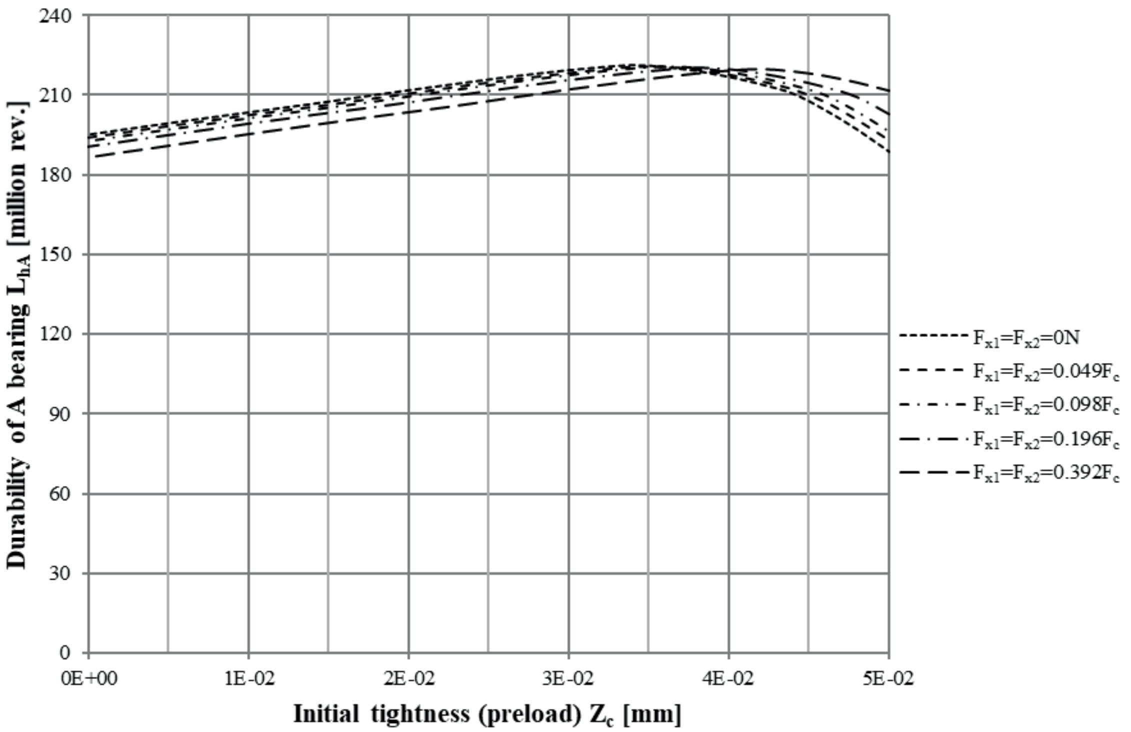

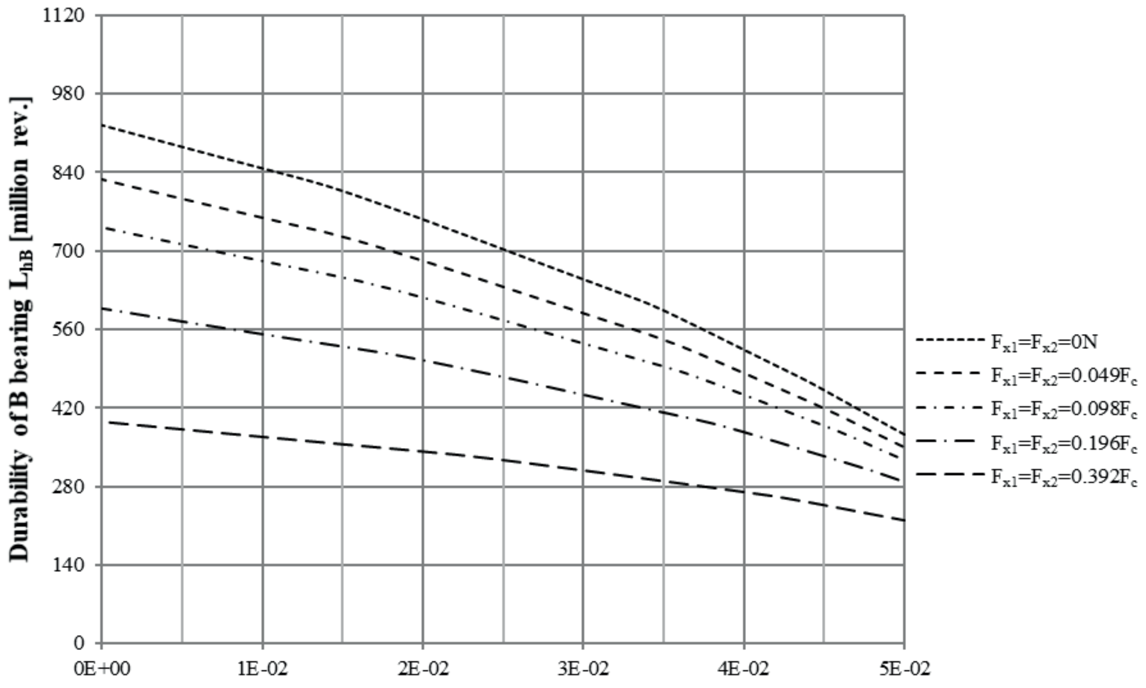

***Figure 14** Durability of bearings A and B for the load plane $x_L = 0.4\ L_W$ for variant I of the load*

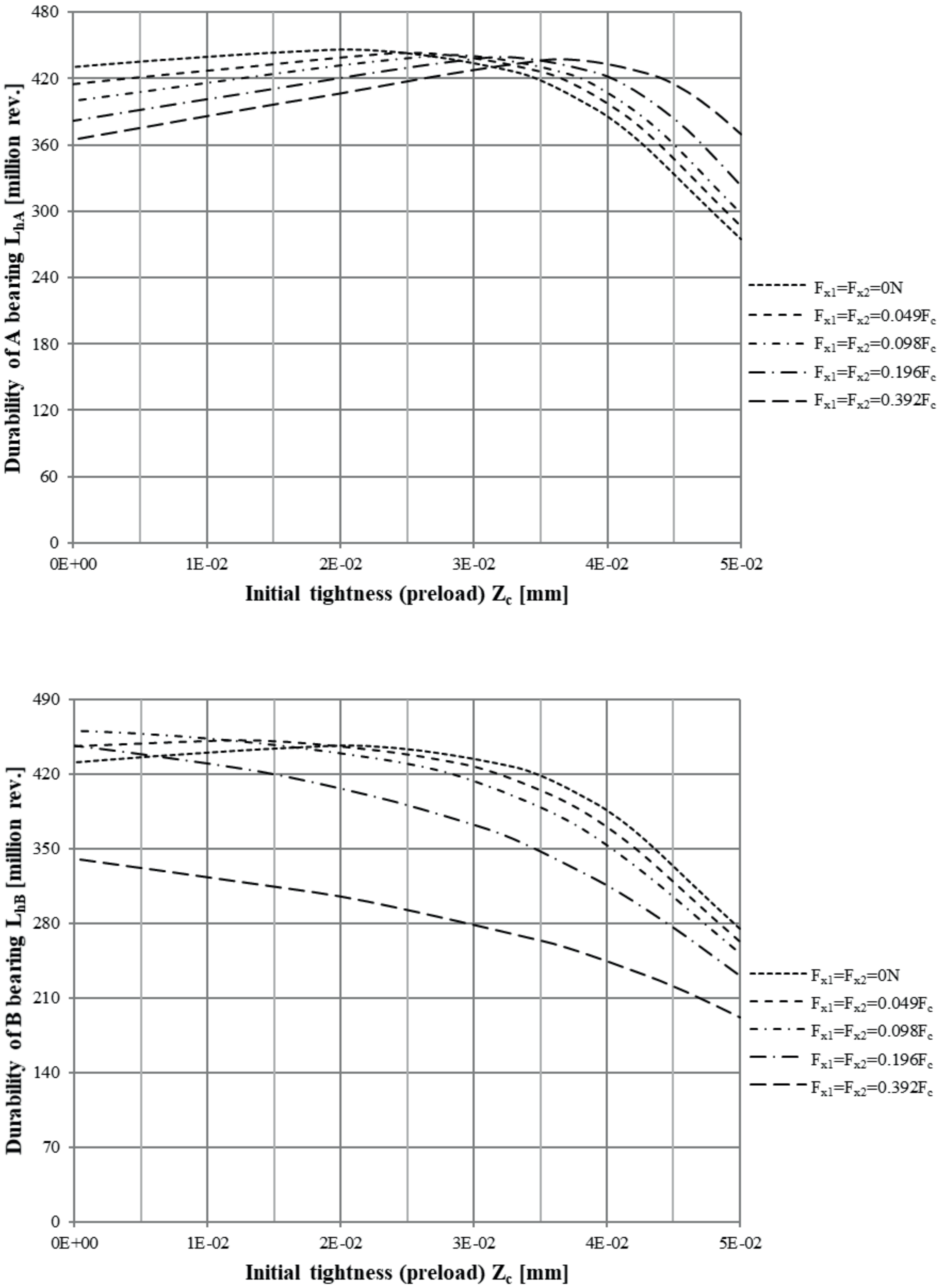

Figure 15 *Durability of bearings A and B for the load plane $x_L = 0.5\ L_W$ for variant I of the load*

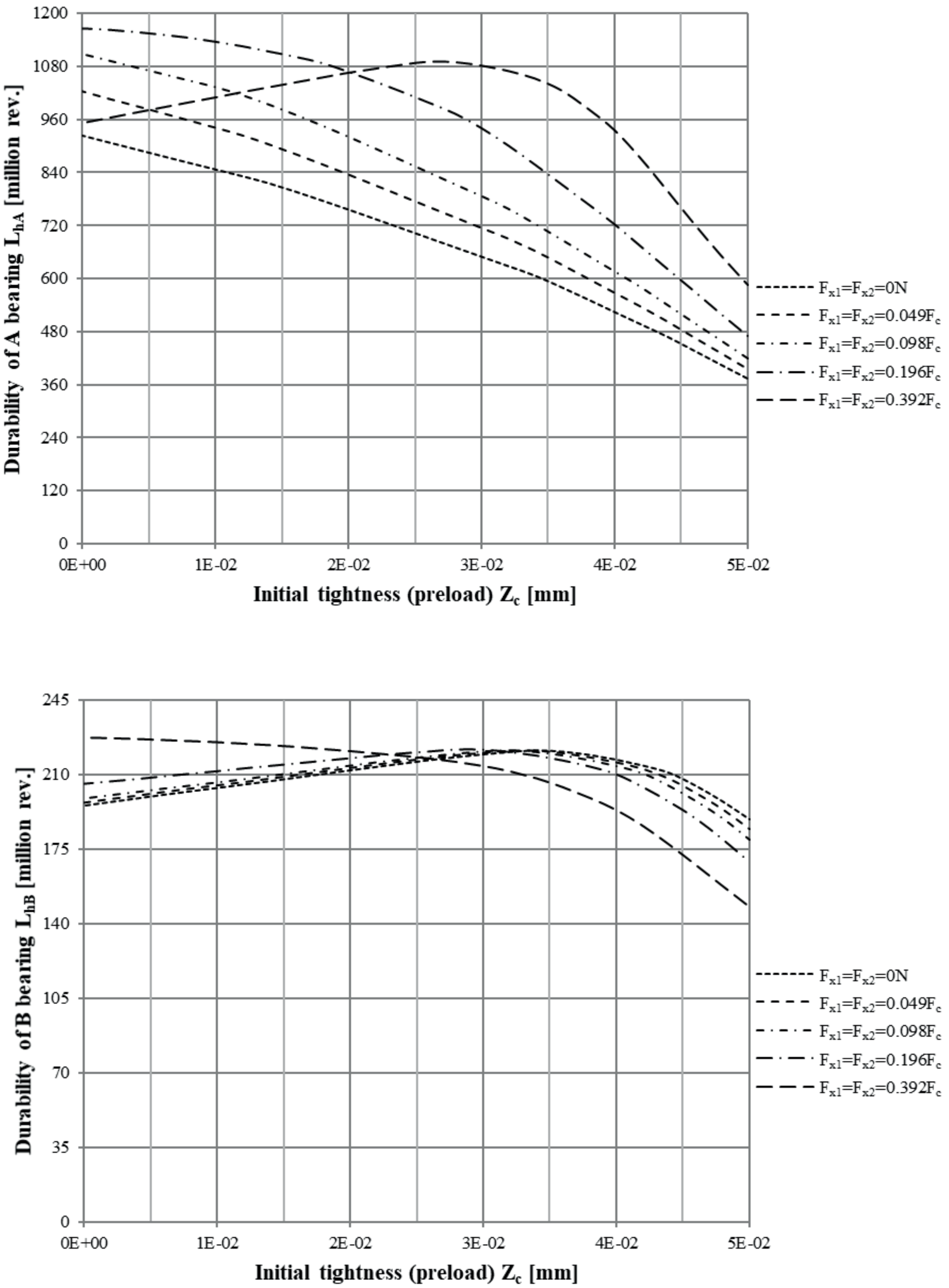

Figure 16 *Durability of bearings A and B for the load plane $x_L = 0.6\ L_W$ for variant I of the load*

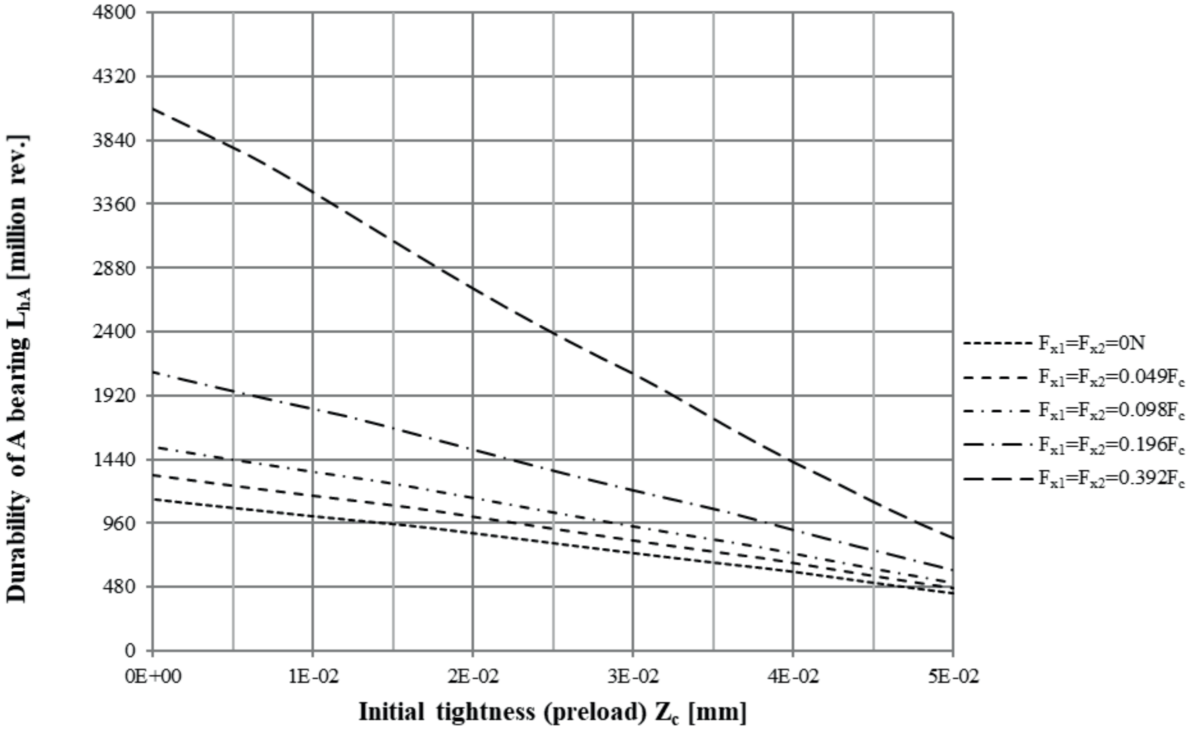

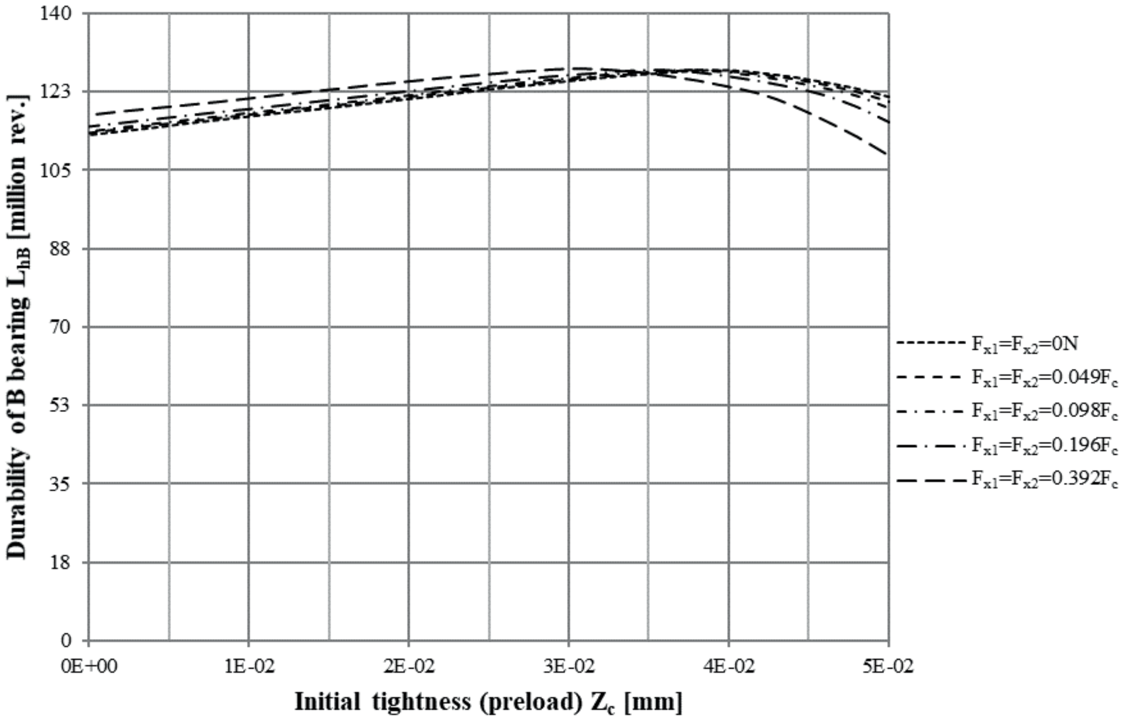

Figure 17 *Durability of bearings A and B for the load plane $x_L = 0.7\ L_W$ for variant I of the load*

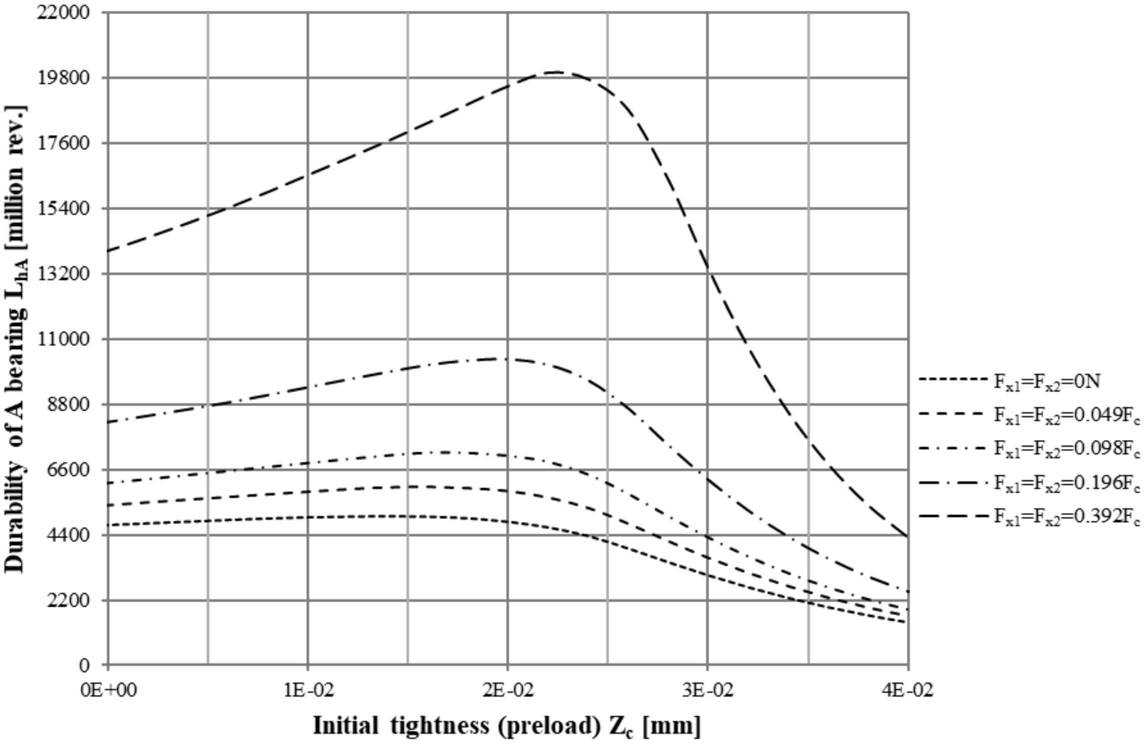

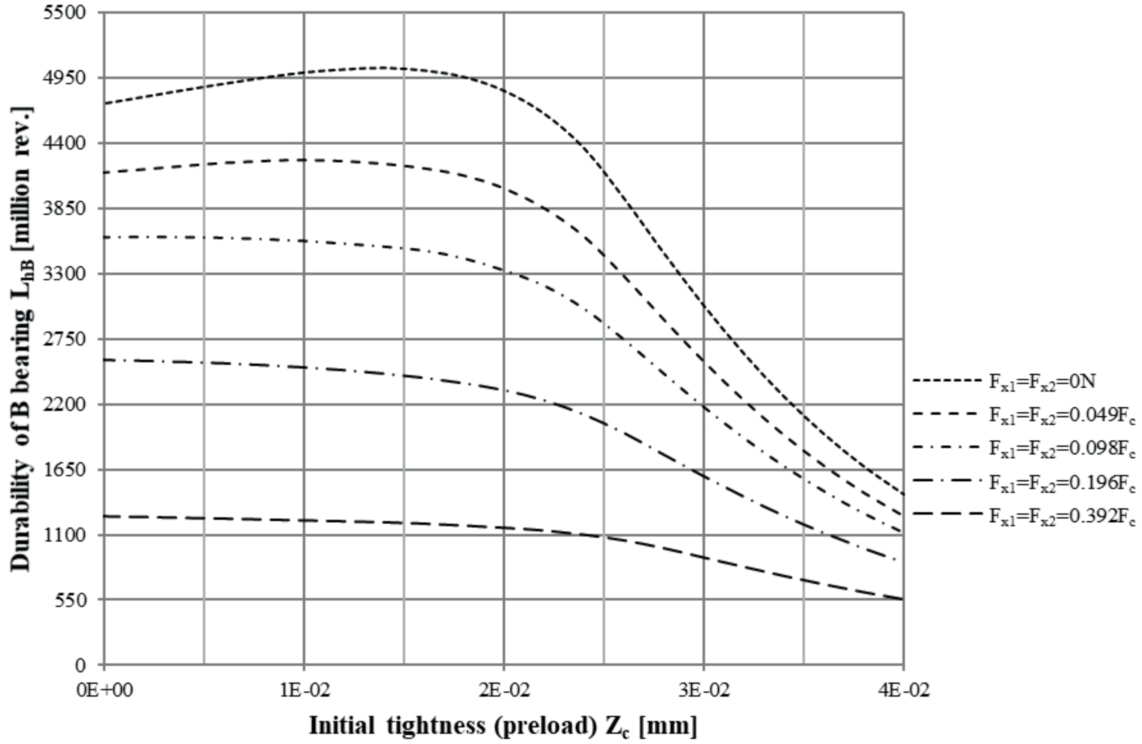

Figure 18 *Durability of bearings A and B for variant II of the loading and for the angles of the load applications* $\beta_1 = 90^o$, $\beta_2 = 90^o$

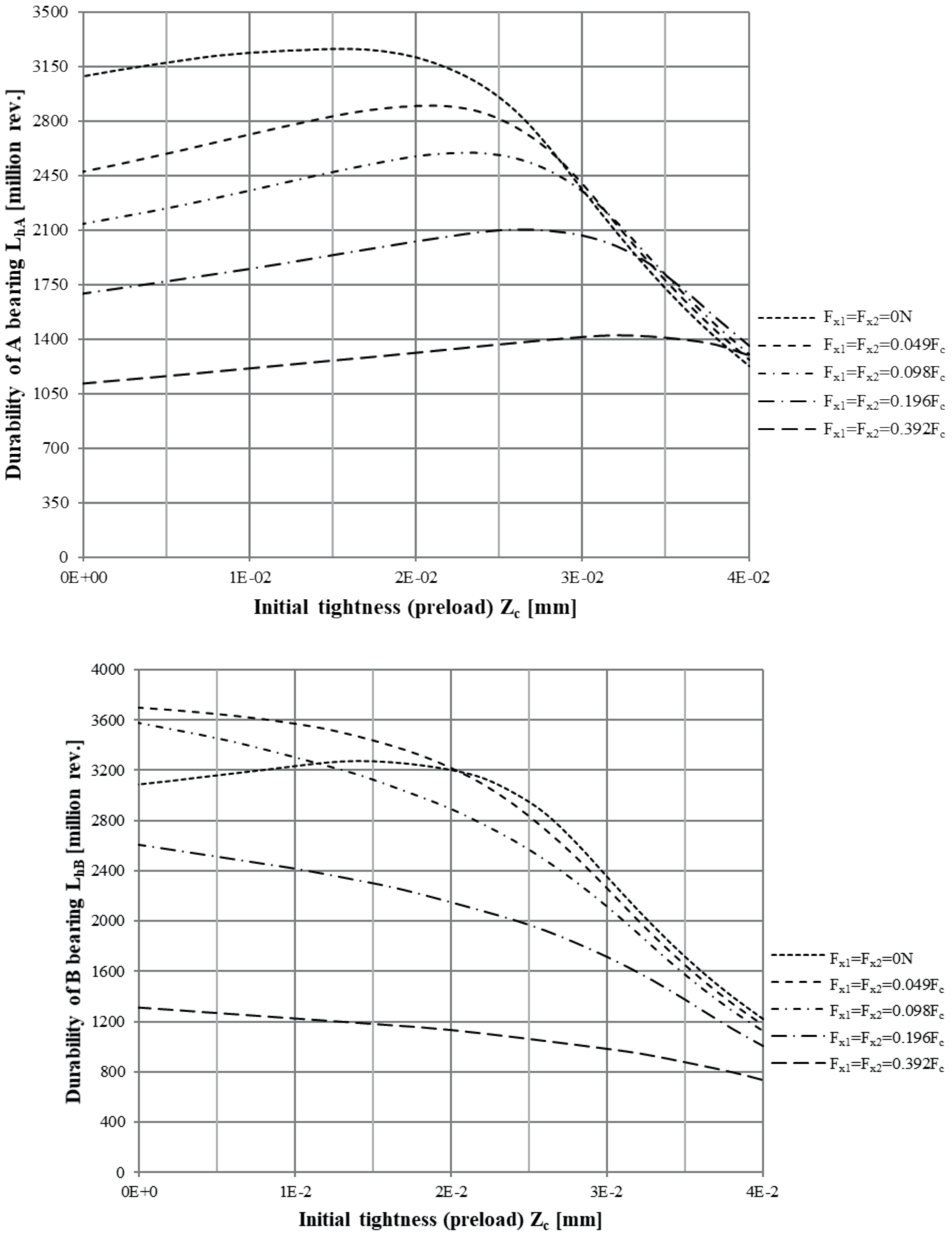

Figure 19 *Durability of bearings A and B for variant II of the loading and for the angles of the load applications* $\beta_1 = 90^o$, $\beta_2 = 180^o$

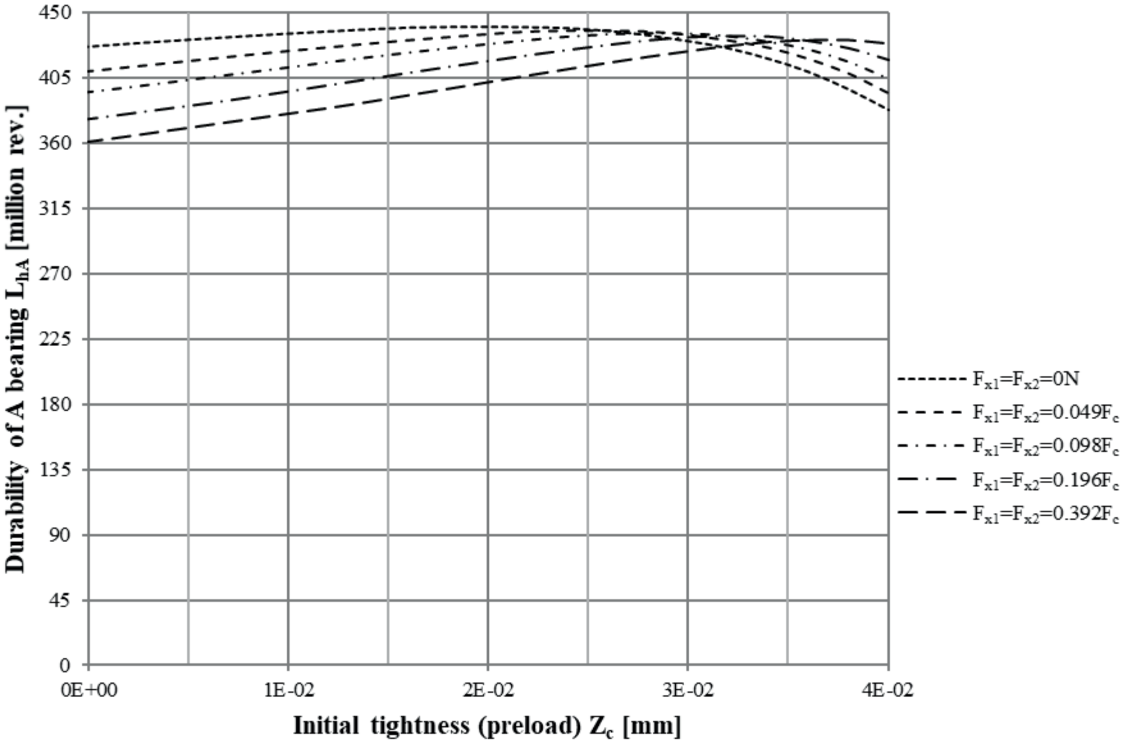

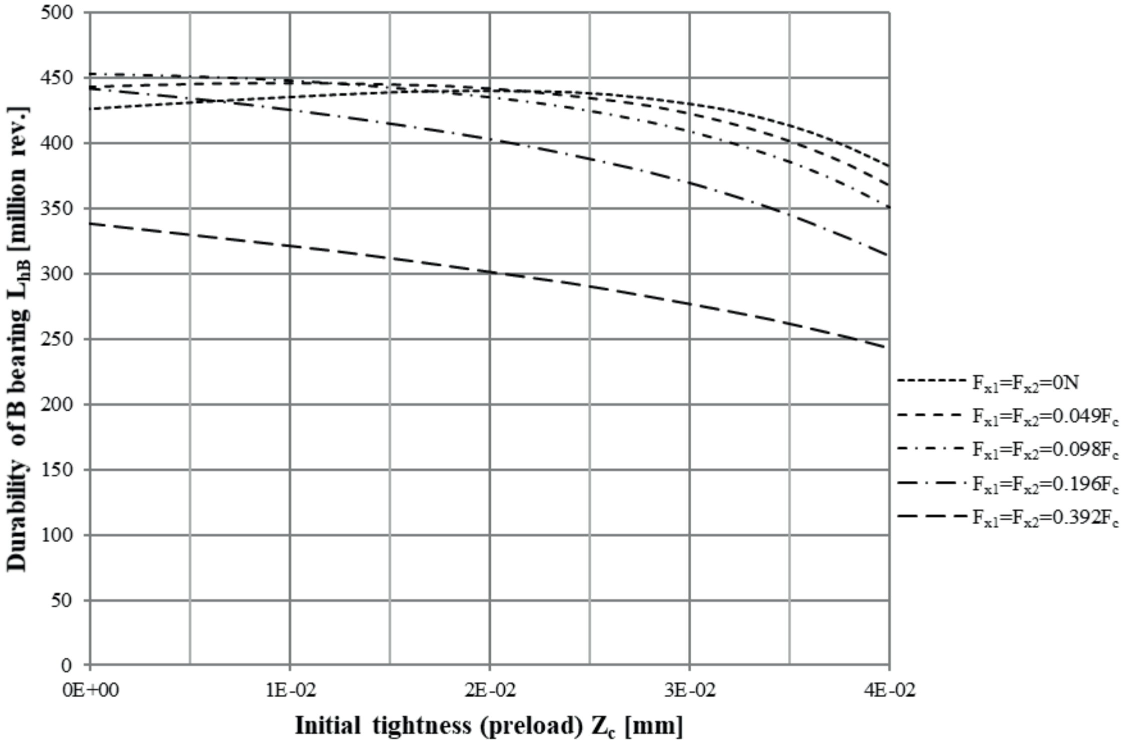

Figure 20 *Durability of bearings A and B for variant II of the loading and for the angles of the load applications* $\beta_1 = 90^{o}$, $\beta_2 = 270^{o}$

4 Deduction

The following observations have been made based on Figures 13÷20:

When loads are applied to the shaft located closer to the left bearing, then, independently of the value of the cross-bending and axial loads, together with the increase of preload $Z_{c,}$ durability of bearing A increases slowly up to a certain value Z_c and then falls rapidly. The maximum value is reached for different Z_c values, depending on the values of loadings. In contrast, the life of the right bearing (B) under these conditions decreases markedly over the entire range of increasing preload. Furthermore, the life curves of bearing B have different levels depending on the axial force, which is understandable since it is directed at the right bearing.

When the forces are applied exactly in the middle between the bearings, the life curve A bearing is similar to the previous case, which means they obtain maximum values. However, in this case these maximum values are visibly "dislocated" in correlation to one another, depending on the axial load values. In contrast to the previous load placement, in this case certain curves of durability of the bearing B (the right one) also obtain maximum values. Those are the curves that correspond to the lowest values of axial force (below 0.1 F_c). For the higher values of axial force, the characteristics of durability of the bearing B have a falling course.

If the loads are applied closer to the bearing on the right side, both the bearing life of bearing A and B vary with the axial force. For a large value of the axial force (above 0.2 Fc), the life curves of bearing A increase to a certain maximum value, but for a smaller axial force these curves decrease monotonically as the preload value increases from 0. On the other hand, the life curves of bearing B behave in the opposite way: the appearance of maximum values can be observed when the axial force is less than 0.2 Fc. When the axial force is higher, the life characteristics of bearing B decrease, but not so sharply.

With the loads applied to the two different wheels, located as in Figure 12, the character of the curves resembles the course characteristic of the position of the load plane exactly in the center of the shaft. All the curves durability of the bearing A demonstrate maxima located in a similar range of preload as in the case of central location of one plane of the load. Whereas out of the durability curves of the bearing B, only the one corresponding to the axial force 0 reaches maximum for the positive value of preload. Other curves are decreasing.

Advantageous durability characteristics for bearings are visible in all the graphs. A small number of lines fall moderately with the increase of preload. However, most of the lines have a rising course, at times, even a significantly rising one.

5 Conclusion

Observations presented above prove, that only when the plane of loading is placed at a half the distance between the bearings and with a low axial load (below 0.1 F_c), a preload enables achieving the increase in durability of both bearings. In all the other cases, the life characteristics of A and B bearings are opposite: when one characteristics increases, the other characteristics simultaneously decreases.

However, it would be too superficial to assume that the use of preload in bearings is usually a harmful factor. It is known that as a result of preload an increase of longitudinal stiffness of a bearing system is obtained, which is beneficial. The observed phenomena mean only that characteristics of durability, when observed separately, will not provide an answer to the question about the optimum value of preload for a specific shaft load.

An application of variable preload is necessary because it has a big impact on bearings' performance, which is shown in [26].

In article [27] a new automatic variable preload system has been proposed. This system fits the preload, however it only depends on the spindle rotational speed. It is crucial to remember that the internal contact feature and thermally induced dynamic preload are essential for a ball bearing which is one of the key problems associated with thermal instability and lock-up problems at high rotational speed.

In [28] is presented a thermo-mechanical coupling model for the angular contact ball bearing with preload and temperature compensation, for the purpose of dynamic preload monitoring.

An interesting solution of the preload has been shown in [29] where the piezoelectric actuators have been used. Furthermore, this article may form the basis for future research into intelligent preload control technology, as well as investigating the thermal-mechanical-dynamic characteristics of the high-speed bearing system.

References

[1] AQUIRREBEITIA, J., PLAZA, J., ABASOLO, M., VALLEJO, J. Effect of the preload in the general static load-carrying capacity of four-contact-point slewing bearings for wind turbine generators: theoretical model and finite element calculations. *Wind Energy* [online]. 2014, **17**(10), p. 1605-1621. eISSN 1099-1824. Available from: https://doi.org/10.1002/we.1656

[2] CHOI, CH.-H., LEE, CH.-M. A variable preload device using liquid pressure for machine tools spindles. *International Journal of Precision Engineering and Manufacturing* [online]. 2012, **13**, p. 1009-1012. ISSN 2234-7593, eISSN 2005-4602. Available from: https://doi.org/10.1007/s12541-012-0131-2

[3] BAI, CH., ZHANG, H., XU, Q. Effects of axial preload of ball bearing on the nonlinear dynamic characteristics of a rotor-bearing system. *An International Journal of Nonlinear Dynamics and Chaos in Engineering Systems* [online]. 2008, **53**(3), p. 173-190. ISSN 0924-090X, eISSN 1573-269X. Available from: https://doi.org/10.1007/s11071-007-9306-2

[4] CAO, H., HOLKUP, T., ALTINTAS, Y. A comparative study on the dynamics of high speed spindles with respect to different preload mechanisms. *The International Journal of Advanced Manufacturing Technology* [online]. 2011, **57**(9), p. 871-883. ISSN 0268-3768, eISSN 1433-3015. Available from: https://doi.org/10.1007/s00170-011-3356-9

[5] CHEHG, H., ZHANG, Y., LU, W., YANG, Z. Research on the effect of structural and material parameters on vibrations based on quasi-static model of bearings. *Journal of the Brazilian Society of Mechanical Sciences and Engineering* [online]. 2020, **42**(11), 578. ISSN 1678-5878, eISSN 1806-3691. Available from: https://doi.org/10.1007/s40430-020-02659-x

[6] GAOFENG, H., WEIGUO, G., YE, CH., DAWEI, Z., YANLING, T., XIANGYANG, Q., HONGIJE, Z. An experimental study on the rotational accuracy of variable preload spindle-bearing system. *Advances in Mechanical Engineering* [online]. 2018, **10**(5), p. 1-14. ISSN 1687-8132, eISSN 1687-8140. Available from: https://doi.org/10.1177/1687814018776171

[7] GU, J., ZHANG, Y., LIU, H. Influences of wear on dynamic characteristics of angular contact ball bearings. *Meccanica* [online]. 2019, **54**(7), p. 945-965. ISSN 0025-6455, eISSN 1572-9648. Available from: https://doi.org/10.1007/s11012-019-00996-3

[8] HU, G., ZHANG, D., GAO, W., CHEN, Y., LIU, T., TIAN, Y. Study on variable pressure/position preload spindle-bearing system by using piezoelectric actuators under close-loop control. *International Journal of Machine Tools and Manufacture* [online]. 2017, **125**, p. 68-88. ISSN 0890-6955. Available from: https://doi.org/10.1016/j.ijmachtools.2017.11.004

[9] HUNG, J.-P., LAI, Y.-L., LUO, T.-L., SU, H.-CH. Analysis of the machining stability of a milling machine considering the effect of machine frame structure and spindle bearings: experimental and finite element approaches. *The International Journal of Advanced Manufacturing Technology* [online]. 2013, **68**(9-12), p. 2393-2405. ISSN 0268-3768, eISSN 1433-3015. Available from: https://doi.org/10.1007/s00170-013-4848-6

[10] HWANG, Y.-K., LEE, CH.-M. A review on the preload technology of the rolling bearing for the spindle of machine tools. *International Journal of Precision Engineering and Manufacturing* [online]. 2010, **11**(3), p. 491-498. ISSN 2234-7593, eISSN 2005-4602. Available from: https://doi.org/10.1007/s12541-010-0058-4

[11] SIM, K., LEE, Y.-B., KIM, T. Effects of mechanical preload and bearing clearance on rotor dynamic performance of lobed gas foil bearings for oil-free turbochargers. *Tribology Transactions* [online]. 2013, **56**(2), p. 224-235. ISSN 1040-2004, eISSN 1547-397X. Available from: https://doi.org/10.1080/10402004.2012.737502

[12] HWAN, Y.-K., LEE, CH.-M. Development of a simple determination method of variable preloads for high speed spindles in machine tools. *International Journal of Precision Engineering and Manufacturing* [online]. 2015, **16**(1), p. 127-134. ISSN 2234-7593, eISSN 2005-4602. Available from: https://doi.org/ 10.1007/s12541-015-0016-2

[13] KIM, D. H., LEE, CH. M. A study on the development of a new conceptual automatic variable preload system for a spindle bearing. *The International Journal of Advanced Manufacturing Technology* [online]. 2013, **65**, p. 817-824. ISSN 0268-3768, eISSN 1433-3015. Available from: https://doi.org/10.1007/s00170-012-4219-8

[14] ZHANG, J., FANG, B., ZHU, Y., HONG, J. A comparative study and stiffness analysis of angular contact ball bearings under different preload mechanisms. *Mechanism and Machine Theory* [online]. 2017, **115**, p. 1-17. ISSN 0094-114X. Available from: https://doi.org/10.1016/j.mechmachtheory.2017.03.012

[15] LI, J., ZHU, Y., YAN, K., YAN, X., LIU, Y., HONG, J. Research on the axial stiffness softening and hardening characteristics of machine tool spindle system. *International Journal of Advanced Manufacturing Technology* [online]. 2018, **99**, p. 951-963. ISSN 0268-3768, eISSN 1433-3015. Available from: https://doi.org/10.1007/s00170-018-2456-1

[16] KACZOR, J., RACZYNSKI, A.The effect of preload of angular contact ball bearings on durability of bearing system. *Proceedings of the Institution of Mechanical Engineers, Part J: Journal of Engineering Tribology* [online]. 2015, **229**(6), p. 723-732. ISSN 1350-6501, eISSN 2041-305X. Available from: https://doi.org/10.1177/1350650114562485

[17] KACZOR, J., RACZYNSKI, A. The selection of preload in angular contact ball bearings according to the durability criterion. *Tribologia* [online]. 2018, **1**(277), p. 25-34. ISSN 0208-7774, eISSN 1732-422X. Available from: https://doi.org/10.5604/01.3001.0011.8284

[18] HARRIS, T. A. *Rolling bering analysis*. London: John Wiley and Sons, 2006. ISBN 9780849381676.

[19] KACZOR, J. Analysis of the influence of shaft load on the value of acceptable preload in a system of angular ball bearings. *Bimonthly Tribologia* [online]. 2020, **290**(2), p. 25-35. ISSN 0208-7774. Available from: https://doi.org/10.5604/01.3001.0014.3737

[20] JANG, G. H, KIM, D. K., HAN, J. H., KIM, C. S. Analysis of dynamic characteristics of a HDD spindle system supported by ball bearing due to temperature variation. *Microsystem Technologies* [online]. 2003, **9**, p. 243-249. ISSN 0946-7076, eISSN 1432-1858. Available from: https://doi.org/10.1007/s00542-002-0260-0

[21] KACZOR, J., RACZYNSKI, A. The selection of preload in angular contact ball bearings according to the criterion of moment of friction. *Tribologia* [online]. 2018, **1**(277), p. 35-44. ISSN 0208-7774, eISSN 1732-422X. Available from: https://doi.org/10.5604/01.3001.0011.8286

[22] KACZOR, J., RACZYNSKI, A. The influence of preload on the work of angular contact ball bearings. *Archive of Mechanical Engineering* [online]. 2016, **63**(3), p. 319-336. eISSN 2300-1895. Available from: https://doi.org/10.1515/meceng-2016-0018

[23] MOHAMMED, A., ABDALLAH, A. Effects of axial preloading of angular contact ball bearings on the dynamics of a grinding machine spindle system. *Journal of Materials Processing Technology* [online]. 2003, **136**(1-3), p. 48-59. ISSN 0924-0136. Available from: https://doi.org/10.1016/S0924-0136(02)00846-4

[24] RACZYNSKI, A. The calculation method of deep groove ball bearings durability with regard to clearance and shaft. *Scientific Problems of Machines Operation and Maintenance*. 1999, **34**(1), p. 111-120. ISSN 0137-5474.

[25] SKF catalog [online]. Available from: http://www.skf.com/group/products/bearings-units-housings/ball-bearings/angular-contact-ball-bearings/single-row-angular-contact-ball-bearings/single-row/index.html?designation=7212%20BEP

[26] LI, T., KOLAR, P., LI, X.-Y., WU, J. Research development of preload technology on angular contact ball bearing of high speed spindle. *International Journal of Precision Engineering and Manufacturing* [online]. 2020, **21**(6), p. 1163-1185. ISSN 2234-7593, eISSN 2005-4602. Available from: https://doi.org/10.1007/s12541-019-00289-5

[27] THAN, V., HUANG, J. H. Nonlinear thermal effects on high-speed spindle bearings subjected to preload. *Tribology International* [online]. 2015, **96**, p. 361-372. ISSN 0301-679X. Available from: https://doi.org/10.1016/j.triboint.2015.12.029

[28] TONG, V.-C., HWANG, J., SHIM, J., OH, J.-S., HONG, S.-W. Multi-objective optimization of machine tool spindle-bearing system. *International Journal of Precision Engineering and Manufacturing* [online]. 2020, **21**(10), p. 1885-1902. ISSN 2234-7593, eISSN 2005-4602. Available from: https://doi.org/10.1007/s12541-020-00389-7

[29] YAN, K.E., YAN, B., WANG, Y., HONG, J., ZHANG, J. Study on thermal induced preload of ball bearing with temperature compensation based on state observer approach. *The International Journal of Advanced Manufacturing Technology* [online]. 2016, **11**, p. 3029-3040. ISSN 0268-3768, eISSN 1433-3015. Available from: https://doi.org/10.1007/s00170-016-9469-4

ULTRASONIC UNIT FOR REDUCING THE TOXICITY OF DIESEL VEHICLE EXHAUST GASES

Adil Kadyrov [1], Bauyrzhan Sarsembekov [1], Alexandr Ganyukov [1,*], Shinpolat Suyunbaev [2], Kirill Sinelnikov [1]

[1]Karaganda Technical University, Kazakhstan
[2]Tashkent State Transport University, Uzbekistan

*E-mail of corresponding author: ganukovktu@mail.ru

Resume

The article presents materials on use of ultrasonic waves to reduce the smoke and toxicity of diesel engine exhaust gases. The results of the experiments are presented. The hypothesis on the reduction of smoke and toxicity of the exhaust gas due to the acceleration of the coagulation of its particles under the action of ultrasound has been confirmed.

The dependences of the degree of turbidity of a diesel car on the number of revolutions of the engine crankshaft per minute and the dependence of the content of harmful impurities in the exhaust gases, without exposure and under the influence of ultrasound, at various revolutions of the engine crankshaft per minute, have been obtained. In addition, graphs of the amount of settled soot in an ultrasonic device on the number of engine revolutions per minute were obtained experimentally without and under the influence of ultrasound.

Article info

Received 25 November 2021
Accepted 7 February 2022
Online 19 April 2022

Keywords:

car
diesel engine
exhaust gases
ultrasonic installation
coagulation
gas analyzer
opacimeter

Available online: https://doi.org/10.26552/com.C.2022.3.B189-B198

ISSN 1335-4205 (print version)
ISSN 2585-7878 (online version)

1 Introduction

Diesel fuel does not have a cost-effective alternative to this day, despite the tightening of environmental standards, it remains in demand in the road transport. Comparison of the energy characteristics of different fuels shows that the operational efficiency of freight transport on existing alternative fuels will require a significant increase in the mass and overall dimensions of a vehicle. When using alternative fuels, the truck would have to carry the additional weight of fuel instead of the cargo being transported. Currently, a car using diesel fuel drives about 2000 km. without refueling. Under the same conditions, the discounts of a car on electric batteries - this distance is reduced by about 80 times [1].

Diesel-fueled car exhaust contains substances that are very harmful to human health - nitrogen oxides, which cause smog and cause respiratory problems and ultrafine soot particles, which increase the risk of cardiovascular diseases and lung cancer [2]. To combat the emission of soot on diesel vehicles, additional catalytic converters are installed, which have a relatively short service life, require additional investment capital and have a high price characteristics. After the failure of this filter, car owners often simply remove it, harming the environment.

Today, there is a number of methods for cleaning exhaust gases from harmful impurities. The most common ones are dry, wet, electric, catalytic and ultrasonic methods of gas cleaning. The dry cleaning method works with filter pipes of different diameters and lengths. The wet method of gas cleaning is carried out due to the interaction of the exhaust gas with water and the subsequent deposition of harmful impurities in the filter elements. This method is most widely used for capturing and further recovering finely dispersed components. Electric gas cleaning uses electrostatic precipitators, the work of which is based on the ionization of molecules. The catalytic gas cleaning method is based on deep cleaning of process gases. The essence of the method is to react with a catalyst. Ultrasonic works by accelerating the process of coagulation of soot particles.

The disadvantages of these methods include: high abrasive wear of the internal parts of the apparatus with a dry cleaning method; dust with low electrical conductivity is not filtered, it is necessary to clean the collecting and corona electrodes, the complexity and high cost of devices with an electric cleaning method;

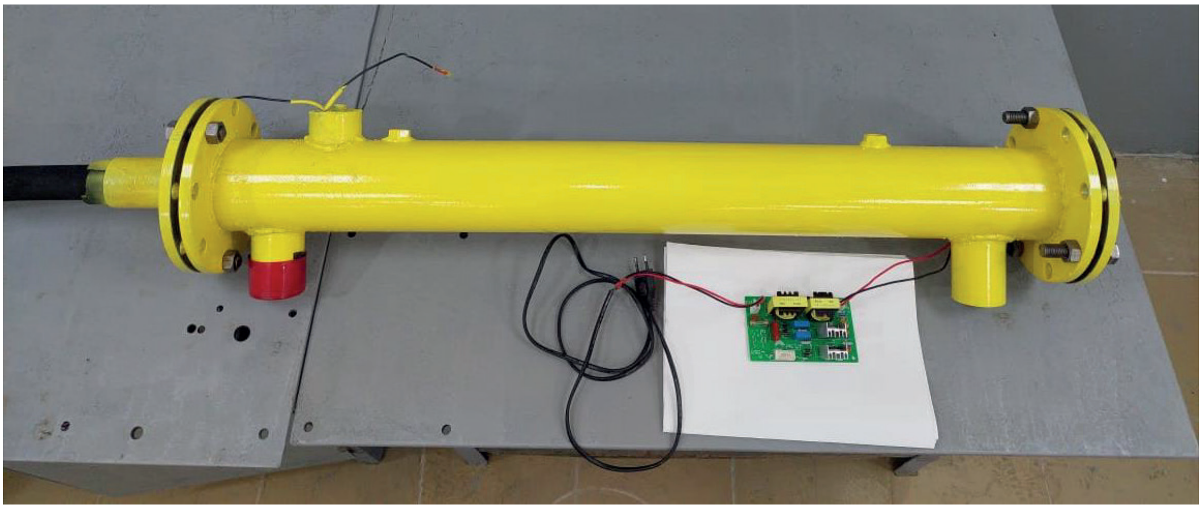

Figure 1 Experimental ultrasound unit (front view)

high consumption of electrical and thermal energy in the catalytic cleaning method.

A method of ultrasonic cleaning is proposed. Authors have developed an ultrasonic unit for reducing the toxicity of diesel vehicle exhaust gases from solid particles, in which an ultrasonic emitter is mounted inside the body. Research is needed to obtain concrete results. In this regard, it is important to conduct an experimental study using modern diagnostic equipment from the manufacturer "BOSCH".

Research has been carried out and results have been obtained on the speed of the ultrasonic wave in different media, the work of standing waves, the process of wave reflection, as well as on the purification of the exhaust gas of a gasoline car [3-10].

The aim of the research was the experimental confirmation of the fact of reducing the smoke and toxicity of the exhaust gas of an internal combustion engine under the influence of ultrasonic waves on it.

Research objectives: analysis of the physics of the process; development of an experimental stand; conducting and analyzing the results of the experiment.

2 Materials and methods

Coagulation (from Latin coagulatio - coagulation, thickening), also flocculation (from Latin flocculi - shreds, flakes) is a physicochemical process of adhesion of small particles of dispersed systems into larger ones under the influence of cohesion forces with formation of coagulation structures. [11-14]

The physics of the exhaust gas cleaning process of a car with ultrasound occurs due to the coagulation process. Coagulation of exhaust gases in a car muffler occurs constantly (orthokinetic coagulation), it is accelerated when exposed to ultrasound, which has a dispersing effect on emulsions and liquid sols and has a coagulating effect on aerosols (smoke, fog, dust) (hydrodynamic coagulation). This is due to the fact that only the longitudinal waves causing compression are possible in gases. In a longitudinal wave, the particles of the medium oscillate about their mean position in the direction parallel to the wave propagation and lead to the appearance of hydrodynamic coagulation [15-16].

The Polish scientist M. Smoluchowski in 1906 proposed the theory of coagulation, which was developed based on the fact that coagulation occurs as a result of the fact that particles of the dispersed phase, performing Brownian motion at a certain moment, approach each other at a distance equal to the radius of the sphere of influence of the particles, equal to the sum of particle radii. In this case, the forces of interaction between the particles create an opportunity for their adhesion (aggregation). Due to the fact that the probability of collision of several particles at once is very small, coagulation occurs, as a rule, between two particles. A binary particle can interact with a single, double, triple, etc. particles, as a result of which large aggregates of particles are formed, which, upon reaching a certain critical mass, lose the ability to perform Brownian motion and settle under the action of gravity [17-19].

The occurring processes are theoretically described by equations of the kinetics of gases [20]

$$n = n_0 \cdot e^{-kt}, \quad (1)$$

where:
n and n_0 - current and initial particle concentration,
k - concentration factor,
t - time coordinate.

It was shown in [17] that, by analogy, it is true:

$$m = m_0 \cdot e^{-kt} \quad (2)$$

where:
m and m_0 - respectively, the current and initial mass of coagulated particles,
k - coagulation coefficient;

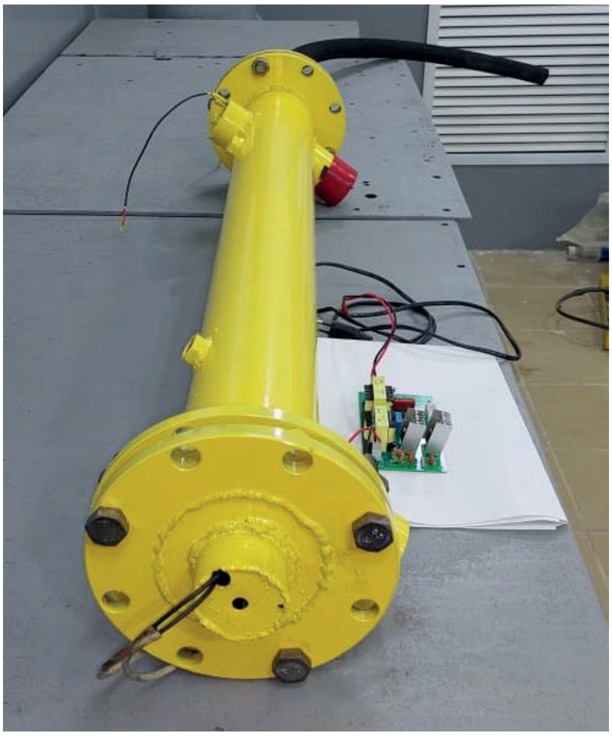

Figure 2 *Experimental ultrasonic unit (side view)*

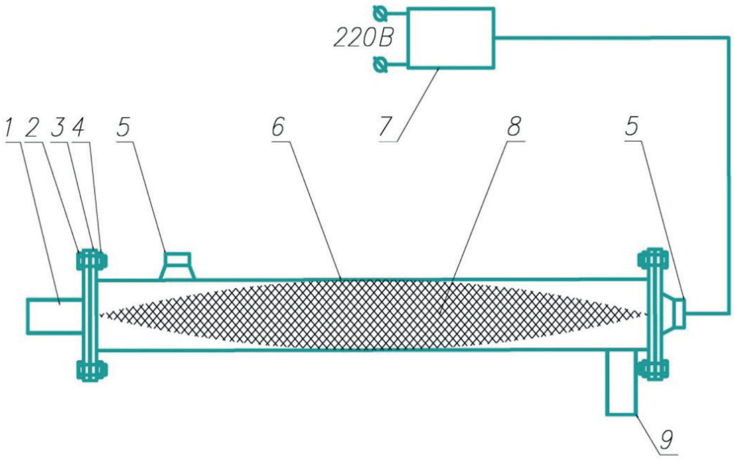

1- exhaust gas inlet branch pipe, 2- bolt, 3- flange, 4- nut, 5- ultrasonic emitter, 6- steel pipe, 7- ultrasonic generator, 8- ultrasonic impact area, 9- exhaust gas outlet branch pipe.

Figure 3 *Scheme of an ultrasonic unit for reducing the toxicity of exhaust gases of a diesel car*

Equation (2) implies:

$$k = \ln\frac{m}{m_0}/t. \quad (3)$$

In work [17], dependences on the change in the transparency of exhaust gases are given.

To carry out the study, a full-size ultrasound unit was manufactured (Figure 1 and Figure 2)

The purpose of the experiment was to determine the opacity of the gas after exposure to an ultrasonic wave, the change in concentration, the ratio of various gases in the exhaust gas and the value of the mass of coagulated particles.

The scheme of an ultrasonic installation for reducing the toxicity of exhaust gases of a diesel vehicle is shown in Figure 3.

An ultrasonic installation for reducing the toxicity of exhaust gases of a diesel vehicle was manufactured according to the scheme in Figure 3 from the following elements:

- steel pipe with a diameter of 110 mm, a length of 1000 mm, a wall thickness of 1.8 mm;
- flat flanges with an outer diameter of 205 mm, an inner diameter of 110 mm and a thickness of 15 mm;
- ultrasonic emitters with a frequency of 40 kHz, a static capacity of ~ 4400 - 4610 pF, a radiating

surface of 45 mm, insulation resistance of 10,000 mΩ and a power of 50 W;
- ultrasonic generator with a frequency of 40 kHz and a power of 100 W.

The body of the installation was made and the two ultrasonic transducers of the longitudinal and transverse directions were mounted, as shown in Figure 3.

To determine the qualitative and quantitative composition of the exhaust gas mixture, the diagnostic complex "BOSCH FSA 740" was used.

The experiment with the ultrasonic installation was carried out as follows:
- to the car Mercedes Benz ML 2.7 CDI, engine capacity 2700 cc.see the production year 2001, fuel grade - diesel, an ultrasonic installation was connected;
- the composition of the exhaust gas was measured by a gas analyzer and the smoke of the exhaust gases was measured without the influence of ultrasound and with the action of a longitudinal ultrasonic wave after 1 minute, depending on the range of rotation of the engine crankshaft (750, 1000 and 1400 (1600) rpm).

The ultrasonic unit was connected to the car using a rubber hose to the inlet pipe 1 for supplying exhaust gases to the unit. In an ultrasonic installation, with the ultrasonic generator turned on, longitudinal ultrasonic waves were applied to the exhaust gas.

In the installation, ultrasonic intensification of coagulation processes and cleaning of exhaust gases took place due to the sedimentation of enlarged particles of exhaust gas at the bottom of the installation. The cleaned exhaust gas was discharged through the outlet pipe 9.

To perform the high-precision measurements of smoke and toxicity in the course of the experiment, the diagnostic complex "BOSCH FSA 740" was used. The BOSCH diagnostic complex includes: KTS 560 diagnostic scanner; gas analyzer "BEA 050"; optical opacimeter "BEA 070". With help of the "KTS 560" scanner, the vehicle engine speed was monitored to record data at a certain moment of the engine crankshaft speed. The gas analyzer "BEA 050" was used to determine the composition of the exhaust gases, namely the

Table 1 *Indications of an autonomous mobile opacimeter for diesel engines "BEA 070"*

Ultrasonic muffler operation	Rotation frequency crankshaft (rpm)	Working time (sec)	Gas turbidity degree (%)
without ultrasound	750		30.6
with ultrasound	750		25.5
without ultrasound	1000	60	27.4
with ultrasound	1000		21.6
without ultrasound	1600		31.6
with ultrasound	1600		30.1

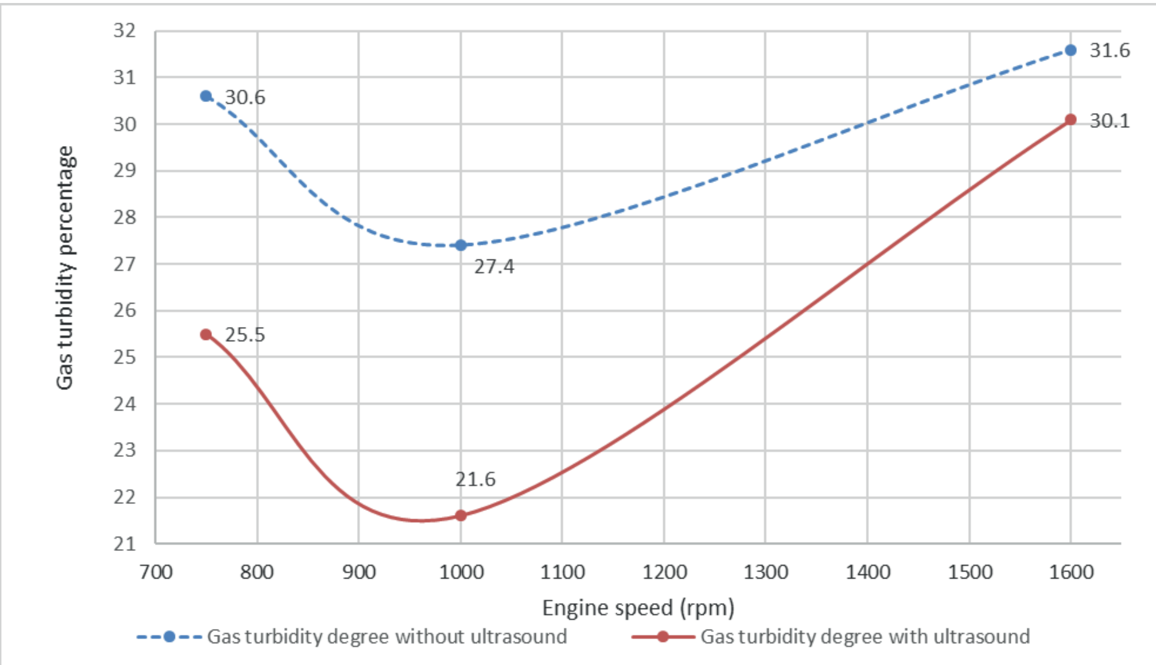

Figure 4 *Graph of the degree of turbidity of diesel exhaust gas at 750, 1000 and 1600 engine rpm*

***Table 2** Experimental data on the degree of turbidity without ultrasonic exposure*

Engine speed (rpm)	Degree of turbidity without ultrasonic exposure (%)	Degree of turbidity without ultrasound exposure, by cubic regression (%)
750	30.6	30.0
800	30	29.6
850	29.3	29.2
900	28.7	28.9
950	28	28.6
1000	27.4	28.5
1050	27.8	28.4
1100	28.1	28.4
1150	28.5	28.4
1200	28.8	28.5
1250	29.2	28.7
1300	29.5	29.0
1350	29.9	29.4
1400	30.2	29.8
1450	30.6	30.3
1500	30.9	30.9
1550	31.3	31.5
1600	31.6	32.3

***Table 3** Experimental data on the degree of turbidity under the influence of ultrasound*

Engine speed (rpm)	Degree of turbidity with ultrasonic exposure (%)	Degree of turbidity with ultrasound exposure, by cubic regression (%)
750	25.5	24.6
800	24.7	24.1
850	23.9	23.7
900	23.2	23.4
950	22.4	23.2
1000	21.6	23.2
1050	22.3	23.2
1100	23	23.4
1150	23.7	23.6
1200	24.4	24.0
1250	25.1	24.5
1300	25.9	25.1
1350	26.6	25.8
1400	27.3	26.7
1450	28	27.6
1500	28.7	28.7
1550	29.4	29.8
1600	30.1	31.1

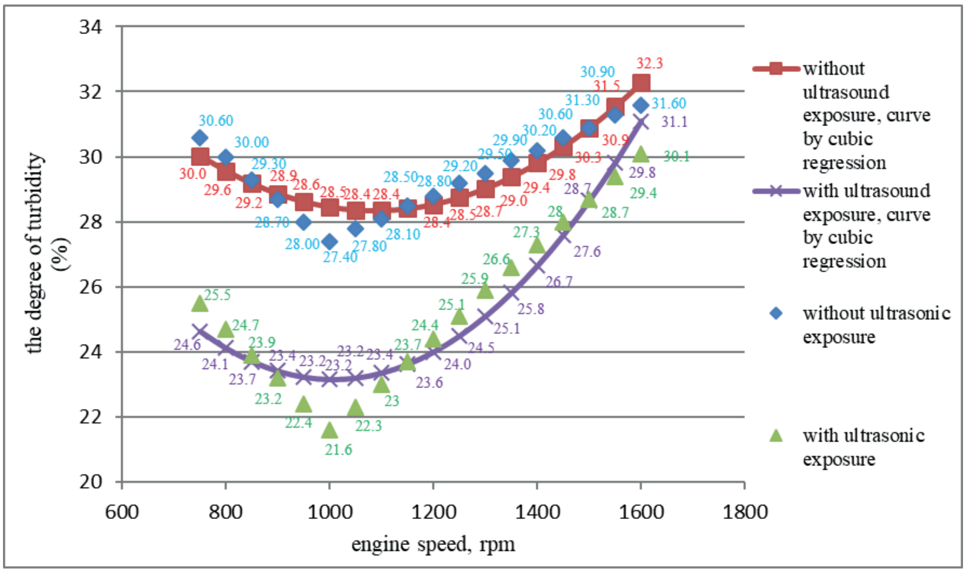

Figure 5 *Experimental turbidity curves*

Table 4 *Readings of the gas analyzer "BEA 050" without ultrasound*

No.	Engine speed (rpm)	O_2 (% vol)	CO_2 (% vol)	HC (ppm vol)	CO (% vol)	Measurement time (sec.)
1	750	17.34	2.25	16	0.027	
2	1000	17.44	2.24	17	0.034	60
3	1400	17.46	2.18	19	0.053	

Table 5 *Readings of the gas analyzer "BEA 050" under the influence of ultrasound on the exhaust gases*

No.	Engine speed (rpm)	O_2 (% vol)	CO_2 (% vol)	HC (ppm vol)	CO (% vol)	Measurement time (sec.)
1	750	17.36	2.26	14	0.022	
2	1000	17.46	2.23	18	0.036	60
3	1400	17.50	2.18	19	0.054	

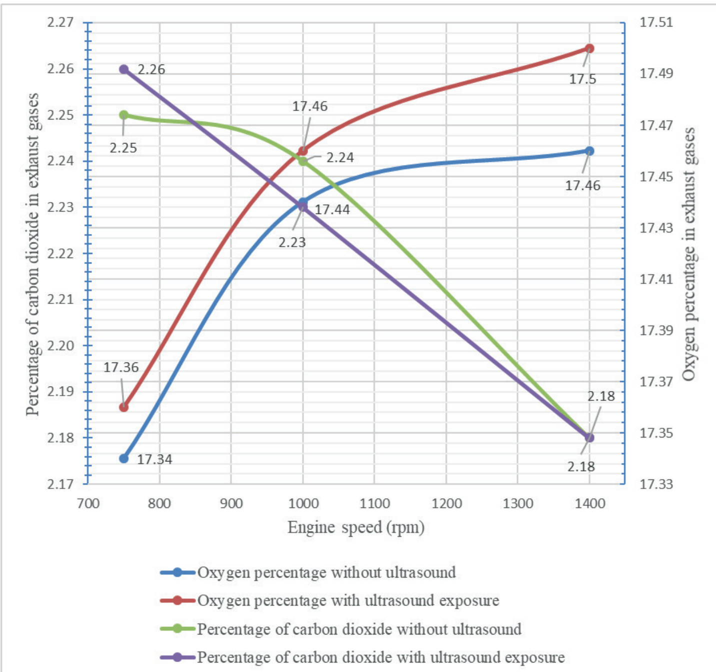

Figure 6 *Graph of the oxygen and carbon dioxide content in the exhaust gases, without exposure and under the influence of ultrasound at 750, 1000 and 1400 engine rpm*

oxygen content in the exhaust gases, carbon dioxide, hydrocarbon and carbon monoxide. The data from the optical opacimeter "BEA 070" was used to determine the percentage of turbidity of the diesel engine exhaust gases.

3 Results

The experiment was divided into three stages. At the first stage of the experiment, the data on influence of ultrasonic waves on the content of the degree of turbidity of the exhaust gases of a diesel car was recorded. Three measurements of exhaust gas opacity without ultrasonic waves and three measurements under the influence of ultrasound were carried out at different ranges of engine operation 750, 1000, 1600 rpm. Recorded readings of the degree of turbidity of exhaust gases are given in Table 1. According to the readings from Table 1, a graph was constructed (Figure 4), demonstrating the significant effect of ultrasound on the degree of turbidity of diesel exhaust gas [15-20].

The significant effect of the ultrasonic wave on the degree of turbidity of the exhaust gas shown in the graph in Figure 4 occurs due to the coagulation of soot particles and their deposition in the ultrasonic installation.

At the first stage of the experiment, the influence of ultrasonic waves on the degree of turbidity of the exhaust gases of a diesel engine was proved in accordance with the graph shown in Figure 4. When ultrasound was applied to the exhaust gas of a car, a decrease in the degree of turbidity was revealed. In particular, at an engine speed of 750 rpm, a decrease in the degree of turbidity by 16.6 % was detected, at 1000 rpm, a decrease of 21.1 % was noted and at an engine speed of 1600 rpm, it decreased by 4.7 %.

As a result of the conducted full-scale experiment, the decrease in the degree of turbidity of the exhaust gas was more than 21 %. The physical process is explained by an increase in the hydrodynamic coagulation of the gaseous medium during the operation of an ultrasonic installation, which has been proven experimentally.

The obtained experimental data were interpolated. A regression analysis of the degree of turbidity was performed and the regression equation was established. From the analysis of the calculations for the largest values of the correlation coefficients, determination and the smallest values of the average approximation error for the process of changing the degree of turbidity of the exhaust gas without ultrasound and under the influence

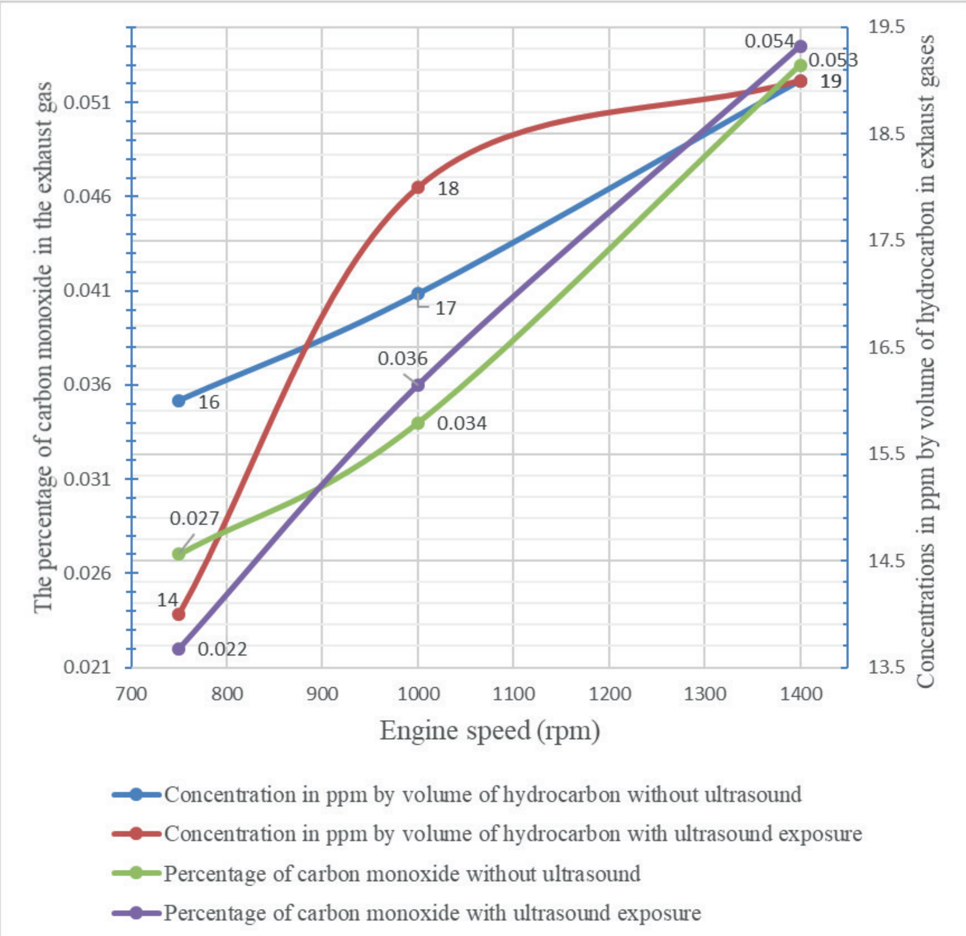

Figure 7 *Graph of the content of hydrocarbon and carbon monoxide in exhaust gases, without exposure and under the influence of ultrasound at 750, 1000 and 1400 engine rpm*

***Table 6** Mass of settled soot at 1000/1250 rpm without ultrasound and under the influence of ultrasound*

Distance (mm.)	At 1000 rpm		Aat 1250 rpm	
	without ultrasound (g.)	with ultrasound (g.)	without ultrasound (g.)	with ultrasound (g.)
100	0.25	0.33	0.70	0.85
200	0.16	0.27	0.39	0.91
300	0.11	0.2	0.12	0.92
400	0.05	0.16	0.62	0.98
500	0.1	0.13	0.31	0.67
Σ	0.67	1.09	2.14	4.33

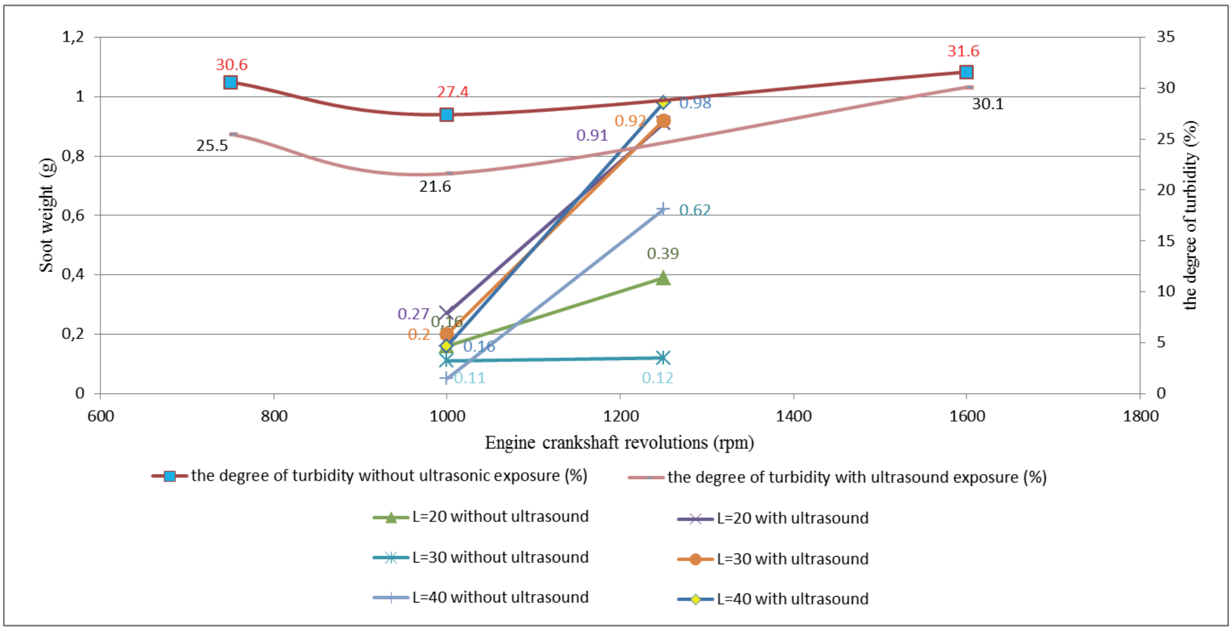

where: L = 200, L = 300, L = 400 is the settling distance of soot particles (mm)

***Figure 8** Dependence of the mass of settled soot and the degree of turbidity on the number of engine revolutions per minute without and under the influence of ultrasound*

of ultrasound, cubic regression equations were used. The values obtained are shown in Tables 2 and 3 and in the graph in Figure 5.

The graphs show that values of the degree of turbidity do not vary much. This indicates the correctness of an experimental study on the purification of diesel vehicle exhaust gas from harmful impurities by ultrasound.

At the second stage of the experiment, six measurements were made to determine the composition of the vehicle's exhaust gases. Measurements were made without the influence of an ultrasonic wave at the engine operating ranges of 750, 1000, 1400 rpm. The data are shown in Table 4. Further, the experiment was carried out with the action of longitudinal ultrasonic waves at the same engine speeds. Measurements of the composition of exhaust gases were recorded, which are presented in Table 5. According to the tables, graphs were built without exposure and under the influence of ultrasound, shown in Figures 6 and 7, which show the composition of the exhaust gases of a diesel engine depending on the crankshaft speed.

According to the data from the graph in Figure 6, an increase was revealed in the oxygen content under the influence of a longitudinal ultrasonic wave on the exhaust gas of a diesel car. When exposed to ultrasound, soot particles coagulate and further precipitate these particles in the ultrasonic installation, thereby increasing the oxygen concentration in the exhaust gases. In the engine operating range of 750 rpm, heavy particles settle to the bottom of the installation, due to which the concentration of carbon dioxide in the exhaust gases increases.

From the data of the graph in Figure 7 one can see the effect of ultrasound on hydrocarbon and carbon monoxide. With an increase in the engine speed, the coagulated hydrocarbon particles deposited by ultrasound are not retained on the walls of the ultrasonic installation. In this regard, the content of hydrocarbon and carbon monoxide increases with increasing engine speed.

During the second stage of the experiment, according to the data from the graphs (Figures 6 and 7), it was revealed that ultrasonic waves affect the composition of the exhaust gases. During the combustion of diesel fuel in an ultrasonic device without ultrasound, excess carbon contributes to the formation of carbon monoxide (CO). According to the data in Table 4, an increase in hydrocarbon (HC) increases the percentage of carbon monoxide (CO). An increase in oxygen (O_2) oxidizes carbon monoxide and forms carbon dioxide (CO_2). There is a change in the ratio of the number of particles of various gases in the process of coagulation. In this regard, the most important factor is the value of the mass of gases at the outlet of the muffler. The experimental data confirm this.

When exposed to ultrasound at 750 rpm. (Table 2) due to the coagulation process, which is enhanced by ultrasound, the picture of the chemical reaction changes and shows a decrease in hydrocarbon (HC), since the inlet pressure of the exhaust gas into the device is small, soot particles have time to increase in size and settle to the bottom of the ultrasonic device.

An increase in engine speed has a less significant effect on the hydrodynamic coagulation process since the length of the device is 1000 mm and is insufficient for effective cleaning of the exhaust gas of a diesel vehicle. According to Table 5, starting from 1000 rpm insufficient radiation occurs in the ultrasonic device, since the inlet pressure of the exhaust gas increases and the soot particles fly out without having time to settle to the bottom.

At the third stage of the experiment, the mass and distance of the deposited soot particles were determined, without exposure and under the influence of ultrasound in an experimental ultrasonic device (Tables 6-7). Figure 8 shows experimental graphs of the dependence of the mass of settled soot and the degree of turbidity on the number of revolutions of the crankshaft per minute without and under the influence of ultrasound.

The graph (Figure 8) shows the dependence of the mass of settled soot and the degree of turbidity on the number of engine revolutions per minute without ultrasound and under the influence of ultrasound. The obtained values of the soot mass generally confirm Equation (3). Thus, despite the sometimes paradoxical picture of the concentration of various gases in the exhaust gas, the mass of coagulated particles (soot) increases and the smokiness decreases.

4 Conclusions

In the course of the research experiment, the possibility of ultrasonic waves' impact on the degree of turbidity, the composition of the exhaust gases of a diesel car and the sedimentation mass of soot particles was determined.

It was found that when exposed to ultrasound, the degree of turbidity of the exhaust gas is significantly reduced by more than 21%. In particular, at an engine speed of 750 rpm, a decrease in the degree of turbidity by 16.6% was detected, at 1000 rpm, a decrease of 21.1% was noted and at an engine speed of 1600 rpm, it decreased by 4.7%.

When measured with a gas analyzer at 750 rpm of the internal combustion engine, due to the coagulation process, the concentration of hydrocarbon (HC) decreased by 12.5%, the mass of deposited soot under the action of ultrasound increased more than 2 times. An increase in the speed of the internal combustion engine does not have a significant effect during the operation of the ultrasonic installation, since the length of the ultrasonic device is not sufficient and the soot particles do not have time to increase in size at the expense coagulation process. The recommended length of the ultrasonic device is at least 3 m [4]. Coagulation of molecules of different gases occurs at different rates, which explains the ratio of their changes in the total volume of exhaust gases.

The hypothesis of reduction of harmful impurities of diesel exhaust gas due to coagulated particles in the ultrasonic device under the action of longitudinal ultrasonic waves on them has been proven.

Experimental data have been obtained, the practical significance of which lies in the possibility of calculating and designing an ultrasonic installation for mufflers of diesel cars of a new type, which allows to qualitatively reduce the toxicity of road transport [3-4].

References

[1] KORABLEV, R. A., BELOKUROV, V. P., ZELIKOV, V. A., LIKHACHEV, D. V., RAZGONYAEVA, V. V., BOYKO, N. I. Environmental safety of vehicles. Voronezh, 2011.

[2] KADYROVA, I. A., MINDUBAEVA, F. A., GRJIBOVSKI, A. M. Prediction of outcomes after stroke: a systematic review. *Human Ecology* [online]. 2015, **22**(10), p. 55-64. ISSN 1728-0869. Available from: https://doi.org/10.33396/1728-0869-2015-10-55-64

[3] KADYROV, A., GANYUKOV, A., PAK, I., SULEYEV, B., BALABEKOVA, K. Theoretical and experimental study of operation of the tank equipment for ultrasonic purification of the internal combustion engine exhaust gases. *Communications - Scientific Letters of the University of Zilina* [online]. 2021, **23**(3), p. B219-B226. ISSN 1335-4205, eISSN 2585-7878. Available from: https://doi.org/10.26552/com.C.2021.3.B219-B226

[4] KADYROV, A., SARSEMBEKOV, B., GANYUKOV, A., ZHUNUSBEKOVA, Z., ALIKARIMOV, K. Experimental research of the coagulation process of exhaust gases under the influence of ultrasound. *Communications - Scientific Letters of the University of Zilina* [online]. 2021, **23**(4), p. B288-B298. ISSN 1335-4205, eISSN 2585-7878. Available from: https://doi.org/10.26552/com.C.2021.4.B288-B298

[5] KADYROV, A., KARSAKOVA, A., DONENBAYEV, B., BALABEKOVA, K. Establishing the strength characteristics of the lifting-leveling device structures of the VPO-3-3000 machines for the track straightening. *Communications - Scientific Letters of the University of Zilina* [online]. 2020, **22**(4), p. 70-79. ISSN 1335-4205, eISSN 2585-7878. Available from: https://doi.org/10.26552/com.C.2020.4.70-79

[6] IBATOV, M. K., KADYROV, A. S., PAK, I. A., KADYROVA, I. A., ASKAROV, B. S. The results of experimental studies of the capacitive equipment of ultrasonic cleaning of exhaust gases of vehicles. *Coal* [online]. 2020, **2**, p. 73-78. ISSN 0041-5790, eISSN 2412-8333. Available from: https://doi.org/10.18796/0041-5790-2020-2-73-78

[7] KADYROV, A. S., KUNAEV, V. A., GEORGIADI, I. V. Prospects for processing of ferrous metallurgical waste based on Arcelormittal Temirtau experience. *Metallurgist* [online]. 2018, **62**(1-2), p. 22-28. ISSN 0026-0894. Available from: https://doi.org /10.1007/s11015-018-0620-3

[8] KADYROV, A. S., KUNAEV, V. A., GEORGIADI, I. V. Ferrous metallurgy waste and waste technical fluids for obtaining the material of road bases. *Ecology and Industry of Russia* [online]. 2017, **21**(12), p. 44-48. ISSN 1816-0395, eISSN 2413-6042. Available from: https://doi.org /10.18412/1816-0395-2017-12-44-48

[9] ZHUNUSBEKOVA, Z. Z., KADYROV, A. S. Study of digging machine flat element loading in clay solution. *Scientific Bulletin of the National Maid University*. 2016, **2**, p. 30-33. ISSN 2071-2227.

[10] VARSHAVSKY, I. L., MALOV, R. V. *How to neutralize car exhaust gases*. Moscow: Transport, 1968.

[11] LOZHKIN, V. N., SHULGIN, V. V., MAKSIMOV, M. A. About modeling of systems for cleaning the exhaust gases of internal combustion engines using neutralizers and heat accumulators of the phase transition. *Technical and Technological Problems of Service*. 2011, **2**(16) p. 42-47.

[12] SHAMIM, T. Effect of engine exhaust gas modulation on the cold start emissions. *International Journal of Automotive Technology* [online]. 2011, **12**(4), p. 475-487. ISSN 1229-9138, eISSN 1976-3832. Available from: https://doi.org/10.1007/s12239-011-0056-2

[13] BALDEV, R., RAJENDRAN, V., PALANICHAMI, P. *Applications of ultrasound*. Moscow: Technosphere, 2006. ISBN 5-94836-088-1.

[14] BERGMAN, L. *Ultrasound and its application in science and technology*. Moscow: Publishing house of foreign literature, 1957.

[15] Patent RK No. 3194. Device for ultrasonic cleaning of exhaust gases. Declared 12/20/2017, publ. 10/02/2018.

[16] KADYROV, A. S., PAK, I. A., KADYROVA, I. A., GANYUKOV, A. A. Physics of the process of ultrasonic coagulation of exhaust gases of internal combustion engines of motor vehicles. *Bulletin of PSU. Energy series*. 2020, **1**, p. 219-230.

[17] IBATOV, M. K., KADYROV, A. S., PAK, I. A., KADYROVA, I. A., ASKAROV, B. S. The results of experimental studies of the operation of capacitive equipment for ultrasonic cleaning of exhaust gases from vehicles. *Coal* [online]. 2020, **2**, p. 73-78. Available from: https://doi.org/10.18796 / 0041-5790-2020-2-73-78

[18] KADYROV, A., GANYUKOV, A., BALABEKOVA, K. Development of constructions of mobile road overpasses. *MATEC Web of Conferences* [online]. 2017, **108**, 16002. ISSN 2261-236X. Available from: https://doi.org /10.1051/matecconf/201710816002

[19] NASAD, T. G., SHEROV, K. T., ABSADYKOV, B. N., TUSUPOVA, S. O., SAGITOV, A. A., ABDUGALIYEVA, G. B., OKIMBAYEVA, A. E. Formation management in parts processing regenerated by surfacing. *News of the National Academy of Sciences of the Republic of Kazakhstan, Series of Geology and Technical Sciences*. 2019, **3**(435), p. 102-108.

[20] BEREZYUK, V. G., KUZEMBAYEV, S. B., SHEROV, K. T., SIKHIMBAYEV, M. R., ALYZHANOV, M. K., MISHNEV, S. A., MAZDUBAY, A. B., GRINEVICH, I. I., SHEROV, A. K., SIKHIMBAYEVA, D. R. Increase of precision of casting blocks by applying acoustical oscillations in gas-impulsive moulding. *Journal of Vibroengineering*. 2015, **17**(5), p. 2178-2186. ISSN 1392-8716, eISSN 2538-8460.

EXPERIMENTAL AND THEORETICAL PERFORMANCE EVALUATION OF BASIN SOLAR STILL WITH LID AFLOAT IN EGYPT CONDITIONS

Amr Mesalem , Ahmed Walaa , Ahmed Elweetedy , Salman Elshamarka

Military Technical College, Cairo, Egypt

*E-mail of corresponding author: amrmesalem@gmail.com

Resume

This paper presents experimental and theoretical work, analyzing the performance of single slope solar still with and without a floating lid, conducted in Cairo, Egypt. A Comparison of the experimental output yield with the theoretical one was carried out. The experimentations without the lid were conducted for 7 days and the daily output yield ranges from (2.8 l/day to 3.15 l/day) with an average output yield of 52.8 % when compared to the theoretical output yield. To improve the output yield of the still, a black fibrous lid was placed on the water surface and its effect on the output yield was studied. Because of its porosity the evaporation surface area of the still was improved, water depth is considered small above its surface. The experimentations with the lid were conducted for 6 days and the daily output yield ranges from (3.1 l/day to 3.3 l/day) with an average output yield of 57.95 % when compared to the theoretical yield.

Article info

Received 25 August 2021
Accepted 4 February 2022
Online 27 April 2022

Keywords:

single slope solar still
passive type
floating lid
output yield
heat transfer

Available online: https://doi.org/10.26552/com.C.2022.3.B199-B210

ISSN 1335-4205 (print version)
ISSN 2585-7878 (online version)

1 Introduction

The Environment is composed of four main components Air, water, soil and energy. Without them there would be an environment, simply there would be life on earth. Water comes clearly in the second place after air for the existence of life. The water covers a huge area of the earth's surface, more than two-thirds of the earth's surface. About 97.5 % of water resources are found in seas and oceans which are not suitable for human consumption as they contain high salty water (3000 ppm to 35000 ppm) and the remaining 2.5 % are freshwater present in the lakes, rivers, polar ice and groundwater. So only a small portion of freshwater is being used in irrigation, industry and fulfilling the domestic demand.

The world is expected to face a problem of shortage of drinking water due to an increase in population and fast industrial development. Pollution of freshwater resources (rivers, lakes and underground water) by industrial wastes has enlarged the problem as well.

One of the most sustainable solutions to provide fresh water for many communities is water desalination. Desalination is a process in which saline water is separated into two parts using various forms of energy, one that has a low concentration of dissolved salts (freshwater) and the other which has a much higher concentration of dissolved salts than the original feed water. Saline water is classified as either slightly salty water or brine water relying on the salinity and water source.

Most of the countries facing water shortage have large commercial desalination plants that use fossil fuel. Only some countries in the world can use fossil fuels to run these plants. But most of the countries have neither the financial nor oil resources to allow them to develop similarly. The production of 1000 m^3 per day of freshwater requires 10,000 tonnes of oil per year [1], which can be considered a highly significant energy consumption, as it involves a recurrent energy expense. The cost of conventional desalination systems operating using fossil fuels keeps increasing due to the increase of world energy prices. Recently, the utilization of renewable energy sources to drive desalination plants appears to be very promising, as it is a sustainable, cheap and clean solution for freshwater supply in regions lacking energy resources. Recently, attention has been directed towards improving the coupling of solar energy systems and desalination technologies.

Extensive research and activities have been conducted for the sake of reaching this goal.

There are two main types of solar still systems which are active solar still and passive solar still. In the active solar still, direct solar radiation and additional thermal energy are fed into the basin. Active distillation systems have been developed to increase the output of distilled water. Raju and Narayana [2] presented experimentally the effect of integrating of flat plate collector (FPC) with solar still. The result showed that connecting two FPCs in series with solar still, provides 41 % more distilled water when compared to a single FPC. Singh et al. [3] discussed the improvement in the performance of a solar still integrated with an evacuated tube collector and showed that the best combination has been attained by integrating 10 evacuated tubes with a water depth of 3 cm with a maximum daily output yield of 3.8 kg/m^2. Sampathkumar et al. [4] discussed the performance of various active solar distillation systems.

In the passive solar still, the water in the basin is heated by solar radiation directly so that the productivity is very low compared to the active solar still. The daily output yield of passive solar still can be increased by changing the design of the conventional still (single slope) or by making modifications in the conventional design. et al. [5] made a comparison between the output yield of triangular basin solar still (TBSS) and conventional basin solar still (CBSS), the experiment revealed that the daily output yield obtained from CBSS and TBSS was found to be 2.7 and 3.2 kg/m^2, respectively. In addition, the daily efficiency of the TBSS was improved by 11.36 % than the CBSS.

et al. [6] designed and fabricated concave type solar still with four glass cover surface (Pyramid shape)

***Table 1** Modifications on conventional solar still*

Reference	Modification	Results
Matrawy et al. [12]	Formed the evaporative surface as a corrugated shape. Decreased the heat capacity by using porous material.	Improvement of about 34 % in the productivity.
Abdallah et al. [13]	Discussed the effect of various absorbing materials on the thermal performance of solar stills. Materials: black coated and uncoated metallic wiry sponges and black rocks.	Distilled water collections were 28 %, 43 % and 60 % for coated and uncoated metallic wiry sponges and black rocks respectively.
Srivastava and Agrawal [14]	Modification is made by incorporating multiple low thermal inertia porous absorbers, floated adjacent to each other.	Increase in the evaporation surface area. On clear days 68 % more distillate output was obtained. 35 % more on cloudy days
Agrawal and Rana [15]	Multiple V-shaped floating wicks are used to enhance the heat absorption and thereby increase productivity.	The evaporative surface area of modified solar still is 26 % larger than that of the conventional one. The maximum daily productivity in one of the clear days is found to be approximately 6.20 kg/m2 in summer and 3.23 kg/m2 in winter with daily efficiencies of 56.62 % and 47.75 %, respectively.
Gawande and Bhuyar [16]	Discussed the Effect of Shape of the Absorber Surface on the Performance of Stepped Type Solar Still. The shape of the absorber surface provided in the basins of solar stills was flat, convex and concave.	When the convex and concave type, the average daily water production is 56.60 % and 29.24 % higher than that of flat type.
Johnson et al. [17]	Performed a theoretical and experimental study on a single-basin solar still when an external solar enhancement is used (Fresnel lens).	A parametric study by varying the water depth showed the Fresnel lens was more effective for larger water depths. The Fresnel lens can aid in improving the overall efficiency of the solar still.
Gupta et al. [18]	Studied the performance of modified solar still using the water sprinkler. Attachment of water sprinkler with constant water flow rate of 0.0001 kg/s on the glass cover.	The distilled water output was recorded 2940 ml and 3541 ml from conventional and modified solar stills, respectively. Water productivity (output yield) of single slope solar still is increased by 20 %. The overall efficiency is increased by 21 % over the conventional solar still.

and studied it experimentally. The results show that the average productivity during the daytime is 4 l/m^2 with a system efficiency of 0.38, higher than the conventional type solar still. Arunkumar et al. [7] made an experimental study on hemispherical solar still which has a higher efficiency than the conventional solar still and compared the daily distillate output with and without flowing water over the cover The efficiency was 34 % and increased to 42 % with the top cover cooling effect (flowing water). Jathar et al. [8] investigated experimentally a concave-type solar still with different temperature and solar intensity and it was noted that The highest daily productivity (3.7 l/m^2/ day) was achieved during march 2020. This may be attributable to the highest average intensity of the radiation (1005 W/m^2) and the most top average temperature difference of 10.5 °C. Gad et al. [9] manufactured and compared the experimental results of conical solar still to the conventional type with the same area. The results showed that the daily productivity for conical and conventional solar stills were 3.38 and 1.93 L/m^2/day, respectively. Many researchers made modifications to the conventional solar still, to increase the output yield even more. Table 1 shows the recent modifications in conventional solar still.

In addition, many researches were made modifications in conventional solar still concerning different parameters and their effects on the yield. Many parameters affect the evaporation rate. Studying the effect of these parameters helped in increasing the evaporation rate. Hence, better yield. One of these parameters is the water depth; it was found out that the evaporation rate is inversely proportional to water depth. grawal et al. [10] made an experimental and theoretical comparison of the daily output yield for different water depths from 200 mm and 10 mm. the experimental value for daily efficiency was around 41.49 % and 32.42 % respectively. It is obvious that to achieve a higher efficiency of a solar still, the heat loss should be minimized by adequate insulation. Khalifa and Hamood [11] studied experimentally the effect of insulation thickness on the productivity of solar still and developed a performance correlation for the effect of insulation on the productivity. Their study showed that the insulation thickness could influence the productivity of the still by over 80 %.

In this paper, a detailed theoretical and experimental work is done on a solar still to get the hourly and daily yield. The work is conducted in the Military Technical College (MTC), Cairo, Egypt. The paper is organized as follows: first, a detailed thermal analysis for a solar still was performed to get the productivity. Then, a physical model for the solar still with net dimensions 1 m * 1 m is constructed. The experimental work was conducted for several days for the solar still with and without a floating lid on the water surface to compare both theoretical and experimental evaluation. Finally, results, discussion and conclusion are introduced.

2 Solar still thermal analysis

A thermal energy balance has been made for the solar still. The following assumptions are considered to simplify the analysis:

- The physical properties of water remain constant with temperature changes.
- Water vapor and dry air are assumed to be ideal gases.
- The outer temperature of the glass equals the inner temperature of the glass.
- The still is assumed to be completely vapor leakage proof.

2.1 Energy balance equations glass cover, water mass and basin linear [10]

The glass receives heat from internal and external sources by different methods, externally from the incident solar radiation and internally from basin water surface through three methods (convection, evaporation and radiation) and reject the received heat to the atmosphere through two methods (convection and radiation).

$$\alpha'_g \; I(t) + q_{twg} = g_{tga}\,, \tag{1}$$

where,

$$q_{twg} = q_{cwg} + q_{ewg} + q_{rwg}\,, \tag{2}$$

$$q_{tga} = q_{cga} + q_{rga}\,, \tag{3}$$

$$\alpha'_g \; I(t) + h_{twg}(T_w - T_g) = h_{tga}(T_g - T_a)\,. \tag{4}$$

The basin water absorbs energy released from the basin liner and consumes it in two ways, some energy is stored in the water due to its specific heat and the rest is transferred to the glass cover through three methods (convection, evaporation and radiation).

$$\alpha'_w \; I(t) + q_{cbw} = q_{twg} + m_w c_w \left(\frac{dT_W}{dt}\right), \tag{5}$$

$$\alpha'_w \; I(t) + h_{cbw}(T_b - T_w) = h_{twg}(T_w - T_g) + m_w c_w \left(\frac{dT_w}{dt}\right). \tag{6}$$

The basin linear absorbs heat energy from the solar radiation transmitted from the glass and releases this energy to the basin water and the rest to the atmosphere by conduction and convection through walls of the still.

$$\alpha'_b \; I(t) = q_{cbw} + q_{tba}\,, \tag{7}$$

$$\alpha'_b \; I(t) = h_{cbw}(T_b - T_w) + h_{tba}(T_b - T_a)\,. \tag{8}$$

By solving Equations (4), (6), (8) one gets,

$$\left(\frac{dT_w}{dt}\right) + aT_w = f(t), \quad (9)$$

where:

$a = U_L/(m_w c_w)$,
$f(t) = M\,I(t) + a\,T_a$,
$M = (\alpha'_{eff} h_{cbw})/m_w c_w (h_{cbw} + h_{tba})$.

The solution of Equation (9) is

$$T_w = \left(\frac{f(t)}{a}\right)(1 - e^{at}) + Tw_0 e^{-at}. \quad (10)$$

The hourly yield equals,

$$M_w = \left(\frac{h_{ewg}(T_w - T_g) * 3600}{L_{ev}}\right) * A_b. \quad (11)$$

To solve the above equations heat transfer analysis for all solar still should be calculated. Equations from (12) to (42) will introduce the heat transfer analysis. Section three introduces the calculation methodology.

The latent heat of evaporation is calculated by [19],

$$L_{ev} = (2501.67 - 2.389 * T_w) * 10^3. \quad (12)$$

2.2 Solar still heat transfer analysis

There are mainly two types of heat transfers taking place in the process of solar still (Internal and external)

Internal heat transfer

It occurs between the basin water surface and inner glass cover through three methods (convection, evaporation and radiation).

The convection heat transfer between the water and the inner glass cover is calculated from,

$$q_{cwg} = h_{cwg}(T_w - T_g). \quad (13)$$

Empirical relation for the convection heat transfer coefficient is given by Dunkle [20].

$$h_{cwg} = 0.884\left[(T_w - T_g) + \frac{(P_w - P_g)(T_w + 273)}{(268.9 * 10^3 - P_w)}\right]^{1/3}. \quad (14)$$

The evaporation heat transfer between water and inner glass cover is calculated from,

$$q_{ewg} = h_{ewg}(T_w - T_g), \quad (15)$$

$$h_{ewg} = \frac{16.28 * 10^{-3} * h_{cwg}(P_w - P_g)}{(T_w - Tg)}. \quad (16)$$

The radiation heat transfer between water and inner glass cover is calculated from,

$$q_{rwg} = h_{rwg}(T_w - T_g). \quad (17)$$

In addition, given by Stefan Boltzmann's equation:

$$q_{rwg} = \varepsilon_{eff}\sigma[(T_w + 273)^4 - (T_g + 273)^4]. \quad (18)$$

From Equations (17) and (18):

$$h_{rwg} = \frac{\varepsilon_{eff}\sigma[(T_w + 273)^4 - (T_g + 273)^4]}{(T_w - T_g)}. \quad (19)$$

Finally, the total internal heat transfer coefficients are:

$$h_{twg} = h_{cwg} + h_{ewg} + h_{rwg}. \quad (20)$$

External heat transfer

External heat transfer is contributed by the top, bottom and sides losses of the solar still.

Top heat losses occur between the outer glass cover and the atmosphere through two methods (convection and radiation).

The radiation heat transfer is

$$q_{rga} = h_{rga}(T_g - T_{sky}), \quad (21)$$

$$q_{rga} = \varepsilon_g\sigma[(T_g + 273)^4 - (T_{sky} + 273)^4]. \quad (22)$$

From Equations (21) and (22)

$$h_{rga} = \frac{\varepsilon_g\sigma[(T_g + 273)^4 - (T_{sky} + 273)^4]}{(T_g - T_{sky})}. \quad (23)$$

The sky temperature is estimated from [21]:

$$T_{sky} = 0.0552 * T_a^{1.5}. \quad (24)$$

The convective heat transfer is

$$q_{cga} = h_{cga}(T_g - T_a). \quad (25)$$

where from [22]

$$h_{cga} = 2.8 + 3.0\,V_w, \quad (26)$$

if $V_w \le 5\,m/s$ & $6.15 * (V_w)^{0.8}$ if $V_w > 5\,m/s$.

Finally, the total top heat transfer coefficients are

$$h_{tga} = h_{cga} + h_{rga}. \quad (27)$$

The bottom and side heat losses occur between the water in the basin and the outer atmosphere through the insulation on the sides and base through three methods (conduction, evaporation and radiation).

$$q_{tba} = h_{tba}(T_b - T_a). \quad (28)$$

***Table 2** Attenuation (Att) factors for varying water depth*

d_w(m)	Attenuation factor
0.02	0.6756
0.03	0.6441
0.04	0.6185
0.05	0.6124
0.06	0.5858
0.08	0.5648
0.10	0.5492

***Table 3** Design parameters*

Parameters	Numerical values
Basin area, A_b	1 m^2
Glass absorptivity, α_g	0.04
Glass reflectivity, R_g	0.06
Glass emissivity, ε_g	0.9
Water reflectivity, R_w	0.05
Water emissivity, ε_w	0.95
Water heat capacity, c_w	4180 J/kg K
Time, t	3600 s
The thickness of glass cover, L_g	0.008 m
Glass thermal conductivity, K_g	1.03 W/m K
The thickness of insulation, L_i	0.02 m
Insulation thermal conductivity, K_i	0.035 w/m K
Stefan Boltzmann's constant, σ	5.6697*10^{-8} w/m^2.K^4
h_w	250 W/m^2 K
Water depth, d	0.03 m
h_{ba}	2.8 W/m^2 °C
h_{cbw}	250 W/m^2 °C (summer) 200 W/m^2 °C (winter)

The heat loss coefficient from basin liner to the atmosphere

$$h_{tba} = \left[\left(\frac{L_i}{K_i}\right) + \left(\frac{1}{h_{ba}}\right)\right]^{-1}, \tag{29}$$

where:

$$h_{ba} = h_{rba} + h_{cba}. \tag{30}$$

Side heat loss is,

$$h_{sa} = h_{tba} * \left(\frac{A_s}{A_b}\right). \tag{31}$$

Solar radiation fractions [23]

The water temperature T_w and the glass temperature T_g depend on the solar radiation fractions, which are defined as the fraction of solar energy absorbed for both water and glass.

The fraction absorbed by glass cover is

$$\alpha'_g = (1 - R_g)\alpha_g. \tag{32}$$

The fraction absorbed by water without attenuation factor is,

$$\alpha'_w = (1 - \alpha g)(1 - R_g)(1 - R_w)\alpha_w. \tag{33}$$

The fraction absorbed by water with attenuation factor is,

$$\alpha'_w = (1 - \alpha g)(1 - R_g)(1 - R_w)\alpha_w * \left[1 - \sum \mu_j EXP(-n_j d_w)\right], \tag{34}$$

where, $\left[1 - \sum \mu_j EXP(-n_j d_w)\right]$ is the attenuation factor that depends on water depth [20]. Table 2 represents the attenuation factor variation.

Then, the glass temperature is

$$T_{gi} = \frac{\alpha'_g\ I(t) + h_{twg} * T_w + U_{tga} * T_a}{h_{twg} + U_{Tga}}, \tag{35}$$

where, U_{Tga} is calculated from:

$$U_{Tga} = \frac{\frac{K_g}{L_g} * h_{tga}}{\frac{K_g}{L_g} + h_{tga}}. \tag{36}$$

and the partial vapor pressures from:

$$P_w = EXP\left\{25.317 - \frac{5144}{(T_w + 273)}\right\}, \tag{37}$$

$$P_g = EXP\left\{25.317 - \frac{5144}{(T_g + 273)}\right\}. \tag{38}$$

Finally, the overall heat transfer coefficients can be calculated from

$$U_T = \frac{h_{twg} * U_{Tga}}{h_{twg} + U_{Tga}}, \tag{39}$$

$$U_b = \frac{h_w * h_{ba}}{h_w + h_{ba}}, \tag{40}$$

$$U_{ss} = \left(\frac{A_{ss}}{A_b}\right) U_b, \tag{41}$$

$$U_L = U_b + U_t + U_{ss}. \tag{42}$$

The above equations were set and solved by computer using the excel software to get the yield. The design parameters used are given in Table 3.

3 Calculation methodology

A certain procedure must be followed to compute the hourly heat transfer coefficients, water temperature, glass temperature and productivity.

1. First of all, water temperature, glass temperature, ambient temperature, solar radiation intensity and wind velocity must be measured and use these values to evaluate the partial vapor pressures P_w & P_g Equations (36) and (37), convection heat transfer coefficient between water and glass h_{rwg} Equation (14), evaporation heat transfer coefficient between water and glass h_{twg} Equation (16), radiation heat transfer coefficient between water and glass h_{rwg} Equation (19) and then deduce the total heat transfer coefficient between water and glass h_{ewg} Equation (20).
2. Use the value of h_{twg} to get the value of overall heat transfer coefficients Equations (38) to (41) from these values calculate the new value of T_w.
3. From evaporation heat transfer coefficient h_{ewg} calculate the hourly yield M_w from Equation (11).
4. From the value of T_w get a new value of T_g Equation (34) and repeat the previous steps.

4 Experimental work

The solar still is designed and constructed to compare the productivity with and without the floating lid. The work is conducted in Military Technical College (MTC), Cairo, Egypt (Latitude: 30, Longitude: 31). The solar still takes the design of a box with dimensions of 1.3 m length, 1.1 m breadth and 0.9 m height. The box is made of plywood with 0.05 m thickness. It has four sides, two of these sides are rectangular and the other two are trapezoidal. The area available for water is 1 m * 1 m. The basin has three holes one for feeding water, one for impure water outlet and the third for distilled water output. The outside walls are insulated with glass wool with thermal conductivity K = 0.035 w/mK. The distillate channel is covered with polyester fabric with a slope of 1/10 to ease the flow of distilled water through the hole to reach the graduated flask insulated with the same material as still. The distilled water passes from the PVC pipe to the flask through a U-tube which acts as a manometer to prevent any air from entering the still. The condensing surface is a normal glass with a thickness of 8 mm, emissivity = 90 %, reflectivity = 6 % and absorptivity = 4 %. The glass is inclined at an angle of 30°, which is equal to the latitude of Cairo. Silicon rubber was used to fill the gaps between plywood edges. The basin was coated with black painted polyester fabric to enhance the absorptivity of solar radiation. Figure 1 shows the constructed physical model. Figure 2 shows the instruments used in the experiment. Figure 3

Figure 1 *Photograph of the constructed solar still*

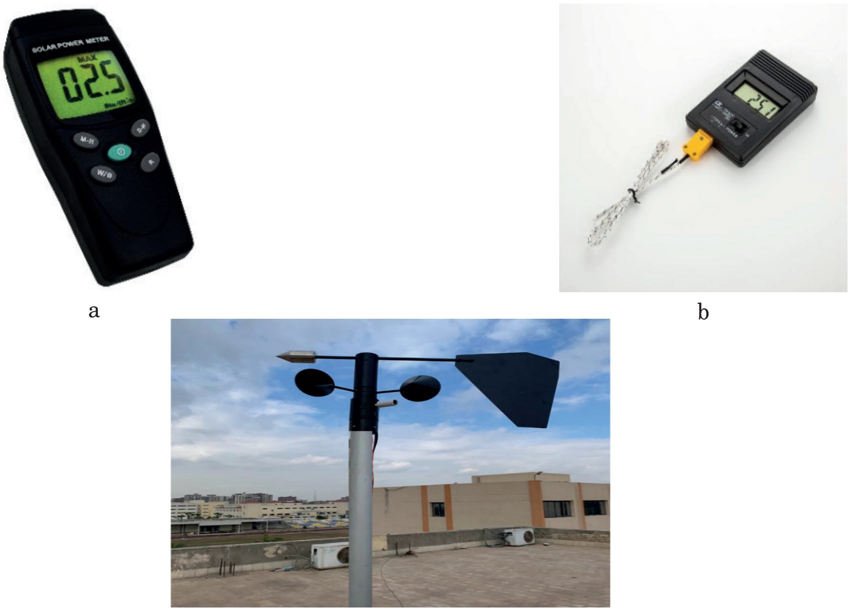

a b

c

Figure 2 *Instruments for experimentation: a-solar power meter, b- digital thermometer, c- wind speed meter*

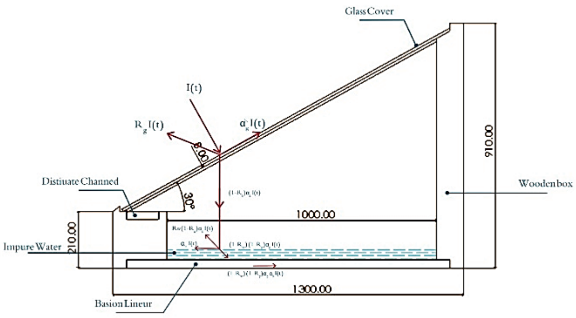

Figure 3 *Schematic diagram of the solar radiation*

shows the schematic diagram of solar radiation in the experiment and the main parts of the solar still.

The experimental work was conducted for two cases; solar still without the lid and solar still with the lid afloat.

For the solar still without lid afloat, the experiments were conducted for seven days of the summer season, 2021 from July 1st to July 7th. The still was placed in the south direction. Solar radiation intensity was measured by using a pyrometer. Wind velocity was taken from the website: timeanddate.com and compared to the measured velocity in MTC and the two readings are the same. These data were used in the theoretical calculation. Both water temperature and glass cover temperature were measured with Ni/Cr electric thermometer and were compared to the theoretical values. The water depth was set to be 30 mm at the beginning of each experimental day. The condensed water was collected in a graduated flask. The yield was considered every 24 hours starting at 7:00 am. The measured solar radiation intensity range was (0 to 990.8 w/m^2) and wind velocity was (0 to 7.78 m/s).

For the solar still with the lid afloat, the experiments were conducted for six days starting from July 8th to July 13th. A black fibrous lid was placed on the surface of the water. The distilled water was measured every 24 hours starting from 7:00 am. Solar radiation intensity range was taken as (0 to 989.7 w/m^2) and wind velocity was taken as (1.11 to 7.78 m/s).

5 Results and discussion

The outputs of the experiment were recorded and compared to the theoretical values, by following the methodology of calculations in section 3.

Figure 4 shows the ambient and sky temperature along the first day of experimentation, which is used in calculations to get the output yield. The ambient temperature was in the range from 26 °C to 38 °C.

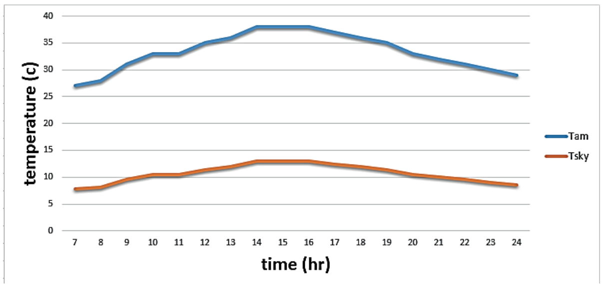

Figure 4 *Ambient and sky temperature from for the first day of calculations (1-7-2021)*

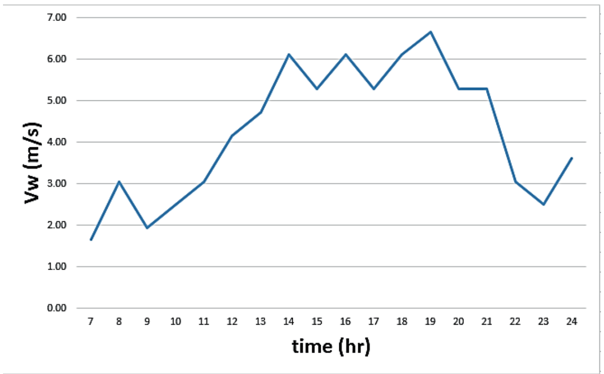

Figure 5 *Wind velocity from the website for the first day of calculations (1-7-2021)*

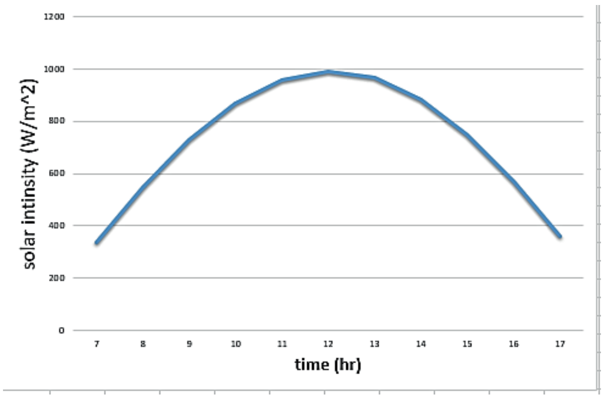

Figure 6 *The solar intensity measured by pyrometer on the first day of calculations (1-7-2021)*

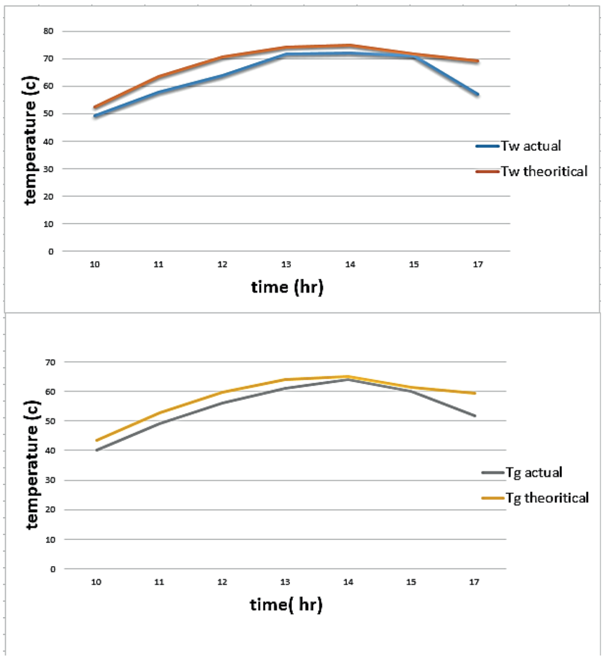

Figure 7 *The temperature comparison between the actual and theoretical water and glass temperatures on the first day of calculations (1-7-2021)*

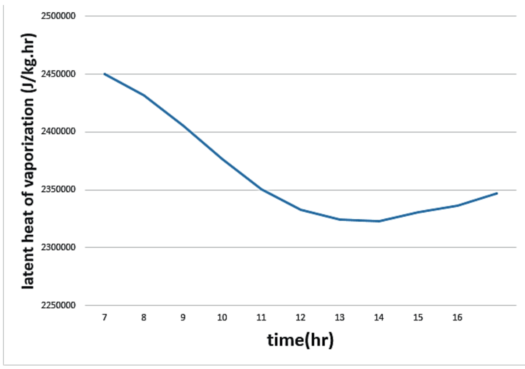

Figure 8 *The variation of latent heat of vaporization with the hours of the day*

Figure 5 shows the wind velocity variation along the day. For the first experimental day, it varies from 4.2 to 6.8 m/s.

Figure 6 shows the solar radiation intensity measured along the day. It varies from 390 to 999 W/m^2.

Figure 7 shows the difference between the measured and theoretical temperatures of both water and glass. The difference between both ranged from 3 to 5 °C.

Figure 8 shows the variation of latent heat of vaporization along the day.

Figure 9 shows the variation of different heat transfer coefficients. It gives a relation between the heat transfer coefficient between the water and glass and the time along the day.

Figure 10 shows the hourly yield output throughout the day. It gives the relation between the hourly yield and the time of the day. Its value 0.012 l/m^{2}hr at 7:00 am and reaches a peak of 0.92 L/m^{2}hr at 1:00 pm with an accumulated value of 5.6 l/m^2.day.

Figure 11 shows the difference between the actual and the theoretical yield of the solar still. It shows that the average actual yield is about 52 % of the theoretical yield. Theoretical daily output is higher than the experimental values due to different heat losses from the still.

For the solar still with a floating lid, the experimental output yield values were compared to the results obtained without the floating lid to indicate the effect of the floating lid on the productivity of the solar still. Figure 12 shows the comparison. It was found that the ratio increased to 58 % with about 6 % of the first condition. This is due to the porosity of the lid; the evaporative surface area of the still was increased.

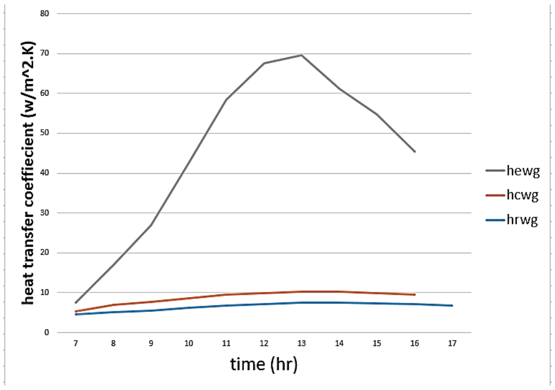

Figure 9 *The variation of heat transfer coefficients between water and glass along the time of the day*

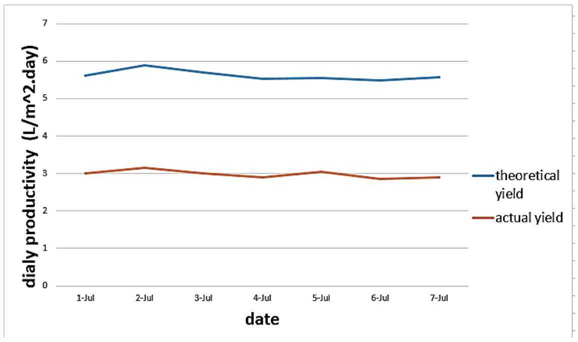

Figure 11 *Yield comparison without a lid on seven days from (July 1st to July 7th) shows that the actual yield is about 52 % of the theoretical yield*

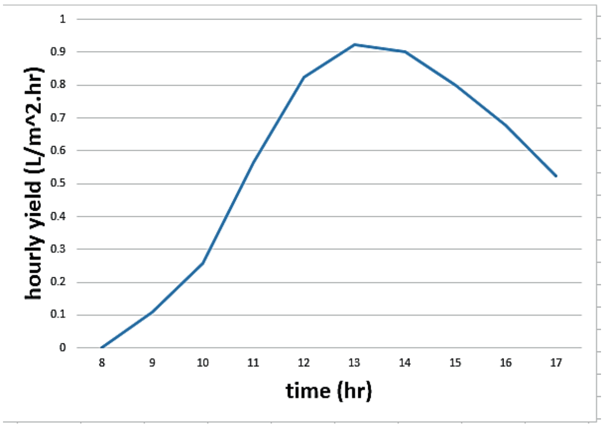

Figure 10 *The hourly variation of the output yield of the solar still along this day*

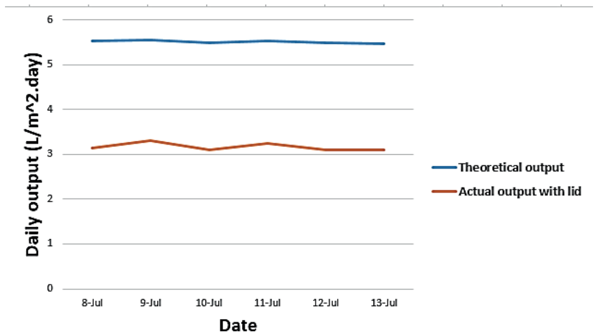

Figure 12 *Yield comparison with a lid on six days from (July 8th to July 13th) shows that the actual yield is about 58 % of the theoretical yield*

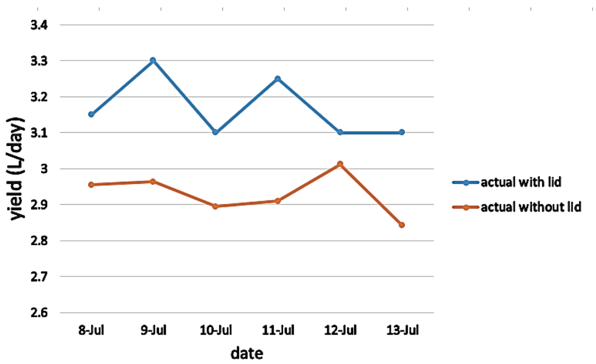

Figure 13 *Comparison between the actual yield with lid and the actual yield without lid*

Figure 13 shows the effect of using a lid afloat and the comparison between the actual yield with and without the lid.

6 Conclusions

The single slope solar still was fabricated and investigated. Different parameters as glass temperature, water temperature and output yield were measured and compared to the theoretically calculated values. In addition, this work shows the effect of placing a floating lid (black fibrous lid) which is porous material on the output yield of the solar still. The output yield of the still with a floating lid was compared to the ratio of the experimental and theoretical output yield. It was found that:

1. The output without a lid was 52 % of the theoretical output.
2. The output with lid was 58 % from the theoretical output.
3. Placing a porous material on the surface of the water increased the productivity by 6 % of the regular output.

4. The porous material works as a heat absorber and increases the evaporative area of water because of the surface area of water balls that pass throw the holes of the material by capillary effect.

References

[1] KALOGIROU, S. A. Seawater desalination using renewable energy sources. *Progress in Energy and Combustion Science* [online]. 2005, **31**(3), p. 242-281. ISSN 0360-1285. Available from: https://doi.org/10.1016/j.pecs.2005.03.001

[2] RAJU, V. R., NARAYANA, R. L. Effect of flat plate collectors in series on performance of active solar still for Indian coastal climatic condition. *Journal of King Saud University - Engineering Sciences* [online]. 2015, **30**(1), p. 78-85. ISSN 1018-3639. Available from: https://dx.doi.org/10.1016/j.jksues.2015.12.008

[3] SINGH, R. V., KUMAR, S., HASAN, M. M., KHAN, M. E., TIWARI, G. N. Performance of a solar still integrated with evacuated tube collector in natural mode. *Desalination* [online]. 2013, **318**, p. 25-33. ISSN 0011-9164. Available from: https://doi.org/10.1016/j.desal.2013.03.012

[4] SAMPATHKUMAR, K., ARJUNAN, T. V., PITCHANDI, P., SENTHILKUMAR, P. Active solar distillation - a detailed review. *Renewable and Sustainable Energy Reviews* [online]. 2010, **14**(6), p. 1503-1526. ISSN 1364-0321. Available from: https://doi.org/10.1016/j.rser.2010.01.023

[5] PRASAD, A. R., SATHYAMURTHY, R., SUDHAKAR, M., MADHU, B., MAGESHBABU, D., MANOKAR, A. M., CHAMKHA, A. J. Effect of design parameters on fresh water produced from triangular basin and conventional basin solar still. *International Journal of Photoenergy* [online]. 2021, **2021**, 6619138. ISSN 1110-662X, eISSN 1687-529X. Available from: https://doi.org/10.1155/2021/6619138

[6] PRADEE, M., VEMBATHURAJESH, A., SUNDARAM, C. M., SIVAGANESAN, V., NAGARAJAN, B. Design, fabrication and performance analysis of concave solar still. In: 2013 IEEE Energytech: proceedings [online]. IEEE. 2013. eISBN 978-1-4673-4444-9. Available from: https://doi.org/10.1109/EnergyTech.2013.6645306

[7] ARUNKUMAR, T., JAYAPRAKASHA, R., DENKENBERGER, D., AHSAN, A., OKUNDAMIYA, M. S., KUMAR, S., TANAKA, H., AYBARG, H. S. An experimental study on a hemispherical solar still. *Desalination* [online]. 2012, **286**, p. 342-348. ISSN 0011-9164. Available from: https://doi.org/10.1016/j.desal.2011.11.047

[8] JATHAR, L. D., GANESAN, S., GORJIAN, S. An experimental and statistical investigation of concave-type stepped solar still with diverse climatic parameters. *Cleaner Engineering and Technology* [online]. 2021, **4**, 100137. ISSN 2666-7908. Available from: https://doi.org/10.1016/j.clet.2021.100137

[9] GAD, H. E., EL-DIN, S. S., HUSSIEN, A. A., RAMZY, K. Thermal analysis of a conical solar still performance: an experimental study. *Solar Energy* [online]. 2015, **122**, p. 900-909. ISSN 0038-092X. Available from: https://doi.org/10.1016/j.solener.2015.10.016

[10] AGRAWAL, A., RANA, R. S., SRIVASTAVA, P. K. Heat transfer coefficients and productivity of a single slope single basin solar still in Indian climatic condition: experimental and theoretical comparison. *Resource - Efficient Technologies* [online]. 2017, **3**(4), p. 466-482. ISSN 2405-6537. Available from: https://doi.org/10.1016/j.reffit.2017.05.003

[11] KHALIFA, A. J. N., HAMOOD, A. M. Effect of insulation thickness on the productivity of basin type solar stills: an experimental verification under local climate. *Energy Conversion and Management* [online]. 2009, **50**(9), p. 2457-2461. ISSN 0196-8904. Available from: https://doi.org/10.1016/j.enconman.2009.06.007

[12] MATRAWY, K. K., ALOSAIMY, A. S., MAHROUS, A. F. Modeling and experimental study of a corrugated wick type solar still: comparative study with a simple basin type. *Energy Conversion and Management* [online]. 2015, **105**, p. 1261-1268. ISSN 0196-8904. Available from: https://doi.org/10.1016/j.enconman.2015.09.006

[13] ABDALLAH, S., ABU-KHADER, M. M., BADRAN, O. Effect of various absorbing materials on the thermal performance of solar stills. *Desalination* [online]. 2009, **242**(1-3), p. 128-137. ISSN 0011-9164. Available from: https://doi.org/10.1016/j.desal.2008.03.036

[14] SRIVASTAVA, P. K., AGRAWAL, S. K. Experimental and theoretical analysis of single sloped basin type solar still consisting of multiple low thermal inertia floating porous absorbers. *Desalination* [online]. 2013, **311**, p. 198-205. ISSN 0011-9164. Available from: https://doi.org/10.1016/j.desal.2012.11.035

[15] AGRAWAL, A., RANA, R. S. Theoretical and experimental performance evaluation of single-slope single-basin solar still with multiple V-shaped floating wicks. *Heliyon* [online]. 2019, 5(4), e01525. eISSN 2405-8440. Available from: https://doi.org/10.1016/j.heliyon.2019.e01525

[16] GAWANDE, J. S., BHUYAR, L. B. Effect of shape of the absorber surface on the performance of stepped type solar still. *Energy and Power Engineering* [online]. 2013, **5**(8), p. 489-497. ISSN 1949-243X, eISSN 1947-3818. Available from: https://doi.org/10.4236/epe.2013.58053

[17] JOHNSON, A., MU, L., PARK, Y. H., VALLES, D. J., WANG, H., XU, P., KOTA, K., KURAVI, S. A thermal model for predicting the performance of a solar still with fresnel lens. *Water* [online]. 2019, **11**(9), 1860. eISSN 2073-4441. Available from: https://doi.org/10.3390/w11091860
[18] GUPTA, B., SHARMA, R., SHANKAR, P., BAREDAR, P. Performance enhancement of modified solar still using water sprinkler: an experimental approach. *Perspectives in Science* [online]. 2016, **8**, p. 191-194. ISSN 2213-0209. Available from: https://doi.org/10.1016/j.pisc.2016.04.029
[19] FATH, H. E. S., HOSNY, H. M. Thermal performance of a single-sloped basin still with an inherent built-in additional condenser. *Desalination* [online]. 2002, **142**(1), p. 19-27. ISSN 0011-9164. Available from: https://doi.org/10.1016/S0011-9164(01)00422-2
[20] DUNKLE, R. Solar water distillation: the roof type still and the multiple effect diffusor still. In: International Developments in Heat Transfer ASME: proceeding. Part V. 1961. p. 895.
[21] PEARCE, J. M., Denkenberger, D. Numerical simulation of the direct application of compound parabolic concentrators to a single effect basin solar still. In: 2006 International Conference of Solar Cooking and Food: proceedings. 2006.
[22] WATMUFF, J. H., CHARTERS, W. W. S., PROCTOR, D. Solar and wind induced external coefficients - solar collectors. 1977.
[23] TIWARI, A. K., TIWARI, G. N. Thermal modeling based on solar fraction and experimental study of the annual and seasonal performance of a single slope passive solar still: the effect of water depths. *Desalination* [online]. 2007, **207**, p. 184-204. ISSN 0011-9164. Available from: https://doi.org/10.1016/j.desal.2006.07.011

Annex - Nomenclatures

A_b Basin liner surface area of the still (m^2)
A_s Basin sidewall area of the still (m^2)
A_{ss} Area of the solar still (m^2)
q_{cba} Convective heat transfer from the bottom of the basin to ambient (W/ m^2)
q_{rba} Radiative heat transfer from the bottom of the basin to ambient (W/ m^2)
q_{cwg} Convective heat transfer from the basin water to glass cover (W/ m^2)
q_{ewg} Evaporative heat transfer from the basin water to glass cover (W/ m^2)
q_{rwg} Radiative heat transfer from the basin water to glass cover (W/ m^2)
q_{twg} Total heat transfer from the basin water to glass cover (W/ m^2)
q_{cga} Convective heat transfer from the glass cover to ambient (W/ m^2)
q_{rga} Radiative heat transfer from the glass cover to ambient (W/ m^2)
q_{tga} Total heat transfer from the glass cover to ambient (W/ m^2)
q_{cbw} Convective heat transfer from the basin liner to water (W/ m^2)
q_{tba} Total heat transfer from the basin liner to ambient (W/ m^2)
q_{ba} Total heat transfer from the bottom of the basin to ambient (W/ m^2)
R_g Reflectivity of the glass cover
R_w Reflectivity of the basin water
R_b Reflectivity of the basin liner
h_{cwg} Convective heat transfer coeffcient from the basin water to glass cover (W/m^2 °C)
h_{ewg} Evaporative heat transfer coeffcient from the basin water to glass cover (W/m^2°C)
h_{rwg} Radiative heat transfer coeffcient from the basin water to glass cover (W/m^2°C)
h_{twg} Radiative heat transfer coeffcient from the basin water to glass cover (W/m^2°C)
h_{cga} Convective heat transfer coeffcient from the glass cover to ambient (W/m^2 °C)
h_{rga} Convective heat transfer coeffcient from the glass cover to ambient (W/m^2°C)
h_{tga} Total heat transfer coeffcient from the glass cover to ambient (W/m^2 °C)
h_{cbw} Convective heat transfer coeffcient from the basin liner to water (W/m^2 °C)
h_{tba} Total heat transfer coeffcient from the basin liner to ambient (W/m^2°C)
h_{ba} Total heat transfer coeffcient from the bottom of the basin to ambient (W/m^2°C)
h_{cba} Convective heat transfer coeffcient from the bottom of the basin to ambient (W/m^2°C)
h_{rba} Radiative heat transfer coeffcient from the bottom of the basin to ambient (W/m^2°C)
h_{sa} side heat transfer coefficient (W/m2°C)
U_b Overall bottom heat transfer coeffcient from bottom to ambient (W m^2 °C)
U_{Tga} Overall heat transfer coefficient from glass to ambient (W/m^2 °C)
U_t Overall top heat transfer coeffcient from basin water to ambient (W/m^2 °C)
U_L Overall heat transfer coeffcient for still (W m^2 °C)

U_{SS} Overall side heat transfer coefficient between water and surrounding (W/m^2 °C)
T_g Glass cover temperature (°C)
T_b Basin water temperature (°C)
T_a Ambient temperature (°C)
T_b Basin liner temperature (°C)
T_{sky} Sky temperature (°C)
V_w Velocity of Wind (m/s)
$I(t)$ Solar Intensity (W/m^2)
L_{ev} Latent heat of vaporization of water (J/kg)
m_w Mass of water in the basin (Kg)
d_w Water depth in the basin (m)
t_g Glass cover thickness (m)
t Time interval (s)
K_i Thermal conductivity of insulation (W/m°C)
K_g Thermal conductivity of glass(W/m°C)
L_i Thickness of insulation (m)
L_g Thickness of glass (m)
C_i Specific heat of insulation in still (J/kg °C)
C_w Specific heat of the water in solar still (J/kg °C)
P_w Partial saturated vapor pressure at a basin water temperature (N/m^2)
P_g Partial saturated vapor pressures at glass cover temperature (N/m^2)
M_w Hourly distillate output per unit basin area (l/m^2/h)
M'_w Daily distillate output per unit basin area (l/m^2/d)

Greek symbols
α_g Absorptivity of the glass cover
α_w Absorptivity of the basin water
α_b Absorptivity of the basin liner
α'_g Fraction of solar flux absorbed by a glass cover
α'_w Fraction of solar flux absorbed by basin water
α'_b Fraction of solar flux absorbed by basin liner
α_{eff} effective absorptivity
ε_g Emissivity of the glass cover
ε_w Emissivity of the basin water
ε_b Emissivity of the basin liner
ε_{eff} Effective emissivity between the water surface and glass cover
σ Stefan-Boltzmann constant
μ_j Fraction of the solar flux having extinction coeffcient
η_j Extinction coeffcient

subscripts
a ambient
g Glass cover
w Basin water
b Basin liner
i internal

DEVELOPMENT OF A MODEL FOR CALCULATING THE SLIP COEFFICIENTS OF A MECHANICAL WHEELED VEHICLE WITH TWO STEERING AXLES

Tassybek N. Bekenov [1], Zhanibek T. Nussupbek [2,*], Zhandos T. Tassybekov [3], Zamira K. Sattinova [4],

[1]Department of Transportation Organization, Traffic and Transport Operation, L. N. Gumilyov Eurasian National University, Nur-Sultan, Republic of Kazakhstan
[2]Department of Transport Engineering and Technology, S. Seifullin Kazakh Agrotechnical University, Nur-Sultan, Republic of Kazakhstan
[3]Department of Design and Engineering Graphics, L. N. Gumilyov Eurasian National University, Nur-Sultan, Republic of Kazakhstan
[4]Department of Thermal Power Engineering, L. N. Gumilyov Eurasian National University, Nur-Sultan, Republic of Kazakhstan

*E-mail of corresponding author: nussupbek@murdoch.in

Resume

The purpose of the study is to perform appropriate calculations of the values of the total slip coefficients alternately on the sides of a vehicle, depending on the angles of rotation of its axles, using the single slip coefficients of its individual wheels directly when turning. The basis of the methodological approach in this study is a combination of system analysis of the principles of calculating the slip coefficients of a mechanical wheeled vehicle with an analytical investigation of problematic aspects of developing a model for calculating the slip coefficients of a vehicle with two steering axles. The results obtained indicate the presence of a persistent relationship between the slipping coefficients of a mechanical wheeled vehicle and the rotation angles of its two steering axles, including a number of other parameters that are important from the standpoint of traffic safety.

Available online: https://doi.org/10.26552/com.C.2022.3.B211-B218

Article info

Received 7 December 2021
Accepted 30 March 2022
Online 18 May 2022

Keywords:

mechanical wheeled vehicle
steering axle
complex slipping coefficients
model for calculating slipping coefficients
slipping of a mechanical wheeled vehicle

ISSN 1335-4205 (print version)
ISSN 2585-7878 (online version)

1 Introduction

Mobile and manoeuvrable mechanical wheeled mechanisms are widely used in various branches of modern industry for the qualitative solution of issues of the cargo transportation and mechanisation of lifting, construction and road works. The scope of their practical application is determined by their types and design features, which are steadily expanding. Due to the mass use of wheeled vehicles, the issues of conducting the large-scale scientific research aimed at improving the already developed and creating the latest designs of mechanical vehicles are becoming increasingly relevant [1].

In modern economic conditions, the issues of gradual increase in the productivity of technological units are given priority. At the same time, the quality of mechanical wheeled vehicles and their performance are of great importance, since they are the most important elements of the technological chain. Very often, when operating such vehicles in the mining industry and a number of other industrial sectors, a decrease in their productivity, conditioned by difficult operating conditions, is observed [2]. Thus, in relation to the existing types and sizes of transport equipment, operational issues are becoming highly relevant, since the proper organisation of transport and technological processes can significantly increase their efficiency in the current conditions of the road and transport loads. It is also necessary to consider the fact that the optimal organisation of the mechanical wheeled vehicles' operation cannot be carried out without a theoretical analysis of their operational characteristics. This means that with the practical use of such machines in difficult road conditions, the analysis of their most important operational qualities, such as traction capability and cross-country ability, becomes particularly relevant [3]. Considering the fact that the operating conditions of mechanical wheeled vehicles assume a variety of very different road situations, the compliance of the traction capability of such machines and their cross-country capability will largely determine the effectiveness of their use. The use of mechanical wheeled vehicles with all-wheel drive for operation in the most severe road conditions and with limited space implies the need for effective resolution of a number of tasks directly related to the issues of increasing their patency in terms and profile and power circulation in their transmission. This determines the relevance of evaluating and selecting rational types and parameters of mechanical machines for their subsequent practical application in industrial enterprises and to determine their main traction parameters [4].

It is a well-known fact that when mechanical wheeled vehicles with two driving axles are moving, there is a redistribution of traction forces between these axles and this is especially important when turning mechanical vehicles. This determines the essential relevance of the study of problems of traction forces redistribution that arise directly during the movement of such vehicles, at any stage of movement. For this reason, studies of various aspects of the development of a model for calculating the slip coefficients of a mechanical wheeled vehicle with two steering axles have significant practical significance in terms of the prospects for creating new models of modern equipment capable of withstanding a large number of load cycles in difficult operating conditions, without the need for major repairs and replacement of components [5].

The main problems of research conducted within the framework of the subject matter are the lack of computational information regarding the quality of the mathematical model being created for calculating the slip coefficients of a mechanical wheeled vehicle with two steering axles. In this study, the task was set to create a qualitative model for calculating these coefficients, as close as possible to the real conditions and reflecting the real prospects for creating a full-drive mechanical vehicle in the future, capable of effectively solving the problems of the passenger and cargo transportation in the most difficult operating conditions.

2 Materials and methods

The basis of the methodological approach in this study is a combination of system analysis of the principles of calculating the slip coefficients of a mechanical wheeled vehicle with an analytical investigation of problematic aspects of developing a model for calculating the slip coefficients of a vehicle with two steering axles. This combination of research methods assumes the establishment of the necessary theoretical basis and the subsequent application of mathematical modelling techniques to create a qualitative model for calculating the slip coefficients of a mechanical vehicle with two steering axles. The study uses equations for determining the slip coefficients of mechanical vehicles with 4x4 wheel arrangement with two steering axles and an on-board blocked transmission and equations for calculating the angles of turns of the driving axles of a mechanical wheeled vehicle.

The theoretical basis of this study is made up of numerous research papers by various authors devoted to creation of mathematical models for determining the slip coefficients of mechanical vehicles with several steering axles and topics related to the subject matter. To form the most complete and reliable picture of research and to facilitate the perception of the information provided, all the developments of foreign authors, taken in the order of citation and presented in this research paper, have been translated into English. Thus, the theoretical basis of this study is the foundation for further research, carried out in strict accordance with all the issues raised in its subject matter.

The study was carried out in several main stages. At the first stage, a theoretical analysis of research papers available within the framework of the stated topics was carried out, which contributes to the development of a high-quality research base for further investigation in this area. In addition, this stage involved a systematic analysis of the principles of calculating the slip coefficients of a mechanical wheeled vehicle, the results of which formed the basis for the study of the principles of constructing a calculation model of the slip coefficients of a mechanical wheeled vehicle with two steering axles.

At the next stage, an analytical investigation of problematic aspects of the development of a model for calculating the slip coefficients of a mechanical wheeled vehicle with two steering axles was carried out. At the same time, this stage included an analytical comparison of the preliminary results obtained to the results and conclusions of other researchers on a similar subject or related to them. This is done to create an objective picture of scientific research, considering the maximum amount of results obtained during a detailed investigation of the issues included in the topic. At the final stage, based on the results obtained, the final conclusions were formulated, acting as an objective reflection of study results and summing up the entire complex of research efforts.

3 Results

The movement of mechanical wheeled vehicles in general and during the turns, in particular, is associated with the periodically arising need to determine the loss of speed due to slipping. As a rule, the slipping of a mechanical wheeled vehicle implies some loss of speed of the centre of the drive axle - the slipping of a conditional dummy wheel, which has a free radius equal to the radius of the driving wheels and is located in the centre of the drive axle [6-7]. A similar definition of slipping is applicable for cases of rectilinear motion. The movement of a wheeled vehicle directly during rotation can be estimated by the movement of its centre of mass. Therefore, the slipping of a wheeled vehicle, when making a turn, should be considered as a loss of speed of its centre of mass (1):

$$\delta = (v_{TC} - v_C)/v_{TC}, \tag{1}$$

here v_{TC}, v_C - theoretical and actual velocities of the centre of mass of the vehicle, respectively.

This study considers a 5VS-15M mechanical vehicle used for transporting rock, having a 4x4 wheel arrangement, two drive axles and an on-board blocked transmission. In this study, the slipping of a mechanical wheeled vehicle on a turn is investigated. In the case under consideration, the angular velocities of the driving wheels and the dummy wheel located at the centre of mass of the 5VS-15M vehicle are the same and equal to $w = w_1 = w_2$. The values of angular velocities can be expressed in terms of linear speeds and rolling radii of the wheels. Then:

$$r_{ki} = r_{ki}^0 (1-\delta_i), \tag{2}$$

where r_{ki} and r_{ki}^0 - the rolling radii of the wheel i - valid and free, δ_i - slipping of the car wheel.

As a result, the following relations are obtained:

$$\begin{aligned} \frac{v_C}{1-\delta_B} &= \frac{v_2'}{1-\delta_2'} = \frac{v_1'}{1-\delta_1'}; \\ \frac{v_C}{1-\delta_H} &= \frac{v_2''}{1-\delta_2''} = \frac{v_1''}{1-\delta_1''}, \end{aligned} \tag{3}$$

where, v_1', (δ_1'), v_1'', (δ_1'') - parameters of the speeds (slipping) of the lagging and running wheels of the front axle, v_2', (δ_2'), v_2'', (δ_2'') - the corresponding parameters for the rear axle.

Based on the data presented above, the equations for determining the values of the slip coefficients of mechanical wheeled vehicles with 4x4 wheel arrangement, with two drive axles and an on-board blocked transmission will have the following form:

$$\delta_B = 1 - \frac{(1-\delta_1')\cos(\varepsilon_1 - \alpha_1') + (1-\delta_2')\cos(\varepsilon_2 - \alpha_2')}{\cos(\varepsilon_2 - \eta_M) + \cos(\varepsilon_1 + \eta_M)}, \tag{4}$$

$$\delta_H = 1 - \frac{(1-\delta_1'')\cos(\varepsilon_1 - \alpha_1'') + (1-\delta_2'')\cos(\varepsilon_2 - \alpha_2'')}{\cos(\varepsilon_2 + \eta_M) + \cos(\varepsilon_1 - \eta_M)}. \tag{5}$$

Equations (4) and (5) determine the parameters of wheel slipping along the sides of a mechanical vehicle (lagging and running), while these equations include angles that are determined by the design of this machine and the angle that makes up the velocity vector of the centre of mass with its longitudinal axis and the rotation angles of the lagging and running wheels, respectively, of the front (rear) axles. The following equations are used to calculate the angle values:

$$\varepsilon_1 = \arccos\frac{a}{\sqrt{a^2 + (0.5B)^2}}, \tag{6}$$

$$\varepsilon_2 = \arccos\frac{b}{\sqrt{b^2 + (0.5B)^2}}, \tag{7}$$

$$\eta_M = arctg\frac{btg\alpha_1 - atg\alpha_2}{L}, \tag{8}$$

where a and b - the distance from the centre of mass of the car to the front and rear wheels, respectively; B - track; L - longitudinal base; a_1 and a_2 - angles of rotation of the front and rear axles, respectively.

With a fixed value of the angles of rotation of the axles, there is a significant difference in the corresponding angles of rotation of the inner and outer wheels of a vehicle, relative to the centre of rotation. Equations are used to calculate these differences:

$$tg\alpha_i' = \frac{Ltg\alpha_i}{L - 0.5B(tg\alpha_1 + tg\alpha_2)}, \tag{9}$$

$$tg\alpha_i'' = \frac{Ltg\alpha_i}{L - 0.5B(tg\alpha_1 + tg\alpha_2)}, \tag{10}$$

here, a_1 and a_2 - the values of the rotation angles of the inner and outer wheels, respectively.

Thus, based on the obtained equations, it is possible to carry out the theoretical calculation of the slip coefficients of mechanical wheeled vehicles with two driving axles directly when turning. Respectively, all the possible losses, both speed and power, can be sequentially set [8]. To determine the value of the traction force of the wheels of the 5VS-15M mechanical vehicle under consideration, it is necessary to experimentally establish values of the moments in the drive of the machine by using strain-gauging techniques. Oscilloscopes H-117 were used to measure the values of the turning angles of the vehicle. The angles of rotation of the wheels of the 5VS-15M mechanical vehicle were set using a selsyn sensor of angular deviations. According to certain parameters of traction forces, the slipping coefficients are established. The results of calculations of the slip coefficients are presented in Table 1.

Since the location of the centre of gravity of a mechanical wheeled vehicle is not strictly between the front and rear drive axles (a = 1.47; b = 1.53), there will be significant differences in the values of the angles of rotation of these axles relative to each other directly when turning the car [9]. Therefore, the angles of rotation of the axles are in strict proportion to the distances of the corresponding axles for the three control actions and will be: a) $\alpha_1 = 4.9°$; $\alpha_2 = 5.1°$; b) $\alpha_1 = 9.8°$; $\alpha_2 = 10.2°$; c) $\alpha_1 = 14.7°$; $\alpha_2 = 15.3°$.

At a given angle of rotation of the axles, the

Table 1 Parameters of the wheel slip coefficient of a mechanical vehicle

Mechanical vehicle	Value of the angle rotation of axles, °.	δ_1	δ_2	δ_3	δ_4
5VS-15M	5	0.120	-0.0646	0.0551	0.0549
	10	0.233	-0.0699	-0.0552	0.0406
	15	0.231	-0.0709	-0.0371	0.0400

Table 2 Calculation data of rotation angles of the inner and outer wheels of the 5VS-15M mechanical vehicle

α_1, deg.	α_2, deg.	α_1', deg.	α_2', deg.	α_1'', deg.	α_2'', deg.
4.9	5.1	5.14	5.35	4.68	4.87
9.8	10.2	10.8	11.2	8.97	9.33
14.7	15.3	17.05	17.7	12.9	13.4

Table 3 The results of calculations of the coefficients of slipping on the inner and outer sides of the mechanical vehicle

Mechanical vehicle	Angle of rotation of axles, deg.	δ_B	δ_H	Angle of structure, deg.
5VS-15M	5	-0.028	0.057	0.08
	10	-0.02	0.115	0.0145
	15	-0.0137	0.2354	0.11085

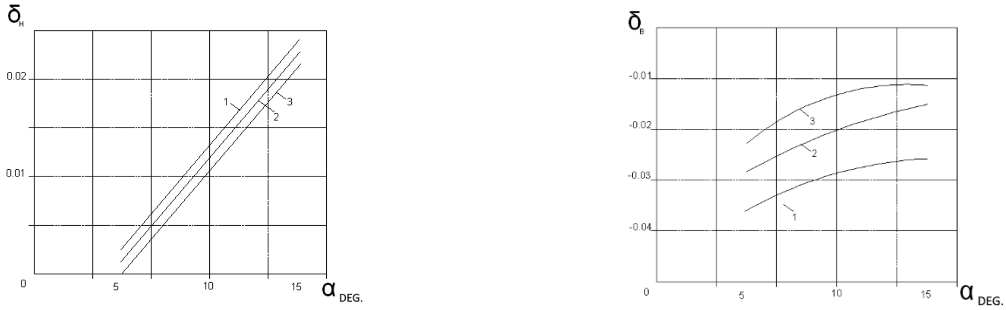

Figure 1 *The dependence of certain parameters of the on-board slip coefficients of a 5VS-15M mechanical vehicle on the angle of rotation of the wheels*
Note: 1 - at a = 1.25; 2 - at a = 1.47; 3 - at a = 1.75

corresponding angles of rotation of the inner and outer wheels of the 5VS-15M mechanical vehicle have significant differences relative to the centre of rotation. Equations (9) and (10) are used to calculate this difference. The calculation data are presented in Table 2.

Equations (4) and (5) allow calculating the parameters of the slip coefficients on the sides of a mechanical wheeled vehicle (internal and external). The data of these calculations are presented in Table 3.

A comparative analysis of the results obtained during the calculations and presented in Table 3 is presented in the form of a graphical dependence in Figure 1.

Comparison of the obtained results with the previous results clearly demonstrates that with the value of the turning angles of the axle of the vehicle at 10° and a = 1.47, the value of δ_H = 0.115, while with a = 1.25, δ_H = 0.122. At the same time, when a = 15° and a = 1.47, δ_H = 0.2354; at a = 1.25, δ_H = 0.24; at a = 1.75, δ_H = 0.2363. The comparative analysis indicates that when a = 10° and a = 1.25, δ_H is 6% higher, while a = 1.47; despite the fact that when a = 1.75, this figure is lower by 12%, than at a = 1.47 and lower by 11%, than when a = 1.25.

This is despite the fact that if a = 15° and a = 1.25, this parameter is 2% higher than in the case when a = 1.47. As for the analysis of slipping, when slipping along the inner radius when turning at an angle of a = 11°, the smallest value of the parameter of the slipping coefficient can be obtained only at a = 1.47. This indicates that the displacement of the centre of mass to the rear of the car is most favourable for this factor. A similar situation exists with a = 15°, since the most advantageous option, in this case, is when a = 1.75, but the slippage does not differ so significantly, namely, only by 13% compared to a = 1.47 and 50% compared to a = 1.25. The question arises why the deviations at

a= 12.5 are higher. The reason is that within the limits of slipping up to δ_H = 0.2, the soil still retains its coupling ability and therefore the redistribution of traction forces is higher with various normal reactions of the wheels.

4 Discussion

Numerous theoretical problems of creating mechanical wheeled vehicles with several driving axles, to improve the cross-country ability and obtain universal vehicles capable of performing their main functions under any road and weather conditions, have long attracted the attention of researchers. In particular, these studies were carried out in relation to road vehicles with a mechanical transmission. The results obtained contribute to establishment of a developed segment of the high-traffic vehicles equipped with all-wheel drive in the modern fleet of vehicles. At the same time, tractors with all-wheel drive and agricultural and special-purpose vehicles are currently quite common. Almost all such equipment is equipped with mechanical transmissions with a step-change in gear ratios. In gearboxes, in addition, either overrunning clutches or differentials are used in transmissions of this kind, which completely exclude the appearance of power fluctuations in transmissions [10].

High efficiency indicators, combined with stable performance characteristics and extreme reliability in conditions of relatively low cost, largely predetermined the further spread of transmissions of this kind on mechanical wheeled vehicles with two or more drive axles. At the same time, on wheeled vehicles in which the number of steering axles exceeds two, at least a pair of driving axles has the maximum convergence between each other. In particular, this is conditioned by the fact that the developers of such vehicles are trying to find the optimal solution to improve the cross-country characteristics and at the same time reduce the variability of rolling conditions of the driving wheels. This is conditioned by the fact that one of the main disadvantages of the differential drive is the loss of the patency of the entire car, in case of problems with the coupling of one of the wheels of the drive axle with the road surface [11]. With the currently existing and implemented design developments of mechanical transmissions of wheeled vehicles with multiple axles, to eliminate the likelihood of problems of wheel coupling with the road, the possibility of forced locking of differentials is provided or differentials with a high internal friction index are used. Both presented options significantly complicate the design of the transmission and negatively affect the overall reliability of the entire car. The practical application of such differentials on mechanical wheeled vehicles with several driving axles is fraught with some difficulties. In a number of situations, in particular, in the case of activation of trailer links of road trains or for some agricultural machines and special-purpose equipment, such difficulties cannot always be overcome. In this context, it is necessary to consider the fact that in the case when developers should make efforts to constructively resolve these difficulties, the situation, as a rule, turns into a significant decrease in the energy efficiency of the developed equipment in practice.

The current situation has turned into the fact that since the second half of the 20th century in a number of Western European countries, adjustable continuously variable transmissions have been actively used in development of the drive design of mechanical wheeled vehicles [12]. As such, electric and hydrostatic transmissions were mainly used, which have significant advantages over conventional mechanical transmissions. In particular, electric transmissions are distinguished by a higher overall efficiency (up to 85 %), ease of installation of the main elements and connections between the aggregate units. A lower value of the cost of electric transmissions has a significant impact on the use of relatively rare alloys and metals in their design. In terms of unit costs, electric transmissions are not significantly superior to hydrostatic transmissions. Mechanical wheeled vehicles with high cross-country capability, equipped with electric transmissions, have structural difficulties with the placement of elements of the air cooling system of electric vehicles, moreover, as with hydrostatic transmissions, the cooling of the body frame is carried out by pumping the working fluid directly through them [13]. The most important feature of an electric transmission should be considered its dynamic external characteristics, in which the internal automatic control is poorly controlled by the gear ratio. In turn, the hydrostatic transmission is much better adapted to automatic regulation, while not creating visible interference to radio communications. At the same time, transmission of this kind has some advantage over an electric one in terms of dimensions, since it is not so bulky.

When creating a mathematical description of the mechanical wheeled vehicle transmission operation, specific mathematical models, describing the operation of individual components of this transmission, should be considered. Such descriptions allow qualitatively assessing the amount of energy losses in transmissions of various kinds and the dependence of these losses on the selected transmission mode. A number of modern studies contain information on the operation of mechanical drives of various vehicles and on the dependencies of energy losses on various aspects of the functioning of these machines. At the same time, it is noted that the definition of such dependencies is fraught with significant difficulties, since there is a largely random nature of changes in the determining parameters that are important from the standpoint of describing the phenomenon of friction in the nodes of mechanical drives. In addition, the issues of describing the processes of viscous friction caused by the presence of lubricant are of considerable complexity from the standpoint of creating a qualitative mathematical description of this process [14].

The use of automatic control systems for the modes of operation of hydrostatic transmissions involves the use of a scheme that ensures the operation of transmissions of this kind in the mode of stable values of transmitted power. The result is a significant increase in the efficiency of such units, when they work on soils of medium and high load-bearing capacity, while when driving on the ground with a low coefficient of adhesion, a gradual increase in the rotational speed of the front wheels of a mechanical vehicle was observed with a slight torque [15]. At the same time, there was intensive milling of the soil under these wheels, a sharp increase in the depth of the natural track, which resulted in a decrease in the cross-country characteristics of this vehicle. This circumstance indicates the fact that the use of simple algebraic solutions, made without considering the quality of the coupling of the wheels of the drive axle with the ground, when creating a mathematical control model of hydrostatic transmissions, in most cases does not allow obtaining the desired result. Notably, to obtain it, it is necessary to conduct a comprehensive study of the automated object, involving the use of the most modern methods of mathematical modelling for qualitative verification of various operating conditions of the projected mechanical vehicles.

The development and industrial production of mechanical wheeled vehicles with low slip coefficient and characterised by increased cross-country ability, operating when placing hydrostatic transmissions on them, will be realistic only if they have no less working efficiency compared to similar models with mechanical-type transmissions, subject to the condition that their operational life will be completely sufficient to recoup all the possible costs associated with the need to equip them with hydrostatic transmissions. Achieving such results will be possible only if such transmissions are equipped with modern adaptive automatic control systems, which will be able to accurately select the mode of operation of the hydrostatic transmission from the entire variety of options offered, which can fully ensure the high efficiency of the entire system [16].

Currently, there is practically no production of mechanical wheeled vehicles with hydrostatic transmissions and all-wheel drive in industrial volumes. Dynamic studies of transmissions of this type were carried out at the highest scientific level, involving the development of complex mathematical models. At the same time, the disadvantage of these models was a weak reflection of the operating conditions of hydrostatic transmissions on mechanical transport vehicles that are in operational use at the moment. As a rule, these mathematical models served to describe the processes occurring directly in such machines themselves [17]. Transmissions of the described nature were mainly created using the power supply scheme of all the hydraulic motors from one common station, which implies the creation of a complete hydraulic differentiated drive for the entire driving wheels. At the same time, there was absolutely no provision for any blocking, both inter-wheel and inter-axle, which could contribute to a significant increase in the number of operational parameters of the vehicle.

The assessment of possible losses in various structural elements of a mechanical wheeled vehicle involves considering the functioning of such elements as a gearbox, transfer case, transmission, gimbal pivot and in this context, application of the recommendation is relevant, according to which the mechanical efficiency of various mechanical elements under different operating modes remains unchanged. This becomes possible only with the rectilinear movement of a mechanical machine with equal parameters for regulating the working surfaces and volumes of hydraulic motors [18]. The development of a system of equations necessary to perform a mathematical description of the operation of the hydrostatic transmission of the drive axle wheels under uniform loads involves the sequential creation of a number of algebraic expressions necessary to determine the parameters of losses in high-pressure pipelines and the values of pressure drops in hydraulic engines. At the same time, to calculate special coefficients characterising the magnitude of losses in hydraulic engines, it is necessary to develop special computer software that allows qualitative calculations of these parameters in a given unit of time [19].

Modern mechanical engineers have until recently experienced considerable difficulties with the design and creation of mechanical wheeled vehicles with low values of wheel slip coefficients of driving axles when making turns [20]. In the last few decades, significant progress has been made in this area, in connection with the development and industrial implementation of a hydrostatic transmission of wheels for driving axles of a number of special and transport vehicles [21]. In recent years, promising results have been achieved in terms of an increase in the maximum operating pressure in hydrostatic systems, which contributes to the overall improvement of the operational and mass-dimensional parameters of various elements included in the transmissions of this type [22]. The operating range of speed control of the hydraulic motor shaft is expanding, which improves operating conditions and allows obtaining an optimal combination of the parameters of the hydraulic motor shaft speed to the lowest possible speed of its rotation under load, which allows increasing the efficiency of the system as a whole [23].

In general, the issues of developing an effective model for calculating the slip coefficients of a mechanical vehicle with two steering axles require further research in connection with the introduction of various technical improvements in the design of both such machines themselves and their suspension and transmission elements, which favourably affect their performance characteristics in general.

5 Conclusions

In the course of studies of the kinematic characteristics of a mechanical wheeled vehicle with two driving axles, a mathematical model of equations was obtained for calculating the coefficients of slipping of such machines. Calculations of the slip coefficients of a mechanical wheeled vehicle are performed directly upon entering the turn. The results obtained indicate that there is a clear relationship between the parameters of the slip coefficients of a mechanical wheeled vehicle and the angles of rotation of the axles directly upon entering the turn, which necessitates considering these characteristics when designing the driving axles of such vehicles. In the event that the value of the slipping coefficient exceeds 0.2, there is no significant difference in the slipping of the wheels of the driving axles, since with an increase in the resistance to movement, conditioned by an increase in the angle of rotation of the axles, the traction forces on the wheels increase significantly, which leads to an increase in their slipping. At the same time, the redistribution of forces gradually aligns, regardless of the difference in normal reactions. This is conditioned by the fact that in this case, the plastic properties are already more characteristic of the soil than the elastic ones.

In general, the findings indicate that there is a clear relationship between changes in values of the wheel slip coefficients of a vehicle and the axles' rotation angles, including a number of other parameters that are important from the standpoint of the prospects for development of effective mechanical wheeled vehicles in the future. The results of this study and the conclusions formulated based on them, can serve as a qualitative scientific basis for subsequent research devoted to investigation of the construction of computational models of the slip coefficients of a mechanical wheeled vehicle with two or more steering axles.

References

[1] DU, H., CAO, D., ZHANG, H. *Modelling, dynamics and control of electrified vehicles*. London: Woodhead Publishing, 2017. ISBN 9780128127865, eISBN 9780128131091.

[2] ARORA, S., ABKENAR, A. T., JAYASINGHE, S., TAMMI, K. *Heavy-duty electric vehicles*. Oxford: Butterworth-Heinemann, 2021. ISBN 9780128181263, eISBN 9780128181270.

[3] SAREVSKI, M. N., SAREVSKI, V. N. *Water (R718) turbo compressor and ejector refrigeration/heat pump technology.* Oxford: Butterworth-Heinemann, 2016. ISBN 9780081007334, eISBN 9780081007341.

[4] CHELIDZE, T., VALLIANATOS, F., TELESCA, L. *Complexity of seismic time series*. Oxford: Elsevier, 2018. ISBN 9780128131381, eISBN 9780128131398.

[5] AHMAD, F., KHALID, M., PANIGRAHI, B. K. Development in energy storage system for electric transportation: a comprehensive review. *Journal of Energy Storage* [online]. 2021, **43**, 103153. ISSN 2352-152X. Available from: https://doi.org/10.1016/j.est.2021.103153

[6] WYPYCH, A. *Databook of antiblocking, release and slip additives*. Toronto: ChemTec Publishing, 2021. ISBN 9781895198836.

[7] GORBAN, V. F., ANDREEV, A. O., STOLBOVYI, V. O., FIRSTOV, S. O., KARPETS, M. V. Influence of the lattice parameter on physical properties of high-entropy coatings. *Scientific Herald of Uzhhorod University. Series "Physics"* [online]. 2021, **49**, p. 61-65. ISSN 2415-8038. Available from: https://doi.org/10.24144/2415-8038.2021.49.61-65

[8] ABE, M. *Vehicle handling dynamics*. Oxford: Butterworth-Heinemann, 2015. ISBN 9780081003909, eISBN 9780081003732.

[9] BALKWILL, J. *Performance vehicle dynamics*. Oxford: Butterworth-Heinemann, 2017. ISBN 9780128126936, eISBN: 9780128126943.

[10] BEKENOV, T. N. *The theory of patency and turnability of self-propelled wheeled machines.* Astana: Publishing house of the L. N. Gumilyov Eurasian National University, 2009.

[11] BEKENOV, T. N., NUSUPBEK, Z. T., TASYBEKOV, Z. T. Determination of the redistribution of slipping coefficients of wheels of self-propelled vehicles when assessing their safety when cornering. In: International Scientific and Practical Conference Innovative Ways to Solve Transport and Energy Problems: proceedings. 2014.

[12] ROHIT, A. K., DEVI, K. P., RANGNEKAR, S. An overview of energy storage and its importance in Indian renewable energy sector: part I - technologies and comparison. *Journal of Energy Storage* [online]. 2017, **13**, p. 10-23. ISSN 2352-152X. Available from: https://doi.org/10.1016/j.est.2017.06.005

[13] JABRI, I., MEKKI, T., RACHEDI, A., JEMAA, M. B. Vehicular fog gateways selection on the internet of vehicles: A fuzzy logic with ant colony optimization-based approach. *Ad Hoc Networks* [online]. 2019, **91**, 101879. ISSN 1570-8705. Available from: https://doi.org/10.1016/j.adhoc.2019.101879

[14] RIZZI, A., LUCKRING, J. M. Historical development and use of CFD for separated flow simulations relevant to military aircraft. *Aerospace Science and Technology* [online]. 2021, **117**, 106940. ISSN 1270-9638. Available from: https://doi.org/10.1016/j.ast.2021.106940

[15] ROY, A. G., PEYADA, N. K. Aircraft parameter estimation using Hybrid Neuro Fuzzy and Artificial Bee Colony optimization (HNFABC) algorithm. *Aerospace Science and Technology* [online]. 2017, **71**, 772-782. ISSN 1270-9638. Available from: https://doi.org/10.1016/j.ast.2017.10.030

[16] CUI, J., LIEW, L. S., SABALIAUSKAITE, G., ZHOU. F. A review on safety failures, security attacks and available countermeasures for autonomous vehicles. *Ad Hoc Networks* [online]. 2019, **90**, 101823. ISSN 1570-8705. Available from: https://doi.org/10.1016/j.adhoc.2018.12.006

[17] MCCREARY, L. A satellite mission concept for high drag environments. *Aerospace Science and Technology* [online]. 2019, **92**, p. 972-989. ISSN 1270-9638. Available from: https://doi.org/10.1016/j.ast.2019.06.033

[18] LEVONI, P., ANGELI, D., CINGI, P., BAROZZI, G. S., CIPOLLONE, M. An integrated approach for the analysis and modelling of road tunnel ventilation. Part I: Continuous measurement of the longitudinal airflow profile. *Transportation Engineering* [online]. 2021, **3**, 100039. ISSN 2666-691X. Available from: https://doi.org/10.1016/j.treng.2020.100039

[19] ZHANG, J., LI, F., ZHANG, H., LI, R., Li, Y. Intrusion detection system using deep learning for in-vehicle security. *Ad Hoc Networks* [online]. 2019, **95**, 101974. ISSN 1570-8705. Available from: https://doi.org/10.1371/journal.pone.0155781

[20] LOUKAS, G., KARAPISTOLI, E., PANAOUSIS, E., SARIGIANNIDIS, P., BEZEMSKIJ, A., VOUNG, T. A taxonomy and survey of cyber-physical intrusion detection approaches for vehicles. *Ad Hoc Networks* [online]. 2019, **84**, p. 124-147. ISSN 1570-8705. Available from: https://doi.org/10.1016/j.adhoc.2018.10.002

[21] NYRKOVA, L. I., LABUR, T. M., OSADCHUK, S. O., YAVORSKA, M. R., KOVAL, V. A. Influence of heat treatment on the properties of welded joints of V1341 alloy under modelled operating conditions. *Paton Welding Journal* [online]. 2021, **2**, p. 18-26. ISSN 0957-798X. Available from: https://doi.org/10.37434/tpwj2021.02.04

[22] MOLODETSKA, T. I. Investigation of the stress-strain state of the bending process of coated materials. *Scientific Herald of Uzhhorod University. Series "Physics"* [online]. 2021, **50**, p. 15-24. ISSN 2415-8038. Available from: https://doi.org/10.24144/2415-8038.2021.50.15-24

[23] GORB, S., LEVINSKYI, M., BUDUROV, M. Sensitivity optimisation of a main marine diesel engine electronic speed governor. *Scientific Horizons* [online]. 2021, **24**(11), p. 9-19. ISSN 2709-8877. Available from: https://doi.org/10.48077/scihor.24(11).2021.9-19

RESEARCH INTO THE LOADING OF THE TANK CAR FRAME CONCEPT WITH FILLER IN THE COMPOSITE CENTER SILL

Oleksij Fomin [1], **Juraj Gerlici** [2], **Alyona Lovska** [3], **Kateryna Kravchenko** [2,*]

[1]State University of Infrastructure and Technology, Kiev, Ukraine
[2]University of Zilina, Zilina, Slovak Republic
[3]Ukrainian State University of Railway Transport, Kharkiv, Ukraine

*E-mail of corresponding author: kateryna.kravchenko@fstroj.uniza.sk

Resume

The study deals with determination of the dynamic loading on the frame of a tank car with closed composite center sill filled with elastic-viscous filler. It has been found that the measures for improvements can decrease the dynamic loading of the frame by 3.5% in comparison to that of the structure without a filler. The strength calculation of the frame of a tank car is also presented. It was found that the maximum equivalent stresses occurred in the contact area between the center sill and the body bolster; they amounted to about 284.7 MPa and did not exceed the allowable values. The computer modelling of the dynamic loading of the tank car frame was also conducted. The numerical values of accelerations and the distribution fields of accelerations in the frame of a tank car were determined. The results of the calculation showed that the hypothesis on the adequacy was not rejected. The natural frequencies and oscillation modes of the tank car frame were also determined.

Available online: https://doi.org/10.26552/com.C.2022.3.B219-B227

Article info

Received 13 January 2022
Accepted 20 April 2022
Online 20 May 2022

Keywords:

tank car
frame
center sill
dynamic loading
strength
modal analysis

ISSN 1335-4205 (print version)
ISSN 2585-7878 (online version)

1 Introduction

Integration of the railway transport into the system of international corridors requires development and putting into operation of new generation rail cars with improved technical and economical characteristics [1-3].

A great amount of freight transported along international corridors is liquids. Traditionally, they are transported in tank cars.

It should be noted that these cars carry considerable loads on the bearing structure due to the yielding state of liquid freight in the tank and due to operational loading of the tank. One of the components to bear these loads is the frame, in particular, the center sill. It bears constant sign-alternating loads. One of the great loads on the center sill is the longitudinal loading. The cyclical longitudinal loading results in failures of the center sill and can lead to crack development. This can be hazardous for both the train operation and environmental safety during the freight transportation.

Therefore, improvements in the bearing structure can decrease the dynamic loading on the frame of a tank car in operation, improve the strength characteristics of the frame and provide the safe rail transportation of liquid freight.

2 Analysis of recent research and publications

Study [1] presents an analysis of the longitudinal displacements of the liquid freight in tank cars and their impact on the stability. The article also presents the experimental results of the research into the oscillations of the liquid freight and outlines further areas of the research in the field.

Study [2] reveals the impact of the yielding state of liquid freight on the dynamic loading of a tank car. It was found that the displacement of the freight had a considerable effect on the load distribution between the front and rear bogies. However, these studies did not provide any solutions for decreasing the loading on a tank car in operation.

The results of determination of the strength for the bearing structure made of composite materials are presented in [3]. It was revealed that the preloading impacted the strength of the bearing structure. The article presents the main failures of the tank made of composite materials.

The structural analysis of the main units of a Zans car is given in [4]. The results of the strength calculation for the bearing structure of a car and the most loaded units of the bearing structure are given, as well.

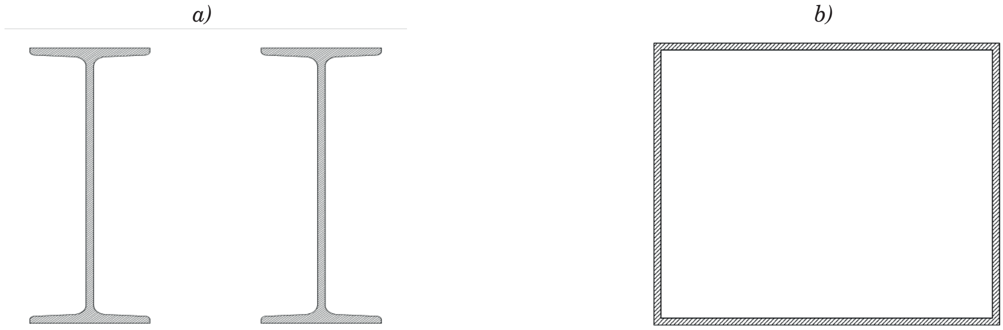

Figure 1 *Section of the center sill of the tank car frame*
a) standard; b) improved

However, this publication does not give any suggestions about improvements in the bearing structure of the tank cars for decreasing the loading.

In [5] authors present determination of the dynamic loading of a tank car moving on the track when the tank is not fully loaded. The effect of the liquid freight displacements on the critical speeds of a tank car was determined.

The experimental determination of the longitudinal loading of a tank for a moving car is given in [6]. The results of experiments were compared to the UIC Standards. Those experiments confirmed the efficiency of structural solutions taken during the designing of a tank car. However, this research does not offer any improvements in the strength characteristics of the tank cars through decreasing their dynamic loading.

Author of [7] presents the results of improvements in the structure of support elements in tank cars for liquid freight. The author developed the finite-element models of tank cars with various structural solutions to the end supports and evaluated the stress state of the support elements.

The ways of how to increase the strength of devices used for fastening the tank to the tank car frame are described in [8]. The authors obtained the dependencies of change in the stresses on the loading of the tank regardless the friction in the end supports. They also gave some recommendations for decreasing the stresses in the areas where the side supports are fastened to the center sill. However, this study does not describe any measures for decreasing the dynamic loading of the bearing structures of tank cars.

Study [9] presents the results of the strength determination for the tank of a tank car during the cyclic loading. The fatigue strength of the tank was evaluated. The impact of cyclic loading on the fatigue strength of the tank was also evaluated.

Similar research into the strength of the tank of a tank car during the cyclic loading is presented in [10]. The research reveals the time characteristics of the main loads and their impact on the fatigue crack development in the tank, which was observed during the technical observation of the tank cars. However, the authors did not propose any solutions for decreasing the effect of cyclical loading on the bearing structures of the tank cars.

The problems of reducing the dynamic loading of the bearing structures of transport facilities in operational modes are described in [11-12]. The results of the research confirmed the efficiency of the engineering solutions suggested.

The analysis of literature [1-12] demonstrates that the issue of improvements in the strength characteristics of the bearing structures of the tank cars, by reducing the loading in operational modes, is rather urgent and requires further investigation.

3 Objective and main tasks of the article

The objective of the article is to present results of determination of the loading on the tank car frame with the closed composite center sill filled with elastic-viscous material. The following tasks were set to achieve the objective:

- mathematical modelling of the dynamic loading on the frame of a tank car with closed composite center sill with elastic-viscous filler;
- strength calculation of the frame of a tank car;
- computer modeling of the dynamic loading on the tank car frame;
- verification of the dynamic loading model of the tank car frame;
- modal analysis of the tank car frame.

4 Research into the loading of the tank car frame concept with filler in the composite center sill

Authors suggest improvements in the frame of a tank car, in particular the application of the closed composite center sill filled with elastic-viscous material to reduce the loading on the tank car frame in operational modes (Figure 1).

Determination of the optimal profile parameters of the center sill was made in accordance with the strength capacity of the standard frame structure. The center sill

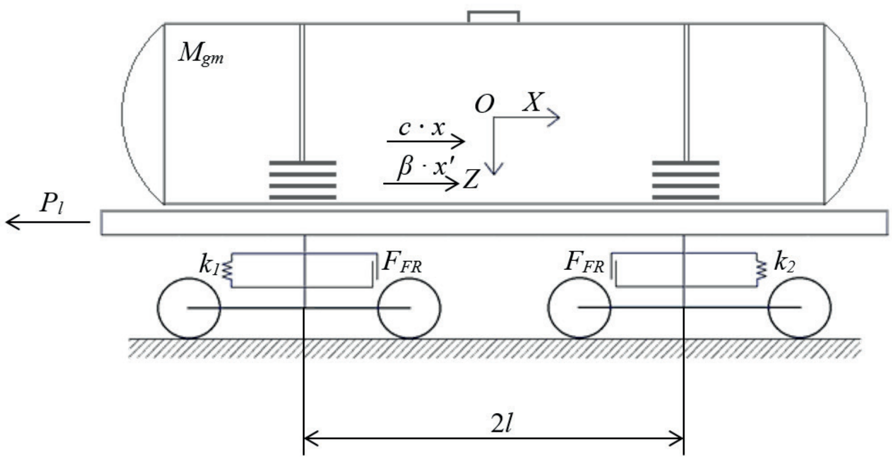

***Figure 2** Design diagram of a tank car*

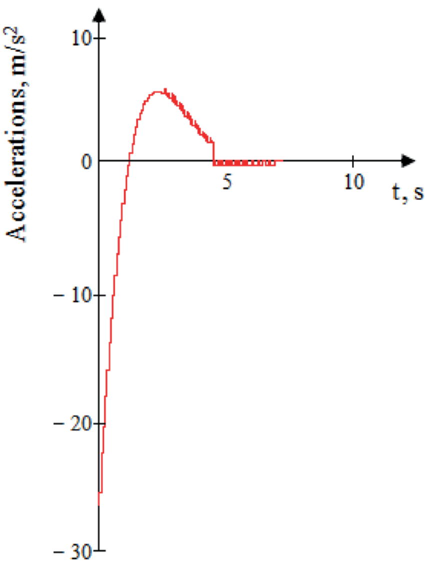

***Figure 3** Accelerations on the bearing structure of a tank car during a jerk*

was made of a composite material. The tare of a tank car was decreased by 2.3% in comparison to that of the standard structure.

The solutions suggested were substantiated through the determination of the dynamic loading of a tank car in the longitudinal plane. Authors used the mathematical model developed by Bogomaz; it describes the dynamic loading on a long-base flat car loaded with four tank containers under the longitudinal force to the rear follower of the coupler [13]. This model was adapted for the research and used for determination of the dynamic loading on a tank car. The design diagram of a tank car is given in Figure 2.

The calculation was made for a jerk. It included the case when the tank car was fully loaded with conditional freight. The restrictions of the mathematical model were zero displacements of the liquid freight in the tank.

$$M_{gm} \cdot \ddot{x} + (M_B \cdot h) \cdot \ddot{\varphi} = P_l - 2P_{fr} - \beta \cdot \dot{x} - c \cdot x, \quad (1)$$

$$I_B \cdot \ddot{\varphi} + (M_B \cdot h) \cdot \ddot{x} - g \cdot \varphi \cdot (M_B \cdot h) = l \cdot F_{FR}(sign\dot{\Delta}_1 - sign\dot{\Delta}_2) + l(k_1 \cdot \Delta_1 - k_2 \cdot \Delta_2), \quad (2)$$

$$M_B \cdot \ddot{z} = k_1 \cdot \Delta_1 + k_2 \cdot \Delta_2 - F_{FR}(sign\dot{\Delta}_1 - sign\dot{\Delta}_2), \quad (3)$$

where

$$\Delta_1 = z - l \cdot \varphi; \; \Delta_2 = z + l \cdot \varphi,$$

M_{gm} - gross mass of a tank car; M_B - mass of the bearing structure of a tank car; I_B - inertia moment of a tank car; P_l - longitudinal force to the front followers of the coupler (P_n = 2.5 MH [14-15]); P_{fr} - friction forces emerging between the center bowls and the body center plates; c - rigidity of the material in the center sill; β - viscous resistance coefficient of the material in the center sill; l - half base of a tank car; F_{FR} - absolute value of the dry friction in a spring group; k_1, k_2 - rigidity of the springs in the spring suspension of the bogies of a tank car; x, φ, z - coordinates describing longitudinal, angular (around the transverse axle) and vertical displacements of a tank car, respectively.

The calculation included the bearing structure of a tank car on the 18-100 bogies. The differential

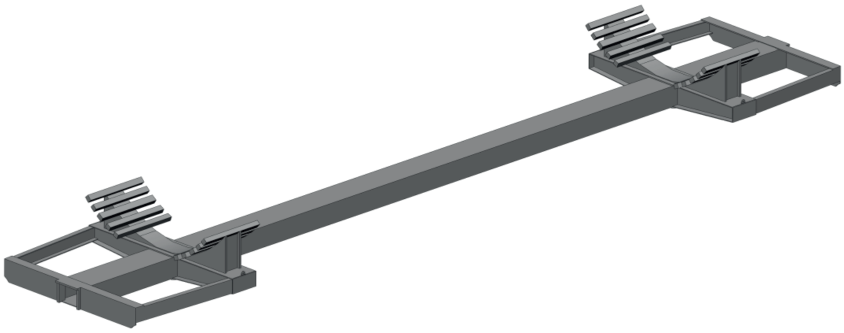

Figure 4 *Spatial model of the tank car frame*

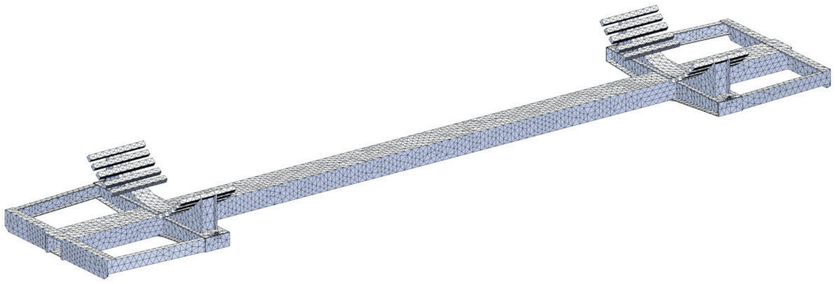

Figure 5 *Finite element model of the tank car frame*

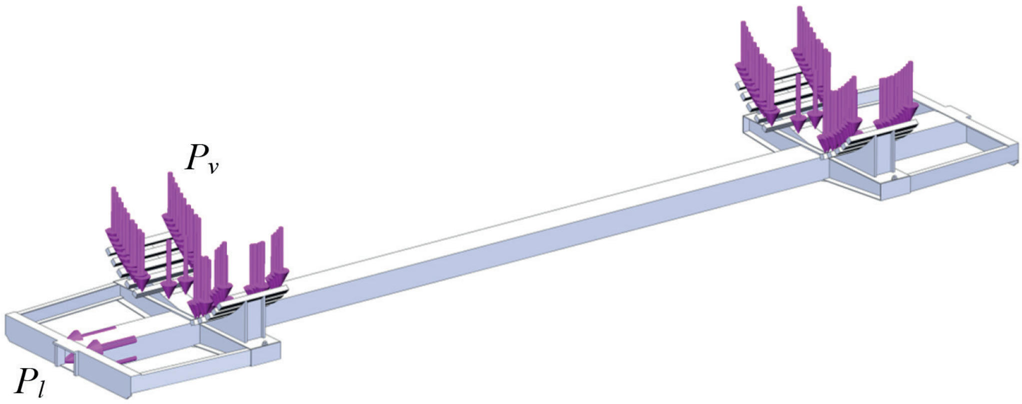

Figure 6 *Design diagram of the tank car frame*

equations of motion were solved with the Runge-Kutta method in MathCad [16-17]. The initial displacements and speeds were taken equal to zero [18-20]. It included a rigidity of the material in the center sill of 82 kN/m and the coefficient of viscous resistance 120 kN·s/m.

The maximum accelerations were 26.4 m/s^2 and occurred at a jerk (Figure 3). After that the acceleration went up and after a gentle jerk it faded. This acceleration value was 3.5 % lower than that obtained for the bearing structure without filler [21].

The accelerations obtained were included in the strength calculation of the frame of a tank car. The calculation was made with the finite element method in SolidWorks Simulation [22-23]. It was based on the spatial model of a tank car (Figure 4).

The finite-element model of the frame was built with isoparametric tetrahedrons [24-26] (Figure 5). The optimal number of the tetrahedrons was calculated by the graphic analytical method [27-28]. The number of the elements in the mesh was 33193 and nodes - 11118. The maximum element size of the mesh was 100 mm, the minimum size - 20 mm, the maximum element side ratio - 109.25; the percentage of elements with the side ratio less than three - 18.1 and more than ten - 25.3. The number of elements in the circle was 9. The element size gain ratio was 1.7.

The design model included the following forces to the frame: vertical static loading in the areas of support of the tank on the frame P_v and longitudinal loading P_l on the front followers of the coupler (Figure 6). The center sill was made of a composite with the titanium matrix reinforced with boron, borsic, silicon carbide, beryllium and molybdenum fabrics. The endurance strength of the composite is: along the fabrics - 1100 -

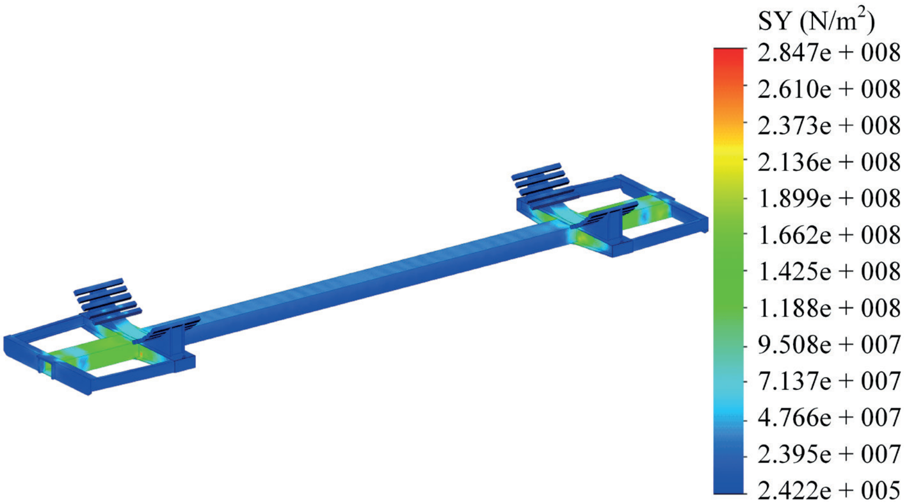

Figure 7 *Stress state of the tank car frame*

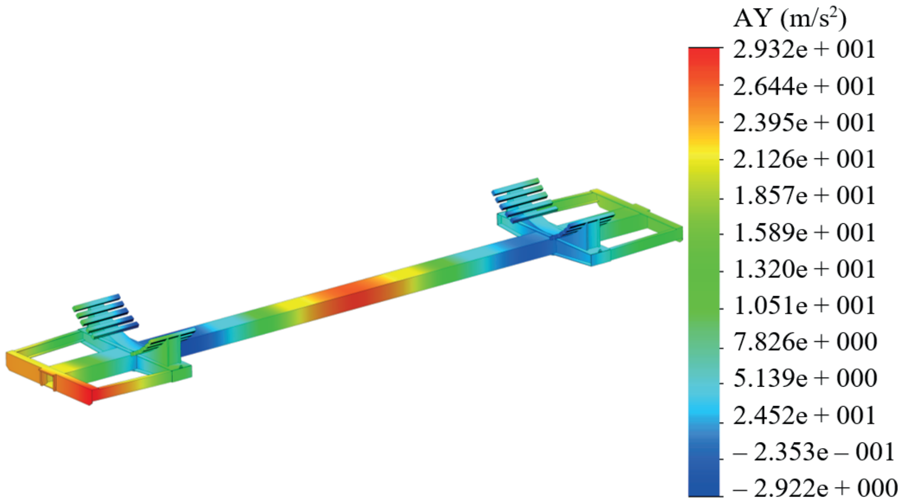

Figure 8 *Accelerations in the tank car frame*

Table 1 *Results of modeling the dynamic loading of the tank car frame*

Longitudinal force, MN	1.8	1.9	2.0	2.1	2.2	2.3	2.4	2.5
Mathematical model	20.1	20.9	21.8	22.7	23.8	24.7	25.6	26.4
Computer model	22.6	23.5	24.3	25.5	26.7	27.5	28.4	29.3

1300 MPa, across the fabrics - 650 MPa. The fixing of the model was carried out in the areas of support on the chassis [29-30].

The elastic viscous material in the frame was modeled through linkages with similar characteristics by choosing appropriate options in the SolidWorks Simulation.

Results of the calculation are presented in Figure 7.

The maximum equivalent stresses were recorded in the contact area between the center sill and the body bolster; they amounted to about 284.7 MPa. These stresses did not exceed the allowable values [14-15, 31].

The distribution fields of accelerations in the tank car frame were determined in accordance with the design diagram given in Figure 6. Results of the calculation are given in Figure 8. The maximum accelerations were recorded in the middle part of the center sill; they amounted to 29.3 m/s^2. In the end parts of the frame the accelerations were about 26 m/s^2. The lowest value of accelerations was recorded in the areas of support of the tank on the frame. It is explained by the securing of the model by the body center plates [32-33].

The mathematical model in Equations (1) - (3) was verified with an F-test [34-35]. The variation parameter was the longitudinal force on the front followers of the coupler. As a result of the calculations, the acceleration acting on the car frame was obtained. The calculation of accelerations was carried out using the mathematical model in Equations (1) - (3) and the computer model is shown in Figure 6. Results of the calculation are given in Table 1. The needed number of static data was found with a Student's t-test.

Results of the calculation demonstrated that at the error mean square S_{sq} = 5.1 and the dispersion of

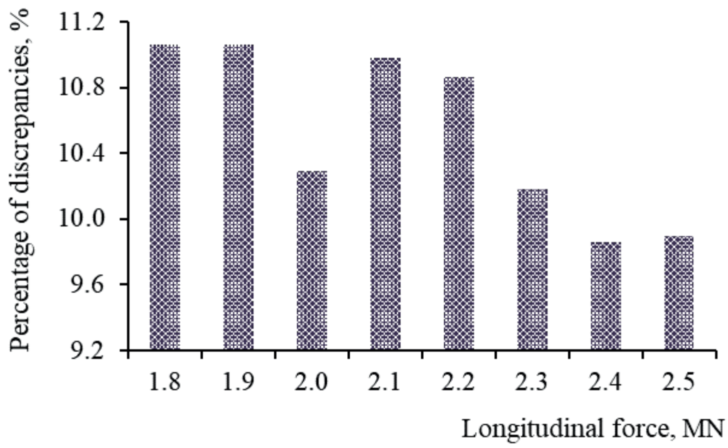

Figure 9 Difference between the results of the mathematical and computer modeling

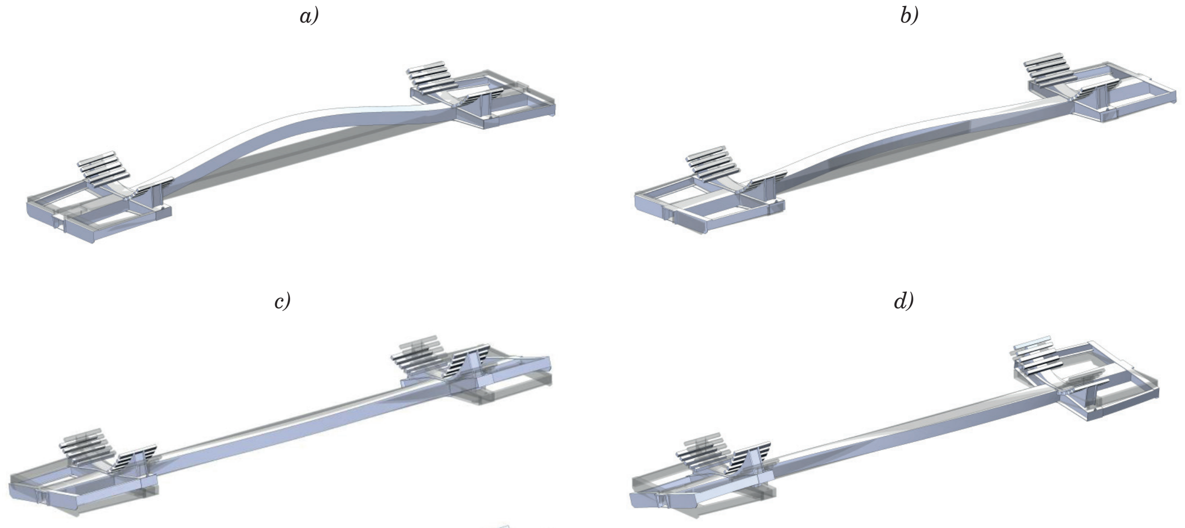

Figure 10 *Some oscillation modes of the tank car frame (scale of deformations 15:1)*
a) Mode 1; b) Mode 2; c) Mode 3; d) Mode 4

Table 2 *Values of the natural oscillation frequencies of the tank car frame*

Mode	Frequency, *Hz*	Mode	Frequency, *Hz*
1	28.0	6	54.1
2	38.9	7	64.4
3	45.1	8	67.0
4	46.3	9	81.9
5	49.2	10	97.9

adequacy S_{ad}^2 = 5.76, the actual value of an F-test was F_a = 1.13, which is lower than the tabular criterion value F_t = 3.07. Thus, the hypothesis on adequacy of the model designed was not rejected.

The difference between the results of the mathematical and computer modeling of the dynamic loading of the frame of a tank car is presented in Figure 9.

The maximum value of this difference was 11.0%; at the longitudinal force on the frame of a tank car it amounted to 1.8 MN and 1.9 MN and the lowest value was about 9.8%, at 2.4 MN.

Besides that, the design diagram of a tank car (Figure 6) was used for determination of the natural frequencies and oscillation modes of the tank car frame.

Some oscillation modes of the tank car frame are given in Figure 10. Transparent color in Figure 10 indicates the stationary position of the frame and matte - the form of vibrations, taking into account the enlarged scale. In this case, each mode shown in Figure 10 corresponds to the numerical value of the frequency indicated in Table 2.

From the results given in Table 2 it can be concluded that the natural frequencies were in a range of the allowable values, as the first frequency exceeded 8 Hz [14-15].

5 Conclusions

1. Authors conducted the mathematic modeling of the dynamic loading of a frame of the tank car with the closed composite center sill filled with elastic-viscous material. It was found that the maximum accelerations were 26.4 m/s^2 and occurred at a jerk. The acceleration value was 3.5% lower than that obtained for the bearing structure without filler.
2. The research included the strength calculation of the frame of a tank car. The maximum equivalent stresses were recorded in the contact area between the center sill and the body bolster; they amounted to about 284.7 MPa. The stresses obtained did not exceed the allowable values.
3. The research also included the computer modelling of the dynamic loading of the frame of a tank car. The maximum accelerations were recorded in the middle part of the center sill and amounted to 29.3 m/s^2. In the end parts of the frame the accelerations were about 26 m/s^2. The lowest accelerations were recorded in the areas of support of the tank on the frame.
4. The designed model of the dynamic loading of the tank car frame was verified. It was found that at the error mean square S_{sq}=5.1 and the dispersion of adequacy S_{ad}^2 = 5.76, the actual value of an F-test was F_a=1.13, which is lower than the tabular criterion value F_t =3 .07. Thus, the hypothesis on adequacy of the model designed was not rejected.
5. The modal analysis was performed for the frame of a tank car. The natural oscillations frequencies of the frame of a tank car were in the range of allowable values. The first natural oscillation frequency exceeded 8 Hz.

The research conducted can be used by those concerned about the development of innovative freight car structures and enhanced efficiency of the railway transport.

References

[1] DIZO, J., HARUSINEC, J., BLATNICKY, M. Computation of modal properties of two types of freight wagon bogie frames using the finite element method. *Manufacturing Technology* [online]. 2018, **18**(2), p. 208-214. ISSN 1213-2489. Available from: https://doi.org/10.21062/ujep/79.2018/a/1213-2489/MT/18/2/208

[2] STASTNIAK, P., MORAVCIK, M., SMETANKA, L., BARAN, P. Strength investigation of main frame in new track friendly railway bogie. *Manufacturing Technology* [online]. 2018, **18**(2), p. 315-320. ISSN 1213-2489. Available from: https://doi.org/10.21062/ujep/98.2018/a/1213-2489/MT/18/2/315

[3] DIZO, J., HARUSINEC, J., BLATNICKY, M. Structural analysis of a modified freight wagon bogie frame. *MATEC Web of Conferences* [online]. 2017, **134**, 00010. ISSN 2261-236X. Available from: https://doi.org/10.1051/matecconf/201713400010

[4] YOUSEFI, S., TAHERI, M. N., SHAHRAVI, M. Analysis of longitudinal fluid sloshing in tank wagon. *International Journal of Heavy Vehicle Systems* [online]. 2019, **26**(2), p. 225-238. ISSN 1744-232X. Available from: https://doi.org/10.1504/IJHVS.2019.098280

[2] SHI, H., WANG, L., NICOLSEN, B., SHABANA, A. A. Integration of geometry and analysis for the study of liquid sloshing in railroad vehicle dynamics. *Proceedings of the Institution of Mechanical Engineers, Part K: Journal of Multi-body Dynamics* [online]. 2017, **231**, p. 608-629. ISSN 1464-4193. Available from: https://doi.org/10.1177/1464419317696418

[3] STREET, G. E., MISTRY, P. J., JOHNSON, M. S. Impact resistance of fibre reinforced composite railway freight tank wagons. *Journal of Composites Science* [online]. 2021, **5**(6), 152. ISSN 2504-477X. Available from: https://doi.org/10.3390/jcs5060152

[4] STASTNIAK, P., SMETANKA, L., MORAVCIK, M. Structural analysis of a main construction assemblies of the new wagon prototype type zans. *Manufacturing technology* [online]. 2018, **18**(3), p. 510-517. ISSN 1213-2489. Available from: https://doi.org/10.21062/ujep/130.2018/a/1213-2489/MT/18/3/510

[5] RAHMATI-ALAEI, A., SHARAVI, M., SAMADIAN ZAKARIA, M. Hunting stability analysis of partially filled tank wagon on curved track using coupled CFD-MBD method. *Multibody System Dynamics* [online]. 2020, **50**, p. 45-69. ISSN 1384-5640. Available from: https://doi.org/10.1007/s11044-019-09715-y

[6] KUBA, E., MORAVCIK, M., PAVELCIK, V. Experimental verification of tank wagon's ability to transmit longitudinal forces in opposite track curves. *Transportation Research Procedia* [online]. 2021, **55**, p. 774-781. ISSN 2352-1457. Available from: https://doi.org/10.1016/j.trpro.2021.07.045

[7] PAVLYUCHENKOV, M. V. Structure rationalization of tank cars support devices for fluids (in Ukrainian). *Science and Transport Progress Bulletin of Dnipropetrovsk National University of Railway Transport* [online]. 2014, **1**(49), p. 151-159. ISSN 2307-3489. Available from: https://doi.org/10.15802/stp2014/22681

[8] SENKO, V. I., SHIMANOVSKIJ, A. O., PUTYATO, A. V. Investigation of ways to increase the strength of

the parts of fastening the boiler to the frame of the railway tank car (in Russian). *Bulletin of Brest State Technical University* [online]. 2004, **4**, p. 54 - 57. eISSN 2706-5812. Available from: https://rep.bstu.by/handle/data/12269

[9] BOYKO, A., KONONOVA, O. Strength calculation for a tank of the tank-car under repeated loading (in Russian). In: XIII International Colloquium Mechanical Fatigue of Metals: proceedings [online]. 2006. ISBN 966-305-027-6, p. 484-490. Available from: http://elartu.tntu.edu.ua/handle/123456789/16833

[10] ZARIPOV, R. Y., VASILEVSKY, V. P. Strength calculation for a tankof the tank-car under repeated loading (in Russian). *The Bulletin of Kazakh Academy of Transport and Communications named after M. Tynyshpaev* [online]. 2017, **1**(100), p. 53-59. ISSN 1609-1817. Available from: https://docplayer.com/58604073-K'azkka-habarshysy-1-100-2017-issn-the-bulletin-of-kazatc-vestnik-kazatk-1-100-vol-100-no.html

[11] LOVSKA, A., FOMIN, O., PISTEK, V., KUCERA, P. Dynamic load and strength determination of carrying structure of wagons transported by ferries. *Journal of Marine Science and Engineering* [online]. 2020, **8**, 902. ISSN 2077-1312. Available from: https://doi.org/10.3390/jmse8110902

[12] LOVSKA, A., FOMIN, O., PISTEK, V., KUCERA, P. Calculation of loads on carrying structures of articulated circular-tube wagons equipped with new draft gear concepts. *Applied Sciences* [online]. 2020, **10,** 7441. ISSN 2076-3417. Available from: https://doi.org/10.3390/app10217441

[13] BOGOMAZ, G. I., MEKHOV, D. D., PILIPCHENKO, O. P., CHERNOMASHENTSEVA, Y. G. Loading of tank containers located on a railway flat wagon when impact into an automatic coupler (in Russian). *Dynamics and Motion Control of Mechanical Systems*. 1992, **1**, p. 87-95.

[14] DSTU 7598:2014. Freight wagons. General requirements for calculations and design of new and modernized wagons of 1520 mm track (non-self-propelled). Kiev: UkrNDNTS:, 2015.

[15] GOST 33211-2014. Freight wagons. Requirements for strength and dynamic properties. Moscow: FGUP "Standartinform": 2016.

[16] KIRYANOV, D. V. *Mathcad 13* (in Russian). Saint Petersburg: BHV Petersburg, 2006. ISBN 5-94157-850-4.

[17] DYAKONOV, V. *Mathcad 8/2000: a special reference book* (in Russian). Saint Petersburg: Piter, 2000. ISBN 5-272-00069-2.

[18] TURPAK, S. M., TARAN, I. O., FOMIN, O. V., TRETIAK, O. O. Logistic technology to deliver raw material for metallurgical production. *Scientific Bulletin of National Mining University* [online]. 2018, **1**, p. 162-169. ISSN 2071-2227. Available fromhttps://doi.org/10.29202/nvngu/2018-1/3

[19] KALANTAIEVSKA, S., PIEVTSOV, H., KUVSHYNOV, O., SHYSHATSKYI, A., YAROSH, S., GATSENKO, S., ZUBRYTSKYI, H., ZHYVOTOVSKYI, R., PETRUK S., ZUIKO, V. Method of integral estimation of channel state in the multiantenna radio communication systems. *Eastern-European Journal of Enterprise Technologies* [online]. 2018, **5/9**(95), p. 60-76. ISSN 1729-3774 Available from: https://doi.org/10.15587/1729-4061.2018.144085

[20] KUCHUK, N., MOHAMMED, A. S., SHYSHATSKYI, A., NALAPKO, O. The method of improving the efficiency of routes selection in networks of connection with the possibility of self-organization. *International Journal of Advanced Trends in Computer Science and Engineering* [online]. 2019, **8**(1), p. 1-6. ISSN 2278-3091. Available from: https://doi.org/10.30534/ijatcse/2019/0181.22019

[21] FOMIN, O., GERLICI, J., GORBUNOV, M., VATULIA, G., LOVSKA, A., KRAVCHENKO, K. Research into the strength of an open wagon with double sidewalls filled with aluminium foam. *Materials* [online]. 2021, **14**(12), 3420. eISSN 1996-1944. Available from: https://doi.org/10.3390/ma14123420

[22] LOVSKA, A. O. Computer simulation of wagon body bearing structure dynamics during transportation by train ferry. *Eastern-European Journal of Enterprise Technologies* [online]. 2015, **3/7**(75), p. 9-14. ISSN 1729-3774. Available from: https://doi.org/10.15587/1729-4061.2015.43749

[23] LOVSKA, A. A. Peculiarities of computer modeling of strength of body bearing construction of gondola car during transportation by ferry-bridge. *Metallurgical and Mining Industry*. 2015, **1**, p. 49-54. ISSN 2076-0507.

[24] FOMIN, O. Modern requirements to carrying systems of railway general-purpose gondola cars. *Metallurgical and Mining Industry*. 2014, **5**, p. 31-43. ISSN 2076-0507.

[25] LOVSKA, A., FOMIN, O., PISTEK, P., KUCERA, P. Dynamic load modelling within combined transport trains during transportation on a railway ferry. *Applied Sciences* [online]. 2020, **10**(16), 5710. eISSN 2076-3417. Available from: https://doi.org/10.3390/app10165710

[26] FOMIN, O., LOVSKA, A. Determination of dynamic loading of bearing structures of freight wagons with actual dimensions. *Eastern-European Journal of Enterprise Technologies* [online]. 2021, **2/7** (110), p. 6-15. ISSN 1729-3774. Available from: https://doi.org/10.15587/1729-4061.2021.220534

[27] VATULIA, G. L., PETRENKO, D. H., NOVIKOVA, M. A. Experimental estimation of load-carrying capacity of circular, square and rectangular CFTS columns. Scientific Bulletin of the National Mining University. 2017, **6**. p. 97- 02. ISSN 2071-2227.

[28] VATULIA, G., KOMAGOROVA, S., PAVLIUCHENKOV, M. Optimization of the truss beam. Verification of the calculation results. *MATEC Web of Conferences* [online]. 2018, **230**, 02037. ISSN 2261-236X. Available from: https://doi.org/10.1051/matecconf/201823002037

[29] FOMIN, O. V., LOVSKA, A. O., PLAKHTII, O. A., NERUBATSKYI, V. P. The influence of implementation of circular pipes in load-bearing structures of bodies of freight cars on their physico-mechanical properties. *Scientific Bulletin of National Mining University*. 2017, **6**, p. 89-96. ISSN 2071-2227.

[30] LOVSKAYA, A., RYIBIN, A. The study of dynamic load on a wagon-platform at a shunting collision. *Eastern-European Journal of Enterprise Technologies* [online]. 2016, **3**, p. 4-8. ISSN 1729-3774. Available from: https://doi.org/10.15587/1729-4061.2016.72054

[31] EN 12663-2. Railway applications - structural requirements of railway vehicle bodies. Part 2: Freight wagons. Bulgaria, 2010.

[32] FOMIN, O. V., BURLUTSKY, O. V., FOMINA, Y. V. Development and application of cataloging in structural design of freight car building. *Metallurgical and Mining Industry* [online]. 2015, **2**, p. 250-256. ISSN 2076-0507.

[33] LOVSKA, A. Simulation of loads on the carrying structure of an articulated flat car in combined transportation. *International Journal of Engineering and Technology (UAE)* [online]. 2018, **7**(4.3), p. 140-146. ISSN 2227-524X. Available from: https://doi.org/10.14419/ijet.v7i4.3.19724

[34] PISTEK, V., KUCERA, P., FOMIN, O., LOVSKA, A. Effective mistuning identification method of integrated bladed discs of marine engine turbochargers. *Journal of Marine Science and Engineering* [online]. 2020, **8**, 379. eISSN 2077-1312. Available from: https://doi.org 10.3390/jmse8050379

[35] BYCHKOV, A. S., KONDRATIEV, A. V. Criterion-based assessment of performance improvement for aircraft structural parts with thermal spray coatings. *Journal of Superhard Materials* [online]. 2019, **41**(1), p. 53-59. ISSN 1063-4576. Available from: https://doi.org/10.3103/S1063457619010088

PREDICTION OF THE ULTRA-LARGE CONTAINER SHIPS' PROPULSION POWER AT THE INITIAL DESIGN STAGE

Piotr Kamil Korlak

Doctoral School of the Maritime University of Szczecin, Szczecin, Poland

*E-mail of corresponding author: 27901@s.am.szczecin.pl

Resume

Container ships represent the fastest growing segment of maritime transport. The need to reduce unit transportation costs and environmental impact has led to development of the most capacious ultra-large container ships operating on the world's major shipping routes. A representative database of ultra-large container ships was created and further subdivided according to the main technical parameters. Using a simple cubic regression model, based on the least squares method, an equation, compliant to the general propeller law, was developed to predict the propulsion power of ultra-large container ships as a function of their sailing speed. The results obtained using the developed equation should be sufficiently close to the results of the exact verification calculations at the technical design stage. Then this prediction would find application in the design of both main propulsion, as well as waste heat and cold recovery systems.

Article info

Received 24 January 2022
Accepted 23 April 2022
Online 23 May 2022

Keywords:

container ship
ULCS
ULCV
ship design
ship propulsion
low-speed engine
two-stroke engine

Available online: https://doi.org/10.26552/com.C.2022.3.B228-B238

ISSN 1335-4205 (print version)
ISSN 2585-7878 (online version)

1 Introduction

Maritime transport currently handles around 80 % of the volume of global trade in goods. Its fastest-growing component is container transport. The weight of cargo transported by containers between 1990 and 2019 recorded a massive nine-fold increase, shown in Figure 1 [1]. The popularity of contenerization results from easier distribution and shorter loading time of cargo on board ships, the protection against external factors and, most importantly, the possibility of transporting further without having to reload the goods in the container - known as intermodal transport [2].

The enormous progress in ship technology has helped to increase the dimensions and performance of container ships. In the period 1968-2021, the loading capacity of the largest container ship increased from 1,530 to 23,992 TEU (Twenty-foot Equivalent Unit), i.e. by a massive 1,468 % (Figure 2). This development continues unabated. In the next few years, new records are expected to be broken and previously unattainable limits of capacity to be exceeded.

The economic benefits of operating ever-larger ships on the world's major shipping routes (East Asia - Northern Europe and East Asia - Northern America) has led to creation of ultra-large container ships (ULCS) of unprecedented size. The ultra-large generation appeared in 2006 with the Emma Maersk, the first container ship with an overall hull length of nearly 400 metres and a cargo capacity of 14,770 TEU [4].

Initially, this generation included all container ships with a cargo capacity of at least 14,501 TEU. However, this criterion has become obsolete with the more effective use of hull space and the location of more and more containers within the same area. The first container ships with dimensions corresponding to the slightly smaller very-large type and with a larger capacity than Emma Maersk were the UASC A15-class (15,000 TEU, delivery year 2014, length overall 368 m, beam 51 m). The largest very-large ones are currently the HMM Nuri-class (16,010 TEU, delivery year 2021, length overall 366 m, beam 51 m). Therefore, when comparing the parameters of all the ultra-large container ships in service, it can be conventionally assumed that their unique feature is a length overall of more than 390 metres. The parameters of the most capacious very- and ultra-large container ships are presented in Table 1 [3].

Despite the constantly growing demand for ultra-large container ships, the literature still does not include methods whereby the propulsion power may be approximately predicted. Available methods of predicting propulsion power are limited to the main engine rated power only and do not take into account the

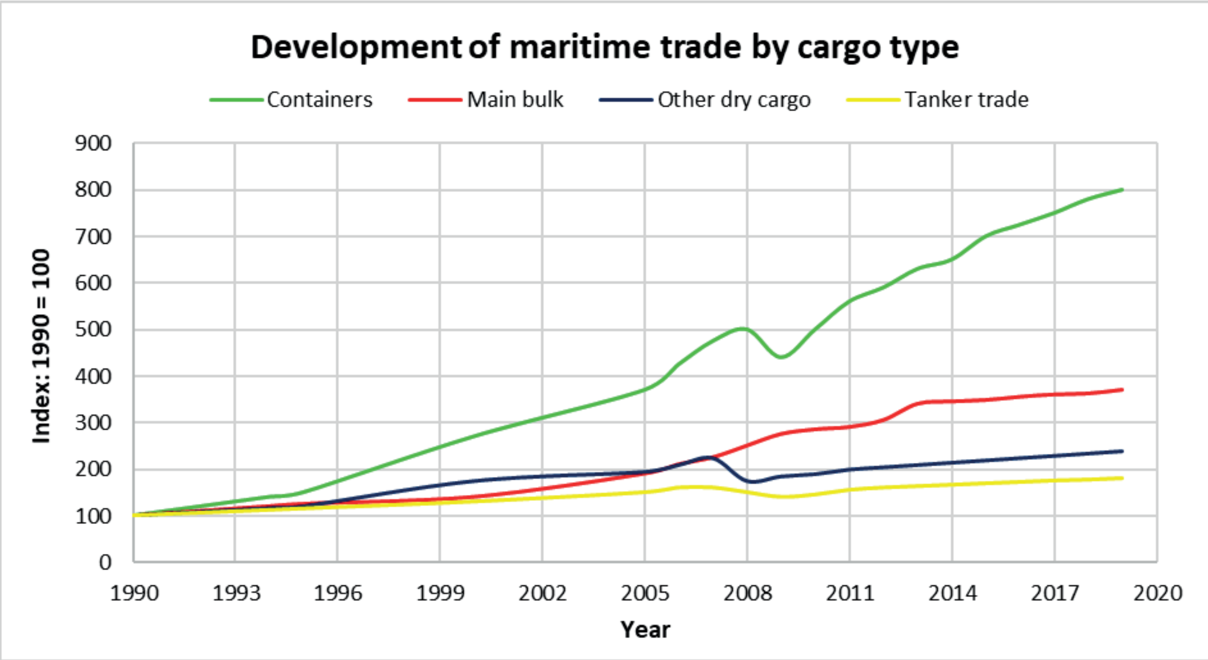

Figure 1 *Development of international maritime trade by cargo type [1]*

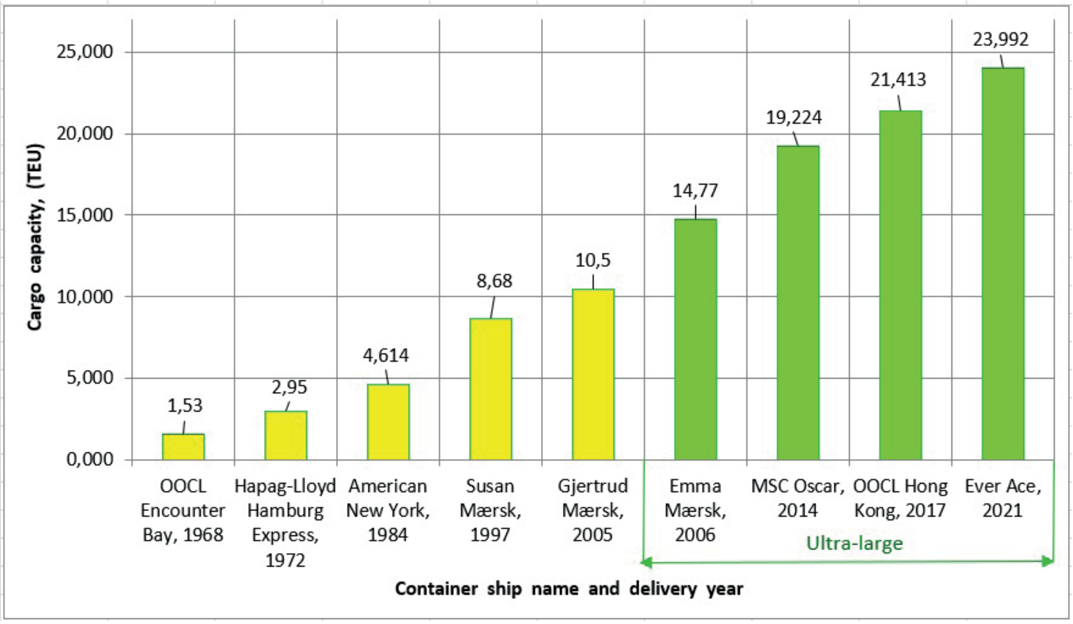

Figure 2 *Increase of the container ships' cargo capacity [3-4]*

Table 1 *The most capacious container ships [3, 5]*

Type	Delivery year	Name	Cargo capacity, (TEU)	Reefer plugs	Length overall, (m)	Beam, (m)	Draft, (m)
Very-large	2021	HMM Nuri	16,010	1,200	366	51	16
Ultra-large	2021	Ever Ace	23,992	2,200	399.9	61.5	16.5

latest ultra-large container ships over 20,000 TEU [6]. It is therefore not feasible on their basis to predict the propulsion power required for any sailing speed, which is particularly important for, among others, calculations of waste heat and cold recovery, whose amount is growing with increasing of the propulsion power [7-8].

At the initial design stage, it is impossible to precisely determine the required propulsion power due to the lack of model tests results [9]. At the same time, decisions made at this stage of a project have a fundamental impact on its total cost and duration. Each mistakenly selected parameter requires adjustments at

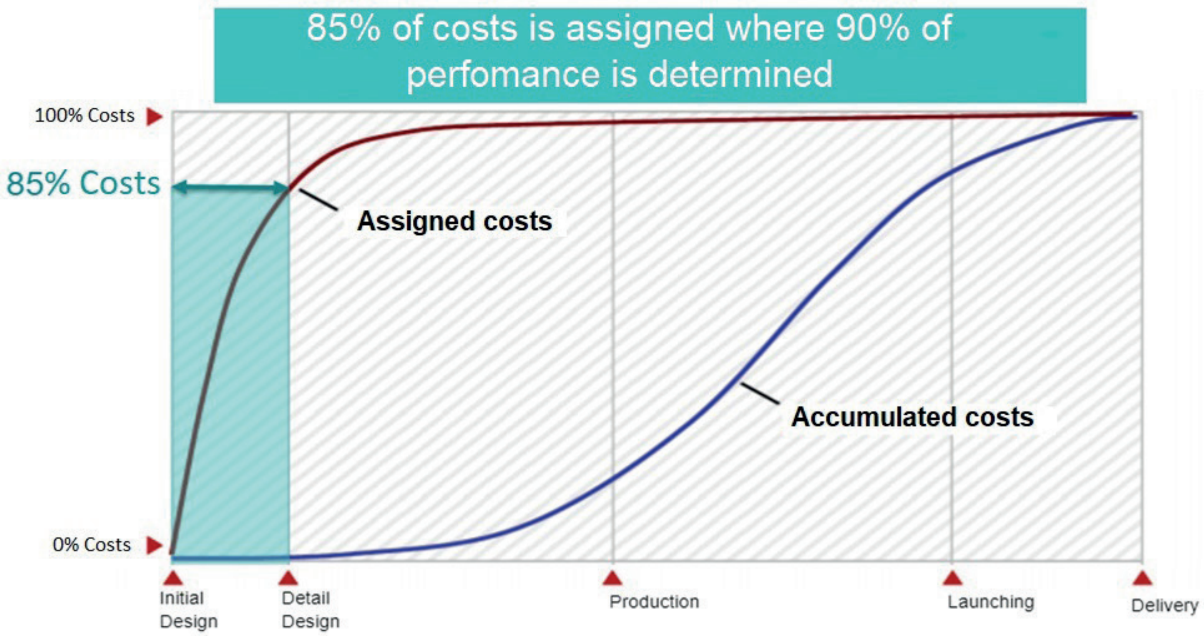

Figure 3 *Stages of the shipbuilding process [11]*

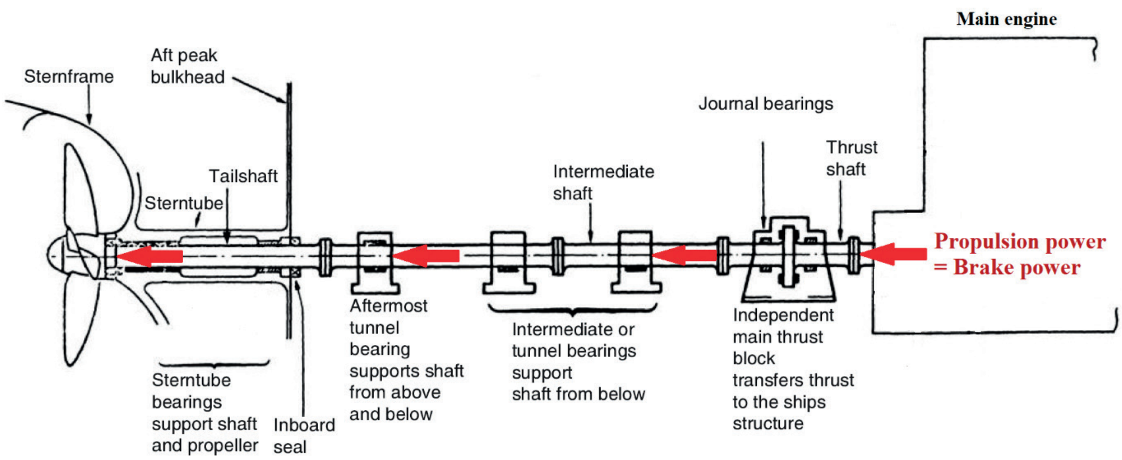

Figure 4 *Conventional direct-drive container ship main propulsion system [13]*

the technical or working design stage, which results in additional work, a significant increase in total costs and a significant delay in delivery. This means that design offices and shipyards cannot afford to have significant errors in the initial design of a given ship [10]. Stages of the shipbuilding process are shown in Figure 3.

Therefore, it was necessary to develop a method for predicting the propulsion power in a quick and simple manner with sufficient accuracy. Methods based on statistical modelling for a specific type of container ship, its cargo capacity, its age and the configuration of its main propulsion system can be an effective tool for predicting the propulsion power of a given ship.

The aim of this paper is to determine the empirical mathematical relationship based on a simple cubic regression model and obtained by comparing the real parameters of actual ultra-large container ships no older than the average age of all the container ships in service - i.e. 13 years [1]. This guarantees both a representative research sample and a focus on configurations of the main propulsion system still in use.

2 Database of the ultra-large container ships

A ship's propulsion power, required for sailing at any service speed, at the initial design stage can be predicted by comparing the actual parameters of ships in operation. For this purpose, a list of selected real parameters was prepared in the form of a database including 20 different classes of the ultra-large container ships, represented by 142 ships, not older than the average 13-year lifetime [1].

The parameters of the ships in service were obtained from the registers of classification societies [12].

This database does not include ships with unconventional main propulsion system configurations - i.e. Maersk Triple-E-class equipped with a pair of main

Table 2 *Representative database of the LNG-fueled ultra-large container ships [14]*

Ship class	CMA CGM Jacques Saade
P_{Bs}, (kW)	57,456
v_s, (kn)	22.00
v_s, (km/h)	40.74
Engine type	WinGD 12X92-DF
	LNG-fueled
P_{Bmax}, (kW)	63,840
P_{Bs}/P_{Bmax}, (%)	90
L_{OA}, (m)	399.9
L_{PP}, (m)	383
Cargo capacity, (TEU)	23,112
Quantity	9
Delivery year	2020

where:

L_{OA} - Length overall, (m),

L_{PP} - Length between perpendiculars, (m),

v_s - Service speed, (kn) or (km/h),

P_{Bs} - Service propulsion power, (kW),

P_{Bmax} - Main engine rated power, (kW).

Table 3 *Representative database of the LNG-ready ultra-large container ships [15-16]*

Ship class	HMM Algeciras	HMM Oslo	MSC Gulsun	MSC Mina
P_{Bs}, (kW)	60,380	59,360	66,650	66,220
v_s, (kn)	22.40	22.25	23.20	23.25
v_s, (km/h)	41.49	41.21	42.97	43.06
Engine type	MAN 11G95ME-C			
	LNG-ready			
P_{Bmax}, (kW)	75,570			
P_{Bs}/P_{Bmax}, (%)	79.90	78.55	88.20	87.63
L_{OA}, (m)	399.9	399.9	399.9	399.9
L_{PP}, (m)	383	383	383	383
Cargo capacity, (TEU)	23,964	23,820	23,756	23,656
Quantity	7	5	6	10
Delivery year	2020	2020	2019	2019

Ship class	COSCO Shipping Universe	COSCO Constellation	UASC A18
P_{Bs}, (kW)	57,900	54,960	41,800
v_s, (kn)	22.00	21.80	19.90
v_s, (km/h)	40.74	40.37	36.86
Engine type	MAN 12S90ME-C	MAN 11S90ME-C	MAN 10S90ME-C
	LNG-ready		
P_{Bmax}, (kW)	69,720	63,910	58,100
P_{Bs}/P_{Bmax}, (%)	83.05	86	71.94
L_{OA}, (m)	399.9	399.7	399.9
L_{PP}, (m)	386	382	385.4
Cargo capacity, (TEU)	21,237	20,119	18,800
Quantity	6	11	6
Delivery year	2018	2017	2015

Table 4 Representative database of the HFO/MGO-fueled ultra-large container ships [5, 12, 14, 16-17]

Ship class	Ever Ace	OOCL G	CMA CGM Antoine de Saint-Exupery	MOL Triumph	Ever Golden	MSC Olympic
P_{Bs}, (kW)	58,600	61,530	59,370	59,160	59,300	56,250
v_s, (kn)	22.20	22.50	22.25	22.20	22.50	21.90
v_s, (km/h)	41.11	41.67	41.21	41.11	41.67	40.56
Engine type	WinGD 11X92	MAN 11G95ME-C	WinGD 11X92	MAN 11G95ME-C		MAN 11S90ME-C
	HFO/MGO-fueled					
P_{Bmax}, (kW)	70,950	75,570	70,950	75,570		63,910
P_{Bs}/P_{Bmax}, (%)	83.01	81.42	83.68	78.29	78.47	88
L_{OA}, (m)	399.9	399.9	399.9	399.9	399.9	395.5
L_{PP}, (m)	393	383	383	383.6	387	379.4
Cargo capacity, (TEU)	23,992	21,413	20,954	20,170	20,160	19,437
Quantity	14	6	3	6	11	6
Delivery year	2021	2017	2017	2017	2017	2016

Ship class	MSC Pegasus	CSCL Globe	CMA CGM Zheng He	CMA CGM Kerguelen	APL Temasek	CMA CGM Marco Polo
P_{Bs}, (kW)	61,530	56,800	54,936	53,960	36,900	63,910
v_s, (kn)	22.65	22.00	21.75	21.60	19.00	23.15
v_s, (km/h)	41.95	40.74	40.28	40.00	35.19	42.87
Engine type	MAN 11G95ME-C	MAN 12S90ME-C	MAN 11S90ME-C			Wartsila 14RT-flex96C
	HFO/MGO-fueled					
P_{Bmax}, (kW)	75,570	69,720	63,910			80,080
P_{Bs}/P_{Bmax}, (%)	81.42	75.16	85.96	84.43	57.73	79.81
L_{OA}, (m)	399.9	399.7	399.2	398	397.9	396
L_{PP}, (m)	383	383	381.4	380	380.1	378.4
Cargo capacity, (TEU)	19,437	19,100	17,859	17,722	17,292	16,020
Quantity	14	5	3	3	8	3
Delivery year	2016	2014	2015	2015	2017 (lengthened)	2012

engines driving two fixed pitch propellers within twin-skeg hull [12]. It includes single-skeg ships with fixed pitch propeller directly-driven by diesel or dual-fuel low-speed main engine (Figure 4).

The created database includes LNG-fueled (Table 2), LNG-ready (Table 3), HFO/MGO-fueled ultra-large container ships' classes (Table 4). It should also be noted that the classes are groups of sister ships. For example, the CMA CGM Jacques Saade class includes 9 ships built to the same design with exactly the same technical parameters. An explanation of LNG-ready term can be found further below Figure 11.

Figure 6 indicates that more than 35 % of the created database consists of ships with a cargo capacity of 23,000 TEU or more, all of which were built in the last three years. Ships of this size are also in the current order books for the coming years as the only ultra-large type. The smallest of these (below 18,000 TEU) are no longer being built due to the steady increase in capacity of the next generation of very-large container ships with an overall length of up to 370 m, which has now already reached 16,010 TEU (HMM Nuri, overall length 366 m, width 51 m, 16,010 TEU). The construction of medium-sized ultra-large container ships of the order of 18,000 ÷ 22,000 TEU is also not continuing due to insufficient compensation for increased investment costs.

As shown in figure 7, ships with a length between perpendiculars equal to 383 m, most often associated with an overall hull length of more than 399 m, constitute 46 % of the created database.

Ships with a service speed of at least 22 knots constitute 74 % of the created database as presented in Figure 8. This group also includes all ships with a capacity of at least 23,000 TEU. Lower service speeds

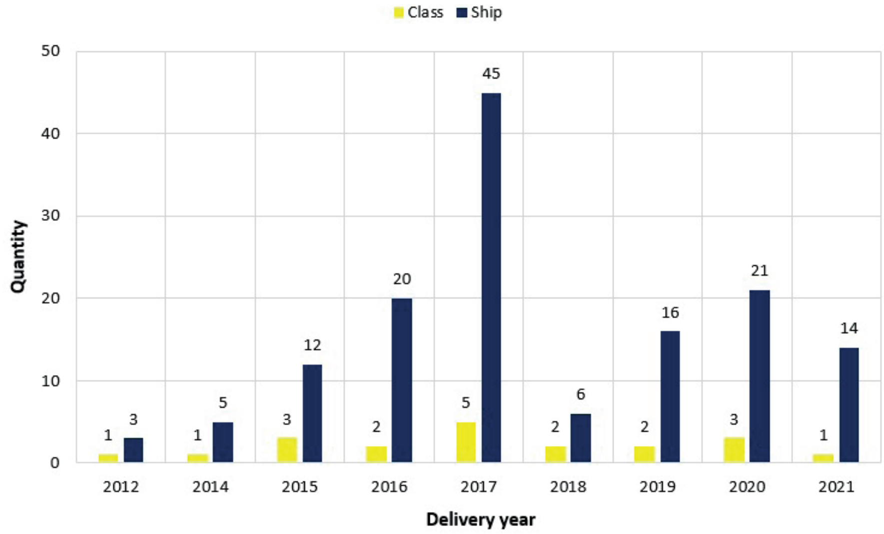

Figure 5 *Database divided into delivery year [3, 5, 12, 14-17]*

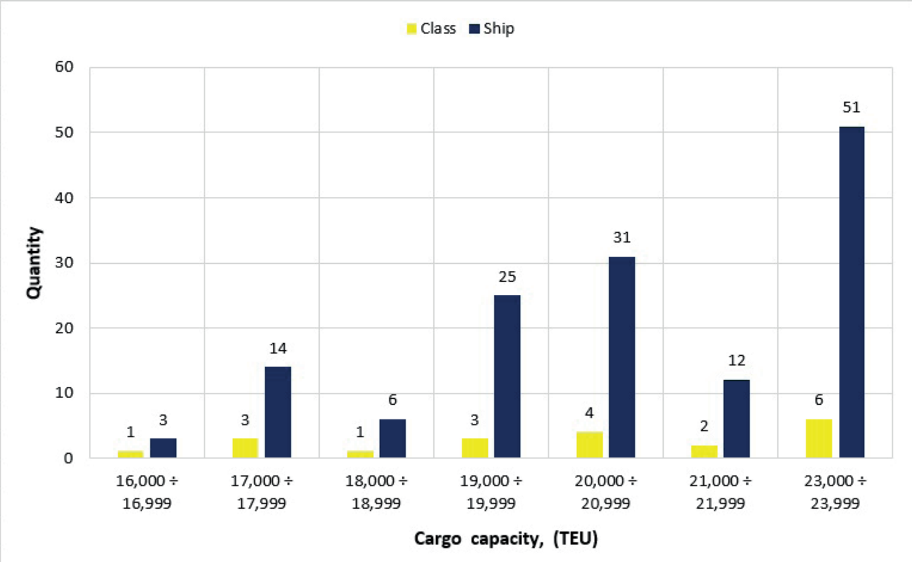

Figure 6 *Database divided into cargo capacity [3, 5, 12, 14-17]*

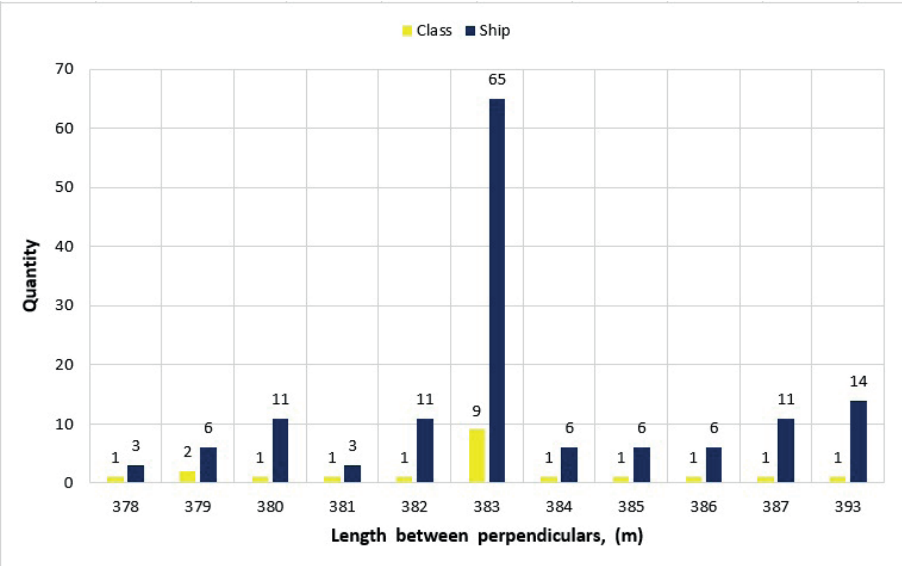

Figure 7 *Database divided into length between perpendiculars [3, 5, 12, 14-17]*

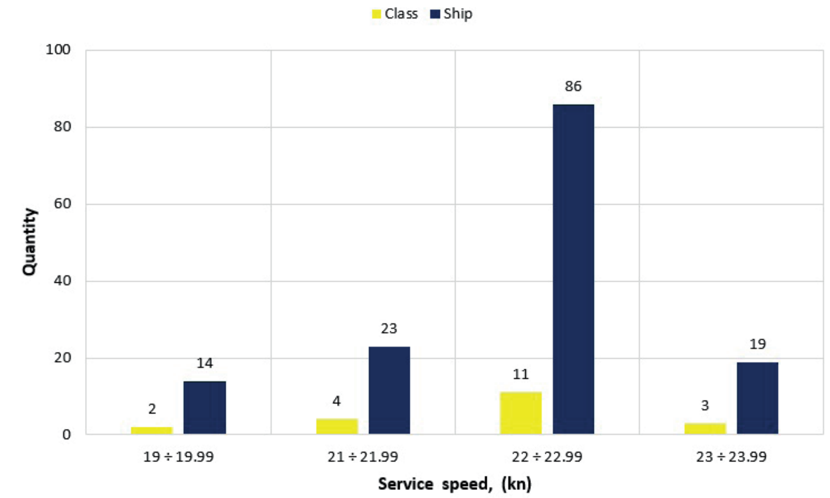

Figure 8 *Database divided into service speed [3, 5, 12, 14-17]*

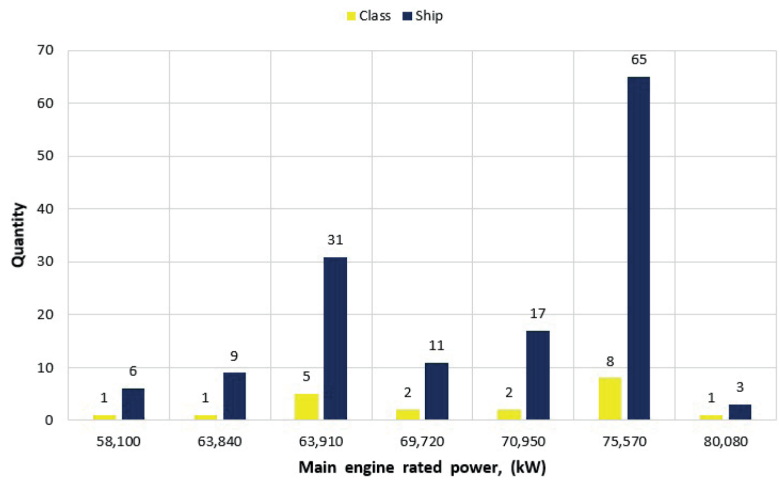

Figure 9 *Database divided into main engine rated power [3, 5, 12, 14-17]*

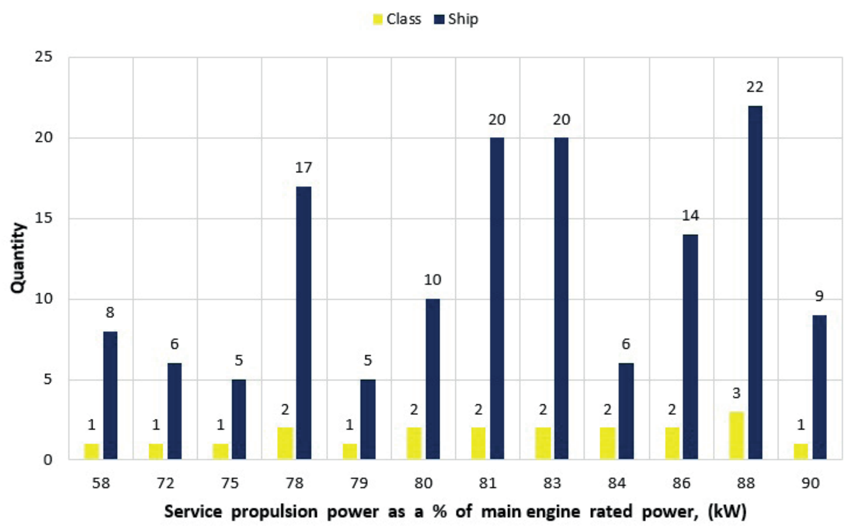

Figure 10 *Database divided into service propulsion power as a % of main engine rated power [3, 5, 12, 14-17]*

are related to slow steaming of the main engine. This parameter was used as the main predictor of the required propulsion power due to its variability over the full range.

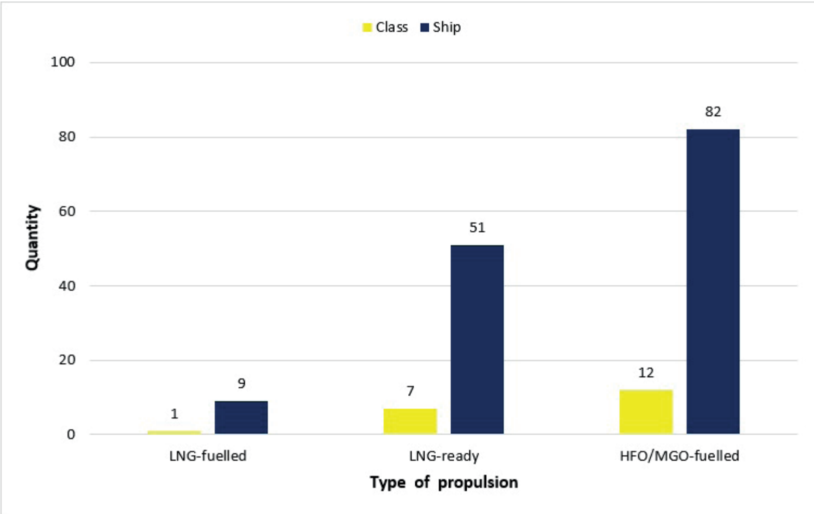

Figure 11 *Database divided into type of propulsion [3, 5, 12, 14-17]*

Table 5 *Values of the propeller curve constant coefficient of all analysed ship classes*

Ship class	Ever Ace	HMM Algeciras	HMM Oslo	MSC Gulsun	MSC Mina
c (kW · kn^{-3})	5.3560	5.3722	5.3889	5.3375	5.3030
Ship class	CMA CGM Jacques Saade	OOCL G	COSCO Shipping Universe	CMA CGM Antoine de Saint-Exupery	MOL Triumph
c (kW · kn^{-3})	5.3959	5.4018	5.4376	5.3899	5.4072
Ship class	Ever Golden	COSCO Constellation	MSC Olympic	MSC Pegasus	CSCL Globe
c (kW · kn^{-3})	5.2060	5.3049	5.3554	5.2952	5.3343
Ship class	UASC A18	CMA CGM Zheng He	CMA CGM Kerguelen	APL Temasek	CMA CGM Marco Polo
c (kW · kn^{-3})	5.3042	5.3392	5.3544	5.3798	5.1513

Figure 9 announces that ships equipped with the MAN 11G95ME-C main engine, whose rated power is 75,570 kW in either a single or dual-fuel version, constitute 46 % of the created database.

The service propulsion power of ultra-large type container ships is usually 78 ÷ 81% or 86 ÷ 90 % of the main engine rated power. These ranges constitute more than 2/3 (68 %) of the created database as demonstrated in Figure 10. The size of the used engine margin results from the applied variant of the main engine work optimisation, in which the specific fuel consumption and pollutant emission are the lowest.

Figure 11 outlines that, in total, 60 of the 142 ships assigned to 8 of 20 classes are equipped with propulsion suitable for running on LNG (Liquified Natural Gas). However, only nine ships CMA CGM Jacques Saade-class are currently LNG-fueled [14]. Ships marked as LNG-ready equipped with dual-fuel engines will burn LNG as soon as LNG tanks and fuel gas supply system are installed within the engine room. The popularity of the LNG as marine fuel will continue to grow due to more and more restrictive limits on the emission of harmful substances (i.e. NO_X, SO_X and CO_2 set by MARPOL Annex VI) and the development of bunkering infrastructure at ports [18].

3 Results and discussion

The values of the propeller curve constant coefficient c, of all the analysed ship classes, c were obtained by transforming Equation (1) resulting from the general propeller law [9, 13, 19]. They are contained in Table 5. The required service propulsion power and service speed values for each ultra-large container ship class were previously included in Table 4.

$$P_B = c \cdot v^3, \tag{1}$$

thus:

$$c = \frac{P_B}{v^3} \tag{2}$$

where:
P_B - Brake power for a given sailing speed, (kW),
c - Propeller curve constant coefficient, constant value for a full range of sailing speed, (kW · kn^{-3}),
v - Sailing speed, (kn).

According to Equation (1), the values of the propulsion power were predicted for all the analyzed ultra-large container ships in the range of sailing speed up to 24 knots. Then, the simple cubic regression model, based on the least squares method, was applied. The following equation was obtained as a result of the calculations:

$$P_B = 5.333 \cdot v^3 \tag{3}$$

Results of the regression analysis and equations describing relations between given parameters are included in Table 6 [20].

Figure 12 shows the propulsion power of the ultra-large container ships' as a function of its sailing speed.

The developed Equation (3) can be applied with very high accuracy to container ships with a length between perpendiculars of 378 ÷ 393 m and a sailing speed not exceeding 24 knots. It facilitates a quick and easy prediction of the ultra-large container ships' propulsion power with sufficient accuracy, which is particularly relevant at the initial design stage, when model tests have not yet been performed.

It is worth noting the very high value of the determination coefficient $R^2 = 0.9959 \cong 1$, obtained when

***Table 6** Regression analysis results [20]*

Parameter	Symbol	Value	Equation	
Sample size	N	500	$N = n_v \cdot n_c$	(4)
Confidence level	CL	0.95	$CL = 1 - p$	(5)
Standard deviation	SD	22,046.57 kW	$SD = \sqrt{\frac{\sum_{i=1}^{N}(P_{Bi} - \overline{P_{Bi}})^2}{N-1}}$	(6)
Determination coefficient	R^2	0.9959	$R^2 = 1 - \frac{\sum_{i=1}^{N}(P_{Bi} - \widehat{P_{Bi}})^2}{\sum_{i=1}^{N}(P_{Bi} - \overline{P_{Bi}})^2}$	(7)
Standard error of propulsion power	SE	985.95 kW	$SE = \frac{SD}{\sqrt{N}}$	(8)

where:
$n_v = 25$ - Total number of points related to sailing speeds between 0 and 24 knots with an interval equal to 1,
$n_c = 20$ - Total number of ship classes, including a total of 142 ships,
$p = 0.05$ - Assumed p-value (probability value),
P_{Bi} - Propulsion power, the actual value of the dependent variable, (kW),
$\widehat{P_{Bi}} = P_B$ - Propulsion power, the predicted value of the dependent variable based on the regression model, (kW),
$\overline{P_{Bi}}$ - Propulsion power, the mean value of the actual dependent variable, (kW).

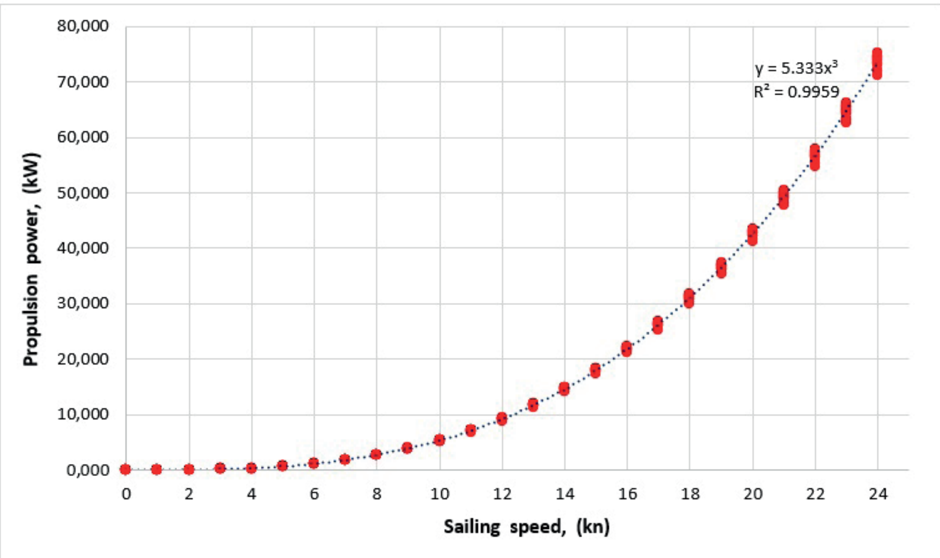

***Figure 12** Propulsion power of the ultra-large container ships' as a function of its sailing speed*

developing an equation for predicting the propulsion power, which indicates a strong relationship between the dependencies under study and choosing the appropriate regression model. This enables the use of Equation (3) with a high probability that the initial calculations would be satisfactorily similar to the results of the exact verification calculations at the technical design stage.

4 Conclusions

A unique feature of all the ultra-large container ships is a length overall of more than 390 meters. The cargo capacity of the most capacious ship has already reached nearly 24,000 TEU and is still growing. The typical configuration of the main propulsion system of the ultra-large container ships consists of a fixed pitch propeller directly-driven by diesel or dual-fuel low-speed main engine. The service speed is the main predictor of the required propulsion power due to its variability over the full range. The calculations based on Equation (3), using a simple cubic regression model, allows the propulsion power to be predicted with sufficient accuracy at the initial design stage, when the model tests results are not yet known. The obtained results would be useful for the design of main propulsion systems, as well as waste heat and cold recovery, whose amount is related to the propulsion power.

References

[1] Review of Maritime Transport 2020 - United Nations Conference on Trade and Development [online] [accessed 2022-01-24]. Available from: https://unctad.org/system/files/official-document/rmt2020_en.pdf

[2] WISNICKI, B. *Vademecum of containerization. Forming the container load unit / Vademecum konteneryzacji. Formowanie kontenerowej jednostki ladunkowej* (in Polish) [online] [accessed 2022-01-24]. 1. ed. Szczecin: Wydawnictwo Link I, 2006. ISBN 83-909749-9-1. Available from: https://www.researchgate.net/profile/Bogusz-Wisnicki/publication/281292577_Vademecum_konteneryzacji_-_Formowanie_kontenerowej_jednostki_ladunkowej/links/578548dd08aec5c2e4e11c3b/Vademecum-konteneryzacji-Formowanie-kontenerowej-jednostki-ladunkowej.pdf

[3] Korean Register of Shipping [online] [accessed 2022-01-24]. Available from: http://www.krs.co.kr/eng/ship_as_address/regist_search.aspx?s_code=0103040500

[4] SAXON, S., STONE, M. Container shipping: the next 50 years - McKinsey and Company [online] [accessed 2022-01-24]. 2017. Available from: https://www.mckinsey.com/~/media/mckinsey/industries/travel%20logistics%20and%20infrastructure/our%20insights/how%20container%20shipping%20could%20reinvent%20itself%20for%20the%20digital%20age/container-shipping-the-next-50-years-103017.pdf

[5] ClassNK Register of Ships [online] [accessed 2022-01-24]. Available from: https://www.classnk.or.jp/register/regships/regships.aspx

[6] CEPOWSKI, T. Prediction of the main engine power of a new container ship at the preliminary design stage. *Management Systems in Production Engineering* [online]. 2017, **2**(25), p. 97-99 [accessed 2022-01-24]. eISSN 2450-5781. Available from: http://dx.doi.org/10.1515/mspe-2017-0014

[7] KORLAK, P. K. Comparative analysis and estimation of amounts of exhaust gas waste heat from the Tier III-compliant dual-fuel low-speed marine main engines. *Scientific Journal of Maritime Research* [online]. 2021, **35**(1), p. 128-140 [accessed 2022-01-24] ISSN 1332-0718, eISSN 1846-8438. Available from: https://doi.org/10.31217/p.35.1.14

[8] KORLAK, P. K. Prediction of the amount of waste cold from liquefied natural gas (LNG) for gas-fueled low-speed main engines. *Scientific Journals of the Maritime University of Szczecin* [online]. 2021, **68**(140) [accessed 2022-01-24]. ISSN 1733-8670, eISSN 2392-0378. Available from: http://repository.scientific-journals.eu/handle/123456789/2688

[9] MOLLAND, A. F., TURNOCK S. T., HUDSON D. A. *Ship resistance and propulsion* [online]. 2. ed. Cambridge: Cambridge University Press, 2017. eISBN 9781316494196. Available from: https://doi.org/10.1017/9781316494196

[10] CHARCHALIS, A., KREFFT, J. Electric power assessment of the container ship in the preliminary design stage. *Scientific Journals of the Maritime University of Szczecin*. 2009, **17**(89), p. 25-31. ISSN 1733-8670, eISSN 2392-0378.

[11] Siemens PLM Automation 2021, Integrated ship design and engineering [online] [accessed 2022-01-24]. Available from: https://www.plm.automation.siemens.com/global/pl/industries/marine/integrated-ship-design-and-engineering-isde.html

[12] American Bureau of Shipping Record [online] [accessed 2022-01-24]. Available from: https://www.eagle.org/portal/#/absrecord/search

[13] MOLLAND, A. F. *The maritime engineering reference book: a guide to ship design, construction and operation*. 1. ed. Oxford: Elsevier Ltd., 2008. ISBN 9780750689878, eISBN 9780080560090.

[14] Bureau Veritas Fleet [online] [accessed 2022-01-24]. Available from: https://marine-offshore.bureauveritas.com/bv-fleet/#/bv-fleet/

[15] China Classification Society Register of Ships [online] [accessed 2022-01-24]. Available from: https://www.ccs.org.cn/ccswzen/internationalShipsList?columnid=201900002000000123

[16] Vessel Register for Det Norske Veritas [online] [accessed 2022-01-24]. Available from: https://vesselregister.dnvgl.com/vesselregister/vesselregister.html

[17] Lloyd's Register Ships in Class [online] [accessed 2022-01-24]. Available from: https://www.lr.org/en/lrofships/

[18] HERDZIK, J. Aspects of using LNG as a marine fuel. *Journal of KONES Powertrain and Transport* [online]. 2012, **19**(2), p. 201-209 [accessed 2022-01-24] ISSN 1231-4005, eISSN 2354-0133. Available from: https://doi.org/10.5604/12314005.1137919

[19] MAN Energy Solutions A/S. 2018. Basic ship propulsion [online] [accessed 2022-01-24]. Available from: https://man-es.com/docs/default-source/marine/5510-0004-04_18-1021-basic-principles-of-ship-propulsion_web.pdf?sfvrsn=5083eaa8_4

[20] JOHNSON, R. A., BCHATTACHARYYA, G. K. *Statistics: principles and methods*. 7. ed. New York: John Wiley and Sons Inc, 2014. ISBN 978-1118967058.

METHODS FOR IDENTIFICATION OF COMPLEX INDUSTRIAL CONTROL OBJECTS ON THEIR ACCELERATING CHARACTERISTICS

Assel Abdullayeva, Aidana Kalabayeva, Andrey Ivanov, Seidulla Abdullayev, Gabit Bakyt *

Academy of Logistics and Transport, Almaty, Republic of Kazakhstan

*E-mail of corresponding author: gaba_b@bk.ru

Resume

Theoretical identification methods for complex industrial control objects give very cumbersome and complex mathematical relations, the use of which for practical purposes is not constructive. In this regard, methods for obtaining mathematical models based on experimental data have now become the main focus of identification theory. In this paper is described the method of identification of industrial control objects developed according to their acceleration characteristics. The structure of the object under study is determined by the type of amplitude-phase frequency response and dynamic parameters are determined by experimental data. The high adequacy of the method is confirmed by similar studies on known (reference) models. The scientific novelty of the work consists in development of a new method for identifying complex industrial control objects by their acceleration characteristics.

Available online: https://doi.org/10.26552/com.C.2022.3.B239-B246

Article info

Received 23 November 2021
Accepted 25 April 2022
Online 26 May 2022

Keywords:

monotone S-shaped acceleration curve
second order inertial link
transfer function
identification
active experiment

ISSN 1335-4205 (print version)
ISSN 2585-7878 (online version)

1 Introduction

Obtaining models based on observations and studying their properties is essentially the main content of science. These models may be more or less formalized, but they all have the main feature that they link observations into a general picture. The problem of obtaining adequate mathematical models of dynamical systems, based on observations of their behaviour is the subject of identification theory. The world around us consists entirely of dynamic systems, so knowledge of identification methods is crucial.

At present, with increasingly high requirements for management processes in various fields of engineering and technology, identification issues are becoming extremely important, since it is impossible to ensure the high-quality management of a system if its mathematical model was not known with sufficient accuracy.

Defining the system characteristics is dual to system management tasks since one cannot manage a system if its characteristics were unknown. Knowledge of the mathematical model before starting the management process significantly affects the effectiveness of its implementation [1-2].

This paper describes the developed methods for adequate identification of complex industrial controls s based on the results of an active experiment (acceleration characteristics).

2 The definition of objects equations by curves of acceleration

To obtain the equations of objects, an experiment is used, which consists in measuring and registering one or more transients. These processes correspond to particular solutions of the desired differential equation. Two types of experiments are most widely used in automation: removal of acceleration curves and removal of frequency characteristics. In the first case, the registered partial solution of the desired equation is the object's response to a standard step change in the input value, which is used to determine the object's equation. In the second case, not one particular solution is registered, but several. These solutions are steady fluctuations in the output value of the object, forced by artificial periodic fluctuations of the input value at various fixed frequencies. These particular solutions -

the frequency characteristics of the object - represent the initial material for the subsequent finding of the equation [3].

If an active experiment cannot be applied on an object, then the statistical dynamics methods are used without using artificial influences on the object [4].

For a linear operator, equation of the form

$$a_0 \cdot x^n + a_1 \cdot x^{n-1} + \ldots + x = b_0 \cdot x_0^m + b_1 \cdot x_0^{m-1} + \ldots + b_m \cdot x_0, \quad (1)$$

where $n > m$; x, x_0 - output and input of the object solution with zero initial conditions and abrupt change in input X_0, can be written analytically, as a function of time and coefficients:

$$x = x_{cm}(t, a_0, a_1, \ldots, a_{n-1}, b_0, b_1, \ldots, b_m); \quad (2)$$

and vice versa, if the order of the object Equation (1) is known and the reaction is obtained experimentally $x_{cm}(t)$ to a step change in input, then you can calculate $n + m + 1$ coefficients a_i, b_i (1). For this, the analytical solution is equated $x(t)$ in (2), in which the coefficients appear a_i and b_i and reaction $x^1_{cm}(t)$ at different times $t = t_i (i = 1, 2, \ldots, m + n + 1)$. The result is a system of $m + n + 1$ equation with unknown coefficients a_i, b_i:

$$x_{cm}(t_i, a_0, a_1, \ldots, a_{n-1}, b_0, b_1, \ldots, b_m) = x'_{cm}(t_i), \quad i = 1, 2, \ldots, n + m + 1, \quad (3)$$

from which the desired coefficients are calculated. In this way $n + m + 1$ discrete ordinates $x^1_{cm}(t)$ acceleration curves allow $m + n + 1$ unknown coefficients. Different variations of this idea are possible, up to the use of other types of reaction. One can take an excess number of ordinates and apply the least squares method.

Knowledge of the order of the object Equation (1) is essential here. The analytical form of solutions of Equation (2) is different for equations of different orders and if the a priori order n is less than the actual one, then this method of equating the ordinates of the analytical solution and the experimental solution; gives incorrect a_i and b_i. If n taken large, then this should not represent a problem, since the extra coefficients will turn to zero. A priori, the order of the object's equation is determined by the number of concentrated containers in the object [5-6].

2.1. Method for identifying the first-order object using an exponential acceleration curve

Figure 1 shows the acceleration curve $y(t)$ of a single-capacitive linear object. At a moment in time $t_0 = 0$ input quantity x changed jumped to a units.

It is necessary to determine numerically the mathematical model of the object.

The required equation has the form

$$T\frac{dy}{dt} + y = Kx \text{ or } \frac{Y(p)}{X(p)} = \frac{K}{Tp + 1} \quad (4)$$

and you need to define constants T and K.

First, an analytical expression is found for the solution of the equation under the given conditions. This solution will contain constants T and K. The resulting acceleration curve is a graphical solution, then comparing the graph with its analytical expression, the constants of this analytical expression are determined. The general form of the solution for conditions $y = 0$ at $t = 0$ and $x = a$ at $t > 0$ is [7]:

$$y(t) = K \cdot a \cdot \left(1 + e^{-\frac{t}{T}}\right). \quad (5)$$

In principle, it is enough to take a couple of any points from the graph, substitute their coordinates into the solution and then from the two obtained equations calculate T and K. However, these equations are transcendental:

$$\left.\begin{array}{l} y_1(t) K \cdot a \cdot \left(1 - e^{-\frac{t_1}{T}}\right) \\ y_2(t) K \cdot a \cdot \left(1 - e^{-\frac{t_2}{T}}\right) \end{array}\right\} \quad (6)$$

and to calculate their roots K and T is difficult.

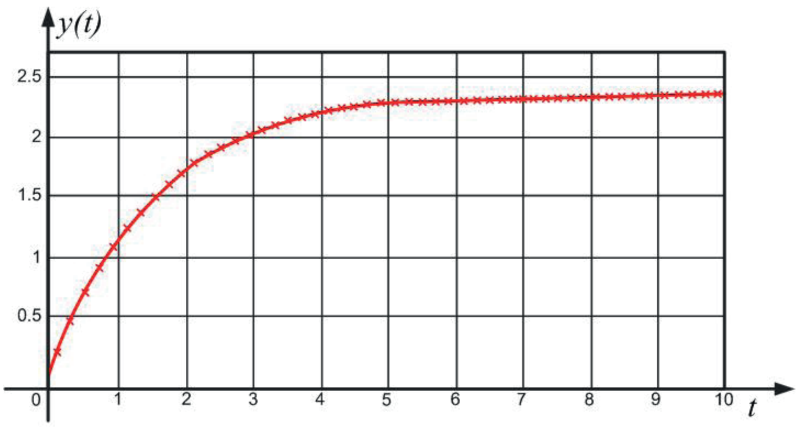

***Figure 1** For definition of the first-order object model along the acceleration curve*

Therefore, one can apply the following technique. In the steady state, is $y\ (t) = k \cdot a$, therefore, the ordinate of the asymptote tends to y, what makes it possible to determine K by simple division by a, i.e.

$$K = \frac{b}{a}. \tag{7}$$

To calculate T, the solution is differentiated with respect to time:

$$\frac{dy(t)}{dt} = K \cdot a \cdot \frac{1}{T} \cdot e^{-\frac{t}{T}} \tag{8}$$

and set t to zero

$$\lim_{t \to 0} \frac{dy}{dt} = K \cdot a \cdot \frac{1}{T} = \frac{b}{T} = tg\alpha, \tag{9}$$

where α is the angle of inclination of the tangent drawn to the graph $y(t)$ at $t = 0$. Therefore,

$$T = \frac{b}{tg\alpha}. \tag{10}$$

Thus, T is numerically equal to the length of the tangent within the range of the origin of coordinates to the point of its intersection with the mentioned asymptote.

This solution is the simplest, but not accurate, since it is difficult to indicate the ordinate of asymptote b. This solution uses only the beginning and end of the graph, while all the intermediate points are dropped from consideration, [8-9].

Now is considered a more accurate technique. The graph is broken equidistant to the interval Δt for ordinates y_0, y_1, y_2 etc. For these points, according to the solution of Equation (5) can be written

$$\left.\begin{aligned} y_0(t) &= K \cdot a \cdot \left(1 - e^{-\frac{0}{T}}\right); \\ y_1(t) &= K \cdot a \cdot \left(1 - e^{-\frac{\Delta t}{T}}\right); \\ y_2(t) &= K \cdot a \cdot \left(1 - e^{-\frac{2\Delta t}{T}}\right); \\ y_3(t) &= K \cdot a \cdot \left(1 - e^{-\frac{3\Delta t}{T}}\right); \end{aligned}\right\} \tag{11}$$

etc.

The previous equations are subtracted from the following ones in pairs:

$$\left.\begin{aligned} y_1 - y_0 &= K \cdot a - K \cdot a \cdot e^{-\frac{\Delta t}{T}}; \\ y_2 - y_1 &= K \cdot a \cdot e^{-\frac{\Delta t}{T}} - K \cdot a \cdot e^{-\frac{2\Delta t}{T}} \\ y_3 - y_2 &= K \cdot a \cdot e^{-\frac{2\Delta t}{T}} - K \cdot a \cdot e^{-\frac{3\Delta t}{T}}; \end{aligned}\right\} \tag{12}$$

etc.

For brevity, $e^{-\frac{\Delta t}{T}}$ is denoted as q, then, one can write:

$$\left.\begin{aligned} y_1 - y_0 &= K \cdot a \cdot (1 - q); \\ y_2 - y_1 &= K \cdot a \cdot q \cdot (1 - q); \\ y_3 - y_2 &= K \cdot a \cdot q^2 q \cdot (1 - q); \end{aligned}\right\} \tag{13}$$

etc.

Dividing each subsequent of these equalities by the previous one, one obtains a series of values for q:

$$\left.\begin{aligned} q_1 &= \frac{y_2 - y_1}{y_1 - y_0}; \\ q_2 &= \frac{y_3 - y_2}{y_2 - y_1}; \\ q_3 &= \frac{y_4 - y_3}{y_3 - y_2}; \end{aligned}\right\} \tag{14}$$

etc.

These numbers differ from one another due to experimental measurement and registration errors $y(t)$.

More accurate is the average value, which gives the arithmetic mean $\bar{q}$ from the calculated individual values q_i. Then the updated time constant $\bar{T}$ is determined from the expression

$$\bar{T} = -\frac{\Delta t}{\ln \bar{q}}. \tag{15}$$

Similarly, according to the known q_i, individual K_i are determined as:

$$\left.\begin{aligned} K_1 &= \frac{y_1 - y_0}{a \cdot (1 - q_1)}; \\ K_2 &= \frac{y_2 - y_1}{a \cdot q_2 \cdot (1 - q_2)}; \\ K_3 &= \frac{y_3 - y_2}{a \cdot q_3^2 \cdot (1 - q_3)}; \end{aligned}\right\} \tag{16}$$

Then the arithmetic means $\bar{K}$ of K_1, K_2, K_3 is K.

2.2 Method for identifying a second - order object with a monotone s-shaped acceleration curve

Figure 2 shows the acceleration curve of the object described by the second-order equation:

$$T_1 \cdot T_2 \cdot \frac{d^2 y}{dt} + (T_1 + T_2) \cdot \frac{dy}{dt} + y = K \cdot x. \tag{17}$$

Constants T_1, T_2 and K, can be calculated if it is known that the perturbation at the input was single $x = a = 1$ at $t > 0$.

As in the previous case, at the beginning, you should write the solution to the equation in general form [10].

Let the general form be, [4]

$$y_{\text{total}}(t) = C_1 \cdot e^{-\frac{t}{T_1}} + C_2 \cdot e^{-\frac{t}{T_2}} + K \cdot a. \tag{18}$$

In this case, it is necessary to determine five unknowns (K, T_1, T_2, C_1, C_2). One can reduce the number of unknowns to three (K, T_1, T_2,).

For this, from the initial conditions $y = 0$; $\frac{dy}{dt} = 0$ for $t = 0$ the arbitrary constants are defined:

$$\left.\begin{aligned} y_{total}(0) &= C_1 \cdot e^{-\frac{0}{T_1}} + C_2 \cdot e^{-\frac{0}{T_2}} + K \cdot a = 0; \\ y'_{total}(0) &= -C_1 \cdot \frac{1}{T_1} \cdot e^{-\frac{0}{T_1}} - C_2 \cdot \frac{1}{T_2} e^{-\frac{0}{T_2}} = 0; \end{aligned}\right\} \tag{19}$$

from

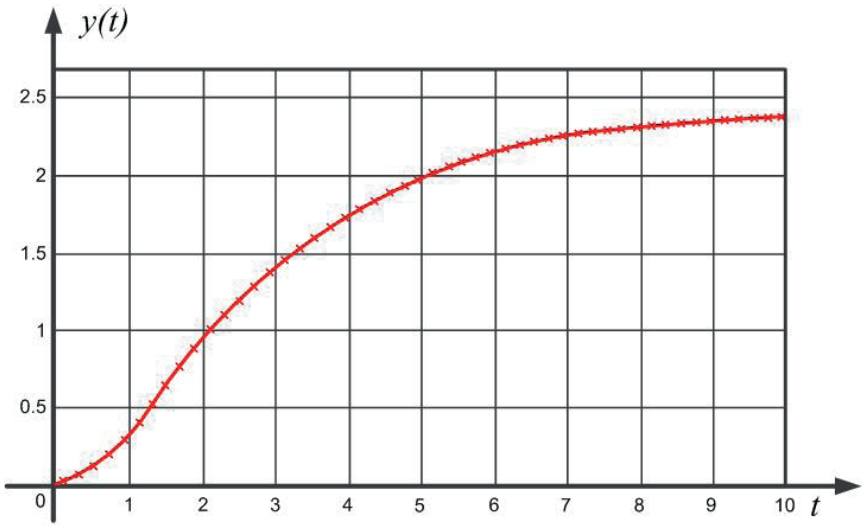

Figure 2 *For definition of the second-order object model with a monotonic acceleration curve S - figurative*

$$C_1 = \frac{k\cdot a\cdot T_1}{T_2 - T_1};\quad C_2 = \frac{k\cdot a\cdot T_2}{T_1 - T_2}. \tag{20}$$

The desired particular solution is obtained in the form

$$y(t) = k\cdot a\cdot\left(\begin{array}{l} 1 + \dfrac{T_1}{T_2 - T_1}\cdot e^{-\frac{t}{T_1}} + \\ + \dfrac{T_2}{T_1 - T_2}\cdot e^{-\frac{t}{T_2}} \end{array}\right). \tag{21}$$

Now, in principle, it is sufficient to take the coordinates y_i, t_i, three arbitrary points from a given graph, substitute them three times into the solution and from the three equations obtained in this way find the roots k, T_1, T_2. However, these equations are transcendental and the roots are difficult to calculate, so it is more convenient to use the following mathematical technique [11].

To do this, the graph *y(t)* is split equidistant to interval Δ *t* for ordinates y_0, y_1, y_2 etc. and one then writes:

$$\left.\begin{array}{l} y_0 = k\cdot a + \dfrac{k\cdot a\cdot T_1}{T_2 - T_1} + \dfrac{k\cdot a\cdot T_2}{T_1 - T_2}; \\ y_1 = k\cdot a\cdot\left(\begin{array}{l} 1 + \dfrac{T_1}{T_2 - T_1}\cdot e^{-\frac{\Delta t}{T_1}} + \\ + \dfrac{T_2}{T_1 - T_2}\cdot e^{-\frac{\Delta t}{T_2}} \end{array}\right); \\ y_2 = k\cdot a\cdot\left(\begin{array}{l} 1 + \dfrac{T_1}{T_2 - T_1}\cdot e^{-\frac{2\Delta t}{T_1}} + \\ + \dfrac{T_2}{T_1 - T_2}\cdot e^{-\frac{2\Delta t}{T_2}} \end{array}\right); \\ y_3 = k\cdot a\cdot\left(\begin{array}{l} 1 + \dfrac{T_1}{T_2 - T_1}\cdot e^{-\frac{3\Delta t}{T_1}} + \\ + \dfrac{T_2}{T_1 - T_2}\cdot e^{-\frac{3\Delta t}{T_2}} \end{array}\right); \end{array}\right\} \tag{22}$$

etc.

By designating $A_1 = K; A_2 = \dfrac{K\cdot T_1}{T_2 - T_1}$; $A_3 = \dfrac{K\cdot T_2}{T_1 - T_2}; p = e^{-\frac{\Delta t}{T_1}}; p = e^{-\frac{\Delta t}{T_2}}$ these equations are rewritten as

$$\begin{array}{l} y_0 = A_1 + A_2 + A_3; \\ y_1 = A_1 + A_2\cdot p + A_3\cdot q; \\ y_2 = A_1 + A_2\cdot p^2 + A_3\cdot q^2; \\ y_3 = A_1 + A_2\cdot p^3 + A_3\cdot q^3; \\ y_4 = A_1 + A_2\cdot p^4 + A_3\cdot q^4; \\ y_5 = A_1 + A_2\cdot p^5 + A_3\cdot q^5. \end{array} \tag{23}$$

We will count the numbers 1, *p* and *q* roots of the cubic equation. Let the first line be multiplied by B_3, the second by - B_2, the third by - B_1, the fourth by - 1 and add them, then the right-hand sides add up to zero, so one gets, [6]:

$$\lambda^3 + B_1\cdot\lambda^2 + B_2\cdot\lambda + B_3 = 0\,. \tag{24}$$

$$y_0\cdot B_3 + y_1\cdot B_2 + y_2\cdot B_1 = 0\,. \tag{25}$$

Then the same is done with the following four lines:

$$y_1\cdot B_3 + y_2\cdot B_2 + y_3\cdot B_1 + y_4 = 0\,. \tag{26}$$

The next four lines will give

$$y_2\cdot B_3 + y_3\cdot B_2 + y_4\cdot B_1 + y_5 = 0\,. \tag{27}$$

In these three equalities, the ordinates y_i, are known from the acceleration curve and the constants B_1, B_2, B_3 are the sought for ones. Having found them, one should then calculate the roots of the cubic equation:

$$\lambda_1 = 1; \lambda_2 = p = e^{-\frac{\Delta t}{T_1}}; \lambda_3 = q = e^{-\frac{\Delta t}{T_2}}, \tag{28}$$

i.e.

$$T_1 = -\frac{\Delta t}{\ln p} \text{ and } T_2 = -\frac{\Delta t}{\ln p}\,. \tag{29}$$

From any equation of system of Equations (23),

***Table 1** Experimental values*

t MIN	0	1	2	3	4	5
$y(t)$	0	0.31	0.80	1.21	1.5	1.7

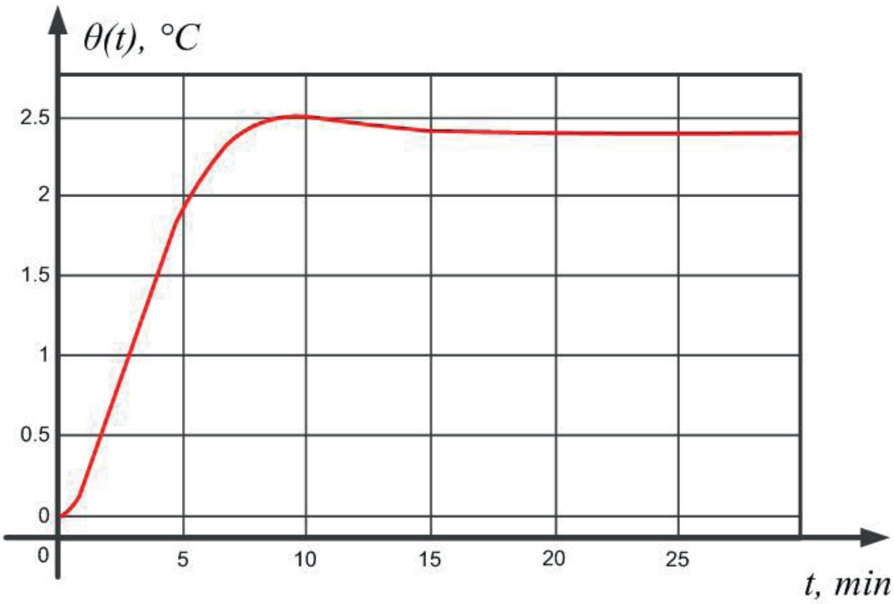

***Figure 3** For definition of the second-order object model with an oscillatory acceleration curve*

except for the first, it is necessary to calculate K.

To increase the accuracy, one cannot take only six initial ordinates, but more than average of the results.

In essence, this method is an approximation of a given graph by the sum of exponential terms [12].

Next is presented a numerical example. Taking = 1 min, six ordinates on the acceleration curve are measured (Figure 2) (Table 1).

From equations

$$0 \cdot B_3 + 0.31 \cdot B_2 + 0.8 \cdot B_1 + 1.21 = 0;$$

$$0.31 \cdot B_3 + 0.8 \cdot B_2 + 1.21 \cdot B_1 + 1.21 = 0;$$

$$0.8 \cdot B_3 + 1.21 \cdot B_2 + 1.5 \cdot B_1 + 1.7 = 0;$$

one calculates $B_1 = -1.97$; $B_2 = -1.19$; $B_3 = -0.222$.

Then, one can find the roots of the cubic equation: $\lambda_1 = 1; \lambda_2 = p = 0.37; \lambda_3 = q = 0.61$. This is relatively easy to do, since one root is known in advance. $(\lambda = 1)$. Then one finds:

$$T_1 = -\frac{\Delta t}{\ln p} = -\frac{1}{\ln 0.37} \approx 1\,\text{min},$$
$$T_2 = -\frac{\Delta t}{\ln p} = -\frac{1}{\ln 0.61} \approx 2\,\text{min}.$$

To calculate K, take one of the lines, except the first, of system in Equation (19), for example, the second:

$$y_1 = A_1 + A_2 \cdot p + A_3 \cdot q = K \cdot a \cdot \left(1 + \frac{K \cdot a \cdot T_1}{T_2 - T_1} \cdot p + \frac{K \cdot a \cdot T_2}{T_1 - T_2} \cdot q\right), \tag{30}$$

and substitute the numeric values

$$0.31 = k \cdot \left(1 + \frac{1}{2-1} \cdot 0.37 + \frac{2}{1-2} \cdot 0.61\right),$$

to get

$$k = 2.07\,.$$

2.3 Method for identifying the second-order object with an oscillatory acceleration curve

Equation of the object is defined according to the reaction of the output Δθ (t) (Figure 3) for the abrupt change in the input value v to the value $v = a$, m/min; Δθ (t) - temperature difference in the last suction chambers, v - belt speed [7].

The acceleration curve has an oscillatory shape and it can be assumed that the sought equation is of the second order with complex roots [9]:

$$\frac{d^2\Delta\theta}{dt^2} - (\gamma_1 + \gamma_2) \cdot \frac{d\Delta\theta}{dt} + \gamma_1 \cdot \gamma_2 \cdot \Delta\theta = \gamma_1 \cdot \gamma_2 \cdot K \cdot v. \tag{31}$$

It is necessary to calculate constants $\gamma_1 \cdot \gamma_2 \cdot K$.

This equation is the same as in the previous case, only the designation of the constants is changed: $\gamma_1 = -\frac{1}{T_1}, \gamma_2 = -\frac{1}{T_2}$, since the time constant here, in the case of an oscillatory system, has no physical meaning. The equation of the oscillatory system is usually written in the form

$$\frac{d^2\Delta\theta}{dt^2} + 2\cdot\varepsilon\cdot\omega_0\cdot\frac{d\Delta\theta}{dt} + \omega_0^2\cdot\Delta\theta = K\cdot w\omega_0^2\cdot\upsilon\,, \quad (32)$$

where ε is the damping coefficient; ω_0 is the natural frequency of the system.

This shows the connection between the physical constants ε,ω_0 and numbers γ_1,γ_2. The latter were introduced for the convenience of calculations.

Using the results of the previous method, one can immediately write the solution to the equation:

$$\Delta\theta(t) = K\cdot a + \frac{K\cdot a\cdot\gamma_2}{\gamma_1-\gamma_2}\cdot e^{\gamma_1 t} + \frac{K\cdot a\cdot\gamma_2}{\gamma_1-\gamma_2}\cdot e^{\gamma_1 t}. \quad (33)$$

Since the control object has vibrational properties, the method of calculating constants used in the previous task will result in non-real numbers γ_1 and γ_2, i.e. complex

$$\gamma_1 = \alpha + j\beta;\ \gamma_2 = \alpha - j\beta. \quad (34)$$

Turning to the real quantities, the form of writing the solution must be accordingly transformed according to the Euler formula; it corresponds to the addition of two harmonics.

$$\Delta\theta(t) = K\cdot a\cdot\left[\begin{array}{l}1+\dfrac{\alpha-j\beta}{2j\beta}\cdot e^{(\alpha+j\beta)\cdot t}+\\ \dfrac{\alpha+j\beta}{-2j\beta}\cdot e^{(\alpha+j\beta)\cdot t}\end{array}\right] =$$
$$K\cdot a\cdot\left\{\begin{array}{l}1+e^{\alpha t}\cdot\\ \left[\begin{array}{l}1+\dfrac{j\alpha+\beta}{-2\beta}\cdot(\cos\beta t + j\sin\beta t)+\\ \dfrac{j\alpha-\beta}{2\beta}\cdot(\cos\beta t - j\sin\beta t)\end{array}\right]\end{array}\right\} = \quad . \quad (35)$$
$$K\cdot a\cdot\left[1+e^{\alpha t}\cdot\left(-\cos\beta t+\frac{\alpha}{\beta}\cdot\sin\beta t\right)\right] =$$
$$K\cdot a\cdot\left[1+e^{\alpha t}\cdot\sqrt{1+\left(\frac{\alpha}{\beta}\right)^2}\cdot\sin\left(\beta t - arctg\frac{\beta}{\alpha}\right)\right].$$

In principle, one could take the coordinates of the three arbitrary points of their graph $\Delta\theta(t)$, putting them in the solution, calculate the real roots from the three equations for *α, β* and *K*. However, since the equations turn out to be transcendental, it is very difficult to solve them and therefore it is more expedient to apply the technique considered in the previous problem [13].

For this, from the acceleration curve one takes six equidistant to the interval Δt = *5 min*, ordinate:

$$\Delta\theta_0 = 0; \Delta\theta_1 = 29.3; \Delta\theta_2 = 69; \Delta\theta_3 = 84.3;$$
$$\Delta\theta_4 = 79.8; \Delta\theta_5 = 71.1.$$

The system of equations is composed for determining the coefficients of the intermediate cubic Equation (21)

$$0\cdot B_3 + 29.3\cdot B_2 + 69\cdot B_1 + 84.3 = 0;$$
$$29.3\cdot B_3 + 69\cdot B_2 + 84.3\cdot B_1 + 79.8 = 0;$$
$$69\cdot B_3 + 84.3\cdot B_2 + 79.8\cdot B_1 + 71.1 = 0.$$

From that one calculates B_1 = -1.1654; B_2 = 1.12; B_3 = - 0.366 and gets the following cubic equation: λ^3 - 1.654 λ^2 + 1.12 λ - 0.366 = 0, the roots of which are then calculated (one root λ_3 = 1 is known in advance):

$$\lambda_1 = 0.327 + j\cdot 0.509; \lambda_2 = 0.327 - j\cdot 0.509; \lambda_3 = 1.$$

The complex roots λ_1 and λ_2 are represent ed in an exemplary form:

$$\lambda_1 = e^{-0.5+j\cdot 1.0}; \lambda_2 = e^{-0.5-j\cdot 1.0}.$$

Next, the constants γ_1 and γ_2 are determined as:

$$\left.\begin{array}{l}\gamma_1 = -\dfrac{1}{T_1} = \dfrac{\ln\lambda_1}{\Delta t} = \dfrac{-0.5+j\cdot 1.0}{5} = \\ -0.1+j\cdot 0.2;\\ \gamma_2 = -\dfrac{1}{T_2} = \dfrac{\ln\lambda_2}{\Delta t} = \dfrac{-0.5-j\cdot 1.0}{5} = \\ -0.1+j\cdot 0.2;\\ (\alpha = -0.1; \beta = 0.2).\end{array}\right\} \quad (36)$$

It remains to calculate the static transfer ratio *K*. This can be easily done by substituting the coordinates of an arbitrary point of the acceleration curve and the calculated constants α and β. Take for example the point *t* = Δt = *5 min*, $\Delta\theta(\Delta t) = \Delta\theta_1 = 29.3$:

$$\Delta\theta = K\cdot 1\cdot\left[1+e^{\alpha t}\cdot\left(-\cos\beta t + \frac{\alpha}{\beta}\cdot\sin\beta t\right)\right] \text{ or}$$

$$29.3 = K\cdot 1\cdot\left[1+e^{-0.1\cdot 5}\cdot\left(-\cos 0.2\cdot 5 + \frac{-0.1}{0.2}\cdot\sin 0.2\cdot 5\right)\right]$$

where one finds *K* = 70 *deg*/(*m*/*hour*).

The required numerical equation of the vibrational object will have the form:

$$\frac{d^2\Delta\theta}{dt^2} + 0.2\cdot\frac{d\Delta\theta}{dt} + 0.05\cdot\Delta\theta = 0.05\cdot 70\cdot\upsilon\,, \quad (37)$$

where υ - *m / hour*; $\Delta\theta$ – °C ; *[t] - min*.

The natural frequency of the object is

$$\omega_0 = \sqrt{\gamma_1\cdot\gamma_2} = 0.224\ rad/min;$$

And the damping factor is

$$\varepsilon = \frac{-\lambda_1-\lambda_2}{2\cdot\omega_0} = \frac{0.2}{2\cdot 0.234} = 0.45\,. \quad (38)$$

When this technique is extended to the higher-order systems, the general scheme of the method remains similar.

3 Conclusion

The article analyses the methods of determination for industrial control devices by the type of amplitude-phase frequency response and substantiates their complex mathematical relations ccording to the data of an active experiment with the means of obtaining acceleration characteristics.

In this paper are developed the methods for identification of industrial control objects. Using the method of statistical dynamics, the frequency characteristics of an industrial facility are determined.

Acceleration indices of the analyzed control object are converted to inertial link of the first order. The result is a mathematical model of an industrial control object in the form of a transfer function.

According to the data of an active experiment, acceleration characteristics are obtained (the object's response to a step input action), which, for the stable linear objects have one of the following types: exponential, S-shaped, or oscillatory. The shape of the acceleration curve determines the structure of the object and its dynamic parameters (transmission coefficients, time constants, delay time) are found by processing the acceleration curve using the special mathematical techniques. For example, a sequential connection of inertial links (an inertial link of the 2nd order) always gives an S-shaped Transition process. Therefore, if an unknown object of research gives an S-shaped acceleration curve, then its mathematical model can be identified as an inertial link of the 2nd order.

Similar conclusions can be drawn for objects with other types of acceleration characteristics.

References

[1] SIMPKINS, A. System identification: theory for the user, 2nd edition (Ljung, L.; 1999) [on the shelf]. *IEEE Robotics and Automation Magazine* [online]. 2012, **19**(2), p. 95-96. ISSN 1070-9932, eISSN 1558-223X. Available from: https://doi.org/10.1109/MRA.2012.2192817

[2] LJUNG, L. *Systems identification (theory for the user)* (in Russian). Moscow: Higher school, 1991.

[3] ZHAN, Z., ZHANG, J., LI, Y., CHUNG, H.-H. PID Control system analysis, design and technology. *IEEE Transactions on Control Systems Technology* [online]. 2005, **13**(4), p. 559-576. ISSN 1063-6536, eISSN 1558-0865. Available from: http://dx.doi.org/10.1109/TCST.2005.847331

[4] ABDULLAYEV, S., TOKMURZINA, N., BAKYT, G. The determination of admissible speed of locomotives on the railway tracks of the republic of Kazakhstan. *Transport Problems International Scientific Journal* [online]. 2016, **11**(1), p. 61-78. eISSN 2300-861X. Available from: https://doi.org/10.20858/tp.2016.11.1.6

[5] MOON, S., KIM, J., SEO, J. Prototyping a remotely-controlled machine for concrete surface grinding operations. *Journal of Civil Engineering and Management* [online]. 2016, **23**(2), p. 1-11. ISSN 1392-3730, eISSN 1822-3605. Available from: https://doi.org/10.3846/13923730.2015.1023349

[6] MUHITOVS, R., MEZITIS, M., KORAGO, I. Development of the railway point electric heating intellectual control algorithm. *Transport Problems International Scientific Journal* [online]. 2020, **15**(1), p. 71-79. eISSN 2300-861X. Available from: https://doi.org/10.21307/tp-2020-007

[7] ADAMBAYEV, M., KUTTYBAEV, A., AUEZOVA, A. Dynamics of dry grinding in two-compartment separator. New developments in mining engineering. In: *Theoretical and practical solutions of mineral resources mining* [online]. PIVNYAK, G., BONDARENKO, V., KOVALEVSKA, I. (Eds.). London: Taylor and Francis Group, 2015. eISBN 9780429225758, p. 435-439. Available from: https://doi.org/10.1201/b19901

[8] GOLNARAGHI, F., KUO, B. *Automatic control systems*. 10. ed. McGraw-Hill Education, 2017. ISBN: 978-1-25-964384-2.

[9] ZAKAMALDIN, A. A., ANDYK, V. S. Parametric identification of control systems using artificial neural networks. *MATEC Web of Conferences*. 2015, **37**, 01064. eISSN 2261-236X. Available from: https://doi.org/10.1051/matecconf/20153701064

[10] LIN, N., ZONG, C., TOMIZUKA, M., SONG, P., ZHANG, Z., LI, G. An overview on study of identification of driver behavior characteristics for automotive control. *Mathematical Problems in Engineering* [online]. 2014, **10**, 569109. ISSN 1024-123X, eISSN 1563-5147. Available from: https://doi.org/10.1155/2014/569109

[11] BELLET, T., MAYENOBE, P., BORNARD, J. C., PARIS, J. C., GRUYER, D., CLAVERIE, B. Human driver modelling and simulation into a virtual road environment. In: *Human modelling in assisted transportation: models, tools and risk methods*. CACCIABUE, P. C., HJALMDAHL, M., LUEDTKE, A., RICCIOLI, C. (Eds.). Milan, Italy: Springer, 2011. ISBN 978-88-470-1821-1, p. 251-262.

[12] IGARASHI, K., MIYAJIMA, C., ITOU, K., TAKEDA, K., ITAKURA, F., ABUT, H. Biometric identification using driving behavioral signals. In: IEEE International Conference on Multimedia and Expo ICME '04: proceedings [online]. Vol. 1. IEEE, 2004. ISBN 0-7803-8603-5, p. 65-68. Available from: https://doi.org/10.1109/ICME.2004.1394126

[13] KUANG, J. M., ZHANG, S. Application of controller with complex zeros in the photoelectric tracking system. *Advanced Materials Research* [online]. 2013, **756-759**, p. 673-677. ISSN 1662-8985. Available from: https://doi.org/10.4028/www.scientific.net/AMR.756-759.673

METHODOLOGY OF FORCE PARAMETERS JUSTIFICATION OF THE CONTROLLED STEERING WHEEL SUSPENSION

Bogdan Sokil [1], Oleg Lyashuk [2], Mariya Sokil [3], Yuriy Vovk [2,*], Iryna Lebid [4], Ivan Hevko [2], Mykhaylo Levkovych [2], Roman Khoroshun[2], Anatoliy Matviyishyn[2]

[1]Department of Engineering Mechanics, Hetman Petro Sahaidachnyi National Army Academy, Lviv, Ukraine
[2]Department of Automobiles, Ternopil Ivan Puluj National Technical University, Ternopil, Ukraine
[3]Department of Transport Technologies, Lviv Polytechnic National University, Lviv, Ukraine
[4]Department of International Transportation and Customs Control, National Transport University, Kyiv, Ukraine

*E-mail of corresponding author: vovkyuriy@ukr.net

Resume

The methodology for selecting the main force parameters of nonlinear non-conservative suspension for the main performance characteristics of wheeled vehicles has been developed based on the longitudinal-angular oscillations. The following has been established: a) change limits of static deformation of the elastic suspension system and its other parameters at which the basic operational characteristics for various ranges of amplitude change are satisfied; b) the amplitude of the initial perturbation of oscillations depending on the shape of the inequality and its entry speed; c) the influence of the main characteristics of damping devices on the amplitude-frequency characteristics. The results of this work can be a basis for the choice of such parameters of the considered controlled suspension, which ensure the stability of the vehicle along the curved sections of the road, its controllability, etc.

Article info

Received 20 March 2022
Accepted 25 April 2022
Online 21 June 2022

Keywords:

longitudinal-angular oscillations
sprung
suspension system
static deformation

Available online: https://doi.org/10.26552/com.C.2022.3.B247-B258

ISSN 1335-4205 (print version)
ISSN 2585-7878 (online version)

1 Introduction

Modern wheeled vehicles (WV) are increasingly using the so-called controlled (active or semi-active) suspension system (CSS) [1-4]. It, in contrast to traditional suspension systems with linear or nonlinear force characteristics, has the ability to “adjust” the force characteristics to the most optimal conditions of movement along the road with irregularities, its curvilinear sections or maneuvering. It is primarily a question of ensuring the smoothness of the course, the stability of the movement to overturn or shift. The specified “adjustment” of CSS by change of static deformation, rigidity characteristics and damping properties of the suspension system (SS) is carried out [2-4]. To design such CSS, more precisely, to create a software product for controlling the determining force parameters of the SS, the problem is the response of the sprung mass (SM) to changes in the magnitude of the force parameters of SS and various external perturbations caused by WV motion. The latter, within one or another physical and corresponding mathematical models of motion can be obtained based on the analytical dependences that follow from the above mentioned models. As for the mathematical models of the dynamics of WV motion, which are adequate to the force characteristics of the studied SS, they are usually ordinary nonlinear differential equations. It is a problematic task to obtain the analytical dependences on their basis, for creation of a software product. The use of numerical or real experiments for these dynamic models [5-8] does not lead to the desired results due to limited for many cases information about SM dynamics. Only in some cases (for linear and some nonlinear mathematical models of SM dynamics [9-15]) it is possible to obtain analytical dependences that can be the basis for creating a software product for controlling SS force parameters and kinematic parameters of WV motion with CSS [16-17]. Obtaining more general analytical dependences for the SS with non-conservative power characteristics, which would serve as a basis for creating a software product of controlled or semi-controlled SS is the subject of this work, hence its relevance.

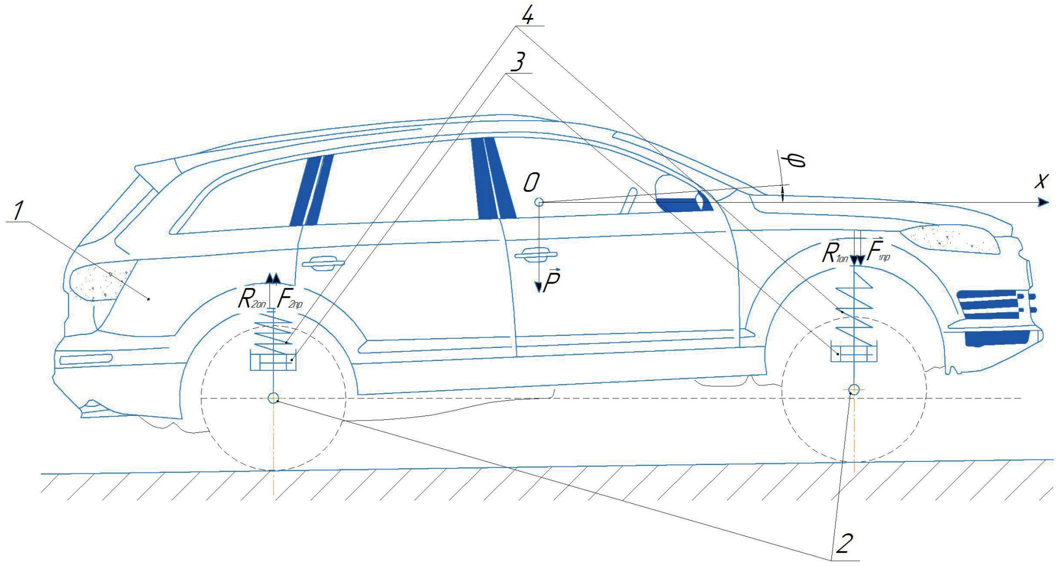

***Figure 1** Calculation scheme for the study of WV longitudinal oscillations with the distribution of forces acting on the SM*

2 Methodology

Longitudinal - angular oscillations of the SM are considered, which, considering the controllability, smoothness, passability are the most important for the vehicle. It has been stated that the restorative forces SS of the front (F_1) and rear (F_2) suspensions are described by more complex dependencies as in [9], namely

$$F_i(\Delta_i, \dot{\Delta}_i) = (\alpha_i + \beta_i(\dot{\Delta}_i)^{\nu_1})(\Delta_i)^{\nu_2+1}, \quad (1)$$

where Δ_i and $\dot{\Delta}_i$ are deformation and deformation rate, respectively, of the front ($i = 1$) and rear ($i = 2$) suspensions; $\alpha_i, \beta_i, \nu_1, \nu_2$ - constant, but ν_1, ν_2 are determined by dependencies $\nu_1 + 1 = (2m+1)/(2n+1)$, ($m,n,p,\ q$ = 0,1,2,...). These conditions are necessary and sufficient conditions for the existence of oscillatory processes in the relevant mechanical systems [18] In particular, the case $\beta_i = 0$ corresponds to the conservative law of change of SS restorative force (progressive - $\nu_2 > 0$ and regressive $-1 < \nu_2 < 0$)] and the case $\beta_i = 0, \nu_2 = 0$ - corresponds to the classical linear law of its change. Various aspects of the SM dynamics for these individual cases have been considered, for example, in [8, 11-12, 19-20]. As for the resistance forces of damping devices (shock absorbers), they, as in most cases of linear or nonlinear systems, depend on the rate of deformation of the elastic elements SS and are described by the dependences $\mathrm{R_{io o \Pi}} = \chi_i \dot{\Delta}_i^{2s+1}$, ($\chi_i$ and s - constants). In addition, the maximum values of these forces are small values compared to the maximum value of the restorative forces. This is a necessary condition for the oscillating motion of the SM during the motion of WV way with irregularities and to ensure the smoothness of WV stroke. At the same time, these conditions reduce the dynamic loads on the driver, passengers or transported goods. The task is to obtain such analytical dependences that describe the effect of the whole set of parameters $\nu_1, \nu_2, \alpha_i, \beta_i, \chi_i$ (including static deformation of the suspension system $\Delta_{cm.}$, as a derivative) on the amplitude-frequency characteristic (AFC) SM oscillations and which would also be the basis for creating a software product for controlling the power parameters of the suspension.

To solve this problem, the calculation model WV is a flat system of two bodies separated in [14] - sprung - 1 and unsprang mass - 2, which are connected by a suspension system (elastic shock absorbers - 3 and damping devices - 4, see Figure 1). In the process of WV movement SM performs longitudinal-angular oscillations. These oscillations play a crucial role in the study of such characteristics of movement as controllability, stability, smoothness, passability of the vehicle [21-26] and are the subject of the study). Therefore, to unambiguously determine the relative position of the SM at two moments of time, it is sufficient to choose the angle of rotation of it around the transverse axis, which passes through the centre of mass (point O) and perpendicular to the velocity vector of the specified point (angle)- $\varphi(t)$).

Notes.

1. The positive direction of the SM angle rotation is taken as in [26].
2. It is considered that during the movement by elastic deformations of tires caused by external factors are much smaller than the deformations of the suspension elements and therefore they are neglected in the mathematical model.

As for the static deformation of elastic elements, which determines the position of the centre of mass relative to the unsprang mass and hence to some extent the return path, it is, as follows from equation (1), determined as:

$$\Delta_{cm.} = \sqrt[\nu_2+1]{\frac{mg}{\alpha_1 + \alpha_2}}, \quad (2)$$

where m - the mass of the sprung part.

The above generally allows deformation of the SS elastic elements at any time to be presented in the form $\Delta_1 = a\varphi(t) - \Delta_{cm.}, \Delta_2 = b\varphi(t) + \Delta_{cm.}$. As a result, from the basic ratio for the relative motion of a body around an axis passing through its centre of mass is as following

$$I_0\ddot{\varphi} = -a(F_1\cdot(a\varphi - \Delta_{cm.}, a\dot{\varphi}) - R_{1on.}(\dot{\Delta}_1)) - b(F_2\cdot(b\varphi - \Delta_{cm.}, b\dot{\varphi}) - R_{1on.}(\dot{\Delta}_2)), \quad (3)$$

where I_0 - the moment of inertia of the sprung mass relative to the above transverse axis; a and b - the WV base.

Taking into account Equation (1), the last ratio is transformed into a form

$$I_o\ddot{\varphi} = -a\begin{pmatrix}(\alpha_1 + \beta_1(a\dot{\varphi})^{\nu_1})(a\varphi - \Delta_{\tilde{n}\grave{o}.})^{\nu_2+1} \\ +\chi_1(a\dot{\varphi})^{2s+1}\end{pmatrix} - b\begin{pmatrix}(\alpha_2 + \beta_2(a\dot{\varphi})^{\nu_1})(b\varphi - \Delta_{\tilde{n}\grave{o}.})^{\nu_2+1} \\ +\chi_2(b\dot{\varphi})^{2s+1}\end{pmatrix}. \quad (4)$$

Below, for simplicity, the angle $\varphi(t)$ is subtracted from the horizontal equilibrium position of SM and therefore the parameters α_1, α_2 associated with WV base and static deformation of the SM dependence $a\alpha_1(\Delta_{cm.})^{\nu_2+1} = b\alpha_2(\Delta_{cm.})^{\nu_2+1}$. In this case, the differential equation of longitudinal-angular oscillations for the first approximation can be represented as

$$\ddot{\varphi} + \frac{1}{I_o}(\beta_1 a^{\nu_1+\nu_2+2} + \beta_2 b^{\nu_1+\nu_2+2})\dot{\varphi}^{\nu_1}\varphi^{\nu_2+1} = \frac{1}{I_o}\begin{Bmatrix}-(\chi_1 a^{s+2} + \chi_1 b^{s+2})\dot{\varphi}^{2s+1} - \\ (\alpha_1 a^{\nu_2+2} + \alpha_1 b^{\nu_2+2})\varphi^{2\nu+1} + (\nu_2+1)\Delta_{cm.} \\ (\beta_1 a^{\nu_1+\nu_2+1} + \beta_2 b^{\nu_1+\nu_2+1})\dot{\varphi}^{\nu_1}\varphi^{\nu_2}\end{Bmatrix}. \quad (5)$$

Thus, the solution of the problem has been reduced to finding and studying the solution of the nonlinear Equation (5). The above restrictions on the recovery force of the suspension system and the resistance force of the damping devices (shock absorbers) will help to find it. From these limitations it follows that the maximum value of the right-hand side of Equation (5) is a small value in comparison to the main part of the nonlinear reducing force SS (arc term of the left-hand side of this equation). This is the basis for application of the general ideas of perturbation methods [26-27] adapted in [28] to construct an asymptotic solution of a similar class of nonlinear equations. According to those, first of all it is necessary to describe the undisturbed motion of SM. These SM oscillations correspond to the differential equation

$$\ddot{\varphi} + \frac{1}{I_o}(\beta_1 a^{\nu_1+\nu_2+2} + \beta_2 b^{\nu_1+\nu_2+2})\dot{\varphi}^{\nu_1}\varphi^{\nu_2+1} = 0, \quad (6)$$

and they are described using the periodic Ateb functions [28-30] in the form

$$\varphi(t) = a_\varphi ca(\nu_2 + 1, (1-\nu_1)^{-1}, \omega(a_\varphi)t + \theta)), \quad (7)$$

where a_φ - of amplitude, $\omega(a_\phi)t + \theta$ - phase, θ - initial phase, $\omega(a_\varphi)$ - natural frequency of oscillations. The latter, as for the most nonlinear oscillatory systems, depends on the amplitude and is determined by the ratio

$$\omega(a_\varphi) = \frac{\nu_2+2}{2}\left(\frac{\frac{1}{I_o}(\beta_1 a^{\nu_1+\nu_2+2} + \beta_2 b^{\nu_1+\nu_2+2})}{\frac{2-\nu_1}{(1-\nu_1)(\nu_2+2)}}\right)^{\frac{1}{2-\nu_1}} a_\varphi^{\frac{\nu_1+\nu_2}{2-\nu_1}}. \quad (8)$$

3 Results

If it was supposed that the SM mass WV is distributed along its entire “area” evenly, then the moment of SM inertia is determined by the dependence $I_0 = \frac{m}{3}\left(\frac{a^3}{a+b} + \frac{b^3}{a+b} + c^2/4\right)$ and to describe the frequency of natural oscillations, a more convenient dependence, which takes into account the static deformation of SM can be used. Static deformation is one of the control parameters of the SM oscillatory process in order to provide the most comfortable conditions for the WV movement way with irregularities. In this case, equation (8) takes the form

$$\omega(a_\varphi) = \frac{\nu_2+2}{2}\Theta a_\varphi^{\frac{\nu_1+\nu_2}{2-\nu_1}}, \quad (9)$$

where

$$\Theta = \left[\frac{\frac{2-\nu_1}{(1-\nu_1)(\nu_2+2)}}{\frac{3g(\beta_1 a^{\nu_1+\nu_2+2} + \beta_2 b^{\nu_1+\nu_2+2})}{(\alpha_1+\alpha_2)\Delta_{cm.}^{\nu_2+1}(a^2+b^2-ab+c^2/4)}}\right]^{\frac{1}{2-\nu_1}}.$$

Figure 2 shows the dependences of SM natural oscillation frequency in hertz $f = \frac{\omega(a_\varphi)}{2\Pi}$ from static deformation at different values of the amplitude of longitudinal-angular oscillations and parameters ν_1, ν_2 (Figure 3), Π - the half period of the Ateb functions used, i.e. $\Pi = \Gamma\left(\frac{1-\nu_1}{2-\nu_1}\right)\Gamma\left(\frac{1}{\nu_2+2}\right)\Gamma^{-1}\left(\frac{1-\nu_1}{2-\nu_1} + \frac{1}{\nu_2+2}\right)$.

Therefore, for a suspension system with a non - conservative law of change of the regenerative force of elastic shock absorbers, for the case of their greater static deformation, the frequency of natural longitudinal - angular oscillations is lower. Moreover, a larger value of the amplitude of oscillations corresponds to a larger value of the frequency, except when ν_1, ν_2, are approaching -1. At the same time in the case $\nu_1 = -\nu_2$, resulting from the Equation (9), the natural frequency is determined only by the power characteristics of the SS, that is, a similar phenomenon occurs as for linear systems (isochronous oscillations of SM). As for the dependence

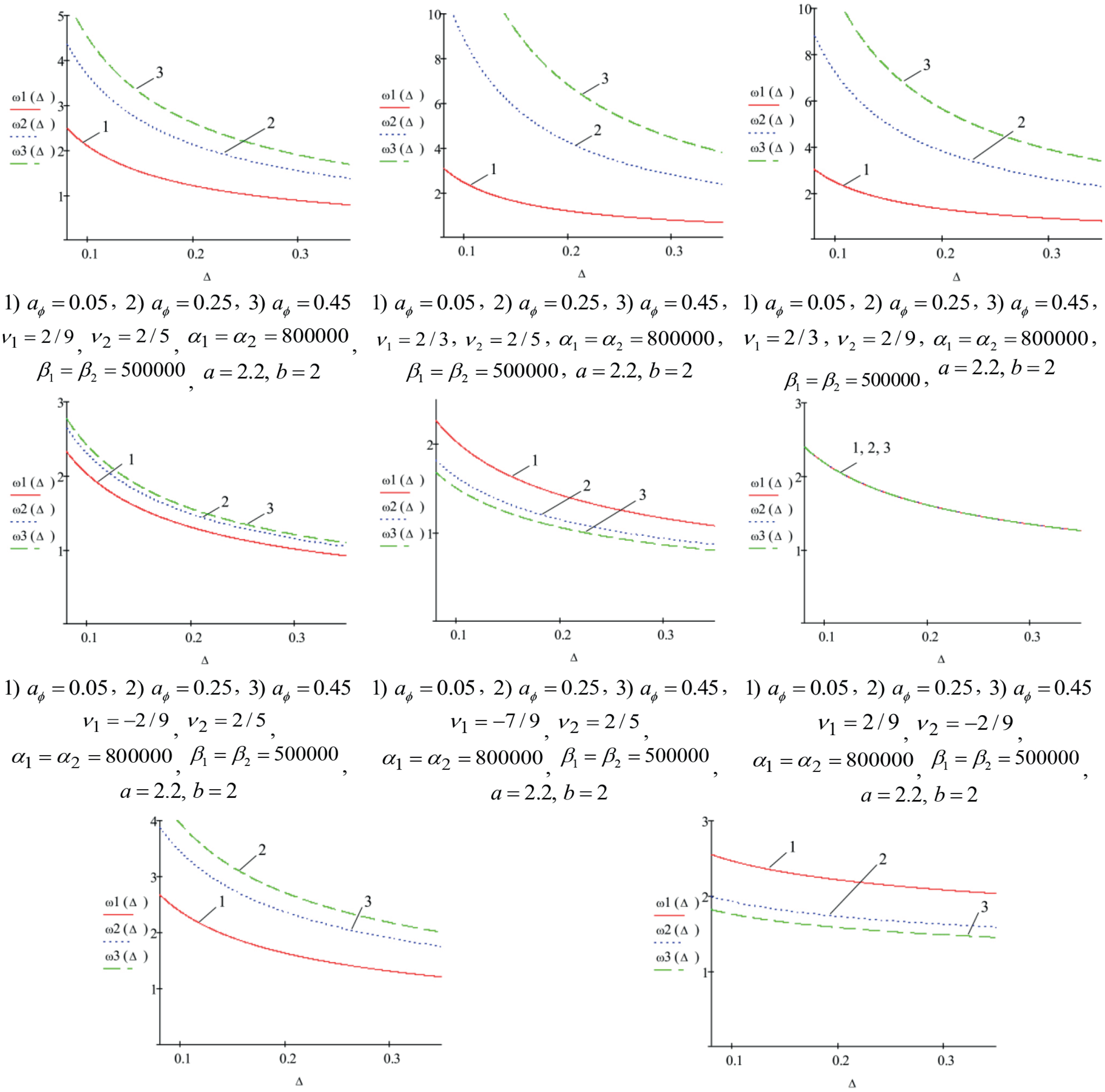

1) $a_\phi = 0.05$, 2) $a_\phi = 0.25$, 3) $a_\phi = 0.45$; $\nu_1 = 2/9$, $\nu_2 = 2/5$, $\alpha_1 = \alpha_2 = 800000$, $\beta_1 = \beta_2 = 500000$, $a = 2.2,\ b = 2$

1) $a_\phi = 0.05$, 2) $a_\phi = 0.25$, 3) $a_\phi = 0.45$, $\nu_1 = 2/3$, $\nu_2 = 2/5$, $\alpha_1 = \alpha_2 = 800000$, $\beta_1 = \beta_2 = 500000$, $a = 2.2,\ b = 2$

1) $a_\phi = 0.05$, 2) $a_\phi = 0.25$, 3) $a_\phi = 0.45$, $\nu_1 = 2/3$, $\nu_2 = 2/9$, $\alpha_1 = \alpha_2 = 800000$, $\beta_1 = \beta_2 = 500000$, $a = 2.2,\ b = 2$

1) $a_\phi = 0.05$, 2) $a_\phi = 0.25$, 3) $a_\phi = 0.45$; $\nu_1 = -2/9$, $\nu_2 = 2/5$, $\alpha_1 = \alpha_2 = 800000$, $\beta_1 = \beta_2 = 500000$, $a = 2.2,\ b = 2$

1) $a_\phi = 0.05$, 2) $a_\phi = 0.25$, 3) $a_\phi = 0.45$, $\nu_1 = -7/9$, $\nu_2 = 2/5$, $\alpha_1 = \alpha_2 = 800000$, $\beta_1 = \beta_2 = 500000$, $a = 2.2,\ b = 2$

1) $a_\phi = 0.05$, 2) $a_\phi = 0.25$, 3) $a_\phi = 0.45$; $\nu_1 = 2/9$, $\nu_2 = -2/9$, $\alpha_1 = \alpha_2 = 800000$, $\beta_1 = \beta_2 = 500000$, $a = 2.2,\ b = 2$

1) $a_\phi = 0.05$, 2) $a_\phi = 0.25$, 3) $a_\phi = 0.45$; $\nu_1 = 5/9$, $\nu_2 = -2/9$, $\alpha_1 = \alpha_2 = 800000$, $\beta_1 = \beta_2 = 500000$, $a = 2.2,\ b = 2$

1) $a_\phi = 0.05$, 2) $a_\phi = 0.25$, 3) $a_\phi = 0.45$; $\nu_1 = 5/9$, $\nu_2 = -7/9$, $\alpha_1 = \alpha_2 = 800000$, $\beta_1 = \beta_2 = 500000$, $a = 2.2,\ b = 2$

Figure 2 *Dependence of the SM natural oscillations frequency on static deformation at different values of oscillations amplitudes and parameters* ν_1, ν_2

of the frequency (period) of oscillations on the amplitude, it is for cases $\nu_1 > 0, \nu_2 > 0; \nu_1 > 0, -1 < \nu_2 < 0$ and $-1 < \nu_1 < 0, \nu_2 > 0$ a larger value of the amplitude corresponds to a larger value of frequency (smaller period); in case $-1 < \nu_1 < 0, -1 < \nu_2 < 0$ corresponds to an increase in frequency when the amplitude remains. If it is taken into account that the dynamic loads, acting on passengers and (cargo) transported for larger values of frequency and amplitude are large, then based on the choice of SS characteristics given the dynamic loads for the case of WV movement along the road with significant irregularities, it is advisable to choose parameters adaptive suspension that satisfy the condition: $-1 < \nu_1 < 0, -1 < \nu_2 < 0$.

Equation (9) is used simultaneously to solve the inverse problem - to determine the relationship between the amplitude of perturbation of longitudinal - angular oscillations $\overline{a}_\varphi$, which are caused by the collision of WV on the inequality of the way at which the frequency of these oscillations takes values $\overline{\omega}_n$. Assuming that the vehicle is moving at a constant speed V hitting the uneven way of a smooth shape $y = g(x)$ at a point with a coordinate x_0 at inseparable contact of a wheel and a way, it has been receive that speed of perturbation of longitudinal-angular fluctuations $\hat{V}$ of the mounting points of the shock absorbers and SM is determined by

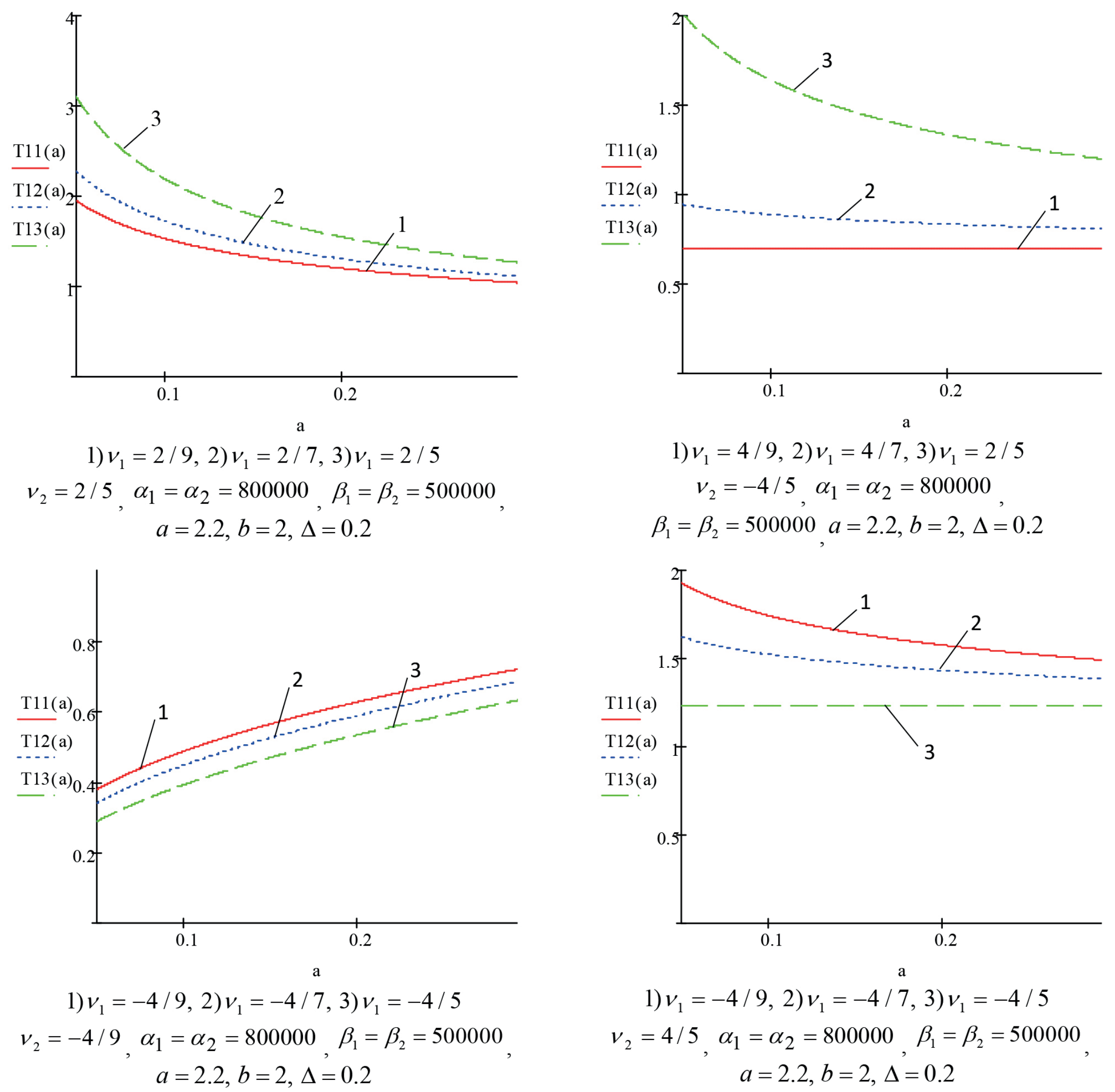

Figure 3 *Dependence of the period of the SM natural oscillations on the amplitude of longitudinal-angular oscillations at different values* ν_1, ν_2

the dependence $\hat{V} = V\sin\phi$ (ϕ - the angle of inclination of the tangent to the inequality of the path at the point with the coordinate x_0). Obviously that $tg\phi = \dfrac{dg}{dx_{|x=x0}}$. On the other hand, the value of the specified component of the speed of the mounting point of the shock absorbers and SM is equal $\hat{V} = \omega_{|x=x0} h$, h - the distance of the specified point to the axis of SM relative rotation around the point passing through the centre of mass of the specified part and, therefore, $h = \sqrt{a^2 + c^2}$.

On the other hand

$$\omega_{|x=x0} = \frac{d\varphi(t)}{dt} = \overline{a}_\varphi \times \times \frac{d(ca(\nu_2+1,(1-\nu_1)^{-1},\omega(a_\varphi)t+\theta)))}{dt}_{|t-t0} = \overline{a}_\varphi \overline{\omega}_n(\overline{a}_\varphi) \frac{d(ca(\nu_2+1,(1-\nu_1)^{-1},\psi))}{d\psi}_{|t-t0}, \quad \psi = \omega(a_\varphi)t + \theta, \tag{10}$$

where t_0- the moment of wheel entry on the unevenness. Limited in Equation (10) to the extreme value of the function $\dfrac{d(ca(\nu_2+1,(1-\nu_1)^{-1},\psi))}{d\psi}$ the ratio that relates the required values has been obtained

$$\frac{1}{\Theta}\overline{a}_\varphi^{\frac{\nu_1+\nu_2}{2-\nu_1}} - \frac{\nu_2+2}{2\overline{\omega}_n}\overline{a}_\varphi = 0. \tag{11}$$

It determines the amplitude of longitudinal - angular oscillations perturbation as parameters function of the suspension and frequency in the form

$$\overline{a}_\varphi = \left(\frac{\nu_2+2}{2\overline{\omega}_{n.}}\Theta\right)^{\frac{\nu_1-2}{\nu_2+2}}. \tag{12}$$

If in the last expression it is passed to the velocity WV and the inequality profile, then the above is equivalent to the following

$$\overline{a}_\varphi = \left(\frac{2V\dfrac{dg}{dx_{|x=x0}}}{(\nu_2+2)h\Theta}\right)^{\frac{2-\nu_1}{2+\nu_2}} \tag{13}$$

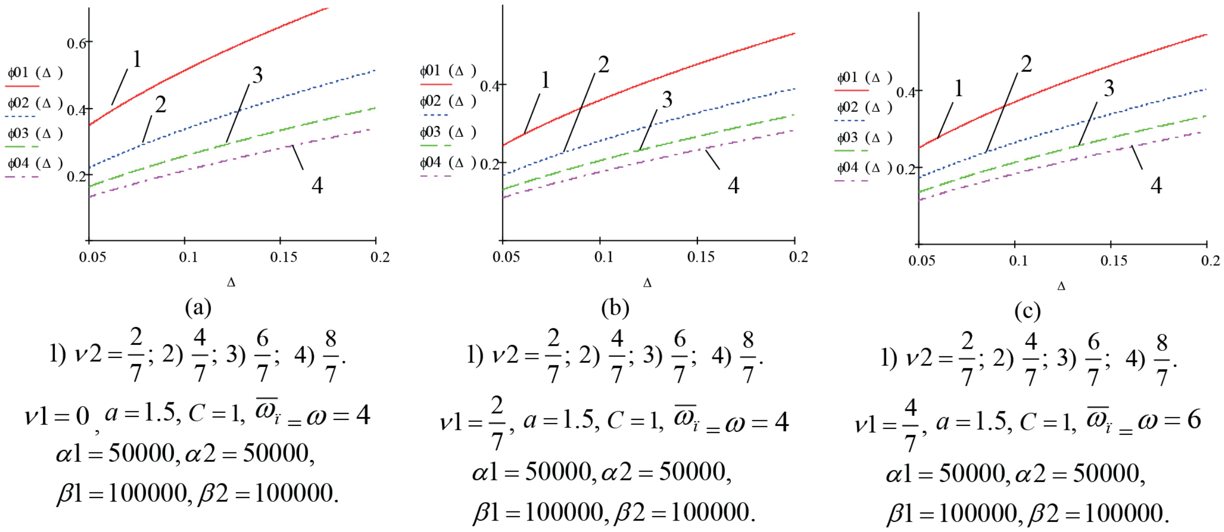

Figure 4 *Dependence of amplitudes of undisturbed motion of longitudinal - angular oscillations on static deformation of the suspension system, provided that the frequencies of these oscillations take the specified values* $\overline{\omega}_n = \omega = 4$ *(a), (b) and* $\overline{\omega}_n = \omega = 6$ *(c)???*

Figure 4 shows the dependence of the amplitude on the static deformation to the Equation (12) for various parameters that characterize WV controlled suspension, provided that the angular velocity, along the angular oscillations, takes a given value $\overline{\omega}_n$.

As expected, for an SS with a progressive law of change of regenerative force, as well as in the case of $\nu_1 > 0, \nu_2 > 0$, a larger value of static deformation corresponds to a larger value; of the amplitude of transverse-angular oscillations at which their frequency takes a given value, in addition, in the case of larger values of the parameter ν_2 it is smaller.

The above Equations (8), (11) serve as a basis for creating a CSS software product. Indeed, if for the base value of the specified suspension system to choose static deformation, it is a function of kinematic and force parameters SS is determined by the ratio

$$\Delta_{st.} = \left(\frac{\nu_2+2}{2\overline{\omega}_{n.}}\right)^{\frac{\nu_1-2}{\nu_2+1}} \times \frac{\left(\begin{matrix}(\alpha_1+\alpha_2)(1-\nu_1)(\nu_2+2)\times \\ (a^2+b^2-ab+c^2/4)\end{matrix}\right)^{\frac{1}{1+\nu_2}}}{(3g(2-\nu_1)(\beta_1 a^{\nu_1+\nu_2+2}+\beta_2 b^{\nu_1+\nu_2+2}))^{\frac{1}{1+\nu_2}}} \times . \\ \times \overline{a}_{\varphi}^{\frac{\nu_2+2}{\nu_2+1}}. \qquad (14)$$

Figure 5 presents the dependence of the static deformation on the amplitude of transverse-angular oscillations at which their frequency takes values $\overline{\omega}_s$.

The presented graphical dependences show that for the considered suspension system in a wide range of changes of amplitudes of longitudinal-angular oscillations the SS with small values of its static deformation satisfies ergonomic operating conditions for small amplitudes of oscillations. With increasing amplitudes of oscillations, the magnitude of static deformation should increase and the growth rate of static deformation is less for the progressive and regressive characteristics of the SS with a smaller value of the parameter ν_2; in case $\nu_1 < 0, \nu_2 < 0$ - greater for smaller values of the parameter values ν_2; in case $\nu_1 < 0, \nu_2 > 0$ - smaller for larger parameter values ν_2.

The influence of the power characteristics of the damping devices (shock absorbers) SS on the AFC oscillations SM has been determined. This can be done based on the solution of the perturbed Equation (5). The influence of these SS elements is manifested, as for all the suspensions, in time reduction of oscillations amplitude. The latter automatically causes a change in the frequency of oscillations. This change can be analytically determined based on the asymptotic solution of Equation (5). The simplest way to find it for the approximation under consideration is the method, which is based on the basic idea of the Van der Paul method [26]. According to the main idea of the abovementioned method, the perturbed motion SM is described by the dependence

$$\varphi(t) = a_{\varphi} ca\left(\begin{matrix}\nu_2+1, \frac{1}{1-\nu_1}, \\ \omega(a_{\varphi}(t))t+\theta(u)\end{matrix}\right). \qquad (15)$$

The problem arises in describing the law how the unknown functions $a_{\varphi}(t)$ and $\theta(t)$ change depending on the form of the right-hand side of equation (5). For this purpose, by differentiating Equation (15) with respect to time, it has been obtained

$$\dot{\varphi}(t) = \dot{a}_{\varphi}(t) ca\left(\begin{matrix}\nu_2+1, \frac{1}{1-\nu_1}, \\ \omega(a_{\varphi})t+\theta(t)\end{matrix}\right) - \\ \frac{2}{\nu_2+2} a_{\varphi}(t)(\omega(a_{\varphi})t)+\dot{\theta}(t)) sa^{\frac{1}{1-\nu_1}} \times \\ \left(\frac{1}{1-\nu_1}, \nu_2+1, \omega(a_{\varphi})t+\theta(t)\right). \qquad (16)$$

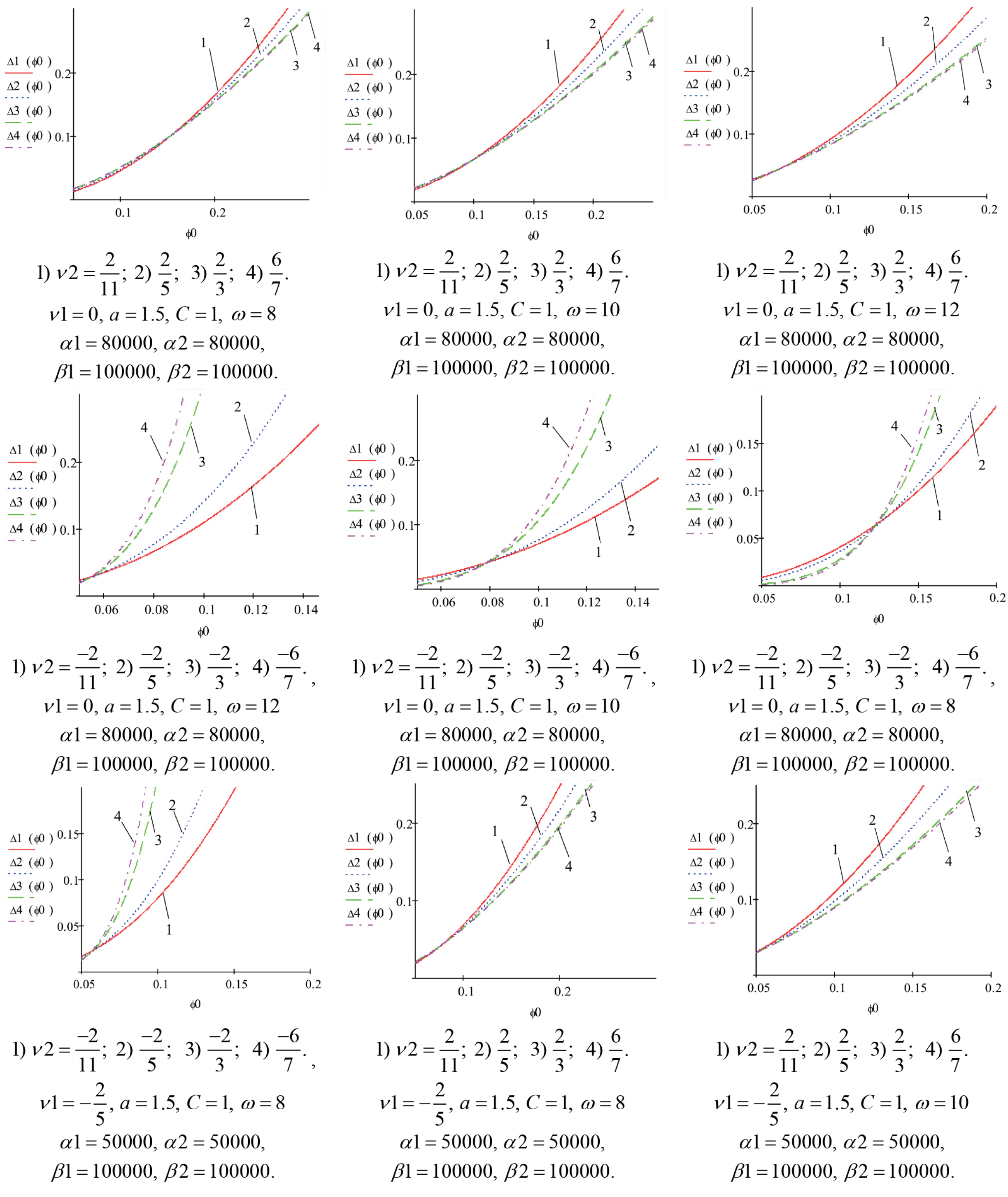

***Figure 5** Values of the SS static deformation at which the frequency of transverse angular oscillations takes set values at different oscillation amplitudes*

The following differentiation by the independent variable and taking into account the undisturbed case $\dot{\varphi}(t) = -\frac{2}{\nu_2+2}a_\varphi\omega(a_\varphi)sa^{\frac{1}{1-\nu_1}}((1-\nu_1)^{-1},\nu_2+1,\psi))$, $\psi = \omega(a_\varphi)t+\theta(t)$, one obtains:

$$\ddot{\varphi}(t) = \frac{4}{(\nu_2+2)(2-\nu_1)}a_\varphi(t)\omega(a_\varphi(t))sa^{\frac{\nu_1}{1-\nu_1}}((1-\nu_1)^{-1},\nu_2+1,\psi))ca^{\nu_2+1}\begin{pmatrix}\nu_2+1,\\(1-\nu_1)^{-1},\psi)\end{pmatrix}\times$$
$$(\omega(a_\varphi(t))+\dot{\theta}(t)) - \frac{2\dot{a}_\varphi(t)}{\nu_2+2}\begin{pmatrix}\omega(a_\varphi(t))+\\a_\varphi\frac{d\omega(a_\varphi(t))}{da_\varphi}\end{pmatrix}sa^{\frac{1}{1-\nu_1}}((1-\nu_1)^{-1},\nu_2+1,\psi). \quad (17)$$

If taking into consideration the form of the relation that describes the natural frequency of SM oscillations, then the dependence $\omega(a_\varphi) + a\frac{d\omega(a_\varphi)}{da_\varphi}$ y in Equation (17) can be replaced by a simpler one, namely: $\omega(a_\varphi) + a_\varphi\frac{d\omega(a_\varphi)}{da_\varphi} = \frac{2+\nu_2}{2-\nu_1}\omega(a_\varphi)$. Taken together allows to obtain a system of the first-order differential equations, from Equation (5), that describe the laws of change of amplitude and frequency of perturbed motion

$$\begin{aligned}&\dot{a}_\varphi(t)ca\left(\nu_2+1,(1-\nu_1)^{-1},\psi\right)\right) - \frac{2}{\nu_2+2}\times\\&a_\varphi(t)\dot{\theta}(t)sa^{\frac{1}{1-\nu_1}}\left((1-\nu_1)^{-1},\nu_2+1,\psi\right)\right) = 0,\\&\frac{2+\nu_2}{2-\nu_1}\dot{a}_\varphi(t)sa\left((1-\nu_1)^{-1},\nu_2+1,\psi\right) + \frac{2}{(2-\nu_1)}\times\\&a_\varphi(t)\dot{\theta}(t)ca^{\nu_2+1}\left(\nu_2+1,(1-\nu_1)^{-1},\psi\right)\right) = \frac{\nu_2+2}{2\omega(a_\varphi)}\times\\&sa^{\frac{\nu_1}{\nu_1-1}}\left((1-\nu_1)^{-1},\nu_2+1,\psi\right)\right)f(a_\varphi,\dot{a}_\varphi,\psi)\end{aligned} \tag{18}$$

where $f(a_\varphi,\dot{a}_\varphi,\psi)$ corresponds to the value of the right-hand side of Equation (5), provided that $\varphi(t)$ and $\dot{\varphi}(t)$ take the main values. From the above system of differential equations, it has been found

$$\begin{aligned}&\dot{a}_\varphi(t) = -\frac{2-\nu_1}{2\omega(a)}sa\left((1-\nu_1)^{-1},\nu_2+1,\psi\right)\right)\times\\&f(a_\varphi,\dot{a}_\varphi,\psi)\\&\dot{\theta}(t) = -\frac{(\nu_2+2)(2-\nu_1)}{4a_\varphi\omega(a_\varphi)}ca\begin{pmatrix}\nu_2+1,\\(1-\nu_1)^{-1},\psi)\end{pmatrix}\times\\&sa^{\frac{\nu_1}{\nu_1-1}}\left((1-\nu_1)^{-1},\nu_2+1,\psi\right)\right)f(a_\varphi,\dot{a}_\varphi,\psi).\end{aligned} \tag{19}$$

It can be greatly simplified based on the following considerations: the speed (rate) of amplitude change and oscillations parameter $\dot{\theta}(t)$ are slowly changing functions of time and therefore the maximum values of their change over the period of oscillations SM are insignificant. This is the basis for averaging the right-hand sides of Equations (19) by the phase of oscillations. Thus, for the first approximation, the differential equations describing the basic parameters of the SM oscillations take the form

$$\begin{aligned}&\dot{a}_\varphi(t) = -\frac{2-\nu_1}{4\omega(a_\varphi)\Pi}\left(-\frac{2}{\nu_2+2}a_\varphi(t)\omega(a_\varphi)\right)^{2s+1}\\&\times\frac{2\Gamma\left(\frac{2(s-\nu_1)+1}{2-\nu_1}(1-\nu_1)\right)\Gamma\left(\frac{1}{\nu_2+2}\right)}{\Gamma\left(\frac{1}{\nu_2+2}+\frac{2(s-\nu_1)+1}{2-\nu_1}(1-\nu_1)\right)}\\&\frac{d\psi}{dt} = \omega(a_\varphi).\end{aligned} \tag{20}$$

Figures 6 and 7 present (for different parameters that describe the force characteristics of the suspension system) the laws of change in time of the amplitude and frequency of longitudinal-angular SM KTZ oscillations.

The presented graphical dependences show that the qualitative picture of the decrease (decline) of the amplitude of the longitudinal-angular parameters of the main suspension system has a negligible effect. As for the quantitative side, then, for example, for cases $\nu_1 < 0, \nu_2 > 0; \nu_1 > 0, \nu_2 < 0; \nu_1 > 0, \nu_2 > 0$ a larger value of the parameter ν_2 corresponds to a lower rate of decline in time of oscillations amplitude; for the case $\nu_1 > 0, \nu_2 > 0$ a larger value of the parameter ν_2 - lower rate of decrease of oscillations amplitude.

As for the change in time of the frequency of damped longitudinal-angular oscillations, then the parameters that characterize the suspension system affect not only the qualitative, as well as the quantitative characteristics of the change in the frequency of natural oscillations. So, for the case $\nu_1 < 0, \nu_1 > 0$ a larger value of ν_2 corresponds more to the value of the natural frequency and for cases $\nu_1 < 0, \nu_2 < 0; \nu_1 > 0, \nu_2 < 0; \nu_1 > 0, \nu_2 > 0$ a larger value of parameter ν_2 correspond to the lower values of natural frequencies. In particular, when $\nu_1 = \frac{2}{3}, a_\varphi = 0.25, \Delta_{st} = 0.2$ increasing the value of the parameter ν_2 from $\frac{2}{9}$ to $\frac{2}{5}$ causes a decrease in the frequency of oscillations in 2.65 times and at the amplitude of oscillations $a_\varphi = 0.05$ for all other values of the specified parameters - in 1.02 times.

4 Conclusion

The proposed research methodology of basic parameters influence, which characterize the nonlinear nonconservative system of suspension of a WV, has been proposed in the study and allows with accuracy necessary for engineering research, to receive analytical dependences of an estimation of their influence on defining parameters of longitudinal-angular fluctuations. The non-protection of the oscillatory process is a peculiarity of the latter, as for almost all the nonlinear oscillatory systems. Despite this, the methodology also allows to establish the influence of the main kinematic parameters of a vehicle, the main external factors of traffic disturbance on the amplitude-frequency characteristics of the longitudinal-angular oscillations of the sprung part. The latter is the basis for assessing and maximizing the WV performance, such as smoothness, dynamic stability along curved sections of road and during maneuvering, the passability of the load on the crew and passengers (transported goods), etc. Therefore, the obtained results can serve as a basis for creation of a software product of the adaptive suspension system with the studied SS power characteristics. In particular, based on the dynamic loads during the collision with the unevenness of the road, in order to minimize the latter, it is necessary that the parameters that characterize the nonlinear conservative force change within: $-1 < \nu_1 < 0, -1 < \nu_2 < 0$, at the same time, after overcoming the unevenness of the path, the adaptive suspension system must switch to their values within $\nu_1 > 0, \nu_2 > 0$.

As for the specific results that follow from the obtained results and relate to the choice of another important parameter for controlling the dynamics of SM - static deformation, the ergonomic operating conditions

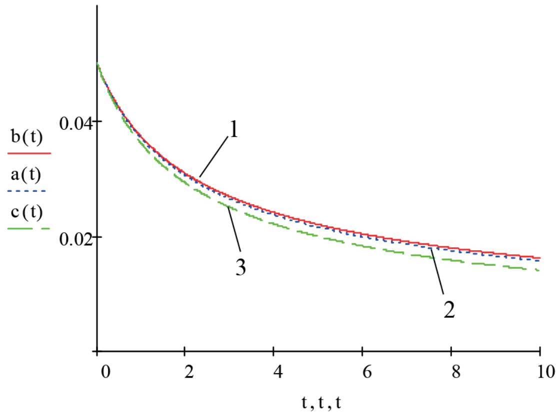

1) $\nu_2 = \nu 21 = 2/7$; 2) $\nu 22 = 2/9$; 3) $\nu 23 = 0$.

$\alpha_1 = \alpha_2 = 800000 ... \Delta = 0.30$

$\beta_1 = \beta_2 = 500000, \nu_1 = -2/5$

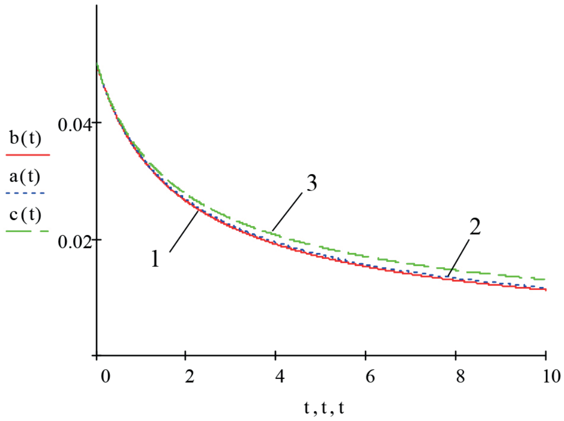

1) $\nu_2 = \nu 21 = -2/7$; 2) $\nu 22 = -2/9$; 3) $\nu 23 = 0$.

$\alpha_1 = \alpha_2 = 800000 ... \Delta = 0.25$

$\beta_1 = \beta_2 = 500000, \nu_1 = -2/5$

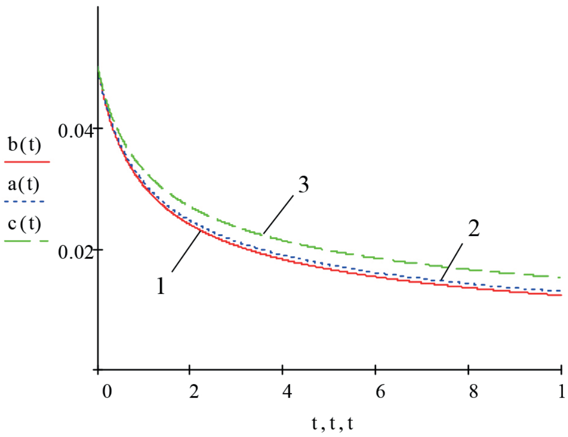

1) $\nu_2 = \nu 21 = -2/7$; 2) $\nu 22 = -2/9$; 3) $\nu 23 = 0$.

$\alpha_1 = \alpha_2 = 800000 ... \Delta = 0.25$

$\beta_1 = \beta_2 = 500000, \nu_1 = 2/5$

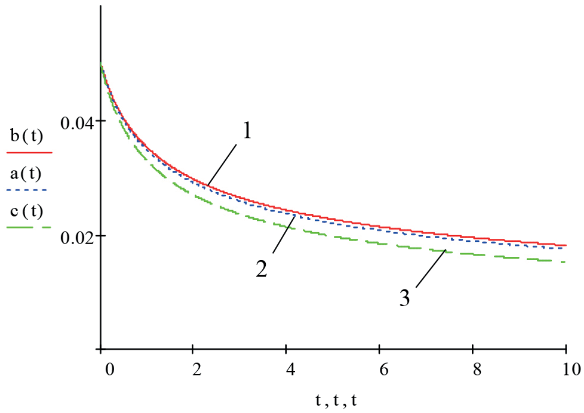

1) $\nu_2 = \nu 21 = 2/7$; 2) $\nu 22 = 2/9$; 3) $\nu 23 = 0$.

$\alpha_1 = \alpha_2 = 800000 ... \Delta = 0.25$

$\beta_1 = \beta_2 = 500000, \nu_1 = 2/5$

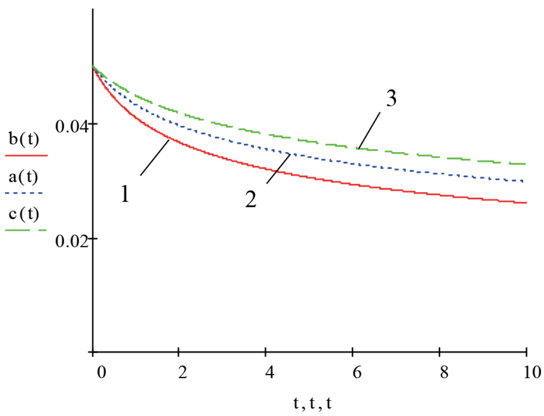

1) $\nu_2 = \nu 21 = 2/7$; 2) $\nu 22 = -2/9$; 3) $\nu 23 = 0$.

$\alpha_1 = \alpha_2 = 800000 ... \Delta = 0.25$

$\beta_1 = \beta_2 = 500000, \nu_1 = 2/5$

Figure 6 *Laws of decreasing amplitude of transverse-angular oscillations of the inverter at different values of its SS force characteristics*

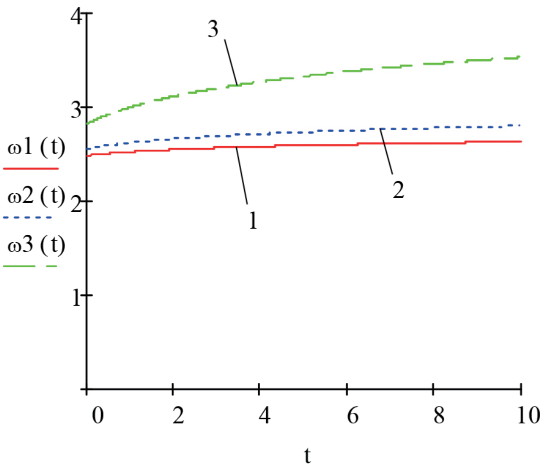

1) $\nu_2 = \nu 21 = 2/7;\ 2)\nu 22 = 2/9;\ 3)\nu 23 = 0.$

$\alpha_1 = \alpha_2 = 800000 ... \Delta = 0.25$

$\beta_1 = \beta_2 = 500000, \nu_1 = -2/5$

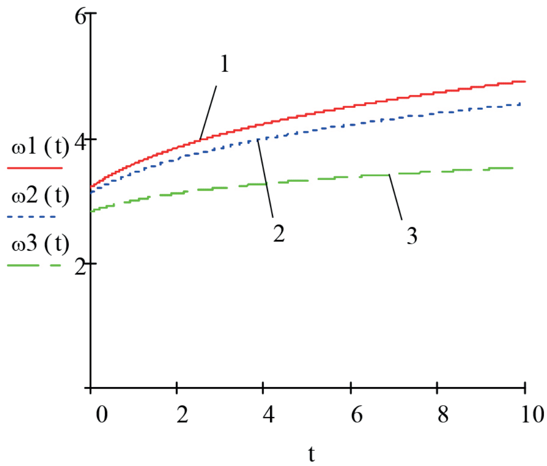

1) $\nu_2 = \nu 21 = -2/7;\ 2)\nu 22 = -2/9;\ 3)\nu 23 = 0.$

$\alpha_1 = \alpha_2 = 800000 ... \Delta = 0.25$

$\beta_1 = \beta_2 = 500000, \nu_1 = -2/5$

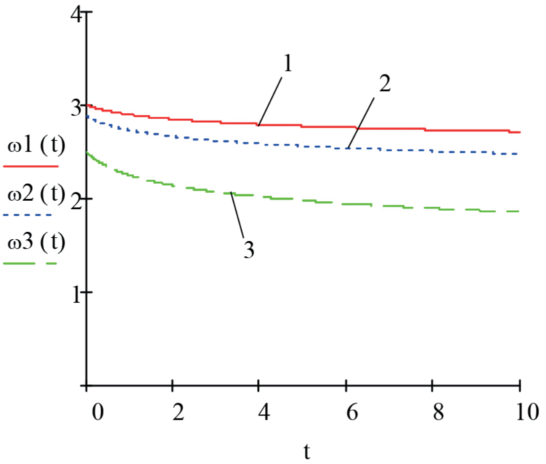

1) $\nu_2 = \nu 21 = -2/7;\ 2)\nu 22 = -2/9;\ 3)\nu 23 = 0.$

$\alpha_1 = \alpha_2 = 800000 ... \Delta = 0.25$

$\beta_1 = \beta_2 = 500000, \nu_1 = 2/5$

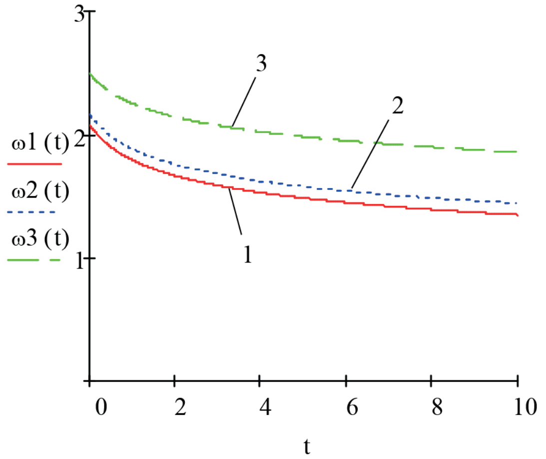

1) $\nu_2 = \nu 21 = 2/7;\ 2)\nu 22 = 2/9;\ 3)\nu 23 = 0.$

$\alpha_1 = \alpha_2 = 800000 ... \Delta = 0.25$

$\beta_1 = \beta_2 = 500000, \nu_1 = 2/5$

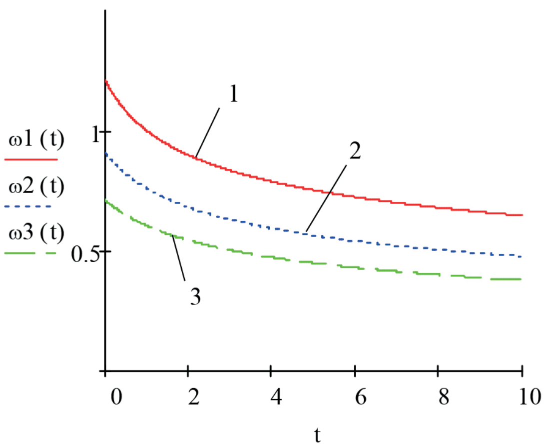

1) $\nu_2 = \nu 21 = 8/7;\ 2)\nu 22 = 8/5;\ 3)\nu 23 = 2.$

$\alpha_1 = \alpha_2 = 800000 ... \Delta = 0.25$

$\beta_1 = \beta_2 = 500000, \nu_1 = 2/5$

Figure 7 *Laws of change in time of the frequency of transverse-angular oscillations of the inverter at different values of its force characteristics* are more satisfied with suspensions with the following values of the nonlinearity parameters $\nu_1 > 0, \nu_2 > 0$ - for small amplitudes of oscillations and suspension deformation of elastic shock-absorbers, which change within $0.2m < \Delta_{st.} < 0.35m$ and $-1 < \nu_1 < 0,\ \nu_2 > 0$ - for large oscillation amplitudes. If the dynamic process of SM is considered as a continuous (damped oscillations after hitting the uneven path) in a wide range of changes in the amplitude of oscillations, so a controlled suspension with the following characteristics is the most favourable from the ergonomic side: $0.2m < \Delta_{st.} < 0.3m$ for $0 < \nu_1 < 2/5$ and $0 < \nu_2 < 8/7$.

The results obtained above will serve as a basis for solving no less important tasks - the study of resonant SM WV phenomena with a controlled suspension system, stability and controllability of vehicles.

References

[1] MANDRIKA, V. R., SHLYKOVA, V. G. Controllability and stability of the B-class car with ESP system. *Bulletin of the National Technical University "KhPI". Series: Transport and Machine Building*. 2013, **31**(1004), p. 69-65. ISSN 2079-0066.

[2] PAVLENKO, V. M., KRYVORUCHKO, O. O. The current state of development of active suspensions of cars. *Bulletin of the National Technical University "KhPI". Series: Automobile and Tractor Construction.* 2014, **9**(1052), p. 54-60. ISSN 2078-6840.

[3] DERBAREMDIKER, A. D., MUSARSKY, R. A., STEPANOV, I. O., YUDKEVICH, M. A. Self-adjusting shock absorber with programmed damping characteristics. *Automotive Industry* [online]. 1985, **1**, p. 13-15. ISSN 0005-2337. Available from: https://www.booksite.ru/promych/1985/1985_1.pdf

[4] Adaptive suspension. Device, principle of operation [online]. Available from: http://www.autoobserver.ru/sistemi-auto/76-adaptivnaya-podveskaustroystvo-i-princip-deystviya-aktivnoypodveski.html

[5] DUSHCHENKO, V. V. Disadvantages, reasons for their occurrence and contradictions in the development of the known physical principles of action of elastic elements of suspension systems for military tracked and wheeled vehicles. *Bulletin of NTU "KhPI». Collection of Scientific Papers. Thematic Issue: Transport Engineering* [online]. 2007, **33**, p. 46-52. ISSN 2079-0066. Available from: http://repository.kpi.kharkov.ua/handle/KhPI-Press/3044

[6] MELNYCHUK, S. V., PODCHASHIVSKY, Y. O., VITYUK, I. V., BOVSUNIVSKY, I. A. Determination of smoothness parameters of the suspension model based on a four-link lever mechanism. *Bulletin of ZhSTU* [online]. 2010, **4**(55), p. 25-27. ISSN 2409-7470. Available from: https://doi.org/10.33405/2409-7470/2020/1/35/207354

[7] PAVLENKO, V. P. State of development of methods of car suspension diagnostics. *Bulletin of NTU "KhPI". Series: Automobile and Tractor Construction* [online]. 2012, **64**(970), p. 63- 69. ISSN 2078-6840. Available from: http://repository.kpi.kharkov.ua/bitstream/KhPI-Press/11412/1/vestnik_HPI_2012_64_Pavlenko_Stan.pdf

[8] LOBAS, L. G., VERBITSKY, V. G. *Qualitative and analytical methods in the dynamics of wheeled vehicles*. Kyiv, Ukraine: Naukova dumka, 1990.

[9] KUZIO, I. V., SOKIL, B. I., PALYUKH, V. M. Influence of parameters on a non-linear basis of transport vehicles. *Bulletin of NU "LP" Series: Dynamics, Technology and Design of Machines and Attachments*. 2007, **588**, p. 49-52. ISSN: 0321-0499. Available from: https://ena.lpnu.ua/handle/ntb/3468

[10] PISARYEV, V. P., GORBUNOV, A. P. Possibility of the layout of new spring elements, with progressive characteristics, in the boundaries of the existing design solution of the BTR-60. *Mechanics and Machinery*. 2009, **2**, p. 51-56. ISSN 2078-7766.

[11] SOKIL, B. I., GRUBEL, M. G., NANIVSKIY, R. A., YALNITSKIY, O. D. Infusion of characteristics of special purpose vehicles on the cross-angular of the addressable mass. *Avtoshliakhovyk Ukrayiny*. 2015, **1-2**, p. 18-20. ISSN 0365-8392.

[12] SOKIL, B. I., NANIVSKYI, R. A., PARASHCHUK, D. L., GRUBEL, M. G. Infusing the power characteristics of the addressing system on the smooth running of the vehicles. *Avtoshliakhovyk Ukrayiny*. 2017, **1-2**, p. 38-41. ISSN 0365-8392.

[13] ANDRUKHIV, A. I., SOKIL, B. I., SOKIL, M. B. Basic principles for the approval of elective parameters of the adaptive surface of collected vehicles of special purpose. *Military Technical Collection* [online]. 2018, **19**, p. 38-51. ISSN 2312-4458, eISSN 2708-5228. Available from: https://doi.org/10.33577/2312-4458.19.2018.3-8

[14] ANDRUKHIV, A., SOKIL, B., SOKIL, M., VOVK, Y., LEVKOVYCH, M. The influence of the cinematic parameters of movement and sprung mass vibrations of wheeled vehicles on the move along the curved linear sections of the way. In 1st International Scientific Conference ICCPT 2019: Current Problems of Transport: proceeding [online]. 2019. ISBN 978-966-305-101-7, p. 259-264. Available from: https://doi.org/10.5281/zenodo.3387627

[15] SOKIL, B., LYASHUK, O., PERENCHUK, O., SOKIL, M., POPOVICH, P., VOVK, Y. Dynamic effect of cushion part of wheeled vehicles on their steerability. *International Journal of Automotive and Mechanical*

Engineering [online]. 2018, **15**(1), p. 4880-4892. ISSN 2229-8649, eISSN 2180-1606. Available from: https://doi.org/10.15282/ijame.15.1.2018.1.0380

[16] BOZHKOVA, L. V., RYABOV, V. G., NORITSINA, G. I. Influence of transverse forced vibrations on car rollover when driving around obstacles. *Transport Business in Russia*. 2009, **3**, p. 65-73. ISSN 2072-8689

[17] PODRIGALO, M. A., VOLKOV, V. P., STEPANOV, V. Y., DOBROGORSKY, M. V. *Stability of wheeled vehicles against skidding during braking and ways of increasing it*. Kharkiv, Ukraine: HNADU, 2006.

[18] SOKIL, B. I. Asymptotic representation of the solution of a nonlinear system with resonance. *Ukrainian Mathematical Journal* [online]. 1983, **35**(3), p. 339-341. ISSN 0041-5995, eISSN 1573-9376. Available from: https://doi.org/10.1007/BF01092191

[19] ROTENBERG, R. V. *Car suspension*. Moscow: Mechanical Engineering, 1972.

[20] VASILENKO, N. V. *Theory of oscillations*. Kyiv: Vyshcha schkola, 1992.

[21] ARTYUSHCHENKO, A. D., SUYARKOV O. G. Investigation of the influence of small class car suspension characteristics on smoothness and its modernization. *Bulletin of the National Technical University "KhPI". Series: Transport Engineering.* 2013, **32**(1004), p. 21 -27. ISSN 2079-0066.

[22] TSON, O. Analytical evaluation of technical and operational indicators impact on the transportation technology by automobile trailers. *Journal of Sustainable Development of Transport and Logistics* [online]. 2016, **1**(1), p. 23-26. ISSN 2520-2979. Available from: https://doi.org/10.14254/jsdtl.2016.1-1.4

[23] PODRIGALO, M. A., KOROBKO, A. I., KLETS, D. M. Estimation of dynamic stability of the car. *Bulletin of the National Technical University "KhPI". Series: Automobile and Tractor Construction* [online]. 2008, **58**, p. 134-137. ISSN 2078-6840. Available from: http://repository.kpi.kharkov.ua/handle/KhPI-Press/35141

[24] SAFONAU, A., VOVK, Y., LYASHUK, O., KHUDOBEI, R. Blending control of the trolleybus traction and brake drives to enhance the braking efficiency of a vehicle. *Journal of Sustainable Development of Transport and Logistics* [online]. 2020, **5**(2), p. 49-61. ISSN 2520-2979. Available from: https://doi.org/10.14254/jsdtl.2020.5-2.5

[25] AIZERMAN, M. A. *Classic mechanics*. Moscow: Nauka, 1974.

[26] BOGOLYUBOV, N. N., MITROPOLSKIY, Y. A. *Asymptotic methods in the theory of nonlinear oscillations*. Moscow: Nauka, 1974.

[26] MOISEEV, N. N. *Asymptotic methods of nonlinear mechanics*. Moscow: Nauka, 1981.

[27] SENIK, P. M., SMEREKA, I. P., SOKIL, B. I. *Asymptotic method and periodic Ateb-functions in the theory of essentially nonlinear oscillations*. Kyiv: Institute of Mathematics, 1977.

[28] SENIK, P. M. Inversion of the incomplete beta function. *Ukrainian Mathematical Journal* [online]. 1969, **21**(3), p. 325-333. ISSN 0041-5995, eISSN 1573-9376. Available from: https://doi.org/10.1007/BF01085368

[29] NAZARKEVYCH, M. Investigation of dependences of Beta and Ateb functions. *Bulletin of the National University "Lviv Polytechnic". Series: "Computer Sciences and Information Technologies* [online]. 2012, **732**, 207-216. ISSN 0321-0499. Available from: https://vlp.com.ua/node/9438

[30] OLSHANSKY, V. P., BURLAKA, V. V., VLIPCHENKO, M. V., MALETS, O. M. On oscillator oscillations with cubic-nonlinear stiffness. *Bulletin of the National Technical University "KhPI". Series: Dynamics and Strength of Machines.* 2017, **39**, p. 177-184. ISSN 2078-9130.

CALCULATION OF BASIC INDICATORS OF RUNNING SAFETY ON THE EXAMPLE OF A FREIGHT WAGON WITH THE Y25 BOGIE

Ján Dižo [1,*], Miroslav Blatnický [1], Denis Molnár [1], Anatoliy Falendysh [2]

[1]Faculty of Mechanical Engineering, University of Zilina, Zilina, Slovak Republic
[2]Pryazovsky State Technical University, Mariupol, Ukraine

*E-mail of corresponding author: jan.dizo@fstroj.uniza.sk

Resume

Freight wagons are among the most widely used means of transporting goods by land. Such a number of wagons and transported material and amount of material need to meet requirements in terms of safety and reliability. A wagon bogie is a key element in the wagon running safety point of view. The Y25 bogie is a most used bogie for freight wagons in the region of the central and west Europe. As this bogie was developed several decades ago, it is interesting to evaluate its running properties according to current standards. The presented research brings results of calculation of chosen basic indicators in terms of running safety. The calculations of the freight wagon with the Y25 bogie was performed by means of a multibody model. Simulation computations were carried out for an empty and loaded wagon, which has been running in curves with various radii and at several running speeds.

Available online: https://doi.org/10.26552/com.C.2022.3.B259-B266

Article info

Received 10 January 2022
Accepted 13 April 2022
Online 21 June 2022

Keywords:

Y25 bogie
freight wagon
running safety
multibody model

ISSN 1335-4205 (print version)
ISSN 2585-7878 (online version)

1 Introduction

Recently, large amount of goods is transported by railways. There are relatively many types of freight wagons for transportation of various kinds of goods, e.g. hopper wagons, tank wagons, wagons for transportation of steel coils, intermodal transport, cars transport and others [1-3]. The most of them are equipped by a two-axle bogie. As regards wagons used in the Central and West Europe, there are wagons with the Y25 bogie. Its development dates back to the sixties of the previous century. The objective of this work was to approach some specific features of this bogie and to calculate the basic indicators related to the running safety [4-6]. They must meet the given criteria for safety operation of freight wagons, as well as an entire train set [7-9].

From the historical point of view, the two main lines of development of freight wagons can be recognized. The European line is typical, that these bogies use a primary suspension system and do not have installed the secondary suspension system. The main advantage of these bogies is lower unsprung mass. Usually, the suspension system contains coil springs. On the other hand, the American development line of bogies is characterized that these bogies have higher unsprung mass due to missing the primary suspension system and they are equipped only with the secondary suspension system [10].

The French technical solution of railway freight wagons of the Y type comes from a realization of the primary suspension system by means of a couple of double coil springs, which are placed on a axlebox sides. One of the double coil spring (nearer to a bogie centre) is supplemented with the friction damper (a SNCF Lenoir patent) [10]. Friction force is generated between an axlebox and a guidance. More detailed description of this friction damper can be found below (section 2).

As a railway wagon is subjected to complicated dynamic influences during the operation, dynamic properties of a railway wagon have to be evaluated and investigated in terms of running safety. From the point of view of railway wagons themselves, the main demands are placed on their quality of running and derailment safety [11-13]. The running safety is affected by number of factors, among them are track irregularities, running speed, track geometry, technical conditions of a wagon, the load of wagons and others [14-17].

2 The Y25 bogie

The French national railways initiated the development of the Y25 bogie in 1960. The goal was

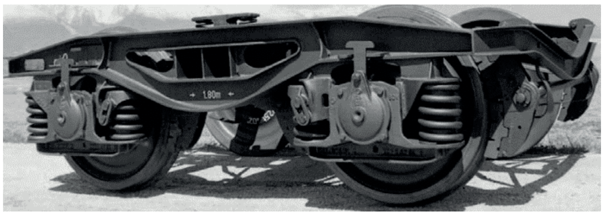

Figure 1 The Y25 bogie [7]

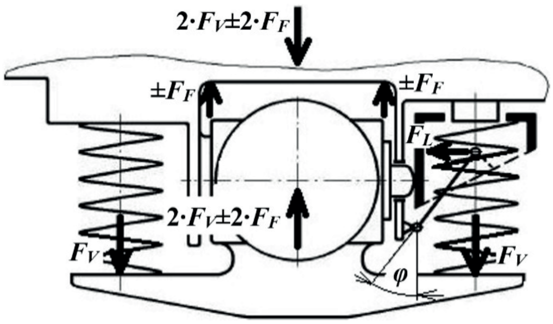

Figure 2 A scheme of a friction damper [10]

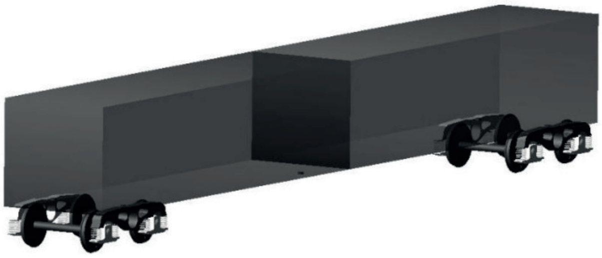

Figure 3 A multibody model of the investigated freight wagon

to design a bogie, which would occupate less space and which would have lower weight in comparison to the one used at the time, the Type 931. The efforts resulted in the Y25 bogie. It has the wheelbase of 1800 mm and the wheels' radius of 920 mm. Its suspension consists of duplex coil springs with a bilinear characteristics and they are combined with friction dampers, typical just for this bogie. The body of a wagon is connected with the bogie by means of a central pivot and with a couple of side bearers. The central pivot includes a special pad of a relatively high stiffness. Yaw oscillation of the bogie is eliminated by suspended side bearers. The bogie is usually designed for maximal running speed of 100 km/h at the maximal axle load of 22.5 t (or 25 t) or for the maximal running speed of 120 km/h at the maximal axle load of 20 t [7, 18-19].

The structure of the bogie is typical by the two longitudinal girders and one central lateral girder supplemented by ending lateral supports. Increasing demands on the noise level, total weight of wagons, running safety and others led to a modified Y25 bogie design, which does not use ending supports. Therefore, one can meet recently two basic bogie frame designs. An example of the Y25 bogie is shown in Figure 1.

A vertical load of the bogie is absorbed by vertical coil springs. The friction damper works on the principle of the Lenoir link. The Lenoir link ensures a generation of a friction forces between friction surfaces of an axlebox and a guidance. In this type of a bogie, the values of these forces depend on operational load of a freight wagon, thus on the load of the system (fully loaded, partially loaded) [20-22].

A scheme of the friction damper is shown in Figure 2. The friction damper is composed of an axlebox and a guidance.

If one considers that the force F_L acts in the Lenoir link, the force of one friction couple F_F is given as following:

$$F_F = F_L \cdot f = F_V \cdot f \cdot \tan\varphi \,, \qquad (1)$$

where F_V is the force in a coil spring, f is a friction coefficient and φ is an angle of a Lenoir link inclination. However, one axlebox includes two friction couples, therefore, the total force for one axlebox is doubled [23-24].

The friction forces in the friction damper are described by the Coulomb friction law. However, this formulation often leads to numerical problems during the simulation computations due to a discontinuous course of the force. Hence, the force is modelled as a continuous function.

3 Computer simulation of a freight wagon

A computational model of a freight wagon and simulations of its running on a track have been performed by a multibody software. A complex multibody model is described by differential-algebraic equations (DAE) [25-28].

A virtual multibody model (Figure 3) of a freight wagon consists of three subsystems:

- A front bogie (Y25 bogie),
- A rear bogie (Y25 bogie),
- A wagon body.

During the modelling of a freight wagon in a multibody software, it is necessary to pay attention to proper locations of individual components of a wagon [29-30]. Components are located in these positions

***Table 1** Parameters of bogie components*

Bogie components	m [kg]	I_{XX} [kg·m²]	I_{YY} [kg·m²]	I_{ZZ} [kg·m²]
Frame	2220	1975	1560	2850
Wheelset	1300	688	688	100
Axleload	20	5	5	5

***Table 2** Parameters of suspension components*

Suspension components	k_X [N/m]	k_Y [N/m]	k_Z [N/m]
Coil springs	700000	700000	500000
Centre pivot	$6\cdot10^6$	$6\cdot10^6$	$6\cdot10^6$
Sidebearers	$3.1\cdot10^5$	$5.8\cdot10^3$	$1.9\cdot10^5$

***Table 3** Parameters the freight wagon*

Wagon body	m [kg]	I_{XX} [kg·m²]	I_{YY} [kg·m²]	I_{ZZ} [kg·m²]
Empty	7900	$8.6\cdot10^3$	$2.8\cdot10^4$	$2.8\cdot10^3$
Loaded	40000	$4.8\cdot10^4$	$5.1\cdot10^5$	$5.0\cdot10^5$

to each other and they are interconnected by spring-damper modelling elements. The centre pivots distance of bogies is 15.7 m.

Parameters of individual components of the Y25 bogie, entering to simulations, are listed in Tables 1 and 2.

The body of the wagon has been created by the two rigid bodies connected by torsion spring with defined a torsion stiffness and by rotational joint (with a longitudinal axis of rotation). Parameters are introduced in Table 3.

3.1 Evaluation of the rail vehicles' dynamics

The UIC 518 standard was the first UIC standard describing the running tests of the rail vehicles, which was gradually supplemented [31-32]. This standard has become the basic for European standard 14 363 and other standards and some of its requirements are included in TSI standards. Measurement and evaluation of the vertical wheel forces Q and lateral wheel forces Y are the part of commissioning of new vehicles, according to UIC 518 standard, EN 14 363 standard and TSI [31-32].

Regarding the evaluation of tests of rail vehicles for commissioning, three main areas are defined:

- running safety,
- track load,
- running characteristics and vehicle vibrations.

The running safety is evaluated by several parameters. Quantities, which evaluate forces between a wheel and a rail, can be divided, according to EN 14 363, as follows [31]:

- quantities determining derailment safety:
  - ❑ (Y/Q) - a ratio of a lateral wheel force (Y) and a vertical wheel force (Q),
  - ❑ $(\sum Y)$ - resulting the lateral wheel on one wheelset,
  - ❑ lateral acceleration on a bogie frame in a wheelset axis location.

More information regarding the evaluation and commissioning of the rail vehicles are introduced in standards (UIC 518, EN 14 363, TSI).

3.2 Evaluation of a freight wagon dynamics

In this work, the quantities of a freight wagon are evaluated in terms of the running safety, which wagon was analysed in the loaded as well as in empty state at.

The calculation part of the work has consisted of performing the simulation computations in a commercial multibody software. Parameters of the freight wagon have been defined, as it is described in the previous section. Two loading conditions have been modelled, i.e. the empty wagon and the loaded wagon. The entire investigation process of the wanted outputs indicators has been running based on simulations computations. Parameters of the running conditions are described below.

3.2.1 Derailment quotient *Y/Q*

The ratio Y/Q is called the derailment safety and it is one of the running safety criteria. The derailment safety was evaluated for the freight wagon running in a curve with various radii and at various running

Table 4 Maximal calculated values of the derailment quotient Y/Q

Wagon state	R [m]	v [m/s]	Y/Q [-]
Loaded	400	11	0.180
	200	11	0.489
	60	6	0.607
Empty	400	11	0.348
	200	11	0.502
	60	6	0.623

Table 5 Lateral wheel forces between the wheel and a rail

Wheelset 1st Wagon state	R [m]	Lateral wheel force Left wheel [kN]	Right wheel [kN]	$\sum Y$ [kN]	$(\sum Y)_{lim}$ [kN]
Loaded	1000	6.13	5.01	1.12	70.9
Loaded	400	38.56	22.82	15.74	70.9
Empty	200	66.73	32.16	34.58	70.9
Empty	200	22.20	9.25	12.65	18.8

speeds. The limited value of 0.8 is valid for curves with a radius greater than 250 m and the limited value of 1.2 is valid for curves with radius less than 250 m and for superelevation ramps [31-34]. Based on these facts, three different curve radii have been chosen, namely 400 m, 200 m and 60 m. Subsequently, the freight wagon has been running on a track in these curves at speeds of 11 m/s (39.6 km/h) and 6 m/s (21.9 km/h). The values of the derailment quotient have been identified in the PostProcessor of the used software. The obtained values and results of the simulation computations are listed in Table 4.

The values presented in Table 4 indicate that the highest percentage difference of the derailment quotient for a comparison of the loaded wagon and the empty wagon is for the curve of 400 m and the running speeds of 11 m/s (39.6 km/h). This percentage is of 48.28 %. Other comparisons bring the percentage of 2.59 % for the curve of 200 and the running speed of 11 m/s (39.6 km/h) and finally of 3.37 % for the curve of 60 m, but the running speed has been of 6 m/s (21.9 km/h).

Graphs in Figure 4 show waveforms of the derailment safety for an outer wheel of the first wheelset for an empty wagon for running in a curve of 400 m at the speed of 11 m/s. Figure 5 shows a graph of the derailment ratio of an outer wheel of an empty wagon in a curve of 60 m at the speed of 6 m/s and a graph of the derailment ratio of a loaded wagon in a curve of 200 m at the speed of 11 m/s. Negative values of the derailment ratio are caused by an orientation of lateral wheel forces in a global coordinate system.

From values of the derailment ratio (Table 5) one can conclude that the biggest risk of derailment of a wagon during running in a curve occurs on the outer wheel of the first wheelset (in the wagon running direction). This ratio increases with a smaller curve radius. Further, it is obvious that this ratio indirectly depends on the wagon weight, i.e. in the case of an empty wagon running in a curve it is higher than in the case of the loaded wagon in a curve of the same radius. Comparing the Y/Q values for considered conditions one can conclude that the most unfavourable case in terms of safety is when the empty wagon runs in a curve with a small radius.

3.2.2 Sum of lateral forces $\sum Y$

Values of the lateral forces in the wheel/rail contact must be within certain limits.

The results for the limited value for a wheelset depends on an axleload and it is given as following:

$$(\sum Y)_{\text{lim}} = \sum(Y_L + Y_R) = \alpha \cdot \left(10 + \frac{Q}{3}\right)[\text{kN}], \tag{2}$$

where Q [N] is the maximal force on an axle, α is a coefficient and for freight wagons α = 0.85 [-].

An empty freight wagon has a considered axleload of 36.35 kN and for it, the following limit value is valid:

$$(\sum Y)_{\text{lim}}^{\text{empty}} = \alpha \cdot \left(10 + \frac{Q^{\text{empty}}}{3}\right) = 0.85 \cdot \left(10 + \frac{36.35}{3}\right) = 18.8\,\text{kN}. \tag{3}$$

The limit value for the loaded freight wagon by the same manner (the axleload of 220.24 kN) has also been calculated according to the formulation:

$$(\sum Y)_{\text{lim}}^{\text{loaded}} = \alpha \cdot \alpha \cdot \left(10 + \frac{Q^{\text{empty}}}{3}\right) = 0.85 \cdot \left(10 + \frac{220.24}{3}\right) = 70.9\,\text{kN}. \tag{4}$$

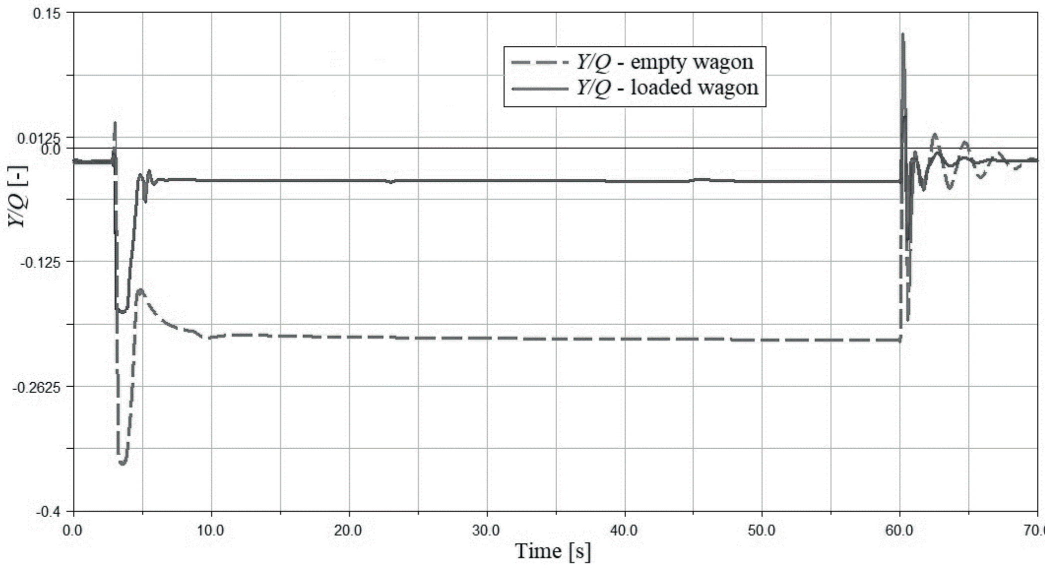

Figure 4 *Derailment ratio - comparison of the loaded and empty wagon, R = 400 m, v = 11 m/s*

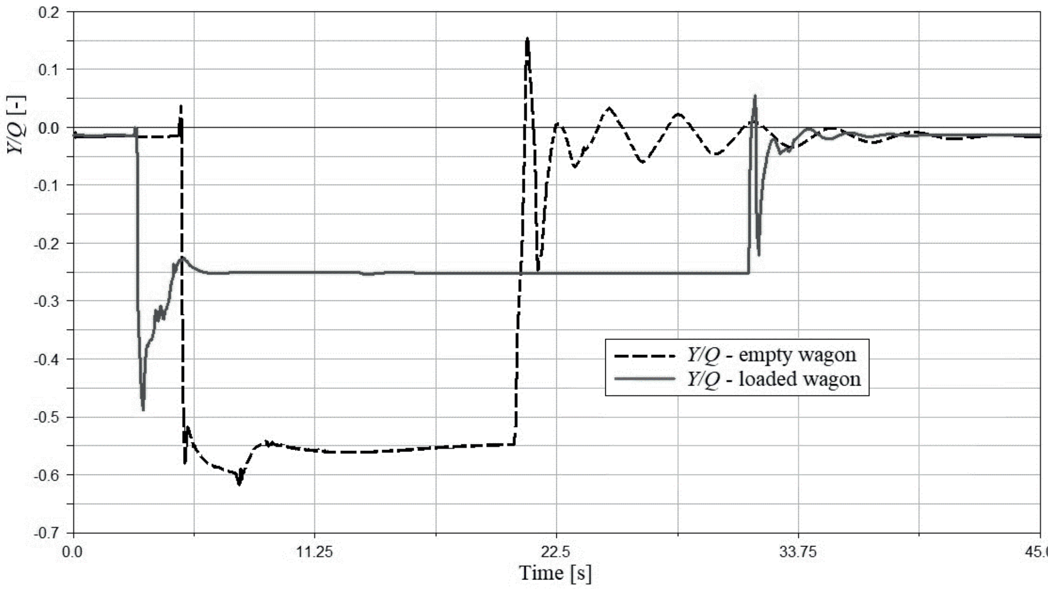

Figure 5 *Derailment ratio for various running conditions: a dashed line - the empty wagon, R = 200 m, v = 11 m/s, a solid line - the loaded wagon, R = 400 m, v = 6 m/s*

Similar to the assessment of the running safety, several simulation calculations were performed to evaluate the sum of lateral forces for various running regimes. The sum of lateral forces was assessed for the first wheelset in the running direction. These sums were compared to the limited value according to Equations (3) and (4). The results are listed in Table 4. The determined limited values of the sum of lateral forces were not exceeded.

The railway transportation of goods is being and in the future will be needed. It has specifics, which predetermine it for longer distances [35-36]. It is connected with the development of newer and more effective wagons and their structural units [37-42]. Therefore, the future research in this field will be focused on investigation of a wagon under various operational conditions. It will be important to know which operational characteristics will be reached on tracks with a real geometry. It relates to development of other realistic models of railway wagons, which will help to reveal positive properties in terms of operational safety. On the other hand, they will be helpful for indication of negative effects without a risk of damage of a final wagon design directly during the operation [43-48].

4 Conclusion

The article presented evaluation of some parameters of a freight wagon equipped by the Y25 bogie, according to the selected criteria. The research was performed by means of a multibody model and by simulation calculations. The reference freight wagon was tested at various conditions and that for the loaded state corresponding to the maximal axleload of 22.5 t as well as for the empty wagon. The wagon was run in various curves and at various speeds. The wagon properties were assessed based on some criteria introduced on the UIC 518 standard (or EN 14 363).

The derailment safety was evaluated for a wheel with the most unfavourable properties. It is the wheel of the first wheelset in the running direction (an outer wheel). Similarly, the first wheelset has the most unfavourable properties in terms of the sum of lateral forces. Evaluation of results of both criteria has shown that the calculated values did not exceed the limited values.

Acknowledgement

This research was supported by the Cultural and Educational Grant Agency of the Ministry of Education of the Slovak Republic in the project No. KEGA 023ZU-4/2020: "Development of advanced virtual models for studying and investigation of transport means operation characteristics".

References

[1] POLOM, M., TARKOWSKI, M., PUZDRAKIEWICZ, K. Urban transportation in the context of rail transport development: the case of a newly built railway line in Gdansk (Poland). *Journal of Advanced Transportation* [online]. 2018, **2018**, 1218041. ISSN 0197-6729, eISSN 2042-3195. Available from: https://doi.org/10.1155/2018/1218041

[2] MASEK, J., KENDRA, M., MILINKOVIC, S., VESKOVIC, S., BARTA, D. Proposal and application of methodology of revitalization of regional railway track in Slovakia and Serbia. Part 1: Theoretical approach and proposal of methodology for revitalization of regional, railways. *Transport Problems* [online]. 2015, **10**, p. 85-95. eISSN 2300-861X. Available from: https://doi.org/10.21307/tp-2015-052

[3] RYBICKA, I., STOPKA, O., LUPTAK, V., CHOVANCOVA, M., DROZDZIEL, P. Application of the methodology related to the emission standard to specific railway line in comparison with parallel road transport: a case study. *MATEC Web of Conferences* [online]. 2018, **244**, 03002. ISSN 2261-236X. Available from: https://doi.org/10.1051/matecconf/201824403002

[4] SHVETS, A. O., BOLOTOV, O. M., PERCEVOJ, A. K., GHLUKHOV, V. V., BOLOTPV, O. O., SAPAROVA, L. S. Research of dynamic indicators and influence of different types of rolling stock on railway track. *IOP Conference Series: Materials Science and Engineering* [online]. 2020, **985**, 012010. ISSN 1757-8981, eISSN 1757-899X. Available from: https://doi.org/10.1088/1757-899X/985/1/012010

[5] LOVISA, A. C., GARACK, O., CLARKE, J., MICHAEL, M. A workflow for the dynamic analysis of freight cars using Simpack. In: 25th Symposium of the International Association of Vehicle System Dynamics IAVSD 2017: proceedings. 2017.

[6] OPALA, M. Evaluation of bogie centre bowl friction models in the context of safety against derailment simulation predictions. *Archive of Applied Mechanics* [online]. 2018, **88**, p. 943-953. ISSN 0939-1533, eISSN 1432-0681. Available from: https://doi.org/10.1007/s00419-018-1351-4

[7] MORAVCIK, M., BASISTA, E., TOMAS, M. Innovative bogie for railway freight wagon. *Acta Mechanica Slovaca* [online]. 2017, **21**(3), p. 46-51. ISSN 1335-2393. Available from: https://doi.org/10.21496/ams.2017.026

[8] SEBESAN, I., ZAHARIA, N.-L., SPIROIU, M. A., FAINUS, L. Rubber suspension, a solution for the future for railway vehicles. *Materiale Plastice*. 2015, **52**(1), p. 93-96. ISSN 0025-5289, eISSN 0025-5289.

[9] HARUSINEC, J., SUCHANEK, A., LOULOVA, M., STRAZOVEC, P. Design of a device to simulate environmental influences on the course of brake tests. *MATEC Web of Conferences* [online]. 2018, **157**, 02013. ISSN 2261-236X. Available from: https://doi.org/10.1051/matecconf/201815702013

[10] HELLER, P., DOSTAL, J. *Rail vehicles II*. Pilsen: West Bohemian Pilsen University, 2009, ISBN 978-80-7043-641-7.

[11] PAGAIMO, J., MAGALHAES, H., COSTA, J. N., AMBROSIO, J. Derailment study of railway cargo vehicles using a response surface methodology. *Vehicle System Dynamics* [online]. 2022, **60**(1), p. 309-334. ISSN 0042-3114, eISSN 1744-5159. Available from: https://doi.org/10.1080/00423114.2020.1815810

[12] LAI, J., XU, J., WANG, P., YAN, Z., WANG, S., CHEN, R., SUN, J. Numerical investigation of dynamic derailment behavior of railway vehicle when passing through a turnout. *Engineering Failure Analysis* [online]. 2021, **121**, 105132. ISSN 1350-6307. Available from: https://doi.org/10.1016/j.engfailanal.2020.105132

[13] SHVETS, A. O. Dynamic interaction of a freight car body and a three-piece bogie during axle load increase. *Vehicle System Dynamics* [online]. 2021, Latest Articles. ISSN 0042-3114, eISSN 1744-5159. Available from: https://doi.org/10.1080/00423114.2021.1942930

[14] DIMITROVOVA, Z. Two-layer model of the railway track: analysis of the critical velocity and instability of two moving proximate masses. *International Journal of Mechanical Sciences* [online]. 2022, **217**, 107042. ISSN 0020-7403. Available from: https://doi.org/10.1016/j.ijmecsci.2021.107042

[15] KLIMENDA, F., SOUKUP, J., SKOCILAS, J., SKOCILASOVA, B. Vertical vibration of the vehicle when crossing over transverse speed bumps. *Manufacturing Technology* [online]. 2020, **20**(1), p. 55-59. ISSN 1213-2489, eISSN 2787-9402. Available from: https://doi.org/10.21062/mft.2020.020

[16] DVORAK, Z., LEITNER, B., NOVAK, L. Software support for railway traffic simulation under restricted conditions of the rail section. *Procedia Engineering* [online]. 2016, **134**, p. 245-255. ISSN 1877-7058. Available from: https://doi.org/10.1016/j.proeng.2016.01.066

[17] SVENTEKOVA, E., LEITNER, B., DVORAK, Z.: Transport critical infrastructure in Slovak Republic. In: 8th International Multi-Conference on Complexity, Informatics and Cybernetics IMCIC 2017: proceedings., 2017.

[18] FOMIN, O., LOVSKA, A., PISTEK, V., KUCERA, P. Determination of the vertical load on the carrying structure of a flat wagon with the 18-100 and Y25 bogies. *Applied Sciences* [online]. 2021, **11**(9). ISSN 2076-3417. Available from: https://doi.org/10.3390/app11094130

[19] FOMIN, O., LOVSKA, A. Determination of vertical dynamics for a standard Ukrainian boxcar with Y25 bogies. *Scientific Bulletin of the National Kirnych University / Naukovyi Visnyk Natsionalnoho Kirnychoho Universytetu* [online]. 2021, **2021**(5), p. 67-72. ISSN 2071-2227, eISSN 2223-2362. Available from: https://doi.org/10.33271/nvngu/2021-5/067

[20] LACK, T., GERLICI, J. Y25 freight car bogie models properties analysis by means of computer simulations. *MATEC Web of Conferences* [online]. 2018, **157**. eISSN 2261-236X. Available from: https://doi.org/10.1051/matecconf/201815703014

[21] LACK, T., GERLICI, J., MANUROVA, M. Freight car bogie properties analysis by means of simulation computations. *Manufacturing Technology* [online]. 2016, **16**(4), p. 25-26. ISSN 1213-2489, eISSN 2787-9402. Available from: https://doi.org/10.21062/UJEP/X.2016/A/1213-2489/MT/16/4/733

[22] MOLATEFI, H., HECHT, M., KADIVAR, M. H. Critical speed and limit cycles in the empty Y25-freight wagon. *Proceedings of the Institution of Mechanical Engineers, Part F: Journal of Rail and Rapid Transit* [online]. 2006, **220**(4), p. 347-359. ISSN 0954-4097, eISSN 2041-3017. Available from: https://doi.org/10.1243/09544097JRRT67

[23] BOSSO, N., GUGLIOTTA, A., SOMA, A. Simulation of a freight bogie with friction dampers. In: 5th ADAMS/Rail User's Conference: proceedings. 2000.

[24] SPIROIU, M. A. Reliability model of freight bogie damper based on real field data. *IOP Conference Series: Materials Science and Engineering* [online]. 2021, **1037**, 012056. ISSN 1757-8981, eISSN 1757-899X. Available from: https://doi.org/10.1088/1757-899X/1037/1/012056

[25] GERLICI, J., NOZHENKO, O., CHERNIAK, G., GORBUNOV, M., DOMIN, R. The development of diagnostics methodological principles of the railway rolling stock on the basis of the analysis of dynamic vibration processes of the rail. *MATEC Web of Conferences* [online]. 2018, **157**. eISSN 2261-236X. Available from: https://doi.org/10.1051/matecconf/201815703007

[26] GORBUNOV, M., GERLICI, J., KARA, S., NOZHENKO, O., CHERNYAK, G., KRAVCHENKO, K., LACK, T. New principle schemes of freight cars bogies. *Manufacturing Technology* [online]. 2018, **18**(2), p. 233-238. ISSN 1213-2489, eISSN 2787-9402. Available from: https://doi.org/10.21062/ujep/83.2018/a/1213-2489/MT/18/2/233

[27] WANG, Y., DIMITROVOVA, Z., YAU, J.-D. Dynamic responses of vehicle ballasted track interaction system for heavy haul trains. *MATEC Web of Conferences* [online]. 2018, **148**, 05004. eISSN 2261-236X. Available from: https://doi.org/10.1051/matecconf/201814805004

[28] IZVOLT, L., HARUSINEC, J., SMALO, M. Optimisation of transition areas between ballastless track and ballasted track in the area of the tunnel Turecky Vrch. *Communications - Scientific Letters of the University of Zilina* [online]. 2018, **20**(3), p. 67-76. ISSN 1335-4205, eISSN 2585-7878. Available from: https://doi.org/10.26552/com.C.2018.3.67-7

[29] STASTNIAK, P., SMETANKA, L., MORAVCIK, M. Structural analysis of a main construction assemblies of the new wagon prototype type Zans. *Manufacturing Technology* [online]. 2018, **18**(3), p. 510-517. ISSN 1213-2489, eISSN 2787-9402. Available from: https://doi.org/10.21062/ujep/130.2018/a/1213-2489/MT/18/3/510

[30] STASTNIAK, P., SMETANKA, L., DROZDZIEL, P. Computer aided simulation analysis of wear investigation of railway wheel running surface. *Diagnostyka* [online]. 2019, **20**(3), p. 63-68. eISSN 2449-5220. Available from: https://doi.org/10.29354/diag/111569

[31] EN 14363: Railway applications. Testing for the acceptance of running characteristics of railway vehicles. Testing of running behaviour and stationary. European Standard. 2005.

[32] UIC CODE: 518 OR Testing and approval of railway vehicles from the point of view of their dynamic behaviour - Safety - Track fatigue - Running behaviour. 4th ed. 2009.

[33] MIKHAILOV, E., GERLICI, J., KLIUIEV, S., SEMENOV, S., LACK, T. Mechatronic system of control position of wheel pairs by railway vehicles in the rail track. In: 17th International Scientific Conference on Dynamics of Rigid and Deformable Bodies 2019: proceedings [online]. AIP Conference Proceedings. 2019, 2198, 020009. ISBN 978-0-7354-1949-0Available from: https://doi.org/10.1063/1.5140870

[34] MIKHAILOV, E., SAPRONOVA, S., TKACHENKO, V., SEMENOV, S., SMYRNOVA, I., KHOLOSTEMKO, Y. Improved solution of guiding of railway vehicle in curves. In: 23rd International Scientific Conference on Transport Means: proceedings. 2019. ISSN 1822-296X, eISSN 2351-7034.

[35] KOSTRZEWSKI, M., KOSTRZEWSKI, A. Analysis of operations upon entry into intermodal freight terminals. *Applied Sciences* [online]. 2019, **9**(12), 2558. eISSN 2076-3417. Available from: https://doi.org/10.3390/app9122558

[36] KOSTRZEWSKI, M. Analysis of selected vibroacoustic signals recorded on EMU vehicle running on chosen routes under supervised operating conditions. *Vibroengineering Procedia* [online]. 2017, **13**, p. 153-158. ISSN 2345-0533, eISSN 2538-8479. Available from: https://doi.org/10.21595/vp.2017.18958

[37] PAVLIK, A., GERLICI, J., LACK, T., HAUSER, V., STASTNIAK, P. Prediction of the rail-wheel contact wear of an innovative bogie by simulation analysis. *Transportation Research Procedia* [online]. 2019, **40**, p. 855-860. ISSN 2352-1465. Available from: https://doi.org/10.1016/j.trpro.2019.07.120

[38] MIKHAILOV, E., SEMENOV, S., TKACHENKO, V., SAPRONOVA, S. Reduction of kinematic resistance to movement of the railway vehicles. *MATEC Web of Conferences* [online]. 2018, **235**, 00033. eISSN 2261-236X. Available from: https://doi.org/10.1051/matecconf/201823500033

[39] MELNIK, R., SOWINSKI, B. The analysis of rail vehicle model eignevalues for suspension fault detection method. Mini Conference on Vehicle System Dynamics, Identification and Anomalies: proceedings. 2014. p. 39-46.

[40] OPALA, M., KORZEB, J., KOZIAK, S., MELNIK, R. Evaluation of stress and fatigue of rail vehicle suspension component. *Energies* [online]. 2021, **14**(12), 3410. eISSN 1996-1073. Available from: https://doi.org/10.3390/en14123410

[41] ZVOLENSKY, P., KASIAR, L., VOLNA, P., BARTA, D. Simulated computation of the acoustic energy transfer through the structure of porous media in application of passenger carriage body. *Procedia Engineering* [online]. 2017, **187**, p. 100-109. ISSN 1877-7058. Available from: https://doi.org/10.1016/j.proeng.2017.04.355

[42] KASIAR, L., ZVOLENSKY, P., BARTA, D., BAVLNA, L., MIKOLAJCIK, M. Diagnostics of electric motor of locomotive series 757. *Diagnostyka*. 2016, **17**(3), p. 95-101. ISSN 1641-6414, eISSN 2449-5220.

[43] CABAN, J., NIEOCZYM, A., GARDYNSKI, L. Strength analysis of a container semi-truck frame. *Engineering Failure Analysis* [online]. 2021, **127**, 105487. ISSN 1350-6307. Available from: https://doi.org/10.1016/j.engfailanal.2021.105487

[44] FIGLUS, T., KUCZYNSKI, L. Selection of a semi-trailer for the haulage of long oversize loads, taking into account an analysis of operational damage. In: 11th International Science and Technical Conference Automotive Safety: proceedings [online]. 2018. p. 1-5. Available from: https://doi.org/10.1109/AUTOSAFE.2018.8373342

[45] NIEOCZYM, A., CABAN, J., VRABEL, J. The problem of proper cargo securing in road transport - case study. *Transportation Research Procedia* [online]. 2019, **40**, p. 1510-1517. ISSN 2352-1465. Available from: https://doi.org/10.1016/j.trpro.2019.07.209

[46] BUREIKA, G., GAIDAMAUSKAS, E., KUPINAS, J., BOGDEVICIUS, M., STEISUNAS, S. Modelling the assessment of traffic risk at level crossing of Lithuanian railways. *Transport* [online]. 2017, **32**(3), p. 282-290. ISSN 1648-4142. ISSN 1648-4142, eISSN 1648-3480. Available from: https://doi.org/10.3846/16484142.2016.1244114

[47] HARUSINEC, J., MANUROVA, M., SUCHANEK, J. Optimalization of a brake unit in terms of control range. *Manufacturing Technology* [online]. 2016, **16**(5), p. 917-923. ISSN 1213-2489, eISSN 2787-9402. Available from: https://doi.org/10.21062/ujep/x.2016/a/1213-2489/MT/16/5/917

[48] STEISUNAS, S., BUREIKA, G. Study of freight wagon running dynamic stability taking into account the track stiffness variation. *Transport Problems*. 2014, **9**(4), p. 131-143. ISSN 1896-0596, eISSN 2300-861X.

A MATHEMATICAL MODEL OF OPERATION OF A SEMI-TRAILER TRACTOR POWERTRAIN

Ján Dižo [1,*], Miroslav Blatnický [1], Rafał Melnik [2], Oleksandr Kravchenko [3]

[1]Faculty of Mechanical Engineering, University of Zilina, Zilina, Slovak Republic
[2]Faculty of Computer Science and Food Science, Lomza State University of Applied Sciences, Lomza, Poland
[3]Faculty of Mechanical Engineering, Zhytomyr Polytechnic State University, Zhytomyr, Ukraine

*E-mail of corresponding author: jan.dizo@fstroj.uniza.sk

Resume

The mathematical modelling is an inseparable part of mechanical engineers' activities. It is applied in design, optimization, verifying, as well as modifying of products. The approach of creating virtual models and their analyzing without having real products is applied in several domains. A mathematical model is given by equations of motion. The main objective of this work is to present the way how a mathematical model of a car powertrain operation is derived and applied in practical applications. A semi-trailer tractor with a standard powertrain was chosen as a reference car. The derived equations of motion are written in a matrix form and subsequently they are solved by means of a technical programming language Matlab. Parameters of the solved tractor mechanical system come from the real data and they are supplemented by the empirical data.

Article info

Received 10 January 2022
Accepted 24 May 2022
Online 21 June 2022

Keywords:

a mathematical model
a powertrain
a semi-trailer tractor
dynamic properties

Available online: https://doi.org/10.26552/com.C.2022.3.B267-B274

ISSN 1335-4205 (print version)
ISSN 2585-7878 (online version)

1 Introduction

Presently, the lorry transport belongs to the most common transport of goods in Europe. Lorry transport is provided by the combination vehicles. In the most European countries, road combination vehicles usually consist of a tractor and one semitrailer or a lorry with one trailer. Although these two types of combination vehicles differ by the maximal permissible length, their maximal permissible weight is of 40 t (Figure 1a). The exception are Scandinavian countries (Norway, Finland, Sweden, Denmark). In these countries, the standard maximal weight is of 60 t and combination vehicles can comprise more trailers (or semitrailers) (Figure 1b, c). The maximal permissible weight of combination vehicles in UK is also slightly higher than in the rest of European countries, namely of 48 t. As the Europe countries have different geographic and climatic conditions, topology of roads, roads networks and other factors and the goods is very often transported through many countries (e.g. from the north to the south and from the east to the west), it is needed to ensure fast enough and reliable movement of goods on roads. One of the key factors is sufficient performance of a powertrain vehicle [1-3].

The data mentioned above lead to the fact, that current tractors of combination vehicles the most often use engines with power of 300 kW to 400 kW and with the torque of 2000 Nm to 2700 Nm [4]. The power is transmitted to the driving axle from an engine through a gearbox, either manual or automatic. Thus, in principle, a powertrain of a standard two-axle semi-trailer tractor consists of a combustion engine, a gearbox, optionally an additional gearbox, further the drive shaft, a differential and the drive axle (the rear axle).

The objective of engineers and designers of lorries is to reach optimal driving characteristics of powertrain and thus the entire combination vehicles. The combustion engine works efficiently at certain range of operational conditions, which include engine speed, engine load and others. These parameters are influenced by a road topology, i.e. whether a vehicle moves on a plane road, in climbs, on highways, in urban environment etc. [5-7]. Therefore, tractors are equipped by engines with various maximal powers to reach sufficient speed at low fuel consumption. In order to be able to predict the waveforms of important powertrain parameters in the design process, it is necessary to create a suitable model [8-9].

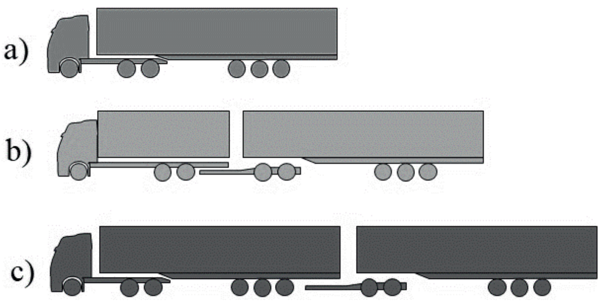

Figure 1 *Possible configurations of combination vehicles in Europe [10]*

Figure 2 *An illustration of the solved semitrailer tractor [11]*

Table 1 *Parameters of the solved vehicle*

Parameter	Designation	Value	Unit
Curb weight	m_c	7250	kg
Total weight of a combination vehicle	m_{tot}	40000	kg
Maximal power	P_{max}	337 (460)	kW (HP)
Maximal torque	M_{max}	2600	Nm
Engine displacement	V	13	l

This work is focused on derivation of a mathematical model of powertrain operation, which belongs to a chosen semi-trailer tractor. Following sections include description of a selected tractor, the derivation of a drive-train mathematical model by means of the Lagrange's equations of motion of the second kind method, its solution using the Matlab software and presentation of the reached results.

2 Derivation of mathematical model of a tractor powertrain

2.1 Description of the semi-trailer tractor

An analysed semitrailer tractor is intended for towing semitrailers with maximal weight of 24 tons. The total weight of the combination vehicles is considered of 40 tons.

It is a two-axle tractor with chassis configuration 4x2, i.e. the rear axle is a drive axle and the front axle is a steering axle. It is considered that the tractor is powered by a diesel combustion engine with the swept volume of 13 litres. The maximum toque is of 2600 Nm and the maximum power is of 337 kW (460 HP). The torques is transmitted to the rear axle by an automatic gearbox. It has installed a hydrodynamic converter of torque [11].

The curb weight of a solo tractor is considered of 7250 kg. All the needed parameters of the tractor are listed in Table 1. An illustration of the solved semitrailer tractor is depicted in Figure 2.

2.2 A mathematical model

A powertrain of the solved semitrailer tractor is a mechanical system with certain typical properties [12-14]. In this case, the work is focused on investigation of running-up the powertrain. For this, it is necessary to set-up a mathematical model. It will consist of equations of motion and a suitable method should be applied for their derivation. The Lagrange's equations of motion of the second kind method was chosen. It is known and widely applied method for derivation of dynamical models of various mechanical systems [15-17]. It is suitable for mechanical systems performing translational, rotational or combined motions. Its general form is:

$$\frac{d}{dt}\frac{\partial E_K}{\partial \dot{q}_j} - \frac{\partial E_K}{\partial q_j} + \frac{\partial E_D}{\partial \dot{q}_j} + \frac{\partial E_P}{\partial q_j} = Q_j, \quad j = 1, 2, \ldots, n, \tag{1}$$

where E_K, E_D and E_P are kinetic, dissipative and potential energy of the system, respectively, q_j, $\dot{q}_j$ are generalized coordinates and their time derivatives of the system, respectively, Q_j is a vector of external loads and n determines number of degrees of freedom. Based on Equation (1), it is certain that number of equations of motion depends on degrees of freedom of a mechanical system. Moreover, using of this method requires to determine proper values of individual energies [18-21].

Therefore, the first step for application of the method is creation of a dynamical model. It comes from a scheme depicted in Figure 3. The solved powertrain of the tractor composes of several components marked

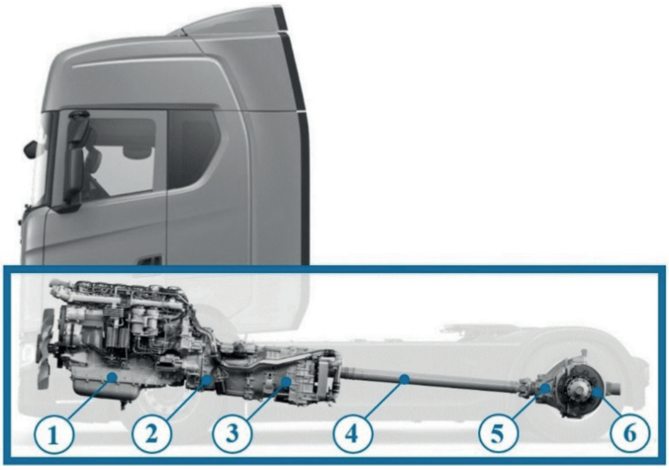

Figure 3 *Components of the solved tractor powertrain: 1 - engine, 2 - hydrodynamic converter, 3 - gearbox, 4 - propeller shaft, 5 - differential, 6 - drive wheels [22]*

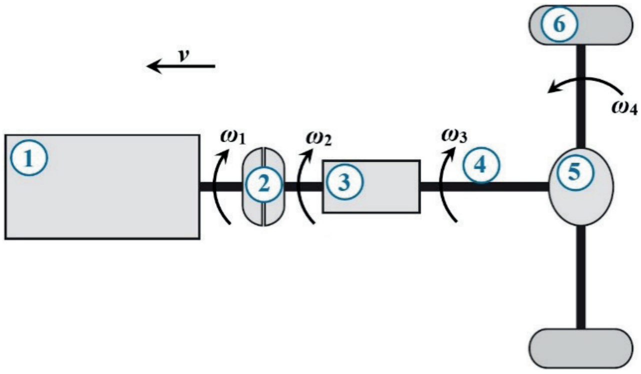

Figure 4 *Scheme of the powertrain with marking of velocities of individual components [5]*

by numbers 1 to 6: 1 - an engine, 2 - a hydrodynamic converter, 3 - a gearbox, 4 - a propeller shaft, 5 - a differential, 6 - drive wheels.

The hydrodynamic converter has two main moving rotating parts - a pump and a turbine. Angular velocity of a pump is ω_P and angular velocity of a turbine is ω_T. Other angular velocities are marked as following: ω_1 - angular velocity of an engine crankshaft, ω_2 - angular velocity of an input shaft to a gearbox, ω_3 - angular velocity of an output shaft of a gearbox (a propeller shaft), ω_4 - angular velocity of a drive axle shaft. When the angular velocities are expressed using the angular coordinates, one gets $\omega_1 = \dot{\varphi}_1, \omega_2 = \dot{\varphi}_2, \omega_3 = \dot{\varphi}_3$ and finally $\omega_4 = \dot{\varphi}_4$.

It is considered that all the connecting shafts of the mechanical system are rigid. This means, that $\omega_P = \omega_1$ and $\omega_T = \omega_2$ or that $\varphi_P = \varphi_1$ and $\varphi_T = \varphi_2$. Angular velocities of individual rotating components are shown in Figure 4.

Thus, it is supposed that the mechanical system has two degrees of freedom (2 DOF) and generalized coordinates are φ_1 and φ_2, i.e. angular deviation of the input shaft to the gearbox (the same with the engine crankshaft and the pump shaft) and angular deviation of the output shaft from the gearbox (the same with the turbine shaft).

Kinetic energy of the system is:

$$E_K = \frac{1}{2} \cdot I_E \cdot \omega_1^2 + \frac{1}{2} \cdot I_P \cdot \omega_1^2 + \frac{1}{2} \cdot I_T \cdot \omega_2^2 + \frac{1}{2} \cdot I_4 \cdot \omega_3^2 + \frac{1}{2} \cdot I_5 \cdot \omega_4^2 + \frac{1}{2} \cdot m_{tot} \cdot v^2, \quad (2)$$

where I_E - moment of inertia of the engine crankshaft, I_P - moment of inertia of the pump, I_T - moment of inertia of the turbine, I_4 - moment of inertia of the shaft between the gearbox and the rear axle differential (a propeller shaft), I_5 - moment of inertia of the drive axle shafts and v - tractor velocity. As can be seen, the kinetic energy includes besides the generalized coordinates φ_1 and φ_2 other coordinates, as well. Hence, the following relations are considered:

$$\omega_3 = \frac{\omega_2}{i_G}, \omega_4 = \frac{\omega_3}{i_C} = \frac{\omega_3}{i_G \cdot i_D}, v = R \cdot \omega_4 = \frac{R \cdot \omega_2}{i_G \cdot i_D}, \quad (3)$$

where i_G - the gear ratio of the activated speed gear, i_D - the permanent gear ratio of the differential and R - the drive wheel radius, which leads to the modified form of the kinetic energy:

$$E_K = \frac{1}{2} \cdot (I_M + I_P) \cdot \omega_1^2 + \frac{1}{2} \cdot \left(I_T + \frac{I_4}{i_G^2} + \frac{I_5}{(i_G \cdot i_D)^2} + \frac{m_{tot} \cdot R^2}{(i_G \cdot i_D)^2} \right) \cdot \omega_2^2, \quad (4)$$

Oror

$$E_K = \frac{1}{2} \cdot I_{1red} \cdot \omega_1^2 + \frac{1}{2} I_{2red} \cdot \omega_2^2, \tag{5}$$

where I_{1red} and I_{2red} are moments of inertia of rotational components reduced to the pump shaft and the turbine shaft, respectively.

Dissipative energy expresses viscous losses in the system and it is given as:

$$E_D = \frac{1}{2} \cdot b_1 \cdot \dot{\varphi}_1^2 + \frac{1}{2} \cdot b_2 \cdot \dot{\varphi}_2^2, \tag{6}$$

where b_1 and b_2 are the viscous losses coefficients.

It should be note, that in the solved task, the tractor moves on a straight road without a climb. Therefore, the potential energy is not being changed, i.e. $E_P = 0$.

Further, in the mechanical system of the powertrain the load moments act, namely the drive moment of the engine M_E and moment of the driving resistance M_R. Besides those, moments of the pump M_P and the moment of the turbine M_T, are considered as well. These moments have also to be reduced to the corresponding shafts, i.e. to the pump shaft and to the turbine shaft.

For coordinate φ_1:

$$M_{1red} \cdot \omega_1 = M_E \cdot \omega_1 - M_P \cdot \omega_P. \tag{7}$$

Thus

$$M_{1red} = M_E - M_P. \tag{8}$$

For coordinate φ_2 is considered a simplified situation, namely, the tractor runs-up from the zero speed, i.e. the drag can be neglected and only the weight of the tractor is considered:

$$M_{2red} \cdot \omega_2 = M_T \cdot \omega_2 - m_{tot} \cdot g \cdot \omega_4 \cdot R = \left(M_T - m_{tot} \cdot g \cdot \frac{R}{i_G \cdot i_D}\right) \cdot \omega_2. \tag{9}$$

Thus

$$M_{2red} = M_T - M_R. \tag{10}$$

Now, one can perform the partial derivations of kinetic and dissipative energies with respect to the generalized coordinates φ_1 and φ_2; the right-hand sides of the equations of motion include reduced moments described above.

Hence, one gets the equations of motion of the semitrailer tractor powertrain in the following form:

$$\begin{aligned} &(I_M + I_P) \cdot \ddot{\varphi}_1 + b_1 \cdot \dot{\varphi}_1 = M_E - M_P \\ &\left(I_T + \frac{I_4}{i_G^2} + \frac{I_5}{(i_G \cdot i_D)^2} + \frac{m_{tot} \cdot R^2}{(i_G \cdot i_D)^2}\right) \cdot \ddot{\varphi}_2 + b_2 \cdot \dot{\varphi}_2 = \\ &M_T - M_R, \end{aligned} \tag{11}$$

or in a shortened form:

$$\begin{aligned} I_{1red} \cdot \ddot{\varphi}_1 + b_1 \cdot \dot{\varphi}_1 = M_{1red} \\ I_{2red} \cdot \ddot{\varphi}_2 + b_2 \cdot \dot{\varphi}_2 = M_{2red}, \end{aligned} \tag{12}$$

where I_{1red} and I_{2red} are the moments of inertia reduced to the shaft rotating at the angular velocity $\dot{\varphi}_1$ and to the shaft rotating at the angular velocity $\dot{\varphi}_2$, respectively. They are:

$$\begin{aligned} I_{1red} &= (I_M + I_P) \\ I_{2red} &= \left(I_T + \frac{I_4}{i_G^2} + \frac{I_5}{(i_G \cdot i_D)^2} + \frac{m_{tot} \cdot R^2}{(i_G \cdot i_D)^2}\right). \end{aligned} \tag{13}$$

Matrix forms of Equations (11) and (12) are:

$$\begin{bmatrix} I_M + I_P & 0 \\ 0 & I_T + \frac{I_4}{i_G^2} + \frac{I_5}{(i_G \cdot i_D)^2} + \frac{m_{tot} \cdot R^2}{(i_G \cdot i_D)^2} \end{bmatrix} \cdot \begin{bmatrix} \ddot{\varphi}_1 \\ \ddot{\varphi}_2 \end{bmatrix} + \begin{bmatrix} b_1 & 0 \\ 0 & b_2 \end{bmatrix} \cdot \begin{bmatrix} \dot{\varphi}_1 \\ \dot{\varphi}_2 \end{bmatrix} = \begin{bmatrix} M_E - M_P \\ M_T - M_R \end{bmatrix} \tag{14}$$

and

$$\begin{bmatrix} I_{1red} & 0 \\ 0 & I_{2red} \end{bmatrix} \cdot \begin{bmatrix} \ddot{\varphi}_1 \\ \ddot{\varphi}_2 \end{bmatrix} + \begin{bmatrix} b_1 & 0 \\ 0 & b_2 \end{bmatrix} \cdot \begin{bmatrix} \dot{\varphi}_1 \\ \dot{\varphi}_2 \end{bmatrix} = \begin{bmatrix} M_{1red} \\ M_{2red} \end{bmatrix}. \tag{15}$$

3 Obtaining the calculations' results

Equations of motion derived in the previous section (Equations (11), or (12)) have been solved in the Matlab software. However, these equations of motion should be adapted for demands of this software. Firstly, accelerations (in this case angular accelerations) must be independent. Thus, one gets:

$$\begin{aligned} \ddot{\varphi}_1 &= \frac{1}{I_{1red}} \cdot (M_{1red} - b_1 \cdot \dot{\varphi}_1) \\ \ddot{\varphi}_2 &= \frac{1}{I_{2red}} \cdot (M_{2red} - b_2 \cdot \dot{\varphi}_2). \end{aligned} \tag{16}$$

The next modification relates to the fact, that the used software is not able to solve differential equations of the second order. Therefore, Equations (16) must be substituted by the differential equations of the first order.

For coordinate φ_1, we consider the following substitution:

$$\theta_1 = \dot{\varphi}_1, \quad \theta_2 = \varphi_1. \tag{17}$$

Then, their derivations are:

$$\theta_1' = \ddot{\varphi}_1, \quad \theta_2' = \dot{\varphi}_1 = \theta_1 \tag{18}$$

It is similar for the coordinate φ_2:

$$\theta_3 = \dot{\varphi}_2, \quad \theta_4 = \varphi_2, \tag{19}$$

$$\theta_3' = \ddot{\varphi}_2, \quad \theta_4' = \dot{\varphi}_2 = \theta_3 . \tag{20}$$

When the derived equations of motion in Equation (11) of the tractor powertrain are rewritten by considering formulations in Equations (17) to (20), one obtains four differential equations of the first order:

$$\begin{aligned}
\theta_1' &= \frac{1}{(I_M + I_P)} \cdot (M_E - M_P - b_1 \cdot \theta_1) \\
\theta_2' &= \theta_1 \\
\theta_3' &= \frac{1}{\left(I_T + \frac{I_4}{i_G^2} + \frac{I_2}{(i_G \cdot i_D)^2} + \frac{m_{tot} \cdot R^2}{(i_G \cdot i_D)^2} \right)} \cdot \\
&(M_T - M_R - b_2 \cdot \theta_3) \\
\theta_4' &= \theta_3 .
\end{aligned} \tag{21}$$

Figure 5 shows the obtained results of calculation of Equation (21). The output values are calculated in the time interval of 15 s. Figure 6 additionally depicts details of the results obtained in the time interval of 2.5 s.

Figure 5 includes two parts. Torque of the used combustion engine (M_E) and moments of the hydrodynamic converter for the pump part (M_P) and the turbine part (M_T) are in the upper part of the figure.

Rotational speed of the input shaft (n_P) and of the output shaft (n_T) together with tractor speed (v) are shown in the lower part of Figure 5.

After starting the combustion engine and reaching the sufficient torque, the pump of the converter begins to increase; thus the torque of the turbine also begins to increase. In the turbine torque, the moment of loads (i.e. driving resistance) is included. After certain time interval, in this case approx. after 2.8 s, the equilibrium of the torques is reached and then the torques are practically identical.

A similar situation is detected for the rotational speeds of the pump shaft and the turbine shaft. Rotational speed of the pump shaft n_P begins to increase with the engine torque M_E. The rotational speed of the turbine shaft n_T is lower than the n_P, because the hydrodynamic converter causes certain decreasing of the rotational speed due to losses. The tractor velocity v is stabilized at the value of 26.64 km/h (a purple curve).

Waveforms of the outputs are calculated for one particular activated gear ratio in the gearbox. In the real operation of the tractor, a driver (either manually of automatically) would change the gear ratio, values of torques would decrease (in the case of driving on the

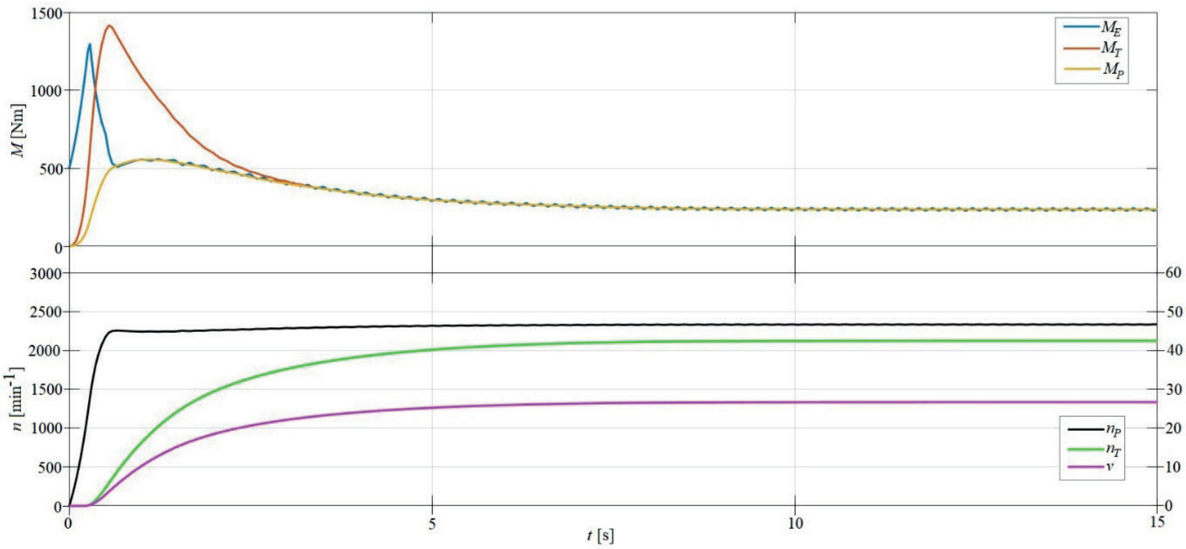

Figure 5 *The results of calculation of the tractor powertrain mathematical model, the time interval 0 to 15 s*

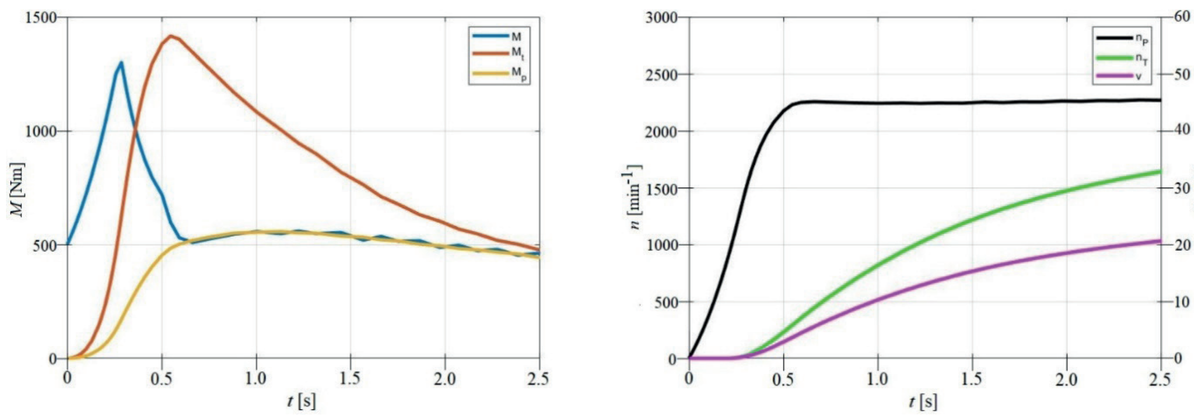

Figure 6 *The detail of waveforms of the obtained results, the time interval 0 to 2.5 s*

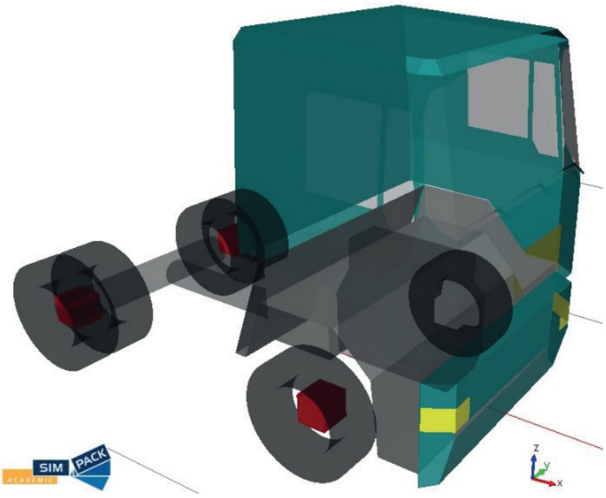

***Figure 7** An illustration of a semi-trailer tractor trailer created in the Simpack software*

flat road, without climb) and the driving speed would be higher. In the case of driving at the higher speed, the drag should be already considered in the mathematical model and it would be incorporated within the moment of driving resistance M_R.

The future research will be focused on modelling the operation of the semitrailer tractor powertrain. The modified mathematical model will be more difficult. It will include other parts for simulation of all the driving resistances, driving in a climb, comparison of outputs values for driving with fully loaded semitrailer etc. As the other step of the future research, challenge for the authors will be to set-up a multibody model (MBS model) of the considered combination vehicle. On one hand, the modelling of the multibody model in the MBS software does not need to derive equations of motion, they are created automatically by a software. On the other hand, it is not possible to check and compare the equations of motion derived by the researcher (let say "manually") with equations of motion derived by the software during the modelling process. Figure 7 shows an ongoing state of the semi-trailer tractor model created in the Simpack software. The research will continue in order to reach a representative MBS model of the tractor and it will serve for performing the simulation computations and evaluation of wanted quantities.

4 Conclusion

The presented research has brought an overview of a creation of the mathematical model for investigation of dynamical properties of a semi-trailer tractor powertrain. This particular tractor uses the hydrodynamic converter of torque. The mathematical model was derived by means of the Lagrange's equations of motion of the second kind method. Calculated values have included output torques and rotational speed of shafts of the powertrain. The achieved results show their graphical waveforms, which are essential for evaluation of the tractor behavior during operation. Tractor's acceleration leads to increase of torque on the drive shaft. After certain time, the mechanical system reaches the equilibrium. It means that the torques of the drive shaft and the driven shaft have the same characteristics in terms of their waveforms. Hence, values of torques are identical. Further change of torques, rotational speeds of driving speed ,will happen after a change of the gear ratio of a change of the external loads (e.g. a change of driving resistance). These driving resistances include mainly the drag at higher driving speeds, inertia resistance during accelerations and the resistance due to climbs. Another important driving resistance is the rolling resistance. It appears at any driving speed and depends on the rolling friction coefficient and on the total weight of the tractor (or of the entire combination vehicle).

The main objective of the performed researchs activities has been to create a basic mathematical model of a semi-trailer tractor powertrain. The further step in the research is to set-up a more complex model, which will also include effects of other phenomena, like flexibility of shafts, a change of weight of a vehicle, driving in climbs and others. An intention of researchers is, besides the mathematical model solved in the Matlab software to set-up a multibody model of the tractor or the entire combination vehicles. The advantage of having two independent mathematical models of a mechanical system in two different software is the possibility to compare the obtained results to each other. Then, it will be possible to investigate the operational properties of the vehicle (with various parameters) and to reveal possibilities to improve some parameters, mainly in terms of the required power during the operation, fuel consumption and others, which influence effective and economical operation of a vehicle.

Acknowledgement

This research was supported by the Cultural and Educational Grant Agency of the Ministry of Education of the Slovak Republic in the project No. KEGA 023ŽU-4/2020: Development of advanced virtual models for studying and investigation of transport means operation characteristics.

References

[1] GNAP, J., SENKO, S., KOSTRZEWSKI, M., BRIDZIKOVA, M., CZODOROVA, R., RIHA, Z. Research on the relationship between transport infrastructure and performance in rail and road freight transport - a case study of Japan and selected European countries. *Sustainability* [online]. 2021, **13**(12), 6654. ISSN 2071-1050. Available from: https://doi.org/10.3390/su13126654

[2] VARJAN, P., GNAP, J., DURANA, P., KOSTRZEWSKI, M. Research on the relationship between transport performance in road freight transport and revenues from excise duty on diesel fuel in selected European countries. In: 13th International Scientific Conference on Sustainable, Modern and Safe Transport TRANSCOM 2019: proceedings [online]. 2019. ISSN 2352-1457, p. 1216-1223. Available from: https://doi.org/10.1016/j.trpro.2019.07.169

[3] PUKALSKAS, S., KRIAUCIUNAS, D., RIMKUS, A., PRZYBYLA, G., DROZDZIEL, P., BARTA, D. Effect of hydrogen addition on the energetic and ecologic parameters of an SI engine fuelled by biogas. *Applied Sciences* [online]. 2021, **11**(2), p. 1-17. ISSN 2076-3417. Available from: https://doi.org/10.3390/app11020742

[4] New powertrain from Scania [online] [accessed-2021-12-20]. Available from: https://www.dieselprogress.com/news/scania-invests-2-billion-on-new-powertrain-platform-improvements/8016254.article

[5] SAHLHOLM, P. *Iterative road grade estimation for heavy duty vehicle control*. Licentiate Thesis. Stockholm, Sweden: KTH School of Electrical Engineering, 2008. ISBN 978-91-7415-186-2.

[6] LEITNER, B. Autoregressive models in modelling and simulation of transport means working conditions. In: 14th International Conference on Transport Means 2010: proceedings. 2010. ISSN 1822-296X, p. 21-24.

[7] KASPAREK, J., JONAK, M. Advanced approaches for modelling of a virtual terrain. In: 19th International Scientific Conference on Transport Means 2015: proceedings. 2015. ISSN 1822-296X, p. 47-50.

[8] LUQUE, P., MANTARAS, D. A., ROCES, J., CASTEJON, L., MALON, H., VALLADARES, D. Optimization of the powertrain of electric vehicles for a given route. In: 14th Conference on Transport Engineering CIT 2021: proceedings [online]. 2021. ISSN 2352-1457. Available from: https://doi.org/10.1016/j.trpro.2021.11.034

[9] SPANOUDAKIS, P., MOSCHOPOLOUS, G., STEFANOULIS, T., SARANTINOUDIS, N., PAPADOKOKOLAKIS, E., IOANNOU, I., PIPERIDIS, S., DOITSIDIS, L., TSOURVELOUDIS, N. C. Efficient gear ratio selection of a single-speed drivetrain for improved electric vehicle energy consumption. *Sustainability* [online]. 2020, **12**(21), 9254. ISSN 2071-1050. Available from: https://doi.org/10.3390/su12219254

[10] DUO2 - We decrease the fuel consumption with up to 20% per transported unit of load - DUO2.NU [online] [accessed-2021-12-29]. Available from: https://duo2.nu/?page_id=221&lang=en

[11] Scania - HLSmith [online] [accessed 2021-12-30]. Available from: https://www.hlsmith.co.uk/scania

[12] RABINOVICH, E., GRITSUK, I. V., ZUIEV, V., EVGENY, E. Y., GOLOVAN, A., ZYBTSEV, Y., VOLKOV, V., GERLICI, J., KRAVCHENKO, K., VOLSKA, O., RUDNICHENKO, N. Evaluation of the powertrain condition based on the car acceleration and coasting data. *SAE Technical Papers* [online]. 2018. ISSN 0148-7191, eISSN 2688-3627. Available from: https://doi.org/10.4271/2018-01-1771

[13] NOUH, A., CHAMI, M., MOHAMED, F. A. Modelling and simulation for powertrain design and control of unconventional vehicles. In: 6th International Renewable Energy Congress: proceedings [online]. 2015. ISBN 978-1-4799-7947-9. Available from: https://doi.org/10.1109/IREC.2015.7110934

[14] LEITNER, B. A new approach to identification and modelling of machines dynamic systems behaviour. In: 14th International Conference Transport Means 2010: proceedings. 2010. ISSN 1822-296X, p. 17-20.

[15] FILO, M., LUKAC, M.: *Modelling and simulation of mechanisms with computer aid* (in Slovak). Zilina: University of Zilina, 2005. ISBN 80-8070-466-X.

[16] LUKAC, M., BRUMERCIK, F., KRZYWONOS, L., KRZYSIAK, Z. Transmission system power flow model. *Communications - Scientific Letters of the University of Zilina* [online]. 2017, **19**(2), p. 27-31. ISSN 1335-4205, eISSN 2585-7878. Available from: https://doi.org/10.26552/com.C.2017.2.27-31

[17] BRUMERCIK, F., LUKAC, M., CABAN, J. Unconventional powertrain simulation. *Communications - Scientific Letters of the University of Zilina* [online]. 2016, **18**(2), p. 30-33. ISSN 1335-4205, eISSN 2585-7878. Available from: https://doi.org/10.26552/com.C.2016.2.30-33

[18] GOMEZ, E. R., SJOSTRAND, J., KARI, L., ARTEAGA, I. L. Torsional vibrations in heavy-truck powertrains with flywheel attached centrifugal pendulum vibration absorbers. *Mechanism and Machine Theory* [online]. 2022, **167**, 104547. ISSN 0094-114X. Available from: https://doi.org/10.1016/j.mechmachtheory.2021.104547

[19] GORBUNOV, M., GERLICI, J., KARA, S., NOZHENKO, O., CHERNYAK, G., KRAVCHENKO, K., LACK, T. New principle schemes of freight cars bogies. *Manufacturing Technology* [online]. 2018, **18**(2), p. 233-238. ISSN 1213-2489. Available from: https://doi.org/10.21062/ujep/83.2018/a/1213-2489/MT/18/2/233

[20] GERLICI, J., SAKHNO, V., YEFYMENKO, A., VERBITSKII, V., KRAVCHENKO, A., KRAVCHENKO, K. The stability analysis of two-wheeled vehicle model. *MATEC Web of Conferences* [online]. 2018, **157**, 01007. ISSN 2261-236X. Available from: https://doi.org/10.1051/matecconf/201815701007

[21] LACK, T., GERLICI, J. Analysis of vehicles dynamic properties from: The point of view of passenger comfort. *Communications - Scientific Letters of the University of Zilina* [online]. 2008, **10**(3), p. 10-18, ISSN 1335-4205, eISSN 2585-7878. Available from: https://doi.org/10.26552/com.C.2008.3.10-18

[22] WILLIAMSSON, D., SELLGREN, U., SODERBERG, A. The hunt for proper relation weights in product architecture clustering. In: NordDesign 2018: proceedings. 2018. ISBN 978-91-7685-185-2.

SMOTE VS. RANDOM UNDERSAMPLING FOR IMBALANCED DATA- CAR OWNERSHIP DEMAND MODEL

Wuttikrai Chaipanha, Patiphan Kaewwichian*

Department of Civil Engineering, Faculty of Engineering, Rajamangala University of Technology Isan, Khon Kaen, Thailand

*E-mail of corresponding author: patiphan.ka@rmuti.ac.th

Resume

Because the numbers of cars reflect each person's travel behaviors for each specific location, the car ownership demand model plays a dominant role in analysis of the travel demand in order to understand each area's individual and household travel behaviors. However, the study project for the master plan of the Khon Kaen expressway represented imbalanced data; namely, the majority class and the minority class were not equal. Before developing a machine learning model, this study suggested a solution to balance the data by using oversampling and under-sampling techniques. The data, which had been improved with SMOTE (Synthetic Minority Oversampling Technique) and kNN (k-nearest neighbors) (k = 5), demonstrated a better effect than the other algorithms that were studied. The TPR (true positive rate) for the rural and suburban areas, which are types of regions with very different imbalance ratios, was calculated before balancing the data at 46.9% and 46.4%. As a result, the TPR values were 63.5% and 54.4%, respectively, following the data balancing.

Article info

Received 28 July 2021
Accepted 31 January 2022
Online 25 March 2022

Keywords:

tour-based model
multiclass classification
k-nearest neighbors
activity-based model

Available online: https://doi.org/10.26552/com.C.2022.3.D105-D115

ISSN 1335-4205 (print version)
ISSN 2585-7878 (online version)

1 Introduction

The most dominant mode of personal travel for a city in extended metropolitan regions is the private car since it is more convenient and flexible. For example, using a vehicle to travel from a suburban or rural area to do business in a CBD (Central Business District) is either a primary destination or an intermediate stop [1]. However, traveling by car influences energy consumption and air quality in an urban area, as well as health problems [2-3].

Regarding the travel demand prediction for transportation planning, household car ownership affects the prognosis of trip frequency choice, destination choice and the mode choice for each trip or tour according to the objectives. It also affects the tour type. Nevertheless, a household's car ownership from each area typically consists of balanced data and imbalanced data [4]. The imbalanced household car ownership was used to predict the Machine Learning Models' travel demand, which represents a state-of-the-art approach [5]. This affects the algorithm training process; specifically, the accuracy and true positive rate would be lower. In the case of the balanced data, the results would be reversed.

Class imbalance is commonly found when the datasets have different members, as most of the minority class contains essential data [6]. Using this imbalanced data to create a model would give an ineffective predicted result due to the decision of the Machine Learning algorithm to rely more on the majority class because it equally focuses on those two classes. In other words, the minority class may be misclassified as the majority class [7-8]. This class disparity is a significant issue in the medical science [9], marketing, banking and manufacturing industries [10], among other fields of study. However, it is still uncommon in transportation planning and is mainly employed when a machine learning model is used to predict car ownership in a household. There has been only one study on Discrete Choice Analysis to analyze the travel demand for business planning, as mentioned in [11]. Therefore, the data imbalance might naturally occur by itself or in limited datasets since a survey require high costs.

A 2-class problem, found in the household's car ownership model, is called a binary classification problem. For example, if there were 100 household car ownership datasets, they would be classified into two groups: 1) households with cars and 2) households without cars. Meanwhile, if the first group contained 90 datasets and another group had ten datasets, the first group's data with more datasets would be called the majority class. By comparison, the group with fewer datasets would be called the minority class. Using this data to create a model with the classification technique and the machine learning model's basic and standard algorithms (including decision trees (DT), k-nearest neighbors (kNN) and Naive Bayes algorithm), the predicted results might be biased by the majority class.

In contrast, the prediction of another group with fewer datasets seems to be an error and is called data misclassification. It was impossible to correctly classify the datasets in the minority class, or the results might be rarely correct. At the same time, the group with large numbers of sample data has accurate prediction results and an overall high efficiency.

Nevertheless, when the imbalanced data contains more than a 2-class problem; it might be a three-class problem, which is called a multiclass classification. The multiclass classification problem would be transformed into a binary classification problem by assembling every majority class into 1 class. In contrast, the minority class would remain [12].

In order to solve the imbalanced data with an adverse effect on the data classification performance on the minority class before processing the data at a data level, this research offers a helpful technique to improve the data classification for household car ownership with a 3-class problem via two techniques: up-sampling and down-sampling. Weight optimization used these two techniques with feature selection to choose the first ten parameters, which had the optimal weights that could be compared before and after balancing the data. The data classification performance was measured from recall, sensitivity, or from the true positive rate (TPR), F-measure, accuracy and fall-out or false-positive rate (FPR).

Even though the present approach to deal with imbalanced data is well-known, in author's opinion such a strategy has yet to be proven in forecasting a household's automobile ownership with machine learning algorithms. In addition, the Imbalance Ratio (IR), k-fold cross-validation and the variables' main attributes from trip and tour-based models were used in this research. Moreover, it can be used to achieve several vital goals for learning classification by using imbalanced data in travel demand forecasting for transportation planning, such as destination selection and mode selection for each trip or for tour based on the objectives.

This article is composed of the following: an Introduction; Sections 1 and 2, which describe the problem of the imbalanced datasets and the classification performance indicators; Section 3, which presents the solutions to the class imbalance problem at a data level; Section 4, which presents the algorithms selected for the study and the datasets; Section 5, which offers the outcomes; and finally, Section 6, which contains the concluding thoughts, as well as the recommendations for further research.

2 Imbalanced datasets

This section sets forth the imbalanced datasets and later presents the indicators to evaluate the data classification problems in a different manner than a regular classification evaluation.

2.1 The class imbalance problem

In some cases of the data classification problem, the numbers of sample data in every class could differ, especially when the datasets had only 2-class or had more than 2-class transportation planning problems (See [13] for more details). However, it could be stated that the imbalanced data existed when one or more classes had had more datasets than other studies, which would be called the majority class. In contrast, the different types had had fewer datasets, as seen in Figure 1.

This imbalanced dataset had significantly affected the model's prediction performance. Most of the essential and outstanding data had been found in the minority class, such as medical science, marketing, banking, production and in transportation (e.g. choice prediction) [14].

Generally, the data classification algorithm had affected excellent decisions and shown biased results following the majority class. In contrast, the minority class seemed to be misclassified. The machine learning algorithm could not classify the data within the minority class because it had correctly categorized the majority class, showing its high performance. Accordingly, it was challenging to train the algorithm and to accurately predict the data when the datasets were imbalanced. This article focused on the minority class or those households without a car (Class 0). In contrast, the families with one and 2+ vehicles (Class 1 and 2) were determined to be the majority class.

2.2 Evaluation in the imbalanced territory

The performance evaluation of the data classification model from the confusion metrics table, which is one of the broadly used approaches, is typically focused on accuracy, the true positive rate (TPR), the false-positive rate (FPR) and the F-measure.

Namely, accuracy was the accurate value from the model after considering all classes; each class was considered one by one. The TPR was the exact value from the model after considering each category one by one. The F-measure was an evaluation of the precision and the TPR from the model altogether. Each type was

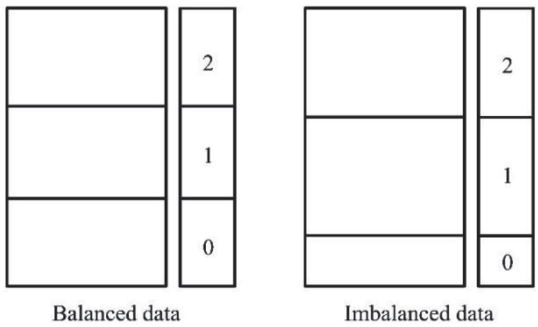

Figure 1 *The illustration of balanced and imbalanced data sets*

Table 1 *The confusion matrix for multiclass classification (for class 0)*

Predicted label classes	True label classes		
	0	1	2
0	TP	FP	FP
1	FN	TN	TN
2	FN	TN	TN

Table 2 *The five-fold cross-validation*

Iteration 1: train on	2	3	4	5	Test on	1
Iteration 2: train on	1	3	4	5	Test on	2
Iteration 3: train on	1	2	4	5	Test on	3
Iteration 4: train on	1	2	3	5	Test on	4
Iteration 5: train on	1	2	3	4	Test on	5

considered one by one. The minority class performance was evaluated mainly from the TPR in the imbalanced datasets since this TPR had described the actual travel distribution [15].

However, this article has mentioned that the TPR had provided an accurate prediction ratio of the minority class (Class 0) and has presented another value for the model's performance evaluation - FPR, which was used to indicate the misclassified majority class ratio.

Table 1 shows the multiclass confusion matrix for Class 0, which was adapted from [16]. True Positive (TP) was the number of the correctly classified data in the target class, Class 0 and it was Class 0. False Positive (FP) was the number of classified data as Class 0, but it was another class. True Negative (TN) was the number of the correctly classified data in any type other than Class 0. False Negative (FN) was the number of the classified data in other categories, but was actually in Class 0. Notably, TN was the opposite of TP and FN was the opposite of FP.

Expression

$$TP+TN/(TP+FN+FP+TN) \quad (1)$$

may be used to calculate accuracy. TPR = TP/(TP+FN) *100; FPR = FP/(FP+TN) *100; and F-measure = (2 * precision * TPR)/(precision + TPR). If these figures were high, precision and TPR would be high as well.

2.3 K-fold cross-validation

The classification model accuracy analysis using the k-fold cross-validation is employed to validate an error in the model's prediction. The K-fold cross-validation was a sampling method, which classified the datasets into several sections (k-fold). Some were tested with the model, while the remainder were used to create the model. After that, the outcomes from the model test were selected for the model's performance evaluation.

The K-fold cross-validation, the datasets were classified equally into several k-folds, e.g., five-folds would find the errors five times. In every calculation round, 1 of 5 folds was singled out to test the model's performance. In contrast, the other four folds were used for algorithm training or model creation. The example is given in Table 2.

3 Solutions in the data level

Before creating the model according to the imbalanced data, the researcher decided to study and balance the data. Therefore, this research suspended the data at a data level by using the Synthetic Minority Oversampling Technique (SMOTE) compared to a random under-sampling technique.

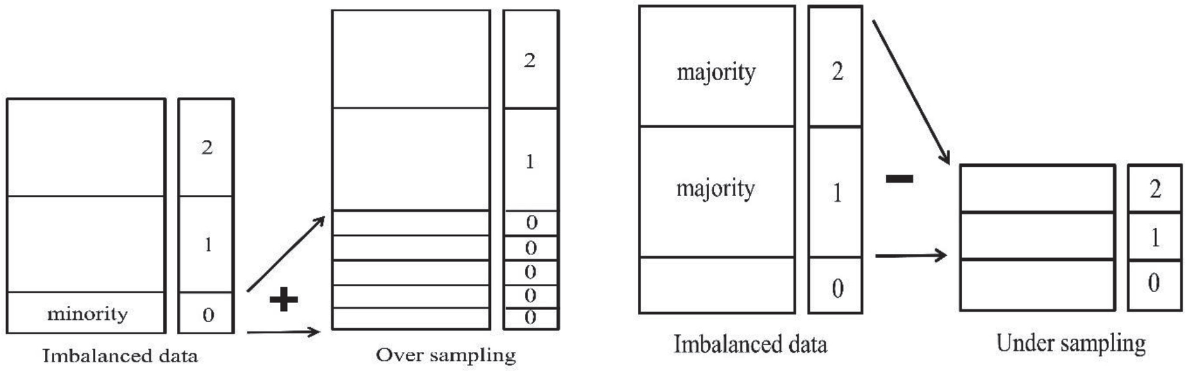

(a) (b)

Figure 2 *The concept of balancing imbalanced datasets: (a) the oversampling technique and (b) the under-sampling technique*

3.1 Oversampling and under-sampling

Balancing training data is an integral part of data processing. Data imbalances usually exist when the dataset's classes are unequally distributed, which may be a risk while training the model. There are several methods for balancing the data and overcoming the imbalanced training data, which could be performed at either a data level or an algorithm level.

SMOTE, or Synthetic Minority Oversampling Technique, which is a sampling method that is mainly used to fix the imbalanced data with the best results, was developed by [17]. Moreover, it is widely used to solve the imbalanced data sets with statistical knowledge. The SMOTE algorithm is a technique for oversampling the minority classes and minimizing the imbalanced data or equalizing the datasets within the target classes. In contrast, random under-sampling is an approach that is utilized to balance the dataset distribution at each level by randomly deleting the majority class examples. Yet, the major disadvantage of the approach is that some of the necessary and valuable measures might be deleted.

Figure 2 depicts the concepts of the oversampling and under-sampling techniques, which increase the minority class examples (as shown in Figure 2a) and decrease the majority class examples (as shown in Figure 2b). If there were 110 examples in Class 1, there would be 100 examples in Class 2 and 30 examples in Class 0.

4 Experimental framework

In this section, is suggested that the suitable algorithms for study and later describes more imbalanced datasets and related parameters. The final part mentions the statistical test to compare the outcomes from each of the classification algorithms.

4.1 Algorithms selected for the study

When the machine learning model trained the data, it was able to create a model from any of the following three major groups: 1) Geometric models - the models are used for mathematic calculations to define length or weight, including neural network (NN) and k-nearest neighbors (kNN); 2) Probabilistic models - the models are created from the training data probability (e.g. Naive Bayes); and 3) Logical models - these models are used to present data in different logical conditions, (e.g., decision tree (DT)).

4.1.1 k-Nearest Neighbors (kNN)

The kNN algorithm compares the unknown sample to the k training sample, which is the new sample's nearest neighbor. Preliminary theoretical results were published by [18], while a thorough summary was published by [19]. Finding the k closest training examples was the first step in applying the kNN algorithm to a new instance. Then, depending on the number of characteristics in the training example, the "proximity" was calculated from a distance in n-dimensional space.

The distance between the new example and the training examples could be calculated using several metrics, such as the

$$\text{Euclidean distance} = [(x_1-y_1)^2+(x_2-y_2)^2+\ldots+(x_L-y_L)^2]^{1/2}, \quad (2)$$

where x_1 was attributed as 1 of data 1 and y_1 was attributed as 1 of data 2. Thus, the attribute of both data (x and y) was L. However, since the length is frequently based on an absolute value, the data must be normalized before training and using the kNN method.

The kNN algorithm then categorizes the unknown sample by voting on the majority of the neighbors it discovers. In the event of a regression, the predicted value is equal to the average of the neighbor's found values.

An example of a small class appears scarce in the data space of an imbalanced training dataset. The estimated closest neighbor k is highly likely to identify a sample from a common type given the testing dataset. Small class sizes meant that the test cases would be more likely to be misclassified. This notice is based on research by [20] and [21].

4.1.2 Naive Bayes

Naive Bayes is a method for creating the high-bias, low-variance classifiers and establishing a good model even within a limited dataset. It is a probabilistic classifier that is based on Bayes' theorem. The estimation of a specific component for a given class variable is assumed to be independent by Naive Bayes classifiers;

$$P(C|A) = P(A|C)*P(C)/P(A), \quad (3)$$

in which P(C|A) is the probability that the data with the attribute A will have Class C. P(A|C) is the chance that attributes A will have Class C in the training data. P(A) is the probability of attribute A, while P(C) is the probability of Class C.

It performs pretty well on large datasets, in which this condition is assumed and holds, even though it demands an unrealistic need that the attribute values are restrictively free [22].

4.1.3 Decision trees (DT)

The DT is an explanation strategy that builds the rule of the DT by summarizing truths or related materials. This method has been used the most frequently because it aids the model in interpreting and making the data more understandable [23]. In this case, repetitive attribute partitioning was used to build the model.

The approach would find each attribute or feature's information gain ratio (IG) at each tree level (starting at the root node) and would then compare it to the class to identify the attribute with the highest IG. It would then be assigned as the decision tree's root (the chosen feature might categorize the data samples for model building and assign them to the same class if it were feasible (maximizing class homogeneity)). The ultimate objective of the decision trees algorithm is to divide all the data into subgroups with similar responses or classes (i.e. the sequence of slicing data to create appropriate if-then rules). The resultant rules can be used to explain an example from root to leaf. All of the information, which is provided, is accurate. In other words, this procedure is repeated until the last node (leaf node). Each node can categorize the sample into separate subgroups with a homogenous class. This procedure then comes to a halt and a decision tree model is generated.

Trees are usually trimmed to increase the predictability of decision structures and to minimize overfitting (See [24] for more details.).

4.2 Datasets

The trip data from the Khon Kaen Expressway Master Plan 2015 (Thailand) Engineering, Economical, Financial and Environmental Feasibility Study was used in this study. Since the population of the research region shares comparable features, systematic random sampling was utilized to obtain a total of 2,015 households consisting of 2 percent of the total households in the target area (4,757 people provided travel information, 616 people provided no travel information). In addition, face-to-face interviews were conducted to obtain information. The participants were

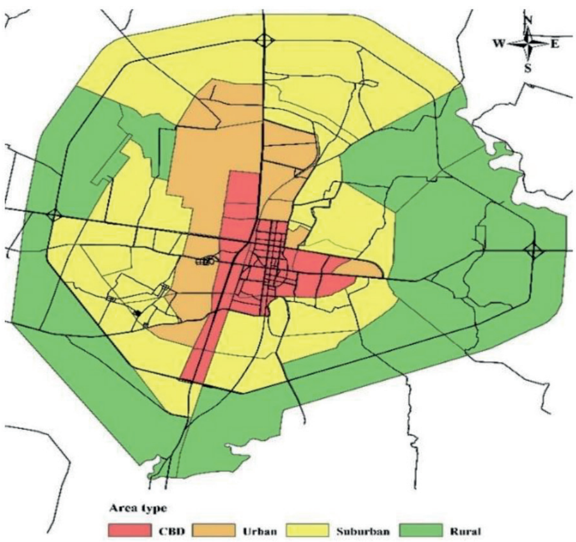

Figure 3 *The Area types in Khon Kaen, Thailand*

Table 3: The explanatory variables

Variables[1]	Definitions	Values
Socio-demographic attributes		
Gender	Gender of traveler	Male; female
TDwelling	Type of dwelling	Detached house; commercial buildings; townhouse; condominium/flat, etc.
HHT#	Household type	Two categories of worker vs. non- worker variable and two groups of dwelling type
Income	Household income (US$.)	No income; 0.029-74.5; 74.53-149.0; 149.03-223.5; 223.53-299.0; 299.03-448.5; 448.53-598.0; 598.03-747.5; 747.53-897.0; 897.03-1196.0.; 1196.03-1495.0; 1495.03-2242.5; 2242.53-2990.0; 2990.03-4485.0; >4485
Empstatus	Employment status	A number of full-time workers in the HH; Non-workers; Self-employed; Students; etc.
Apptype	Type of appointment	Number of CEOs; white-collar, blue-collar, red-collar, pink-collar, student, etc.
Kids	Number of children in HH	Numbers
HHS	Household size	Numbers
AGE	Number of people within an age category	<6; 7-19; 20-39; 40-59; 60-79; >80
Zone attributes		
Areatype	Origin or destination area type	CBD (central business district); urban; suburban; rural
PoDwell	Percentage of detached houses	Percentage
HHSlow[2]	Percentage of low-income households	PHHS1to2; PHHS3to4; PHHS5to6
Tour attributes		
Tour type	Number of stops on a tour	1: 1 (more) stop; 0: no stop
Main mode	Mode choice in a tour	Car; motorcycle; motor tricycle; minibus; train; bicycle; walking; other
Numbtrip	Number of trip segments within each tour	Numbers
Accessibility attributes		
Accessibility[3]	Accessibility Measurement	Acci; aij time

Note: [1]The factors were divided into socio-demographic characteristics, tour characteristics and accessibility characteristics. These variables were used to build and assess the models' performance. [2] The percentage of HHS had 2, 4, or 6 family members and the average income was less than 448.5, 897.0, or 1495.0, respectively. [3] A commuter's attempt to overcome the physical and time barrier between zones was measured by accessibility. The aij was the free-flow travel time between traffic zones i and j; acci was the average journey time between location i and a random place within the region [26].

recruited from 73 zones. The GIS information was utilized to categorize the research region. In addition, 10 more zones from suburban and urban areas were included, which increased the number of zones to 83. As illustrated in Figure 3, the residential density divided these zones into four area types: the central business district (CBD), the urban region, the suburban area and the rural area. These area types indicated the source region type and primary destination location for each trip under one tour. Thus, they were variables that indicated the source region type for each trip and the primary destination location under one tour.

The variables' main attributes from the tour and trip-based models were used in this research to create the model shown in Table 3.

4.2.1 Parameters

Each model used the kNN, Naive Bayes and decision trees algorithms to classify the data and the RapidMiner Studio Educational 9.7 Software Tool's default parameters. That is, the default parameters for the decision tree algorithm consisted of "criterion, gain ratio, 20 maximal depth of a tree, 0.25 the confidence level, 0.1 the minimal gain of a node and 2.0 minimal leaf size". The default parameters for the kNN algorithm were "k = 5 [25], measure types: mixed measures, mixed measure: Euclidean Distance"; and the default parameters for Naive Bayes algorithm were "5.0 number of neighbors, 1000 up-sampling size and a 0.5 nominal change rate".

***Table 4** The details of the imbalanced data sets for each area type*

Area types	Instances	Class0	Class1	Class2	Imbalance ratio, IR
Rural	809	211	373	225	2.83
Total	4852	874	2321	1657	4.55
Urban	1054	177	472	405	4.95
CBD.	1358	223	667	468	5.09
Suburban	1631	263	809	559	5.20

Note: As the consideration values for each region type, the imbalance ratio (IR) is defined as the negative class example or majority class divided by the number of positive class examples or minority class. If the IR was more than 9 [27], the dataset would have been significantly skewed. If the IR was less than 9, the dataset imbalance would have been considered as mild or low.

The car ownership ratio for the households in the study area is presented in Table 4, in which Class 0 was the minority class and Classes 1 and 2 were in the majority classes. The data was primarily used to construct and test the performance of the car ownership demand model via each machine learning algorithm before and after the data balancing. In addition, all of the data was compared using the statistical significance tests (T-Test) (alpha = 0.05).

5 Results

This research used a Synthetic Minority Oversampling Technique, SMOTE, to make the minority class datasets equal to the majority class and employed random under-sampling to balance the datasets after the data normalization.

Simultaneously, the weight optimization was selected to choose the first ten variables with the optimal weight to create the model. Meanwhile, the k-fold cross-validation was used to create and validate the data classification models with kNN, Naive Bayes and DT algorithms. Finally, the commission mainly considered the model's performance from balancing and from the imbalanced data in order to predict Class 0 as the minority class.

5.1 The results before and after the data balancing

The results from the model's performance validation, which were obtained by using different algorithms before the data was balanced, is presented in Table 5. The kNN algorithm showed high performance in predicting the minority class (Class 0) when considering the optimal accuracy and the TPR of all the area types and the FPR was low. However, the TPR percentage of each area-type was still low (the lowest = 44.3% for the total area type), in which the data analysis indicated that this problem had occurred due to the imbalanced data as the Imbalanced Ratio (IR) [28]. In each area, the type was in the range between 2.83 - 5.20.

After determining the best performing algorithm, the researcher solved the imbalanced dataset with a 2-part validation. In Part 1, the problem was solved at a data level using SMOTE and random under-sampling. In Part 2, the optimal k-parameter of the kNN algorithm was defined in order to improve the model performance so that the data in Part 1 could be classified.

By using the kNN algorithm to create a model for household car ownership, by performing the data balancing with SMOTE and by employing an under-sampling technique in each area type, the model's performance to predict Class 0 was illustrated as shown in Table 6. From the table, it can be seen that SMOTE demonstrated a higher TPR when compared to the time prior to balancing, but it was lower than the under-sampling technique. The TPR values for each area type were 63.5%, 64.0%, 67.2%, 66.4%, 54.4% and 78.7%, 83.2%, 85.9%, 85.2% and 74.5% for SMOTE and the under-sampling technique, respectively. Nevertheless, the under-sampling techniques might have deleted some important data, resulting in a high FPR value. Therefore, even though the TPR from the under-sampling technique was higher than the results from SMOTE, several misclassified cases were often found (FPR value was high.) [29].

In conclusion, after balancing the dataset with SMOTE and using the kNN algorithm to create the model for household car ownership demand, the model performed highly when predicting the minority class (Class 0) with the essential data compared to the imbalanced data and the balanced data with the under-sampling technique. Furthermore, an oversampling approach was found to be superior to an undersampling strategy for the inadequate data [30]. After balancing the data with SMOTE, another critical problem was selecting the appropriate k value for the kNN method because the neighbors from the k nearest neighbors had been chosen randomly depending upon the amount of oversampling desired.

This step began with a fixed size k = 5 (k-neighborhood) as the default parameter that was used to classify the training data by calculating the distance between the examples and adjusting the other measures for the following calculations (adding different k parameters). Any k parameter lower than 5 (e.g. 1 or 3) would not be counted due to low discrimination power [31]. Finally,

Table 5 *The performance before balancing the training data for the minority class (Class 0)*

Algorithms	Area types	Accuracy (%)	TPR (%)	FPR (%)	F-measure (%)
K-nearest neighbors (kNN)	Rural	63.4	46.9	9.2	54.2
	Total	67.7	44.3	6.7	50.6
	Urban	70.0	53.6	6.1	58.3
	CBD.	69.0	53.8	6.6	57.4
	Suburban	67.2	46.4	7.2	50.5
Naive Bayes	Rural	50.3	20.8	5.8	30.3
	Total	50.5	20.1	5.5	27.7
	Urban	52.8	28.2	7.7	33.9
	CBD.	50.4	36.7	10.5	38.7
	Suburban	51.2	25.1	8.3	29.9
Decision tree	Rural	52.3	15.1	0.3	26.1
	Total	47.8	0.8	0.2	1.6
	Urban	48.3	13.5	0.2	23.6
	CBD.	50.6	8.0	0.6	14.5
	Suburban	50.3	0.0	0.0	0.0

Table 6 *The results of TPR and FPR, when balancing the training data with the kNN algorithm*

Algorithms	Area types	TPR_n (%)	FPR_n (%)	TPR_o (%)	FPR_o (%)	TPR_u (%)	FPR_u (%)
K-nearest neighbors (kNN)	Rural	*46.9*	9.2	*63.5*	16.0	*78.7*	45.0
	Total	*44.3*	6.7	*64.0*	11.0	*83.2*	43.9
	Urban	*53.6*	6.1	*67.2*	7.7	*85.9*	34.7
	CBD.	*53.8*	6.6	*66.4*	9.4	*85.2*	41.7
	Suburban	*46.4*	7.2	*54.4*	12.3	*74.5*	50.1

Note: Subscript "n" refers to the pre-balancing data set, "o" refers to the balancing method by the SMOTE method and "u" refers to the balancing method using a random under-sampling technique

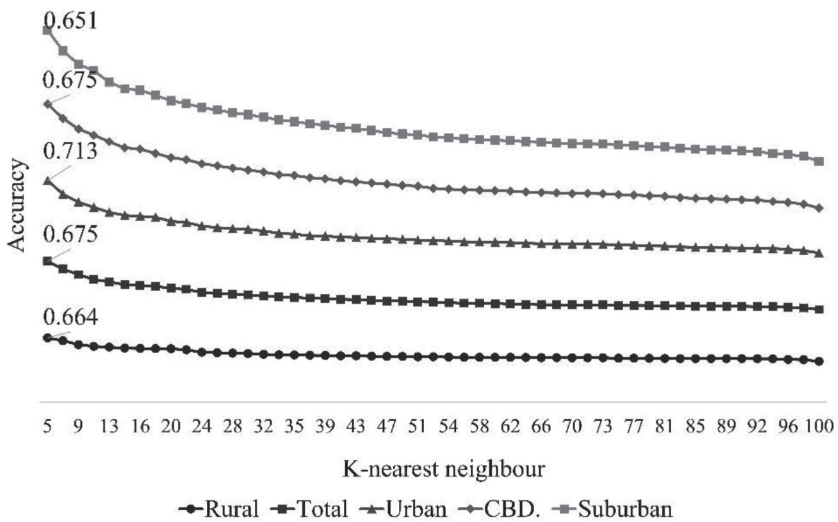

Figure 4 *The results of k-neighborhood parameterization as appropriate for each area type*

the outcome affirmed that the k neighborhood algorithm was suitable with 5 points for the training datasets in all the area types (IR= 2.83 - 5.20) within the study area, as illustrated in Figure 4, representing accuracy from all the area types with different k parameters.

Additionally, when k = 5 in all the area types, it was observed to give the best accuracy for the classification of household car ownership; the accuracy values for each area type were 65.1%, 67.5%, 71.3%, 67.5% and 66.4% for a rural area, the total area, an urban area, CBD and the suburban area, respectively.

It is likely that the target class label had not been uniformly distributed among the categorization jobs. A dataset like this is described as "imbalanced data." Data imbalances might make training a data science model difficult. For example, if the model is trained primarily on the majority class in imbalanced class problems, it will bias the model's prediction towards the majority class.

As a result, it was found that dealing with the imbalanced class is necessary before moving onto the modeling process. Many class balancing approaches tackle class imbalance by either sampling the minority class once again or by eliminating some samples from the majority class. The method for handling class balance strategies is divided into two categories: over-sampling and under-sampling.

One consequence of utilizing under-sampling approaches is that many majority class data points are lost in balancing the class. Over-sampling strategies do compensate for this flaw. However, producing several samples within the minority class may lead to model overfitting.

SMOTE is a common and well-known oversampling technique, which is used by data scientists to generate false minority data points within a cluster of minority class samples. The research outcomes also affirmed that balanced data facilitates the machine learning model, which leads to a more accurate minority class classification.

6 Conclusions and future work

This research created a helpful model for the classification of household car ownership in 5 area types with the imbalanced datasets. However, more than 2-class problems had affected the model's classification of the minority class (Class 0). The researcher recognized the significance of the preparatory step. Therefore, the parameters from the trip-based and tour-based models with weight optimization were selected to find the first ten parameters with optimal model creation. Later, cross-validation was used to create and test the performance of the data classification model before using the over and under-sampling technique to balance the datasets.

Using a geometric model, the k-Nearest Neighbors (kNN) algorithm created a model with balanced data by using SMOTE or the oversampling technique. As a result, the model was able to better classify the datasets because the data balancing had prevented biased results from occurring when the data was imbalanced. Consequently, the efficiency of the classification of the minority class was higher.

Future work should focus on developing the model to have better performance in order to solve the class imbalance with a hybrid sampling method at the data level, at the ensemble classifier, at the semi-supervised classifier at an algorithm level and in the feature selection at the feature level. In addition, the findings should be tested in order to find opportunities to improve the data prediction and to define policies for better urban transportation planning via the machine learning model and households with favorable characteristics.

References

[1] KAEWWICHIAN, P., TANWANICHKUL, L., PITAKSRINGKARN, J. Car ownership demand modeling using machine learning: decision trees and neural networks. *International Journal of GEOMATE* [online]. 2019, **17**(62), p. 219-230. ISSN 2186-2982, eISSN 2186-2990. Available from: https://doi.org/10.21660/2019.62.94618

[2] FEI, C., LIU, R., LI, Z., WANG, T., BAIG, F. N. (2021). Machine and deep learning algorithms for wearable health monitoring. In: *Computational intelligence in healthcare* [online]. MANOCHA, A. K., JAIN, S., SINGH, M., PAUL, S. (eds.). Cham: Springer international publishing, 2021. ISBN 978-3-030-68722-9, eISBN 978-3-030-68723-6, p. 105-160. Available from: https://doi.org/10.1007/978-3-030-68723-6_6

[3] JANDACKA, D., DURCANSKA, D., KOVALOVA, D. Concentrations of traffic-related pollutants in the vicinity of different types of urban crossroads. *Communications - Scientific Letters of the University of Zilina* [online]. 2019, **21**(1), p. 49-58. ISSN 1335-4205, eISSN 2585-7878. Available from: https://doi.org/10.26552/com.C.2019.1.49-58

[4] DOUZAS, G., BACAO, F. Effective data generation for imbalanced learning using conditional generative adversarial networks. *Expert Systems with Applications* [online]. 2018, **91,** p. 464-471. ISSN 0957-4174. Available from: https://doi.org/10.1016/j.eswa.2017.09.030

[5] BASU, R., FERREIRA, J. Understanding household vehicle ownership in Singapore through a comparison of econometric and machine learning models. *Transportation Research Procedia* [online]. 2020, **48**, p. 1674-1693. ISSN 2352-1465. Available from: https://doi.org/10.1016/j.trpro.2020.08.207

[6] JOHNSON, J. M., KHOSHGOFTAAR, T. M. Survey on deep learning with class imbalance. *Journal of Big Data* [online]. 2019, **6**(1), p. 1-54. ISSN 2196-1115. Available from: https://doi.org/10.1186/s40537-019-0192-5

[7] SMITH, M. R., MARTINEZ, T. The robustness of majority voting compared to filtering misclassified instances in supervised classification tasks. *Artificial Intelligence Review* [online]. 2018, **49**(1), p. 105-130. ISSN 0269-2821, eISSN 1573-7462. Available from: https://doi.org/10.1007/s10462-016-9518-2

[8] BRANCO, P., TORGO, L., RIBEIRO, R. P. A survey of predictive modeling on imbalanced domains. *ACM Computing Surveys (CSUR)* [online]. 2016, **49**(2), p. 1-50. ISSN 0360-0300. Available from: https://doi.org/10.1145/2907070

[9] MAZUROWSKI, M. A., HABAS, P. A., ZURADA, J. M., LO, J. Y., BAKER, J. A., TOURASSI, G. D. Training neural network classifiers for medical decision making: The effects of imbalanced datasets on classification performance. *Neural Networks* [online]. 2018, **21**(2-3), p. 427-436. ISSN 0893-6080. Available from: https://doi.org/10.1016/j.neunet.2007.12.031

[10] VUTTIPITTAYAMONGKOL, P., ELYAN, E., PETROVSKI, A. On the class overlap problem in imbalanced data classification. *Knowledge-Based Systems* [online]. 2021, **212**, 106631. ISSN 0950-7051. Available from: https://doi.org/10.1016/j.knosys.2020.106631

[11] DENG, J., LORENZINI, K., KRAUS, E., PALETI, R., CASTRO, M., BHAT, C. Business process and logical model to support a tour-based travel demand. 2014.

[12] HOSENIE, Z., LYON, R. J., STAPPERS, B. W., MOOTOOVALOO, A. Comparing multiclass, binary and hierarchical machine learning classification schemes for variable stars. *Monthly Notices of the Royal Astronomical Society* [online]. 2019, **488**(4), p. 4858-4872. ISSN 0035-8711, eISSN 1365-2966. Available from: https://doi.org/10.1093/mnras/stz1999

[13] KAEWWICHIAN, P. Multiclass classification with imbalanced datasets for car ownership demand model - cost-sensitive learning. *Promet – Traffic and Transportation* [online]. 2021, **33**(3), p. 361-371. ISSN 1848-4069. Available from: https://doi.org/10.7307/ptt.v33i3.3728

[14] WANG, S., WANG, Q., ZHAO, J. Deep neural networks for choice analysis: extracting complete economic information for interpretation. *Transportation Research Part C: Emerging Technologies* [online]. 2020, **118**, 102701. ISSN 0968-090X. Available from: https://doi.org/10.1016/j.trc.2020.102701

[15] BIAGIONI, J. P., SZCZUREK, P., NELSON, P., MOHAMMADIAN, A. Tour-based mode choice modeling: using an ensemble of (un-) conditional data-mining classifiers. In: 88th Annual Meeting of the Transportation Research Board: proceedings. 2008.

[16] RIVAS-PEREA, P., COTA-RUIZ, J., PEREZ VENZOR, J. A., CHAPARRO, D. G., ROSILES, J.-G. Lp-SVR model selection using an inexact globalized quasi-newton strategy. *Journal of Intelligent Learning Systems and Applications* [online]. 2013, **5**(1), p. 19-28. ISSN 2150-8402, eISSN 2150-8410. Available from: https://doi.org/10.4236/jilsa.2013.51003

[17] CHAWLA, N. V., BOWYER, K. W., HALL, L. O., KEGELMEYER, W. P. SMOTE: synthetic minority over-sampling technique. *Journal of Artificial Intelligence Research* [online]. 2002, **16**, p. 321-357. ISSN 1076-9757. Available from: https://doi.org/10.1613/jair.953

[18] COVER, T., HART, P. Nearest neighbor pattern classification. *IEEE Transactions on Information Theory* [online]. 2006, **13**(1), p. 21-27. ISSN 0018-9448. Available from: https://doi.org/10.1109/TIT.1967.1053964

[19] AGARWAL, Y., POORNALATHA, G. Analysis of the nearest neighbor classifiers: a review. In: Advances in Artificial Intelligence and Data Engineering: proceedings [online]. 2021. ISSN 2194-5357, eISSN 2194-5365. Available from: https://doi.org/10.1007/978-981-15-3514-7_43

[20] MANI, I., ZHANG, I. kNN approach to unbalanced data distributions: a case study involving information extraction. In: Workshop on Learning from Imbalanced Datasets: proceedings. Vol. 126. 2003.

[21] HRIC, M., CHMULIK, M., JARINA, R. Comparison of selected classification methods in automatic speaker identification. *Communications - Scientific Letters of the University of Zilina* [online]. 2011, **13**(4), p. 20-24. ISSN 1335-4205, eISSN 2585-7878. Available from: http://komunikacie.uniza.sk/index.php/communications/article/view/873

[22] AGRAWAL, R. Predictive analysis of breast cancer using machine learning techniques. *Ingenieria Solidaria* [online]. 2019, **15**(3), p. 1-23. ISSN 2357-6014. Available from: https://doi.org/10.16925/2357-6014.2019.03.01

[23] WOSYKA, J., PRIBYL, P. Decision trees as a tool for real-time travel time estimation on highways. *Communications - Scientific Letters of the University of Zilina* [online]. 2013, **15**(2A), p. 11-16. ISSN 1335-4205, eISSN 2585-7878. Available from: http://komunikacie.uniza.sk/index.php/communications/article/view/648

[24] WETS, G., VANHOOF, K., ARENTZE, T., TIMMERMANS, H. Identifying decision structures underlying activity patterns: an exploration of data mining algorithms. *Transportation Research Record* [online]. 2000, **1718**(1), p. 1-9. ISSN 0361-1981. Available from: https://doi.org/10.3141/1718-01

[25] ZHANG, S., LI, X., ZONG, M., ZHU, X., WANG, R. Efficient kNN classification with different numbers of nearest neighbors. *IEEE Transactions on Neural Networks and Learning Systems* [online]. 2018, **29**(5), p. 1774-1785. ISSN 2162-237X. Available from: DOI: 10.1109/TNNLS.2017.2673241

[26] ALLEN, W. B., LIU, D., SINGER, S. Accessibility measures of U.S. metropolitan areas. *Transportation Research Part B: Methodological*. 1993, **27**(6), p.439-449. ISSN 0191-2615.

[27] GARCIA, S., HERRERA, F. Evolutionary undersampling for classification with imbalanced datasets: proposals and taxonomy. *Evolutionary Computation* [online]. 2009, **17**(3), p. 275-306. ISSN 1063-6560. Available from: https://doi.org/10.1162/evco.2009.17.3.275

[28] BUDA, M., MAKI, A., MAZUROWSKI, M. A. A systematic study of the class imbalance problem in convolutional neural networks. *Neural Networks* [online]. 2018, **106**, p. 249-259. ISSN 0893-6080. Available from: https://doi.org/10.1016/j.neunet.2018.07.011

[29] FERNANDEZ, A., GARCIA, S., HERRERA, F., CHAWLA, N. V. SMOTE for learning from imbalanced data: progress and challenges, marking the 15-year anniversary. *Journal of Artificial Intelligence Research* [online]. 2018, **61**, p. 863-905. ISSN 1076-9757. Available from: https://doi.org/10.1613/jair.1.11192

[30] KRISHNAVENI, C. SOBHA RANI, T. On the classification of imbalanced datasets. *International Journal of Computer Science and Technology IJCST* [online]. 2011, **2**(SP1), p. 145-148. ISSN 0976-8491, eISSN 2229-4333. Available from: https://doi.org/10.13140/RG.2.2.14964.24961

[31] NAPIERALA, K., STEFANOWSKI, J. Types of minority class examples and their influence on learning classifiers from imbalanced data. *Journal of Intelligent Information Systems* [online]. 2016, **46**(3), p. 563-597. ISSN 0925-9902, eISSN 1573-7675. Available from: https://doi.org/10.1007/s10844-015-0368-1

THE COMPARISON OF DYNAMIC EFFECTS ACTING IN THE COMMON CROSSING AND SWITCH UNIT OF A TURNOUT

Jaroslav Smutný, Dušan Janoštík*, Viktor Nohál

Institute of Railway Structures and Constructions, Faculty of Civil Engineering, Brno University of Technology, Brno, Czech republic

*E-mail of corresponding author: janostik.d@fce.vutbr.cz

Resume

The paper presents an analysis and comparison of selected dynamic parameters in the common crossing and switch unit of a railway turnout. The paper includes a description of the measurement methodology, the report of mathematical methods used to evaluate the measured data and comparison of selected parameters describing dynamic processes in individual parts of the structure. The paper also includes a mathematical analysis of the lesser-known Hilbert Huang transformation, including its practical application. From the presented case study, practical experience and recommendations for the railway line managers, research organizations and possibly for the wider technical public are derived.

Article info

Received 16 September 2021
Accepted 10 January 2022
Online 29 March 2022

Keywords:

railway turnout
common crossing unit
switch unit
dynamic effects
nonstationary and nonlinear signals
vibrations analysis in time and frequency domain
Hilbert-Huang transformation

Available online: https://doi.org/10.26552/com.C.2022.3.D116-D125

ISSN 1335-4205 (print version)
ISSN 2585-7878 (online version)

1 Introduction

All the parts of the superstructure and substructure are subject to dynamic loads from the running of trains. When the train is moving, the wheels of the train set not only roll on the rail but also shift tangentially. In addition, slip occurs at small radii of curves. The forces and moments are then not transmitted pointwise, but in the contact area between the wheel and the rail.

The axle forces acting vertically on the rail, derived by the own weight of the trainset, the longitudinal stresses caused by starting and braking, the longitudinal and transverse pressures and the forces generated by passing in a curve, etc., are distributed through the rail fastening to the rail supports, the track bed and the subgrade. The whole process of dynamic loading is accompanied by the propagation of vibrations, changes in motion behavior or deformation of the structure [1].

When passing the axle wheels on rails, it is necessary to consider the uneven distribution of stress in individual and adjacent areas of supports and rail bed. The rails distribute the load caused by the running trainsets to individual sleepers. The magnitude of the forces that the rail transmits on the sleeper is determined by the shape of the rail, the flexibility of the rail mounting on the sleeper, the shape of the sleeper and the distribution of the sleepers. The rail bed is then stressed unevenly depending on how the stress is distributed over the sleeper bed [2]. This is also related to the uneven stress on the bottom of the railway.

The transmission of dynamic forces from the rails to the subsoil is even more complicated in turnout constructions. It is necessary to include the changing position of the rails in the transverse direction on the supports, uneven transmission of dynamic effects in different parts of the turnout structure, changing cross-sections of rails in the tongue, crossing the wheelsets retainer, or the changing longitudinal dimension of the rail supports.

The dynamic effects on the railway structure increase with increasing speed of the trainsets. The dynamic stress of the track is also influenced by properties of all the parts of the railway superstructure, i.e. the quality of the gravel bed, the type of sleepers, the quality of their tamping, the properties of track fittings, the type of fasteners and the quality of the railway sub-ballast layers, as well. Particularly at points of interruption in the continuity of travel and at points of change in track stiffness, there are increased dynamic effects. In those places, there is an irregular settlement of the rail bed, crushing of the aggregate of the rail bed and defects on the running surface of the rails.

One of the main problems of today's railways is to minimize the costs associated with track maintenance. Based on the knowledge of the dynamic processes taking place in it, it is possible to determine appropriate measures that will lead to minimization of the maintenance costs. Effective tools also include vibrodiagnostics, i.e. the analysis of vibrations propagating through the superstructure and substructure. Therefore, one will increasingly encounter phenomena whose satisfactory clarification and technical solution will depend on understanding the dynamic stress of the railway structure [3].

The railway turnout structures represent one of the key points of the railway transport. This is because a turnout structure consists of a number of structural components of different properties, which in summary must fulfil the required functions. Among the most important properties is especially their reliability and safety within the framework of the railway operation. At the same time, the running of trainsets generates large dynamic stress in the turnout area, which is different from the dynamic stress in the rail grid area. Therefore, it is very important to study the dynamic processes in turnouts in order to improve the quality of maintenance work. Application of the new methods of measurement and analysis helps to achieve that goal [4].

A classic simple turnout consists of three main parts - common crossing unit, closure unit and switch unit (Figure 1). The common unit consists of a frog, a retainer and an outer rail. There is a crossing of rails and separation of rails in two different directions. The common crossing unit forms the place where the wheel passes a gap (depression) for the wheel flange of the vehicle, which moves in another direction. In order to avoid an impact or climbing of the flange on the tip of the common crossing unit, the second wheel of the same wheelset is guided by a retaining device, which does not allow it to move away from the outer rail.

The closure unit of the turnout actually forms a tangle of tracks. It connects the switch and the common crossing unit. The interchange is a moving part of the turnout, on which the track branches in two directions. The main parts of the switch unit consist of tongues, supports and a turnout. The tongue forms the only moving structure of the carriageway. The position of the tongues determines the direction of further movement of the train set while driving. The tongues are usually stored on stool bases. Under the normal circumstances, one tongue always rests on the support. A motorized converter is used to adjust the tongues. To secure them in the appropriate position there is a locking device. From the above, it is clear that especially the common crossing and switch units belong to the key parts of turnouts in terms of dynamic effects.

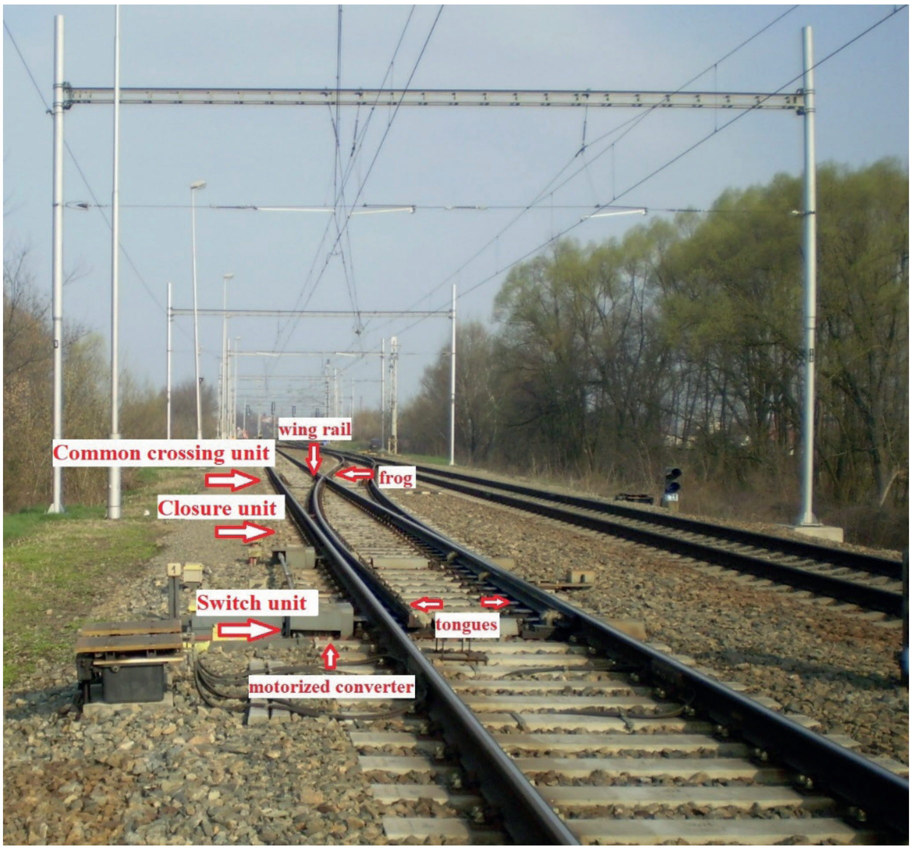

***Figure 1** The picture of a turnout with a description of the most important parts*


(a)


(b)

Figure 2 *The view of the common crossing (a) and a switch (b) unit of turnout*

The dynamic processes in both areas are further briefly considered.

High dynamic forces and high vibrations level can be expected in the area of the train set wheel transition from the wing rail to the tip of the frog, where, depending on the quality of the transition geometry, a dynamic impact occurs.

From theoretical assumptions and computer simulations [5], it is concluded that another area requiring increased attention is the switch unit. The mechanism of vibrations transmission in this case is different from that of the common crossing assembly. At the same time, many theoretical works show a lower level of vibrations propagating through the switch unit into the gravel bed. This is due to the uninterrupted running surface of the rail when the wheel flange gradually approaches and rests on the tongue rail. The intensity of vibrations is damped by the track skeleton, when a small part is damped already in the rail and its rubber pad. Further vibrations damping occurs in the sleeper. The undamped component of the vibrations energy is also transferred to the gravel bed. The question is how much of this energy is compared to the energy propagating in the common crossing unit.

2 Methods of measurement and evaluation

A measurement methodology, certified by the Ministry of Transport of Czech Republic, was used to measure the dynamic effects acting on the turnout [6]. This methodology consists of three parts. The first involves measuring the motion behavior of a structure. The second area involves the propagation of vibrations and shocks from the wheel-rail contact, through the sleeper, into the gravel bed of the common crossing and switch unit. The third area provides information on the forces and deformations acting. Note that a simplified variant of this methodology was used in this paper to present the results.

Before measuring the dynamic characteristics of the turnout, the geometric parameters were measured by a measuring wagon of the infrastructure manager in the Czech Republic. The measurement confirmed that the whole turnout is in excellent condition.

In total, two basic measuring areas with 3 measuring points were set in the measured turnout, to which piezoelectric acceleration sensors from the Bruel&Kjaer company were attached. These locations were chosen so that the measured values could be compared. In the case of the common crossing unit, it was a triaxial acceleration sensor located at the foot of the wing rail in the straight branch of the turnout (labelling outputs A4Z, A5X, A6Y), acceleration sensor located on the sleeper near the tip of the common crossing unit (A3Z) and acceleration sensor located on the rod (waveguide) in a gravel bed (A0Z). In the switch unit, the sensors were placed on the heel of the support (acceleration sensor, labelling A4Z, A5X, A6Y), then on the sleeper in the area of the passage of the wheel from the support to the tongue rail (A3Z) and measuring rod, which was embedded in the gravel bed near the passage of the wheel (A0Z). Simultaneously with the measurement of vibrations characteristics, a large number of other parameters were measured. Their comparison and analysis are not part of this paper.

Time, frequency and time-frequency analysis were used for vibrations analysis. Note that the analysis in the time plane was focused on the one hand to determine the maximum values of vibrations acceleration and on the other hand to calculate the effective value of vibrations acceleration. Within the frequency analysis, the classical Fourier analysis with output to amplitude frequency spectra was used. The formulas and the procedure for calculating the effective value of acceleration or amplitude spectra are not given in the paper, they can be found in many professional publications [7-8].

In the time-frequency analysis, the authors used the Hilbert Huang transform. According to the research and the authors' experience, this type of analysis is particularly advantageous in the case of impact loads. Since this is a less known transformation procedure with specific calculation, its analysis and description are given in the text below.

The Hilbert-Huang transformation is a lesser-known and less widely used method for analysis of the transient, nonlinear and non-stationary signals [9-11]. The procedure for calculating this transformation must be divided into two parts. In the first part, the so-called empirical modal decomposition is performed, followed by the second in the framework, which calculates the so-called Hilbert spectrum. This then represents the propagation of energy in the time-frequency domain and is calculated by applying the well-known Hilbert transformation.

Empirical modal decomposition is used to decompose any nonlinear or nonstationary signal $s(t)$ into a finite number of eigenmodal functions. The Eigen modal functions must satisfy two basic conditions [11-12]:

- The number of extrema (i.e. minima and maxima) must be either equal to, or differ by at most one, the number of passes through the function through zero;
- At any point, the average value defined by the envelope of local maxima and local minima is zero.

The first condition is similar to the narrowband requirement for a stationary Gaussian process, the values must not differ too much. The second condition is local, derived from the first and it ensures that the instantaneous frequency will not have unnecessary fluctuations caused by the asymmetric waveforms. Note that this is essentially a resemblance to the Fourier transformation, which also decomposes into simpler functions, sins and cosines. The disadvantage of the Fourier transformation is that it gives good results only for a signal that is stationary and fully periodic. In the case of calculating the Hilbert-Huang transformation, this limit does not apply. Furthermore, the calculation procedure of the empirical modal decomposition, according to the author of the method of scientist E. Huang, is described [13-14]. The calculation procedure takes place in several steps.

The first step is to find the local extrema (maxima and minima) in the given signal $s(t)$. These extrema are then interpolated with a suitable curve, such as a cubic spline. This creates two envelopes of the original signal - the upper $e_{max}(t)$ and the lower $e_{min}(t)$. The average value of both envelopes is then calculated. Next, one calculates the difference between the signal and the mean value.

$$h_1(t) = s(t) - \mu_1(t). \tag{1}$$

If the calculation does not meet the requirements for the modal function, iterations must be continued. Note that due to the approximation, new extrema can arise, i.e. overshoot or undershoot in the envelope. The calculation procedure must be repeated until the resulting component meets the specified conditions. The procedure can be written by an equation

$$h_{k+1}(t) = h_k(t) - \mu_{k+1}(t). \tag{2}$$

It should be noted here that the iteration process essentially filters the low frequency components and smoothes the different amplitudes. The standard deviation value, which is calculated from the two consecutive results of the iteration process, was used as a criterion for completing the partial calculation of each component for the purposes of this paper. E. Huang determined a typical value of the standard deviation for the end of the iteration in the interval 0.2 and 0.3 [13-14]. Note that the first modal component represents the highest frequency component of the signal $s(t)$. If one separates the calculated component from the signal, we obtain the so-called residue. The residue contains components with lower frequencies. It can be marked as a new signal and the procedure repeated. The original signal is described by the following equation [15].

$$s(t) = \sum_{i=1}^{n} c_i + r_n, \tag{3}$$

where $s(t)$ is the original signal, r_n is the residue and c_i is the component. Equation (3) shows that the original signal can be reconstructed by simply summing all the modal functions and the residual. Note that the decomposition can be terminated based on a predetermined limit of the number of iterations or when the residual is a monotonic function from which it is no longer possible to separate other proper modal functions [16]. If one has calculated the individual components described above by decomposition, the Hilbert transformation can be applied to each and calculate the instantaneous frequency. This procedure can be expressed by the following equation.

$$s(t) = \sum_{k=1}^{n} a_k(t) \cdot e^{j \cdot \int \omega_k(t) \cdot dt}. \tag{4}$$

Thus, Equation (3) expresses the instantaneous amplitude $a_k(t)$ and the instantaneous frequency (angular frequency) $\omega(t)$ as a function of time t, while allowing the amplitude to be expressed as a function of frequency and time. It is therefore the Hilbert amplitude spectrum, which expresses the energy distribution in the time-frequency plane [17-18].

It follows from the above description that the Hilbert-Huang transformation represents an alternative to, for example, the Fourier transformation or the Wavelet transformation [19], or to other time-frequency methods, with the difference that it decomposes the measured signal in a different way. Thus, not into predefined functions such as trigonometric functions, parent wavelet etc. but into functions based on the signal under investigation.

3 The case studies

To compare the dynamic effects in the switch and the common crossing units, turnout No. 59 (Figure 2) was selected in the so-called Pardubice head of

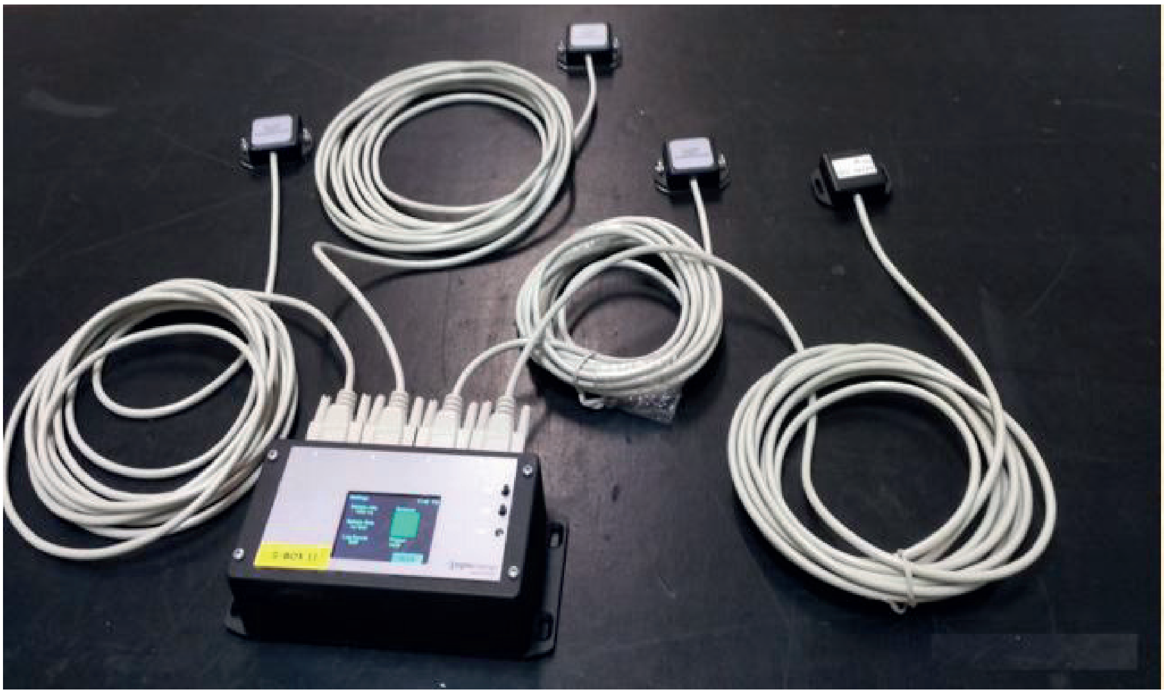

Figure 3 *View of the measuring system with sensors*

the Chocen railway station with a left turn direction (turnout designed for a speed of 80 $km \cdot h^{-1}$). The selected turnout is of the type J60-1:14-760-zlp, L, p, CZP, b, KS, ZPT. Trainsets may pass through this turnout in a straight line at a line speed of 160 $km \cdot h^{-1}$. The turnout is equipped with a system of railway superstructure UIC 60 with Vossloh Skl 24 fastening and concrete sleepers. Note that this is the most common type of turnout used on the corridor lines of the Czech Republic. For this reason, the author's team in this paper focused on the measurement and analysis of this particular structure. At the same time, the same types of turnouts were measured at other localities. In total, there were 20 measuring campaigns.

Two autonomous S-Box dataloggers (Figure 3), developed at the authors‘ workplace, were used for the measurements. The S-Box datalogger has been described in detail in the literature [20]. For measurement purposes, the measuring system was verified using a calibration sensor 8305 from Bruel&Kjaer and a vibrating calibrator V21D from Metra Mess und Frequenz Technik. It is a two-level measuring system consisting of a data logger and a superordinate computer with software for analysis of the measured data. The system provides up to 12-channel recording from various types of sensors (vibrations, noise, displacement, strain gauges, temperature etc.). Within the first level, the data is measured and stored on an SD card. The datalogger is equipped with a system to automatically start and stop recording and also provides the possibility of data wireless transmission to a higher-level system consisting of a computer and the relevant software.

Within the superordinate system (second level), manual, semi-automatic or fully automatic analysis of the measured data takes place according to a set scenario. It should be noted that for this measurement, a Raspberry Pi computer was used as the master system. The data analysis program was developed in Python. The whole setup was powered by a battery, which was recharged from a solar panel when needed. Measured and evaluated data were continuously sent to the NAS storage of the authors' workplace to the database server.

The measuring set-up was supplemented with a trigger module. This consisted of the two infrared gates mounted on a small tripod at a height of 150 mm above the top of the rail and an evaluation module. The first barrier was placed at 30 m in front of the measuring station, the second at 30 m behind it. The principle of starting and ending the measurement was based on the principle of counting and comparing the passing axles. The evaluation module simultaneously measured the running speed of the train set. This data was also transferred to the master computer.

The data filtering and classification of the trainsets into predefined categories was performed automatically on the master computer after downloading the data from the measuring system.

The evaluation software in the master computer includes implementation of the support vector machine method for recognizing the train sets. The authors of the paper have very good implementation experience with this method. The input to the method is the measured vibrations acceleration values from three sensors - on the wing rail, on the sleeper and in the gravel bed.

It should be noted that the classification software contains a database of locomotives, passenger cars and entire train sets including the gauge for more accurate recognition. The classifier was set up before the measurement.

As a part of the measurement campaign, the passage

***Table 1** The comparison of the effective values of vibrations acceleration [m.s^{-2}]*

Train set	Turnout	A0Z ^	A3Z ^	A4Z ^	A5X †	A6Y ‡	Travel speed [km/h]
Leo Express	59, Common crossing unit	20	43	108	25	32	155
	59, Switch unit	2	38	40	10	17	155
Pendolino	59, Common crossing unit	22	45	110	28	30	163
	59, Switch unit	4	39	42	12	13	162
RegioJet	59, Common crossing unit	10	26	95	17	26	140
	59, Switch unit	3	24	49	11	20	140
Train set with 151 engine	59, Common crossing unit	7	16	46	12	13	120
	59, Switch unit	2	25	42	10	14	120
Train set with 150 engine	59, Common crossing unit	2	10	33	6	10	82
	59, Switch unit	2	40	65	15	25	82

Legend: ^ in the vertical direction
† in the longitudinal direction
‡ in the transverse direction

of a total of 60 trains was recorded, for which, in addition to the time course of vibrations acceleration, their other parameters were also recorded - travel time, running speed, number of railway cars and type of locomotive and direction of travel.

For their own evaluation, these trains were divided into suitable categories. In the article, the authors focused on evaluation of selected train sets. Those were divided into three main categories. The first category includes EC trainsets. This category includes both light complete trains sets of the Pendolino and LeoExpress type, as well as classic RegioJet train sets with the E630 series locomotive. The second category is represented by the passenger trains with a locomotive of the 151 series. The third category is represented by the freight train sets hauled by relatively old locomotives of the 150 series.

The global maxima and minima were automatically subtracted in the superordinate computer, then the basic vibrations characteristics (effective acceleration values a_{ef} and amplitude frequency spectra) were calculated for each acceleration sensor and for each category of trainsets. The calculated characteristics were organized in a table and graphs for comparison. Note that the effective acceleration values shown in Table 1 are the result of averaging the partial values from all the measurements made for a given category of train set.

It is clear from Table 1 that significantly higher effective acceleration values were obtained when the EC category trainsets (Pendolino, LeoExpress and RegioJet) passed in the common crossing unit of the turnouts compared to the switch unit. Relatively similar dynamic effects were also found for passenger trains hauled by 151 series locomotives. For the trainsets hauled by Class 150 series locomotives this is different. In most of the measured parameters, higher values were obtained in the area of the exchange of the measured turnout compared to the frog part. It should be noted that this fact was also demonstrated by a more detailed analysis in the time and frequency plane, including the comparison of time records and their amplitude frequency spectra.

To compare the dynamic load found in the frog and switch unit of the turnout, the passage of a RegioJet train set at a speed of 140 kmh^{-1} was selected for the paper (Figures 4 and 5). Due to the limited space of the paper, the authors focused on a more detailed analysis of measured data from sensors that were in the gravel bed near the rail attachment. It should be noted that the RegioJet train consists of railcars from the Austrian and Swiss Federal Railways. The wagons are hauled by modernized Škoda locomotives and TRAXX MS 2e locomotives from the manufacturer Bombardier.

The top graph of each figure shows the time course of vibrations. The left graph shows the amplitude spectrum of the vibrational response. The middle graph shows the 3D representation of the time-frequency waveform of the vibrations amplitude spectrum.

The values of the spectra are expressed in decibel scale by different colours (or grayscale). Note that the maximum value is the colour black. Again, it should be mentioned that for a more detailed insight into the dynamic characteristics, time and frequency slices can be displayed within the middle graph. In the former case, those are the plots providing individual frequency spectra at different times, while in the latter case; they are the time histories of selected frequency components.

From the comparison of time records it is clear that higher values of vibrations acceleration (up to 360 m·s^{-1})

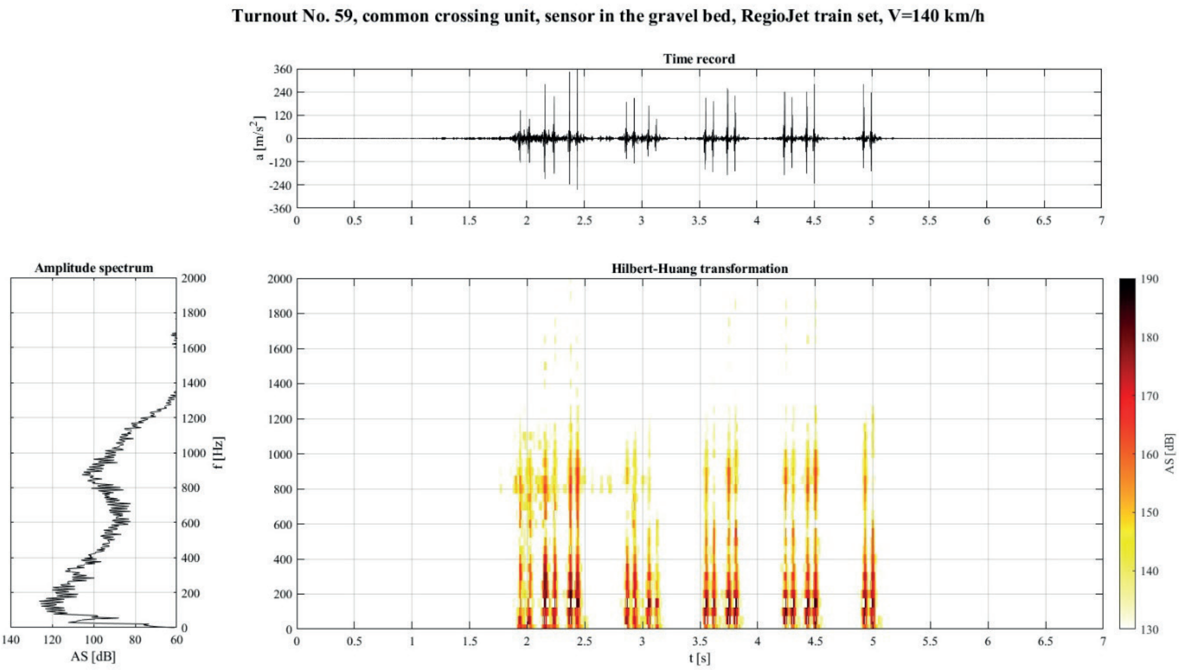

Figure 4 *Time, frequency and time-frequency characteristics of the vibrations, sensor in the gravel bed, turnout no. 59 - common crossing unit, vertically direction, RegioJet, speed 140 km·h^{-1}*

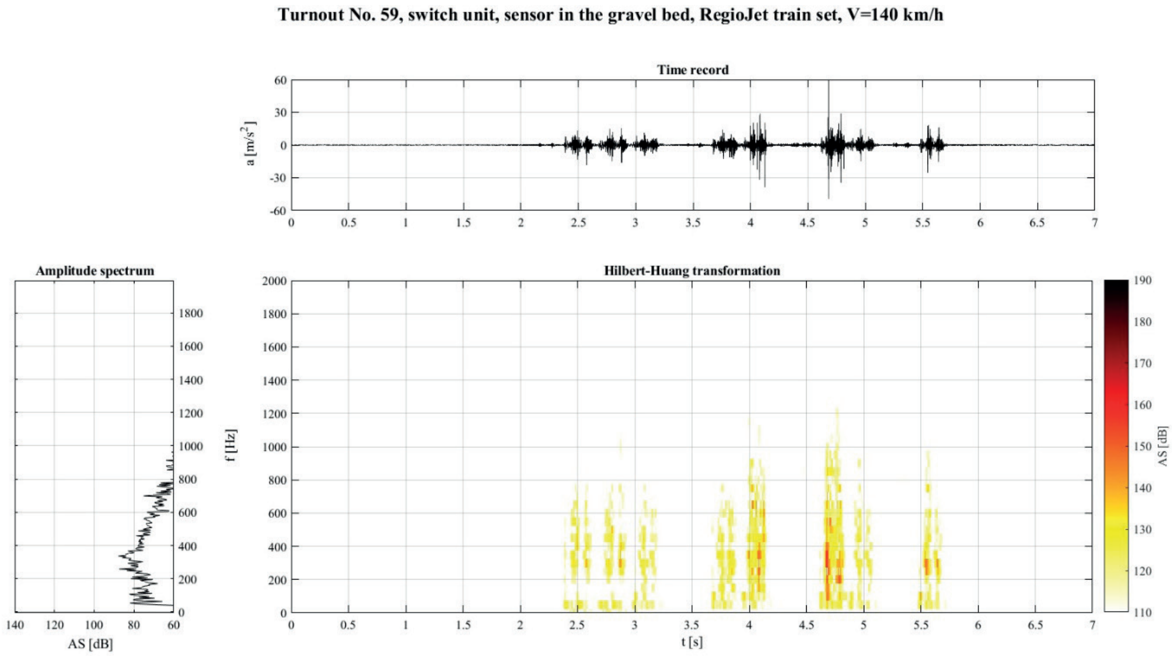

Figure 5 *Time, frequency and time-frequency characteristics of the vibrations, sensor in the gravel bed, turnout no. 59 - switch unit, vertically direction, RegioJet, speed 140 km·h^{-1}*

were measured when the set wheel passes from the wing rail to the common crossing unit tip (Figure 4) compared to the passage of the train set through the switch unit (60 m·s^{-1}) (Figure 5). The time recording of vibrations from the common crossing unit shows the course of the signal composed of a series of very narrow shocks from the wheels of a passing train set. Thus, a relatively large part of the vibrational energy is transferred to the gravel bed.

From the time course found in the switch unit of the turnout, it is clear that the course of acceleration has a different character. The course is much smoother, there are not so outlined individual passages of the wheels of the set.

The frequency spectrum (Figure 4) obtained from the running of the trainset through the common crossing unit shows several frequency clusters with maximum values at the frequencies 30 Hz, 150 Hz, 230 Hz, 320 Hz, 520 Hz, 880 Hz and 1.7 kHz. The highest spectrum value (125 dB) was reached at a frequency of 150 Hz. The frequency spectrum obtained from the running of the trainset through the switch unit (Figure 5) also shows several significant frequency components (80 Hz, 110 Hz, 200 Hz, 260 Hz, 340 Hz and 700 Hz). The highest value of the spectrum (87 dB) was reached at a frequency of 340 Hz.

The same conclusions are drawn with the time-frequency analysis by the Hilbert Huang transform method (middle graphs of Figures 4 and 5). In contrast to the classical frequency analysis performed using the Fourier transform, the time distribution of significant frequency components is also evident from these graphs.

Even in the case of this analysis, it is clear that a higher peak in the time-frequency plane was achieved in the case of passing the wheels of the trainset through the railway common crossing unit. Note that the graphs show a very accurate time localization of individual frequency components.

4 Conclusions

The paper was devoted to the comparison of dynamic effects from the train sets acting on the common crossing and switch unit of the turnout. To compare the selected dynamic parameters excited by the train set, turnout No. 59 was selected. This turnout is located in the Chocen railway station. The paper presents a simplified variant of a certified methodology focused on analysis of the vibrations propagation of turnout structures.

The paper also includes a theoretical analysis and practical application of the Hilbert-Huang transform for evaluation of dynamic phenomena occurring in a turnout. This lesser-known and less used transform belongs to the group of time-frequency procedures particularly suitable for analysis of the nonlinear, transient and non-stationary signals.

The Hilbert-Huang transform represents a certain alternative to, for example, the Fourier transform or the Wavelet transform, or to other time-frequency methods. Note that the Hilbert-Huang transform analyses the signal in a different way, i.e. not by decomposing it into predefined functions such as trigonometric functions, mother wavelet, etc., but into functions defined based on the signal under investigation.

Thanks to the calculation method, it can be used in a wide range of applications. For example, the removal of noise in the measured signal, the visualization of various sources and mechanisms, the analysis of image data etc. It can be reasonably assumed that this transformation will also find significant application in the field of railway engineering, especially in evaluation of the short-term dynamic effects from passing trains. The outputs of the Hilbert-Huang transform can be very well coupled with selected machine classification and identification methods.

According to the performed analysis, it is obvious that in most cases the higher acceleration values were obtained in the common crossing unit of the turnout in the passing railway sets than in the switch unit. Only for the trains pulled by locomotives of the 150 and 151 series the case was opposite. It can be assumed that this fact is influenced by the technical condition of the locomotives of the 150 and 151 series, as well as their different dynamics of passing through the turnout sections in question. This fact has also been observed at other locations during other measurement campaigns. Certainly, this fact is very significantly influenced by different mechanisms of dynamic effects in the heart and change of turnouts, as well, leading to vibrations propagation.

The Hilbert Huang transform generally offers a comprehensive tool for the analysis of transient and non-stationary signals. Based on the experience gained by the authors, its use can also be recommended for the time-frequency analysis of short-term dynamic phenomena occurring in railway structures. This method can be successfully applied not only in the analysis of railway superstructure samples measured in the laboratory, but in the evaluation of real structures, as well.

Based on the analyses performed, it can be concluded that the methodology used provides good results and conclusions. The measured and calculated quantities are characterized by sufficient accuracy and interpretability. The time and frequency analysis tools of the signals have also contributed very well to the quality of the measured data.

The authors recommend continuing the work performed, focusing on turnouts of various types and geometric parameters and focusing on both the common crossing and the switch unit of the turnout. Further analysis and development of the research methods will contribute to a better understanding of the dynamic stress of turnouts from passing trainsets, which will lead to development of the new structures with longer service life and with lower maintenance costs.

Acknowledgements

This paper was supported by the project FAST-S-21-7401, "Evaluation of dynamic effects acting on a structure by advanced mathematical analysis methods".

References

[1] MORAVCIK, M. Analysis of vehicle bogie effects on track structure - nonstationary analysis of dynamic response. *Communications - Scientific Letters of the University of Zilina* [online]. 2011, **13**(3), p. 33-40. ISSN 1335-4205, eISSN 2585-7878. Available from: http://komunikacie.uniza.sk/index.php/communications/article/view/860

[2] KAEWUNRUEN, S., REMENNIKOV, A. M. Field trials for dynamic characteristics of railway track and its components using impact excitation technique. *NDT & E International* [online]. 2007, **40**(7), p. 510-519. ISSN 0963-8695. Available from: https://doi.org/10.1016/j.ndteint.2007.03.004

[3] KASSA, E., ANDERSON, C., NIELSEN, J. Simulation of dynamic interaction between train and railway turnout. *Vehicle System Dynamics* [online]. 2006, **44**(3), p. 247-258. ISSN 0042-3114, eISSN 1744-5159. Available from: https://doi.org/10.1080/00423110500233487

[4] KAEWUNRUEN, S. Monitoring structural deterioration of railway turnout systems via dynamic wheel/rail interaction. *Case Studies in Nondestructive Testing and Evaluation* [online]. 2014, **1**, p. 19-24. ISSN 2214-6571. Available from: https://doi.org/10.1016/j.csndt.2014.03.004

[5] KOLLMENT, W., O'LEARY, P., HARKER, M., OSSBERGER, U., ECK, S. Towards condition monitoring of railway points: instrumentation, measurement and signal processing. In: 2016 IEEE International Instrumentation and Measurement Technology Conference: proceedings [online]. IEEE. 2016. p. 612-617. Available from: https://doi.org/10.1109/I2MTC.2016.7520434

[6] SMUTNY, J., PAZDERA, L., VUKUSIC, I. Dynamic effects on turnouts evaluation. The certified methodology. Ministry of Transportat of Czech Republic. 124/2014-710-VV/1, 2014.

[7] CHAMPENEY, D. C. *A handbook of Fourier theorems*. New York: Cambridge University Press, 1987. ISBN 9780521265034.

[8] SMUTNY, J. Measurement and analysis of dynamic and acoustic parameters of rail fastening. *NDT & E International* [online]. 2004, **37**(8), p. 119-129. ISSN 0963-8695. Available from: https://doi.org/10.1016/j.ndteint.2003.08.003

[9] HUANG, N. E., SHEN, Z., LONG, S. R., WU, M. C., SHIH, H. H., ZHENG, Q., YEN, N. C., TUNG, C. C., LIU, H.-H. The empirical mode decomposition and the Hilbert spectrum for nonlinear and non-stationary time series analysis. *Proceedings of the Royal Society A* [online]. 1998, **454**(1971), p. 903-995. ISSN 1364-5021, eISSN 1471-2946. Available from: https://doi.org/10.1098/rspa.1998.0193

[10] HUANG, N. E. New method for nonlinear and nonstationary time series analysis: empirical mode decomposition and Hilbert spectral analysis. In: Wavelet Application VII SPIE 4056: proceedings [online]. 2000. p. 197-210. Available from: https://doi.org/10.1117/12.381681

[11] HUANG, N. E., SHEN, S. S. P. *Hilbert-Huang transform and its applications* [online]. World Scientific Publishing, 2005. ISBN 978-981-256-376-7, eISBN 978-981-4480-06-02, p. 1-24. Available from: https://doi.org/10.1142/5862

[12] HUANG, N. E., WU, Z. A review on Hilbert-Huang transform method and its applications to geophysical studies. *Reviews of Geophysics* [online]. 2008, **46**(2), p. 1-23. eISSN 1944-9208. Available from: https://doi.org/10.1029/2007RG000228

[13] HUANG, N. E., CHEN, X., LO, M.-T., WU, Z. On Hilbert spectral representation: a true time-frequency representation for nonlinear and nonstationary data. *Advances in Adaptive Data Analysis* [online]. 2011, **3**(01n02), p. 63-93. ISSN 1793-5369, eISSN 1793-7175. Available from: https://doi.org/10.1142/S1793536911000659

[14] TORRES, M. E., COLOMINAS, M. A., SCHLOTTHAUER, G. S., FLANDRIN, P. A complete ensemble empirical mode decomposition with adaptive noise. In: IEEE International Conference on Acoustic, Speech and Signal Processing ICASSP 2011: proceedings [online]. IEEE. 2011. p. 4144-4147. Available from: https://doi.org/10.1109/ICASSP.2011.5947265

[15] JUNSHENG, C., DEJIE, Y., YU, Y. Research on the intrinsic mode function (IMF) criterion in EMD method. *Mechanical System and Signal Processing* [online]. 2004, **20**(4), p. 817-824. ISSN 0888-3270. Available from: https://doi.org/10.1016/j.ymssp.2005.09.011

[16] ZHANG, R. R., MA, S., SAFAK, E., HARTZELL, S. Hilbert-Huang transform analysis of dynamic and earthquake motion recordings. *Journal of Engineering Mechanics* [online]. 2003, **129**(8), p. 861-875. ISSN 0733-9399, eISSN 1943-7889. Available from: https://doi.org/10.1061/(ASCE)0733-9399(2003)129:8(861)

[17] CHIANG, W. L., CHIOU, D. J., CHEN, C. W., TANG, J. P., HSU, W. K., LIU, T. Y. Detecting the sensitivity of structural damage based on the Hilbert-Huang transform approach. *Engineering Computations* [online]. 2010, **27**(7), p. 799-818. ISSN 0264-4401. Available from: https://doi.org/10.1108/02644401011073665

[18] RILLING, G., FLANDRIN, P., GONCALVES, P. On empirical mode decomposition and its algorithms. In: IEEE-EURASIP Workshop on Nonlinear Signal and Image Processing NSIP2003: proceedings. IEEE. 2003.

[19] PUTRA, T., ABDULLAH, S., NUAWI, M. Z., YUNOH, M. F. M. The Morlet and Daubechies wavelet transforms for fatigue strain signal analysis. *Applied Mechanics and Materials* [online]. 2018, **471**, p. 197-202. ISSN 1662-7482. Available from: https://doi.org/10.4028/www.scientific.net/AMM.471.197

[20] JANOSTIK, D., NOHAL, V., SEELMANN, H., SMUTNY, J. The continuous monitoring of selected railway structures using the autonomous data logger. *Communications - Scientific Letters of the University of Zilina* [online]. 2020, **22**(2), p. 88-96. ISSN 1335-4205, eISSN 2585-7878. Available from: https://doi.org/10.26552/com.C.2020.2.88-96

A SIMULATION APPROACH FOR EVALUATING CONGESTION AND ITS MITIGATION MEASURES ON URBAN ARTERIALS OPERATING WITH MIXED TRAFFIC CONDITIONS

Chintaman Santosh Bari, Tanmayee V. Gunjal, Ashish Dhamaniya*,

Department of Civil Engineering, Sardar Vallabhbhai National Institute of Technology, Surat, India

*E-mail of corresponding author: adhamaniya@gmail.com

Resume

Present study evaluates the various congestion indexes in terms of speed performance index, volume to capacity ratio and congestion index based on travel time on the urban roadway network of 5.7 km in length, operating with mixed traffic conditions (traffic with varying static and dynamic characteristics of vehicles). The mitigations measures have been proposed to cater to the present traffic demand by converting the uncontrolled intersection to a partially controlled or signal-controlled intersection. In order to check the effectiveness of such mitigation measures, various scenarios have been generated in the developed and a well calibrated simulation model. It has also been observed that the speed performance index has improved by 8.88 percent while providing channelized intersection at one of the point elements and 11.52 %when the two-point elements have converted to channelizing intersection.

Article info

Received 25 October 2021
Accepted 7 February 2022
Online 4 May 2022

Keywords:

congestion
intersection
simulation
speed

Available online: https://doi.org/10.26552/com.C.2022.3.D126-D140

ISSN 1335-4205 (print version)
ISSN 2585-7878 (online version)

1 Introduction

Rapid urbanization in cities has intensified urban infrastructure requirements creating pressure on the sustainable and efficient development of transport facilities. There has been an increase in the world's urbanization by 13% in the last three decades and it is expected that it will reach up to 66% around 2050 [1]. Further, the growth rate of urbanization in developing countries is rapid compared to developed countries [2]. It is well described in the literature that road densities increase with an increase in population density and vice versa [3]. The higher road density leads to higher additional infrastructure per worker [4], causing the migration of the rural population towards the urban lands creating the new residential zones outside the city land. With an increase in population, a substantial increase in the vehicular growth rates is observed. The growth rate in vehicle population made the traffic problems more critical and complicated. The trip rates increased along with the population growth, as well, causing the rise in traffic on the road network and thus creating bottleneck situations with congestions and vehicular delays in metropolitan cities. Traffic congestion is now a severe urban problem and is one of the significant concerns of traffic engineers, as well as travelers.

The congestion can occur due to the frequent change in macro and micro level parameters looking to the present traffic demand [5]. The micro-level parameters are related to the traffic plying on a particular facility, while the macro-level parameter is related to the overall demand of the facility [6]. The congestion mostly gets set off due to the micro-level parameters, while its effect on the macro level is operated by the parameters that provide the occurrence of congestion. While dealing with the micro-level parameters, the congestion may be caused by the exceedance of the traffic demand over the road capacity, causing the reduction in traffic stream speed. These speed reductions cause longer trip times and also vehicular queuing, mostly at intersections. Longer trip delays may occur due to frequent events such as road accidents, breakdown of vehicles in the traffic stream, traffic signal timings, the geometry of the intersections, etc. [7]. Some special events also cause traffic congestions, such as political rallies, bad weather conditions, social gatherings, etc., but are not frequent. Further, looking towards the macro-level demand, the demand is the function of the land use pattern, employment status, employment opportunities, income level of the particular people causing the demand, car ownership and other regional, political, or historical background of the city.

This increase in congestion level leads to the extra delay to the road users and the personage tension and high amount of emissions [8-10]. Traffic in developing countries such as India, Taiwan and Vietnam is highly heterogeneous in nature, characterized by a broad mix of vehicles with diverse static and dynamic features in the absence of a lane discipline. This mixed traffic nature promotes extra challenges for dealing with the congestion, starting from finding the reasons behind it to the field applications of the mitigation measures. To deal with congestion, mitigation measures such as a change in intersection geometry, signal timings, etc. must be undertaken. These measures are costly and time-intensive to apply in the field. Hence, in the present study, the simulation tool is applied to study the congestion and emission level for different geometric improvements for an urban arterial network.

2 Literature review

Literature regarding the cause of congestion and the mitigation measures was being reviewed and is given below.

In 1975, Glover and Simon [4] concluded that the higher population density leads to massive road construction and thus a substantial increase in the road density was observed. Similar observations were given by Ji et al. [11] for Beijing province in China. They also concluded that the built-up area is more intense near the highways (expressway considered in the study). Tripathi [12] suggested that there may not be a significant effect on the population agglomeration due to the improvement of the infrastructure facilities with the help of the estimated regression equation for India. Dingil et al. [13] concluded that less congestion is observed for cities with higher Gross Domestic Product (GDP). In addition, cities with a high-density population may face lower congestion if there is high rail infrastructure per person. Cleveland et al. [3] concluded a nonlinear relationship between the population density and road length per resident. Das and Saw [14] developed a mixed traffic congestion model using the speed drop factor and the Mixed Traffic Impedance (MTI) applying the speed profile. The developed method can also consider roadside disruptions, such as parking, pedestrian encroachment, land-use impacts and vendor areas. Asaithambi et al. [15] investigated the impact of lane discipline, intraclass variability and composition on traffic flow characteristics under heterogeneous traffic conditions in India using the microscopic simulation model. They found that the stream speed was affected by composition, intraclass variability and lane discipline in a statistically significant way. He et al. [16] used the speed performance index, road segment and network congestion indexes to measure congestion levels on the urban road network. The traffic congestion modeling is done in the study using a congestion index based on journey time and the volume to capacity (v/c) ratio to analyze congestion. Gautam and Jain [17] divided the route into independent segments to apply the aggregate traffic behavior to estimate congestion on urban arterial and sub-arterial roads in a metropolis with heterogeneous traffic conditions. Wang et al. [18] considered the travel time for representing traffic congestion along with saturation degree, average speed, travel efficiency, low-speed proportion, total delay and average halting number. They found that the traffic congestion increases as the number of vehicles on the road increases due to reduced vehicle speed. Made and Wedagama [19] concluded that the impact of different types of vehicles on the road congestion is necessary to study for defining the traffic management goal in mixed traffic situations.

Afrin and Yodo [20] analyzed existing road traffic congestion measures and offered helpful suggestions for establishing a long-term, robust traffic management system. Comparison of seven congestion measures: speed, travel time, Level of Service (LOS), delay, relative congestion index, road segment congestion index, congested hour, travel time index and planning time index was done. Results showed that the speed can be easily comprehensible but did not consider nonrecurring conditions. Further, travel time can account for both time and space but does not include capacity. Fellendorf and Vortisch [21] illustrated the detailed methodology for calibration and validation of simulation models both at microscopic and macroscopic level in VISSIM. They concluded that the distribution of intended speeds was one of the essential input parameters for the lane usage. The paper's findings revealed that simulation tools based on the psychophysical car-following model could accurately simulate traffic flow under a variety of real-world scenarios. Jie et al. [22] revealed that the preferred speeds, top-end mean values of the acceleration and deceleration patterns observed in the field were significantly lower than VISSIM's default parameter. The results showed that drivers are less aggressive in real compared to simulation default parameters in VISSIM. Rao and Rao [6] developed the measure for identifying the congestion on the urban arterials operating with mixed traffic conditions in India. They observed the congestion stream speed ranging between 18 km/h to 22 km/h. Sun et al. [23] evaluated the traffic congestion occurring on urban arterial using the travel time and traffic volume in China. They concluded that the travel time-based measure gives noticeable results about congestion. Samal et al. [9] studied the traffic congestion on the urban arterial in India using the travel time reliability measures. They found that the users were wasting 50 % of the time in the congestion.

From the literature review, it can be summarized that Congestion Index (CI), such as speed performance index, index based on travel time, volume to capacity (V/C) ratio etc. are the measures for evaluating the traffic congestion. Further, it is better to know prior the congestion level occurring after improvement in terms of geometric characteristics for network-level analysis. The present study is taken to select the best suitable measures for congestion mitigation occurring on the urban arterial road by changing the geometry of the intersections. The microsimulation approach is used to study the congestion and emission level for different geometric improvements for an urban arterial network as it is a cost-effective approach [24]. From literature, it can be seen that the VISSIM can represent the mixed traffic and non-lane based traffic nature and therefore, it is used in the present analysis.

3 Description of the study stretch

In the present study, an urban arterial network in the city of Surat has been considered as a case study. Surat is considered in the present study because it is the fastest-growing city with rank fourth in 2016 among all the cities in the world. It had an annualized Gross Domestic Product (GDP) growth rate of 11.5% over the seven fiscal years between 2001 and 2008. Surat had a population of 4.46 million, according to the 2011 India census. Vehicle registered in Surat raised to 3 600 000 in 2011-12. Further, it is one of the smart cities under the Smart City Mission of India.

The selected arterial is the busiest route in the southwest zone of Surat. It connects the busiest Athwa Gate intersection on one end and Dumas (a tourist attraction) on the other end. It is the main corridor for reaching the Surat Airport and the Kandla Port (one of the major ports of India). In addition, shopping malls and other recreational activities are mostly present along this corridor. For all these reasons, the demand exceeds the capacity of the arterial and frequent congestion was observed in the peak hours. The study was conducted along with a 5.7-kilometer long road network of six-lane urban arterial road that consists of six different links. The network begins at the Athwa Gate Circle and concludes at the Rahul Raj Mall. The whole stretch has been divided into six segments (Figure 1), as Athwa Gate to Police Parade Ground (Section-1), Police Parade Ground to Parle Point (Section-2), Parle Point to Sargam (Section-3), Sargam to Sardar Vallabhbhai National Institute of Technology (SVNIT) (Section-4), SVNIT to Kargil Chowk (Section-5) and Kargil Chowk to Rahul Raj Mall (Section-6).

In this road network, one signalized intersection is present between Section-1, recognized by the name Chopati. Two major rotaries are at Kewal Chowk and Kargil Chowk, while one minor rotary is at Parle Point, also an intersection near Police Parade ground named as Synergy Group point. For convenience, in further discussions, they are referred to as intersections 1, 2, 3, 4 and 5 for Chopati, Synergy intersection, Parle Point, Kewal Chowk and Kargil Chowk intersection, respectively.

4 Data collection and extraction

Data collection serves as a foundation to carry out further research work. It was important to measure the traffic load on the field in order to construct an accurate picture of the current scenario in the VISSIM simulation. In this study, data collection basically consisted of three parts. As the first was speed data collection using the radar gun; the second was the volume data collection by the process of video recording

Figure 1 *Study Stretch from Athwa Gate to Rahul Raj Mall*

2 (a) Videographic survey

2 (b) Spot speed survey

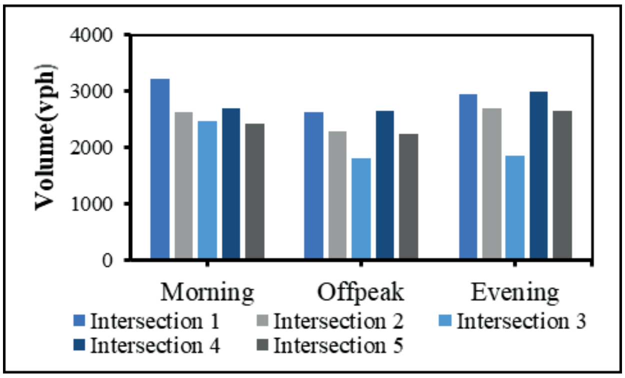

2 (c) Variation of volume for each intersection

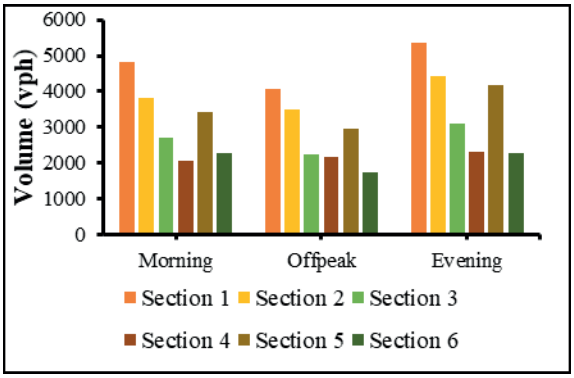

2 (d) Variation of volume for each midblock

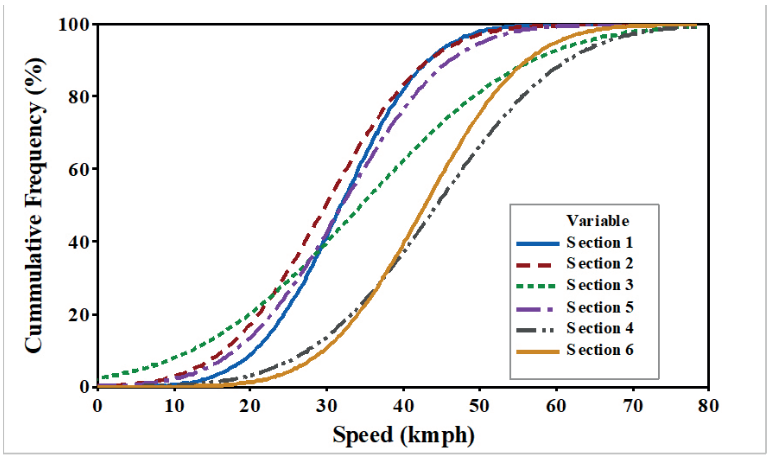

2 (e) Speed CDF at different midblock sections for 2W

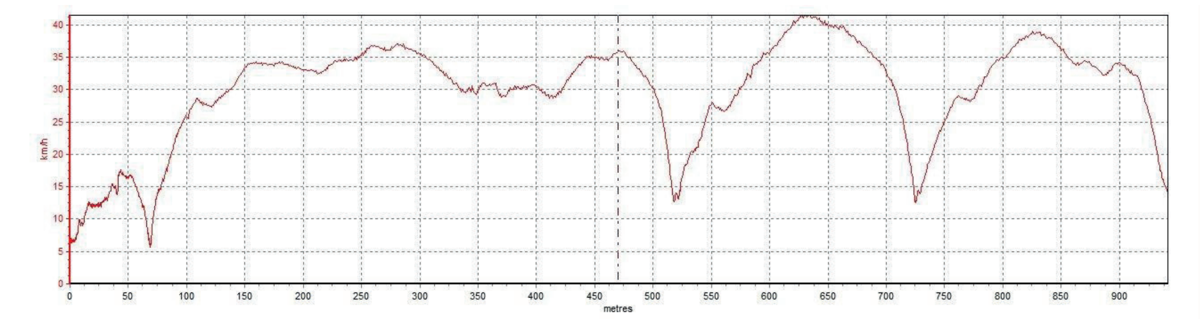

2 (f) Sample Speed-Distance plot from P-box survey

Figure 2 *Field Data Collection*

using a video camera in the field and lastly, the travel time data collection with the help of a performance box (P-box) instrument. Collected data was extracted to give input to the developed simulation model. MS Excel, Minitab and Performance box software were used to analyze the data.

Indian traffic includes various vehicle classes with varying static and dynamic features. Hence, for the study purpose, all the vehicles were classified into five different vehicle classes such as motorized two-wheelers (2W), motorized three-wheelers (3W), small cars (SCs), big cars (BCs) and buses. The vehicle classification is carried out as per the Indian Highway Capacity Manual (Indo-HCM) [25]. The SCs include all the hatchback and sedan cars, while the BCs include all the crossover utility vehicles (XUVs) and sport utility vehicles (SUVs).

4.1 Video graphic survey

A video graphic survey was carried out using a high-resolution video camera in the field for all five intersections and six midblock sections (Figure 2 (a)). The camera is mounted at a high vantage point such that all the turning movements and good view of all the crossroads of the intersection were observable from the position. Data were collected for the morning peak, evening peak and for off-peak separately. Traffic composition and turning movement counts were retrieved from the recorded video footage by playing recorded video on a large screen in the laboratory and data was gathered in 5-minute intervals. The analysis is done independently to look at traffic mix in the morning, off-peak and evening hours.

Figures 2 (c) and (d) show that volume for off-peak is less both for midblock sections and intersections. In addition, it can be observed that the volume observed at Section-1 is higher and for Intersection-1, volume is bigger as compared to the others. Further, from the field observed traffic composition, it is found that 2Ws account for the majority of traffic (averagely 46 %), followed by small cars (averagely 38 %), 3W (averagely 11 %), big cars (averagely 5%) and finally buses. The analyzed volume and composition are provided as input to the prepared model.

4.2 Radar gun survey

Figure 2 (b) shows the field speed data collection by using a radar gun. For Section-5 and Section-6, a dedicated BRTS corridor is available, so there is a negligible variation in the speed of buses both spatially and temporally. Keeping this fact in mind, a sample of buses was skipped for this section. The cumulative density function (CDF) for all the vehicle categories, considering peak and off-peak time, was studied. The graph shows an “S” shaped curve, i.e. the speed follows the normal distribution (Figure 2 (e)).

4.3 Travel time data collection by P-Box Survey

Travel time data was collected with help of the Performance Box (P-Box) instrument. The P-Box is a self-contained Global Positioning System (GPS) data logger and a performance meter. A 10 Hz fully calibrated GPS engine provides accuracy and precision and the data can be stored on a removable SD flashcard. It gives the real-time data of speed, acceleration, latitude, longitude etc. [26]. For recording the real-time data of each vehicle, the antenna is connected to the vehicle’s body part. The data obtained from the P-box instrument was then analyzed using Racelogical P-Box software [27]. Figure 2 (f) shows the sample speed distance plot obtained from the P-box.

5 Development of a simulation model

After acquiring these large datasets of five intersections and six midblock sections with their traffic volume, speed and travel time, the next step is to build the simulation network model in VISSIM. The base network model is developed with the help of links and connectors, as shown in Figure 3. For the link, the length and the number of lanes are provided as an input to the model (Figure 1). The traffic is highly heterogeneous in India. There is a wide variation in composition and volume per 5-minute count and therefore the 5-min count, is found reasonable, to depict the flow rate [25]. Therefore, in the present study also, the 5-min flow rate and traffic composition for that volume (12 x time interval) for an hour, were given as input for simulation. (Figures 2 (c) and (d)).

Figure 3 shows different intersections along the road network developed in the VISSIM. As observed in the field, Intersection-5 was the signalized intersections. The timings of the signals were observed from the field and were given as input. For other intersections, conflict areas were provided at merging and diverging sections.

Speed distribution is provided from collected data for each category of the vehicle separately for morning peak, evening peak and off-peak. Figure 4 (a) represents the default speed distribution given in the VISSIM. Figures 4 (b) and 4 (c) show the sample field observed speed distribution applied for 2W and SC, respectively.

6 Calibration of the model

As the driving behavior in India is significantly different from developed countries, any model built-in VISSIM must be calibrated to represent the field conditions accurately. Wiedemann 74 and Wiedemann 99 are the two psychophysical perception car-following models included in VISSIM. Wiedemann 74 is more typically used to represent urban traffic and hence is

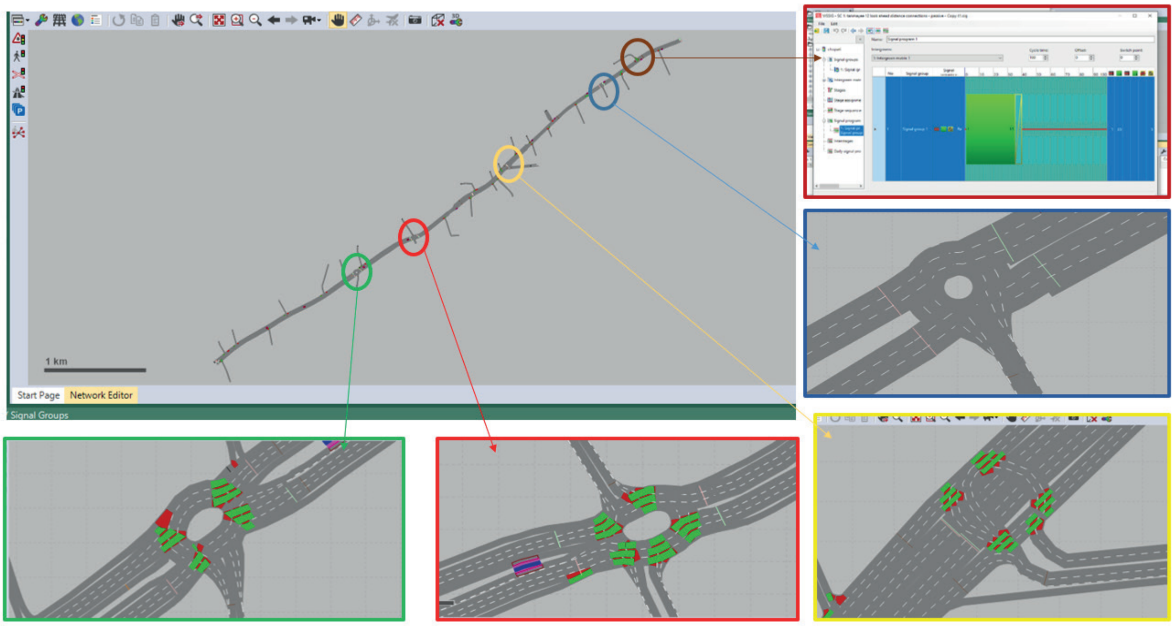

***Figure 3** Established road network in VISSIM*

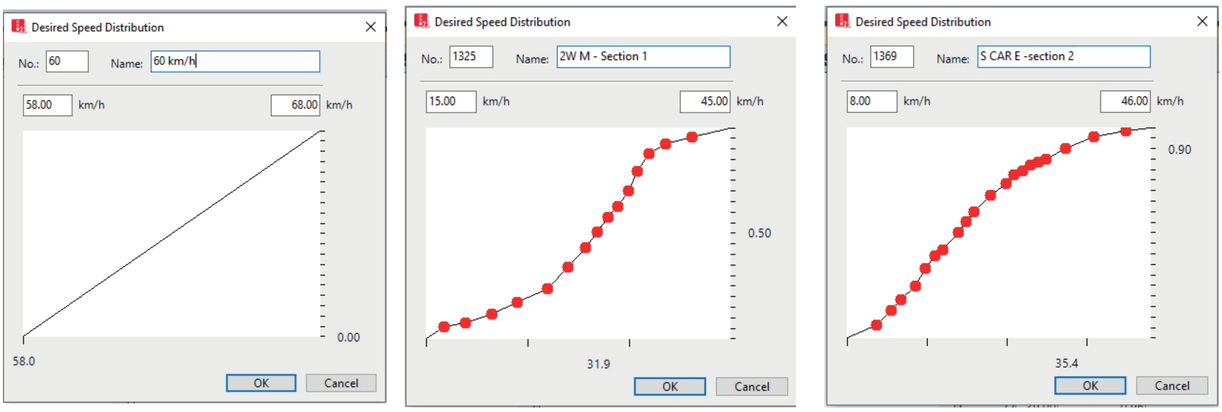

(a) *(b)* *(c)*

***Figure 4** Sample Speed distribution provided as input (a) Default in VISSIM (b) for 2W (c) for SC*

adopted here [28]. The methodology for calibration is shown in Figure 5. Calibration is the process of fine-tuning the model's input parameters to accurately replicate observed traffic circumstances. The manual trial and error method is used for calibration in this study. The simulation run should be performed until no significant difference is found between the observed and the simulated values. In this research, calibration is done using the speed and volume data, whereas validated by the collected field travel time data for the entire network. Firstly, the VISSIM results were generated for the default parameters for three random seeds. It was observed that the VISSIM output did not match the field data and was having a significant error. After that, the default parameter values are updated during the calibration until the difference between the actual and simulated measures, such as flow and speed, was less than the required threshold value. For each vehicle category, the values of driving behavior parameters, obtained after the calibration, are shown in Table 1.

6.1 Calibration by speed

The speed distribution curve obtained from the simulation run was compared to the field data to check the effectiveness of the model. For each intersection, the speed frequency curves are plotted for simulated and field data. From Figure 6 (a), it can be concluded that there is a negligible discrepancy between simulated and field speeds because the two curves are almost similar. Further, the F-test was conducted to determine whether the statistically significant difference exists between the simulated and field data. Here, the F-value is less than $F_{crtical}$ for all time periods and for all intersections and hence, it can be concluded that the simulated speeds can represent the field speeds well.

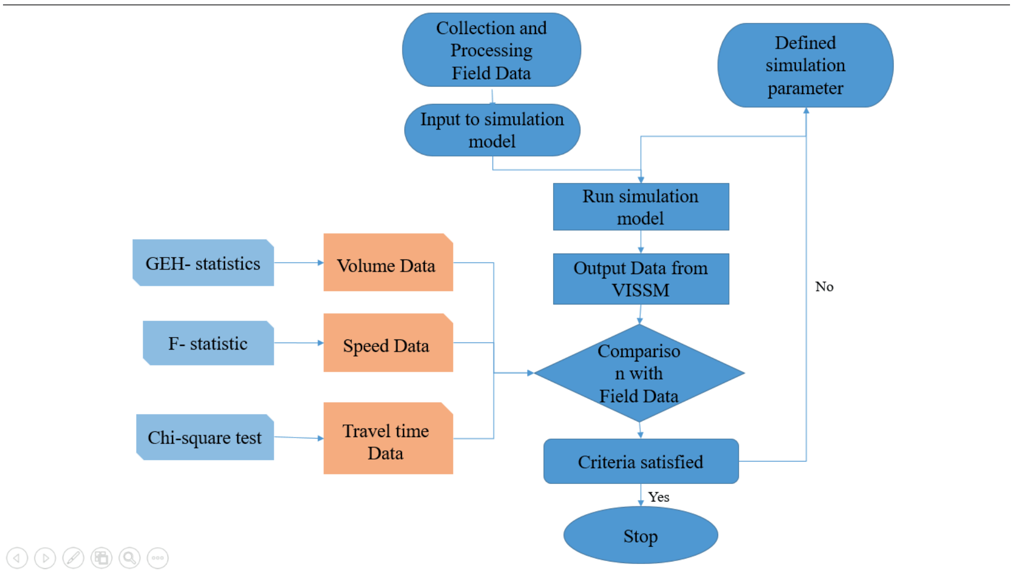

***Figure 5** Flowchart of calibration*

***Table 1** Calibrated values of the traffic parameters*

Parameter		Default	Calibrated parameter				
			2W	SC	3W	BC	Bus
Minimum look ahead distance		0	30	30	30	30	30
Minimum look back distance		0	20	10	10	10	10
Model parameter	Average standstill distance	2	0.2	0.2	0.4	0.4	0.4
	Additive part of safety distance	2	0.1	0.1	0.1	0.1	0.4
	Multiplicative part of safety distance	3	0.5	0.5	0.5	0.7	0.75
Lane change behavior	Minimum clearance	0.5	0.4	0.4	0.5	0.5	0.4
	Safety distance reduction factor	0.6	0.5	0.5	0.5	0.5	0.5
Minimum lateral distance	Distance standing (at 0 kmph)	0.2	0.2	0.2	0.2	0.2	0.2
	Distance driving (at 50 kmph)	1	0.5	0.5	0.5	0.5	0.5

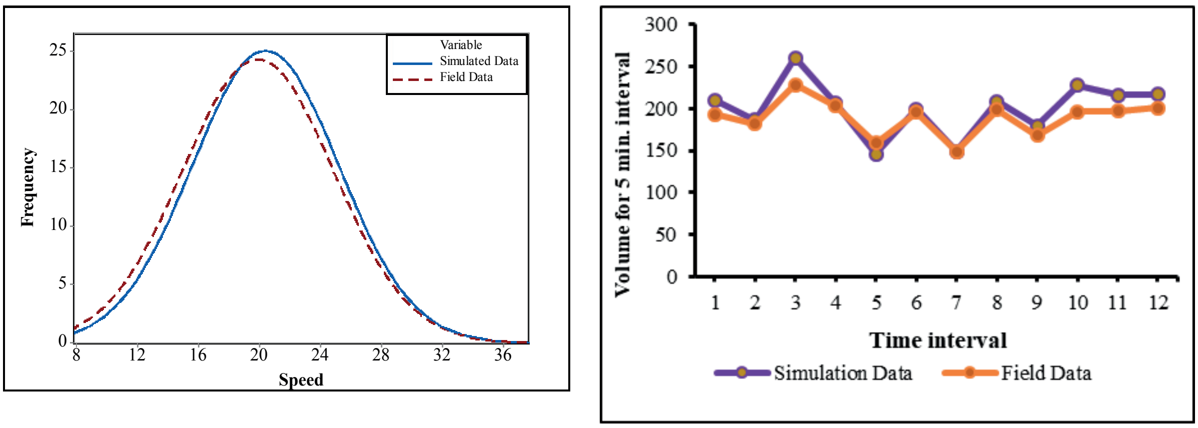

6 (a) Comparison of Speed frequency curve for simulated data and field data

6 (b) Volume count of midblock for evening

***Figure 6** Calibration results*

Table 2 *The GEH values for midblock for section 6*

Time interval (s)	Morning			Off-peak			Evening		
	Field data	Simulated data	GEH value	Field data	Simulated data	GEH value	Field data	Simulated data	GEH value
0-300	193	-		117	115	0.19	235	232	0.20
300-600	182	161	1.60	137	140	0.25	310	310	0.00
600-900	228	215	0.87	141	135	0.51	334	338	0.22
900-1200	203	192	0.78	156	157	0.08	272	273	0.06
1200-1500	159	144	1.22	155	156	0.08	239	218	1.39
1500-1800	195	197	0.14	174	180	0.45	286	284	0.12
1800-2100	149	149	0.00	165	161	0.31	239	223	1.05
2100-2400	198	198	0.00	147	147	0.00	254	256	0.13
2400-2700	168	165	0.23	146	142	0.33	278	281	0.18
2700-3000	196	190	0.43	126	128	0.18	230	230	0.00
3000-3300	197	197	0.00	157	157	0.00	216	218	0.14
3300-3600	201	198	0.21	139	137	0.17	174	175	0.08

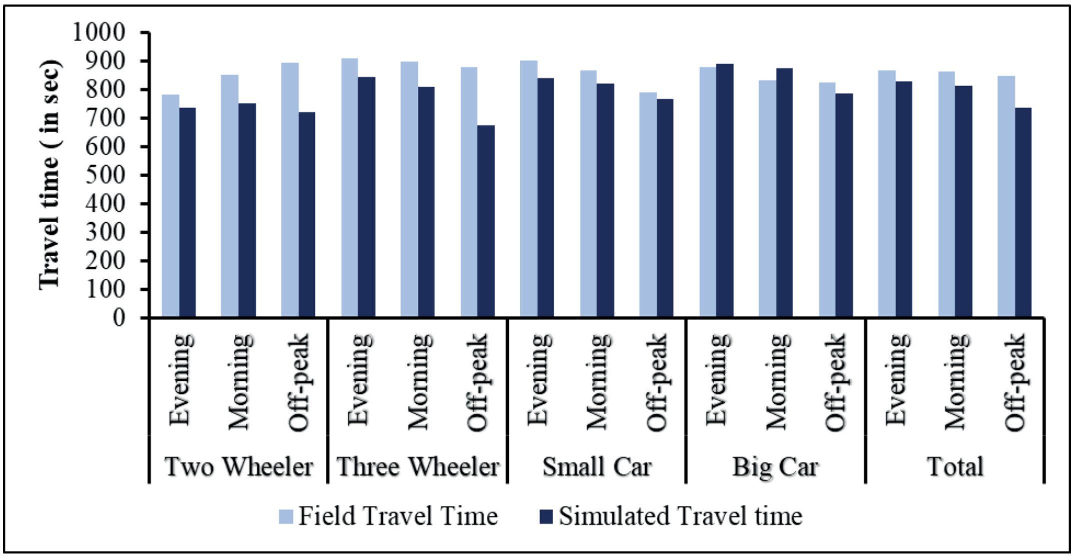

Figure 7 *Validation by the vehicle class-wise travel time*

6.2 Calibration by volume

Volume calibration is carried out for each midblock section of six segments. The analysis for calibration of volume is carried out from the GEH statistics. The formula for the GEH Statistic is given by:

$$GEH = \sqrt{\frac{2(M-C)^2}{M+C}} \quad (1)$$

where: M is the hourly traffic volume from the traffic model and C is the real-world hourly traffic count.

The GEH value less than five is considered as a good match between field and simulated data. At least 85% of volume in the model should have GEH less than 5 [29-30].

From Table 2 is observed that the maximum GEH value is 1.64 and the minimum GEH value is 0.00. The values are within the permissible limits, so it can be concluded that the model is well calibrated for volume at the given midblock. For other midblock sections, the GEH value for all 5-minute time intervals for the morning, off-peak and evening peak were less than 5 and hence it can be said that the model is well-calibrated.

6.3 Validation by the travel time

After calibrating the point and link elements, the entire network is validated using the travel time on the entire network. The chi-square test has been conducted

Table 3 Development adopted in scenarios

Scenario no.	Development adopted	VISSIM Modification
Scenario 1	Existing condition	------
Scenario 2	Signalized intersection at intersection 5.	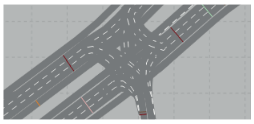
Scenario 3	The channelized intersection at intersection 5.	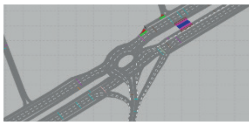
Scenario 4	Signalized intersection at intersection 4	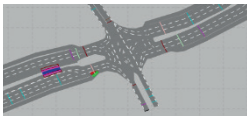
Scenario 5	The channelized intersection at intersection 4	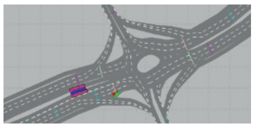
Scenario 6	The channelized intersection at intersections 4 and 5.	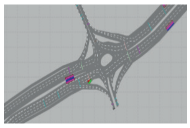 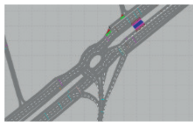
Scenario 7	The signal at intersections 4 and 5.	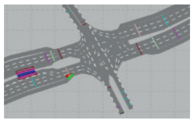 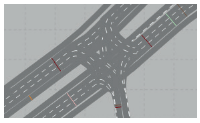
Scenario 8	The channelized intersection at intersection 2.	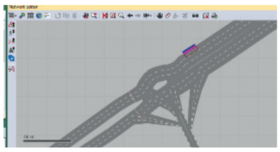
Scenario 9	Re-designing signal timing for intersection 1.	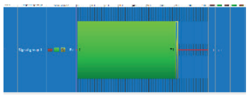
Scenario 10	A signal at intersection 5 and channelized intersection at intersections 4 and 2.	 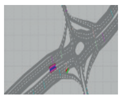 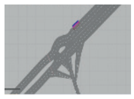

to ensure that there is no significant difference in observed and simulated travel time. The observed data is considered field travel time and expected data is considered simulated travel time. The p-value from the chi-square test is 0.000, which is less than 0.05 for all the vehicle classes and for the morning, evening and off-peak. Thus, it can be said that the model is validated. Figure 7 shows the simulated and field observed travel times for different periods and vehicle classes.

7 Mitigation measures

The present study stretch is composed of various links and nodes with a number of access points. The nodes consist of uncontrolled, partially controlled and uncontrolled intersections and the whole study stretch mostly has commercial and residential land use. Looking to the present traffic demand, the traffic on the entire facility has increased and reached the level of congestion at a certain time of the day and it is very frequent. In order to provide the mitigation measures, the present nodes have been upgraded to a higher category (partially controlled to signal control) based on current traffic demand and various scenarios have been generated in simulation to check their effectiveness to reduce the congestion on the entire facility.

8 Development of scenarios

In order to obtain the satisfactory performance of the entire network (congesting index must be within the acceptable values), various scenarios have been created

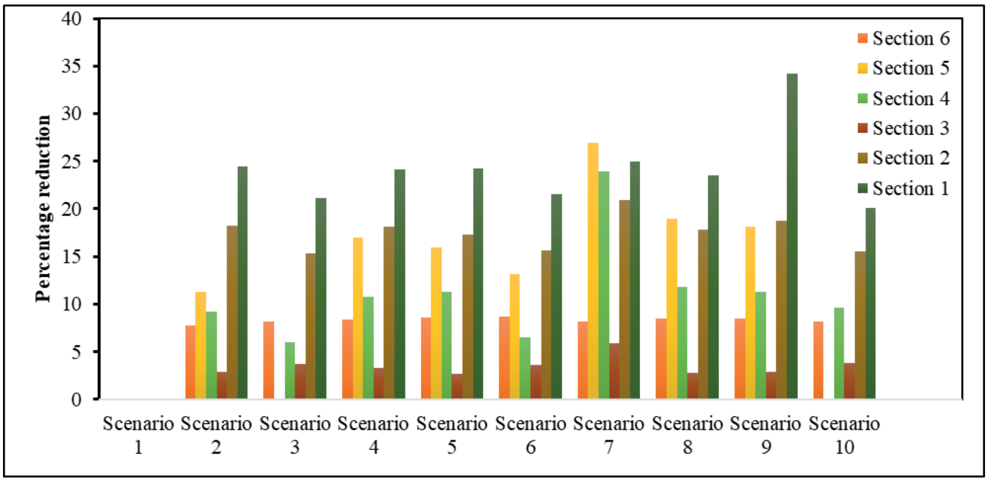

Figure 8 *Percentage reduction of the speed performance index for generated scenarios*

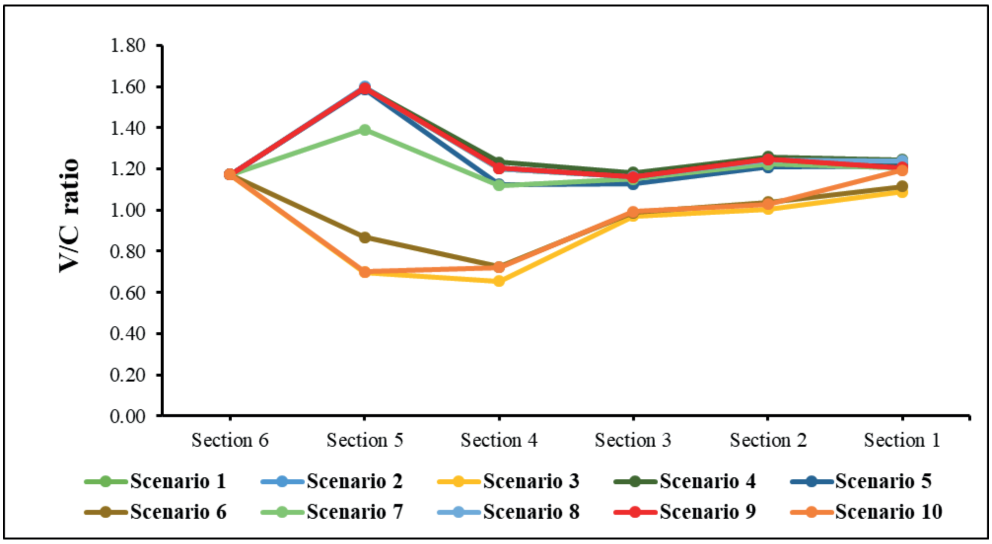

Figure 9 *Graph of the v/c ratio for different scenarios*

in VISSIM and compared to the existing scenario. The geometric developments were made in all the scenarios by providing channelized intersection or providing signalized intersection in the study stretch. The development made in each scenario is shown in Table 3.

The channelized intersection is provided by providing free left turn in rotaries. Signal timing for signalized intersection is adopted by calculating it with Webster's Method [31]. Signal timing is adopted in two phases, in the direction of a minor road and another in the direction of a major road. Scenarios are generated in VISSIM software with the help of the scenario management tool. Scenario 1 is an existing scenario. Nine scenarios are generated by providing a signal at the intersection and channelized intersection at intersections 4 and 5.

9 Results

Level of Congestion is analyzed for each scenario. Congestion is described as an excess of vehicles on a portion of the roadway at a particular time resulting in slower speeds. Congestion can be measured using average speed, flow/density, delay and travel time variability.

9.1 Speed performance index

Vehicle speed is an essential indicator for measuring the road traffic state. Here, the speed performance index is used to measure the level of congestion. The speed performance index is as calculated by:

$$R_V = \frac{v}{V_{\max}} * 100\,, \quad (2)$$

where:

R_v denotes the speed performance index,

v represents the average travel speed, km/h,

V_{max} indicates the maximum permissible road speed, km/h.

The value of the speed performance index lies between 0 to 100. Value 0 indicates heavy congestion, while value 100 shows very smooth traffic. As the

Table 4 *Reduction in travel time (in %) compared to Base Scenario (Scenario-1) for the best result scenarios*

Scenario	Scenario-3	Scenario-6	Scenario-9
Small Car			
Morning-peak	25.30	22.50	22.58
Off-peak	25.47	20.16	22.00
Evening-peak	22.12	22.19	16.89
Three Wheeler			
Morning-peak	21.15	23.68	26.17
Off-peak	19.84	23.14	23.34
Evening-peak	23.44	23.90	22.69
Two-wheeler			
Morning-peak	7.44	26.68	26.45
Off-peak	26.22	28.03	25.89
Evening-peak	28.29	28.21	21.45
Big car			
Morning-peak	19.54	24.79	25.34
Off-peak	16.12	27.87	23.70
Evening-peak	19.45	22.89	21.49

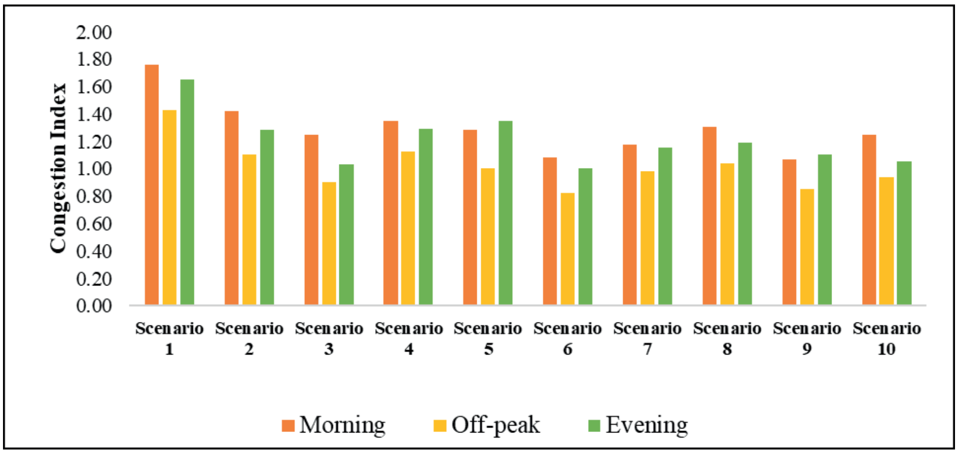

Figure 10 *Congestion index based on the travel time for different scenarios*

value increases from 0 to 100, congestion is reduced. In this study, the speed performance index for midblock between segments is found out. From Figure 8, it can be observed that the maximum speed performance index is for scenario 9. The average percentage increased by 15.6% for this scenario.

9.2 Volume-to-capacity ratio

The volume to capacity (v/c) ratio measures the level of congestion on the road. The v/c ratio can vary from 0 to 1 and as the value of v/c increases, congestion increases. For each road segment, volume is collected from the simulated run and the volume to capacity ratio is thus evaluated. For determining the v/c ratio, the capacity of the urban road is adopted from the recently developed Indian Highway Capacity Manual. From Figure 9, for scenario 3, scenario 6 and scenario 10, the v/c ratio is minimum. Scenarios 3, 6 and 10 provided channelized intersection so the vehicle could take a free left turn, minimizing the chance of queues and delays. Hence, volume on the road is less and provides better performance.

9.3 Congestion index based on travel time

Congestion index based on the travel time is a performance measure of the road network, indicating congestion on the road. The average value of the Congestion Index (CI) is calculated for the whole road stretch as:

$$CI = \frac{T^{L}/V_F}{L/V_F}, \qquad (3)$$

where:

T is the average of the travel times as computed by the model on the validation dataset,

L is the segment length,

V_F is the free-flow speed

Using Equation (3), the congestion index is calculated based on the travel time. Table 4 shows the vehicle class wise travel time reduction in percentage for three best scenarios of all. From Figure 10, it is observed that the congestion index is small for scenarios 6, 9 and 3. The average reduction of travel time congestion index is 35%, 39.64% and 38.56%, respectively, for scenarios 3, 6 and 9. Furthermore, along with the congestion index, a significant reduction in travel time is observed for scenarios 3, 6 and 9. The results show that channelized intersection has an advantage over signalized intersection for the studied road section as for signalized intersection, even if there was no congestion, the driver has to wait until the signal turns green.

9.4 Traffic congestion representation using geographic information system (GIS)

Geographic Information System (GIS) provides visualization of the congestion, which can be easily recognizable for the traveler. The traffic conditions were displayed using ArcGIS software and the volume to capacity ratio and travel time congestion index were used to analyze the road segment congestion. As the congestion level reduces, a delay gets reduced and hence exhaust emission decreases. For all the scenarios, the

Figure 11 *ArcGIS Model for Different scenario*

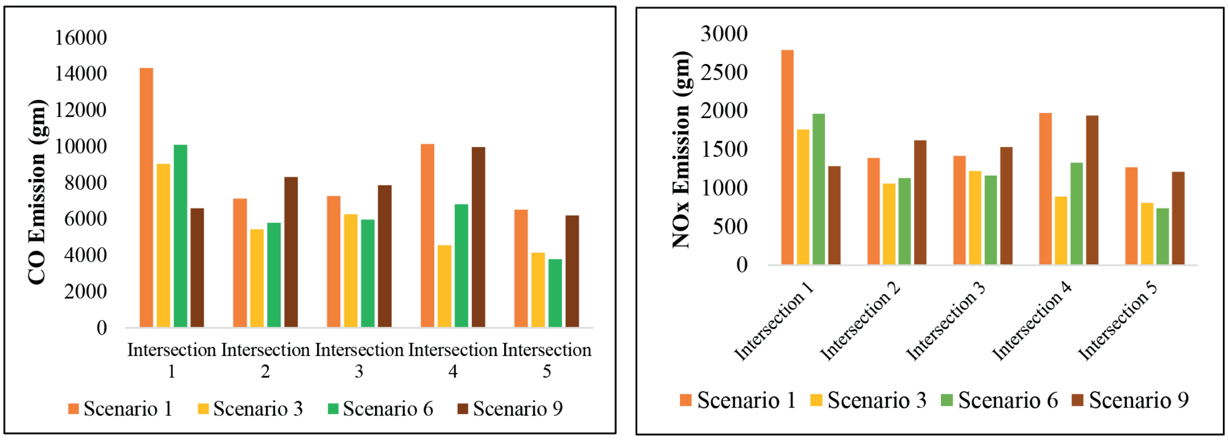

(a) *(b)*

Figure 12 *Emission Observed for different scenarios (a) CO Emission (b) NOx Emission for scenarios*

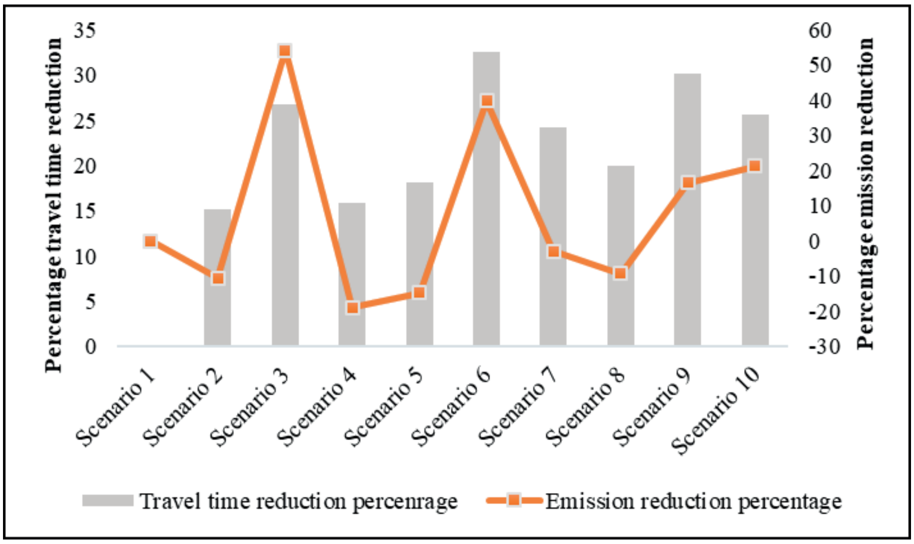

***Figure 13** Relation between delay and emission*

congestion is shown by the v/c ratio because it is used as the primary measure for the planning purpose.

Figure 11 shows the four different scenarios presented using the GIS platform taking the v/c ratio as the measure of effectiveness. Figure 11 (a) shows the existing field condition, which is observed to have large v/c values. Figures 11 (b), 11 (c) and 11 (d) show the GIS representation for scenarios 3, 6 and 9, respectively. It is observed that the congestion relaxes with a maximum decrease in the v/c ratio from 1.27 (for the base scenario) to 0.81 (for scenario 3).

9.5 Emission of gases

In terms of sustainable and energy-efficient transport system options, fuel consumption and air pollution are other vital performance measures. Therefore, the vehicle emission regarding carbon dioxide (CO_2), nitrogen oxides (NO_X) and Volatile Organic Compounds (VOCs) and fuel consumption were measured. Reducing the value of this measure of effectiveness reflects a significant increase in the traffic flow efficiency and safety along the road. As congestion reduces, emissions of these gases are also reduced. The reduction patterns of CO_2 and NOx are shown in Figure 12, respectively.

9.6 Comparison between delay and vehicle emissions

As vehicle travel time is reduced percentage of emission is also reducing. However, the proportions of reduction of emission and travel time are not similar. Figure 13 shows the comparison of the travel time reduction and emission reduction for all the scenarios. For scenario 3, the reduction of travel time is by 26% and emission reduction by 54%. Meanwhile, for scenario 6, travel time reduction is 32% and emission reduction is 39%.

The overall simulation analysis results of three congestion indexes, based on speed, travel time and the v/c ratio, are used to quantify and assess the congestion. Thus, it is observed that scenario 3 (i.e. provide channelized intersection at Intersection 5), scenario 6 (i.e. the channelized intersection at Intersection 4 and Intersection 5) and scenario 9 means (change the signal time for Intersection 1 signal) are performing better than the remaining scenarios. Further, considering the emission reduction and the travel time reduction, scenario-3 can be given as the rank-1 due to consideration of sustainability. Moreover, for scenario-3, only one intersection has to change, which will be more economical than making the other improvements. It is recommended that scenario-9 be implemented in the field as it deals only with the signal timings that will be easy to deal with.

10 Conclusions

The traffic congestion is the biggest challenge of the current era, especially on urban road networks. The problem of congestion becomes very tedious in heterogeneous non-lane-based traffic streams. An arterial road network is considered in the present study, where the frequent traffic congestion has been observed in the recent past. In order to provide mitigation measures for congestion, geometrical improvements of various nodes have been suggested. Therefore, the entire network has been simulated in VISSIM microscopic simulation software that is calibrated for heterogeneous non-lane-based traffic movement by collecting field data on the study stretch. The geometric improvement has been suggested and hence 10 different scenarios have been generated in VISSIM and various congestion measures have been determined. After a comprehensive analysis of the congestion measures, such as the speed performance index, congestion index by travel time and the v/c ratio, it is observed that the channelized intersection is performing better for most indexes' values than a signalized intersection. Out of 10 scenarios generated, it is observed that 3 scenarios give favorable results of the less congestion on the road. These three scenarios are respectively for providing channelized intersection at intersection 5, providing channelized intersection at intersection 4 and intersection 5 and providing a signal at intersection 4; channelized intersection at intersection 5 and interstation 2. The results show that providing channelizing intersection at two of the point elements (intersection) would reduce the travel time congestion index from 1.61 to 0.97. It has also been observed that the speed performance index has improved by 8.88% while providing channelized intersection at one of the point elements and 11.52% when the two-point elements have converted to channelizing intersection. The whole outcome, in terms of the congestion measures, has been graphically shown in the GIS environment. The GIS-based outcome is easy to understand the scenarios and effective countermeasures provided to reduce congestion.

Acknowledgment

The authors would like to thank TEQIP-III, a Government of India initiative, for sponsoring this project. The project is entitled "Operational Efficiency of Urban Roadway Links using Performance Box" (Project number SVNIT/CED/AD/TEQIPIII/2119/2019). The present study is a part of the project.

References

[1] SHI, G., SHAN, J., DING, L., YE, P., LI, Y., JIANG, N. Urban road network expansion and its driving variables: a case study of Nanjing city. *International Journal of Environmental Research and Public Health* [online]. 2019, **16**(2318), p. 1-16. ISSN 1660-4601. Available from: https://doi.org/10.3390/ijerph16132318

[2] COHEN, B. Urbanization in developing countries: current trends, future projections and key challenges for sustainability. *Technology in Society* [online]. 2006, **28**, p. 63-80. ISSN 0160-791X. Available from: https://doi.org/10.1016/j.techsoc.2005.10.005

[3] CLEVELAND, T., DEC, P., RAINHAM, D. Shorter roads go a long way: the relationship between density and road length per resident within and between cities. *Canadian Planning and Policy / Amenagement et Politique au Canada* [online]. 2020, **2020**, p. 71-89. ISSN 2562-122X. Available from: https://doi.org/10.24908/cpp-apc.v2020i0.13406

[4] GLOVER, D. R., SIMON, J. L. The effect of population density on infrastructure: the case of road building. *Economic Development and Cultural Change*. 1975, **23**(3), p. 453-468. ISSN 0013-0079, eISSN 1539-2988.

[5] KARTHIK, S., LOUI, T. R. Development of traffic congestion model to evaluate the level of congestion and its associative cost for an urban arterial road: a case study. *Journal of The Institution of Engineers (India): Series A* [online]. 2021, **102**(2), p. 623-632. ISSN 2250-2157. Available from: https://doi.org/10.1007/s40030-021-00526-z

[6] RAO, A. M., RAO, R. K. Identification of traffic congestion on urban arterials for heterogeneous traffic. *Transport Problems* [online]. 2016, **11**(3), p. 131-142. ISSN 1896-0596. Available from: https://doi.org/10.20858/tp.2016.11.3.13

[7] OLAYODE, I. O., SEVERINO, A., CAMPISI, T., TARTIBU, L. K. Prediction of vehicular traffic flow using Levenberg-Marquardt artificial neural network model: Italy road transportation system. *Communications - Scientific Letters of the University of Zilina* [online]. 2022, **24**(2), p. E74-E86. ISSN 1335-4205, eISSN 2585-7878. Available from: https://doi.org/10.26552/com.C.2022.2.E74-E86

[8] JANDACKA, D, DURCANSKA, D., KOVALOVA, D. Concentrations of traffic related pollutants in the vicinity of different types of urban crossroads. *Communications-Scientific Letters of the University of Zilina* [online]. 2019, **21**(1), p. 49-58. ISSN 1335-4205, eISSN 2585-7878. Available from: https://doi.org/10.1088/1757-899X/661/1/012152

[9] SAMAL, S. R., KUMAR, P. G., SANTHOSH, C. J., SANTHAKUMAR, M. Analysis of traffic congestion impacts of urban road network under Indian condition. *IOP Conference Series: Materials Science and Engineering* [online]. 2020, **1006**(1), 012002. ISSN 1757-899X. Available from: https://doi.org/10.1088/1757-899X/1006/1/012002

[10] BARI, CH. S., NAVANDAR, Y. V., DHAMANIYA, A. Vehicular emission modeling at Toll Plaza using performance box data. *Journal of Hazardous, Toxic and Radioactive Waste* [online]. 2020, **24**(4), p. 1-19. ISSN 2153-5493, eISSN 2153-5515. Available from: https://doi.org/10.1061/(ASCE)HZ.2153-5515.0000550

[11] JI, W., WANG, Y., ZHUANG, D., SONG, D., SHEN, X., WANG, W., LI, G. Spatial and temporal distribution of expressway and its relationships to land cover and population: a case study of Beijing, China. *Transportation Research Part D: Transport and Environment* [online]. 2014, **32**, p. 86-96. ISSN 1361-9209. Available from: https://doi.org/10.1016/j.trd.2014.07.010

[12] TRIPATHI, S. Relationship between infrastructure and population agglomeration in urban India: an empirical assessment. *ADBI Working Paper Series*. 2017, **731**, p. 1-25. ISSN 1655-5252.

[13] DINGIL, A. E., SCHWEIZER, G., RUPI, F., STASISKIENE, Z. Transport indicator analysis and comparison of 151 urban areas, based on open source data. *European Transport Research Review* [online]. 2018, **10**(58), p. 1-9. ISSN 1866-8887. Available from: https://doi.org/10.1186/s12544-018-0334-4

[14] DAS, A., SAW, K. Traffic congestion modelling under mixed traffic conditions through fuzzy logic approach: an Indian case study of arterial road. 2004.

[15] ASAITHAMBI, G., KANAGARAJ, V., SRINIVASAN, K. K., SIVANANDAN, R. Characteristics of mixed traffic on urban arterials with significant volumes of motorized two-Wheelers: role of composition, intraclass variability and lack of lane discipline. *Transportation Research Record* [online]. 2012, **2317**(2317), p. 51-59. ISSN 0361-1981. Available from: https://doi.org/10.3141/2317-07

[16] HE, F., YAN, X., LIU, Y., MA, L. A traffic congestion assessment method for urban road networks based on speed performance index. *Procedia Engineering* [online]. 2016, **137**, p. 425-433. ISSN 1877-7058. Available from: https://doi.org/10.1016/j.proeng.2016.01.277

[17] GAUTAM, L., JAIN, K. Study on mixed traffic flow behavior on arterial road. International *Journal of Engineering Research and Technology (IJERT)*. 2018, **6**(11), p. 1-7. ISSN 2278-0181.

[18] WANG, W.-X., GUO, R.-J., YU, J. Research on road traffic congestion index based on comprehensive parameters: taking Dalian city as an example. *Advances in Mechanical Engineering* [online]. 2018, **10**(6), p. 1-8. ISSN 1687-8132, eISSN 1687-8140. Available from: https://doi.org/10.1177/1687814018781482

[19] MADE, D., WEDAGAMA, P. The influence of mixed traffic on congestion level. *International Journal of GEOMATE*. 2019, **17**(64), p. 18-25. ISSN 2186-2982, eISSN 2186-2990.

[20] AFRIN, T., YODO, N. A survey of road traffic congestion measures towards a sustainable and resilient transportation system. *Sustainability* [online]. 2020, **12**(11), p. 1-23. ISSN 2071-1050. Available from: https://doi.org/10.3390/su12114660

[21] FELLENDORF, M., VORTISCH, P. Validation of the microscopic traffic flow model VISSIM in different real-world situations. In: 80th Annual Meeting of Transportation Research Board: proceedings. 2001. p. 1-9.

[22] JIE, L., FANGFANG, Z., VAN ZUYLEN, H., SHOUFENG, L. Calibration of a micro simulation program for a Chinese city. *Procedia - Social and Behavioral Sciences* [online]. 2011, **20**, p. 263-272. ISSN 1877-0428. Available from: https://doi.org/10.1016/j.sbspro.2011.08.032

[23] SUN, D. J., LIU, X., NI, A., PENG, CH. Traffic congestion evaluation method for urban arterials: case study of Changzhou, China. *Transportation Research Record* [online]. 2014, **2461**, p. 9-15. ISSN 0361-1981. Available from: https://doi.org/10.3141/2461-02

[24] CELKO, J., KOVAC, M., HUSZAROVA, K. Influence of selected vehicle maneuvers on reduction of the urban roads capacity. *Communications - Scientific Letters of the University of Zilina* [online]. 2019, **21**(4), p. 81-89. ISSN 1335-4205, eISSN 2585-7878. Available from: https://doi.org/10.26552/com.C.2019.4.81-89

[25] INDO-HCM. Indian Highway Capacity Manual (Indo-HCM). 2017.

[26] CHARLY, A., MATHEW, T. V. Evaluation of driving performance in relation to safety on an expressway using field driving data. *Transportation Letters* [online]. 2020, **12**(5), p. 1-9. ISSN 1942-7875. Available from: https://doi.org/10.1080/19427867.2019.1591075

[27] Racelogic Limited. Performance Box-III 100Hz GPS Data Logger User Guide. Unit 10, Swan Business Centre, Osier Way, Buckingham MK18 1TB. United Kingdom.: Racelogic Limited., 2014.

[28] PAUL, G., RAJU, N., ARKATKAR, S., EASA, S. Can segregating vehicles in mixed-traffic stream improve safety and throughput? implications using simulation. *Transportmetrica A: Transport Science* [online]. 2021, **17**(4), p. 1-25. ISSN 2324-9935. Available from: https://doi.org/10.1080/23249935.2020.1826595

[29] MITKAS, D. Z., POLITIS, I. Evaluation of alternative ramp metering scenarios on freeway on-ramp with the use of microscopic simulation software Vissim. *Transportation Research Procedia* [online]. 2020, **45**(2019), p. 483-490. ISSN 2352-1465. Available from: https://doi.org/10.1016/j.trpro.2020.03.042

[30] BARI, CH S., GUPTA, U., CHANDRA, S., ANTONIOU, C., DHAMANIYA, A. Examining effect of electronic toll collection (ETC) system on queue delay using microsimulation approach at Toll Plaza -a case study of Ghoti Toll Plaza, India. In: 7th International IEEE Conference on Models and Technologies for Intelligent Transportation Systems: proceedings. 2021. p. 1-6.

[31] MATHEW, T. V., RAO, K. V. K. Traffic signal design-II. In: *Introduction to Transportation Engineering*. NPTEL, 2007.

ENERGY-SAVING THERMAL STABILIZATION SYSTEM AND ASSESSMENT OF TEMPERATURE LOADINGS OF A BRIDGE DECK PAVEMENT

Sergey A. Kostenko *, Aleksandr A. Piskunov, Nikita A. Ganin, Galina A. Emelianova

Federal State Autonomous Educational Institution of Higher Education, Russian University of Transport (MIIT), Moscow, Russia

*E-mail of corresponding author: skostenko1973@mail.ru

Resume

To improve the general traffic safety in conditions of winter ice at traffic interchanges and to extend the overall service life of the roadway, it is proposed to use energy-saving thermal stabilization of a bridge deck pavement by transferring the low-temperature geothermal energy by heat pumps. The practical and computational parts of the pilot plant work are demonstrated and discussed. In order to analyze the need to use additional thermal joints, computer simulation was performed in the LIRA-CAD-2018 software package with subsequent extrapolation to a real bridge span.

Article info

Received 10 February 2022
Accepted 25 April 2022
Online 1 June 2022

Keywords:

de-icing
thermal stabilization of the roadway span
heat pumps
computer simulation
thermal joints
ESG-investing

Available online: https://doi.org/10.26552/com.C.2022.3.D141-D149

ISSN 1335-4205 (print version)
ISSN 2585-7878 (online version)

1 Introduction

Currently, there are several ways to solve the problem of comfortable travel through traffic interchanges in winter:

1. Traditional mechanical cleaning method combined with the use of chemical reagents [1]. However, in order to ensure the traction between the wheel and the road surface, snowplows must work constantly during the snowfalls, which creates additional difficulties for the movement of vehicles and, on the other hand, traffic makes it difficult for specialized equipment for cleaning the roadway. The use of chemical reagents negatively affects tires and metal parts of cars. At the same time, such cleaning often forms snow dumps on the side of the track, hindering the movement of vehicles [2].
2. Installation of liquid's sprayers of emulsified chemical reagents in the base of the bridge deck pavement. This is a technologically complex module-system, which is responsible for the treatment of the roadway with chemical reagents in automatic mode. At the same time, the scattering density is calculated based on empirical estimates that are not always optimal [3].

Despite the fact that the quality of the de-ice chemical products used is constantly being improved, the composition of the reagents is being updated, the direction of their action remains unchanged - a decrease of the melting point temperature of ice and snow [4].

Obviously, both approaches are not without drawbacks, the main of which are the following:

- limited duration of the chemical reagent exposure;
- the coefficient of the car tires' adhesion with a road surface drops by 30 percent in comparison with a wet surface [5];
- the chemical reagents used are biotoxicants and allergens [6-7];
- oily brine sprayed by moving vehicles, which is formed after melting the ice and snow, reduces visibility and contributes to an increase in road accidents [8].

To eliminate these drawbacks, the authors propose a fundamentally different approach to solving the problem for de-icing of traffic interchanges and roads at subzero temperatures - low-temperature geothermal thermal stabilization of bridge deck pavement with the heat pumps' use.

The process of thermal stabilization maintains the temperature of the roadway surface part in a fairly narrow interval, optimal both for stabilizing the rheological characteristics of asphalt concrete and for safe ice-free exploitation. At the same time, the main bearing structure of the bridge crossing perceives the thermal loads that differ from the heated surface pavement coating. Therefore, it is necessary to additionally analyze the unevenness of the resulting thermal loads (and, accordingly, possible deformations) and assess the need for additional thermal joints.

This work is devoted to the study of the thermal stabilization technology applicability as part of the implementation of the Russian Federation federal program "Safe High-quality Roads", "Best Available Technologies", which accords with the concept of ESG-investing (Environmental, Social and Governance).

2 Experimental model and equipment

Based on the Federal State Autonomous Educational Institution of Higher Education "Russian University of Transport" (MIIT) research laboratory, the authors' team of the department "Bridges and Tunnels" has developed an experimental model of a bridge deck pavement with a size of ≈1.15 m^2, built on a scale of 1:20 in relation to the size of the object being modeled (Figures 1, 2).

The model is a rectangular heat- and waterproofing concrete slab with plywood framework, with the plan dimensions of 1520×755 mm and a height of 220 mm.

The heat exchanger pipeline made from metal-polymer pipe d 20×2 mm is laid in a serpentine course.

Temperature parameters were read from the surface of the experimental model with an infrared pyrometer.

The schematic diagram of the installation for the thermal stabilization is shown in Figure 3.

In the experiment the assembled unit was responsible for the thermal stabilization of the bridge deck pavement research model, in which the heating of the heat-transfer agent (water) in the closed circulation circuit of the model slab was performed according to the heat exchange scheme in a heat-insulated heat exchange reservoir. Heat was injected into this heat exchanger due to heat transfer performed by the compressor. The heat was taken away by the compressor from another heat exchanger simulating a geothermal source with a maintained temperature of 11±1 °C. The thermostating (thermal recharge) of this heat exchanger was performed by a flow heater.

Preliminary evaluations of heat exchangers were performed according to the Equation [9]:

$$Nu_s = 1.4\left(\mathrm{Re}_p \frac{d}{l}\right)^{0.4} \cdot \mathrm{Pr}_p^{0.33} \cdot (\mathrm{Pr}_p/\mathrm{Pr}_r)^{0.25}, \quad (1)$$

where: Nu_s - Nusselt number for the system;
Re_p - Reynolds number for the flow of water in the pipe;
Pr_p - Prandtl criterion for water in the pipe (6.52 at 22 °C);
Pr_r - Prandtl criterion for water in a reservoir (3.93 at

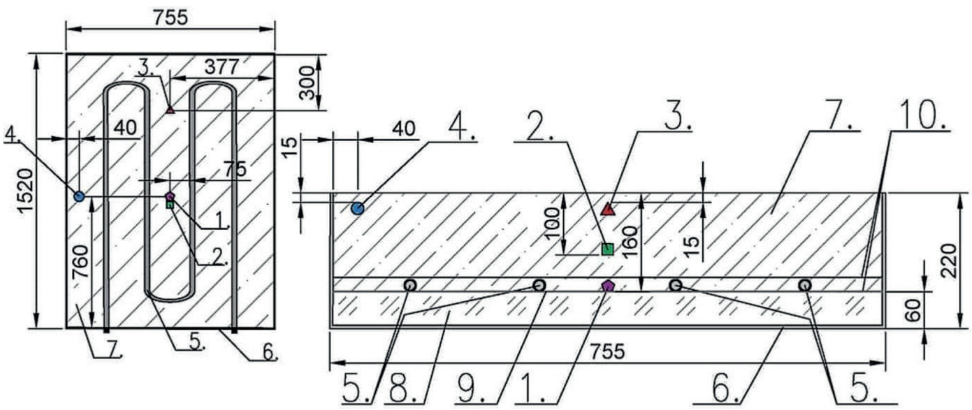

1-4 - Remote thermal sensors; 5 - Metal-polymer pipe d 20×2 mm; 6 - Plywood framework; 7 - Sand-gravel concrete; 8 - Thermal insulation sheet; 9 - Polyethylene film 0.3 mm; 10 - Structural steel netting 70×70 mm

***Figure 1** Scheme of the experimental model for the bridge deck pavement and the arrangement of remote temperature sensors*

***Figure 2** View of the bridge deck pavement experimental model before and after the sand-concrete filling*

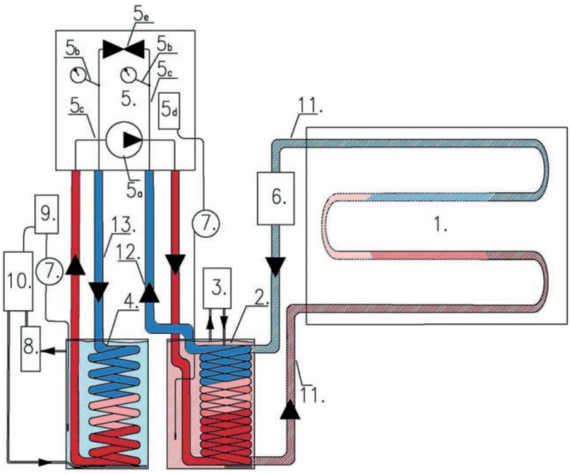

1 - Model slab; 2 - Heating circuit heat exchanger; 3, 8 - Mixers; 4 - Heat exchanger for heat recovery circuit; 5 - Compressor block; 6 - Circulation pump; 7 - Thermostat; 9 - Power contactor; 10 - Instantaneous water heater; 11 - Heating circuit of the model slab; 12 - Compressor heat supply circuit (condenser); 13 - Compressor heat removal circuit (evaporator)

Figure 3 *Installation schematic diagram*

Figure 4 *View of the bridge deck pavement experimental model before and after the research experiment with imitation of icing*

45 °C);
d - pipe diameter, m;
l - pipe length, m.

Amendment for the pipe curvature was made by introducing a correction factor as a multiplier, which is determined for the coil pipes by the ratio:

$$\varepsilon_r = 1 + 1.77\frac{d}{R}, \quad (2)$$

where: d - pipe diameter ($1.5\cdot10^{-2}$ m);
R - coil radius (0.2 m).

Calculations have shown that a copper tubular heat exchanger with a diameter of 15 mm and a length of 15 m is sufficient to remove/return heat at the level of 7 kW.

The temperature of 45 °C in the heat exchanger of the model slab was kept constant using a thermostat. The temperature of 11±1 °C, kept constant in the compressor heat exchanger, simulates the real temperature of geothermal sources. Thus, the selected thermal mode of the installation corresponds to the standard thermal load, as close as possible to full-scale conditions.

The water volume in the circuit of the pattern slab was about 6 liters, in the heat exchangers tanks it was about 80 liters.

Such a scheme of the experimental unit was necessary for testing the model's construction parts and the thermophysical assessment of the entire scheme as a whole, including thermal loads and losses.

3 Experimental part

The pattern slab was moved outdoor (at a temperature of -17 °C) 20 hours before the start of the experiment, the surface was covered with water, thereby simulating the icing of the bridge deck pavement. The thickness of the ice cover ranged from 0.7 to 1.5 mm, the longitudinal slope of the surface was 30 ‰ (Figure 4).

The wind speed on the day of measurements was 3-5 m/s.

The temperature difference of the heat-transfer agent in the supply and return branches in the established stationary mode (after ~ 4 hours from the start of the experiment) was 0.3-0.4 °C. The graph of the change in the temperature difference of the heat-transfer agent over time (similar dependency with the heating power removed by the external circuit) is shown in Figure 5. The estimated power output varied in the

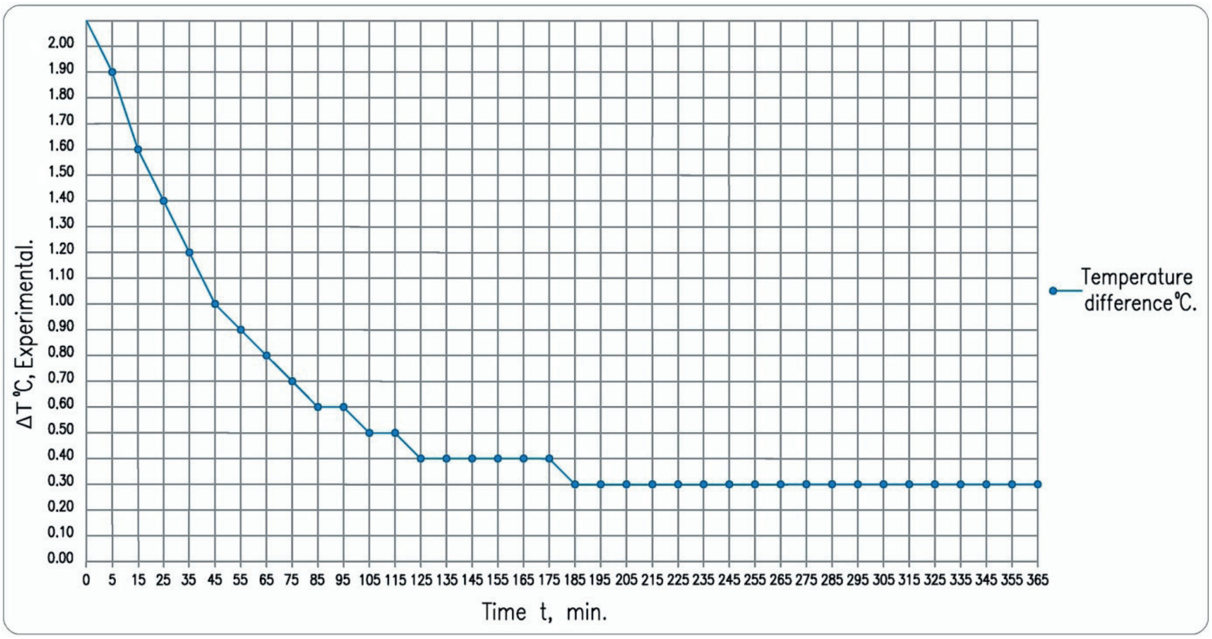

Figure 5 *Graph of the change in the temperature difference of the heat-transfer agent (forward/reverse flow) in time*

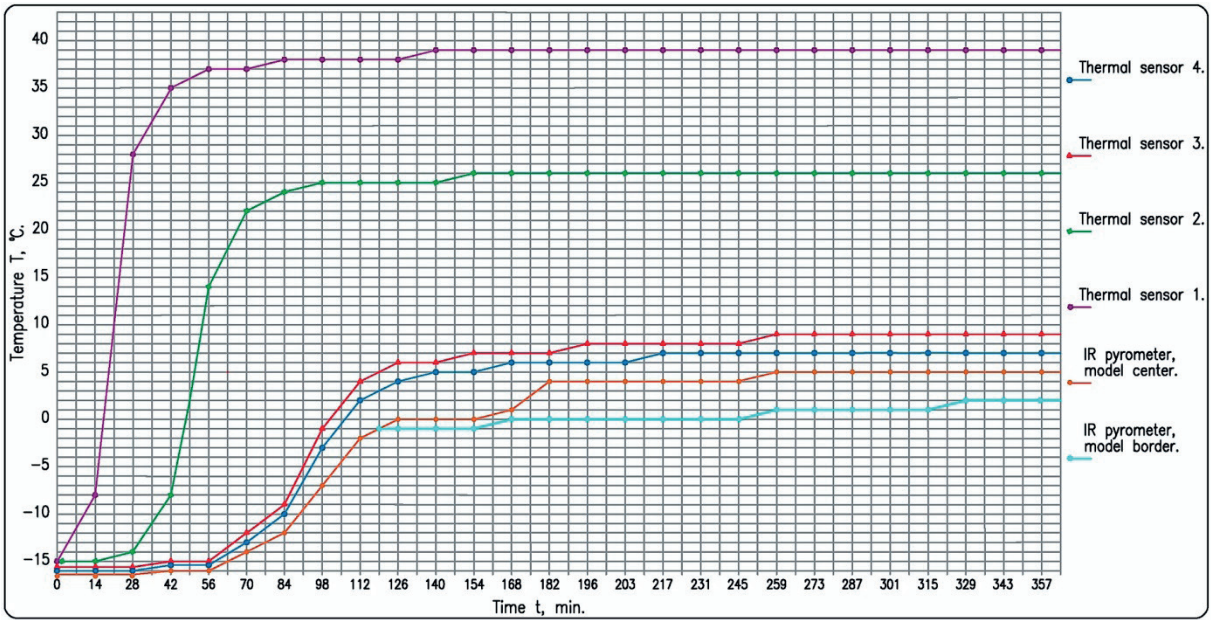

Figure 6 *Graph of the temperature changes process on surfaces and in layers over time on the bridge deck pavement experimental model*

approximate range from 4.2 to 0.5 kW.

The results of the experiment showed that the beginning of ice melting occurred after $t_{exp} \approx$ 2-2.5 hours and it took $t_{exp} \approx$ 4-4.5 hours to completely surface thawing of the bridge deck pavement experimental model (Figure 6).

As follows from the shown graphs of the change in the temperature difference (Figures 5, 6), the process of the heat wave dispersion in the solid is non-stationary and, in general, can be described by a rather complex system of differential equations with definite boundary conditions [10].

After 4-4.5 hours of the experiment to be started, the heat transfer process assumes the character of a stationary one.

After 6 hours from the beginning of the research the experiment is terminated and accomplished.

4 Analytical solution

To describe the process of thermal stabilization of the bridge deck pavement experimental model in winter during the surface ice thawing, estimated calculations of the heat flows were performed to establish a correlation with the above mentioned experimental results.

Since the calculations are evaluative, the following assumptions were made:

1. In the period after the set of a stationary heat flow, the temperature dependence on the vertical coordinates is described by a linear dependence; the temperature gradient is constant;
2. Radiation thermal emission from the heated surface of the unit into the environment is not taken into account due to insignificance;
3. To account for the uneven heating along the horizontal coordinate, a concrete block can be represented as a superposition of 3 elements insulated along the perimeter and not interacting with each other through the side walls;
4. The heat transfer equations are considered in integral form;
5. Heating of the unit bottom part is uniform over the entire surface;
6. The values of thermodynamic coefficients are taken as averaged tabular [11].

Taking into account the accepted assumptions, the allocation scheme of the stationary heat flow for a parallelepiped with thermally insulated side walls (excluding phase transitions) consists of:

1. Heat transfer from the heater through the concrete solid to the surface;
2. Convective heat transfer from the block surface to the air.

Thus, the equation of the system stationary state for each highlighted element must satisfy the equality of two heat flows - heat-conducting through the volume of the concrete parallelepiped (Fourier equation) and then convective through the surface layer (Newton-Richman equation):

$$P = (\lambda \cdot S \cdot (T_2 - T_1))/h = \alpha \cdot S \cdot (T_1 - T_a), \quad (3)$$

where:

P - total heat-loss power (heat flow), W;
S - the cross-sectional area of the parallelepiped (block), m^2;
T_2 - the temperature of the heated (bottom) block surface, K;
T_1 - the temperature of the cooled (top) block surface, K;
T_a - ambient air temperature, K;
h - block height, m;
λ - coefficient of thermal conductivity (specific conductivity), W/(m·K);
α - heat transfer coefficient, W/(m^2·K).

From this equation it is possible to find the surface temperature of the block with an established heat transfer process:

$$T_1 = (\lambda \cdot T_2 + h \cdot \alpha \cdot T_a)/(h \cdot \alpha + \lambda). \quad (4)$$

The heat transfer coefficient α - is calculated in accordance with requirements of the Russian Federation building regulations code (SNiP 2.03.04.84 part 2) according to the formula:

$$\alpha = 5.8 + 11.6\sqrt{v}, \quad (5)$$

where

v - wind speed in m/s.

According to equation (4), the calculated temperature of the top block surface should be set at +5.7 °C, which correlates with the experimental data of ≈5.0-5.5 °C in the central part and confirms the correctness of the estimating calculations.

The steady-state specific heat flow P (specific heat consumption) will be - about 0.5 kW/m^2 in accordance with equation (3).

The specific amount of heat given off by the heat-transfer agent over a period of time Δt will be:

$$Q = V_{sp} \cdot \rho \cdot c_{sp} \cdot \Delta T \cdot \Delta t \quad (6)$$

where:

Q - the total amount of heat given, J;
V_{sp} - specific volume (flow rate) of the passing heat-transfer agent, m^3;
ρ - the heat-transfer agent density, kg/m^3;
C_{sp} - specific heat capacity of the heat-transfer agent, kJ/(kg·deg);
ΔT - change in the temperature of the heat-transfer agent, K.

Thence it is possible to assess the evaluated flow rate of the heat-transfer agent for the steady-state stationary mode of the heat transfer, which should be 1.64 m^3/hour. During the time from the 4th to the 6th hour, the leaked volume of the heat-transfer agent was 3.55 m^3, which correlates with the calculated 3.28 m^3.

The process of melting the surface snow/ice layer, which requires additional heat spending, is divided into 3 stages:

- ice heating from T_a to 0 °C;
- phase transition;
- water heating from 0 °C to T_1

The evaluated value of the correction for the specific heat losses related to the melting of the surface ice layer of a thickness of 1 mm is about 95 W·h.

If one takes the above calculated specific power for a steady heat exchange flow of 500 W/m^2 (i.e., power consumption of 0.5 kW·h /m^2), then the energy consumption increases to about 0.6 kW·h /m^2 or by 20% in the case of melting of a thin (1 mm) ice crust.

Assuming the density of freshly fallen dry snow of 40-60 kg/m^3 [12], one can say that power consumption increases by 20% for every 15 mm of precipitation in winter at temperatures below -10 °C.

In the stationary mode, the energy consumption of the entire model object for the last 2 hours of the experiment should be ~ 1.15 kW·h (specific heat extraction power ~ 500 W/m^2, slab surface area ~ 1.15 m^2, measurement time - 2 hours). The experimentally recorded integral energy consumption of the compressor (measured by a direct-on electric meter) was 0.33 kW·h. Thus, the increasing coefficient of the heat pump in the experiment was ~ 3.5.

5 Computer simulation model

With the introduction of thermal stabilization technology, the load-bearing spans and surface layers of the roadway are staying under conditions of significantly different temperature loadings. This imbalance can lead to material's degradation, materialized in the appearance of cracks in the pavement. In order to analyze the reasonable need to install additional elements in the roadway structure, computer modeling for the experimental model was performed in the LIRA-CAD-2018 software package [13], with subsequent extrapolation to the real span section.

An increase in temperature leads to the transition of atoms (molecules) to a higher energy level, which means an increase in the oscillating atoms' amplitudes of when heated. However, the oscillation anharmonicity caused by the asymmetry of the real potential energy curve of the atoms' interaction leads to an increase in the distance between atoms and, accordingly, to the thermal expansion of solids [14].

The fundamental law of thermal expansion states that a body with a linear dimension L in the corresponding measurement, when its temperature increases by ΔT and there are no external mechanical forces, expands by an amount ΔL equal to:

$$\Delta L = \alpha \cdot L \cdot \Delta T, \tag{7}$$

where:
α - coefficient of linear thermal expansion.

Asphalt concrete pavements arranged on a rigid (cement concrete) base have a coefficient of linear thermal expansion several times different from the concrete of the base bearing layer, therefore, reflected cracks appear atop the joints and cracks of the rigid base, which are intensively developing, lead to untimely destruction of the pavement.

The most radical way to rapidly retard of the asphalt concrete pavements cracking processes is to reinforce them with flexible rolled geogrids in combination with solid nonwoven geotextiles [15].

In the software package, the model of the road pavement piece with the base heating possibility is adopted in the dimensions of 1520 × 755 mm. The grid of the model nodes is adopted 75×75 mm. The layers of the road pavement fragment are modeled by linking a set of isosceles rectangular triangles with 75 mm legs made using the finite element No. 42 (triangular plate) into three composite slabs of 1520 × 755 mm. The nodes of composite slabs modeling the road pavement layers are connected by rod elements made of rod finite element No. 10, which is assigned infinitely large stiffness to imitate the joint effort of composite slabs. Figure 7 shows a general view of the calculation scheme in plane and in axonometry.

The model of the road pavement fragment is fixed by each bottom layer node from movement along the Z axis. For the possibility of modeling the slab deformations from temperature influences, the border line of the bottom slab nodes located along the slab long side is fixed to avoid displacing along the Y axis and the border line of nodes located along the short side of the slab is fixed to avoid displacing along the X axis. The fastenings combination allows the slab model to deform easily from temperature influences in the X0Y plane. The scheme for fixing the nodes of the bottom slab is shown in Figure 8.

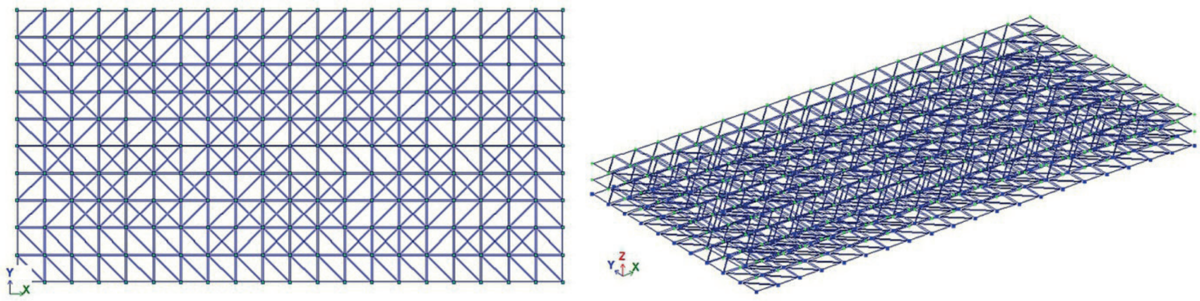

Figure 7 *General view of the design scheme in plan and axonometry (LIRA-CAD-2018)*

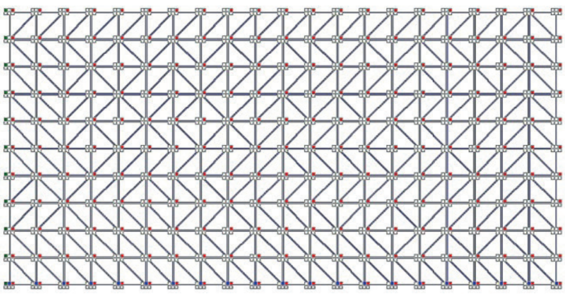

Figure 8 *The scheme for fixing the nodes of the model bottom slab (LIRA-CAD-2018)*

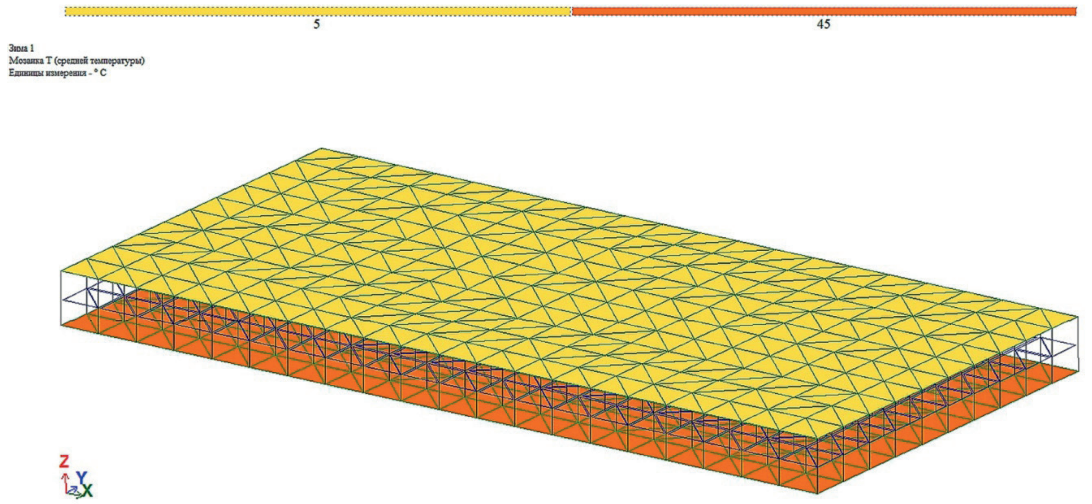

Figure 9 *Mosaic of temperature loadings according to the "Winter-1" scheme (LIRA-CAD-2018)*

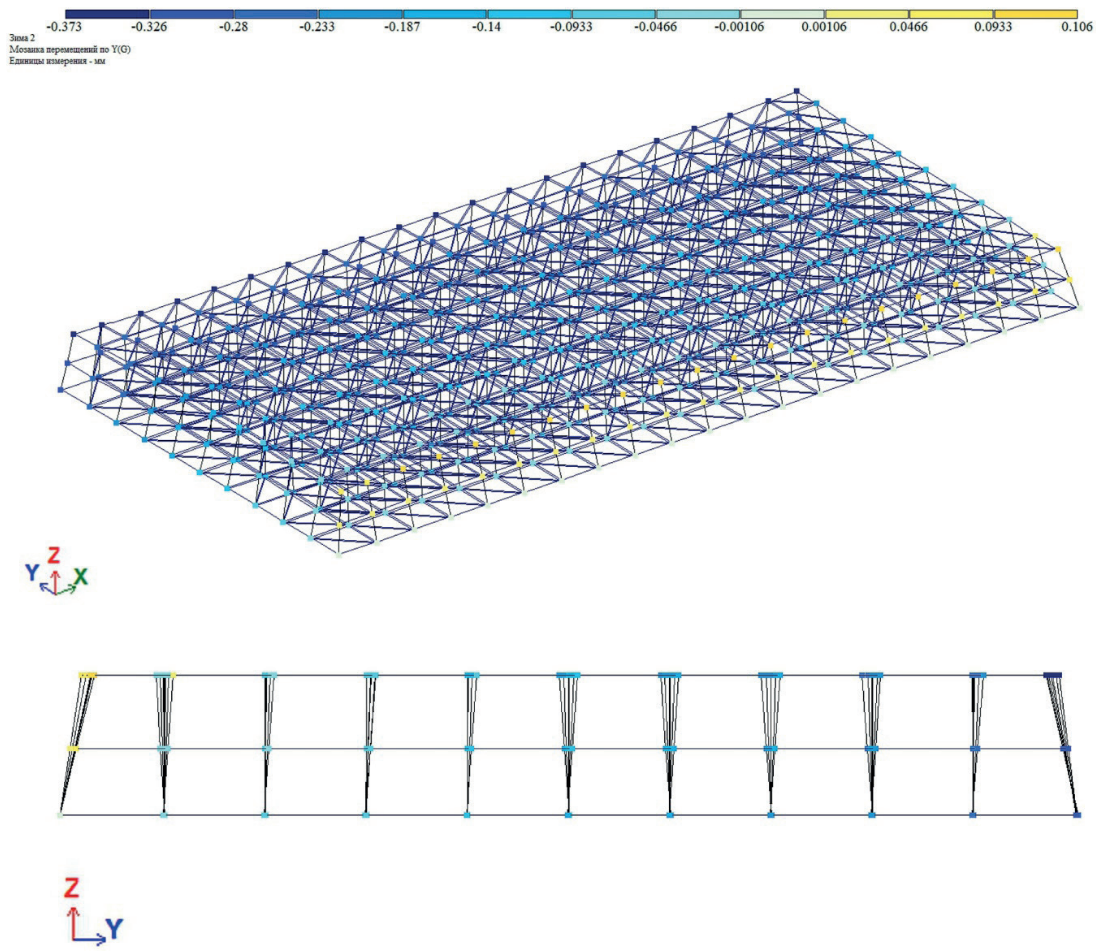

Figure 10 *Calculation mosaics of model nodes displacements along the Y axis for temperature loadings of the "Winter-2" scheme (LIRA-CAD-2018)*

Table 1 *Displacement mosaic for model slab*

Scheme	X-axis maximum	Y-axis maximum	X-axis summ	Y-axis summ
Winter-1	0.817	0.414		
Winter-2	-0.680	-0.373		
Winter mode			1.497	0.787

The design scheme contains two different temperature loadings:

- "Winter-1" - the transition from 45 °C in the bottom part of the slab to 5 °C in the top part at ambient temperature from -16 °C to -12 °C (heating mode).
- "Winter-2" - a slab in a stationary uniformly cooled state at the beginning of the experiment (the temperature of the bottom part is -16 °C, the top part is -16 °C).

Reference temperatures are taken from experimental data:

- 45 °C - corresponds to the heat-transfer agent temperature;
- 5 °C - plate surface temperature after completion of the ice melting process;
- – 16 °C - temperature of the ambient air and the model at the beginning of the experiment.

In the LIRA-CAD-2018 software package the following conditions are accepted as normal: T = 273.15 K (0 °C), P = 101 325 Pa (1 atm, 760 mm Hg)

The mosaic of temperature loading according to the "Winter-1" scheme is shown in Figure 9.

Each loading provides for both temperature effects on the bottom and top layers of the model and the effect on the plates of the slab's body.

As a result of computer simulation, calculated mosaics of the model nodes' displacements along the X and Y axes were obtained for all the variants of temperature loadings.

Figure 10 shows as an example a mosaic of the nodes' geometry deformation of the slab for the loading "Winter-2".

The results of the displacement mosaics for a model slab with a length of 1520 mm are shown in Table 1 (according to the maximum values for each scheme and for the total values by period, mm).

Taking the standard span length of 64 m, one obtains the possible range for additional thermal extensions of the bridge deck pavement for this gauge - up to +63 mm.

The obtained results confirm the need to install additional modular multiprofile deformation thermal joints during the thermostabilized blocks' assembly on the bridge deck pavement.

6 Conclusions

The results obtained in the experiment on the thermal stabilization of a bridge deck pavement prototype, in combination with the analysis of the efficiency of underground heat collectors [16], allow to capture the ability of the proposed method practical application.

As follows from the results of the experiment, with an average winter temperature range in the Central Russia, the power consumption to maintain the roadway in a safe condition is about 0.5 kW·h/m^2.

Further development of the thermal stabilization technology with application of the modern geothermal heat pumps with an efficiency coefficient of up to 4.5-5.5, in the future would reduce energy consumption by 4-5 times and reach 100-150 W/m^2 per hour.

The obtained experimental results are satisfactorily correlated to the calculated ones, which makes it possible to perform preliminary estimates in laboratory conditions.

The modelling of seasonal temperature loadings for the roadway on the bridge spans confirms the need to install additional compensatory thermal joints when using the thermal stabilization technique.

Overall, the obtained results indicate the economic efficiency and expediency of introduction and practical application of the thermal stabilization technology for the bridge structures' safe operation.

References

[1] RUSSELL, G. A. Anti-icing coatings and methods - *Michigan Tech Patents,* 122 [online]. 2014. Available from: https://digitalcommons.mtu.edu/patents/122

[2] SELL, S., REHFELD, N. Anti-icing coatings and de-icing technical approaches and status - Winterwind Ostersund [online]. 2013. Available from: https://windren.se/WW2013/52_Sell_Stephan_Winterwind_2013.pdf

[3] BRODARD, P.-A. Surface condition management. A global concept for winter maintenance operations. In: 12th International Road Weather Conference SIRWEC 2004: proceedings. 2004. ISBN 3-88148-399-3, ISSN 0072-4122.

[4] GLUSHKO, A. N., BESSARABOV, A. M., ZAREMBA, G. A., GLADKAJA, A.A., STOYANOV, O.V. Systemic studies of the anti-icing agents melting ability / Sistemnye issledovaniya plavyashchej sposobnosti protivogololednyh reagentov (in Russian). *Bulletin of Kazan Technological University* / *Vestnik Kazanskogo Tekhnologicheskogo Universiteta.* 2015, **18**(1), p. 119-122. ISSN 2072-6007.

[5] CASEY, P. C., ALWAN, C. W., KLINE, C. F. Impacts of using salt and salt brine for roadway deicing. Review prepared for Idaho transportation department research program [online]. 2014. Available from: https://professionalsnowfightersassociation.org/wp-content/uploads/2019/04/saltimpacts-copy.pdf

[6] TRUJILLO-GONZALEZ, J. M., TORRES-MORA, A. M. Heavy metal accumulation related to population density in road dust samples taken from urban sites under different land uses. *Science of the Total Environment* [online]. 2016, 553, p. 636-642. ISSN 0048-9697. Available from: https://doi.org/10.1016/j.scitotenv.2016.02.101

[7] MALYSHEVA, A. G., SHELEPOVA, O. V., VODYANOVA, M. A., DONERIAN, L. G., USHAKOVA, O. V., YUDIN, S. M. Ecological and hygienic problems of the application of anti-icing agents in a large metropolis (for example, the territory of Moscow) / Ekologo-gigienicheskie problemy primeneniya protivogololyodnyh reagentov v usloviyah krupnogo megapolisa (na primere territorii goroda Moskvy) (in Russian). *Hygiene and Sanitation*. 2018, 97(11), p. 1032-1037. ISSN 2412-0650. Available from: http://dx.doi.org/10.18821/0016-9900-2018-97-11-1032-37

[8] PAYNE, B. F. Oil and gas well brines for dust control on unpaved roads - part 1: ineffectiveness. *European Scientific Journal* [online]. 2018, 14(27), p. 398-427. ISSN 1857-7881, eISSN 1857-7431. Available from: https://doi.org/10.19044/esj.2018.v14n30p166

[9] MIKHEYEV, M. A., MIKHEYEVA, I. M. *Basics of heat transfer* / *Osnovy teploperedachi* (in Russian). Moscow: Energiya, 1977.

[10] PASCAL, H. A Nonlinear model of heat conduction. *Journal of Physics A: Mathematical and General.* 1992, **25**(4), p. 939-949. ISSN 0305-4470, eISSN 1361-6447. Available from: https://doi.org/10.1088/0305-4470/25/4/029

[11] GURVICH, L. V., VEYTS, I. V., ALCOCK, C. B. *Thermodynamic properties of individual substances*. N.Y.: Hemisphere Pub. Corp., 1989. ISBN 9780891165330.

[12] VIALLON-GALINIER, L., HAGENMULLER, P., LAFYSSE, M. Forcing and evaluating detailed snow cover models with stratigraphy observations. *Cold Regions Science and Technology* [online]. 2020, 180, 103163. ISSN 0165-232X. Available from: https://doi.org/10.1016/j.coldregions.2020.103163

[13] LIRA-CAD-2018 - GK LiraLand (in Russian) [online]. Available from: https://www.liraland.ru/news/update/3987/

[14] PADMAVATHI, D. A. Potential energy curves and material properties. *Materials Sciences and Applications* [online]. 2011, **02**(02), p. 97-104. Available from: https://doi.org/10.4236/msa.2011.22013

[15] DMITRIYEV, I. I. Geosynthetic materials in road construction / Geosinteticheskiye materialy v dorozhnom stroitelstve (in Russian). *Construction of Unique Buildings and Structures* / *Stroitelstvo Unikalnykh Zdaniy i Sooruzheniy* [online]. 2016, **10**(49), p. 35-58. ISSN 2304-6295. Available from: https://unistroy.spbstu.ru/userfiles/files/2016/10(49)/3_dmitriev_49.pdf

[16] KOSTENKO, S. A, PISKUNOV, A. A., GANIN, N. A. Organization of laying an underground heat exchanger circuit when using a low-temperature geothermal system for thermal stabilization of the roadway at multi-level transport junctions / Organizatsiya ukladki podzemnogo kontura teploobmennika pri ispol'zovanii nizkotemperaturnoy geotermal'noy sistemy dlya termostabilizatsii dorozhnogo polotna na mnogourovnevykh transportnykh razvyazkakh (in Russian). *Innovation and Investments* / *Innovatsii i Investitsii.* 2021, **3**, p. 307-313. ISSN 2307-180X.

REVIEWING THE COMPONENTS OF TECHNOLOGY ACCEPTANCE BEHAVIOR IN TRANSPORTATION SECTOR

Waqas Ahmed *, Sheikh Muhamad Hizam, Ilham Sentosa

UniKL Business School (UBIS), Universiti Kuala Lumpur, Kuala Lumpur, Malaysia

*E-mail of corresponding author: waqas.ahmed@s.unikl.edu.my

Resume

Technology integration in transportation enhances the efficiency towards urban mobility management. The effective implementation of such technologies requires exploration of vital factors of acceptance and use. This study synthesizes a review work on the road-transport technologies' literature from 2011 to 2021 by contemplating the adoption mechanism keywords such as "acceptance", "usability", "adoption" of technology in transportation, mobility and numerous transport technologies through Boolean operators. Total of 42 articles from 20 developed and developing countries are enlisted for analysis. Numerous Information System (IS) theories and behavioral dimensions are emanated from surveyed literature. Avoid-Shift-Improve (ASI) framework is also materialized to understand the inferences of reviewed articles. Study conclusions are debated for implications of transport technologies from citizens' perspective.

Available online: https://doi.org/10.26552/com.C.2022.3.E96-E107

Article info

Received 7 September 2021
Accepted 28 March 2022
Online 20 May 2022

Keywords:

technology acceptance
usability
transportation technology
smart mobility
Avoid-Shift-Improve (ASI) framework
Intelligent Transport System (ITS)

ISSN 1335-4205 (print version)
ISSN 2585-7878 (online version)

1 Introduction

Metropolitans, being possessive of the elevated concentrations and growth of business and commercial activities, are multifaceted in nature verily affected by transportation system. As urbanization level upsurges, the mobility features across cities need to be updated, upgraded and integrated. To fortify the development and progress of cities to become smart ones, the smart mobility concept enhances the efficiency, ease of use and access of public modes of transport to mobilize the inhabitants in convenient way by using information and communication technologies [1]. In this era of digital economy and technological disruption, innovation in transportation has updated the mechanism as traditional transport system converted into Intelligent Transportation System (ITS). The ITS based various technologies aim to upgrade system, overcome challenges, and mitigate the risks in transport industry. The role of ITS covers transportation management, infrastructure, operation, policies and control methods [2]. The term, Intelligent Transport System (ITS), as main element of Industrial Revolution 4.0 (IR 4.0) [3], has numerous useful applications, like smart parking system, driver support system, Electronic Toll Collection (ETC), Highway Data Collection (HDC), Traffic Management Systems (TMS), Vehicle Data Collection (VDC) and Emergency Vehicle Preemption (EVP) etc. to make the life easy and manageable on roads. There is a wide array of advantages that can be obtained from the ITS deployments. Intelligent Transportation System (ITS) can perform the prominent role in managing traffic congestion, controlling road risks, reducing high accidents rate, carbon emissions, air pollution and, on the other hand increasing safety and reliability, travel speeds, traffic flow and satisfied travelers for all modes [4], [5]. The ITS has traversed various milestones from Artificial Intelligence (AI) to automated vehicles, from robotics to renewable energy [6] for developing the cities in smart environment towards better and convenient mobility facilities.

Being equipped with such ICT tools, the current situation of transport system still entails with challenges that need to be focused on. Rodrigue [7] explored that in this 21st century, the drivers used to spend three times more time on roads as compared to 20th century due to the high level of urbanization. Another similar report by Kapsch [8] showed that drivers consume an average of four year of their life (mostly time waiting in traffic congestions) in a vehicle. As concentrated urbanized atmosphere has escalated the congestion challenge that further called the issues of parking, fuel consumption, environmental impacts, infrastructures damages, mental health, and low productivity etc.

High integration of technology in transport system can cope with such challenges. As the Boston Consulting Group firmly considers prevalent acceptance of technologies could harvest considerable advantages. Such as eradicating road mortalities, refining travel time up-to 40%, recuperating billions of hours vanished in traveling and congestion and producing overall recompences to public worth $1.3 trillion [9]. The fruitful implementation of Information System (IS) technologies require studying the factors influencing the acceptance and use of such technologies. Various studies have explored that proper adoption of technology in transport system, such as in electronic tolling, has played important role in congestion management [10], [11], smart parking for supporting urban mobility [12]. However, numerous researches pointed out towards the ineptitude of technology integration and challenges due to user's concerns and unwillingness [13]-[16]. Acceptance and integration of technology by users in a transport system is based on certain factors of their perception that primarily control the adoption decision of the technology. Jou et al. [10] considered that user attitude molds the behavior and this behavioral intention is responsible for taking any decision of acceptance and rejection. The attitude can be impacted by various factors to make positive (accept) and negative (reject) feelings [17]. To understand the user behavior and attitude towards innovations, certain expressions of IT theories should be considered.

There are various IT models and theories that facilitate the technology adoption by predicting the technology users' behavior and attitude towards acceptance of a system. Technology Acceptance Model (TAM) by Davis [18] is considered as a pioneer in this field of IT acceptance that also predicted the transport technology acceptance behavior. Unified Theory of Acceptance and Use of Technology (UTAUT) proposed by Venkatesh et.al, [19] undertook various technology adoption studies to fortify the proper acceptance of a system. Theory of Planned Behavior (TPB) deals with systematic drivers of human behavior towards certain innovation acceptance. In transportation sector, TAM and UTAUT models are widely used for acceptance assessment. As the effective realization of innovative transport system necessities to observe and examine the elements shaping the acceptance, a wide-ranging insight of transport technology acceptance studies is a matter of significance. The objective of this study is to determine the imperative aspects affecting the adoption of the road transport system technologies by undertaking a systematic review on the elements impacting the acceptance of technology in this field.

2 Methodology

The selection of keywords was based on objective of a study, which describes the investigation of factors for transport technology infusion among users/drivers. For such an intent authors adopted the keywords search strategies directed by Bramer [20]. It included the search of relevant studies that answer the study's aim and scope. From this preliminary search of papers, the relevant keywords were found that would yield out the related studies for the review. Authors classified two types of keywords that included 1) users behavior's action such as Acceptance, Adoption, Technology Usability and 2) Transportation Technology such as Automated Vehicle (AV), Electric Vehicles (EV), Automated Road Transport System (ARTS), Electronic Toll Collection System (ETC), Car Navigation System, Smartphone Driver Support System, Automated Parking System, Autonomous Vehicles etc. After finalizing above keywords, next step was to select the appropriate databases for searching the relevant studies that included Google Scholar, ACM Digital Library, IEEE Explore, Science Direct, Springer, Scopus and Web of Science (WoS). We used the Boolean operator for searching the required studies such as Acceptance OR Adoption AND Electric Vehicle OR Car Navigation System etc.

The inclusion and exclusion protocols were used to refine and pinpoint the suitable studies for this systematic review work (see Figure 1). The basic inclusion criteria consisted of the article language and timeframe. This catalog hunt was comprised of 256 articles with the timeframe of 2011 to 2021. As technology integration and innovation diffusion were seen prevalently in the last decade and specifically since last couple of years during pandemic era, therefore this timeframe was selected to comprehend and explore the recent and advanced technology diffusion in transportation sector from users' perspective. Only English language articles were considered for the analysis. More inclusion criteria, such as type of study (i.e. empirical and quantitative research work only but no review work or editorial or technical notes), peer reviewed papers (i.e. original articles only and no preprint or repository work) and Journal articles (i.e. complete research work only and no conference proceedings and book chapters) were also considered in literature searching process. As the aim of this work was to synthesize the elements of acceptance and adoption behavior of transport technology users, the theoretically supported studies were considered only. Information System theories supported inferences are more viable in terms of expanding the body of knowledge. Quality of articles was assessed based on peer reviewed nature of studies and respective journal indexing such as only articles from those journals were included for the survey that were indexed in Scopus and/or Web of Science databases for last 5 years, as publications in Scopus and WoS database are aligned with integrity and higher standard of research output. Inclusion criteria also entail the focus of the road technology studies only. Additionally, articles that focused on citizens adoption of transport technology were

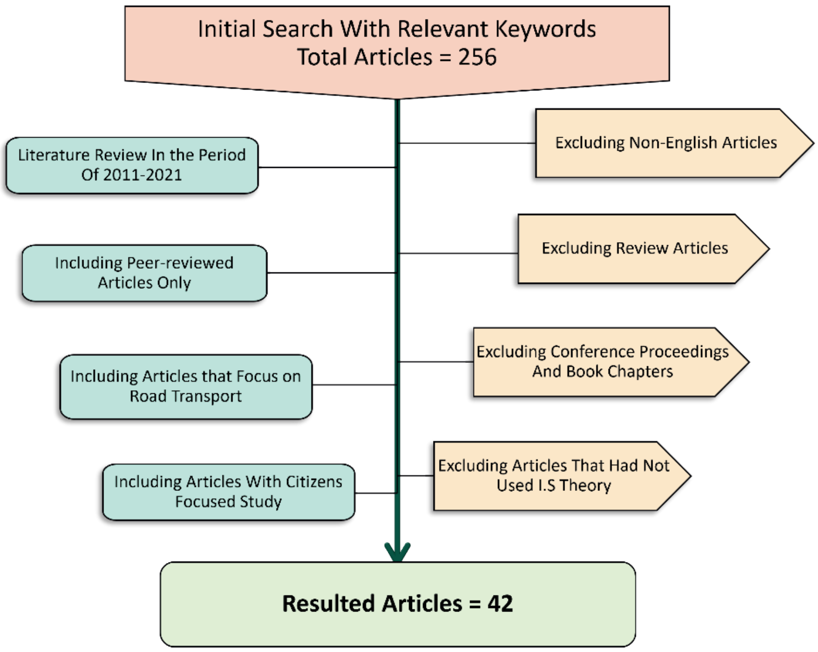

Figure 1 *Inclusion and Exclusion Criteria*

included only. The purpose of the transport technology is to integrate the smart mobility in societies, therefore only citizens' centered studies were included and non-citizens' research work was disregarded for this study. Moreover, the assessment of search criteria and quality to ensure the fairness and reduce the biasness, the STROBE technique is used. This technique is based on 22-items checklist that refers the guidelines for selected article. These guidelines are based on article contents like title, abstract, introduction of matter, methodology techniques, results expressed and conclusion of proper should be according to standards of STROBE.

3 Results and discussion

The total number of articles that considered after inclusion and exclusion criteria for this review research were 42. Table 1 shows the transport technologies that are investigated for this research. Electric cars have 7 studies and automated vehicles technologies are the highest in number with 10 articles. Electronic tolling and car navigation system have 4 studies each and smart parking has 3 and driver support system comprises of 2 studies, while other transportation tools and technologies, such as ridesharing related technologies and public transport linked tools etc. are listed in miscellaneous section and there are 12 studies in this category. Table 1 also explores the usage of IT theory in reviewed articles. Technology Acceptance Model (TAM) has appeared in 20 articles as a suitable IT theory for predicting the user behavior in transportation sector. Unified Theory of Acceptance and Use of Technology (UTAUT) is considered in 7 studies for technology acceptance. Theory of Planned Behavior (TPB) is undertaken by 4 studies to formulate the user behavior. Diffusion of Innovation Theory (IDT) is used by one study. There are 10 studies that had utilized the combination of discussed theories (TAM, TPB, UTAUT, IDT) to formulate better scenario for behavioral intention towards the transportation technology acceptance. To conclude the results of collected data, articles from various databases were published by numerous research publication platforms. Out of 42 articles, majority of papers i.e. n = 24 (57%) was published by Elsevier (see Figure 2). Most researched transport technologies are Autonomous vehicles (n = 10) and Electric vehicles (n = 7) followed by navigation system, e-tolling and smart parking technologies (see Table 1). Around 50% of studies (n=20) considered the TAM model for behavior prediction followed by UTAUT and TPB while higher trend of combining these IS models and adding the external variables is also orchestrated (n = 10) (see Table 1). Among reviewed articles, 8 studies are published in China to comprehend the behavioral modelling for transport technology followed by South Korea (n = 5) and Taiwan (n = 3) (see Figure 3). Geographically, the most part of studies i.e. 54% were conducted in Asia Pacific region (n = 23). Among 42 articles, around 30% of papers (n = 12) were published in 2021 that shows the significance of investigating topic and tendency of research in this segment. It shows the technology integration strategies by government in the region to obtain the sustainable urban mobility.

Numerous technologies of transportation system, such as electric vehicles, automated vehicles, RFID sensors, parking system, car navigation system, etc., are analyzed and observed through selected articles of adoption mechanism. These technologies have become the matter of interest for the governments

***Table 1** Articles searched containing the adoption of transportation system technologies*

Topic	Articles	TAM	TPB	IDT	UTAUT	Combined
Car Navigation System	4	2			1	1
Smart Parking	3	1	1		1	
Electronic Tolling	4	3				1
Driver Support System	2	1				1
Automated Vehicles	10	4			2	4
Electric Vehicles	7	2	2		2	1
Miscellaneous	12	7	1	1	1	2
Total	42	20	4	1	7	10

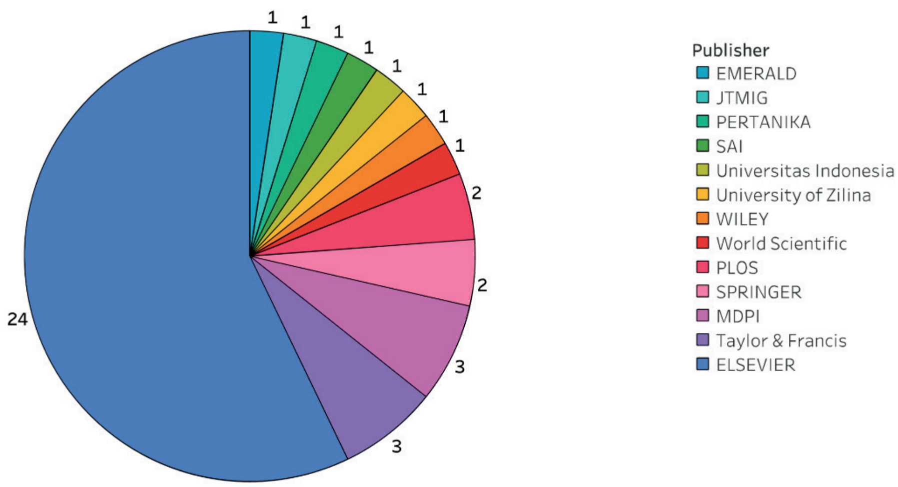

***Figure 2** Articles by Publisher*

and authorities in recent days due to challenges in mega cities are mounting the congestion intensity, fatalities on roads and environment hazardous [21]. Intelligent Transportation System (ITS) provides the solutions for these issues by congestion charging, smart parking system, environment friendly vehicles, internet of things based sensors support system in vehicles [22]-[24]. The studied articles encompass wide variety of ITS technologies that provide the solutions for smart mobility. Besides this, these studies covered the empirical evidence of advanced technology adoption in developed countries and show the urgency of authorities to prioritize the transport-tech for sustainable urban development.

Among studied digital transport services, autonomous vehicles are trendy now a days due to integration of Artificial Intelligence in transport sector that enables the efficiency and accuracy on roads, however, safety is still the main issue in its adoption. The adoption of Autonomous vehicles is mainly investigated in China i.e. a study on unmanned cars' utility assessed by the TAM model where perceived enjoyment and perceived trust in technology found most influencing element towards adoption [25] while another study contemplating TAM and IDT in adoption of autonomous cars concluded with the fact that Perceived Usefulness (PU), relative advantage and result demonstrability can help to integrate the acceptance level [26]. In Slovenia, autonomous vehicles acceptance among millennials was investigated by UTAUT and included the safety concerns at higher level compared to benefits of autonomous cars towards adoption mechanism [27]. Trust as acceptance antecedent was validated in South Korea through the TAM model with significance role PU [28]. The PU and PEOU of TAM models appeared as key predictors of driverless cars in USA [29]. Meanwhile a study pertaining the case of developing country i.e. Vietnam also explored the autonomous vehicle adoption system and showed the financial risk and time risk as the significant factors to manage the acceptance [30]. As autonomous vehicles are not limited to personal cars, but buses, shuttles and other modes of public transport also managed by artificial intelligence and no-driver required to operate. In China, autonomous buses can be accepted by citizen upon perceiving the higher level of trust and perceived usefulness [31]. Similarly, trust and compatibility in accepting the autonomous shuttles as a mode of mobility plays vital role in a German study [32]. Perceived Enjoyment and Performance Expectancy are emerged as important factors in Greek autonomous public transport adoption [12]. In Ireland, adoption of the autonomous public transport and driverless shared vehicles underlined the TAM and TPB and found that Perceived Behavioral Control, Perceived Usefulness

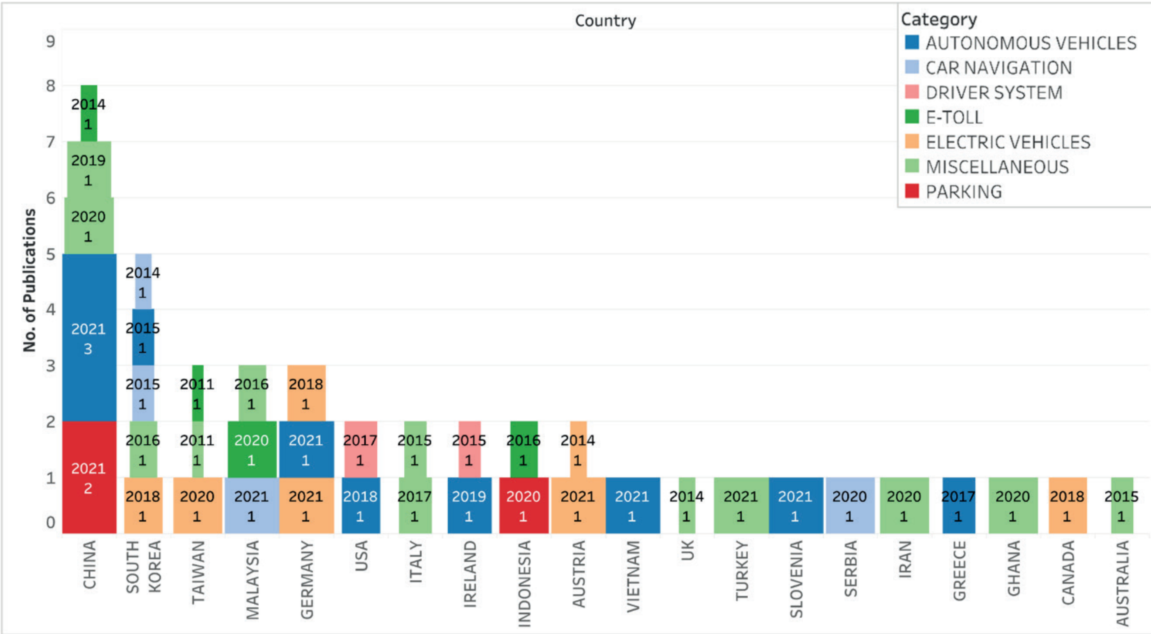

***Figure 3** Reviewed Articles by Countries w.r.t Category and Year*

and Subjective Norms were the main elements to shape the behavioral intention of citizens [33]. Autonomous vehicles adoption mainly depends on trust level of technology and the safety concerns associated with the system can be addressed by more efficient and sustainable system integrity, rules and regulation by authorities and distinct lane and route distribution of driverless cars at trial basis for the long-term benefits and mass integration.

Electric vehicles are hot topic in transportation technology and sustainable mobility. They include the personal cars, public buses, tri-wheelers and two wheelers (scooters and bicycles). Electric vehicles recognition is also interpreted as widely used technology of transport system in reviewed papers. Being environment friendly and convenient one, electric vehicle adoption positively influenced by perceived usefulness, satisfaction and attitude while perceived cost found as hurdle in acceptance of electric vehicle technology [34]. While using the TPB theory, the Attitude and Perceived Behavior Control emerged as strong stimulators of early adopters in Canada for electric vehicles [35]. In Germany, the early adopters showed Perceived Organizational Usefulness and Social Norms as main ingredients of electric vehicles acceptance through the Structural Equation Modeling [36]. Towards electric bicycle in Austria, the Perceived Usefulness, Perceived Ease Of Use and Environmental factor, possessed the significance towards shaping adoption behavior [37]. To comprehend the citizens behavior towards acceptance of e-scooters for urban and short-distance mobility in Germany, UTAUT model was used to validate the behavior modelling by expounding the personal benefit and convenience as vibrant behavior predictor [38]. E-Scooters' adoption studies in Taiwan [39] and Austria [37], [40] predominantly used the TPB theory where Perceived Behavioral Control and Social Influence played main role to shape the behavior. Electric mobility resources are prevailing in developed countries by considering the sustainable urban mobility a crucial for future cities. Minimizing the dependency on gasoline-powered cars, buses and two-wheelers by promoting environment friendly e-cars, green buses and e-scooters to protect the environment, cities livelihood and healthy urban atmosphere. To attain this milestone, the adoption of e-vehicles is mainly dependent on the word-of-mouth about usability scenario because perceived enjoyment and usefulness of technology are largely acknowledged by citizens in reviewed articles and infusing the "good word" at mass level could help for higher level integration. By keeping this in mind, government should promote it through multiple ways as transforming the public transport to electric ones, encouraging the e-vehicles import or production capacity and motivate the micro-level usability of e-scooters for better future.

As urban and highway mobility entails the tolling and parking mechanism, the transportation technology orchestrates the advanced technology for system integration, safety and time saving tools to support the government in toll collection, on road vehicles, managed parking and travel behavior of citizens. Such technology supports the vehicles to ploy on roads with organized intelligent transport system. In such a way, Taiwan implemented electronic tolling on its highways to enhance the efficiency of tolling and combat the congestion issue in 2006. However, the proper adoption was not achieved until the government understood the crucial factors impacting the decision making of highways users to adopt RFID tags. The TAM model and Theory of Planned Behavior with external constructs were assessed that concluded in prominence of role of media and word of mouth towards adoption of e-tolling [10].

Figure 4 *Word Cloud of Most Impact Variables in Reviewed Papers*

Indonesian study on e-toll established the significance of Perceived Usefulness and Perceived Behavioral Control [11]. In Malaysia, the RFID tag for e-toll, smart parking and electronic road pricing is being implanted and to understand the netizens behavior towards its adoption was assessed by TAM model which in result explored the vibrant role of Attitude (backed by PU and PEOU) and Subjective Norms [41]. Similarly, a TAM-based Chinese study validated the E-toll adoption through the TAM model and resulted in presenting the Social Influence and individual characteristics as the main antecedents of behavior shaping of individuals [42]. The sensor-based technologies in vehicles inside the urban spaces possess the quite a prominence regarding the parking purpose. Using the UTAUT, an Indonesian study towards urban parking technology acceptance showed the Facilitating Conditions as a key predictor among netizens [43]. More studies on parking technologies revealed that Perceived Usefulness with Perceived Network Externality in shared parking [44], Perceived Risk with role of gender for deciding the shared parking versus conventional parking [45] can play important part in adopting the smart parking tool.

Technologies inside the vehicles play noteworthy part to engage the citizens on road with complete information of surroundings, connectivity and safety assurance such as car navigation system, driver support system etc. Usability of these tools was mainly validated by the TAM and UTAUT models. According to multiple studies from South Korea, Quality features of car navigation system [46] and Perceived Usefulness of such tools [47] can become the adopting triggers among citizen while in Serbia, installing telematics for cars insurance purpose was supported by Facilitating Conditions [48]. Social Influence and Usefulness can change the netizen behavior in Malaysia to use dashboard cam [49]. Adoption of Smartphone driver assistance mechanism in Ireland was also backed by Perceived Gain and Usefulness with Social Influence [50]. In a similar study in USA, to prevent the accident on highways, advanced driver assistance system was validated through TAM variables [51]. Technology to assist the drivers on roads and prevent the unfavorable situation are backed by quality features, perception of benefits and views of society to accept or resist. However, the road safety measurement should encourage to utilize the in-vehicle digital tools for safe and managed travelling.

In miscellaneous category, there were assorted studies on public transit technology, ridesharing apps, sustainable mobility tools for netizens etc. These studies had analyzed the citizens behavior through TAM, TPB and UTAUT and most of the articles were describing the public transport digital tool. Such as for public transit commuters in Taiwan, [52] and UK [53], and mobile payment for public transport in Italy [54] were resulted in importance of potential significance of system. While towards car drivers, in Australia, ITS tool for railway crossing system was measured for adoption through the combined theoretical framework where PBC and SN were prominent behavioral factor [55]. Similarly, system quality of the ITS mechanism in Malaysian roads was accepted through its usefulness (PU) [56]. To manage the bicycles detection on roads, drivers acceptance was measured by the TAM model in Italy [57]. Travelers adoption of variable message signs on roads in China was also validated by TAM model [58]. Ridesharing is the most famous digital transportation service and its adoption through various social and contextual elements is important for sustainable mobility. Muti-modal trip-planning app in Turkey [59] and ride-sharing service in China [60] were mainly adopted through the PU. To accept the bicycle sharing system in Iran, Facilitating Conditions from UTAUT emerged as vibrant factor of adoption [61]. Ridesharing in a less-economically developed country i.e. Ghana, depended on level of education of respondents [62].

Higher level of acceptance of the ITS solutions (as explored in reviewed papers) ensures the management of mobility tasks. Technology Acceptance Model is used by substantial number of studies in innovation or information system adoption. Lai [63] conducted the review of technology adoption by theory studies and found that the TAM model was the most used one for any type of technology acceptance. He further explained that TAM model defined the ways, why do the acceptance and rejections of respective system occur. Taherdoost [64] conducted the technology acceptance review and found the importance of TAM among several models. Therefore, in transportation system, the TAM model is also prevailing in most studies. However, assessing the technology adoption through blending the multiple models also apparent and evident in the study [65].

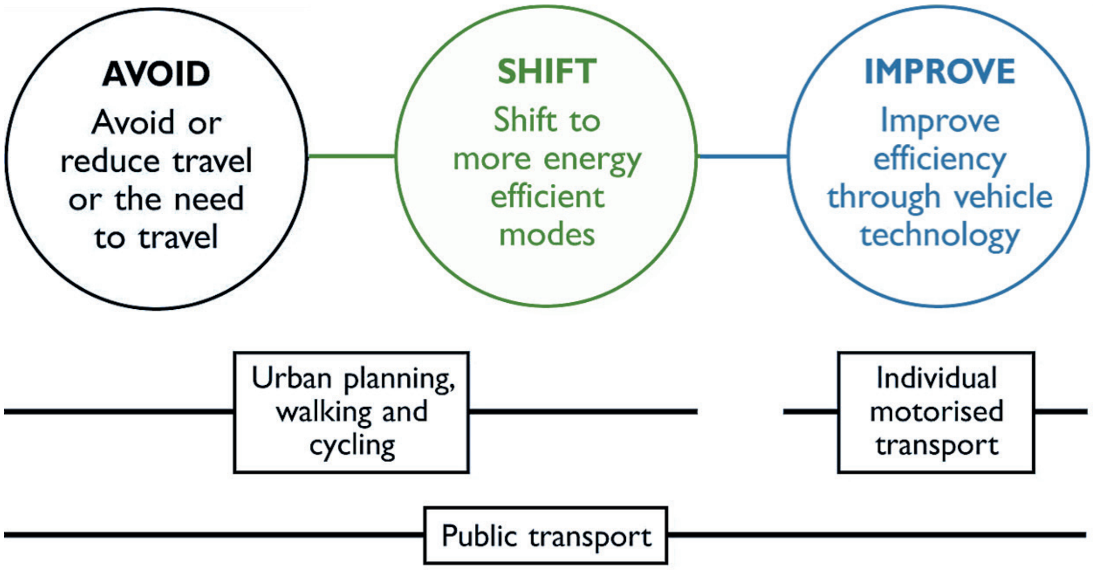

Figure 5 *Avoid Shift Improve (ASI) framework*

However, combing the TAM , TPB and UTAUT model also resulted in TAM notoriety for predicting behavior for technology adoption [51].

Perceived Usefulness (PU) is the main construct in TAM model that depicts about the advantageous nature of technology while another construct of TAM is Perceived Ease of Use (PEOU) which talks about the convenience usage of that technology. Both of these factors are major contributor towards impact on attitude and behavioral intention of users. Attitude refers to positive or negative assessment due to features of a system that intended to use. Behavioral Intention of user is considered as the behavior of user towards the certain innovation or system acceptance or rejection. Social Norms are the societal influence to accept and adopt the technology. Perceived Behavioral Control is provocation of human behavior that enables to accept the system based on certain stimulators. Performance Expectancy in UTAUT model is parallel to Perceived Usefulness of TAM model, which relates with efficiency in performance by usability of the specific system. Table 1 explores the transport technology adoption as per theory to assess the user behavior. Here, the TAM model is prevalent, UTAUT and TPB also have strong influence towards behavioral shaping. There are various variables reviewed in the papers, which had significant impact on behavioral intention. A word cloud is shaped in Figure 4 to follow most impacted variables across the reviewed articles.

As adoption of any technology is a basic step towards future oriented pattern of usability therefore understanding the antecedents and factors of significance will help the stakeholders to fortify the plan of action. The rationale of this study is to understand the infusion of technological pattern according to users' behavior, which in return will help to improve the sustainable mobility practices. This impression is based on the Avoid-Shift-Improve (A-S-I) framework, which is modelled by German authorities in 1990s era to develop the sustainable urban mobility strategies [66]. The A-S-I framework, as depicted in Figure 5, is based on the three strategies i.e. Avoid the travel activity through certain modes of transport such as prevent cars usability in cities and Shift to public transport or Avoid the gasoline powered vehicles and Shift to electric vehicles or Avoid the mobility activity through any vehicles and Shift to walking or cycling inside the city for sustainable mobility practices. When Avoid and Shift are not feasible then Improve strategy is implemented by managing the technology for individual motorized mobility such as connectivity, automation and sensors in the vehicles. In this study, the Shift and Improve strategy (specifically) is being focused by contemplating the factors that play significant role to support stakeholder for sustainable mobility strategy.

The analysis of reviewed articles explores that in order to implement the autonomous vehicles (the Improve strategy of A-S-I framework), safety, security and assurance of managed control should be kept in mind. Driverless cars or semi-autonomous vehicles are merely adopted based on the safety measures, while autonomous public transport such as shuttles, buses or trains are smoothly accepted by the netizen due to trust level in authorities. To infuse the autonomous public mobility initiatives, it is suggested to focus on quality of services and ease of use of service for mass integration. Similarly, sensors and devices in the cars for parking, e-tolling, navigations and support gadgets are infused by their perception of benefits, facilitating circumstances, and quality of service. Such tools are also backed by society influence where people adopt the respective technology by realizing its usage worth among other people's action. While choosing technological services for ridesharing, mobility as a service (MaaS) and trip planner, the usefulness and usability ease can enhance the individuals' choice of mobility patterns. Regarding electric vehicles which support the Shift strategy of A-S-I framework, the mechanism is already diffused by early adopter in many developed countries in the shape of personal conveyance and micro-mobility scooters etc. A better word of mouth regarding the benefits of e-vehicles in the society would be quite resourceful for the mass adoption. E-scooters for micro mobility would be the solution for heavily car-congested urban roads. Stakeholders should promote the usability of such practices by encouraging the mobility startup towards e-scooter initiatives. Authorities would also gain the useful outcomes by e-buses implementation, since as per users' point of view, innovative technology with less effort is suitable for mass adoption.

4 Conclusion

The objective of this study was to determine the imperative aspects affecting the adoption of road transport system technologies by undertaking a systematic review on the elements impacting the acceptance of technology in this field. This systematic review is led by searching of numerous keywords such as adoption, usability, acceptance of IT in transportation, highways and information system models in transport services through the Boolean operators. Authors also examined the different vital technologies, such as Autonomous Vehicle (AV), Electric Vehicles (EV), Automated Road Transport System (ARTS), Electronic Toll Collection System (ETC), Car Navigation System, Smartphone Driver Support System, Automated Parking System and other technologies (i.e. in vehicles and on roads) in the 2011-2021 period. There are 42 articles enlisted in this study that shrouded adoption mechanism of advance technology in the transport system in 20 developed and developing countries. The technology acceptance model (TAM) has appeared to be the most significant model used to predict and point out the determinants influencing the acceptance of technologies in road transport system; in addition the Unified Theory of Acceptance and Use of Technology (UTAUT) model and Theory of Planned Behavior (TPB) have also covered many applications in recent years in the transportation system. Perceived usefulness, convenience in usability, social influence, facilitating circumstances, attitude and behavioral control and behavioral intentions of end-users are effective in the adoption of modern transport system. By contemplating numerous factors like usefulness, ease of use and social influence, the adoption rate of transport technologies can be amplified to make better achievement of smart mobility.

The study elaborated the phenomenon of adopting the smart mobility solutions and key determinants of smooth acceptance of technology in transportation. The TAM model demonstrated its eminence in technology adoption literature, particularly its nature of combining with external variables and other theories made it forerunner towards advanced technologies. The Unified Theory of Acceptance and Use of Technology (UTAUT) model, being an advanced extension of TAM, also showed the significance in predicting the digital technologies in transportation. The study encapsulates the suitability of combining the TAM and UTAUT models for better assessment of behavioral intention of technology users. The research fortified the value of main construct of the TAM, i.e. Perceived Usefulness as key determinant of transport technologies. Social influence has also captured the prominent place in behavior shaping in reviewed studies.

As per A-S-I framework, the inferences will support in Shift and Improve strategy as majority of reviewed article were discussing and pointing towards adoption of individualized transport technology to Improve the vehicle technology and some articles also discussing how to Shift to energy efficient mode of mobility. The research will support the authorities to devise the effective policies for technology implementation through the ASI framework, as to implement Shift strategy, the positive word of mouth of technological gain should be focused. To implement Improve strategy, privacy concerns in automation and social influence with service quality in sensors should be concentrated. The vital features and elements of technology should be communicated through the mass media and word of mouth. The sense of significance of technology enhances the technology adoption. Technology cannot be diffused in organization without willingness of individual behavioral system. As this research has reviewed the articles, which are condensing the mobility challenges and solutions of developed countries, it would contribute to literature for future studies of developing nations to foresee the mobility solutions. The study is the first step towards realizing the technology and human behavior in road transportation; however, further work in this field would outcome in more useful and resourceful inferences. The study is limited to road transport technologies; future studies should consider the other modes of transportation such as logistic, rail, air and maritime for more concentration of diverse technology integration, such as maritime autonomous surface ships, blockchain adoption in the aviation industry, LNG as an alternative fuel, port digitalization, automated road transport logistics and road freight transport mechanism etc.

References

[1] KASSIM, N. S. Smart city - introduction [online]. 2016. Available from: https://www.mcmc.gov.my/skmmgovmy/media/General/pdf/Sesi-5-Rangkakerja-Berteraskan-Aspek-Informasi-%28PLANMalaysia%29.pdf

[2] PATEL, P., NARMAWALA, Z., THAKKAR, A. A Survey on intelligent transportation system using internet of things. *Middle-East Journal of Scientific Research* [online]. 2019, **15**(5), p. 231-240. ISSN 1990-9233. Available from: https://doi.org/10.5829/idosi.mejsr.2013.15.5.11215

[3] SHUKRI, S., EMBONG, B. Future trend in transportation [online]. 2017. Available from: https://www.llm.gov.my/doc/Paper%204%20(MIMOS)-Future%20Trend%20In%20Transportation.pdf

[4] Intelligent transportation systems for sustainable development in Asia and the Pacific - UN ESCAP [online]. 2015. Available from: https://www.unescap.org/sites/default/files/ITS.pdf

[5] QURESHI, K. N., ABDULLAH, A. H. A Survey on intelligent transportation systems. *Middle-East Journal of Scientific Research* [online]. 2013, **15**(5), p. 629-642. ISSN 1990-9233. Available from: https://doi.org/10.5829/idosi.mejsr.2013.15.5.11215

[6] Conference Newsletter ITS Seminar and Exhibition 2017 - ITS [online]. 2017. Available from: http://itsasia-pacific.com/wp-content/uploads/2017/03/ITS-Conference-2017-Newsletter.pdf

[7] RODRIGUE, J.-P. Urban transport challenges. In: *The geography of transport systems* [online]. RODRIGUE, J.-P. London: Routledge, 2020. ISBN 978-0-367-36463-2, p. 439. Available from: https://doi.org/10.4324/9780429346323

[8] Smart urban mobility - Kapsch [online]. 2016. Available from: https://www.kapsch.net/

[9] TORTORELLA, J. The road to autonomous vehicles must be paved with collaboration among all stakeholders - The Boston Consulting Group [online] [accessed 2019-05-23]. 2015. Available from: https://www.globenewswire.com/news-release/2015/09/08/924237/0/en/The-Road-to-Autonomous-Vehicles-Must-Be-Paved-With-Collaboration-Among-All-Stakeholders.html

[10] JOU, R. C., CHIOU, Y. C., KE, J. C. Impacts of impression changes on freeway driver intention to adopt electronic toll collection service. *Transportation Research Part C: Emerging Technologies* [online]. 2011, **19**(6), p. 945-956. ISSN 0968-090X. Available from: https://doi.org/10.1016/j.trc.2011.05.002

[11] IRAWAN, H., HENDAYANI, R., WIDYANI, D. Adoption of electronic toll application analysis. *International Journal of Economics and Management*. 2016, 10(S1), p. 211-222. ISSN 1823-836X, eISSN 2600-9390.

[12] MADIGAN, R., LOUW, T., WILBRINK, M., SCHIEBEN, A., MERAT, N. What influences the decision to use automated public transport? Using UTAUT to understand public acceptance of automated road transport systems. *Transportation Research Part F: Traffic Psychology and Behaviour* [online]. 2017, **50**, p. 55-64. ISSN 1369-8478. Available from: https://doi.org/10.1016/j.trf.2017.07.007

[13] WRIGHT, S., CELLINA, F., BULGHERONI, M., CARTOLANO, F., LUCIETTI, L., VAN EGMOND, P., VAN WIJNGAARDEN, L. Public acceptance of SocialCar, a new mobility platform integrating public transport and car-pooling services: insights from a survey in five European cities. In: 7th Transport Research Arena TRA 2018: proceedings. 2018.

[14] WANG, Y., WANG, S., WANG, J., WEI, J., WANG, C. An empirical study of consumers' intention to use ride-sharing services: using an extended technology acceptance model. *Transportation* [online]. 2020, **47**, p. 397-415. ISSN 0049-4488, eISSN 1572-9435. Available from: https://doi.org/10.1007/s11116-018-9893-4

[15] OOI, K. B., FOO, F. E., TAN, G. W. H. Can mobile taxi redefine the transportation industry? A systematic literature review from the consumer perspective. *International Journal of Mobile Communications* [online]. 2018, **16**(3), p. 341-359. ISSN 1470-949X, eISSN 1741-5217. Available from: https://doi.org/10.1504/IJMC.2018.10004694

[16] NAWEED, A., ROSE, J. Assessing technology acceptance for skills development and real-world decision-making in the context of train driving. *Transportation Research Part F: Traffic Psychology and Behaviour* [online]. 2018, **52**, p. 86-100. ISSN 1369-8478. Available from: https://doi.org/10.1016/j.trf.2017.11.003

[17] ZOLOTOV, M. N., OLIVEIRA, T., CASTELEYN, S. E-participation adoption models research in the last 17 years: a weight and meta-analytical review. *Computers in Human Behavior* [online]. 2018, **81**, p. 350–365. ISSN 0747-5632. Available from: https://doi.org/10.1016/j.chb.2017.12.031

[18] DAVIS, F. D. Perceived usefulness, perceived ease of use and user acceptance of information technology. *Management Information Systems Quarterly* [online]. 1989, **13**(3), p. 319-340. ISSN 0276-7783, eISSN 2162-9730. Available from: https://doi.org/10.2307/249008

[19] VENKATESH, V., MORRIS, M. G., DAVIS, G. B., DAVIS, F. D. User acceptance of information technology: toward a unified view. *Management Information Systems Quarterly* [online]. 2003, **27**(3), p. 425-478. ISSN 0276-7783, eISSN 2162-9730. Available from: https://doi.org/10.2307/30036540

[20] BRAMER, W. M., DE JONGE, G. B., RETHLEFSEN, M. L., MAST, F., KLEIJNEN, J. A systematic approach to searching: an efficient and complete method to develop literature searches. *Journal of the Medical Library Association* [online]. 2018, **106**(4), p. 531-541. eISSN 1558-9439. Available from: https://doi.org/10.5195/jmla.2018.283

[21] MAKINO, H., TAMADA, K. SAKAI, K., KAMIJO, S., Solutions for urban traffic issues by ITS technologies. *IATSS Research* [online]. 2018, **42**(2), p. 49-60. ISSN 0386-1112. Available from: https://doi.org/10.1016/j.iatssr.2018.05.003

[22] ALI, M., MANOGARAN, S., YUSOF, K. M., SUHAILI, M. R. M. Analysing vehicular congestion scenario in Kuala Lumpur using open traffic. *Indonesian Journal of Electrical Engineering and Computer Science* [online]. 2018, **10**(3), p. 875-882. ISSN 2502-4752, eISSN: 2502-4760. Available from: https://doi.org/10.11591/ijeecs.v10.i3.pp875-882

[23] NOOR, N. M., SAM, S. M., FIRDAUS, N., AZMI, M., CHE, R., YUSOFF, M. RFID-based electronic fare toll collection system for multi-lane free flow - a case study towards Malaysia toll system improvement. *Journal of Telecommunication, Electronic and Computer Engineering* [online]. 2016, **8**(4), p. 71-76. ISSN 2180-1843, eISSN 2289-8131. Available from: https://jtec.utem.edu.my/jtec/article/view/1175

[24] YAU, K.-L. A., LAU, S. L., CHUA, H. N., LING, M. H., IRANMANESH, V., KWAN, S. C. C. Greater Kuala Lumpur as a smart city: a case study on technology opportunities. In: 2016 8th International Conference on Knowledge and Smart Technology (KST): proceedings [online]. IEEE. 2016. p. 96-101. Available from: https://doi.org/10.1109/KST.2016.7440496

[25] HUANG, T. Research on the use intention of potential designers of unmanned cars based on technology acceptance model. *PLoS ONE* [online]. 2021, **16**(8), e0256570. eISSN 1932-6203. Available from: https://doi.org/10.1371/journal.pone.0256570

[26] YUEN, K. F., CAI, L., QI, G., WANG, X. Factors influencing autonomous vehicle adoption: an application of the technology acceptance model and innovation diffusion theory. *Technology Analysis and Strategic Management* [online]. 2021, **33**(5), p. 505-519. ISSN 0953-7325, eISSN 1465-3990. Available from: https://doi.org/10.1080/09537325.2020.1826423

[27] MANFREDA, A., LJUBI, K., GROZNIK, A. Autonomous vehicles in the smart city era: an empirical study of adoption factors important for millennials. *International Journal of Information Management* [online]. 2021, **58**, 102050. ISSN 0268-4012. Available from: https://doi.org/10.1016/j.ijinfomgt.2019.102050

[28] CHOI, J. K., JI, Y. G. Investigating the importance of trust on adopting an autonomous vehicle. *International Journal of Human - Computer Interaction* [online]. 2015, **31**(10), p. 692-702. ISSN 1044-7318, eISSN 1532-7590. Available from: https://doi.org/10.1080/10447318.2015.1070549

[29] KOUL, S., EYDGAHI, A. Utilizing technology acceptance model (TAM) for driverless car technology adoption. *Journal of Technology Management and Innovation* [online]. 2018, **13**(4), p. 37-46. eISSN 0718-2724. Available from: https://doi.org/10.4067/S0718-27242018000400037

[30] ESCANDON-BARBOSA, D., SALAS-PARAMO, J., MENESES-FRANCO, A. I., GIRALDO- GONZALEZ, C. Adoption of new technologies in developing countries: the case of autonomous car between Vietnam and Colombia. *Technology in Society* [online]. 2021, **66**, 101674. ISSN 0160-791X. Available from: https://doi.org/10.1016/j.techsoc.2021.101674

[31] WU, Z., ZHOU, H. XI, H., WU, N. Analysing public acceptance of autonomous buses based on an extended TAM model. *IET Intelligent Transport Systems* [online]. 2021, **15**(10), p. 1318-1330. eISSN 1751-9578. Available from: https://doi.org/10.1049/itr2.12100

[32] NORDHOFF, S., MALMSTEN, V., VAN AREM, B., LIU, P., HAPPEE, R. A structural equation modeling approach for the acceptance of driverless automated shuttles based on constructs from the unified theory of acceptance and use of technology and the diffusion of innovation theory. *Transportation Research Part F: Traffic Psychology and Behaviour* [online]. 2021, **78**, p. 58-73. ISSN 1369-8478. Available from: https://doi.org/10.1016/j.trf.2021.01.001

[33] ACHEAMPONG, R. A., CUGURULLO, F. Capturing the behavioural determinants behind the adoption of autonomous vehicles: conceptual frameworks and measurement models to predict public transport, sharing and ownership trends of self-driving cars. *Transportation Research Part F: Traffic Psychology and Behaviour* [online]. 2019, **62**, p. 349-375. ISSN 1369-8478. Available from: https://doi.org/10.1016/j.trf.2019.01.009

[34] PARK, E., LIM, J., CHO, Y. Understanding the emergence and social acceptance of electric vehicles as next-generation models for the automobile industry. *Sustainability* [online]. 2018, **10**(3), 662. ISSN 2071-1050. Available from: https://doi.org/10.3390/su10030662

[35] MOHAMED, M., HIGGINS, C. D., FERGUSON, M., REQUIA, W. J. The influence of vehicle body type in shaping behavioural intention to acquire electric vehicles: a multi-group structural equation approach. *Transportation Research Part A: Policy and Practice* [online]. 2018, **116**, p. 54-72. ISSN 0965-8564. Available from: https://doi.org/10.1016/j.tra.2018.05.011

[36] GLOBISCH, J., DUTSCHKE, E., SCHLEICH, J. Acceptance of electric passenger cars in commercial fleets. *Transportation Research Part A: Policy and Practice* [online]. 2018, 116, p. 122-129. ISSN 0965-8564. Available from: https://doi.org/10.1016/j.tra.2018.06.004

[37] WOLF, A., SEEBAUER, S. Technology adoption of electric bicycles: A survey among early adopters. *Transportation Research Part A: Policy and Practice* [online]. 2014, **69**, p. 196-211. ISSN 0965-8564. Available from: https://doi.org/10.1016/j.tra.2014.08.007

[38] KOPPLIN, C. S., BRAND, B. M., REICHENBERGER, Y. Consumer acceptance of shared e-scooters for urban and short-distance mobility. *Transportation Research Part D: Transport and Environment* [online]. 2021, **91**, 102680. ISSN 1361-9209. Available from: https://doi.org/10.1016/j.trd.2020.102680

[39] ECCARIUS, T., LU, C. C. Adoption intentions for micro-mobility - Insights from electric scooter sharing in Taiwan. *Transportation Research Part D: Transport and Environment* [online]. 2020, **84**, 102327. ISSN 1361-9209. Available from: https://doi.org/10.1016/j.trd.2020.102327

[40] BREZOVEC, P., HAMPL, N. Electric vehicles ready for breakthrough in MaaS? Consumer adoption of E-car sharing and E-scooter sharing as a part of mobility-as-a-service (MaaS). *Energies* [online]. 2021, **14**(4), 1088. eISSN 1996-1073. Available from: https://doi.org/10.3390/en14041088

[41] AHMED, W., HIZAM, S. M., SENTOSA, I., AKTER, H., YAFI, E., ALI, J. Predicting IoT service adoption towards smart mobility in Malaysia: SEM-neural hybrid pilot study. *International Journal of Advanced Computer Science and Applications* [online]. 2020, **11**(1), p. 524-535. ISSN 2158-107X, eISSN 2156-5570. Available from: https://doi.org/10.14569/IJACSA.2020.0110165

[42] GAO, L., BAI, X. A unified perspective on the factors influencing consumer acceptance of internet of things technology. *Asia Pacific Journal of Marketing and Logistics* [online]. 2014, **26**(2), p. 211-231. ISSN 1355-5855. Available from: https://doi.org/10.1108/APJML-06-2013-0061

[43] ILHAM, R., SHONHADJI, N., YUTANTO, H., EKANINGTYAS, D. Analysis of the acceptance factor of android-based parking information systems in Indonesia. *Communications - Scientific Letters of the University of Zilina* [online]. 2020, **22**(2), p. 97-106. ISSN 1335-4205, eISSN 2585-7878. Available from: https://doi.org/10.26552/com.C.2020.2.97-106

[44] NING, Y., YAN, M., XU, S. X., LI, Y., LI, L. Shared parking acceptance under perceived network externality and risks: theory and evidence. *Transportation Research Part A: Policy and Practice* [online]. 2021, **150**, p. 1-15. ISSN 0965-8564. Available from: https://doi.org/10.1016/j.tra.2021.05.009

[45] NIU, Z., HU, X., QI, S., YANG, H., WANG, S., AN, S. Determinants to parking mode alternatives: a model integrating technology acceptance model and satisfaction-loyalty model. *Transportation Research Part A: Policy and Practice* [online]. 2021, **152**(73), p. 216-234. ISSN 0965-8564. Available from: https://doi.org/10.1016/j.tra.2021.08.010

[46] PARK, E., KIM, K. J. Driver acceptance of car navigation systems: integration of locational accuracy, processing speed and service and display quality with technology acceptance model. *Personal and Ubiquitous Computing* [online]. 2014, **18**(3), p. 503-513. ISSN 1617-4909, eISSN 1617-4917. Available from: https://doi.org/10.1007/s00779-013-0670-2

[47] PARK, E., KIM, H., OHM, J. Y. Understanding driver adoption of car navigation systems using the extended technology acceptance model. *Behaviour and Information Technology* [online]. 2015, **34**(7), p. 741-751. ISSN 1362-3001, eISSN 0144-929X. Available from: https://doi.org/10.1080/0144929X.2014.963672

[48] MILANOVIC, N., MILOSAVLJEVIC, M., BENKOVIC, S., STARCEVIC, D., SPASENIC, Z. An acceptance approach for novel technologies in car insurance. *Sustainability* [online]. 2020, **12**(24), 10331. ISSN 2071-1050. Available from: https://doi.org/10.3390/su122410331

[49] VAFAEI-ZADEH, A., NG, S.-X., HANIFAH, H., TEOH, A. P., NAWASER, K. Safety technology adoption: predicting intention to use car dashcams in an emerging country. *International Journal of Innovation and Technology Management* [online]. 2021, **18**(05), 2150022. ISSN 0219-8770, eISSN 1793-6950. Available from: https://doi.org/10.1142/S021987702150022X

[50] KERVICK, A. A., HOGAN, M. J., O'HORA, D., SARMA, K. M. Testing a structural model of young driver willingness to uptake smartphone driver support systems. *Accident Analysis and Prevention* [online]. 2015, **83**, p. 171-181. ISSN 0001-4575. Available from: https://doi.org/10.1016/j.aap.2015.07.023

[51] RAHMAN, M. M., LESCH, M. F., HORREY, W. J., STRAWDERMAN, L. Assessing the utility of TAM, TPB and UTAUT for advanced driver assistance systems. *Accident Analysis and Prevention* [online]. 2017, **108**, p. 361-373. ISSN 0001-4575. Available from: https://doi.org/10.1016/j.aap.2017.09.011

[52] CHEN, C. F., CHAO, W. H. Habitual or reasoned? Using the theory of planned behavior, technology acceptance model and habit to examine switching intentions toward public transit. *Transportation Research Part F: Traffic Psychology and Behaviour* [online]. 2011, **14**(2), p. 128-137. ISSN 1369-8478. Available from: https://doi.org/10.1016/j.trf.2010.11.006

[53] DONALD, I. J., COOPER, S. R., CONCHIE, S. M. An extended theory of planned behaviour model of the psychological factors affecting commuters' transport mode use. *Journal of Environmental Psychology* [online]. 2014, **40**, p. 39-48. ISSN 0272-4944. Available from: https://doi.org/10.1016/j.jenvp.2014.03.003

[54] DI PIETRO, L., GUGLIELMETTI MUGION, R., MATTIA, G., RENZI, M. F., TONI, M. The integrated model on mobile payment acceptance (IMMPA): an empirical application to public transport. *Transportation Research Part C: Emerging Technologies* [online]. 2015, **56**, p. 463-479. ISSN 0968-090X. Available from: https://doi.org/10.1016/j.trc.2015.05.001

[55] LARUE, G. S., RAKOTONIRAINY, A., HAWORTH, N. L., DARVELL, M. Assessing driver acceptance of intelligent transport systems in the context of railway level crossings. *Transportation Research Part F: Traffic Psychology and Behaviour* [online]. 2015, **30**, p. 1-13. ISSN 1369-8478. Available from: https://doi.org/10.1016/j.trf.2015.02.003

[56] HASSN, H. A. H., ISMAIL, A., BORHAN, M. N., SYAMSUNUR, D. The impact of intelligent transport system quality: drivers' acceptance perspective. *International Journal of Technology* [online]. 2016, **7**(4), p. 553-561. ISSN 2086-9614, eISSN 2087-2100. Available from: https://doi.org/10.14716/ijtech.v7i4.2578

[57] DE ANGELIS, M., PUCHADES, V. M., FRABONI, F., PIETRANTONI, L., PRATI, G. Negative attitudes towards cyclists influence the acceptance of an in-vehicle cyclist detection system. *Transportation Research Part F: Traffic Psychology and Behaviour* [online]. 2017, **49**, p. 244-256. ISSN 1369-8478. Available from: https://doi.org/10.1016/j.trf.2017.06.021

[58] DIOP, E. B., ZHAO, S., VAN DUY, T. An extension of the technology acceptance model for understanding travelers' adoption of variable message signs. *PLoS One* [online]. 2019, **14**(4), e0216007. eISSN 1932-6203. Available from: https://doi.org/10.1371/journal.pone.0216007

[59] ALTAY, B. C., OKUMUS, A. User adoption of integrated mobility technologies: the case of multimodal trip-planning apps in Turkey. *Research in Transportation Business and Management* [online]. 2021, in press, 100706. ISSN 2210-5395. Available from: https://doi.org/10.1016/j.rtbm.2021.100706

[60] WANG, Y., WANG, S., WANG, J., WEI, J., WANG, C. An empirical study of consumers' intention to use ride-sharing services: using an extended technology acceptance model. *Transportation* [online]. 2020, **47**(1), p. 397-415. ISSN 0049-4488, eISSN 1572-9435. Available from: https://doi.org/10.1007/s11116-018-9893-4

[61] JAHANSHAHI, D., TABIBI, Z., VAN WEE, B. Factors influencing the acceptance and use of a bicycle sharing system: applying an extended unified theory of acceptance and use of technology (UTAUT). *Case Studies on Transport Policy* [online]. 2020, **8**(4), p. 1212-1223. ISSN 2213-624X. Available from: https://doi.org/10.1016/j.cstp.2020.08.002

[62] ACHEAMPONG, R. A., SIIBA, A., OKYERE, D. K., TUFFOUR, J. P. Mobility-on-demand: An empirical study of internet-based ride-hailing adoption factors, travel characteristics and mode substitution effects. *Transportation Research Part C: Emerging Technologies* [online]. 2020, **115**, 102638. ISSN 0968-090X. Available from: https://doi.org/10.1016/j.trc.2020.102638

[63] LAI, P. The literature review of technology adoption models and theories for the novelty technology. *Journal of Information Systems and Technology Management* [online]. 2017, **14**(1), p. 21-38. ISSN 1807-1775. Available from: https://doi.org/10.4301/s1807-17752017000100002

[64] TAHERDOOST, H. A review of technology acceptance and adoption models and theories. *Procedia Manufacturing* [online]. 2018, **22**, p. 960-967. ISSN 2351-9789. Available from: https://doi.org/10.1016/j.promfg.2018.03.137

[65] KIANPISHEH, A., MUSTAFFA, N., SEE, J. M. Y., KEIKHOSROKIANI, P. User behavioral intention toward using smart parking system. *Communications in Computer and Information Science*. 2011, **252**(2), p. 732-743. ISSN 1865-0929.

[66] BONGARDT, D., STILLER, L., STWAR, A., WAGNER, A. Sustainable urban transport: avoid-shift-improve (A-S-I) [online]. 2019. Available from: https://www.transformative-mobility.org/assets/publications/ASI_TUMI_SUTP_iNUA_No-9_April-2019.pdf

DEVELOPMENT OF MODE-WISE SPEED PREDICTION MODELS FOR URBAN ROADS WITH SIDE FRICTION CHARACTERISTICS

Shishodiya Ghanshyam Singh , S. Vasantha Kumar *

School of Civil Engineering, Vellore Institute of Technology (VIT), Vellore, Tamil Nadu, India

*E-mail of corresponding author: svasanthakumar1982@gmail.com, svasanthakumar@vit.ac.in

Resume

The present study has developed regression models to study the impact of side friction factors on speeds of vehicles in urban roads. The factors that were considered are on-street parking, pedestrian movement, water stagnation, encroachment, poor road condition and wrong side driving. Three locations from Vellore and Chikmagalur cities in India were selected and vehicle speeds, side friction parameters and flow were collected through videographic survey for 6 hours duration. It was found that the speeds of vehicles were in the range of only 11-23 km/h due to side friction. The study has proposed a "simple arithmetic operand" method to overcome the multicollinearity problem and it predicts well, the speeds with mean absolute percentage error (MAPE) between 8-29%. The arithmetic operand method proposed in the present study can be applied in other fields as well to overcome the multicollinearity problem.

Article info

Received 1 February 2022
Accepted 9 May 2022
Online 13 June 2022

Keywords:

side friction
vehicle speed
prediction
regression
multicollinearity
principal component regression

Available online: https://doi.org/10.26552/com.C.2022.3.E108-E121

ISSN 1335-4205 (print version)
ISSN 2585-7878 (online version)

1 Introduction

An efficient transportation system should ensure easy mobility by free flow of vehicles without any traffic congestion [1-3]. Properly maintained carriageways are essential to meet this goal as there are features on carriageway, which normally hinder the traffic flow. Popularly called as side friction in literature can be in the form of pedestrian walking on the carriageway, on-street parking, road side encroachment, bus stops, wrong movement of vehicles, etc. These side friction elements occupy some portion of the carriageway and thus result in reduction of carriageway width. This phenomenon leads to reduced capacity of the highway and poor level of service (LOS) besides affecting the speeds of vehicles. As seen in Figure 1, due to non-availability of proper sidewalk, the pedestrians are forced to walk on the carriageway and this causes the vehicles to reduce their speeds as the carriageway width has got reduced. These side frictions not only reduce the speeds of vehicles and capacity of the roads but they raise the safety concerns as well, especially for the pedestrians [4].

Studies have been carried out worldwide on the effect of side friction on vehicle speeds and they are reviewed in Table 1. It can be seen that the side friction is a common phenomenon in most of the countries, especially in the developing ones as there are studies reported from India, Indonesia, Africa etc. From the review of literature, one can figure out that the roadside friction activities such as pedestrians, bus stops, entry/exit maneuvers, wrong movement of vehicles, non-motorized traffic and on-street parking were considered mostly and their impacts on the vehicular speeds were analyzed. However, there are other side friction elements, such as water stagnation on roads owing to lack of proper drainage system, carriageway encroachment through road side shops and poor road condition due to improper maintenance. The impact of these side frictions, which likely tends to obstruct the traffic flow, has not been studied before in any of the reported studies. This was one of the main motivations aimed for carrying the present work in which each of these side frictions were taken into account and their impact was studied. One common thing, observed from Table 1, is that in many studies, statistical analysis of explanatory variables was not seriously taken into consideration. For example, R^2 and p-values were not reported in many studies. Even if the R-square was less and/or p-values were more than 0.05, but still the variables were considered and the models were used. The possible reason for not achieving the expected R^2 and p-value is due to the existence of redundancy in the form of multicollinearity

Figure 1 *Side friction on Indian roads*

Table 1 *Studies on side friction*

Sl. No	Authors	Side friction considered	Model fitting based on R^2 value*	Statistical significance of the variables based on p-values**	Whether the problem of Multicolli-nearity addressed	Country where the study was carried out
1	Biswas et al. [5]	On-street parking, Pedestrian movement and Non-motorized vehicles (NMV)	N/A	N/A	No	India
2	Alkaissi and Kamoona [6]	On-street parking, Pedestrians movement	Good	N/A	No	Iraq
3	Mahendra et al. [7]	Pedestrian movement, On-street parking, Entry/ Exit of vehicles, Slow moving vehicles	Moderate	N/A	No	Indonesia
4	Patkar and Dhamaniya [8]	Bus stops, NMV and Pedestrian movement	Good	Significant	No	India
5	Yeboah et al. [9]	Pedestrian movement	N/A	N/A	No	Ghana
6	Bitangaza and Bwire [10]	Pedestrian movement, On-street parking	Good	N/A	No	Rwanda
7	Chauhan et al. [11]	NMV, Roadside parking	N/A	N/A	No	India
8	Najid [12]	NMV, Pedestrian movement, Left-Right Access, Roadside parking	N/A	N/A	No	Indonesia
9	Hidayati et al. [13]	Pedestrian movement, Roadside parking vehicles, Entry/Exit of vehicles	N/A	N/A	No	Indonesia
10	Gulivindala and Mehar [14]	Wrong movement of vehicles, Pedestrian movement, Stopped vehicles and Entry/ Exit manoeuvre	N/A	Moderate	No	India
11	Salini et al. [15]	Bus Stops, Pedestrian movement and Roadside parking	Good	Not Significant	No	India
12	Rao et al. [16]	Pedestrian movement, Roadside parking, NMV, Entry/Exit of vehicles	Poor	Not Significant	No	India
13	Bansal et al. [17]	Bus stops	Poor	Significant	No	India
14	Chiguma [18]	Pedestrian movement, NMV, Roadside parking	Moderate	Not Significant	No	Tanzania
15	Munawar [19]	Pedestrian movement, Roadside Parking, Entry/Exit of Vehicles, Bus Stops	N/A	N/A	No	Indonesia

*R^2 value > 0.7 is Good, 0.5 - 0.7 is Moderate, < 0.5 is Poor [20]

**p- value < 0.05 means the independent variable is significant; N/A = Not Available.

in the dataset, i.e. higher inter-correlations between the two or more independent variables (IVs) in the model. However, none of the studies reviewed before have studied this multicollinearity effect and the ways to overcome it. Hence, in the present study after analyzing the conventional methods like principal component regression (PCR), a new method called "simple arithmetic operand" was proposed to remove this multicollinearity effect and achieve the desired R^2 and p-values. This was one of the main contributions of the present study, i.e. a new method to remove the multicollinearity among the independent variables, which can be applied in other fields, as well, where the multicollinearity is a potential problem while regressing the variables. The details of study area, data collection and data extraction are explained in the following section.

2 Study area

The problem of side friction can be mainly seen in cities and busy towns where the commercial activities are predominant. Hence, in the present study, a city called Vellore located in Tamil Nadu state of India and a busy town in Karnataka state of India called Chikmagalur were considered. Vellore, which has a population of around 0.5 million is one of the fast-growing cities in the state and it is considered as an important educational hub as VIT University and Christian Medical College and Hospital (CMCH) are located in Vellore. In addition, the golden temple and Vellore fort attracts large number of tourists in recent years. The other study area, called Chikmagalur, is a famous hill station in the state of Karnataka and it attracts tourists in huge amounts

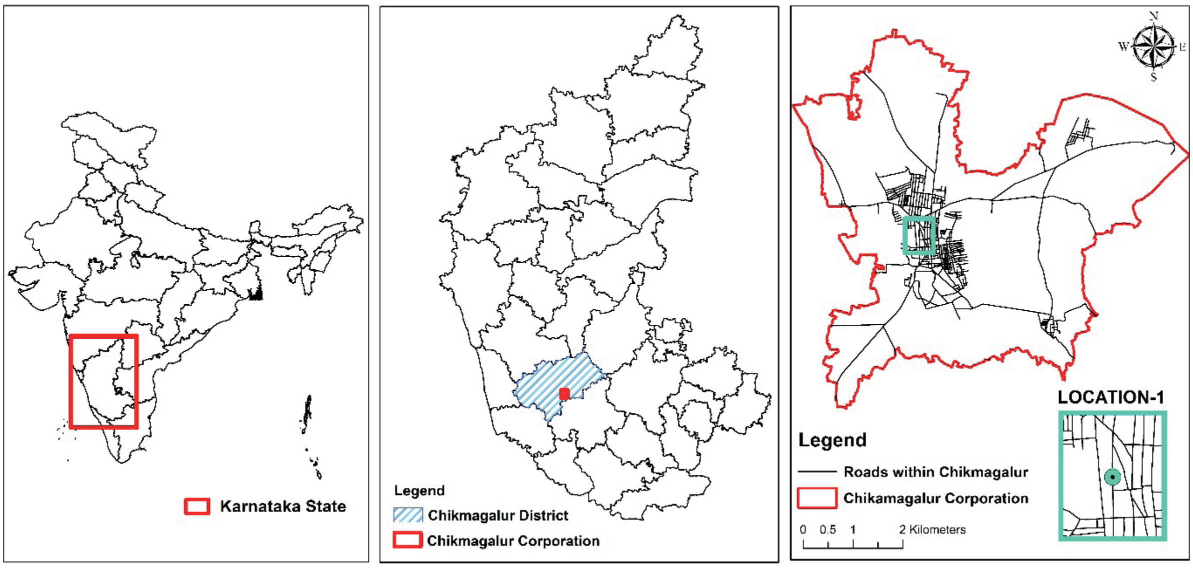

Figure 2 *Map showing the location - 1 in Chikmagalur town in Karnataka, India*

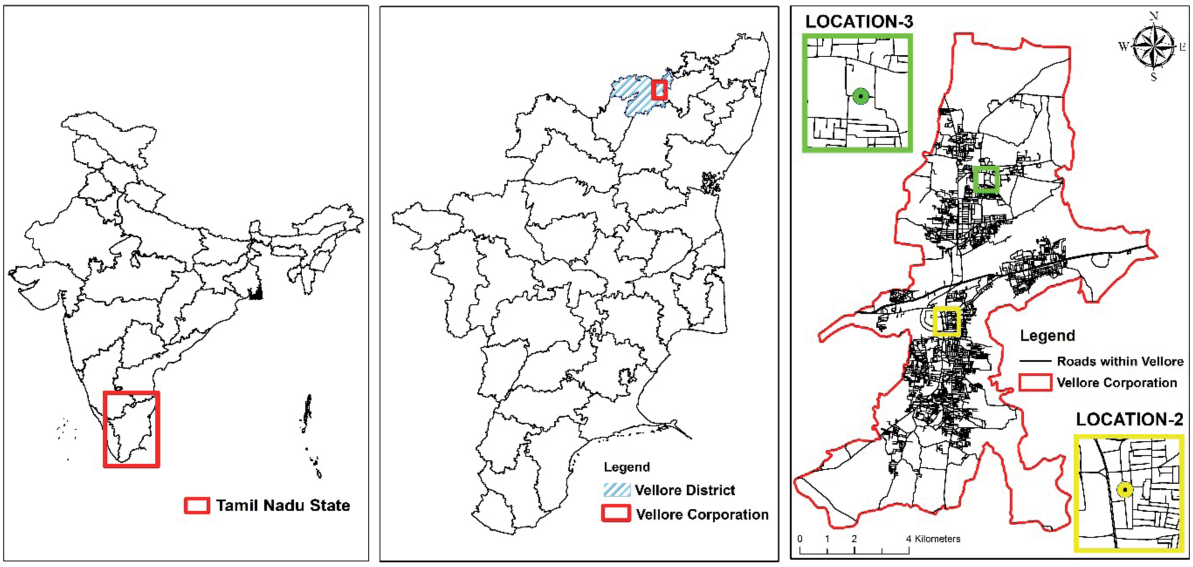

Figure 3 *Map showing the locations - 2 and 3 in Vellore city in Tamil Nadu, India*

***Table 2** Description of the study area*

Name of the study location	Nature of road	Type of side friction
Indira Gandhi (IG) Road, Chikmagalur (Location - 1)	Intermediate undivided arterial road with 10 m wide carriageway (including both directions)	Water stagnation on road, Pedestrian movement, Wrong-side driving.
Long Bazzar Road, Vellore (Location - 2)	4 lane divided road with two lanes per direction (7.5 m wide carriageway per direction)	Encroachments in the form of road-side shops, On-street parking, Pedestrian movement, Wrong-side driving.
VG Rao Nagar Road, Vellore (Location - 3)	Intermediate undivided collector street with 5.5 m wide carriageway	Poor road condition.

***Figure 4** Photos showing the study locations (a) IG road, Chikmagalur; (b) Long bazaar road, Vellore; (c) VG Rao nagar road, Vellore*

almost throughout the year. After careful investigation, three locations were selected as study stretches - one in Chikmagalur and two in Vellore. Figures 2 and 3 shows the maps of three locations selected for the present study and details of the selected locations such as nature of the road and type of the side friction are given in Table 2.

The locations were chosen in such a way that they cover the side frictions, which have not been studied before. For example, in Indira Gandhi (IG) road of Chikmagalur, water stagnation on carriageway is a major side friction, as seen in Figure 4a. It can be noticed that due to water stagnation, almost two thirds of the carriageway in one direction is not utilized, as the vehicles are not using the road space covered with water. This creates a kind of bottleneck situation where the vehicles are forced to reduce its speed when passing through this area. In addition to water stagnation, pedestrian movement on carriageway and wrong-side driving were also noticed in IG road and hence were taken into account. This IG Road is considered as the main commercial hub for the tourists coming to Chikmagalur as it contains the hotels, restaurants, shopping malls and the presence of Karnataka State Road Transport Corporation (KSRTC) bus station makes this road one of the busiest roads in Chikmagalur.

In the case of Vellore, two locations were taken, one amidst of the main inner city comprising CBD (central business district), namely the Long bazaar road, in addition to other one in a residential area called VG Rao Nagar. The study stretch in Long bazaar of Vellore is basically a four-lane divided urban arterial with dual lanes per direction of travel but presence of encroachments in the form of road-side shops and on-street parking occupied almost one whole lane in each direction, as can be seen in Figure 4b. In order to put restrictions on these encroachments, the civic authorities have constructed a median few years ago. However, this median does not serve its original purpose and encourages illegal parking as the two-wheelers have parked their vehicles on both the sides of the median, as seen in Figure 4b. As like in IG road of Chikmagalur, in Long bazaar of Vellore also pedestrians were found to walk on the carriageway and wrong side movement were observed. Hence, these two variables were considered as the side frictions in addition to the road-side encroachment and on-street parking. The two-lane collector street, located in a residential area called VG Rao Nagar, was another study stretch from Vellore. A photograph of the location is shown in Figure 4c. As seen from the photo, there is no proper road constructed with asphalt or concrete and only earthen road is available for the motorists to use. Such a poor road condition is one of the side frictions, which can be seen in interior streets of tier-2 cities in India like Vellore. Though the VG Rao Nagar comes under Vellore municipal corporation (selected for smart city mission by Government of India), the roads are very poor and act as a speed barrier for the vehicles. Such bumpy roads not only cause the vehicles to reduce their speed while passing through the section, but they cause many health-related problems, as well, like the back pain and spinal cord damage especially for the two-wheelers. These earthen roads, where thousands of vehicles plying on it every day, create a dusty environment in the entire location. All the three study stretches from Chikmagalur and Vellore are midblock sections without any intersections nearby, thus, the drop in vehicles' speeds would be mainly due to the prevailing side frictions activities.

3 Data collection and extraction

The data for all the three locations was collected using videographic method with a handycam mounted on the tripod. High rise buildings, which are just adjacent to the study stretch were chosen as the vantage points to get a clear vision of traffic stream. As traffic and side friction activities would be generally more during weekdays, the video data collection also was carried out on typical working days, i.e. 16th August 2019 (Friday), 10th February 2020 (Monday) and 5th February 2020 (Wednesday) for the locations-1, 2 and 3 respectively. As various commercial activities begin from 10 a.m. in IG road of Chikmagalur and Long Bazaar of Vellore, the vehicular and pedestrian population will also start increasing from 10 a.m. onwards. Hence, the data collection was carried out from 10 a.m. to 12 p.m. for a duration of 2 h at these two locations (1 and 2). For the study stretch in VG Rao Nagar of Vellore, the video recording was carried out for a period of 8 a.m. to 10 a.m. The reason for choosing this particular time is VG Rao Nagar is basically a residential area with many schools and colleges nearby. Hence, the educational and office trips were found to be more during this period of 8-10 a.m. and so the data collection was done during this time using a tripod mounted handycam.

The extraction of required data from video depends on variables that are going to be used in the regression model. In this study, the velocity of a specific class of vehicle has been taken as the dependent variable (DV) and the speed corresponding to other classes of the vehicles, side friction elements and flow of vehicles, were considered as independent variables (IV's). Hence, for building up the regression model, the data required are speed, side friction parameters and flow corresponding to different categories of vehicles (four wheeled, three wheeled and two wheeled). The traffic volume count (flow) was done manually by counting class-wise categories of vehicles for every 5 minutes time interval by using the recorded video. Speed of vehicles can be obtained by dividing the distance by the corresponding travel times of vehicles. In order to get the travel times, a length of 63 m, 34 m and 60 m were marked on the road at the three study locations, namely, IG Road, Long Bazaar road and VG Rao Nagar road, respectively. The video taken at the study locations was played and the travel times of vehicles to cover the above mentioned lengths were then noted down using a digital stop watch. With the known distance and time of travel, speed of vehicles was then determined. As the side frictions, namely, the water stagnation, poor road condition and encroachment were taken as categorical variables with presence or absence, there is no data required to be extracted from the video. However, the side frictions like pedestrian movement and wrong movement vehicles were calculated manually for each 5 min time interval.

4 Methodology

The present study has developed the mode-wise regression models with help of data collected from study stretches in Chikmagalur and Vellore. Since each vehicle type exhibit different speed characteristics, separate multiple linear regression equations were built corresponding to each mode. The two wheeled vehicles would generally drive fast, despite having compact space available between other modes of vehicles, due to the smaller vehicle sizes, which may not be possible with three wheeled and four wheeled vehicles. The general form of the regression models that are developed for each mode are given below.

a) The four wheeled vehicles

$$y_{FW} = \alpha_0 + \alpha_1 x_1 + \alpha_2 x_2 + \alpha_3 x_3 + \alpha_4 x_4 + \alpha_5 x_5 + \alpha_6 x_6 + \alpha_7 x_7 + \alpha_8 x_8 + \alpha_9 x_9, \quad (1)$$

where:

y_{FW} = mean speed of the four wheeled vehicles (km/h) for each 5 min. duration,

x_1 = mean speed of the three wheeled vehicles (km/h) for each 5 min. duration,

x_2 = mean speed of the two wheeled vehicles (km/h) for each 5 min. duration,

x_3 = categorical variable (1 if poor road condition, 0 otherwise),
x_4 = categorical variable (1 if road-side encroachment and on-street parking, 0 otherwise),
x_5 = number of pedestrians moving on the carriageway in each 5 min. interval,
x_6 = number of wrong-side driving vehicles in each 5 min. interval,
x_7 = number of the four wheeled vehicles (flow) observed for each 5 min. duration,
x_8 = number of the three wheeled vehicles (flow) observed for each 5 min. duration,
x_9 = number of the two wheeled vehicles (flow) observed for each 5 min. duration.

b) The three wheeled vehicles

$$y_{ThW} = \beta_0 + \beta_1 x_1 + \beta_2 x_2 + \beta_3 x_3 + \beta_4 x_4 + \beta_5 x_5 + \beta_6 x_6 + \beta_7 x_7 + \beta_8 x_8 + \beta_9 x_9, \tag{2}$$

where:
y_{ThW} = mean speed of the three wheeled vehicles (km/h) for each 5 min. duration,
x_1 = mean speed of the four wheeled vehicles in (km/h) for each 5 min. duration,
x_2 = mean speed of the two wheeled vehicles in (km/h) for each 5 min. duration.
x_3 to x_9 as defined before in Equation (1).

(c) The two wheeled vehicles

$$y_{TW} = \gamma_0 + \gamma_1 x_1 + \gamma_2 x_2 + \gamma_3 x_3 + \gamma_4 x_4 + \gamma_5 x_5 + \gamma_6 x_6 + \gamma_7 x_7 + \gamma_8 x_8 + \gamma_9 x_9, \tag{3}$$

where:
y_{TW} = mean speed of the two wheeled vehicles (km/h) for each 5 min. duration,
x_1 = mean speed of the four wheeled in (km/h) for each 5 min. duration,
x_2 = mean speed of the three wheeled in (km/h) for each 5 min. duration.

In the above equations, α_0, β_0 and γ_0 are the regression constants and α_1 to α_9, β_1 to β_9 and γ_1 to γ_9 are the regression coefficients for the independent variables of the four wheeled, three wheeled and two wheeled vehicles, respectively. The independent variables that were chosen indicate that the speed of a particular category of vehicles in a traffic stream is influenced by speeds of other vehicles, flow or volume and the available side frictions. As per traffic flow theory, for a given flow there could be two extreme cases possible one in the free-flowing state and the other one in the congested state [21]. This says that, just based on flow alone, one cannot ascertain the type of the traffic state. Hence, in the present study, while selecting the independent variables, speeds of other categories of vehicles were also taken into account in addition to flow, because for a given flow, if the traffic is free flowing, the vehicles would go at high speeds, whereas if it is congested, the speeds would be less. As seen from Figure 4, the presence of side frictions also plays a major role in speeds of vehicles. Hence, they were taken into account in the regression models, as seen from Equations (1) to (3). There are total of five side frictions, namely, poor road condition, road-side encroachment and on-street parking, water stagnation, pedestrians movement and wrong-side driving. Out of these five side frictions, the first 3 were taken as categorical variables (presence or absence) and the last 2 were taken as continuous variables. Normally in regression analysis, if there are "n" levels to represent as dummy or categorical variable, then there will be "n-1" dummy variables in the regression model [22]. In the present study, there are 3 categorical responses, which are need to be incorporated and so 2 variables were included, namely, x_3 and x_4. If both x_3 and x_4 were zero, then that indicates the water stagnation condition. A total of 720 observations for each vehicular mode were taken into account for generating the multiple linear regression equations [12 data points/h × 2 h × 3 locations × 10 variables (1 dependent variable and 9 independent variables)]. Thus, an aggregate of 2160 set of measurement points (720×3) was considered for development of all the three multiple linear regression models. While regressing the independent variables, if a specific type of roadside friction activity is absent, then it was treated to be zero. Such as, in VG Rao Nagar data, x_3 (poor road condition) was taken as 1, whereas for the other two locations, it was zero.

Once the regression models were built, the R^2 and p-values were checked to know the strength of the models developed. If R^2 is exceeding the value of 0.70 and probability value remains below 0.05, then the proposed model is reliable and it is statistically significant [20]. However, sometimes, due to the high correlation among the independent variables, popularly called as multicollinearity, the p-values of some variables may exhibit values more than 0.05. The problem with multicollinearity is that the regression coefficient estimates become imprecise and fluctuate drastically and may lead to poor predictions, as well [23-24]. Multicollinearity may result in indeterminate estimates as explained below.

The two variable case is assumed, expressed in the standardized form (subtracting mean and dividing by standard deviation).

$$y_i = \beta_0 + \beta_1 x_{1i} + \beta_2 x_{2i} \tag{4}$$

where: i (*observation*) = 1, 2, ... , n (*sample size*).

As $\overline{y} = \beta_0 + \beta_1 \overline{x_1} + \beta_2 \overline{x_2}$, Equation (4) becomes

$$\begin{aligned} y_i - \overline{y} &= \beta_0 + \beta_1 x_{1i} + \beta_2 x_{2i} - (\beta_0 + \beta_1 \overline{x_1} + \beta_2 \overline{x_2}) \\ &= \beta_1 (x_{1i} - \overline{x_1}) + \beta_2 (x_{2i} - \overline{x_2}). \end{aligned} \tag{5}$$

If one divides Equation (5) by standard deviation on both sides

$$\frac{y_i - \overline{y}}{S_y} = \left(\beta_1 \frac{S_{x1}}{S_y}\right)\frac{x_{1i} - \overline{x_1}}{S_{x1}} + \left(\beta_2 \frac{S_{x2}}{S_y}\right)\frac{x_{2i} - \overline{x_2}}{S_{x2}}. \quad (6)$$

Equation (6) can be denoted as

$$y_i{}^* = \beta_1{}^* z_1 + \beta_2{}^* z_2 , \quad (7)$$

where: $y_i{}^* = \frac{y_i - \overline{y}}{S_y}, z_{1i} = \frac{x_{1i} - \overline{x_1}}{S_{x1}}, z_{2i} = \frac{x_{2i} - \overline{x_2}}{S_{x2}}$.

Equation (7) is the standardized form of dependent and independent variables with mean zero and standard deviation one. The matrix form of Equation (7) is $Y^* = Z\beta^*$, w where:

$$Y^* = \begin{bmatrix} y_1{}^* \\ y_2{}^* \\ \cdot \\ \cdot \\ \cdot \\ y_n{}^* \end{bmatrix}, Z = \begin{bmatrix} Z_{11} & Z_{21} \\ Z_{12} & Z_{22} \\ \cdot & \cdot \\ \cdot & \cdot \\ \cdot & \cdot \\ Z_{1n} & Z_{2n} \end{bmatrix}, \beta^* = \begin{bmatrix} \beta_1{}^* \\ \beta_2{}^* \end{bmatrix}..$$

The least square estimator of β^* is

$$\beta^* = (Z'Z)^{-1} Z'Y^* = \frac{1}{(n-1)(1 - r_{z1z2}{}^2)} \times \begin{bmatrix} 1 & -r_{z1z2} \\ -r_{z1z2} & 1 \end{bmatrix} \begin{bmatrix} (n-1) r_{z1y^*} \\ (n-1) r_{z2y^*} \end{bmatrix} = \frac{1}{(1 - r_{z1z2}{}^2)} \times \begin{bmatrix} r_{z1y^*} - r_{z1z2} \cdot r_{z2y^*} \\ r_{z2y^*} - r_{z1z2} \cdot r_{z1y^*} \end{bmatrix}. \quad (8)$$

Thus, the standardized regression coefficients are

$$\beta_1{}^* = \frac{r_{z1y^*} - r_{z1z2} \cdot r_{z2y^*}}{1 - r_{z1z2}{}^2}, \quad (9)$$

$$\beta_2{}^* = \frac{r_{z2y^*} - r_{z1z2} \cdot r_{z1y^*}}{1 - r_{z1z2}{}^2}, \quad (10)$$

where, r_{z1y^*} is the correlation coefficient between z_1 and y^*, r_{z2y^*} is the correlation coefficient between z_2 and y^* and r_{z1z2} is the correlation coefficient between z_1 and z_2. $\beta_1{}^*$ and $\beta_2{}^*$ can also be obtained directly using $\beta_1 \frac{S_{x1}}{S_y}$ and $\beta_2 \frac{S_{x2}}{S_y}$ respectively as seen in Equations (6) and (7). From Equations (9) and (10), can be seen that, if the independent variables are highly correlated, $|r_{z1z2}| \to 1$, what would result in poor estimates of $\beta_1{}^*$ and $\beta_2{}^*$ as denominators in Equations (9) and (10) would approach zero. In addition, the variances $Var\beta^* = (Z'Z)^{-1}\sigma^2$ will become very large and approach ∞ when $|r_{z1z2}| \to 1$. Such large variances imply the poor and indeterminate estimates of the regression coefficients. Hence, if there exists highly correlated variables with one another in a regression model, multicollinearity pose a serious issue that has to be estimated for accuracy of the models.

Detection of multicollinearity can be achieved by calculating "tolerance" for each independent variable. Tolerance is computed by subtracting R^2 from 1. HereR^2 is obtained by regressing an independent variable over the remaining IV's. Whenever the least correlation exists between considered IV's, it indicates R^2 to be small and, thus, the tolerance become large. On the other hand, if strong correlation is found among the independent variables, R^2 would be high and the tolerance would be low. Thus, the terms tolerance and multicollinearity are inversely proportional to each other. In general, any tolerance value less than 0.2 indicates the presence of high degree of multicollinearity in the dataset used for model development [25-26]. Hence, the tolerance value of 0.2 was considered as a benchmark for indicating the existence or non-existence of multicollinearity in the dataset for the present study also. If the multicollinearity is detected, methods like principal component regression (PCR) can be done to remove the multicollinearity. In the present study, a new method, called "simple arithmetic operand" method, was proposed by defining a new set of independent variables obtained by adding, subtracting, multiplying or dividing the existing independent variables. Both the PCR and the proposed method were evaluated for its statistical significance by checking the R^2, p-values and tolerance. The model was then validated by taking only 75% of the data and predicting for the remaining 25% data. Predicted speeds were then checked with the observed speeds for similarity and the accuracy of prediction was reported through one of the popular error measures called "Mean Absolute Percentage Error (MAPE)". The reason for choosing MAPE is that it has many advantages when compared to other error measures, such as mean absolute error (MAE) or root mean squared error (RMSE). For example, MAPE is scale independent, whereas the other two error measures are scale dependent, i.e. they depend on the range of the target variable and hence cannot be compared across the datasets. As the present study compares the performance of the mode-wise regression models, it would be advantageous if one uses MAPE rather than MAE or RMSE. In addition, if the value of MAPE is below 10%, then prediction can be considered excellent, 10-20% is considered good and if MAPE ranges between 20-50% then its reasonable, whereas MAPE exceeding more than 50% is unacceptable [27-28]. Thus, based on MAPE, one can ascertain how good the prediction results are, which may not be possible with MAE or RMSE. Results are discussed in the following section.

5 Results and discussion

In this section, the findings were presented in two parts. The first part explains the basic descriptive statistics for the collected data. The second part deals with development of multiple linear regression model, treatment for multicollinearity, which is then

***Table 3** Descriptive statistics*

	Indira Gandhi (IG) road, Chikmagalur			
	Mean	Std. Dev.	Min.	Max.
Mean speed of the four wheeled vehicles	15.11	2.31	9.43	19.34
Mean speed of the three wheeled vehicles	17.47	2.74	10.61	22.29
Mean speed of the two wheeled vehicles	21.37	1.01	19.7	23.26
Number of pedestrians (x_5)	49.38	11.5	32	77
Wrong-side driving (x_6)	16.33	3.76	10	24
Number of the four wheeled vehicles (x_7)	52.33	10.01	33	78
Number of the three wheeled vehicles (x_8)	33.92	4.56	25	42
Number of the two wheeled vehicles (x_9)	84.46	9.94	67	103
	Long bazzar road, Vellore			
	Mean	Std. Dev.	Min.	Max.
Mean speed of the four wheeled vehicles	2.67	4	0	10.68
Mean speed of the three wheeled vehicles	10.6	1.85	7.99	14.85
Mean speed of the two wheeled vehicles	16.5	3.05	11.31	21.89
Number of pedestrians (x_5)	72.42	12.84	46	97
Wrong-side driving (x_6)	27.92	7.57	10	44
Number of the four wheeled vehicles (x_7)	0.96	1	0	3
Number of the three wheeled vehicles (x_8)	6.88	2.64	3	13
Number of the two wheeled vehicles (x_9)	44.83	10.13	27	63
	VG Rao nagar road, Vellore			
	Mean	Std. Dev.	Min.	Max.
Mean speed of the four wheeled vehicles	9.3	1.17	7.35	11.97
Mean speed of the three wheeled vehicles	5.76	5.08	0	12.67
Mean speed of the two wheeled vehicles	13.66	1.07	11.95	16.03
Number of pedestrians (x_5)	0	0	0	0
Wrong-side driving (x_6)	0	0	0	0
Number of the four wheeled vehicles (x_7)	5.88	2.82	1	13
Number of the three wheeled vehicles (x_8)	1.42	1.64	0	5
Number of the two wheeled vehicles (x_9)	32.83	7.8	20	48

followed by validation of the developed model.

5.1 Descriptive statistics

The statistics, like mean, standard deviation (SD), minimum and maximum values, were calculated location-wise for the speed, flow and side friction data collected and the results are shown in Table 3. The categorical variables x_3 and x_4 were not considered for calculation of descriptive statistics, as they take the values of 0 or 1. Many interesting results can be obtained by looking into Table 3. Overall, the two-wheeled vehicles speeds were high when compared to that of other vehicle categories in all the 3 locations considered. As said before, the two-wheeler being the smallest vehicle in terms of size, possesses the ability to freely maneuver between the large seized vehicles and, hence, the average speed is high when compared to others. Due to this phenomenon, the two-wheelers did not exhibit completely stopped condition ("zero" speed) in any of locations, whereas other vehicles have stopped completely and reported zero speed under the "minimum speed" category as seen from Table 3. One can notice in Table 3 that the maximum speed ranges between 19-23 km/h, 11-22 km/h and 12-16 km/h, for IG road, Long bazaar road and VG Rao nagar road, respectively. Though the central government has raised the speed limits of cars and two-wheelers in Indian cities to 70 km/h and 50 km/h respectively [29], however the maximum speeds of cars and two-wheelers were found to be only 19 km/h and 23 km/h, respectively, as seen from Table 3. This is mainly due to the presence of different side frictions on the urban roads and unless they are removed it is difficult to achieve increment in the speed of vehicles in India. The results suggest that the minimum, maximum and average speed of vehicles were different for different vehicle categories and this clearly indicates the need for the mode-wise speed prediction models as attempted in the present study.

Table 4 *Results of the mode-wise regression models*

	Four wheeled (R^2 = 0.815)			Three wheeled (R^2 = 0.720)			Two wheeled (R^2 = 0.811)		
Variable	Reg. Coeff. value	p value	Tolerance	Reg. Coeff. value	p value	Tolerance	Reg. Coeff. value	p value	Tolerance
Intercept	35.494	1.84E-05	-	-0.672	0.952	-	28.106	6.05E-08	-
x_1	0.008	0.936	0.280	0.012	0.936	0.184	-0.055	0.500	0.185
x_2	-0.131	0.500	0.189	0.578	0.016	0.206	0.154	0.016	0.307
x_3	-21.041	0.000	0.014	-1.321	0.865	0.011	-13.997	0.000	0.014
x_4	-21.829	6E-06	0.022	1.840	0.780	0.016	-7.673	0.021	0.017
x_5	-0.007	0.831	0.072	0.0009	0.984	0.072	-0.067	0.003	0.082
x_6	-0.114	0.104	0.131	-0.057	0.520	0.127	0.034	0.460	0.127
x_7	-0.045	0.407	0.058	-0.045	0.515	0.057	-0.018	0.600	0.057
x_8	-0.165	0.129	0.039	0.292	0.032	0.041	-0.099	0.165	0.039
x_9	-0.088	0.016	0.135	-0.012	0.790	0.123	-0.017	0.480	0.123

"-" implies not applicable

From the descriptive statistics was found that, though the Long bazaar road of Vellore has bigger carriageway width, compared to the IG road, the average speeds of vehicles were smaller than those of IG road. The possible reason for that is presence of the side friction activities in the form of roadside shops and on-street parking in the Long bazaar road, as seen in Figure 4b. When the effective carriageway width available at Long bazaar was measured using the tape, it was shocking to notice that out of 7.5 m carriageway, only 2.74 m was available for vehicles to go. The remaining portion was completely encroached by the side friction activities and this may be the reason for lower speeds in the Long bazaar road. The average speed of the four wheelers was found to be only 2.67 km/h in Long bazaar, which is far less when compared to other locations' four-wheelers speeds. The possible reason for this is that the Long bazaar is a market area where more pedestrians walk on the carriageway due to absence of proper footpath. This has been shown in Table 3 where the pedestrian count was higher (72 pedestrians/5 min) in the Long bazaar than in any other location. In such a scenario, considering the pedestrians' safety, the drivers of the four-wheelers are forced to reduce their speed drastically, as the pedestrians walk on the carriageway. The results indicate the need for proper sidewalks also in locations where there are pedestrian activities, in addition to removal of side frictions like the on-street parking and roadside shops.

5.2 Development of the speed prediction models

Table 4 shows the multiple linear regression model results obtained for all the modes (four wheeled, three wheeled and two wheeled vehicles). It includes the coefficient of determination (R^2), estimated regression coefficients, p-value for each of the independent variables, as well as the tolerance values. It was found that R^2 was good as it is more than 0.7 in all the three modes. In addition, the signs of the coefficients were logical as most of the side friction and flow variables exhibited negative sign. For example, the negative coefficients of categorical variables x_3 and x_4 indicate that if the road is poor in condition or encroached by the road-side shops with on-street parking or water stagnation is there, then speeds will get reduced. Similarly, if the flow is increasing then speeds of vehicles would get reduced. Though the developed mode-wise regression models have good R^2 values and logical signs, however the explanatory variables are not statistically significant, as most of the coefficients have p-values more than 0.05, as seen from Table 4. In addition, the tolerance was found to be less than 0.2 in 24 out of 27 tolerance values calculated and this indicates the presence of multicollinearity in the given dataset. It is logical to expect multicollinearity, i.e. correlation among the independent variables because if there are road-side shops, it may attract people to purchase the goods, which in turn leads to gathering of people, on-street parking and pedestrian movement and finally leading to reduction of vehicles speed in that road stretch.

In order to break the multicollinearity between the independent variables in the model, the conventional approach is to use methods like principal component regression (PCR) or ridge regression. In this study, the PCR was used to check whether it can remove the multicollinearity or not. The PCR involves basically the conversion of given data of independent and dependent variables to standardized form and then calculating the covariance matrix. The covariance matrix was then used to calculate the eigen values and vectors, which were then used to calculate the principal components. The results of the PCR, done using NCSS 2020 statistical software [30], is shown in Table 5. As before, the R^2 values were good as they are more than 0.7 for all the three models. Since some degree of bias is added to the regression estimates in the PCR, it is not meaningful

Table 5 *Results of mode-wise regression models developed using PCR*

	Four wheeled (R^2 = 0.762)			Three wheeled (R^2 = 0.719)			Two wheeled (R^2 = 0.781)		
Variable	Reg. Coeff. value	p value	Tolerance	Reg. Coeff. Value	p value	Toleance	Reg. Coeff. value	p value	Tolerance
Intercept	6.139	-	-	1.876	-	-	14.509	-	-
x_1	-0.007	0.949	0.280	-0.006	0.962	0.244	0.075	0.326	0.249
x_2	0.206	0.305	0.228	0.555	0.011	0.247	0.173	0.011	0.310
x_3	1.323	0.466	0.174	-3.145	0.136	0.162	-3.251	0.010	0.143
x_4	-5.480	0.026	0.097	0.371	0.889	0.099	1.798	0.196	0.115
x_5	0.018	0.661	0.074	-0.0007	0.988	0.073	-0.069	0.005	0.082
x_6	-0.064	0.413	0.135	-0.063	0.469	0.135	0.077	0.108	0.139
x_7	0.055	0.317	0.071	-0.052	0.398	0.071	0.032	0.348	0.072
x_8	0.152	0.087	0.077	0.269	0.006	0.081	0.052	0.349	0.073
x_9	-0.041	0.288	0.149	-0.017	0.685	0.148	0.014	0.535	0.150

Table 6 *Results of multiple linear regression model developed using simple arithmetic operand method*

Variable	p value	Tolerance
	Four wheeled (R^2 = 0.702)	
Intercept	7.03E-21	N/A
Variable-1	0.000	0.349
Variable-2	1.74E-05	0.712
Variable-3	0.014	0.354
	Three wheeled (R^2 = 0.700)	
Intercept	4.39E-05	N/A
Variable-1	1.13E-06	0.623
Variable-2	0.013	0.505
Variable-3	0.016	0.400
	Two wheeled (R^2 = 0.707)	
Intercept	1.96E-18	N/A
Variable-1	0.009	0.258
Variable-2	0.006	0.923
Variable-3	0.014	0.248

to infer the statistical significance based on the t-stat (coefficient divided by standard error) and p-value for PCR models [31]. However, the tolerance must be more than 0.2 for all the variables to ensure that the multicollinearity is removed. However, results in Table 5 show that tolerance was less than 0.2 for majority of the variables and this clearly indicates that the PCR failed to remove the multicollinearity in the dataset. The present study tried a new method called "simple arithmetic operand" to remove the multicollinearity, which is explained below.

The proposed approach, named as "simple arithmetic operand" is quite simple and straightforward, as the name suggests. Because in this method, the independent variables were added, differenced or ratioed to create new variables, until the desired results were achieved, i.e. R^2 exceeding 0.70, p values of new IV's (independent variables) less than 0.05 accompanied by tolerance of more than 0.2. While developing the regression model using the proposed approach, 75% of the data were used so that the remaining 25% can be used for validation. The developed models are shown below in Equations (11)-(13).

a) Four wheeled vehicles

$$y_{FW} = 14.210 + 4.530\underbrace{[(x_1/x_2) - (x_3 + x_4)]}_{\text{Variable} - 1} - 0.061\underbrace{[(x_5 + x_6)]}_{\text{Variable} - 2} + 0.098\underbrace{[(x_7) + (x_8 - x_9)]}_{\text{Variable} - 3}. \quad (11)$$

b) Three wheeled vehicles

$$y_{ThW} = -8.722 + 0.452[(x_1 + x_2) + (x_3 + x_4)] + 0.041[(x_5 + x_6)] - 0.099[(x_7 - x_9) - (x_8)]. \quad (12)$$

(c) Two wheeled vehicles

$$y_{TW} = 10.425 + 0.157[(x_1 + x_2) - (x_3 + x_4)] + 0.020[(x_5 + x_6)] + 0.024[(x_7) + (x_8 + x_9)]. \quad (13)$$

It can be seen from Equations (11)-(13) that the regression model has been reduced from 9 variables to 3 variables, by adding, subtracting or ratioing the given independent variables. Sometimes, the combinations were applied, as well. For example, x_3 and x_4 were added and subtracted from the ratio of x_1 and x_2. As seen from Table 6, R^2 values were 0.7 and above, p-values were less than 0.05 and tolerance values were above 0.2. Tolerance of above 0.2 indicates that the proposed approach has removed the multicollinearity, which was not possible with the conventional methods like the PCR. The proposed approach is simple, does not require any specialized softwares like NCSS and produces the desired results finally. In addition, no independent variables were dropped as seen from Equations (11)-(13). Thus, with the proposed approach no variables are missing. The only limitation with this approach is that it involves the "trial and error" practice, that is done manually until the expected results are obtained. If a separate tool is developed in MSEXCEL to automate this trial-and-error procedure, then there will be no limitation for this method.

With the aim of validating the potential of the developed model in forecasting the mode wise vehicular speeds, the remaining 25% data were used for comparing the actual/observed speeds with the predicted ones. The results shown in Figure 5 clearly exhibit the similar trend of observed speed to that of the predicted speed. In addition, R^2 was greater than 0.7 for all the three modes, which says that the results were acceptable. The MAPE calculated between actual and predicted were 17.26%, 29.60% and 8.23% for the four wheeled, three wheeled and two wheeled vehicles respectively. Generally, the value of MAPE below 10% is considered to be excellent, 10-20% termed as good and a range of 20-50% is considered to be reasonable, but any value exceeding more than 50% is unacceptable [27- 28]. With the obtained results, one can draw a conclusion that the prediction accuracy is excellent in the case of the two wheeled vehicles, good for the four wheeled and reasonable for the three wheeled vehicles.

In Figure 5 was noticed that the predicted and observed values were in good agreement for the two wheeled and four wheeled vehicles, whereas for the three wheeled vehicles, the predicted speeds were lower than the actual ones. The possible reason for this could be that the three-wheelers include the normal autos and the shared type autos both of which have different characteristics in terms of its size, as well as operation.

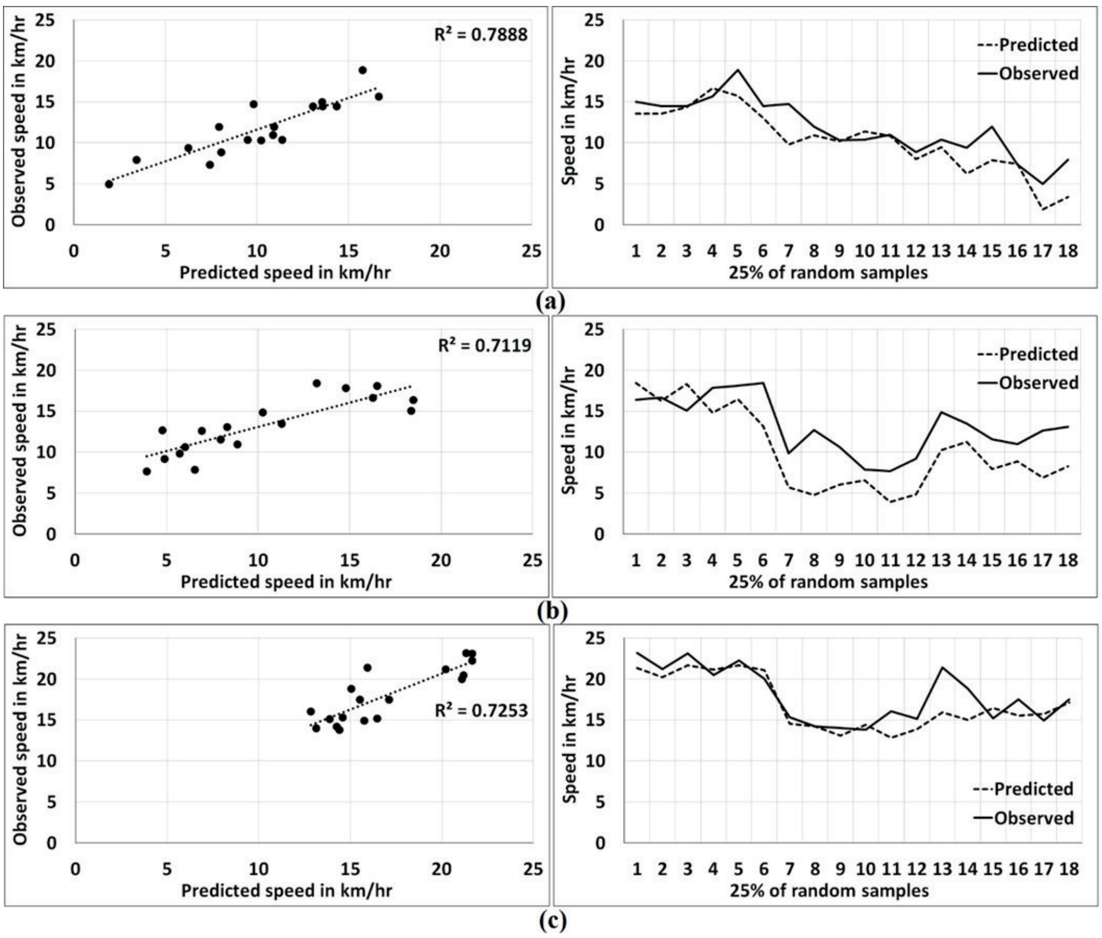

Figure 5 *Observed vs. Predicted Speed for (a) Four wheeled (b) Three wheeled (c) Two wheeled vehicles*

In addition, the normal autos were only present in Chikmagalur, whereas the shared type autos were counted more in Vellore. In model development, both types of autos have considered as one class and the data from all the locations were combined to develop the regression model. Perhaps it may likely to be the probable cause for three wheeled vehicles alone to exhibit slightly higher range of MAPE when compared to other modes. Overall, the MAPE and R^2 are within the acceptable limits for the all the three modes and, hence, the developed models could be considered for predicting the mode-wise speeds using speed corresponding to other vehicular classes, side friction activities data and traffic volume count.

6 Concluding remarks

One of the important factors that causes reduction in speed of vehicles on urban roads of India is the side friction. The carriageway, which is meant for vehicles to go has not been utilized properly for the purpose for which it has been constructed, because of these side frictions. Studies on investigating the impact of side frictions on vehicular speeds have been mostly focused on common type of roadside frictional activities like curb side bus stops, on-road parking, movement of pedestrians, etc. However, there are other side frictions like water stagnation, road-side shops and poor road condition, which are not studied before. Present study attempted this by collecting data from cities like Vellore and Chikmagalur in India and developed mode-wise speed prediction models using the regression analysis. One of the main highlights of the present study is that it has proposed a method to remove the multicollinearity, which is a common problem in the regression analysis. Even the popular methods, like the PCR, failed to remove multicollinearity in the dataset. However, the simple arithmetic operand method proposed in this study performs well, as it finally results in a model with only few variables, good R^2, low p-values and acceptable tolerance values. The mode-wise regression models, developed using the simple arithmetic operand method, were found to predict well the speeds of various categories of vehicles if the side friction and other causative variables are given as inputs. The arithmetic operand method that has been proposed in the present study can be applied in other fields, as well, to overcome the multicollinearity problem. The main limitation of the present study is that the traffic and side friction data were collected during the peak hours on selected working days. If one collects the data during the off-peak hours or weekends, the results may be slightly different as the impact of the side friction would be minimum during those times. Again, it depends on which side friction one considers, for example, poor road condition will not change on a weekday or weekend, whereas the on-street parking would be high during the weekdays when compared to weekends. Another limitation is that the present study considered cars, light commercial vehicles (LCVs) and buses under "four-wheelers" category, while extracting the flow data. If one considers them as separate classes, it may be possible to see how the speeds of those four-wheeled vehicle categories are influenced by different side frictions, which is the future scope of the present work.

References

[1] SOLTESZ, T., KOZEL, M., CSISZAR, C., CENTGRAF, T., BENYO, B. Information system for road infrastructure booking. *Periodica Polytechnic Transportation Engineering* [online]. 2011, **39**(2), p. 55-62. ISSN 0303-7800, eISSN 1587-3811. Available from: https://doi.org/10.3311/pp.tr.2011-2.02

[2] BALAKRISHNAN, S., SIVANANDAN, R. Influence of lane and vehicle subclass on free-flow speeds for urban roads in heterogeneous traffic. *Transportation Research Procedia* [online]. 2015, **10**, p. 166-175. ISSN 2352-1465. Available from: https://doi.org/10.1016/j.trpro.2015.09.066

[3] SILVA, D., FOLDES, D., CSISZAR, C. Autonomous vehicle use and urban space transformation: a scenario building and analysing method. *Sustainability* [online]. 2021, **13**(6), 3008. ISSN 2071-1050. Available from: https://doi.org/10.3390/su13063008

[4] ANIS, S., CSISZAR, C. Management of potential conflicts between pedestrians and autonomous vehicles. In: IEEE Smart City Symposium Prague SCSP 2019: proceedings [online]. 2019. ISBN 978-1-7281-0498-0, eISBN 978-1-7281-0497-3, p.1-6. Available from: https://doi.org/10.1109/SCSP.2019.8805678

[5] BISWAS, S., CHANDRA, S., GHOSH, I. Side friction parameters and their influences on capacity of Indian undivided urban streets. *International Journal of Transportation Science and Technology* [online]. 2021, **10**(1), p. 1-19. ISSN: 2046-0430. Available from: https://doi.org/10.1016/j.ijtst.2020.03.007

[6] ALKAISSI, Z., KAMOONA, W. Influence of roadside impedance on speed and capacity of urban streets. *IOP Conference Series: Materials Science and Engineering* [online]. 2021, **1090**, p. 1-13. ISSN 1757-8981, eISSN 1757-899X. Available from: https://doi:10.1088/1757-899X/1090/1/012121

[7] MAHENDRA, M., WICAKSONO, A., DJAKFAR, L. The effect of side friction on delays in one-way urban road sections. *Journal of Southwest Jiaotong University* [online]. 2021, **56**(5), p. 265- 274. ISSN 0258-2724. Available from: https://doi: 10.35741/issn.0258-2724.56.5.24

[8] PATKAR, M., DHAMANIYA, A. Influence of nonmotorized vehicles on speed characteristics and capacity of mixed motorized traffic of urban arterial midblock sections. *Journal of Transportation Engineering, Part A: Systems* [online]. 2020, **146**(4), p. 1-11. ISSN 2473-2907, eISSN 2473-2893. Available from: https://doi.org/10.1061/JTEPBS.0000325

[9] YEBOAH, A., AMOAH, A., KOVE, M. Analysis of congestion on some road link sections using roadside friction in congestion index in Kumasi. *International Journal for Traffic and Transport Engineering* [online]. 2020, **10**(1), p. 31-40. ISSN 2217-544X, eISSN 2217-5652. Available from: http://dx.doi.org/10.7708/ijtte.2020.10(1).03

[10] BITANGAZA, M., BWIRE, H. Effects of roadside friction elements on travel performance and level of service in Kigali. *International Journal for Traffic and Transport Engineering* [online]. 2020, **10**(2), p. 236-251. ISSN 2217-544X, eISSN 2217-5652. Available from: http://dx.doi.org/10.7708/ijtte.2020.10(2).09

[11] CHAUHAN, R., DHAMANIYA, A., ARKATKAR, S., SAHU, P. K., VIKRAM, D. Effect of side friction parameter on urban road traffic: under mixed traffic scenario. *Journal of the Eastern Asia Society for Transportation Studies* [online]. 2019, **13**, p. 314-330. eISSN 1881-1124. Available from: https://doi.org/10.11175/easts.13.314

[12] NAJID. Evaluation of side friction in IHCM for highway two lanes two ways. In: 2nd International Symposium on Transportation Studies in Developing Countries ISTSDC 2019: proceedings [online]. Vol. 193. Advances in Engineering Research. 2019. ISBN 978-94-6252-913-7, p. 116-119. Available from: https://doi.org/10.2991/aer.k.200220.024

[13] HIDAYATI, N., SUNARJONO, S., AWAD, S., MAGFIRONA, A. Different impact of side friction condition on traffic flow along Yosodipuro street Surakarta. *AIP Conference Proceedings* [online]. 2019, **2114**(1), 040011. ISSN 0094-243X, eISSN 1551-7616. Available from: https://doi.org/10.1063/1.5112440

[14] GULIVINDALA, P., MEHAR, A. Analysis of side friction on urban arterials. *Transport and Telecommunication* [online]. 2018, **19**(1), p. 21-30. eISSN 1407-6179. Available from: https://doi.org/10.2478/ttj-2018-0003

[15] SALINI, S., GEORGE, S., ASHALATHA, R. Effect of side frictions on traffic characteristics of urban arterials. *Transportation Research Procedia* [online]. 2016, **17**, p. 636-643. ISSN 2352-1465. Available from: https://doi.org/10.1016/j.trpro.2016.11.118

[16] RAO, A. M., RAO, K. R. Free speed modelling for urban arterials - a case study on Delhi. *Periodica Polytechnica Transportation Engineering* [online]. 2015, **43**(3), p. 111-119. ISSN 0303-7800, eISSN 1587-3811. Available from: https://doi.org/10.3311/PPtr.7599

[17] BANSAL, P., AGRAWAL, R., TIWARI, G. Impacts of bus-stops on the speed of motorized vehicles under heterogeneous traffic conditions: a case-study of Delhi, India. *International Journal of Transportation Science and Technology* [online]. 2014, **3**(2), p. 167-178. eISSN 2046-0430. Available from: https://doi.org/10.1260/2046-0430.3.2.167

[18] CHIGUMA, M. Analysis of side friction impacts on urban road link-case study, Dar-Es-Salaam. Doctoral thesis in traffic and transport planning. infrastructure and planning. Sweden: Royal Institute of Technology Stockholm, 2007. ISBN 978-91-85539-17-8.

[19] MUNAWAR, A. Speed and capacity for urban roads, Indonesian experience. *Procedia - Social and Behavioral Sciences* [online]. 2011, **16**, p. 382-387. eISSN 1877-0428. Available from: https://doi.org/10.1016/j.sbspro.2011.04.459

[20] MOORE, D., NOTZ, W., FLIGNER, M. *The basic practice of statistics*. 7. ed. New York, USA: W. H. Freeman, 2015. ISBN 978-1464142536.

[21] ROESS, R. P., PRASSAS, E. S., MCSHANE, W. R. *Traffic engineering*. 5. ed. London, UK: Pearson Education; 2019. ISBN 9780134599717.

[22] DEVORE, J. L. *Probability and statistics for engineering and the sciences*. 9. ed. Boston, USA: Brooks/Cole Cengage Learning, 2010. ISBN 978-0-538-73352-6.

[23] MONTGOMERY, D. C., RUNGER, G. C. *Applied statistics and probability for engineers*. 6. ed. New York, USA: John Wiley and Sons, Inc., 2016. ISBN 9788126562947.

[24] LEVINE, D. M., STEPHAN, D. F., SZABAT, K. A. *Statistics for managers using microsoft excel*. 8. ed. London, UK: Pearson Education Limited, 2016. ISBN 0134173058.

[25] KIM, J. H. Multicollinearity and misleading statistical results. *Korean Journal of Anaesthesiology* [online]. 2019, **72**(6), p. 558-569. ISSN 2005-6419, eISSN 2005-7563. Available from: https://doi.org/10.4097/kja.19087

[26] WEISBURD, D., BRITT, C. *Statistics in criminal justice*. New York, USA: Springer, 2014. ISBN 9781461491699.

[27] KUMAR, S. V., VANAJAKSHI, L. Short-term traffic flow prediction using seasonal ARIMA model with limited input data. *European Transport Research Review* [online]. 2015, **7**(21), p. 1-9. eISSN 1866-8887. Available from: https://doi.org/10.1007/s12544-015-0170-8

[28] BHARADWAJ, N., KUMAR, P., ARKATKAR, S., MAURYA, A., JOSHI, G. Traffic data analysis using image processing technique on Delhi-Gurgaon expressway. *Current Science* [online]. 2016, **110**(5), p. 808-822. ISSN 0011-3891. Available from: https://doi.org/10.18520/cs/v110/i5/808-822

[29] The Times of India. It's legal now: cars allowed to go up to 70 km/h in cities [online]. 2018. Available from: https://timesofindia.indiatimes.com/india/its-legal-now-cars-allowed-to-go-up-to-70km/h-in-cities/articleshow/63308093.cms

[30] Statistical Software - NCSS [online]. 2020. Available from: ncss.com/software/ncss

[31] Statistical software. Principal components regression. Chapter 340 - NCSS [online]. 2020. Available from: https://www.ncss.com/wp-content/themes/ncss/pdf/Procedures/NCSS/ Principal_Components_Regression.pdf

ANALYSIS AND EVALUATION OF THE EFFECTIVENESS OF SAFETY SYSTEMS AT RAILROAD CROSSINGS IN POLAND

Piotr Gorzelańczyk [1,*], Aleksandra Borkowska [1], Pawel Szubert [1], Tomáš Kalina [2], Martin Jurkovič [2]

[1]Stanislaw Staszic University of Applied Sciences in Pila, Pila, Poland
[2]Department of Water Transport, Faculty of Operation and Economics of Transport and Communications, University of Zilina, Zilina, Slovak Republic

*E-mail of corresponding author: piotr.gorzelanczyk@puss.pila.pl

Resume

The number of vehicles on the road is growing every year and each year too many people lose their lives and health on Polish roads. The number of accidents, including at level crossings, is very high. Despite the construction of new, safer roads, the number of collisions continues to grow and about three thousand accident participants die each year. The main causes of accidents are inadequate speed to the prevailing road conditions or regulations, driving under the influence of alcohol and random events. For this reason, the article analyzes the safety at railroad crossings in Poland. In the next stage, an exemplary system improving safety at railroad crossings is presented. The new solution was analysed using a survey. The research results presented may be applicable to other countries.

Article info

Received 13 October 2021
Accepted 7 December 2021
Online 25 March 2022

Keywords:

railway infrastructure
train
railroad crossing
safety
railway

Available online: https://doi.org/10.26552/com.C.2022.3.F46-F61

ISSN 1335-4205 (print version)
ISSN 2585-7878 (online version)

1 Introduction

Railroad crossings are a very characteristic element of the railway infrastructure because two types of traffic flows (road and rail) intersect here. Due to the steady increase in traffic, the frequency of crossings is also increasing, which increases the likelihood of accidents at level crossings.

Safety is undoubtedly a very important element in the life of every human being. For years, it has been a specific object against which statistical research or various types of analyzes are conducted. Their aim is to increase the comfort in the sphere of safety of all the road users. The problem of accidents at level crossings is repeatedly mentioned on the radio and television. Social media also touches on this topic in order to reach the largest possible audience. This is to make people of all ages aware of the risk of carelessness and lack of concentration when approaching the railway crossings. However, it should be remembered that the safety itself at the railroad crossings depends mainly on behavior of the road users, as well as on the proper performance of tasks by rail and road infrastructure managers [1].

A sense of security is an integral part of the daily life of public transport users. There are many definitions of safety in the literature. One of them defines it as freedom from all the threats and such freedom of action in which we do not feel threatened [2]. There are many accidents at level crossings every year. The causes of accidents can be very different, they can be dependent on weather conditions or simply the carelessness of road users.

Safe road travel means following a number of established rules and regulations that should not be taken lightly [3]. The improvement of road safety is influenced by many elements related not only to the promotion of correct behavior among drivers [4-6], but to the proper organization of traffic, the appropriate technical condition of roads and vehicles, as well [7-11]. Training and examinations for future drivers are equally important. Road safety is a research field covering not only the above-mentioned aspects, as well as issues related to traffic supervision, emergency medical services and transport psychology [10]; road traffic safety in the analyzed city [12]; problems with the course of the procedure related to the proceeding of inflows in the first publication of [13-20].

Some publications focus on assessing the safety of level crossings in terms of detection and monitoring [21-22], others address safety using ultrasound and wireless

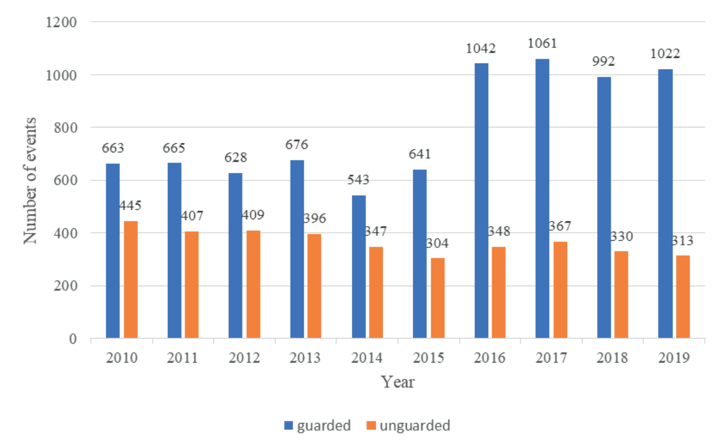

Figure 1 *Number of incidents at guarded and unguarded railroad crossings in Poland in 2010-2019 [35]*

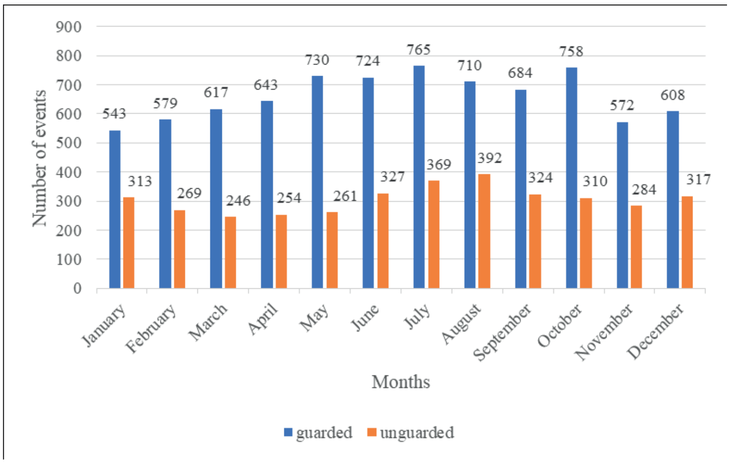

Figure 2 *The average number of incidents in individual months on guarded and unguarded level crossings in Poland in 2010-2019 [35]*

communication [23]. The possibility of increasing safety at road crossings is also discussed in Saunders et al. [24], which analyzes active elements at road and level crossings. In Widyastuti et al. [25], the authors address the safety of level crossings in Blitar on a model case. The probability of accidents at railway crossings also increases with the intensity of traffic, which is also pointed out by the publications Gasparik [26-27] and Mesko [28], which deal with capacity problems in railway transport. Addabbo et al. assess safety and safety analysis by targeted measurement. [29]. The authors of [30] investigated different situations and analyze them. Warnings for drivers before arriving at level crossings are addressed in Read et al. [31], where the authors focused on the warning alarm systems for drivers approaching the automatic level crossings. Zaman et al. dealt with map modelling of accidents at the railway crossings [32]. Another factor that affects safety at level crossings is the human factor. The reason may be carelessness, inexperience of drivers or violation of road traffic regulations. These factors are investigated by Akaateba et al. [33] and Salmon et al. [34]. The authors focused on the analysis of psychological factors that affect professional drivers and new drivers.

2 Safety at railroad crossings

Analyzing the data in Figure 1, one can see that more events take place at guarded crossings. These are crossings where the safety is ensured by people (railway crossing - category A). The increase in the number of accidents on guarded crossings as compared to unguarded ones, may result from the fact that in these places there is a man guard, who may faint at any moment, or simply forget to activate the barrier. In Poland, guarded crossings constitute 17.5 and unguarded crossings - 82.5 of all the crossings. The largest number of accidents on guarded level crossings (74 of events in a given year) took place in 2017, while the largest number of accidents on unguarded level crossings (40 of events in a given year) occurred in 2010. An incident at the unguarded level of crossings may also be caused by a careless driver who ignores the half-barriers at the level crossings. These are very dangerous situations and pose a threat to other road users, because the driver of the car does not comply with the road traffic regulations.

Most accidents at guarded level crossings in Poland (Figure 2) occurred in July (67% of events in a given month). In turn, the fewest events took place in

January (63% of events in a given month). At unguarded crossings, most accidents took place in August (36% of incidents in a given month), while the lowest number of accidents in March (29% of incidents in a given month). The reason for the increased number of accidents during the holiday months may be the fact that most people travel during this time, which is causing the increased traffic on the roads.

The largest number of persons who died on guarded crossings (Figure 3) was in 2010 (15 persons), seriously injured in 2017 (18 persons) and slightly injured in 2010 (18 persons). The smallest number of persons died in 2013 (4 persons), seriously injured in 2012 (4 persons), slightly injured in 2018 (3 persons).

Most persons died at unguarded railway crossings (Figure 4) in 2012 (33 persons), seriously injured in 2015 (24 persons) and slightly injured in 2011 (70 persons). The smallest number of persons died in 2010 and 2014 (18 persons), seriously injured in 2011 (16 persons), slightly injured in 2019 (17 persons).

The most common cause of accidents at guarded railway crossings in Poland was running into a railway barrier (72.83 %). The incident may have occurred because the drivers were rushing ahead of the oncoming train. Running an animal was the rarest cause of accidents (0.08 %). It can also be seen that the most common side collisions at rail and road crossings were sideways (45.46 %). The rarest animal was run over (0.20 %). The average number of incidents on guarded level crossings was 661 and at unguarded level crossings 326 [35].

The most common type of vehicles in incidents on guarded and unguarded railway crossings in Poland is a passenger car (50.56% - guarded crossings, 70.56% - unguarded crossings). The reason why a passenger car is most often involved in the incidents may be the fact that, according to GUS (Central Statistical Office) data, the number of registered vehicles increases every year [39]. The least frequent incidents involving a motorcycle with a capacity of up to 125 cm3 occur on guarded and unguarded crossings (0.05% - guarded crossings, 0.02% - unguarded crossings). The average number of vehicles on guarded crossings was 676 and on unguarded crossings - 342 [35].

As can already be seen from the above statistical data, the situation at the rail and road crossings in Poland is not ideal in terms of safety. To improve safety, a solution should be applied that will enthusiastically

Figure 3 *Number of persons who died, seriously injured and slightly injured on guarded railway crossings in Poland in 2010-2019 [35]*

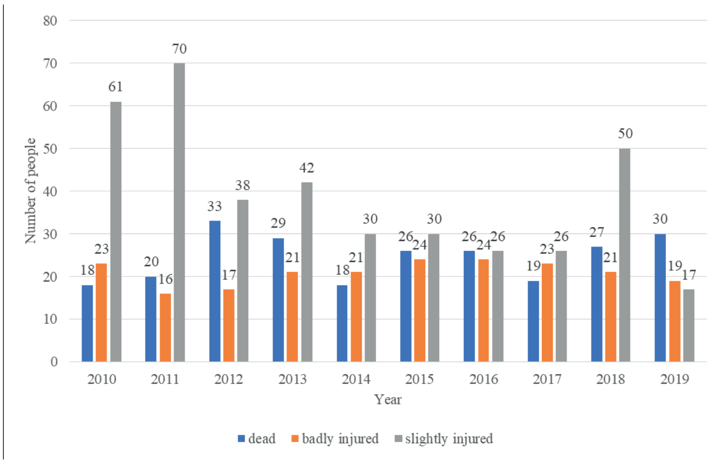

Figure 4 *The number of persons who died, seriously injured and slightly injured on unguarded railway crossings in Poland in 2010-2019 [35]*

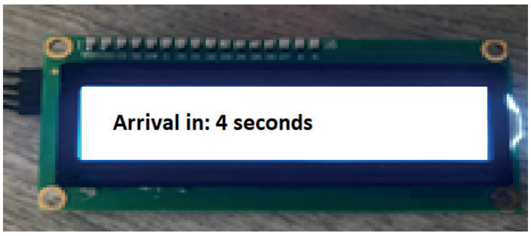

Figure 5 *Time display used in the demonstration model*

Figure 6 *Demonstration model with time display*

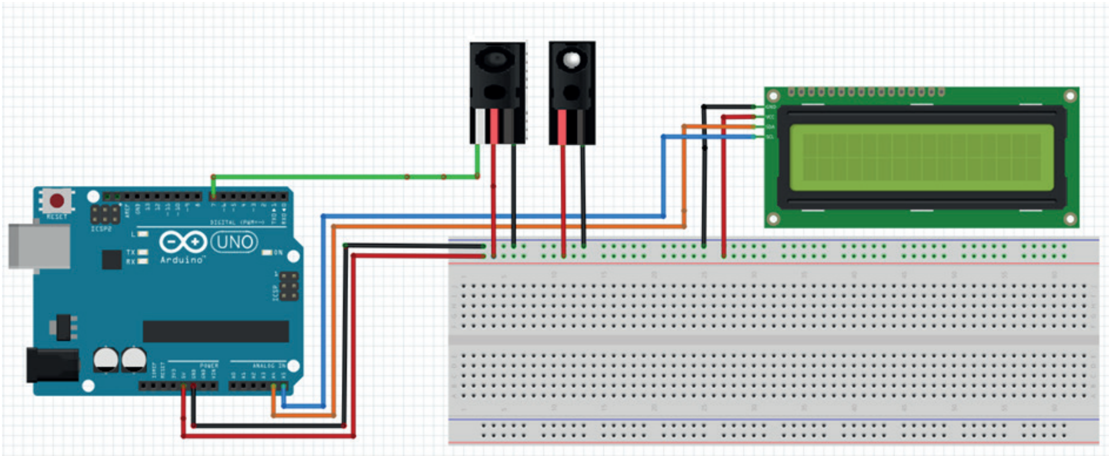

Figure 7 *Connection diagram*

encourage road users to improve conditions in such a dangerous place as the railroad crossing. For this reason, the authors propose to use the time display on the railroad crossings and it has not been tested or described anywhere. This is the basis for the implementation of the new solution as a test facility to improve safety at the railroad crossings.

A device that can improve safety at railroad crossings is a time display (Figure 5), which would count down the seconds until the front of the train appears at the railroad crossing. The solution would be placed at the single-track crossings. It can be a supplement to the already existing level crossing signals, e.g. at level crossings with traffic lights only. It could also be the main warning device at the D level crossings, because, according to PKP (Polish State Railways) data, these are the most numerous crossings in Poland [36]. Level crossings and level crossings are classified into the following categories [37]:

- category A - level crossings for public use with horned barriers,
- category B - level crossings of public use with automatic traffic lights and half barriers,
- category C - level crossings of public use with automatic traffic lights,
- category D - level crossings of public use without horns and half-gates and without automatic traffic lights
- category E - level crossings for public use,
- category F - crossings and level crossings of non-public use.

The inspiration for creating such a device was the already existing time display, which was used at road intersections. It tells drivers in how many seconds the light color will change. In European countries, exhibitions of this type are slightly less popular than in Asian countries, but there are, among others, in Greece, Belgium and Croatia [38]. There are two types of counters in Poland: for drivers and for pedestrians. The most frequently used counters in Poland are solutions attached to the siren. For the first time, the exhibition at intersections appeared in Opole in 2007. From that moment, more and more cities began to decide on this type of solution, including Torun, Poznan, Wroclaw, Zielona Gora and Szczecin [39].

3 Assumptions for the project

The time display counts down 6 seconds before the front end of the train reaches the level crossing. The train covers the entire length of the track in 9.8 seconds. The total length of the track is 280 cm. The train speed is 0.29 m/s. All the rail vehicles at the railroad crossing point move at the same speed. The sensors that the train must pass through for the display to start counting down are 174 cm from the railroad crossing. Figure 6 shows the demonstration model.

4 Connection diagram

The display and the infrared sensor (Figure 7) are connected via the contact plate to the 5 V (red) and GND (ground) (black) power supply. Signals that allow text to be displayed on the LCD (Liquid-crystal display) are connected to the SDA (data line) -> A1 and SCL (clock line) -> A0 connectors. The light barrier sends the obstacle signal with a green wire to connector 7 on the Arduino Uno. Arduino UNO is a board for learning electronics and programming.

5 The principle of operation of the device (on the mock-up)

The receiver and the transmitter of the infrared sensor are placed opposite to each other on both sides of the tracks (Figure 8). During the normal operation, both elements "see each other". When a train passes through them, the light barrier is broken and a signal is sent to the microcontroller during this time. Arduino uno, after receiving information about an obstacle, starts the time countdown algorithm. At the same time, the display shows information about the time remaining until the train arrives at the railroad crossing. After the train has passed through the crossing, the measuring device returns to the rest mode and waits for the next signal from the infrared sensor.

6 Assumptions for the actual use of the time display

The time display counts down 60 seconds before the front end of the train reaches the level crossing. The train speed is 70 km/h. All the rail vehicles at the railroad crossing point move at the same speed. The load cells through which the train must pass in order for the display to start counting down are 1166 meters from the railroad crossing and the inductive sensors are 1366 meters away.

7 The principle of operation of the device at the selected intersection

On the Pila - Ulikowo railway line, on which there is a railroad crossing, the maximum axle loads for the wagon and locomotive are 221 kN (approx. 25 tons) [36]. In this case, for the display to work properly, one needs

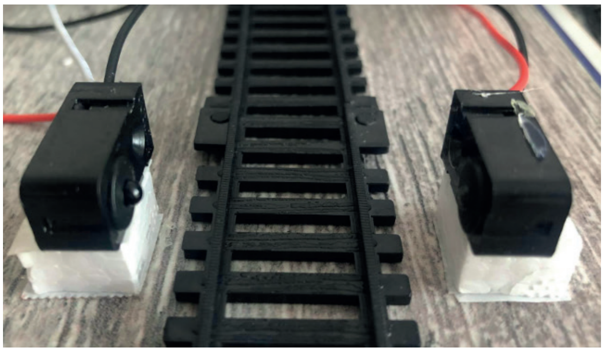

Figure 8 *Setting the sensors*

Figure 9 *Visualization of the device installation on the railroad crossing*

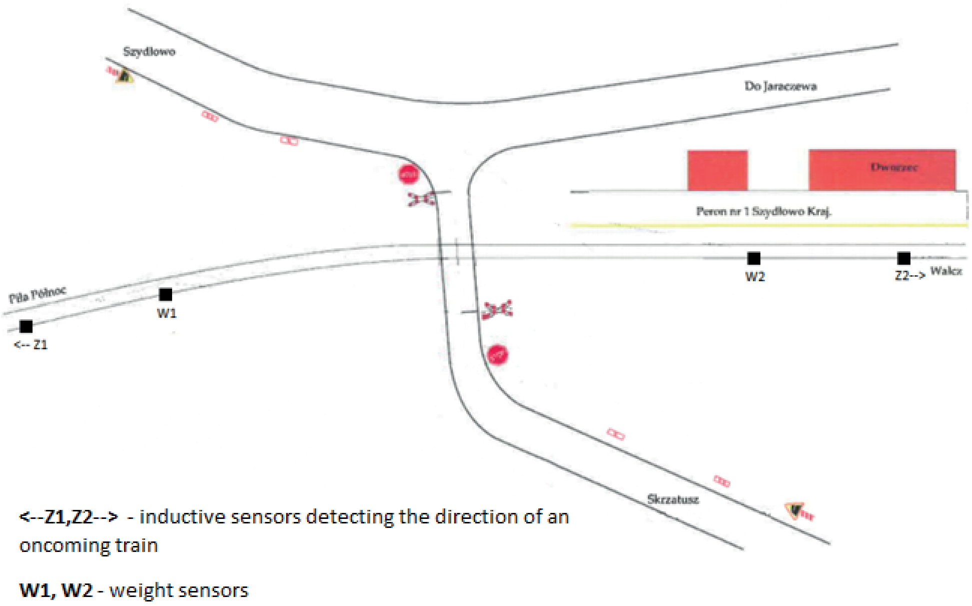

Figure 10 *Arrangement of sensors on the railroad crossing*

to use weight sensors. The infrared sensor could not be connected, as a passing animal or human may interrupt the light beam at any time, which would disturb the display. Another element that is actually used is an inductive (proximity) sensor that detects the direction of the train. This is necessary because the solution was applied at a single-track crossing where trains run in two directions. The inductive sensor sends a signal to the weighing sensor about the approaching train from the direction of the inductive sensor. Figure 10 shows the arrangement of strain gauges and inductive sensors. Arduino uno, after receiving information about exceeding the weight, starts the time countdown algorithm. At the same time, the display (Figure 9) shows information about the time remaining until the train's arrival at the railroad crossing. After passing the railway crossing, the measuring device returns to the ready state and waits for the next signal from the weighing cell.

8 Materials and methods

The survey technique was used to conduct this research. This was due to the prevailing COVID-19 pandemic from February to April 2021. The survey form is a deliberately created set of properly formulated questions that are then asked to the surveyed group of people. The survey was anonymous and consisted of 17 questions - including one on respondent's age. Before conducting the targeted research, a pilot one was carried out on a selected group of respondents. People were asked questions prepared for the target survey. Then, appropriate conclusions were developed, which showed that it is possible to conduct the study on a larger number of respondents. They could choose one of the answers provided or enter their own. The survey also included an open-ended question. The results obtained from the study are aimed at checking the level of knowledge in the field of behavior on the railroad crossings and checking whether drivers and pedestrians feel safe on the railroad crossings with the use of modern hazard warning systems, opinions on the proposed solution.

9 Object of research

The respondents constitute: 69.5% of women and 30.5% of men. The questionnaire was completed by 3.6% of women and 3.28% of men under the age of 18, 36.69% of women and 36.07% of men aged 18-25, 26.6 2% of women and 29.51% of men aged 18-25. 26-36 years of age, 18.71% of women and 11.48% of men aged 37-46, 14.39% of women and 19.67% of men over 47 years of age (Table 1). The greater number of answers given by women may result from the fact that, according to the latest data of the Central Statistical Office, the number of women in Poland is dominant (51.63%) [26].

According to the data in Table 2, 82% of the respondents have a driving license and 18% do not. The majority of both men and women holding a driving license were aged 18-25 (women - 29.50%, men - 32.79

Table 1 *Gender and age structure*

	Woman	Man	Woman	Man
Under 18	5	2	3.60%	3.28%
18 - 25	51	22	36.69%	36.07%
26 - 36	37	18	26.62%	29.51%
37 - 46	26	7	18.71%	11.48%
Over 47 years old	20	12	14.39%	19.67%
Sum	139	61	100.00%	100.00%

Table 2 *Answers to the question: "Do you have a driving license?"*

Woman, %					
Answer / Age	Under 18	18 - 25	26 - 36	37 - 46	Over 47 years old
Yes	0.00	29.50	23.74	15.83	10.07
No	3.60	7.19	2.88	2.88	4.32
Sum	3.60	36.69	26.62	18.71	14.39
Man, %					
Answer / Age	Under 18	18 - 25	26 - 36	37 - 46	Over 47 years old
Yes	0.00	32.79	27.87	9.84	18.03
No	3.28	3.28	1.64	1.64	1.64
Sum	3.28	36.07	29.51	11.48	19.67

Table 3 Place of residence

Woman, %					
Answer / Age	Under 18	18 - 25	26 - 36	37 - 46	Over 47 years old
Pila	0.72	10.07	12.95	9.35	6.47
5 - 12 km from the city center	1.44	3.60	2.88	2.16	2.16
13 - 25 km from the city center	0.72	6.47	5.04	2.16	1.44
More than 25 km from the city center	0.72	0.72	5.76	0.72	4.32
Sum	3.60	20.86	26.62	14.39	14.39
Man, %					
Answer / Age	Under 18	18 - 25	26 - 36	37 - 46	Over 47 years old
5 - 12 km from the city center	0.00	14.75	9.84	4.92	4.92
13 - 25 km from the city center	0.00	4.92	0.00	3.28	3.28
More than 25 km from the city center	1.64	6.56	4.92	0.00	6.56
Sum	1.64	1.64	14.75	1.64	4.92
5 - 12 km from the city center	3.28	27.87	29.51	9.84	19.67

Table 4 Means of transport

Woman, %					
Answer / Age	Under 18	18 – 25	26 - 36	37 - 46	Over 47 years old
Bike	1.44	2.16	1.44	0.72	0.72
Car	0.00	30.94	20.86	12.23	9.35
Train	0.72	1.44	0.72	1.44	0.72
Bus	1.44	2.16	3.60	4.32	2.88
Others - scooter	0.00	0.00	0.00	0.00	0.72
Sum	3.60	36.69	26.62	18.71	14.39
Man, %					
Answer / Age	Under 18	18 - 25	26 - 36	37 - 46	Over 47 years old
Bike	3.28	1.64	0.00	0.00	0.00
Car	0.00	29.51	26.23	9.84	16.39
Train	0.00	0.00	1.64	0.00	0.00
Bus	0.00	4.92	1.64	1.64	1.64
Others - scooter	0.00	0.00	0.00	0.00	1.64
Sum	3.28	36.07	29.51	11.48	19.67

%). The overwhelming number of men may result from the fact that, according to the Central Register of Vehicles and Drivers, 17.6 million people have a category B driving license, of which 60% are men and 40% are women [35].

The data in Table 3 present the places of residence of the research group. According to the information, 38% of respondents live in Pila, 12% of persons are 5-12 km from the city center, 17% of persons live 13-25 km from the city center and 33% of respondents live more than 25 km from the city center. Most of the respondents living in Pila are women (12.95%) aged 26-36 and men (14.75%) aged 18-25. The highest number of answers was given by women from Pila (39.57 %), which may be because, according to the Central Statistical Office, 73,139 persons live in Pila, of which 52.2% are women [40].

10 Results

The first question asked to the respondents concerned the most frequently used means of transport (Table 4). According to the data, most of the respondents, both women (30.94%) and men (29.51%) aged 18-25, drive a car. The second place was taken by the group of persons aged 26-36 (women - 20.86%, men - 26.23 %). Most road users use a car (Figure 11) (76 %). The next most frequently used means of transport is the bus (13 %), 6% use the bicycle, 4% choose the train, 0.5% of the research group walk and 0.5% use the scooter.

The next question was whether the respondent witnessed an accident at the railroad crossing. Reading the data in Table 5, one can see that 12.50% of respondents participated in an accident at a railroad crossing, while the vast majority of respondents did not participate in such an event (87.50 %). The discrepancy may be because not all the railroad crossings with accidents are located in places with high traffic. Most women (4.32%) aged 18-25 participated in accidents.

Another question was about persons who were involved in an accident at a railroad crossing. According to the information contained in Table 6, it can be seen that a greater number of respondents did not answer this question (88.50 %), although 11% were observers of events at railroad crossings and 1 person was injured in an accident at the crossing. The group of observers was dominated by women (4.32%) aged 18-25.

Another question was posed to persons who witnessed an accident at the crossing and it was at which railroad crossing the accident took place. Most of the respondents (Table 7) witnessed an accident on a single-track crossing (54.17 %), while 45.83% saw an accident on a double-track crossing. The greatest number

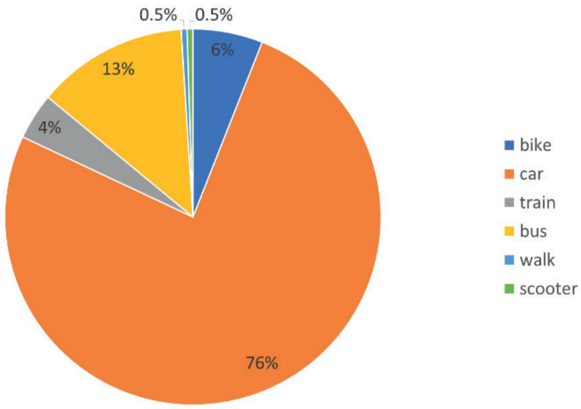

Figure 11 *Means of transport of the respondents*

Table 5 *Responses to the question: "Have you been / have you witnessed an accident at a railroad crossing?"*

		Woman, %			
Answer / Age	Under 18	18 - 25	26 - 36	37 - 46	Over 47 years old
Yes	0.72	4.32	3.60	2.88	1.44
No	2.88	32.37	23.02	15.83	12.95
Sum	3.60	36.69	26.62	18.71	14.39
		Man, %			
Answer / Age	Under 18	18 - 25	26 - 36	37 - 46	Over 47 years old
Yes	0.00	3.28	3.28	1.64	3.28
No	3.28	32.79	26.23	9.84	16.39
Sum	3.28	36.07	29.51	11.48	19.67

Table 6 *Responses to the question: "During the incident, what were you?"*

		Woman, %			
Answer / Age	Under 18	18 - 25	26 - 36	37 - 46	Over 47 years old
An observer	0.72	4.32	3.60	2.16	1.44
The injured	0.00	0.00	0.00	0.00	0.00
Perpetrator	0.00	0.00	0.00	0.00	0.00
Not applicable	2.88	32.37	23.02	16.55	12.95
Sum	3.60	36.69	26.62	18.71	14.39
		Man, %			
Answer / Age	Under 18	18 - 25	26 - 36	37 - 46	Over 47 years old
An observer	0.00	1.64	3.28	0.00	3.28
The injured	0.00	0.00	0.00	1.64	0.00
Perpetrator	0.00	0.00	0.00	0.00	0.00
Not applicable	3.28	34.43	26.23	9.84	16.39
Sum	3.28	36.07	29.51	11.48	19.67

Table 7 Responses to the question about the crossing which the incident took place on

Woman, %					
Answer / Age	Under 18	18 - 25	26 - 36	37 - 46	Over 47 years old
Monorail	0.00	11.11	11.11	16.67	5.56
Two-track	5.56	22.22	16.67	5.56	5.56
Multi-track	0.00	0.00	0.00	0.00	0.00
Sum	5.56	33.33	27.78	22.22	11.11
Man, %					
Answer / Age	Under 18	18 - 25	26 - 36	37 - 46	Over 47 years old
Monorail	0.00	16.67	16.67	16.67	33.33
Two-track	0.00	0.00	16.67	0.00	0.00
Multi-track	0.00	0.00	0.00	0.00	0.00
Sum	0.00	16.67	33.33	16.67	33.33

Table 8 Responses to the question: "What was the cause of your accident?"

Woman, %					
Answer / Age	Under 18	18 - 25	26 - 36	37 - 46	Over 47 years old
Driver error	0.00	29.41	23.53	5.88	11.76
Malfunctioning warning devices against railroad crossing	5.88	5.88	5.88	11.76	0.00
Other	0.00	0.00	0.00	0.00	0.00
Sum	5.88	35.29	29.41	17.65	11.76
Man, %					
Answer / Age	Under 18	18 - 25	26 - 36	37 - 46	Over 47 years old
Driver error	0.00	0.00	0.00	0.00	33.33
Malfunctioning warning devices against railroad crossing	0.00	16.67	33.33	16.67	0.00
Other	0.00	0.00	0.00	0.00	0.00
Sum	0.00	16.67	33.33	16.67	33.33

of accidents was observed at single-track crossings, because according to statistical data on events at railway crossings, there are more single-track crossings [36]. Most of the surveyed women (16.67%) aged 37-46 and men (33.33%) over 47 saw the event while traveling. None of the respondents saw an accident on a multi-track crossing.

According to the respondents' answers in Table 8, 39.13% answered that the cause of the accident was a faulty warning device at railroad crossings, while 60.87% assessed the situation as a driver's error. The majority of women (29.41%) aged 18-25 and men (33.33%) aged over 47 stated that the cause of the accident was driver's error, while 11.76% of women aged over 47 and men (33.33%) aged 26-36 believed that the event occurred as a result of incorrect operation of warning devices at the railroad crossing.

In the next question, the respondents who witnessed the accident at the railroad crossing could present in writing what the accident looked like. Below are the most common descriptions provided by respondents:

- "The lights were off and a car was crossing the tracks. The train was approaching and began to warn with siren/honk. The passenger car sped up, but the train hit the rear of the car, pushing it to the side of the road. Nobody was hurt, but the entire rear of the car was crushed "
- "The driver did not stop in front of a stop sign and the train hit the back of the trailer"
- "We were driving with my brother-in-law and the traffic lights allowed us to cross the tracks. Suddenly, a train came around the bend. My brother-in-law sped up and drove into the ditch"- response of the injured person,
- "The driver did not adjust the speed and stopped at a stop sign and there was a collision"
- "There was a train and the gates did not close"
- "The barrier were almost deserted and the driver has pulled into the crossing. He survived, but it didn't look good. "
- "The barrier began to close and the traffic lights were on and the passenger car still wanted to pass before the gates were closed"
- "The machine reached the intersection, the warning lights were not flashing and the train was approaching"

Analyzing the answers of the respondents, one can see that incidents at the level crossings are caused both by drivers and by improperly operating warning systems of the oncoming trains. The participants in the accident also responded to an open question. The person should not place complete confidence in the safety system, i.e. not rely only on its proper functioning.

The next three questions concerned the behavior of drivers at the railroad crossings. According to the answers given by the respondents (Table 9), most of them always stick to the signs placed in front of the railroad crossing (88.5 %). 11% of respondents said that they "sometimes follow the signs". Out of the entire research group (0.5%) of persons replied that they never obey the signs placed there. Most women (33.81%) aged 18-25 and men (24.59%) aged 18-25, 26-36 replied that they always obey the signs at the railroad crossing. This may be because they are young drivers, which makes them more sensitive to dangerous situations and the things around them.

Another question was about the behavior at a railroad crossing equipped with barriers and traffic lights. Analyzing the answers of the respondents (Table 10), one can see that most road users know how to behave at an intersection equipped with barriers and traffic lights. As many as 84.5% of respondents replied: "I am waiting for the barrier to lift completely, the red light will stop flashing and only then I am crossing the railway crossing". It proves. that both pedestrians and drivers are particularly careful, which means that they obey traffic regulations [41] and that their own safety is important to them. Another answer was: "I check that nothing is coming and I cross the railroad". This answer was chosen by 15% of the respondents. Another answer

Table 9 *Responses to the question: "Do you follow the road signs placed there before entering / entering the railroad crossing?"*

Woman, %					
Answer / Age	Under 18	18 - 25	26 - 36	37 - 46	Over 47 years old
Always	3.60	33.81	23.74	16.55	14.39
Sometimes	0.00	2.88	2.16	2.16	0.00
Never	0.00	0.00	0.72	0.00	0.00
Sum	3.60	36.69	2.88	2.16	14.39
Man, %					
Answer / Age	Under 18	18 - 25	26 - 36	37 - 46	Over 47 years old
Always	3.28	24.59	24.59	9.84	18.03
Sometimes	0.00	11.48	4.92	1.64	1.64
Never	0.00	0.00	0.00	0.00	0.00
Sum	3.28	36.07	29.51	11.48	19.67

Table 10 *Responses to the question: How do you behave at the railroad crossing equipped with barriers and traffic lights?*

Woman, %					
Answer / Age	Under 18	18 - 25	26 - 36	37 - 46	Over 47 years old
I wait for the turnstiles to go up completely. the red light to stop blinking and I pass	3.60	33.81	23.74	14.39	11.51
I check that nothing is coming and I am crossing the railroad crossing	0.00	2.88	2.88	4.32	2.88
Otherwise (the respondent could enter his/her answer here)	0.00	0.00	0.00	0.00	0.00
Sum	3.60	36.69	26.62	18.71	14.39
Man, %					
Answer / Age	Under 18	18 - 25	26 - 36	37 - 46	Over 47 years old
I wait for the turnstiles to go up completely. the red light to stop blinking and I pass	1.64	22.95	22.95	11.48	19.67
I check that nothing is coming and I am crossing the railroad crossing	1.64	13.11	4.92	0.00	0.00
Otherwise (the respondent could enter his/her answer here)	0.00	0.00	1.64	0.00	0.00
Sum	3.28	36.07	29.51	11.48	19.67

Table 11 *Responses to the question: How do you behave at the railroad crossing equipped with traffic lights?*

Answer / Age	Under 18	18 - 25	26 - 36	37 - 46	Over 47 years old
Woman, %					
I check if the train is coming. If not - I pass	1.44	9.35	5.04	6.47	0.72
I stop and I wait for the blinking lights to go out	2.16	27.34	21.58	12.23	13.67
Otherwise (the respondent were able to enter their answer here)	0.00	0.00	0.00	0.00	0.00
Sum	3.60	36.69	26.62	18.71	14.39
Man, %					
Answer / Age	Under 18	18 - 25	26 - 36	37 - 46	Over 47 years old
I check if the train is coming. If not - I pas	3.28	14.75	8.20	1.64	1.64
I stop and I wait for the blinking lights to go out	0.00	21.31	21.31	9.84	18.03
Otherwise (the respondent were able to enter their answer here)	0.00	0.00	0.00	0.00	0.00
Sum	3.28	36.07	29.51	11.48	19.67

Table 12 *Response to the question: "Do you ever enter the railroad crossing without being particularly careful?"*

Answer / Age	Under 18	18 - 25	26 - 36	37 - 46	Over 47 years old
Woman, %					
Always	0.00	1.44	0.72	1.44	1.44
Sometimes	0.00	9.35	5.76	2.16	0.72
Never	3.60	25.90	20.14	15.11	12.23
Sum	3.60	36.69	26.62	18.71	14.39
Man, %					
Answer / Age	Under 18	18 - 25	26 - 36	37 - 46	Over 47 years old
Always	0.00	1.64	1.64	0.00	0.00
Sometimes	0.00	19.67	14.75	1.64	2.88
Never	3.28	14.75	13.11	9.84	5.76
Sum	3.28	36.07	29.51	11.48	8.63

was chosen by a man aged 26-36 and it was: "I am waiting for the gate to rise high enough for my car to fit and I am going through." It can be concluded that the person who marked this answer does not pay attention to the safety systems used at the level crossings. It is therefore necessary to continuously educate road users to minimise the risks at the level crossings.

The next question was concerned with behavior of the road users on crossings equipped with traffic lights. The information provided by the respondents, given in Table 11, shows that as many as 75% of the respondents replied, "I stop and wait until the flashing lights go out". Such an answer was given by the greatest number of women (27.34%) aged 18-25 and men (21.31%) aged 18-25 and 26-36. This proves that both pedestrians and drivers care about their own safety and pay attention to the safety systems used. On the other hand, 25% of respondents only check that the train is not coming and if it does not they pass.

The next question was, "Do you ever enter a railroad crossing without being careful?" Analyzing the responses (Table 12), one can see that the majority of respondents (70%) are particularly cautious at the railroad crossings. As many as 25.5% of the research group persons sometimes forget the said rule, which is the cause of undesirable events at the railway crossings. The questionnaire was also completed by persons who are not particularly careful (4.5%) and thus pose a threat to themselves and other road users. Persons with the answer "always" are mostly women. The greatest number of "never" answers was given by women (25.9%) and men (14.75%) aged 18-25. This is evidenced by the fact that the majority of students in this age group obtain their knowledge on the road safety at school.

Another question, related to the sense of security, was: "Do you think that the current safety devices at the railroad crossings (traffic lights, gates, sound devices) provide sufficient safety?" According to the answers given by the respondents (Table 13), most of them do not feel completely safe using the current security

Table 13 *Responses to the question: "In your opinion, do you think the currently used safety devices at the railroad crossings (traffic lights, barriers, sound devices) ensure sufficient safety?"*

	Woman, %				
Answer / Age	Under 18	18 - 25	26 - 36	37 - 46	Over 47 years old
Yes - I feel safe	2.16	15.83	9.35	7.19	3.60
I do not know - despite the devices used. I still do not feel safe entering the railroad crossing	0.00	17.27	13.67	8.63	7.19
No	1.44	3.60	3.60	2.88	3.60
Sum	3.60	36.69	26.62	18.71	14.39
	Man, %				
Answer / Age	Under 18	18 - 25	26 - 36	37 - 46	Over 47 years old
Yes - I feel safe	3.28	11.48	4.92	1.64	4.92
I do not know - despite the devices used. I still do not feel safe entering the railroad crossing	0.00	18.03	18.03	9.84	6.56
No	0.00	6.56	6.56	0.00	8.20
Sum	3.28	36.07	29.51	11.48	19.67

Table 14 *Responses to the question: "What do you think about the use of an additional device before the railroad crossing, which is a time display, which would count down seconds (e.g. 20 seconds) until the train enters the railroad crossing?"*

	Woman, %				
Answer / Age	Under 18	18 - 25	26 - 36	37 - 46	Over 47 years old
Absolutely - I am open to new technological solutions that will improve safety at railroad crossings	3.60	32.37	23.74	16.55	11.51
I do not know	0.00	0.72	1.44	2.16	1.44
No - I don‘t see the need for such a device	0.00	3.60	1.44	0.00	0.72
Other (here the respondent was able to enter his/her answer)	0.00	0.00	0.00	0.00	0.72
Sum	3.60	36.69	26.62	18.71	14.39
	Man, %				
Answer / Age	Under 18	18 - 25	26 - 36	37 - 46	Over 47 years old
Absolutely - I am open to new technological solutions that will improve safety at railroad crossings	1.64	32.79	24.59	11.48	14.75
I do not know	1.64	0.00	3.28	0.00	1.64
No - I don‘t see the need for such a device	0.00	3.28	1.64	0.00	3.28
Other (here the respondent was able to enter his/her) answer	0.00	0.00	0.00	0.00	0.00
Sum	3.28	36.07	29.51	11.48	19.67

systems (48.5 %). The answer "No" was given by 17% of the respondents, while 34.5% of the research group answered "Yes". The majority of both women (17.27%) aged 18-25 and men (18.03%) aged 18-25 and 26-36 do not feel safe using the current security systems. This proves that road users are waiting for new safety systems' improvements that will increase their safety comfort when approaching a railway crossing.

Another question posed to the respondents was: "What do you think about the use of an additional device before the railroad crossing, which is the time display proposed by the authors, which would count down seconds (e.g. 20 seconds) until the train enters the railroad crossing?" According to the answers of the respondents (Table 14), one can see that most of them (87%) are interested in a new technological solution, which is a time display. The answer "I do not know" in the survey was given by 6% of the respondents and 6.5% saw no need to use such a device. 0.72% of women over 47 believed that the application of the above solution would pose a threat as it would provoke careless drivers to pass in front of the train. To dispel any doubts, the new solution could be implemented on a single level crossing in conjunction with a camera to observe the behavior of drivers and then consider whether the device is completely safe.

Table 15 *Responses to the question: "If an additional device was used that could improve safety at railroad crossings, would you pay attention to it?"*

Woman, %					
Answer / Age	Under 18	18 - 25	26 - 36	37 - 46	Over 47 years old
Yes	2.16	32.37	24.46	17.99	12.95
Maybe	1.44	4.32	2.16	0.72	1.44
No	0.00	0.00	0.00	0.00	0.00
sum	3.60	36.69	26.62	18.71	14.39
Man, %					
Answer / Age	Under 18	18 - 25	26 - 36	37 - 46	Over 47 years old
Yes	1.64	31.15	29.51	11.48	19.67
Maybe	1.64	4.92	0.00	0.00	0.00
No	0.00	0.00	0.00	0.00	0.00
sum	3.28	36.07	29.51	11.48	19.67

The last question asked by respondents was: "If an additional device was used that could improve safety at railroad crossings, would you pay attention to this?" Analyzing the responses (Table 15) of the respondents, the majority, as many as 91% of respondents, declared that they would pay attention to a new, additional device and 9% of the respondents answered "Perhaps". Neither person gave a negative answer. The majority of both women (32.37%) and men (31.15%) aged 18-25 answered "yes", while 4.32% of women and 4.92% of men aged 18-25 answered "maybe".

11 Discussion

When assessing a new safety system, first of all, attention should be paid to the annual number of accidents. Among other things, it was this factor that prompted authors to propose the time display as a security solution. One should constantly strive to reduce the accident statistics from year to year. The answers of the respondents play a key role in this case, because, as one can see in the question about what traffic users think about the new, additional device, as many as 87% of respondents said that they are most open to new technological solutions that would improve safety at the level crossings - road traffic. If the road users accept the new solution, the time display could also be used on crossings of other categories, not only D. However, the priority is given to crossings of this category, as they are dominant by the number of unfortunate events.

Another way to reduce the number of accidents is to focus on reducing the number of the level crossings, which can be achieved through cooperation between the state, regions and municipalities. The modernization of the level crossings must be in line with national and international standards and norms, as declared by the research of Luptak et al. [42]. Another solution is to take technical measures aimed at clarifying and simplifying the traffic situation at the level crossings, as proposed and recommended in several studies [43-45]. For this reason, it makes sense to introduce this solution at one of the level crossings and to observe the behaviour of drivers crossing the crossing. Will they respect the timer or will they enter the crossing despite the countdown to the train's arrival?

12 Conclusion

The main goal of improving the safety at the railroad crossings is to significantly reduce the risk for life and health in rail and road traffic. In most cases, haste and lack of care for security systems lead to material losses at best.

The poor technical condition of the pavement at the intersection of public roads and railroads should be repaired as soon as possible from the moment the pavement damage is reported. However, in majority of cases, the retrofitting occurs at the time of an accident.

According to statistical data, most accidents occur at level D level crossings. These crossings are only equipped with a "Stop" warning sign. Equipping D category crossings with the new technological solutions, such as a time display, can significantly improve safety in such difficult places. The new system can also complement the existing systems (e.g. at level C level crossings). Modernization or additional auxiliary systems may lead to a gradual lowering of the accident curve at the railroad crossings.

Another important aspect is educating the public and future road users about the dangers and rules of behaviour at the railway crossings. An example of such activities are special actions conducted by PKP. Increasing the awareness of young drivers that stopping a vehicle before each railroad crossing is an obligation to save lives. Eliminating behaviours leading to accidents will definitely improve the level of safety at the railroad crossings.

The research results presented may be applicable to other countries. Authors of the article propose an improvement in safety at a single-track crossing where the train moves at a set speed. In the next stage, the authors plan to extend the research to double-track crossings where the trains would move at different speeds.

References

[1] Accident and collision record system [online] [accessed 2021-06-15]. Available from: www.sewik.pl

[2] ANTONOWICZ, M., MAJEWSKI, J. On safety in land transport. *Railway Market*. 2014, **10**. eISSN 2081-1454.

[3] CELINSKI, I. Mobile diagnostics of vehicles as a means to examine and define speed limits in a road. *Diagnostic*. 2017, **18**(1), p. 67-72. eISSN 2449-5220.

[4] TOPOLSEK, D., OJSTERSEK, T. C. Do drivers behave differently when driving a car or riding a motorcycle? *European Transport / Trasporti Europei*. 2017, **66**, 7. ISSN 1825- 3997.

[5] GOLAKIYA, H. D., CHAUHAN, R., DHAMANIYA, A. Evaluating safe distance for pedestrians on urban midblock sections using trajectory plots. *European Transport / Trasporti Europei*. 2020, **75**, 2. ISSN 1825- 3997.

[6] MOHANTY, M., SAMAL, S. R. Role of young drivers in road crashes: a case study in India. *European Transport / Trasporti Europei*. 2019, **74**, 1. ISSN 1825- 3997.

[7] OLEGAS, P., PRENTKOVSKIENE, R., LUKOSEVICIENE, O. Investigation of potential deformations developed by elements of transport and pedestrian traffic restricting gates during motor vehicle-gate interaction. *Transport* [online]. 2007, **22**(3), p. 229-235. ISSN 1648-4142, eISSN 1648-3480. Available from: https://doi.org/10.3846/1648 4142.2007.9638130

[8] OLEGAS, P., SOKOLOVSKIJ, E., BARTULIS, V. Investigating traffic accidents: a collision of two motor vehicles. *Transport* [online]. 2010, **25**(2), p. 105-115. ISSN 1648-4142, eISSN 1648-3480. Available from: https://doi.org/10.3846/transport.2010.14

[9] GIANLUCA, D., DE`LUCA, M., PRATO, C., PRENTKOVSKIS, O., JUNEVICIUS, R. The impact of vehicle movement on exploitation parameters of roads and runways: a short review of the special issue. *Transport* [online]. 2016, **31**(2), p. 127-132. ISSN 1648-4142, eISSN 1648-3480. Available from: https://doi.org/10.3846/1648 4142.2016.1201912

[10] LUKE, R., HEYNS, G. J. Reducing risky driver behavior through the implementation of a driver risk management system. *Journal of Transport and Supply Chain Management* [online]. 2014, **8**(1) (a146), p. 1-10. ISSN 2310-8789, eISSN 1995-5235. Available from: https://doi.org/10.4102/jtscm.v8i1.146

[11] Reflectors for vulnerable road users - Driving school portal [online] [accessed 2021-06-15]. Available from: https://www.portalnaukikuje.pl/aktualnosci/odblaski-dla-niechrononych ucznikowruchu-road-2152.html

[12] GORZELANCZYK, P., PYSZEWSKA, D., KALINA, T., JURKOVIC, M. Analysis of road traffic safety in the Pila poviat. *Scientific Journal of Silesian University of Technology. Series Transport* [online]. 2020, **107**, p. 33-52. ISSN 0209-3324, eISSN 2450-1549. Available from: https://doi.org/10.20858/sjsutst.2020.107.3

[13] NOVALES, M., BERTRAND, D., FONTAINE, L. A proposed new approach to light rail safety management in Spain and other countries. *Safety Science* [online]. 2019**, 11**8, p. 740-751. ISSN 0925-7535. Available from: https://doi.org/10.1016/j.ssci.2019.06.010

[14] DJORDJEVIC, B., KRMAC, E., MLINARIC T. J. Non-radial DEA model: a new approach to evaluation of safety at railway level crossings. *Safety Science* [online]. 2018, **103**, p. 234-246. ISSN 0925-7535. Available from: https://doi.org/10.1016/j.ssci.2017.12.001

[15] VAEZI, A., DALAL, J., VERMA, M. Designing emergency response network for rail hazmat shipments under uncertainties: optimization model and case study. *Safety Science* [online]. 2021, 141, 105332. ISSN 0925-7535. Available from:https://doi.org/10.1016/j.ssci.2021.105332

[16] DUNCAN, D., KLOCKNER, K. Development of the contributing factors Framework interview guide (CFF-IG): all aboard the rail safety truth train. *Safety Science* [online]. 2020, **129**, 104853. ISSN 0925-7535. Available from: https://doi.org/10.1016/j.ssci.2020.104853

[17] READ, G. J. M, COX, J. A., HULME, A., NAWEED, A., SALMON, P. M. What factors influence risk at rail level crossings? A systematic review and synthesis of findings using systems thinking. *Safety Science* [online]. 2021, **138**, 105207. ISSN 0925-7535. Available from: https://doi.org/10.1016/j.ssci.2021.105207

[18] HADJ-MABROUK, H. Analysis and prediction of railway accident risks using machine learning. *AIMS Electronics and Electrical Engineering* [online]. 2020, **4**(1), p. 19-46. ISSN 2578-1588. Available from: https://doi.org/10.3934/ElectrEng.2020.1.19

[19] SANTARREMIGIA, F., DOLORES MOLERO, G., POVEDA-REYES, S., AGUILAR-HERRANDO, J. Railway safety by designing the layout of inland terminals with dangerous goods connected with the rail transport system. *Safety Science* [online]. 2018, **110**(B), p. 206-216. ISSN 0925-7535. Available from: https://doi.org/10.1016/j.ssci.2018.03.001

[20] YAN, H., GAO, C., ELZARKA, H., MOSTAFA, K., TANG, W. Risk assessment for construction of urban rail transit projects. *Safety Science* [online]. 2019, **118**, p. 583-594. ISSN 0925-7535. Available from: https://doi.org/10.1016/j.ssci.2019.05.042

[21] MCHUGH, K., KLOCKNER, K. Learning lessons from rail safety storytelling: telling safety like it is. *Safety Science* [online]. 2020, **122**, 104524. ISSN 0925-7535. Available from: https://doi.org/10.1016/j.ssci.2019.104524

[22] AMBROS, J., PERUTKA, J., SKLADANY, P., TUCKA, P. Enhancing the insight into Czech railway level crossings' safety performance. *International Journal of Rail Transportation* [online]. 2020, **8**(1), p. 99-108. ISSN 2324-8378, eISSN 2324-8386. Available from: https://doi.org/10.1080/23248378.2019.1612791

[23] CAI, N., CHEN, H., LI, Y., PENG, Y. Intrusion detection and tracking at railway crossing. In: 2019 International Conference on Artificial Intelligence and Advanced Manufacturing, AIAM 2019: proceedings [online]. 2019. Art. n. 57. ISBN 978-1-4503-7202-2, p. 1-6. Available from: https://doi.org/10.1145/3358331.3358388

[24] SAUDERS, W. J., MOUSA, S. R., CODJOE, J. Market basket analysis of safety at active highway-railroad grade crossings. *Journal of Safety Research* [online]. 2019, **71**, p. 125-137. ISSN 0022-4375, eISSN 1879-1247. Available from: https://doi.org/10.1016/j.jsr.2019.09.002

[25] WIDYASTUTI, H., UTAMI, A., DZULFIQAR, Z. M. Model of queuing in the railway level crossing (case study: Imam Bonjol railway level crossing in Blitar). *IOP Conference Series: Materials Science and Engineering* [online]. 2019, **650**, 012053. ISSN 1757-8981, eISSN 1757-899X. Available from: https://doi.org/10.1088/1757-899X/650/1/012053

[26] GASPARIK, J., ABRAMOVIC, B., HALAS, M. New graphical approach to railway infrastructure capacity analysis. *Promet - Traffic and Transportation* [online]. 2015, **27**, p. 283-290. ISSN 0353-5320, eISSN 1848-4069. Available from: https://doi.org/10.7307/ptt.v27i4.1701

[27] GASPARIK, J., ABRAMOVIC, B., ZITRICKY, V. Research on dependences of railway infrastructure capacity. *Tehnicki Vjesnik – Technical Gazette* [online]. 2018, **25**(4), p. 1190-1195. ISSN 1330-3651, eISSN 1848-6369. Available from: https://doi.org/10.17559/TV-20160917192247

[28] MESKO, P., GASPARIK, J., LALINSKA, J. Railway capacity issues on Slovak international corridors. In: 21st International Scientific Conference Transport Means: proceedings. 2017. p. 436.

[29] ADDABBO, T., DELLA GIOVAMPAOLA, C., FORT, A., MUGNAINI, M., POZZEBON, A., TOCCAFONDI, A., VIGNOLI, V. Target measurements influence on level crossing detection system safety determination. *Measurement* [online]. 2019, **135**, p. 547-554. ISSN 0263-2241. Available from: https://doi.org/10.1016/j.measurement.2018.11.059

[30] TAILLANDIER, V. Smart level crossing. In: 2018 16th International Conference on Intelligent Transport System Telecommunications ITST 2018: proceedings. IEEE. 2018.

[31] READ, G. J. M., BEANLAND, V., STANTON, N. A., GRANT, E., STEVENS, N., LENNE, M. G., THOMAS, M., MULVIHILL, C. M., WALKER, G. H., SALMON, P. M. From interfaces to infrastructure: extending ecological interface design to re-design rail level crossings. *Cognition, Technology and Work* [online]. 2021, **23**, p. 3-21. ISSN 1435-5558, eISSN 1435-5566. Available from: https://doi.org/10.1007/s10111-019-00583-2

[32] ZAMAN, S. U., HOSSAIRR, S., SHAHNAZ, C. Automatic rail crossing alarming system. In: 2018 IEEE International WIE Conference on Electrical and Computer Engineering WIECON-ECE 2018: proceedings. IEEE. 2018. p. 129.

[33] AKAATEBA, M. A., AMOH-GYIMAH, R., AMPONSAH, O. Traffic safety violations in relation to drivers' educational attainment, training and experience in Kumasi, Ghana. *Safety Science* [online]. 2015, **75**, p. 156-162. ISSN 0925-7535. Available from: https://doi.org/10.1016/j.ssci.2015.02.010

[34] SALMON, P. M., READ, G. J. M., STANTON, N. A., LENNE, M. G. The crash at Kerang: investigating systemic and psychological factors leading to unintentional non-compliance at rail level crossings. *Accident; Analysis and Prevention* [online]. 2013, **50**, p. 1278-1288. Available from: https://doi.org/10.1016/j.aap.2012.09.029

[35] Central register of vehicles and drivers [online] [accessed 2021-06-15]. Available from: http://www.cepik.gov.pl/

[36] List of maximum axle loads - PKP Polskie Linie Kolejowe [online] [accessed 2021-06-15]. Available from: https://www.plksa.pl/files/public/user_upload/pdf/Reg_przydzielania_tras/Regulamin_2013_2014/zmiana_7_02_2014/P_13-14_Z_2.2_20140207122952.pdf

[37] Classification of level crossings - Crossing of railway lines with public roads. Regulation of the Minister of Transport and Maritime Economy of 10 January 1991 on the crossing of railway lines with public roads. [online] [accessed 2022-02-22]. Available from: https:// https://sip.lex.pl//

[38] WENGEL, M. Displays of signal transmission time at intersections with traffic lights. Evaluation of the Regulation Dz. of Laws of May 31, 2017. item 1062.

[39] BUDA, M., FALWARSKI, T., KRUKOWICZ, T. Problems of using time counters in traffic lights. Urban and Regional Transport. 2016, **9**. ISSN 1732-5153.

[40] Central Statistical Office [online] [accessed 2021-06-15]. Available from: https://stat.gov.pl/

[41] Road traffic law. Journal of Laws. 2021.0.450, Art. 28. on road traffic [online] [accessed 2021-06-15]. Available from: https:// https:// https://lexlege.pl///

[42] LUPTAK, V., STOPKOVA, M., JURKOVIC, M. Proposed methodology for the calculation of overview distances at level crossings and the inclusion thereof in national standards. *Sustainability* [online]. 2020, **12**(14), 5684. eISSN 2071-1050. Available from: https://doi.org/10.3390/su12145684

[43] KUBO, J. Rationalization of railroad crossings in the South Bohemian Region / Racionalizace zeleznicnich prejezdu na uzemi Jihoceskeho kraje (in Czech) [online] [accessed 2020-02-05]. Bachelor thesis. Ceske Budejovice: Institute of Technology and Business in Ceske Budejovice, 2019. Available from: https://is.vstecb.cz/th/vfulx/

[44] SMOCZYNSKI, P., GILL, A., KADZINSKI, A. Modelling of railway accidents with accimap - case study. In: 23rd International Scientific Conference Transport Means: proceedings. 2019. p. 113.

[45] LARUE, G. S., WATLING, C. N., BLACK, A. A., WOOD, J. M. Getting the attention of drivers back on passive railway level crossings: evaluation of advanced flashing lights. *Transportation Research Record: Journal of the Transportation Research Board* [online]. 2019, **2673**, p. 789-798. ISSN 0361-1981, eISSN 2169-4052. Available from: https://doi.org/10.1177/0361198119828679

UNIVERSITY OF ŽILINA

In its over 65 years of successful existence, the University of Žilina (UNIZA) has become one of the top universities in Slovakia.

COOPERATION INNOVATION TECHNOLOGY TRANSFER 2022

The main goal of this year's COINTT conference will be to raise the profile of academic workplaces in the eyes of entrepreneurs

The third week of October (October 18-19) this year will once again open the gates of the largest Slovak conference on technology transfer, which will take place for the third year under the name COOPERATION INNOVATION TECHNOLOGY TRANSFER 2022 (hereinafter „COINTT"). For the first time, the conference will take place in-site in the conference rooms of the Saffron Hotel in Bratislava. It will traditionally take place on three stages: TECHNOLOGY TRANSFER, INNOVATION and COOPERATION.

In addition to technology transfer, the event also focuses on intellectual property protection, innovation and business support. The thematic focus of this year is to simplify the contact between the adacemia and business in the area of technology transfer. Within the topic, individual program inputs will try to answer the questions of whether open access and easy access are beneficial for the commercial use of intellectual property or not, how to simplify technology transfer at Slovak research institutes, what methods of contact and cooperation with the commercial sphere they use, how to make its activities more attractive for the private sector, what is the role of the Technology Transfer Office at the Slovak Centre of Scientific and Technical Information (SCSTI) and what is the role and importance of local technology transfer offices at universities.

The event also includes a ceremony to announce the results of the Slovak Technology Transfer Award, Scientists, researchers, R&D teams are awarded in three categories: INNOVATION, INNOVATOR, THE BIGGEST ACHIEVEMENT OF THE YEAR IN THE FIELD OF TECHNOLOGY TRANSFER. Slovak Technology Transfer Award 2022 is prepared by the organizer in the form of a gala evening.

COINTT 2022 is already under the auspices of the Slovak Minister of Education, Science, Research and Sports - Branislav Gröhling. The event is organized by the SCSTI. The co-organizers are the Slovak Innovation and Energy Agency (SIEA), a consulting company supporting startups - Civitta Slovakia and the National Association for Technology Transfer of the Slovak Republic associating 7 public academic institutions to support technology transfer in Slovakia and its systematization. Negotiations with other event partners are still ongoing. The COINTT conference is organized within the implementation of the national project National Infrastructure to Support Technology Transfer in Slovakia II - NITT SK II / Investment in your future / This project is supported by the European Regional Development Fund / www.opii.gov.sk.

ASSESSING THE PROPENSITY TO CAR SHARING SERVICES IN UNIVERSITY CITIES: SOME INSIGHTS FOR DEVELOPING THE CO-CREATION PROCESS

Vincenza Torrisi [1], Tiziana Campisi [2,*], Matteo Ignaccolo [1], Giuseppe Inturri [3], Giovanni Tesoriere [2]

[1]Department of Civil Engineering and Architecture, University of Catania, Italy
[2]Faculty of Engineering and Architecture, Kore University of Enna, Italy
[3]Department of Electric, Electronic and Computer Engineering, University of Catania, Italy

*E-mail of corresponding author: tiziana.campisi@unikore.it

Resume

Cities are often characterised by the presence of universities and by a greater number of students, often commuters, with an average age of less than 30 years. The study focused on the city of Enna (Italy), where the university students represent a significant percentage of residents and also a good rate of local travel demand. The survey campaign was conducted over a period of more than one year. A bivariate statistical method was applied highlighting significant variables regarding several features of a car sharing system. Additionally, non-parametric statistics and a before and after analysis were performed to evaluate the influence of implementation of the shared transport service. The results can also offer insights into the improvement of transport supply in urban context and the possible implementation of the co-creation actions between the companies managing the service with the end-users.

Article info

Received 20 January 2021
Accepted 6 May 2022
Online 14 June 2022

Keywords:

sharing economy
propensity to car sharing
sustainable transport systems
bivariate analysis
non-parametric test
before and after analysis
co-creation

Available online: https://doi.org/10.26552/com.C.2022.3.G1-G14

ISSN 1335-4205 (print version)
ISSN 2585-7878 (online version)

1 Introduction

The continuous evolution of urban transport models is characterised by different sharing transport systems i.e. car sharing and bike sharing that are particularly attractive and constantly updated themes [1-2].

A correct design of sharing mobility systems provides an optimal basis for implementation of Mobility as a Service (MaaS) systems, useful for all age groups and which make it possible to streamline booking procedures and waiting times in changing the mode of transport, also considering the new transport mobility issues deriving from the COVID-19 pandemic and the evolving transport demand [3-4]. An increasing safety related to this mode of transport can be guaranteed both by carefully studying the variables that characterise the transport demand or further measures to the restriction of the private vehicle use for decarbonisation strategies.

The use of one's own car is also connected to increasing economic, social and environmental costs. In fact, the ever-increasing transport demand, effectively involves enhancing the attention to systems capable of "intelligently" addressing the mobility problems in their entirety, by allowing more effective and efficient overall performance of the system, using appropriate mobility planning and management strategies [5-6] and implementation of innovative transport systems [7]. One strategy, linked to benefit in terms of innovation and low costs, is to create vehicle sharing institutions. Shared transport demand is strongly influenced by some external factors such as population density, age, family size, level of education, proximity to public transport stations, land use, distance from the central business district, distance from services, number of companies close to the stations and vehicle availability. Authors of [8] show the impact of demographic, environmental, economic and travel models on the adoption of vehicle sharing systems. The efficiency of the implemented system is based on the correct design and location of the stations.

The optimisation of the transport offer is done by considering the end user as a user as well as a potential helper during the decision-making process, implementing what is called co-creation. The term co-creation refers to involvement of users and stakeholders during the product design and development process. Co-creation is a very broad term and emphasises the collective creativity of stakeholders, designers, researchers and end users [9]. Some authors have identified the co-creation as the composition of co-production and co-design, while others have referred to co-creation as a particular case of co-design [10].

Several researches have highlighted the importance of networks and configuration of relationships and resources in markets. In particular, the creation of value is a complex and multidimensional process that is best studied in the context of dynamic networks or ecosystems of exchange of services. The concept of co-creation has been advanced by several value research from a service ecosystem view, considering the importance of networks and the configuration of relationships and resources in markets [11-12].

In the field of mobility, a bottom-up approach to participatory planning is essential in order to improve cooperation between citizens and politicians and to take into account the critical issues that users encounter on a daily basis [13-15].

In studies [16] and [17] authors focused their research on the relationship among sharing service, forecasting, optimization and personalization actions.

The evolution of shared mobility starts from traditional forms such as taxi, car rentals and public transport [18] and expands through the diffusion of new business models and concepts. In this perspective, the growing development of new forms of one-way mobility or free-floating car sharing is spreading in Europe and America [19]. Car sharing generates benefits for the community and for certain population groups, such as young people who do not own a car [20]. Indeed, this service allows journeys to be made without a need to purchase a vehicle [21]. Moreover, the diffusion of car sharing service implements a mitigation intervention regarding the dependence on private cars, with economic and environmental impacts as well as potential health benefits that can be obtained from this emerging mode of transport [22-23].

Currently, many systems are adopting electric vehicles that require charging only when battery levels drop below a certain value. In order to improve the service, in accordance with [24], a model was evaluated which considers the assignment of cars to charging stations and the path of staff and service vehicles by optimising the service.

Consequently, to promote a more sustainable development of urban areas characterised by expansion of university centres, it is considered that the diffusion of the shared transport service, in parallel with the diffusion of the public transport service, can improve travel, especially when the student population is almost represented by foreign students or commuters. The attributes of potential users of this system have been studied in this research in order to maximise its effectiveness. A survey of a number of attributes was conducted in order to know and model the propensity of university students to join the car sharing. Mixed data collected from Internet and paper surveys were used to understand the preferences of early adopters for this shared transport service and to assess the subsequent extension of the service to the whole population.

Furthermore, through a before and after analysis, it was possible to compare the results of the survey following the implementation of the car sharing service and influences that this had on the opinions of the interviewees.

The document is divided into 4 sections: Section 2 with the analysis of literature on the evolution of the shared transport system and demand modelling analysis; in Section 3 is defined the sample acquisition methods and the statistical analysis methodology used; in Section 4 the results are compared and finally conclusions and evolutionary hints of this research are provided in Section 5.

2 Literature review: the sustainability of car sharing services implementation

Compared to the last decade, Europe is experiencing a positive development of car sharing in terms of number of cars and number of users. At present, Europe represents around 50 % of the global car sharing market and is expected to reach 15 million users by 2020.

Europe highlights that car sharing is popular in cities with a high level of education or university presence and, in cities where business-to-consumer (B2C) takes place and in cities where there are many people with green ideals and ecologists [25]. In addition, the car sharing is getting less choice in cities where there are many automotive commuters. The introduction of innovative mobility services, such as car sharing, leads to changes in users' travel habits, inducing a shift in travel demand from existing travel arrangements. An analysis of these changes should be performed to promote the car sharing, effectively managing the travel demand.

The recent pandemic has altered the travel habits of users due to both restrictions and the growing fear of contagion [26-27]. The months following the lockdown (March-May 2020) were characterised by an increase in the use of private vehicles, reducing the successes of the decarbonisation campaigns implemented prior to the pandemic [28]. Some categories of users such as students and workers have reduced travel from March to December 2020 due to distance learning and teleworking [29]. A small number of studies have considered future compulsory student travel, which constitutes a large part of daily travel and is crucial for the development of a society, by analysing available travel alternatives and specific risk mitigation measures on vehicles, as well as the promotion of shared or alternative mobility [30].

The variables investigated in this manuscript allow to lay the foundations for an improvement of the service in the post-pandemic phase: in fact, it is known that the car sharing offers a way to stay on the move while maintaining distance during the Coronavirus pandemic, especially without an own car. It also offers the possibility of having one's own car at short notice, without the financial commitment of owning one. This service is optimal for areas, such as the one examined, where the weather conditions together with the high slopes do not allow one to move easily on foot and/or by bicycle. To identify the travel attributes that affect the intention to switch to car sharing, estimates can be used through the decision trees for each mode of transport. In fact, in accordance with [31], it is clear that the threshold values of each variable that induce a modal shift are specific to the mode and therefore provide better information useful for calibrating the best political and economic actions aimed at increasing the benefits of car sharing. The social component, defined by students and in particular by those who attend universities, in general is very receptive to the concept of sharing economy and therefore university students are recognized as a potential group of customers for car sharing operators.

A study focusing on Belgrade university students reveals that the student population has provided a homogeneous response regarding critical aspects of service adoption such as costs, distance from vehicles and convenience of parking. Specific attributes, such as the pricing scheme and vehicle cleaning, are particularly interesting problems in the study market [32].

Some universities in California offer commuter students free use of shared vehicles across campus for a certain period of time, so car-sharing is very popular with bus commuters, college students and women employees [33]. In order to improve the car sharing transport offer for university students it is necessary to consider a series of socio-economic variables, but it is also important to understand both the unique characteristics of academic institutions such as markets for car sharing and the ways to predict the university demand for car sharing services.

The design of a balanced survey, hard-copy and online format, allows researchers to investigate the transport habits and car sharing preferences of university affiliates and the propensity to use the car sharing service. Studies prepared over the past decade showed that the status of an interviewee at the university (e.g. faculty, student or staff) had a strong influence on individual acceptance of car-sharing, even more so than the socioeconomic variables, such as income or property. Vehicles and people's attitudes play an important role in their decision making [23]. Different types of the car sharing services affect the travel behaviour (choice and frequency) and this depends on the type of user. Several factors have changed the travel habits and modal choices over time, e.g. the recent COVID-19 pandemic or the spread of Mobility as a Service (MaaS) platforms.

Several studies in the literature show such trends through before-and-after modelling; in particular, according to [34] the sustainability of shared mobility in the post-pandemic phase has been considered through two levels: at the level of travel behaviour and at the level of urban infrastructure. In contrast, research conducted by [35] investigated the effects of car sharing by considering trends in transport-related emissions at the individual and city level.

With regard to bivariate modelling, a research focused on the city of Turin focused on estimation of cars haring services, estimating the propensity to have a car sharing subscription and substitution patterns between different means of transport for a representative sample of trips made by the population of Turin through the bivariate models [36].

In agreement with [37] an ordered bivariate profit model was implemented to better understand the influence of various exogenous socioeconomic and demographic variables on the frequency of use of ride-sourcing and car-sharing services.

This work is focused on a correlation of variables related to location of the sample's place of residence (distance) by relating this variable to the concept of car-sharing utility and fare selection. The results made it possible to combine the socio-demographic or purely user-specific aspects with typical characteristics of the pricing of the service and the interconnected distance between the places of residence/work and the car parks where the shared cars are parked.

3 Materials and methods

The methodological framework of the research is represented in Figure 1.

First of all, a survey was carried out in order to retrieve a number of information and measures. Then, the obtained data were processed and analyzed through a statistical bivariate analysis (the first step) and a before and after analysis (the second step).

In the first part of the analysis, after the definition of main and secondary variables, the computational procedure for the assessment of multiple dependence or independence between variables was characterised by six steps, including primarily the calculation of the Cronbach alpha.

Subsequently, in the second step, the survey was re-proposed and statistical tests were implemented, i.e. Wilcoxon and Friedmann, by comparing the "before" and "after" answers. Moreover, judgement criteria were identified based on which the percentages of variation in the opinions of the interviewed users were assessed.

The following subsections provide more details on the methodological aspects regarding the structuring and implementation of the questionnaire and the performed statistical analysis.

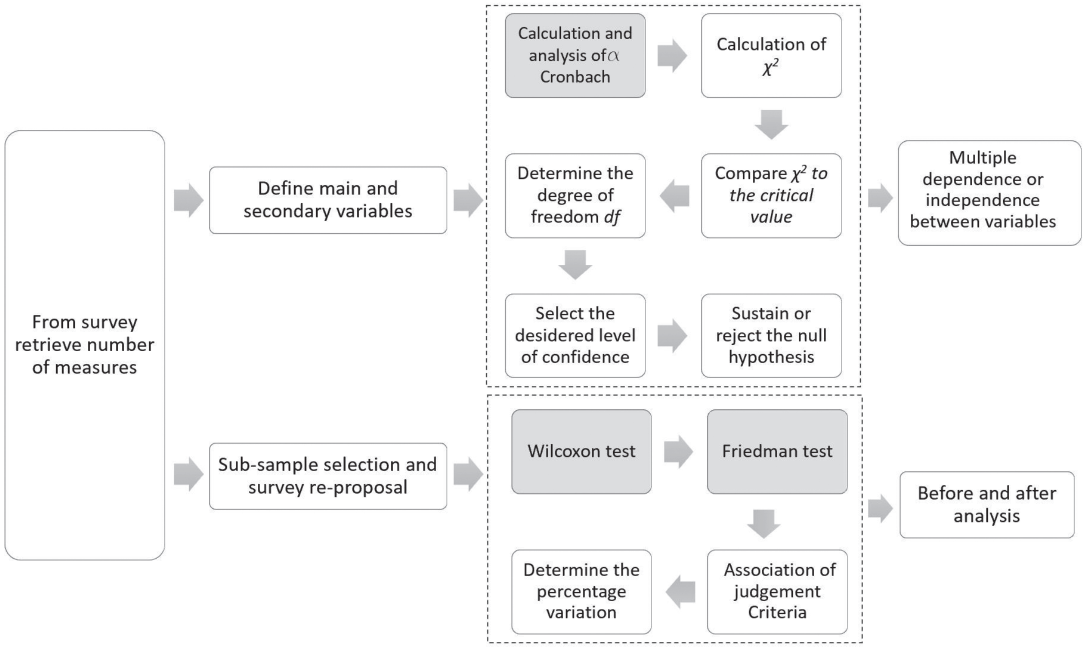

***Figure 1** Methodological framework*

3.1 Questionnaire design and data collection

The questionnaire was structured in four sections, investigating different variables:

- the first section was related to socio-demographic data (i.e. gender, age, car and driver licence ownership; attended university);
- the second one was linked to geographical information (i.e. residence and domicile);
- the third section investigated the travel behaviour (i.e. transport modes for home/school and home/leisure trips; bus use frequency);
- the fourth section analysed the shared mobility experience. This last section investigated previous experiences linked to car sharing (e.g. in Italy; abroad with electric or hybrid vehicles); the propensity to use alternative vehicle power supply; and aspects related to the car sharing service (i.e. way of reservation; rate; service subscription). Finally, the experience and propensity to use the implemented car sharing service in the case study area were evaluated.

The questionnaire was drawn up considering different types of approach to the response, that is, through both Internet and paper surveys and a single, multiple or Likert scale response. The rating system of Likert scale [38-39] was used to structure answers in ordered scale (e.g. "absolutely no", "absolutely yes" for answering the question about the proposal of a new car sharing service), wherever it was possible, in order to assess the subject's perception.

The sample was characterized by a specific group of users consisting of university students. The size of the sample can be considered significant, as it is representative of almost the entire student population. Furthermore, a sub-sample was randomly selected and was subjected to a double investigation before and after the advent of the car sharing service in the study area.

3.2 Bivariate analysis

A bidimensional or bivariate analysis was developed to study the influence of different variables in joint car sharing service, from a sustainable perspective.

The main variables, related to economic, environmental and social points of view, were associated with several secondary variables and Pearson's chi squared test was calculated considering pairs of these variables [40-41]. Selected variables included three major aspects: influence of socio-demographic data (e.g. gender; car ownership), travel behaviour (e.g. transportation mode for daily trips) and attributes related to experiences with car sharing and willingness to join it (e.g. car sharing experience in Italy and abroad; rate selection; car sharing utility). Specifically, three main variables were associated to each combined correlation with several secondary variables, as reported in Table 1.

The concept of probabilistic independence on which this study was based is represented by the following assumptions:

$$H_0: P(AB) = P(A) \times P(B), \quad (1)$$

$$H_1: P(AB) \neq P(A) \times P(B), \quad (2)$$

where:

- H_0 is the null hypothesis;
- H_1 is the alternative hypothesis;
- A and B the two correlated variables.

***Table 1** Bivariate attributes and specific correlations between main and secondary variables*

Correlation	Main variables	Secondary variables
C1- 1		1 - Mode of transport for home/school
C1- 2	1. Place of residence (Distance)	2 - Mode of transport for home/leisure
C1- 3		3 - Car ownership
C2- 1		1 - Gender
C2- 2		2 - Car ownership
C2- 3		3 - Place of residence (Distance)
C2- 4	2. Car Sharing utility	4 - Mode of transport for home/school
C2- 5		5 - Mode of transport for home leisure
C2- 6		6 - Car sharing experience in Italy
C2- 7		7 - Car sharing experience abroad
C3- 1		1 - Gender
C3- 2		2 - Place of residence (Distance)
C3- 3		3 - Mode of transport for home/school
C3- 4	3. Rate selection	4 - Mode of transport for home/leisure
C3- 5		5 - Car sharing experience in Italy
C3- 6		6 - Car sharing experience abroad
C3- 7		7 - Car Sharing utility

To test the association between the two categorical variables and verify the null hypothesis H_0 that the samples are independent, the data were organized in a table of contingency g x k, a chi-square χ^2 was derived from:

$$\chi^2 = \sum_{i=1}^{g} \sum_{j=1}^{k} \frac{(n_{ij} - E_{ij})^2}{E_{ij}} = \sum_{i=1}^{g} \sum_{j=1}^{k} \frac{n_{ij}^2}{E_{ij}} - n, \qquad (3)$$

with $n = \sum_{i=1}^{g} \sum_{j=1}^{k} n_{ij} = \sum_{i=1}^{g} \sum_{j=1}^{k} E_{ij}$

where:

- n_{ij} is the number of observed cases in sample j and which correspond to the i-th mode;
- E_{ij} is the number of expected cases in sample j and for the i-th mode if H_0 is true;
- g is the number of modes in which the main variable is expressed;
- n it is the number of all the samples put together.

Due to the hypothesis of independence of the samples, the number of expected cases was calculated with:

$$E_{ij} = \frac{n_{.j} n_{i.}}{n}, \qquad (4)$$

with:

- $n_{.j} = \sum_{i=1}^{g} n_{ij}$ is the marginal frequency for each of the g modes;
- $n_{i.} = \sum_{j=1}^{k} n_{ij}$ is the number of each sample.

Before calculating the chi-square χ^2, the Cronbach alpha was calculated for each correlation, in order to measure the internal reliability of the questionnaire, Equation (5), [42], with particular reference to the quantitative variables (or items) and using the Likert scale:

$$\alpha = K \cdot \frac{\underline{r}}{1 + (K+1) \cdot \underline{r}}, \qquad (5)$$

where:

- K is the number of items;
- $\underline{r}$ represents the mean of the correlations.

The formulation has been adapted for the case of dichotomous variables (or items), as follows:

$$\alpha = \frac{K}{K-1} \cdot \left[1 - \frac{\sum p \cdot q}{\sigma_t^2}\right], \qquad (6)$$

where:

- K is the number of items;
- p is the proportion of items with coding equal to 1;
- $q = 1 - p$;
- σ_t^2 is the variance.

3.3 Before and after analysis

The before-and-after analysis (B/A analysis) constituted of a non-experimental design, which is very suitable for the purposes of this study, since it is a reasonable option for an evaluation to provide preliminary evidence for an intervention effectiveness [43-44].

Specifically, in this study a B/A analysis of this type "OXO" was applied to assess the level of causality of the two measurements Oi and Oj having in the middle the introduction of the intervention X, i.e. the implementation of the car sharing service in the study area. The percentage of response variation before and after the intervention was calculated and it was compared to a judgement criterion associated with each variable, to be able to assign a negative or positive value, from a multiple perspective (i.e. economic, social and environmental).

Additionally, since the statistical analyzed sub-sample for the B/A analysis was derived from the same group population, the Wilcoxon non-parametric test was applied to verify, in the presence of ordinal values with a continuous distribution, if the judgments undergo a variation following implementation of the intervention X. The test involved calculating the statistical variable U, which has a distribution under the null hypothesis determined by the following equation:

$$U_1 = R_1 - \frac{n_1(n_1+1)}{2}, \quad (7)$$

where:

- n_1 is the sample dimension of the sample interviewed before the intervention X;
- R_1 is the sum of the ranks in the mentioned sample;

Similarly, the statistic variable U_2 was calculated for the sample interviewed after the implementation of intervention X. The smallest value of U_1 and U_2 was used for consulting the significance tables and performing the Wilcoxon test.

3.4 Study area: the car sharing service of Enna city

The analysed area focuses on the municipality of Enna characterised by the presence of 27.000 inhabitants and around 5300 students from two universities respectively Kore University of Enna (about 4800 enrolled) and Dunarea de Jos Galati (about 500 enrolled) in 2020. The city is distributed along three macro areas called Enna Alta, Enna Bassa and Pergusa (Figure 2).

The road infrastructures are mostly classified by local roads without preferential lanes. At present there is no bike sharing service but since 2019 a car sharing service has been activated by the company titled Amat Palermo. The service is provided from 06:00 to 22:30 on weekdays and from 07:00 to 23:00 on holidays every 30 minutes. In April 2019 the city inaugurated a car sharing service with the presence of 6 cars and a minivan.

There are two bus terminals located respectively in Enna Alta and one in Enna Bassa near the universities. There is a taxi service little used by residents due to the high costs.

The Kore University of Enna is located in the centre of Enna Bassa and the surrounding areas are populated by residential neighbourhoods mostly inhabited by university students and commercial activities such as shops and supermarkets (Figure 3). The majority of the student population is commuting while the remaining part has rented, or owned houses scattered in the three ones defined above.

AmiGO is the car sharing service in the Sicilian Region, supplementing public and private transport, intelligent, economic and respectful of the environment. In Enna it has been started for less than a year and provides for the facilitation of travel to and from the areas of the historic centre where many primary schools, banks and offices are located, Enna Bassa, a place of schools and universities and the tourist area of Pergusa (Figure 4). The service is intended as an alternative to use of the private vehicles and provides for the sharing of a car park with low environmental impact among all the registered citizens, limiting the use of the car to the time strictly necessary.

4 Results and discussion

4.1 Statistical analysis results

From May 2018 to January 2020, five investigation campaigns were launched, which involved the paper and online administration of a total of 704 surveys. The investigated population was entirely related to the Kore University with a gender distribution of 48% males and 52% females with an average age between 24 and 29 years (63 %).

After the first part of the survey, related to socio-demographic analysis, the possible itineraries made by the university students for home/school and home/leisure reasons were monitored, considering the location of the different houses and the location of each Faculty of the University of Enna Kore. It has been estimated

***Figure 2** Enna landscape and an overview of Enna Alta, Bassa and Pergusa*

Figure 3 *An overview of Enna Bassa where the University of Enna Kore and relative distribution of each Faculty*

Figure 4 *Dedicated AmiGo parking area and car sharing service in Enna*

that around 62% of the population lives in the district of university faculties located in Enna Bassa (within 1 km), 32% in Enna Alta (considering also cities with similar distance) and 6% in Pergusa. The latter two are respectively 5km and over 6km away from the university area.

The geo-localisation of the University of Enna Kore is barycentric with respect to the area of Enna Bassa and the three districts that characterise it are about 700m from each other. Students are uniformly distributed in the various faculties, i.e. 51% of students attend the Faculty of Psychology and Sociology, 25% attend Engineering and Architecture courses, while the remaining 28% are divided between economics and law studies.

The second part of the questionnaire focused on the driving licence possession and on the use of alternative transport modes, i.e. the frequency of public transport or the propensity to go on foot. In particular, a high percentage of students have a driving licence (over 98% and 51% for over five years). However, a good percentage of them use public transport (41%) or walk (26%) to go to university. Considering home/leisure itinerary, the percentage of car use increases (43%) because the public transport service is active until 10 pm. It is impossible to reach Enna Alta and Bassa on foot due to the high slope and the absence of pavements on many road sections. The third part of the questionnaire allowed to acquire information on the previous experience of the car sharing service (47% in Italy and 26% abroad) and therefore studied the propensity to use it (72% of students thought it very useful to set up a car sharing service).

A part of the sample (about 10% of the entire sample randomly selected) was doubly interviewed and on the completed questionnaires it was possible to implement a before and after analysis. The aggregate results of the individual attributes show almost total interest in the provision of a car sharing system dedicated to students and this result is consistent with those obtained for the attributes relating to the previous experience of car sharing services and willingness to pay for use of this service, distinguishing between low (65 %), medium (28%) and high (7%) rates. This corresponds to use of the small two-seater vehicles in the first case and small vehicles in the second. These choices are supported by Enna's morphology referring to the narrow streets of the historic centre.

4.2 Bivariate analysis results

In order to schematically summarise the obtained results, the Cronbach alpha and the chi-square values for each studied correlation are shown in Table 2. It emerged that in most cases the items are highly

Table 2 *Bivariate attributes and correlations between main and secondary variables*

Correlation	αCronbach	χ^2	p < .01	p < .05	p < .001
C1- 1	0.7691	17.8043	Sign	Sign	Sign
C1- 2	0.6125	13.3779	Sign	Sign	Sign
C1- 3	α < 0.3	6.6885	.0352	Sign	Sign
C2- 1	0.4 < α <0.6	12.8139	Sign	Sign	Sign
C2- 2	0.8467	27.6656	Sign	Sign	Sign
C2- 3	0.6762	11.4428	.0220	Sign	Sign
C2- 4	0.7795	9.1079	.0584	.0584	Sign
C2- 5	α < 0.3	64.6379	Sign	Sign	Sign
C2- 6	0.8194	15.5678	Sign	Sign	Sign
C2- 7	0.6771	17.6167	Sign	Sign	Sign
C3- 1	0.4 < α <0.6	7.56	.02282	Sign	Sign
C3- 2	0.7504	2.5099	.6428	.6428	.6428
C3- 3	0.4 < α <0.6	23.7965	Sign	Sign	Sign
C3- 4	0.4 < α <0.6	32.4531	Sign	Sign	Sign
C3- 5	0.8309	12.6495	Sign	Sign	Sign
C3- 6	0.6645	4.4359	.1088	.1088	.1088
C3- 7	0.7081	14.6545	Sign	Sign	Sign

correlated with each other, as there is a high internal consistency having obtained Cronbach alpha values higher than 0.60, which represent a good level of consistency. In some correlations, the range of variation is between 0.4 and 0.6 and this indicates a tentative and possible consistency. Therefore, it is possible to affirm that each question makes a real contribution to the measure of the construct.

However, the Cronbach alpha represents an indicator to measure the reliability and verify the reproducibility over time. Thus, in the cases of values from 0.4 downwards, this indicates that these correlations are not reproducible over time under the same conditions. The lower reliability in the case study was verified for the correlations corresponding to place of residence (distance) with car ownership. In fact, the results may vary over time if, for example, the user no longer owns a car or vice versa buys a new one. A similar phenomenon was also observed in the case of the correlation between car sharing utility and mode of transport for home/leisure, because evidently it is the shared mode of travel that is more considered by the examined users to go to school or work. Furthermore, since it is a large sample of students, not having a high financial availability, it is possible that they prefer to travel by private car (own or family car) or walking. In particular, in Enna Bassa, the entertainment venues are almost all close to the student residences.

The obtained results for the chi-square are discussed for each analysed main variable.

4.2.1 Place of residence (distance)

The first correlations were referred to the place of residence, which is likely related to the distance travelled during the daily trips. In this case, the city macro-areas and the neighbourhoods were grouped into three categories: a short-travelled distance (i.e. Santa Lucia; Ferrante and Enna Bassa); a medium-travelled distance (i.e. Monte; Lombardia and Enna Alta) and a long-travelled distance (i.e. Pergusa and other locations). It was considered useful to correlate this variable with the transport modes, both for home-school trips and home-leisure trips, in order to understand which mode is chosen by students according to the travelled distance. In addition, car ownership was also taken into account. By analysing the tables of contingency for each of these correlations, it was possible to observe that over 63% of students travel for a short distance, but they were almost equally distributed among the three considered modes, that is, walking, public and private transport. For longer distances, a very small percentage of students walking was obtained; however, those who use the bus were more than double compared to those who use the private car. This denotes good sustainable travel behaviour. Slightly different considerations were found in the case of home/leisure trips: in fact, a good percentage of walkability was registered, equal to 31% of the total; however, at the same time, an increase in the number of trips by car was noted to the detriment of those made by bus. This is consistent with the fact that greater flexibility is required for home-leisure trips, but this also indicates a lack of public transport service to support demand mobility. Finally, it was observed that the number of trips for short, medium and long distances was very similar both in the case of car ownership and no-ownership.

The results associated with the bivariate analysis, with respect to this first main variable, were coherent for the three correlations and allowed to assume a hypothesis of independence between the variables, except in the case of the last correlation, for which there is a dependency at $p < 0.01$ (see Table 3).

4.2.2 Car sharing utility

Evaluation of propensity to join the car sharing was assessed in the opinion of students about the utility associated with the service. Students expressed a rating on a Likert scale from 1 to 5 based on how useful a car sharing service dedicated to Enna's students can be. The analysed correlations with this main variable took into account different aspects relating to socio-demographic data; travel behaviour and car sharing experience.

For the examined sample, equally distributed between men and women, it was not observed a specific propensity for car sharing based on gender. In general, the students' opinions regarding the usefulness of a car sharing service were very positive. The maximum value of 5 was selected in more than 70% of cases and for this reason it was chosen to analyse correlations considering the utility values from 3 to 5. Non-car owners showed a greater propensity towards car sharing, attributing a higher utility rating. The distance also influenced car sharing service, which was deemed proportionally useful up to 4 times more in the case of medium distances than the short ones. As regards the transport modes used for daily trips, higher utility values associated with car sharing were obtained by those who walk, especially in the case of home-leisure trips, which need more flexibility. Through the calculation of the chi-square, a dependence from the variables of a distance and transport mode was found (for $p < 0.01$ and $p < 0.05$) and so they influence reciprocally with the main variable. Finally, any previous experience of using car sharing was taken into consideration, both in Italy and abroad. Certainly, a positive aspect was represented by the fact that almost 50% of the interviewed sample had already used a car sharing service. This percentage rises in the case of experiences abroad. However, the same utility values were also attributed by those who have not yet experienced this service.

4.2.3 Rate selection

The last analysed main variable was the rate selected by students for car sharing service, which in a certain way is representative of the willingness to pay to use this service. The correlations taken into consideration were similar and the influence that the utility, associated with the car sharing service, may have on the willingness to pay a certain rate, was assessed, as well.

The rate was set in three different ranges (i.e. low, medium and high), depending on the service characteristics and on operational attributes (for example the displacement of the vehicle used, the type of power supply, etc.). Considering that, for all the correlations the highest percentage of responses was concentrated in correspondence with the low rate values. It emerged that women were more willing to pay an eventual medium rate to use the service. Analysing the correlation with the distance, from the calculated table of contingency it was possible to observe that as the travel distance increases, the willingness to pay a higher rate decreases, because the total cost of the service is greater due to the increasing number of kilometres. As regards the attribute linked to travel behaviour, represented by the transport mode, it was registered as a willingness to pay a medium rate one third less than a low rate by students travelling by car; for those who walk, this percentage is only reduced by half. In addition, in this case, the willingness to pay for using a car sharing service was demonstrated in the same way by students without previous experience of using car sharing. In the end, from the last correlation it clearly emerged that utilities with a value of 5 were associated with higher percentages of potential increases of the rate, since the utility associated with the car sharing is greater and, therefore, they are willing to pay more.

4.3 Before and after analysis results

A selected group was interviewed the first time before the implementation of car sharing in Enna and the second time after a period of approximately one year after the activation of the service. The before and after analysis (B/A) was based on the comparison of data obtained by dispensing the questionnaire both before and after the car sharing service implementation in Enna (mentioned in the methodology section as intervention "X").

The Wilcoxon test was performed considering the three variables related to: (i) the car sharing utility; (ii) the willingness to pay and thus the rate of the service; (iii) the recommendation of the car sharing service. The results of the statistical test are reported in Table 3.

Since the test proves non-significance, then it can be argued that the null hypothesis cannot be rejected. This implies that the randomly selected values of the items associated to the population interviewed before the implementation of the car sharing service is assumed to be equal to the randomly selected values of the items associated to the population interviewed after implementing the intervention.

The results indicate a measure of how similar the random sample is and how close it is to the entire population. Therefore, the judgments of the considered sub-sample, both before and after the implementation of the service, remain almost similar considering the three examined variables. In fact, the students interviewed have shown that they tend to use alternative and less polluting forms of mobility regardless of the

Table 3 *Wilcoxon test results*

Items	p-value	Z	p < .01	p < .05	p < .10
Utility	0.06619	-1.8371	Not Sign	Not Sign	Not Sign
Rate	0.127	1.5259	Not Sign	Not Sign	Not Sign
Recommendation	0.272	-1.0984	Not Sign	Not Sign	Not Sign

Table 4 *Percentage variation of B/A analysis and criteria evaluation*

B/A variables	Percentage variation %	Criteria
Place of residence	11	Travel distance
mode of transport for home / school	14	Sustainability
mode of transport for home / leisure	2	Sustainability
Bus use frequency	0	Sustainability
Car sharing experience in Italy	0	Increasing experience
Car sharing experience abroad	5	Increasing experience
Electric/hybrid vehicle experience	4	Technological Innovation
Propensity to use electric/hybrid vehicles	0	Technological Innovation
Car Sharing utility	11	Willingness
Car sharing reservation methods	0	Innovation
Main reason for using car sharing	2	Motivation Convenience
Rate selection	16	Willingness to pay
Service subscription	8	Customer; Loyalty

implementation of these shared service types. This evidence could be partly attributed to the fact that there is a widespread participation in dissemination campaigns and surveys regarding shared mobility. Furthermore, even the preventive planning actions by the local government in the context of SUMPs can trigger the propensity to use these forms of mobility [45].

With regard to the B/A analysis, almost all of the significant variables reported in the investigation were subject to the B/A analysis and specifically the percentage of response variation was calculated. This percentage was compared to a judgement criterion associated with each variable, so as to be able to assign a negative or positive judgement to the variation, from a multiple perspective. Table 4 shows the results of the B/A analysis highlighting the aspects and variables most sensitive to the introduction of the car sharing service in Enna:

As regards the place of residence, there was a total variation of 11%. The real appreciable variation of this variable, if analysed with respect to the "travel distance" criteria, can be reduced to 3% since the other residence displacements concerned the two neighbourhoods of Ferrante and Santa Lucia, which are quite close between them and therefore comparable. Therefore, no major changes from this point of view are appreciable.

Another significant variable related-to the mode of transport, both for home/school and home/leisure daily trips. In this case, an overall variation of 14% was obtained. In detail, for home/school 7% stopped using the bus and started walking and 3% changed mode of transport from private car to bus, while the remaining percentage started using the car or the bus instead of walking. Considering the sustainability criteria, a positive variation of this variable can be assumed. With reference to home/leisure trips, a positive percentage variation of 2% was obtained. No variation was obtained with respect to the bus use frequency.

Evaluating the sharing mobility experience, the percentage variation related to car sharing experience in Italy is zero, but considering experience abroad it was registered an increase of 5%, which represents a positive aspect as this could lead to a greater propensity to use the car sharing service implemented at Enna.

Concerning the experience of using electric or hybrid vehicles, there was registered an increase of 4% in favour of these new innovative forms of alimentation. No variation was observed relating to the willingness to use an electric or hybrid car sharing service.

An important aspect is represented by the value associated with the usefulness of a dedicated university car sharing service.

As a matter of fact, by comparing the answers obtained before and after the implementation of the car sharing service in Enna, there was a response percentage variation equal to 11%. This would seem to suggest that student opinion has changed. However, this can be denied because analysing in detail the answers, it was a variation of the utility judgement, which varied between the values of 4 and 5 on the Likert scale. In fact, there was a 5% variation from value 5 to value 4 and a 6% from 4 to 5. So, it can be said that there was no change in thinking of students that could affect the willingness to use the car sharing service. Moreover, the preferred way of reservation represented for the majority by the use of an APP has not undergone changes. Instead, only 2% of response variation was registered in the motivation to use car sharing. In this case, this variation derives from a change in the convenience of using car sharing, first associated with flexibility and subsequently with an economic aspect. Therefore, it was possible to attribute a slightly negative judgement, as the economic aspect is prevailing the idea of the availability of a vehicle that allows you to move more flexibly, instead of owning a car. This consideration was also found in the subsequent significant variable analysed, that was the rate selection for car sharing service. The total percentage variation is equal to 16% and specifically 13% corresponds to a declaration of intent to pay less, moving from a high to medium rate, or from medium to low rate. This negatively affects the willingness to pay for the car sharing service.

In a certain way, a similar consideration made for the car sharing can be associated with the variable linked to the kind of typology service subscription to car sharing. In fact, the response variation of 8% can be considered null as the number of students who expressed a preference for non-subscription is the same as the number that expressed a change in favour of activating a subscription.

A final consideration that can be made in relation to this B/A analysis is that, by performing a cross-observation of the response variation before and after the implementation of car sharing and of the experience related to amiGO, half of these observed variations derived from users of the service. Therefore, any kind of recorded change is only partially attributable to a direct experience of the car sharing service.

5 Conclusion

Car sharing services play an active role in keeping congestion at bay by meeting the current short-term demand for private cars. As long as people have the possibility to share a car, they will be more likely to continue using the public transport in the future. Therefore, it is important to analyse how certain factors increased or decreased the propensity to use car sharing in the pre-pandemic phase in order to understand the correlation between the variables analysed and those arising from the pandemic and to be able to optimise the service.

This work was focused on evaluating the implementation of a car sharing service in the city of Enna, involving students through a large consultation survey featuring mixed data from Internet/paper surveys. The results made it possible to analyse students' propensity to use the shared mobility and to provide an opinion on the current car sharing service implemented by the Municipality of Enna in collaboration with a transport company. A detailed analysis was performed, segmenting the sample, in order to study the heterogeneity of preferences and model the propensity to the car sharing.

The data processing took place through a bivariate statistical analysis and through a before and after method on a portion of the sample investigated. The Cronbach alpha computation was used in order to measure the internal reliability of the questionnaire. Then, the chi-square test was calculated to analyse different combinations of attributes and their correlations. Different combinations of the socio-demographic parameters, experience with shared mobility and the propensity to use a university car sharing service have been taken into consideration. Moreover, a non-parametric test (i.e. Wilcoxon test) was performed and through the B/A analysis it was possible to investigate the judgement of the student population regarding the service implemented in Enna.

Based on the research on the transfer model of the optimization of the future car sharing service implemented in Enna, this document has reached the following conclusions:

- a lack of public transport service to support mobility demand can generate a greater propensity to use private cars for daily trips, especially in the case of home-leisure trips, which need more flexibility. In this context, a car sharing service could help to make the journeys more sustainable, without necessity to own a car;
- despite having carried out an extensive investigation campaign, there seems to be no high gender influence in the analysed correlations. However, it would be interesting to deepen this aspect with reference to other case studies;
- previous experiences of using car sharing can influence a greater propensity to join this service. Since the analysed sample is represented by students (high percentage of 18-30 years old), it is possible to affirm that a young age group tends to be more willing to try a new experience, in this case a shared mobility service;
- the highest percentage of responses was concentrated in correspondence with the low rate values associated with car sharing services. It would be interesting to investigate the willingness to pay with reference to the service characteristics and on operational attributes. Furthermore, to encourage the use of car sharing, it would be useful to propose discounted rates for students, also depending on the travelled distance.

The analysis conducted and the selection of the variables analysed allowed evaluation of possible correlations and mutual influences, paving the way for recalibrating the implemented service. It also lays the groundwork for future phases of the research that will consider multiple simultaneous correlations with a multinomial logit analysis. The obtained results from this research highlight some of the factors that optimise the propensity to use car sharing by the student population in the area examined. These results can be implemented and optimised by investigating more variables or by comparing different target groups such as millennials. This approach allows to highlight that the motivation for a stable participation (for a longer period of time) and the collaboration of the user samples is essential to obtain useful results in the process of service optimisation. Through this strategy and the related survey steps both experts and non-experts represent different and often complementary perspectives. The research findings could also be useful for local authorities, university managers and managers of shared mobility services to control the part of the travel demand.

Data availability statement

Some or all data, models, or code generated or used during the study are available from the corresponding authors by request.

References

[1] SHAHEEN, S., COHEN, A., CHAN, N., BANSAL, A. Sharing strategies: cars haring, shared micro mobility (bike sharing and scooter sharing), transportation network companies, micro transit and other innovative mobility modes. In: *Transportation, land use and environmental planning*. DEAKIN, E. 1. ed. Elsevier, 2020. ISBN 9780128151679, p. 237-262.

[2] LIAO, F., CORREIA, G. Electric car sharing and micro mobility: a literature review on their usage pattern, demand and potential impacts. *International Journal of Sustainable Transportation* [online]. 2022, **16**(3), p. 269-286. ISSN 1556-8318, eISSN 1556-8334. Available from: https://doi.org/10.1080/15568318.2020.1861394

[3] HENSHER, D. A., MULLEY, C., HO, C., WONG, Y., SMITH, G., NELSON, J. D. *Understanding mobility as a service (MaaS): past, present and future*. 1. ed. Elsevier, 2020. ISBN 9780128200445.

[4] CAMPISI, T., BASBAS, S., SKOUFAS, A., AKGUN, N., TICALI, D., TESORIERE, G. The impact of COVID-19 pandemic on the resilience of sustainable mobility in Sicily. *Sustainability* [online]. 2020, **12**(21), 8829. eISSN 2071-1050. Available from: https://doi.org/10.3390/su12218829

[5] TORRISI, V., IGNACCOLO, M., INTURRI, G. Estimating travel time reliability in urban areas through a dynamic simulation model. *Transportation Research Procedia* [online]. 2017, **27**, p. 857-864. ISSN 2352-1465. Available from: https://doi.org/10.1016/j.trpro.2017.12.134

[6] TORRISI, V., IGNACCOLO, M., INTURRI, G. Analysis of road urban transport network capacity through a dynamic assignment model: validation of different measurement methods. *Transportation Research Procedia* [online]. 2017, **27**, p. 1026-1033. ISSN 2352-1465. Available from: https://doi.org/10.1016/j.trpro.2017.12.135

[7] HELFERT, M., KLEIN, C., DONNELLAN, B., GUSIKHIN, O. (Eds.). Smart cities, green technologies and intelligent transport systems. In: 8th International Conference, SMARTGREENS 2019 and 5th International Conference VEHITS 2019: proceedings. Vol. 1217. Revised selected papers. Springer Nature: 2021. ISBN 978-3-030-68028-2.

[8] EFTHYMIOU, D., CHANIOTAKIS, E., ANTONIOU, C. Factors affecting the adoption of vehicle sharing systems. In: *Demand for emerging transportation systems: modelling adoption, satisfaction and mobility patterns*. ANTONIOU, C., EFTHYMIOU, D., CHANIOTAKIS, E. (Eds.). 1. ed. Elsevier, 2019. ISBN 9780128150184.

[9] SANDERS, E.B.-N., STAPPERS, P.J. "Co-creation and the new landscapes of design". *CoDesign* [online]. 2008, **4**(1), p. 5-18. ISSN 1571-0882, eISSN 1745-3755. Available from: https://doi.org/10.1080/15710880701875068

[10] DUDAU, A., GLENNON, R. VERSCHUERE, B. Following the yellow brick road? (dis)enchantment with co-design, co-production and value co-creation in public services. *Public Management Review* [online]. 2019, **21**(11), p. 1577-1594. ISSN 1471-9037, eISSN 1471-9045. Available from: https://doi.org/10.1080/14719037.2019.1653604

[11] LUSCH, R. F. Service - dominant logic of marketing. Reactions, reflections, reflections and refinements. *Marketing Theory* [online]. 2006, **6**(3), p. 281-288. ISSN 1470-5931, eISSN 1741-301X. Available from: https://doi.org/10.1177/1470593106066781

[12] VARGO, S. L., LUSCH, R. F. Service-dominant logic: continuing the evolution. *Journal of the Academy of Marketing Science* [online]. 2008, **36**(1), p. 1-10. ISSN 0092-0703, eISSN 1552-7824. Available from: https://doi.org/10.1007/s11747-007-0069-6

[13] GARAU, C. Focus on citizens: public engagement with online and face-to-face participation - a case study. *Future Internet* [online]. 2012, **4**(2), p. 592-606. ISSN 1999-5903. Available from: https://doi.org/10.3390/fi4020592

[14] GARAU, C. Citizen participation in public planning: a literature review. *International Journal of Sciences*. 2012, **1**(12), p. 21-44. ISSN 2305-3925.
[15] GARAU, C. *Plan and participation processes / Processi di piano e partecipazione* (in Italian). Rome: Gangemi Editore Spa, 2013. ISBN 8849226497.
[16] ATASOY, B., AZEVEDO, C. M. L., AKKINEPALLY, A. P., SESHADRI, R., ZHAO, F., ABOU-ZEID, M. SMART mobility via prediction, optimization and personalization. In: *Demand for emerging transportation systems: modelling adoption, satisfaction and mobility patterns*. ANTONIOU, C., EFTHYMIOU, D., CHANIOTAKIS, E. (Eds.). 1. ed. Elsevier, 2019. ISBN 9780128150184.
[17] ACAMPA, G., TICALI, D., PARISI, C. M. Value of travel time: an economic assessment for transport appraisal decision-makers. *AIP Conference Proceedings* [online]. 2019, **2186**(1), 160009. ISSN 0094-243X, eISSN 1551-7616. Available from: https://doi.org/10.1063/1.5138077
[18] SPREI, F. Disrupting mobility. *Energy Research and Social Science* [online]. 2018, **37**, p. 238-242. ISSN 2214-6296. Available from: https://doi.org/10.1016/j.erss.2017.10.029
[19] KUHN, M., MARQUARDT, V., SELINKA, S. "Is sharing really caring?": The role of environmental concern and trust reflecting usage intention of "station-based" and "free-floating" - car sharing business models. *Sustainability* [online]. 2021, **13**(13), 7414. Available from: https://doi.org/10.3390/su13137414
[20] EFTHYMIOU, D., ANTONIOU, C., Modelling the propensity to join car sharing using hybrid choice models and mixed survey data. *Transport Policy* [online]. 2016, **51**, p. 143-149. ISSN 0967-070X. Available from: https://doi.org/10.1016/j.tranpol.2016.07.001
[21] MARTIN, E., SHAHEEN, S. A., LIDICKER, J. Impact of car sharing on household vehicle holdings: Results from North American shared-use vehicle survey. *Transportation research record*, 2010, *2143*(1), 150-158.
[22] KENT, J. L. Car sharing as active transport: What are the potential health benefits? *Journal of Transport and Health* [online]. 2014, **1**(1), p. 54-62. ISSN 2214-1405. Available from: https://doi.org/10.1016/j.jth.2013.07.003
[23] ZHOU, F., ZHENG, Z., WHITEHEAD, J., PERRONS, R. K., WASHINGTON, S., PAGE, L. Examining the impact of car-sharing on private vehicle ownership. *Transportation Research Part A: Policy and Practice* [online]. 2020, **138**, p. 322-334. ISSN 0965-8564. Available from: https://doi.org/10.1016/j.tra.2020.06.003
[24] FOLKESTAD, C. A., HANSEN, N., FAGERHOLT, K., ANDERSSON, H., PANTUSO, G. Optimal charging and repositioning of electric vehicles in a free-floating car sharing system. *Computers and Operations Research* [online]. 2020, **113**, 104771. ISSN 0305-0548. Available from: https://doi.org/10.1016/j.cor.2019.104771
[25] MUNZEL, K., BOON, W., FRENKEN, K., BLOMME, J., VAN DER LINDEN, D. Explaining carsharing supply across Western European cities. *International Journal of Sustainable Transportation* [online]. 2020, **14**(4), p. 243-254. ISSN 1556-8318, eISSN 1556-8334. Available from: https://doi.org/10.1080/15568318.2018.1542756
[26] BASBAS, S., GEORGIADIS, G., CAMPISI, T., TESORIERE, G. Factors influencing public transport demand in Sicily during COVID-19 era: a study of commuters' travel and mode choice behaviors. In: International Conference on Computational Science and Its Applications ICCSA 2021: proceedings [online]. Part VI. Cham: Springer, 2021. ISBN 978-3-030-86978-6, p. 339-353. Available from: https://doi.org/10.1007/978-3-030-86979-3_25
[28] CAMPISI, T., BASBAS, S., AL-RASHID, M. A., TESORIERE, G., GEORGIADIS, G. A region-wide survey on emotional and psychological impacts of COVID-19 on public transport choices in Sicily, Italy. *Transactions on Transport Sciences* [online]. 2021, **2**, p. 1-10. ISSN 1802-9876. Available from: https://doi.org/10.5507/tots.2021.010
[28] MOSLEM, S., CAMPISI, T., SZMELTER-JAROSZ, A., DULEBA, S., NAHIDUZZAMAN, K. M., TESORIERE, G. Best-worst method for modelling mobility choice after COVID-19: evidence from Italy. *Sustainability* [online]. 2020, **12**(17), 6824. eISSN 2071-1050. Available from: https://doi.org/10.3390/su12176824
[29] BELZUNEGUI-ERASO, A., ERRO-GARCES, A. Teleworking in the context of the COVID-19 crisis. *Sustainability* [online]. 2020, **12**(9), 3662. eISSN 2071-1050. Available from: https://doi.org/10.3390/su12093662
[30] CECCATO, R., ROSSI, R., GASTALDI, M. Travel demand prediction during COVID-19 pandemic: educational and working trips at the University of Padova. *Sustainability* [online]. 2021, **13**(12), 6596. eISSN 2071-1050. Available from: https://doi.org/10.3390/su13126596
[31] DIANA, M., CECCATO, R. A multimodal perspective in the study of car sharing switching intentions. *Transportation Letters* [online]. 2019, Latest Articles. ISSN 1942-7867, eISSN 1942-7875. Available from: https://doi.org/10.1080/19427867.2019.1707351
[32] BOJKOVIC, N., JEREMIC, V., PETROVIC, M., TICA, S. Preferences for car sharing service attributes among university students: evidence from an emerging market. *JEEMS Journal of East European Management Studies* [online]. 2019, **24**(4), p. 636-653. ISSN 0949-6181, eISSN 0949-6181. Available from: https://doi.org/10.5771/0949-6181-2019-4-636
[33] ZHOU, J. An analysis of university employee car-sharers in Los Angeles. *Transportation Research Part D: Transport and Environment* [online]. 2012, **17**(8), p. 588-591. ISSN 1361-9209. Available from: https://doi.org/10.1016/j.trd.2012.07.003

[34] TURON, K., KUBIK, A., CHEN, F. Electric shared mobility services during the pandemic: transport modelling aspects. *Energies* [online]. 2021, **14**(9), 2622. eISSN 1996-1073. Available from: https://doi.org/10.3390/en14092622

[35] ARBELAEZ VELEZ, A. M., PLEPYS, A. Carsharing as a strategy to tackle greenhouse gas emissions in the transport system: assessing the effects of carsharing in Amsterdam. *Sustainability* [online]. 2021, **13**(4), 2418. eISSN 2071-1050. Available from: https://doi.org/10.3390/su13042418

[36] CECCATO, R., DIANA, M. Substitution and complementarity patterns between traditional transport means and car sharing: a person and trip level analysis. *Transportation* [online]. 2021, **48**, p. 1523-1540. ISSN 0049-4488, eISSN 1572-9435. Available from: https://doi.org/10.1007/s11116-018-9901-8

[37] DIAS, F. F., LAVIERI, P. S., GARIKAPATI, V. M., ASTROZA, S., PENDYALA, R. M., BHAT, C. R. A behavioural choice model of the use of car-sharing and ride-sourcing services. *Transportation* [online]. 2017, **44**(6), p. 1307-1323. ISSN 0049-4488, eISSN 1572-9435. Available from: https://doi.org/10.1007/s11116-017-9797-8

[38] LIKERT, R., A technique for the measurement of attitudes. *Archives of Psychology*. 1932, **140**, p. 5-55. ISSN 0272-6653.

[39] LOUVIERE, J. J., MEYER, R. J., BUNCH, D. S., CARSON, R., DELLAERT, B., HANEMANN, W. M., HENSHER, D., IRWIN, J. Combining sources of preference data for modelling complex decision processes. *Marketing Letters* [online]. 1999, **10**(3), p. 205-217. ISSN 0923-0645, eISSN 1573-059X. Available from: https://doi.org/10.1023/A:1008050215270

[40] CURTIS, K., YOUNGQUIST, S. T. Part 21: categoric analysis: Pearson chi-square test. *Air Medical Journal* [online]. 2013, **32**(4), p. 179-180. ISSN 1067-991X. Available from: https://doi.org/10.1016/j.amj.2013.04.007

[41] SHARPE, D. Chi-square test is statistically significant: now what? *Practical Assessment, Research and Evaluation* [online]. 2015, **20**(1), 8. ISSN 1531-7714. Available from: https://doi.org/10.7275/tbfa-x148

[42] BLAND, J. M., ALTMAN, D. G. Statistics notes: Cronbach's alpha. *BMJ*. 1997, **314**(7080), 572. ISSN 0959-8138, eISSN 1756-1833. Available from: https://doi.org/10.1136/bmj.314.7080.572

[43] COOK, T., D., CAMPBELL, D., T., *Quasi-experimentation: design and analysis issues for field settings*. Chicago: Rand MacNally, 1979.

[44] SHADISH, W., R., COOK, T., D. AND CAMPBELL, D., T. *Experimental and quasi-experimental designs for generalized causal inference*. Cengage Learning, Inc., 1991. ISBN 978-0395615560.

[45] TORRISI, V., GARAU, C., IGNACCOLO, M., INTURRI, G. "Sustainable urban mobility plans": key concepts and a critical revision on SUMPs guidelines. *Lecture Notes in Computer Science* [online]. 2020, **12255**, p. 613-628. ISSN 0302-9743, eISSN 1611-3349. Available from: https://doi.org/10.1007/978-3-030-58820-5_45

KOMUNIKÁCIE
COMMUNICATIONS

VEDECKÉ LISTY ŽILINSKEJ UNIVERZITY
SCIENTIFIC LETTERS OF THE UNIVERSITY OF ZILINA

VOLUME 24 Number 3

July 2022

Address of the Editorial Office:
University of Zilina
EDIS - Publishing House
Univerzitna 8215/1
010 26 Zilina, Slovakia

E-mail: komunikacie@uniza.sk

Individual issues of the journal can be found on: http://komunikacie.uniza.sk

Each paper was reviewed by two reviewers.

Journal is currently indexed by SCOPUS and DOAJ, and is icluded in portal SJR - SCImago Journal & Country Rank, EBSCO host, ROAD, Crossref (DOI), iThenticate and Google Scholar.

Published quarterly by University of Zilina in EDIS - Publishing House of the University of Zilina.

Registered No: EV 3672/09

ISSN (print version) 1335-4205
ISSN (online version) 2585-7878

ICO 00397 563

The full author quidelines are available at: https://komunikacie.uniza.sk/artkey/inf-990000-0400_Author-guidelines.php

UNIVERSITY
OF ŽILINA

In its over 65 years of successful existence, the University of Žilina (UNIZA) has become one of the top universities in Slovakia.

Scientific conferences

organized by University of Žilina

38th DANUBIA – ADRIA Symposium on Advances in Experimental Mechanics 2022
Date and venue: 20. - 23. 9. 2022, Poros Island (GR)
Contact: frantisek.novy@fstroj.uniza.sk
Web: https://das.tuwien.ac.at/home/

Geosynthetics 2022
Date and venue: 22. - 23. 9. 2022, Žilina (SK)
Contact: filip.gago@uniza.sk
Web: https://www.geosyntetika.sk/

12th International Conference Horizons of Railway Transport 2022
Date and venue: 30. 9. - 1. 10. 2022, conference wagon in special train Praha – Bratislava – Košice – Žilina (CZ, SK)
Contact: jozef.gasparik@fpedas.uniza.sk
Web: https://fpedas.uniza.sk/~horizonty/

31. R-S-P Seminar, Theoretical Foundation of Civil Engineering (31RSP) (TFoCE 2022)
Date and venue: September 2022, Žilina (SK)
Contact: andrea.husarikova@uniza.sk

Transport Infrastructure in Cities
Date and venue: 04. - 05. 10. 2022, Žilina (SK)
Contact: dopravna.infrastruktura@fstav.uniza.sk
Web: https://svf.uniza.sk/kcs/

Globalization and its Socio-Economic Consequences 2022
Date and venue: October 2022, Rajecké Teplice (SK)
Contact: globalizacia@globalizacia.com
Web: https://globalizacia.com/

19th Seminar of Track Management STRAHOS 2022
Date and venue: 13.-14. 10. 2022, Poprad (SK)
Contact: strahos2022@fstav.uniza.sk
Web: https://svf.uniza.sk/strahos/

Solid State Surfaces and Interfaces 2022
Date and venue: 9.-10. 11. 2022, Bratislava (SK)
Contact: juliana.blaskova@fpedas.uniza.sk
Web: www.inair.uniza.sk

11th International Conference on Air Transport INAIR 2022
Date and venue: 21. - 24. 11. 2022, Smolenice (SK)
Contact: stanislav.jurecka@uniza.sk
web: https://www.savsssi.sk/scope/

UNIVERSITY OF ŽILINA
Science & Research Department
Univerzitná 8215/1, 010 26 Žilina, Slovakia
Ing. Janka Macurová
tel.: +421 41 513 5143
e-mail: janka.macurova@uniza.sk